The use of metabonomic profiling approaches for the investigation of complex food fraud

Kate Louise Sidwick

Thesis submitted for the degree of Doctor of Philosophy

March 2019

Keele University

Abstract

Food fraud is a challenge in today's expanding global food industry. Recently weaknesses in current testing methods for meat authentication have been exposed. Labels are assumed to accurately describe the contents of meat products, however these can be easily manipulated. Consumers must have confidence in food products for various reasons, including allergies and religious beliefs. Techniques have been created to target obvious types of fraud, however the more subtle types remain difficult to combat. This work aimed to understand the chemical composition of meat products in order to develop methods that can tackle complex frauds. The development of a data processing and statistical workflow sufficient for vast untargeted metabonomic datasets was also essential for this research.

Liquid chromatography quadrupole time-of-flight mass spectrometry, with robust quality control procedures and multivariate statistics, were used to measure changes in the metabolic profile of meat samples. Specifically, the differentiation between normally slaughtered and dead on arrival chicken was achieved, and sphingosine was identified as a key marker in the muscle tissue. An investigation into the duration of frozen storage and freeze-thaw cycling of meat found the fatty acid degradation pathways were most affected. The adulteration of minced beef products with other meat species yielded the tentative identifications of several markers that could be used to detect adulterated beef products regardless of whether the meat is raw or cooked. Finally, the metabolic changes occuring during the spoilage of chicken were observed, and showed that amino acid and fatty acid concentration could be used to determine the shelf-life of meat products.

The methodologies that have been presented in this work have shown potential to be implemented and developed as robust detection methods to combat subtle food frauds in the future.

Contents

List of Tables

List of Figures

Abbreviations

ANOVA	Analysis of variance
AQ	Aqueous extract
ATP	Adenosine triphosphate
a.u.	Arbitrary units
CE	Capillary electrophoresis
CV	Coefficient of variance
DOA	Dead on arrival
EIC	Extracted ion chromatogram
ELISA	Enzyme linked immunosorbent assay
ESI	Electrospray ionisation
FSA	Food Standards Agency
FT	Freeze-thaw
GC	Gas chromatography
HILIC	Hydrophilic interaction chromatography
HPLC	High performance liquid chromatography
ICP-MS	Inductively coupled plasma mass spectrometry
IR	Infrared
IRMS	Isotope ratio mass spectrometry
MRM	Mechanically recovered meat
MS	Mass spectrometry
MS/MS	Tandem mass spectrometry
$\boldsymbol{m/z}$	Mass-to-charge ratio
NMR	Nuclear magnetic resonance
NS	Normally slaughtered
OR	Organic extract
PAF	Platelet activating factor

PC	Principal component
PCA	Principal component analysis
PCR	Polymerase chain reaction
QC	Quality control
Q-TOF	Quadrupole time-of-flight
RAPD	Random amplified polymorphic DNA
rcf	Relative centrifugal force
RFLP	Restriction fragment length polymorphism
ROS	Reactive oxygen species
SD	Standard deviation
SIM	Selected ion monitoring
TIC	Total ion chromatogram
UHPLC	Ultra high performance liquid chromatography

Acknowledgements

I would like to take this opportunity to thank my supervisor **Dr David Thompson**, for the chance to do this research project, and for helping me grow as a researcher. I would also like to thank **Dr Luisa Pereira** for her advice, and the opportunity to gain invaluable experience at Thermo Fisher Scientific in Runcorn. My thanks also go to **Dr Craig Adam** for his instruction regarding statistical analyses. Thank you to **Dr Tony Edge** and **Professor Ian Wilson** for their professional advice and support during this project. This research project would also not have been possible without the funding from the **BBSRC iCASE studentship BB/L015439/1** and **Thermo Fisher Scientific**.

I am very thankful to everyone I have shared an office with, both past and present, for creating a wonderful environment to work in, and providing a break from research over a cup of tea. I would like to express my thanks to **Dr Steven Wye** for his assistance with all computer-based problems I have encountered. I am particularly grateful to **Amy Johnson** and **Sue Shemilt**, who have given me so much support during my time at Keele, both personally and academically. Thank you for listening to research plans and talking through experiments, and the time spent reading my thesis is greatly appreciated. I will forever be grateful to **Amy** for her incredible help during my second year.

My sincerest thanks go to my family for always being there for me. Their encouragement has motivated me to always work hard, and I would not be where I am today without their love and support. Finally, I would like to thank **Luke Johnson**, whose unwavering optimism and positivity have helped me through the past 4 years, and will continue to do so in the future. Thank you for always believing in me, and assuring me that I've got this.

Chapter 1

Introduction

1.1 Food fraud

1.1.1 Background

Food fraud occurs when food is placed on the market with the deliberate intent of deceiving the customer, whether it is for financial gain or an easier method of producing the product [1]. It includes adulteration, ingredient substitution, and tampering of the label [2] to reduce production costs whilst appearing to offer the same product in the eyes of the consumer. Adulterating with cheap alternatives, stating false information on the labels, and extending the shelf-life of products are all manners in which manufacturers commit food fraud [3]. The increasing globalisation of the food industry creates complex issues when authenticating food products, which means methods need to be developed to detect these fraudulent activities.

Food fraud is generally considered to be an economic issue, however any modification to the food product that the consumer is not aware of may lead to adverse health effects. The criminal is the only person aware of changes to the product not stated on the label, but would not have the expertise to deduce if the changes to the product have any toxic or hazardous effects to the consumer [4]. A change to a food product that remains unknown to the public is also an issue for people with allergies; if the label does not state exactly what is in the product, it could cause serious harm to the consumer. Some religious communities also require the labels on food products to be correct in order to avoid ingredients that are prohibited due to their beliefs [5]. This is why it is crucial that the contents within a food item are specified on the label,

describing exactly what is in the product, enabling the consumer to make an educated decision to buy food items that suit their own particular requirements or religion [6].

Not only do these fraudulent activities affect the consumer, but they also cause an issue for honest producers. The cost of their production remains as expected, and so the profit margin is considerably less than producers who deliberately deceive consumers in order to reduce production costs. This provides additional temptation for more producers to start being dishonest about the production method or contents of their products, especially when many acts of fraud go undetected due to the subtle nature of the changes to the product, and the lack of a method of detection.

The Food Standards Agency (FSA) is a governmental body covering England, Wales and Northern Ireland. They aim to protect the consumer's health and interests in relation to food, and is responsible for the safety and hygiene of food, as well as maintaining the consumers' confidence in the food they purchase. The FSA have carried out 'The Food and You survey' every 2 years since 2010. This questionnaire aids in understanding the public's perception of the food industry. In 2014, only 34% of respondents said they always felt confident in the information on labels of food products, and of those who were not confident, 31% said they read the food labels more carefully [7]. This is evidence that consumers put a large amount of faith into the information on food labels, but unfortunately mislabelling is one of the main methods for food fraud, and it is difficult to detect.

1.1.2 Recent food fraud incidents

There are a vast range of food products that have been targeted by food fraud in recent years. Specifically: honey, olive oil, seafood, meat, dairy products and herbs and spices [8]. Due to the direct impact these incidents can have to the public, many of these fraudulent activities are reported in the news, making the public aware of the

issues within the food industry and decreasing their trust in food products. The Joint Research Centre (JRC) of the European Commission provides a monthly report on the issues that have arisen in media coverage regarding the global food industry [9]. From the 2018 reports, the main acts of fraud are through mislabelling of products, substitution of ingredients and masking of the origin of the product. The main food areas that have been targeted are seafood, meat and wine. Specifically in the UK, fish products were illegally exported through the use of another company's label, an Indian restaurant was found to be selling mutton as lamb and eggs were sold as free-range at a high price despite not meeting the criteria for free-range products [9].

Within these reports, there have also been many cases of fraud that could have posed a health risk to the public had it not been detected. Bakeries in Pakistan were selling products containing possible carcinogenic substances replacing food colours, meat in Brazil had been found to be adulterated with starch at a level above the legal limit and contaminated with listeria, and meat not suitable for human consumption entered the Belgium market as minced meat with falsified expiry dates. The incorrect storage or consumption after the use-by date has severe health implications, as bacteria accumulates on food products, causing food poisoning. Adulteration with unknown compounds can also cause health implications. One of the most known cases of this in recent years was the adulteration of milk with melamine in China in 2008. Melamine is a chemical used in glues and adhesives, and is used in milk to increase the nitrogen concentration. This falsely indicates an increase in protein concentration, despite the dilution of the milk [10]. The health effects of this adulteration were vast, with 52,000 children hospitalised, and 6 infant deaths, caused by the detrimental effects melamine has on the human body [11].

The meat industry appears to be heavily targeted for fraud on a regular basis. The detection of undeclared horsemeat in processed beef products in Europe in 2013 confirmed the vulnerability of this industry. With the vast complexity of the food

supply chain, it became evident that the authentication methods in place were not sufficient to stop a large scale adulteration event to occur. Despite this realisation 5 years ago, undeclared horsemeat has continued to be found in meat products, specifically in the Irish market [9].

1.1.3 Authentication techniques

The authentication of food products confirms the information on the label is correct. This information includes geographical origin, ingredient content, and production and processing methods [12]. Many organisations and governments have been created around the world to provide standardised criteria for higher quality items that can be sold at a more expensive cost. This creates an opportunity for counterfeiting and mislabelling in order to benefit economically. With the advancement of technology, there are several techniques that can be employed to authenticate food products, including genomics and proteomics, chromatography, isotope ratio methods, immunological methods, and spectroscopy [12].

DNA-based techniques have been particularly useful in determining the species in meat and fish products, especially in processed foods [13]. A polymerase chain reaction (PCR) assay is the fundamental approach in DNA-based food authentication methods, where specific small fragments of DNA are amplified to determine the species or origin of a product, usually analysed through the use of gel electrophoresis. This is useful when looking at the adulteration with different species, however it has limited value when meat is adulterated with tissue of the same species. This is an issue when products are represented as 100% chicken breast tissue, for example. Food authentication methods using a proteomic approach involves the use of high resolution mass spectrometry to detect peptide markers associated with different foods. This technique is mostly used for species determination, and as such, complements DNA-based techniques [14]. These techniques were particularly useful

during the investigation of undeclared horsemeat in processed beef products.

Chromatographic methods are able to separate the individual components within a complex mixture that can be encountered during food analyses, and can attempt to identify compounds when coupled to other techniques, such as mass spectrometry. High performance liquid chromatography (HPLC) is able to detect proteins, carbohydrates and lipids, and gas chromatography is more applicable to volatile compounds. Gas chromatography has been used in detecting the adulteration of olive oil based on the fatty acid content, as well as determining the geographical origin of olive oil [15]. HPLC is a fairly new addition to the tools used for authenticating of food products, and has been used to detect the adulteration of milk, and the analysis of triglycerides to differentiate between coffee types. Ultra high performance liquid chromatography (UHPLC) has been successful in quantifying polyphenols in fruit juice, which is important due to the elevated prices associated with fruit juice containing a high concentration of polyphenols based on the health benefits of these compounds [16].

EU legislation [17] provides protection for food products based on geographical origin [18]. Protected Designation of Origin (PDO) is the term used for food items that are associated to a specific region based on exact and unique processing techniques that cannot be carried out in alternative locations. These food products have a higher value associated to them, and therefore analytical techniques are required in order to verify their geographical origin. This aids in preventing mislabelling and origin masking that causes consumers to pay more for a food product that has not originated from a location with associated higher prices. Many techniques have been implemented to determine the geographical origin of products, including gas chromatography mass spectrometry, spectroscopic techniques such as nuclear magnetic resonance (NMR) and infrared (IR) spectroscopy, and HPLC and capillary electrophoresis (CE) [19]. The best approaches for the authentication of

geographical origin, however, are isotope-based techniques, such as isotope ratio mass spectrometry (IRMS), and elemental analysis methods, such as inductively coupled plasma mass spectrometry (ICP-MS) [18]. The isotopic and elemental composition of soil and fodder varies globally, and these properties allow IRMS and ICP-MS to be beneficial in verifying the geographical origin of food products. IRMS has been used to differentiate between cheeses from different regions of Italy based on the carbon and nitrogen isotopes [20], and ICP-MS has been successful in determining the origin of onions based on the mineral composition [21].

Immunoassays are commonly used within the meat industry for authentication purposes due to their high sensitivity and low cost. They use antibodies that bind specifically to a protein of interest in a food sample and are most often used to identify the species of a meat product and any potential adulterant meat. Enzyme Linked Immunosorbent Assay (ELISA) is the most prevalent method for food authentication, and again is mostly used to differentiate between meat species [22]. Despite many advantages, these techniques can give false-positive results, rely on the availability of antibodies for the proteins of interest, and are not useful with processed products that have undergone extreme heat [23].

Spectroscopic techniques are often used in food authentication due to the speed of analysis, cost of equipment, and its non-destructive nature. These methods usually require the use of advanced mathematical and statistical processes to aid in the interpretation of the results. Fluorescence spectroscopy detects polyaromatic hydrocarbons and heterocyclic compounds, and has been used to differentiate between virgin olive oil and other cheaper alternatives. Infrared spectroscopy has been used to authenticate a wide range of food products such as honey, meat and cheese, and it has also been implemented to detect and quantify the adulteration of milk. Raman spectroscopy is not subjected to interference by water like other spectroscopic techniques, and so is particularly useful with food that has a high water

content, such as fruit and vegetables. It has been able to detect the adulteration of honey, olive oil, meat and fish [24].

All of these techniques have been successful in a variety of areas within the food industry, however they all have disadvantages associated with them, and many of them require prior knowledge before analysing samples. The development of techniques that gain a global view of the chemical composition of the food products will provide the fundamental research needed for targeted assays to be developed, that may be more efficient than current methods.

1.1.4 Meat fraud

As previously mentioned, one of the main areas of interest today is meat fraud, mainly stimulated by the detection of horse meat in processed meat in 2013 [6]. Ever since this incident, the consumers trust in meat products has decreased substantially, and it has become evident that there are weaknesses in the testing of the authenticity of meat products. There have been many studies investigating methods to measure the authenticity of meat, as described previously, however, these techniques all have disadvantages, especially when investigating the more subtle changes to food products that currently rely on the information on the label.

It is essential to develop untargeted methods and workflows that are able to provide an insight into the chemical composition of meat products and associated fraudulent products. These will subsequently determine specific markers or types of compounds that are significant to particular types of fraud, which will aid in the development of targeted assays to combat fraud within the increasingly complex food industry.

1.2 The chemistry of meat

1.2.1 Muscle to meat conversion

Animals have three kinds of muscle tissue; skeletal, smooth and cardiac. It is the skeletal muscle that is most commonly used in meat products. Skeletal muscle, the structure of which can be seen in Figure 1.1, consists of long, thin cells called muscle fibres, which contain myofibrils that form the contracting part of the muscle. A number of muscle fibres are gathered together and encased in connective tissue called endomysium, and surrounded by a thin sheet of connective tissue called perimysium [25]. Many of these bundles are held together by a thicker layer of connective tissue called epimysium, and blood vessels run throughout these structures. These blood vessels provide the oxygen necessary for oxidative phosphorylation to occur and energy in the form of adenosine triphosphate (ATP) to be produced for muscle contraction. When muscle contraction occurs there is a delay in the increase of ATP production, so in the meantime creatine phosphate aids in the rapid production of ATP. The blood vessels also transport carbohydrates, proteins and lipids around the body where they are stored in or near the muscle tissue ready to be used for energy once the muscle ATP stores are depleted, particularly during times of exercise [26].

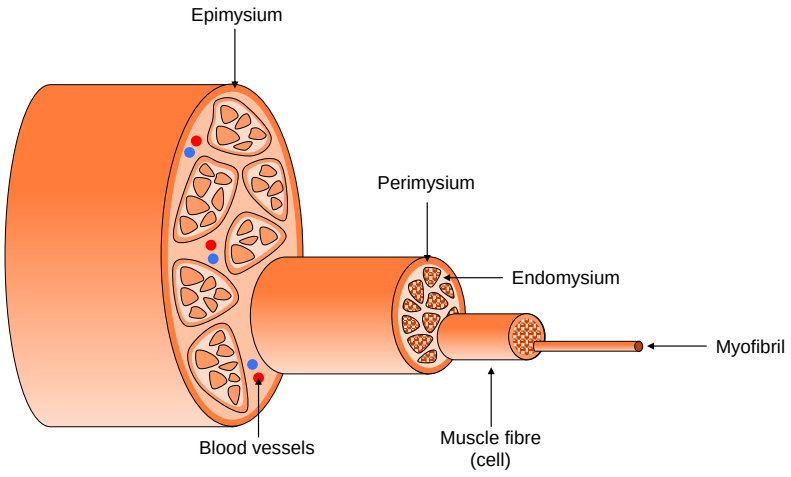

Figure 1.1: Structure of skeletal muscle, adapted from Stanfield and Germann [26]

The conversion of muscle to meat is a complicated biochemical process that happens after death. Once blood circulation stops, anaerobic conditions begin, causing the local energy sources to be used. ATP is immediately generated by the dephosphorylation of creatine phosphate, and then later by glycogenolysis and glycolysis. However, once the concentration of creatine phosphate decreases, ATP decreases and free phosphate groups increase, which causes the accumulation of lactate and a decrease in pH. Rigor mortis is the point in which the muscles become stiff and rigid due to reaching a plateau in the lactate concentration and pH level [27]. This also causes a decrease in the water-holding capacity of the muscle, where water moves into the extracellular space and out of the muscle, resulting in shortening of the myofibrils and shrinkage. Proteases then degrade proteins within the muscle, thus improving the tenderness [27]. The anaerobic conditions in the muscle tissue results in the production of reactive oxygen species, which then cause oxidative damage to proteins. This aids in the tenderisation of the meat, however if it continues, the meat becomes tough and dark, decreasing the quality of the meat product [28]. All of these processes show that vast chemical changes occur after death, and these can be exploited to detect complex fraud within the meat industry.

1.2.2 Different tissue types

Muscle is the most common tissue type used in meat products in the UK. The consumption of other tissue types, such as liver and heart, has increased around the world due to their nutritional benefits. Liver has been found to contain higher amounts of polyunsaturated fatty acids (PUFA), creatine and carnosine compared to muscle tissue [29], and heart tissue has been reported to have a high amount of leucine, lysine and other amino acids [29, 30]. It is also known that the cholesterol content is higher in the organs of animals compared to the muscle tissue.

The chemical composition varies substantially between tissue types, as well as being

affected by environmental influences, such as diet, geographical origin and exposure to light [31]. This can cause the chemical analysis of different tissue types to become very complex.

1.3 Metabonomics

Metabonomics is the study of metabolites, which are low molecular weight compounds (less than 1500 Da); collectively known as the metabolome. They include mainly organic species such as amino acids, fatty acids, carbohydrates, vitamins and lipids [32]. Metabonomics can be defined as the 'quantitative measurement of the dynamic multiparametric metabolic response of living systems to pathophysiological stimuli or genetic modification' [33, 34]. It focusses on the changes in metabolic profile caused by disease or environmental influences. This term can be confused with metabolomics, which is the study of the metabolites present within an organism, cell or tissue [35], and both terms have been used interchangeably [36]. Metabolomics tends to describe the study of metabolites within a single cell, whereas metabonomics studies the full systems biology approach, which encompasses the whole organism, including all organs and cell types, and the changes that occur over time [34]. It can be classified within the 'omics' technologies, which includes genomics, the study of the genome; transcriptomics, the study of gene expression; proteomics, the study of protein expression; and finally metabonomics, the study of the metabolome [36]. Analyses using metabonomic methods can be both targeted, where a specific compound or class of compound can be searched for, and untargeted. The latter is more of an issue due to the vast number of metabolites that can be present within a sample, however, it is a very useful technique for initial investigations [35]. Many metabolites can be found, and any metabolic changes due to diet, environment, disease, or drugs can be monitored over a period of time [37].

Metabonomics has the advantage of analysing the metabolic profile of the whole organism, which increases its usefulness in many fields of research [38], including medicine [39, 40], nutrition [41, 42], environmental sciences [43–45], and toxicology [46–48]. The concept of metabonomics originated from work using nuclear magnetic resonance (NMR) to study the metabolism of metal compounds in human blood [49]. The use of NMR as an analytical technique for metabonomics has been the main focus for research due to the structural information that can be obtained from this method [50]. In the last 10 years, the use of mass spectrometry has become increasingly more popular in the field of metabonomics [51, 52], and it can be coupled with techniques such as gas chromatography, liquid chromatography and capillary electrophoresis [53].

Metabonomics has become a frequently used tool for the quality, processing and safety of food products. Utilising an untargeted approach, a metabolic profile can be obtained, and markers can be found that can be used to detect food fraud [54]. The untargeted approach is particularly beneficial in this field as any changes to the metabolic profile can be detected without any previous knowledge. There are a number of areas within the food industry with the potential to use this technique, including honey, oils, alcohol, fruit juices and meat [55]. Adulteration of fruit juices is a common area of fraud due to the high cost of producing 100% fresh juice, and it is difficult to detect adulterants just by taste or aroma [42]. The metabolic profile of juice can be obtained by analytical methods such as ultra-high performance liquid chromatography coupled with quadrupole time-of-flight mass spectrometry (UHPLC-Q-ToF), and the purity of the juice can be investigated to see if it has been adulterated with other fruit juices, water, or added sugars, to assess the overall authenticity of the juice [56]. There has also been a lot of research in the use of metabonomic techniques for investigating the authenticity of high price items such as honey, oils and wine [57]. It is common to get fraud occurring within the expensive products on the market, due to the manufacturers excluding the ingredient that

makes the product expensive, and replacing it with a cheaper alternative, without the consumers' knowledge. The origin of the ingredients is also a factor when it comes to the price of food items, with certain food products considered to be of better quality originating from one location over another. Many analytical techniques are used in order to determine the geographical origin of food products, including mass spectrometry, spectroscopy, and chromatography [19]. Interestingly, metabonomics has been applied to orange origin discrimination with the use of UHPLC-Q-ToF, using robust quality control protocols, to identify markers for the authentication of Valencia oranges [58].

Focussing on the meat industry, previous metabonomic approaches have been applied to the verification of the origin of meat, the identification of any meat substitution, the identification of meat processing treatments and the detection of any non-meat additives [59]. Specifically, inductively coupled plasma-mass spectrometry (ICP-MS) has been found to be useful in determining the origin of meat products based on the elemental composition. NMR-based metabonomics has also proven useful in determining the geographical origin of beef products [60]. The detection of the illegal act of mechanically recovered meat (MRM) using metabolic profiles obtained from gas chromatography-mass spectrometry (GC-MS) has also been investigated, with specific markers found to show potential in detecting this fraudulent activity [61]. This study included additional extraction processes to ensure all metabolites were obtained, and reproducibility tests to gain reliable data. The application of metabonomics and small molecule profiling to understanding the complex chemical changes that occur in animals prior to and after slaughter, as well as during different storage conditions, could aid in the detection of very subtle and complex frauds that occur within the meat industry. These include the falsification of shelf-life dates, and mislabelled fresh products that have been previously frozen.

1.4 Rationale and aims

The importance of authenticating meat products has reached a critical point in society. The food supply chain has become more complex and global in nature, causing frauds to continue without detection despite tests being in place. The more subtle frauds that rely on trusting the labelling of products are extremely difficult to control due to the lack of methods that can detect them. These subtle frauds can cause many concerns to the consumer as the changes made to the product could defy their personal or religious beliefs, as well as potentially causing negative health effects.

This work aims to address key areas within the meat industry, some of which do not currently have a chemical method of detection. Using an untargeted metabonomic approach, a deeper understanding of the chemical changes that occur within meat products before and after slaughter could aid in the development of more specific targeted assays that can then be used within the meat industry to detect the more subtle changes to food products. This fundamental research aimed to present a workflow suitable for initial small molecule profiling studies that focussed on extremely subtle changes in meat products. This was with the purpose to aid in the development of targeted approaches for the issues specified in this work. The application of the workflows and techniques used in this research could also be implemented to detect other subtle frauds in complex matrices other than meat in the future.

The specific aims for this research are as follows:

- To develop a data processing and statistical workflow suitable for untargeted metabonomic studies
- To investigate the metabolic differences between normally slaughtered and dead on arrival poultry meat

- To examine the changes in metabolic content during frozen storage of chicken muscle, lamb muscle and lamb liver tissue
- To determine the effect that freeze-thaw cycling has on the metabolic content of chicken muscle and lamb liver tissue
- To analyse the effect of adulteration on raw and cooked minced beef with different percentages of minced pork, lamb or turkey meat
- To investigate the metabolic changes that occur during the spoilage process in chicken muscle tissue stored at different temperatures to independently determine the shelf-life of chicken

Chapter 2

Analytical techniques and methodologies

2.1 Chromatography

Chromatography is a technique that is used to separate components within a complex mixture. The method is based on the transport of a mixture suspended in a mobile phase through a stationary phase. The components within the mixture are separated depending on the affinity to both phases [62]. The stationary phase is usually a solid in a small-particle form, and the mobile phase is either a gas (gas-chromatography) or a liquid (liquid chromatography) [63].

2.1.1 High performance liquid chromatography

Liquid chromatography is a technique that can be used to separate a variety of organic compounds. It can provide both a qualitative and quantitative analysis of a mixture, with each component having its own retention time and peak area proportional to the amount of that component [63]. Some components can have the same retention time as each other under the same conditions, and this is known as co-eluting. The basic instrumentation consists of a solvent reservoir, a pump, an injector port, the column, a detector, and a data processing system [64]. The solvent reservoir contains the mobile phase, which usually consists of water and an organic solvent. The mobile phase aids in the transport of compounds within the mixture and affects the separation of individual components. The pump forces the mobile phase through the system at a high pressure. These can be binary in order to pump two different mobile phases at the same time, or quaternary for four mobile phases.

The injector port controls the introduction of the liquid sample and works via a rotating valve system. In the load position, the mobile phase flows from the pump to the column, while the sample is injected and fills the loop, and any excess is removed via the waste line. In the inject position, the mobile phase flows from the pump, through the loop, and to the column, carrying the sample [62].

The column contains the stationary phase, which works with the mobile phase to separate the mixture dependent on how the individual components interact with each phase. Typically, the stationary phase is made up of spherical silica gel beads. The type of liquid chromatography depends on the polarity of the stationary phase; normal phase HPLC will have a polar stationary phase and a less polar mobile phase, and reversed phase HPLC will have a nonpolar stationary phase and a more polar mobile phase.

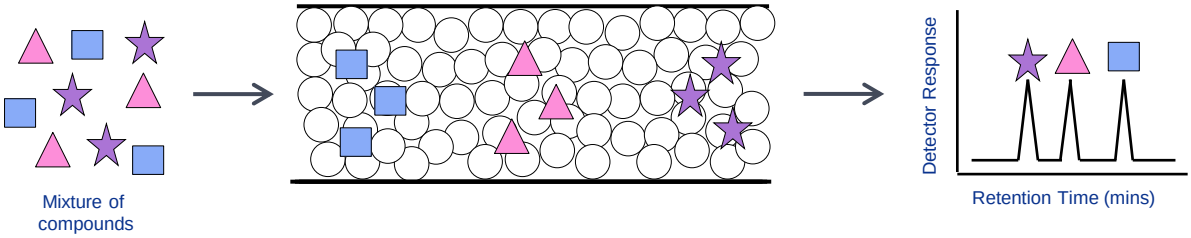

Figure 2.1: Separation of compounds in Reversed Phase Liquid Chromatography, adapted from Bayne and Carlin [64]

A compound that has a higher affinity for the stationary phase than the mobile phase will be retained on the column for longer and so will have a longer retention time. Ideally, individual components within a sample will have differing affinities for the stationary phase, so all compounds will have different retention times and produce a chromatogram containing peaks with good separation, as shown in Figure 2.1. The compounds that have a low affinity for the stationary phase will travel through the column faster, and reach the detector first, causing a peak in the chromatogram.

In reversed phase HPLC, which is the type of chromatography used in this work, the stationary phase consists of silica gel beads that are coated with hydrophobic alkyl chains of varying lengths; C4, C8 and C18. The longer the alkyl chain, the less polar the stationary phase [64]. The mobile phase is made up of an aqueous solvent, and an organic solvent with a stronger eluting power, commonly methanol or acetonitrile. The addition of a buffer is beneficial when analysing ionisable compounds to ensure the pH is kept constant, which helps promote separation. Keeping the concentration of the aqueous and organic solvent constant is known as an isocratic separation, and a varied concentration throughout the analysis is known as a gradient separation. A gradient separation is most likely to be used in reversed phase HPLC, especially during initial analyses when the conditions for a successful separation of a complex mixture are unknown [63]. This usually begins with a low concentration of organic solvent, such as 5%, with a gradual increase to 100% to assess the separation of the components. It is not recommended to use 100% aqueous solvent as this causes the long carbon chains within the stationary phase to collapse. A gradient method can be developed to include varying rates of increasing organic solvent in order to get the best separation in the most efficient amount of time. The most nonpolar compounds will be retained by the stationary phase for longer, and the most polar compounds will elute first. By changing the concentration of the organic solvent, the retention time for compounds can be optimised for a more efficient analysis. Increasing the concentration of the organic solvent in the mobile phase will decrease the polarity of the mobile phase, causing the nonpolar components within the mixture to be less retained on the stationary phase and to elute quicker. The rate in which the organic solvent is increased is also a useful tool when developing an efficient chromatographic separation; by slowing the rate of an increase in organic solvent concentration, compounds that elute close together can be better separated. Once the sample has been separated using chromatography, the individual components can be measured via a variety of detectors, including diode array detectors and mass spectrometers.

2.2 Mass spectrometry

Mass spectrometry (MS) is an analytical technique that determines the molecular masses of individual compounds within a sample [62]. In LC-MS, the sample reaches the mass spectrometer after separation via liquid chromatography. During mass spectrometry, the sample undergoes a series of steps: ionisation, where the sample is converted to a gas and ionised in the ion source; separation, where the ions enter a mass analyser and are separated based on their mass-to-charge ratio (m/z); and detection, where the ions strike the detector and the electrical charge is measured. Finally, a data processing system is used to display the mass spectrum, with an x-axis showing m/z and the y-axis showing the signal intensity. The spectrum can be interpreted to give an indication to the composition and structure of the molecule [62].

2.2.1 Ionisation

There are a number of ion sources that can be utilised in mass spectrometry. In this work, electrospray ionisation (ESI) was used, which is the most commonly used technique for analysing liquid samples due to its compatibility with chromatographic techniques, low chemical specificity, and high ionisation efficiency [65].

2.2.1.1 Electrospray ionisation

During the transition from liquid to gas, the sample solution is subjected to three main processes; generation of charge droplets, solvent evaporation, and the production of gas-phase ions [66]. The solution is passed through a small capillary tube, which has a high voltage, and an aerosol of charged droplets is formed that have the same polarity as the capillary voltage [67]. These droplets are then passed through a curtain of inert gas, usually nitrogen, which causes desolvation of the droplets. The charges in

the droplets are arranged equally on the surface. The surface tension of the charged droplet tries to keep the shape of the droplet, while the charges of the same polarity on the surface of the droplet repel each other, which is known as the Coulomb force [66]. The size of the droplet decreases as desolvation occurs, caused by the presence of a drying gas and an elevated temperature, which leads to a greater charge density. When it reaches the point where the Coulomb force is greater than the surface tension, the droplet breaks apart, which is known as a Coulomb explosion. This causes ions at the surface of the droplet to be ejected into the gaseous phase [67]. These charged ions are then passed through a skimmer cone, to focus the ion beam and ensure the trajectory of the ions is stable [66], and accelerated towards the mass analyser, where their mass-to-charge ratio is measured.

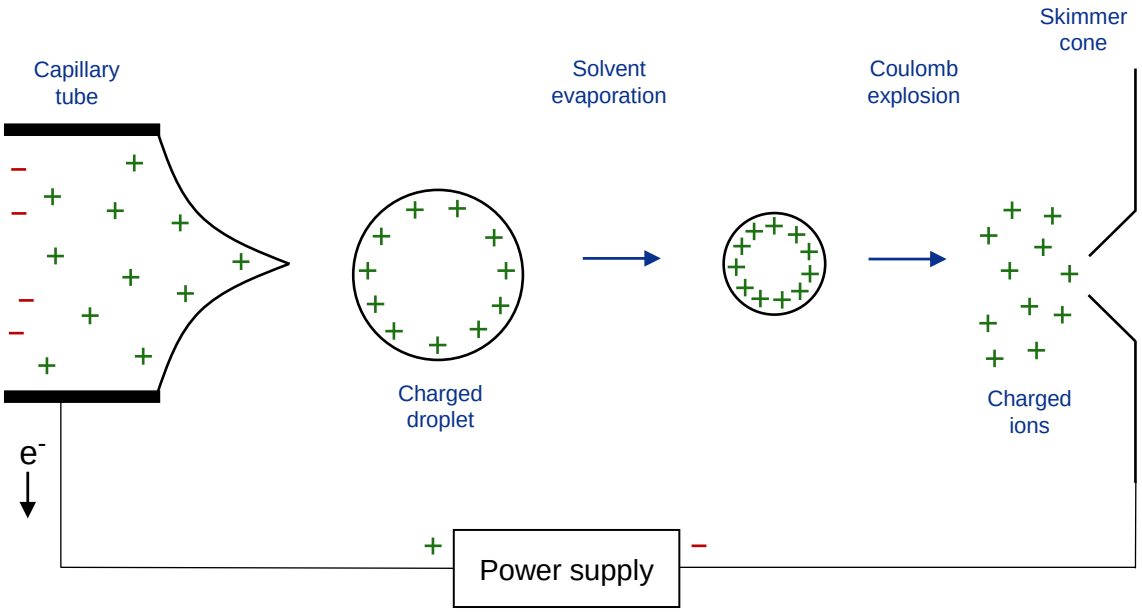

Figure 2.2: Representation of the electrospray ionisation process, showing the generation of a droplet, desolvation, and formation of gas-phase ions. Adapted from de Hoffman and Stroobant [68]

The formation of adducts is commonly observed in electrospray ionisation. A protonated molecule, denoted by M+H, is the most prevalent adduct, however sodium (M+Na) and ammonium ($M+NH_4$) adducts can also be encountered [69]. These adducts usually originate from mobile phase buffers and solvent impurities.

2.2.2 Mass analysers

There are a variety of mass analysers that separate the ions based on different principles, such as trajectory stability and velocity [68].

2.2.2.1 Quadrupole

The quadrupole mass analyser separates ions based on their mass-to-charge ratio using the stability of trajectories within an electric field [68]. It is made up of four parallel cylindrical rods spaced equally around a central void. The rods all have an electrical potential, with the opposite rods having the same charge and adjacent rods having a different charge (Figure 2.3). This creates an area in which only ions with a specific mass-to-charge ratio will be allowed to pass through to the detector, and any other ions will collide with the rods and are therefore removed from the sample stream [64].

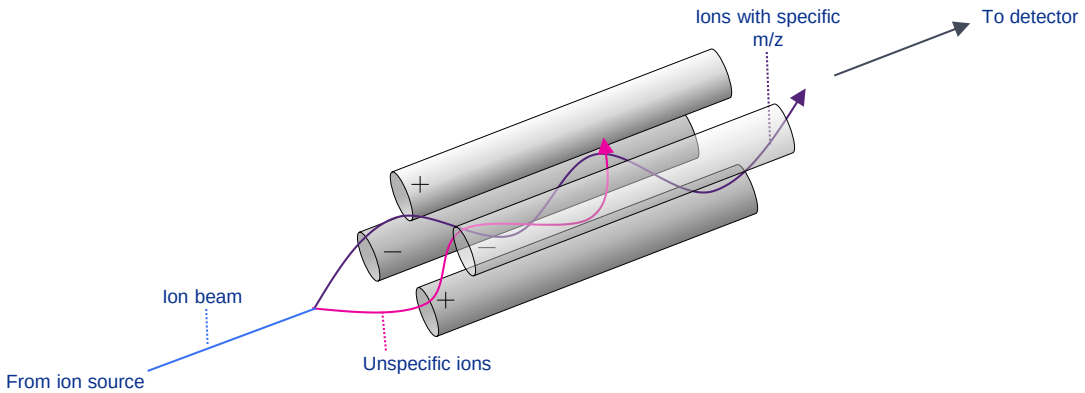

Figure 2.3: Representation of a quadrupole mass analyser, showing ions with a specific m/z passing through to the detector and the removal of unspecific ions

2.2.2.2 Orbitrap

The Orbitrap contains three electrodes; two outer and one central. A voltage is applied between these electrodes, causing an electric field. A pulse injects the ions into this space tangentially, and they begin oscillating around the central electrode. If the correct parameters are set, the ions remain circling in a spiral due to the balance of the attraction to the central electrode and centrifugal force [70]. The shape of the outer electrodes causes the ions to be pushed towards the widest part of the ion trap. Ions with different mass-to-charge ratios will oscillate at different frequencies, and the outer electrodes act as a detector for the ion image current. When all ions of interest have entered the ion trap and moved away from the outer electrodes, the central electrode voltage becomes stable, and this is the point in which the image current of the oscillations can be detected [71]. This image current is then Fourier-transformed into a mass spectrum [72].

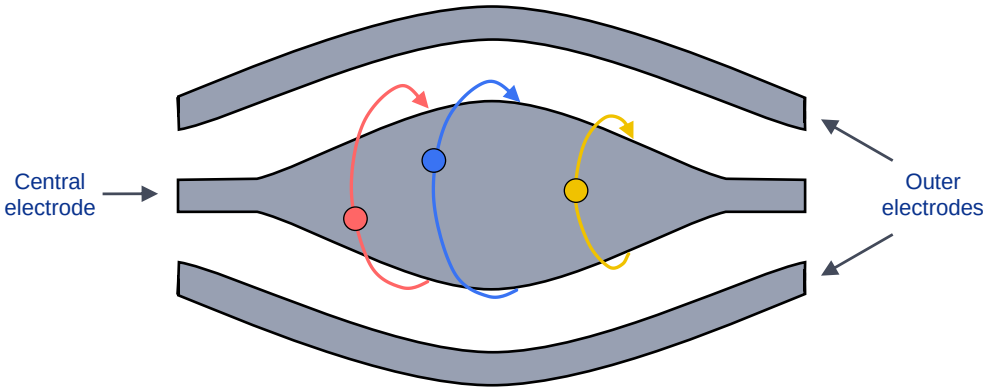

Figure 2.4: Representation of an Orbitrap mass analyser, showing the separation of three ions with different m/z values

2.2.2.3 Time-of-flight

Another type of mass analyser that was used within this project is the time-of-flight mass analyser, which separates ions based on their velocities when drifting in a free-field region known as the flight tube [68]. After ionisation in the ion source, the ions pass through a series of ion optics to narrow the ion beam. When they reach the bottom of the flight tube, the ions flow over the pulser, which produces a high voltage pulse that accelerates the ions upwards, and ions not involved in this continue forward and are removed from the analysis. Not all ions are therefore analysed, which reduces the sensitivity of the technique, but it gives a start point for the timer and attempts to make the kinetic energy the same for all ions, enhancing the mass accuracy and selectivity. Each of the ions will have a different mass-to-charge ratio and so will have different velocities, meaning they will take different times to travel the flight tube and reach the detector [73]. The lower the mass of the ion, the quicker it will reach the detector. This mechanism is represented in Figure 2.5. The ions then reach the detector at the end of the flight tube, and a mass spectrum with each ion represented by a peak is produced.

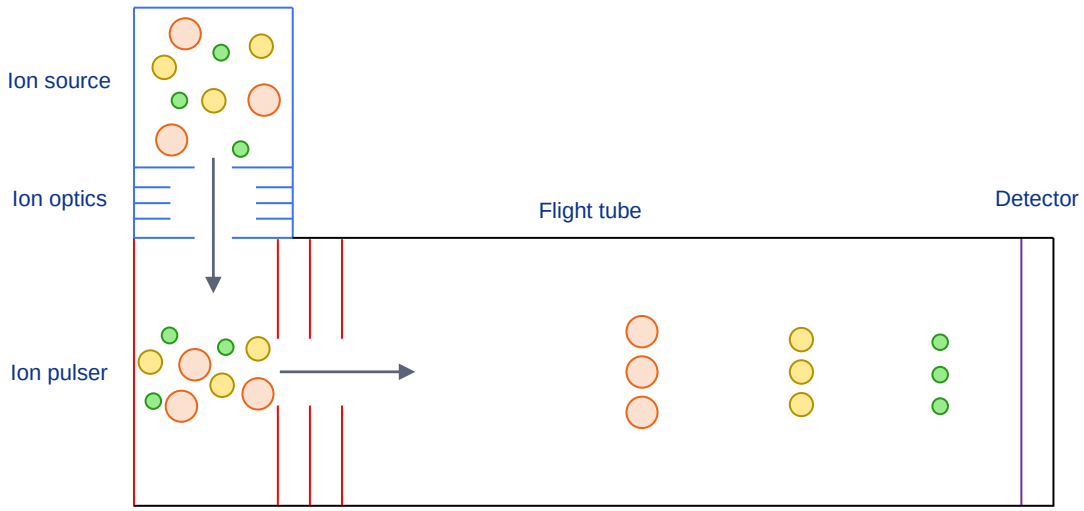

Figure 2.5: Representation of a flight tube in a time-of-flight mass analyser, shown as a linear time-of-flight tube for simplicity. Orange, yellow and green ions have different mass-to-charge ratios

The mass resolution can be improved by the inclusion of a reflectron at the end of the flight tube. The ions travel through the flight tube, and at the end the reflectron acts as an ion mirror, where the ions are deflected back down the flight tube. The detector is placed next to the ion pulser, so the ions can be detected after being reflected (Figure 2.6). The purpose of the reflectron is to compensate for minor velocity differences between ions with the same m/z, by decreasing the spread of flight times, which improves the resolving power. Ions with more kinetic energy and so more velocity will enter the reflectron deeper than ions with a lower velocity, and so will spend more time in the reflectron, causing both ions with the same m/z to reach the detector simultaneously [68].

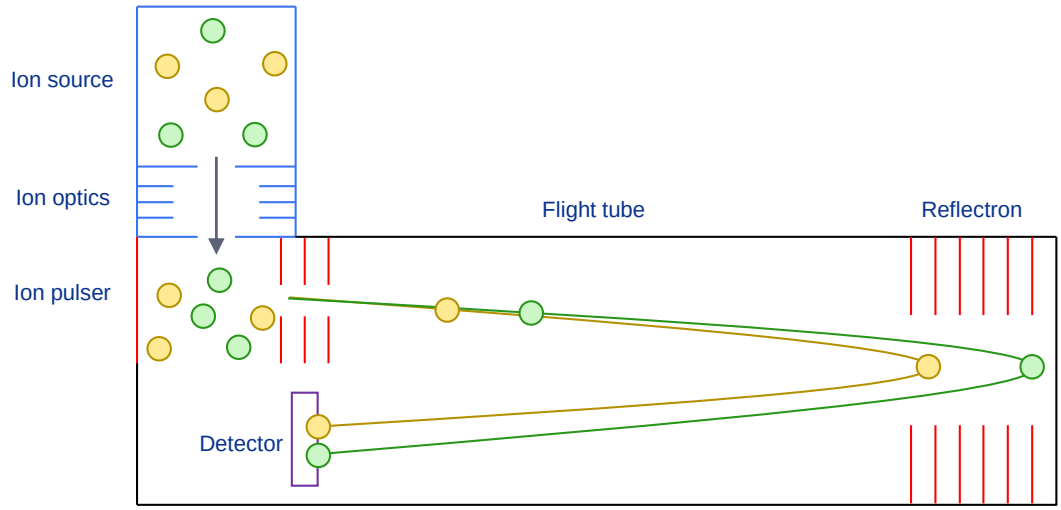

Figure 2.6: Representation of a reflectron in a time-of-flight mass analyser, showing how the reflectron improves mass resolution. Green and yellow ions have same mass-to-charge ratios

2.2.3 Hybrid instruments

2.2.3.1 Quadrupole time-of-flight

The combination of two different types of mass analysers are known as hybrid instruments, which aim to combine the advantages of the two mass analysers for enhanced performance. Within this work, a quadrupole time-of-flight (Q-TOF) mass spectrometer was used, which can be described as the addition of a quadrupole and collision cell to a time-of-flight mass analyser [68]. This combination of mass analysers increases the sensitivity and mass accuracy, and can be utilised in both MS and tandem MS mode. For initial untargeted analyses, single MS mode is most beneficial, where the first quadrupole allows all ions with a range of m/z through, allowing a more holistic approach. A schematic of this instrument can be seen in Figure 2.7.

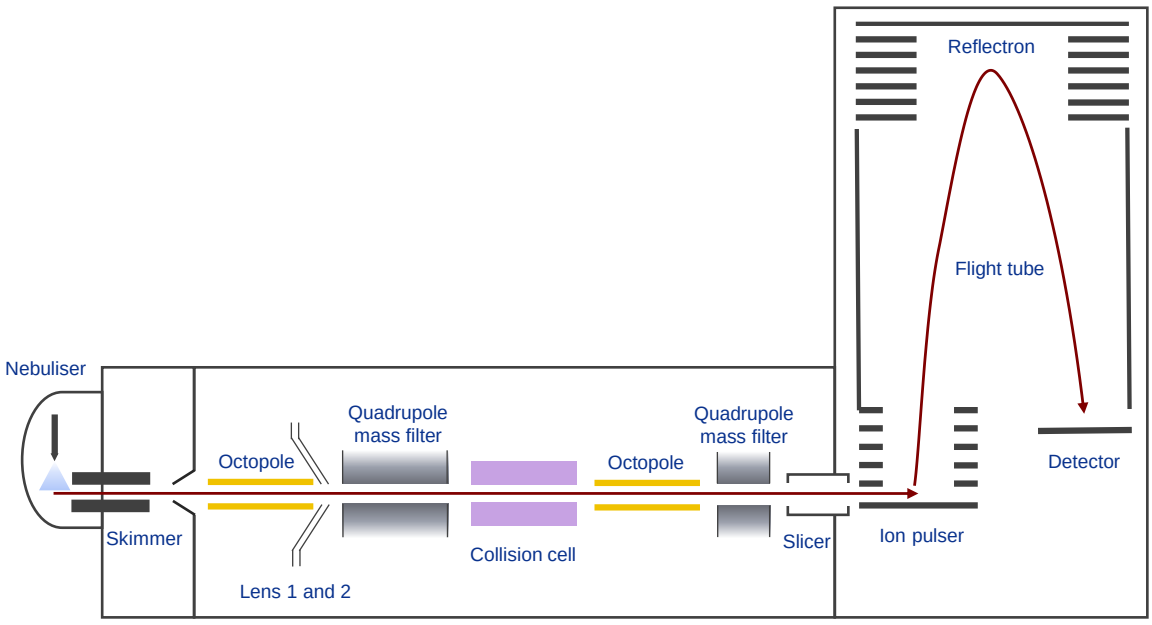

Figure 2.7: Representation of a quadrupole time-of-flight instrument

The ion source consists of two nebulisers; the first nebuliser converts the sample into fine droplets, as described in Section 2.2.1.1, and an additional nebuliser introduces a reference mass solution to maintain a continuous mass accuracy. A counterflow

drying gas reduces the noise related to the incomplete drying of solvent droplets. The skimmer reduces the broadening of the ion beam, which then proceeds into the first octopole ion guide. The two lenses enhance the high mass ion transmission and increases the sensitivity. The quadrupole mass filter allows ions of a specific m/z to pass through and continue to the collision cell, which ensures all ions exit with nearly identical energy. The ions pass through another octopole guide and quadrupole mass filter, until they reach the slicer. This reduces the variations in vertical movement of the ions before entering the bottom of the flight tube. The ions are then separated in the flight tube, as described previously.

2.2.3.2 Quadrupole Orbitrap

In this work, a Q Exactive Plus was used, which is the combination of a quadrupole with an Orbitrap, represented in Figure 2.8.

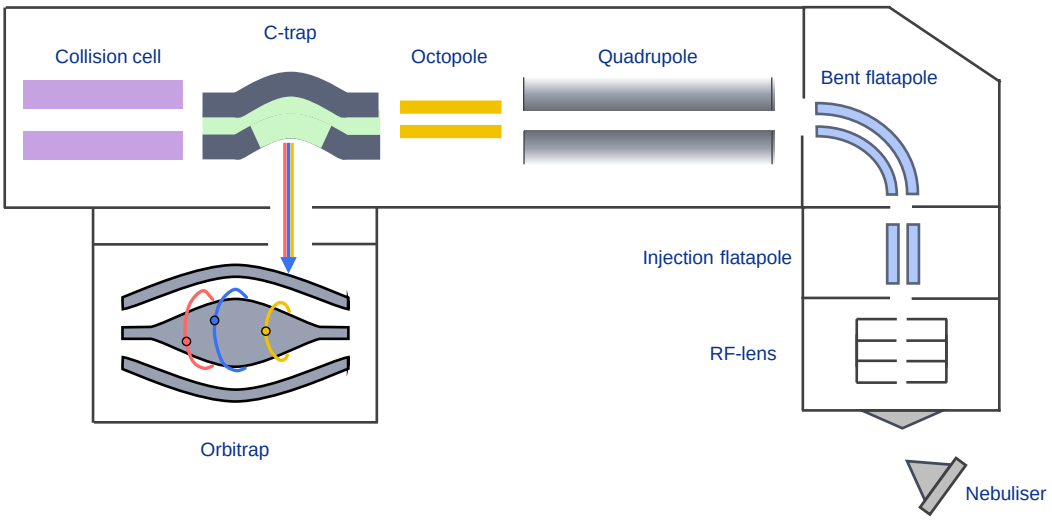

Figure 2.8: Simplified representation of a Q Exactive Plus instrument, adapted from Thermo Fisher Scientific [74]

The sample is ionised via electrospray ionisation, the ions then pass through an RF lens which captures and focusses the ions into a close beam. The two flatapoles aim to continue to guide the ion beam, and attempt to reduce noise by removing neutrals

and any clusters of ions with a high velocity from entering the quadrupole, which allows ions with a specific *m/z* through [74]. This can be used to allow a range of ions through, or ions with a more specific *m/z* for targeted analyses where tandem mass spectrometry (MS/MS) can be carried out. After passing through a short octopole for further focussing of the ion beam, the ions reach the C-trap. This is a curved RF quadrupole ion trap that injects the ions into the Orbitrap mass analyser [72]. The C-trap is filled with nitrogen, so upon entering, ions collide with nitrogen and lose energy. The RF of the electrodes is then decreased, and high-voltage pulses are applied across the trap. This directs the ions to a slot in one of the electrodes, where they are accelerated out of the C-trap and into the Orbitrap mass analyser [72]. The collision cell is used for fragmentation during MS/MS analyses.

2.2.4 Tandem mass spectrometry

Tandem mass spectrometry (MS/MS) is any method that consists of two stages of mass analysis, where the first analyser allows certain ions through, and the second analyser analyses the product ions. Fragmentation of ions in between these two mass analysers occurs in a collision cell that is filled with an inert gas, usually nitrogen. There are four main types of scan modes that can be used in MS/MS; product ion scan, precursor ion scan, neutral loss scan, and selected reaction monitoring (Figure 2.9) [68]. Product ion scan isolates a precursor ion with a specific *m/z*, and analyses all product ions that occur after fragmentation. Precursor ion scan selects a product ion to analyse in order to detect the precursor ions. For this mode, the first analyser is set to scan mode, and the second analyser is set to detect product ions with a specific *m/z*. Neutral loss scan has the first analyser set to scan a specific *m/z* range (x), and the second analyser scans for the same range but offset by the mass of the expected lost neutral molecule (y). Finally, selected reaction monitoring sets both mass analysers to specific *m/z*, where the first analyser is set to detect an ion with a specific *m/z* (a) and the second analyser is set to a specific fragment of that ion (b).

In this work, product ion scan mode has been implemented in order to confirm the identification of a marker by setting the first analyser to the specific m/z of that marker and setting the second analyser to scan mode so that all product ions can be seen. The product ions can then be compared to that of a chemical standard.

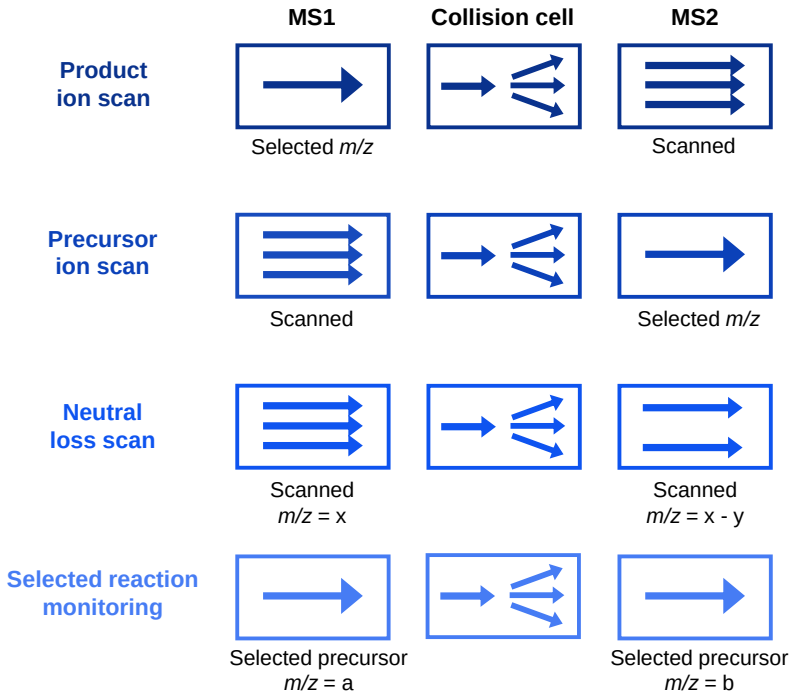

Figure 2.9: Scan modes using tandem mass spectrometry, showing settings for the first mass spectrometer (MS1) and the second mass spectrometer (MS2).
x = specific m/z, y = mass of neutral molecule, a = specific m/z, b = fragment of a.
Adapted from de Hoffman and Stroobant [68]

2.3 Analytical considerations in metabonomic studies

Metabonomic studies are complex, producing vast datasets that are time-consuming to process and interpret. Many features can be detected, however some of these features may not actually be of interest as a marker as they are not statistically significantly different between sample types. For clarity, the term "feature" is for a retention time and m/z ion pair the instrument has detected, and the term "marker" is for any of these features that are statistically significantly different at a p-value of < 0.05.

Often, time is spent investigating markers that appear significant between the analysed sample sets, however this significance could be due to instrumental or analytical bias [75]. It is therefore essential to carefully plan the design of the experiment from the start to ensure the discovered markers are robust and useful, and not just an artefact of the analysis. To do this, several analytical considerations must be addressed and accounted for within the experimental set-up.

2.3.1 Quality control samples

When using chromatographic methods, there is the issue of instrumental drift caused by the length of the analytical run [76], column degradation, temperature change, or instrument contamination. Many studies fail to include a solution to these problems, so it can be questioned whether the data obtained is reliable. Quality control (QC) samples can be used to combat this issue. QC samples in this work are equal aliquots from every sample within the analytical run combined to represent all molecules in all samples [77]. They can be used to condition the column, as well as monitoring the quality of the data. Obtaining repeatable results is vital in order to gain useful data,

especially in metabonomic studies where the datasets are complex and vast. The retention time, signal intensity and mass accuracy are the three main factors that need to be stable throughout a run [75]. The first few injections of a biological sample are usually unrepresentative due to changes in these three factors. Recommendations in literature [75, 78–81] states several injections of the QC samples should be run at the beginning of the main run to stabilise the system. The number of injections depend on the column and instrument used; a different number of QC samples may be required for different analytical runs before the chromatograms appear stable. It has been shown that some analyses require a more thorough procedure for conditioning the column, where a series of QC samples at a high injection at a faster solvent gradient aids in stabilising the system [79].

The QC samples are also used to assess the quality of the data. One QC sample is injected at regular intervals, usually every 5 to 10 samples depending on the length of the analytical run, allowing potential issues such as reducing sensitivity, retention time drift, or reducing mass accuracy to be found [78]. The simplest way to establish whether there was any instrumental instability that would cause the data to be invalid is by using multivariate statistics, such as Principal Component Analysis (PCA), to visualise the clusters of sample groups, including the QC samples. As these QC samples have an identical composition, they should form a tight cluster in the PCA plot, which indicates the data obtained are worthy of more in-depth investigations. Additional statistical tests on individual features within a dataset that assesses the spread of the data within the QC samples also helps to remove any features that are not reliable within the QC samples, and therefore not reliable within the samples.

2.3.2 Analytical run order

In order to remove any bias associated with instrumental drift, the samples can be injected in a random order [78]. This ensures that if there are any issues with the instrument during a long analytical run, partial datasets are still obtained, which can be utilised if there is limited time to repeat the analytical run. QC samples can also be injected throughout the analytical run, and statistical tests carried out on these ensure the retention time and peak area variability is within an acceptable limit. Any features that are not reliable in the QC samples are not considered to be robust and so are not statistically analysed further as a potential marker of interest.

2.4 Data pre-processing and software

There are many openly available platforms online that can be used to pre-process data, including OpenMS, XAlign and MZmine [82], as well as software packages such as MarkerLynx (Waters), Profinder and Mass Profiler Professional (Agilent Technologies), and Compound Discoverer (Thermo Fisher Scientific). The data produced throughout this project was pre-processed using *XCMS Online*, with additional statistical tests carried out on *Microsoft Excel* and *IBM SPSS statistics* software.

XCMS Online is an online platform that allows feature detection, retention time correction, and chromatogram alignment to be carried out [83]. This software allows the pre-processing of metabonomic data in three stages; upload of data, selection of parameters, and interpretation of results. Data files must be in a specific format prior to upload, and so each individual raw data file obtained throughout this work was converted from a .d file to a .mzXML file through the use of *MSConvertGUI* from ProteoWizard, which provides open-source databases for proteomic studies. *XCMS Online* has predefined parameters based on the instrumental setup of a study, with

the option of adapting these parameters to specify signal/noise thresholds, retention time correction, and normalisation of data [84]. The results from these analyses can be viewed online, which also involves interactive plots and additional tools that link to the METLIN database, and the results can also be downloaded. This results folder provides a large feature table, which has retention time and m/z pairs for every feature detected in the samples, with the peak area for each feature in each sample. This feature table can be imported into other programs such as *Microsoft Excel* for manual statistical analyses.

Microsoft Excel was used to visualise the feature table created from *XCMS Online* and carry out manual statistical analyses. Principal component analyses were also carried out with the use of the Multivariate Analysis add-in [85]. *SPSS* was used to carry out additional statistical analyses, including homogeneity of variance, ANOVA and Welch tests, on normalised (peak areas obtained through *XCMS Online*) and raw data (peak areas obtained through extracted ion chromatograms (EICs) in *MassHunter Qualitative Analysis*) throughout this research.

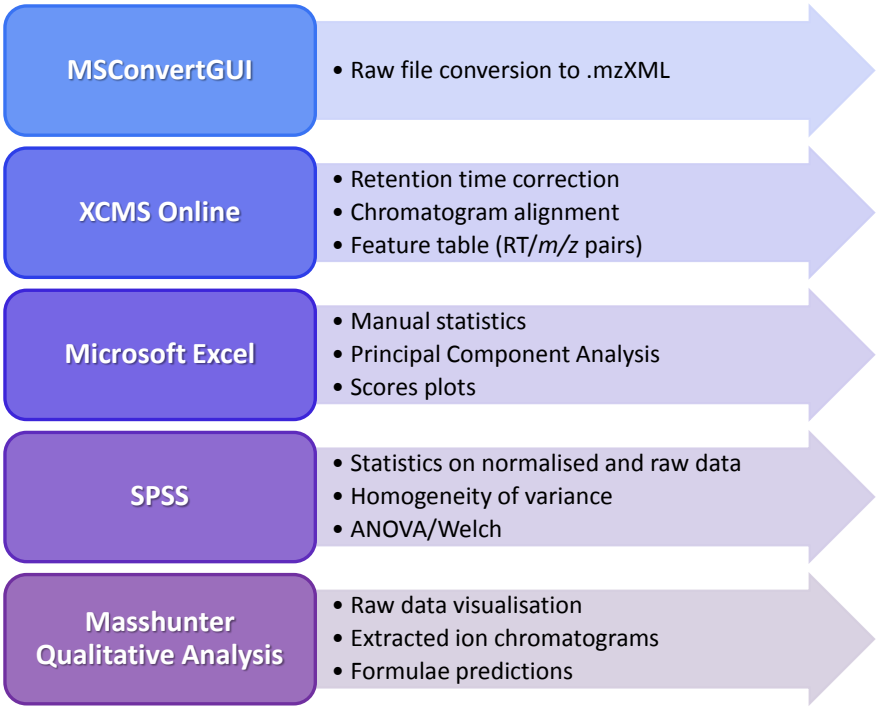

Figure 2.10: Software used within this work for data processing and statistical analysis

2.5 Statistical analysis

2.5.1 Normal distribution

A normal distribution of data, also known as a Gaussian distribution, is determined by the mean and the standard deviation of a data set, and a characteristic feature of this type of distribution is a symmetric bell-shaped curve around the mean [86] (Figure 2.11). The majority of the data, 68%, is expected to fall within one standard deviation of the mean, 95% within two standard deviations, and 99.7% within three standard deviations. The standard deviation controls the spread of the curve, so the higher the standard deviation, the more spread the curve will be around the mean. There are a number of tests that can be performed to check the distribution of data, including Kolmogorov-Smirnov test and the Anderson-Darling test [87]. When a data set follows a normal distribution, parametric tests can be used, however if a data set is not normally distributed, non-parametric tests should be performed.

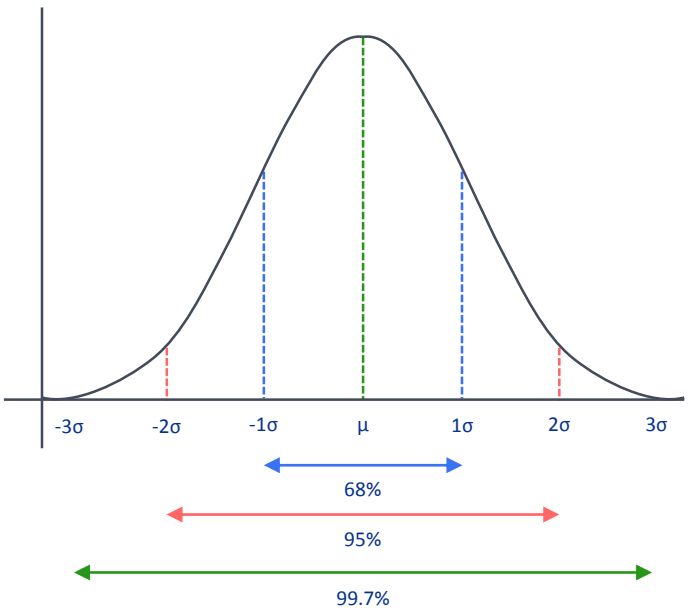

Figure 2.11: Normal distribution curve

Many statistical tests assume the data has a normal distribution, and so tests are required to check the data is indeed normal. These tests, however, are not powerful enough to use on the small data sets that are common in analytical science [88]. It is for this reason that this research has assumed normality in all data sets, and only parametric statistical tests have been used. There is no reason for the data sets to not follow a normal distribution, as only one variable was changed in each experiment, quality control samples were implemented to monitor instrumental drift that may cause bias, and all samples were randomised prior to injection.

2.5.2 Homogeneity of variance

The homogeneity of variance, or equal variance, is an important assumption for many statistical tests. For datasets of the same size, the homogeneity of variance must be tested prior to selecting a statistical technique to use. For example, when analysing two sample sets, a Student's t-test is used, and this can be carried out assuming equal variances, or unequal variances. When more than two sample sets are being analysed, an analysis of variance (ANOVA) test is used for data with equal variances, and Welch's test is used for data with unequal variances. If the sample sizes are unequal, it is appropriate to assume unequal variances and carry out the relevant statistical tests.

A Levene's test is used to calculate the homogeneity of variances. This uses the absolute deviations from group means, or medians, where large variances cause deviations from the group mean, which increases the mean of the absolute deviations [88]. A one-way ANOVA can then be used on these absolute deviations to assess if the difference between the groups is significant, and if so, the data is found to have unequal variances.

2.5.3 Student's t-test

The t-statistic is based on the difference between the population means of two independent groups, with the null hypothesis stating that the two means are equal

(Equation 2.1) and the alternative hypothesis stating the two means are not equal (Equation 2.2).

$$H_0 : \mu_1 = \mu_2 \qquad (2.1) \qquad\qquad H_1 : \mu_1 \neq \mu_2 \qquad (2.2)$$

There are three types of this statistical test; one-sample t-test, used to determine if the mean of a single sample is different to an expected value, a paired t-test, used for seeing differences between two sets of paired observations, and two-sample t-test, or unpaired t-test, used to test differences between two independent sets of measurements [87]. In this work, the unpaired t-test was used as the two datasets were independent from each other.

2.5.4 Analysis of variance/Welch's test

Analysis of variance (ANOVA) is a statistical test that allows the variation between more than two sets of data to be estimated [88]. One-way ANOVA is applicable when only one experimental variable is under investigation; for example, the length of frozen storage. This statistical technique examines the variability of the data, as opposed to the t-test, which examines the mean. Between-group variability is the differences in mean between each group of data, and looks at the difference of each group's mean to the overall mean. Within-group variability is the spread of the data within each group, and ANOVA is a comparison of these two types of variability [87]. It uses the F-test to measure the ratio of these two types of variability. An ANOVA test requires the assumptions that the data is normally distributed and the variances are equal. As previously discussed, normality has been assumed for all datasets in this research. With regards to the variances, if they are found to be unequal, Welch's test can be used. When the variances are unequal, the F-test has been shown to not be robust, and so an alternative test must be used. A Welch's test is the most widely recommended method for correcting the heterogeneity of variances [89]. This test

adjusts the F-test to combat against errors that the original F-test is vulnerable to when the variances are unequal. It is available in many statistical software packages, such as *SPSS*.

2.5.5 Coefficient of variance

The standard deviation (SD) represents the dispersion of the data around the mean. The coefficient of variance (CV), also known as the relative standard deviation, is a ratio of the standard deviation to the mean for a specific set of data. It represents the spread of results as a proportion of the mean value, allowing direct comparisons to be made between datasets that may have means of varying magnitudes [86]. This value is usually expressed as a percentage, and it is calculated using the following formula:

$$CV\% = \frac{Standard\ deviation}{Mean} \times 100 \tag{2.3}$$

The coefficient of variance can be calculated using the peak areas of each feature in the quality control samples run throughout an analytical run, in order to monitor the overall precision of the data and the stability of individual features. Usually a coefficient of variance value of up to 15% is recommended as the accepted value [80], but in metabonomics and the discovery of biomarkers, the coefficient of variance value can have an upper limit of 30% and still be considered adequate due to the untargeted nature of the analyses [90]. Therefore, markers with a CV% of less than 30% in the quality control samples are seen as robust and reliable throughout the analytical run, and could be used to differentiate between sample types.

2.5.6 Multivariate statistics

Metabonomic studies produce vast and complex multivariate data sets, and in order to analyse this data, chemometric methods are required. Chemometrics can be defined as the application of statistical and mathematical methods to chemical analyses [91].

One of the most useful tools within chemometrics is pattern recognition, and the most commonly used multivariate statistical technique is Principal Component Analysis (PCA) [92]. Usually a correlation can be seen between the variables in a dataset, however this information is redundant. PCA condenses large datasets with multiple variables into fewer parameters called Principal Components (PCs), removing any correlations. An eigenvalue corresponds to each PC, which represents the amount of variance in the dataset, with the largest variance in the first component [93]. Principal component analysis generates score and loading values; the scores provide the coordinates of samples in the PC space, allowing visualisation of similarities or differences in samples and any sample groupings, displayed in a scores plot, whereas loadings signify the amount that each original variable contributes to the PCs [94].

During the analysis, it is sometimes appropriate to standardise the data, especially when the variables are measured on different scales, or one variable has a larger variance than others, which would dominate the scores plot [93]. Standardising the data allows the measurement scale to be converted into a relative one [94].

A scores plot, which is how the PCA has been represented in this work, can show if the data can be separated into groups based on the variance between the sample sets. It can also represent the precision of the data by examining the quality control samples and seeing if they are tightly clustered, showing high precision in the dataset, or if they are spread out or in a line, which could mean instrumental drift has had a high impact on the results. The coefficient of variance percentage of the markers,

calculated from the peak areas of the quality control samples for each marker, affects the spread of the data points in the PCA scores plots; the lower the CV%, the more stable that marker is throughout the analytical run.

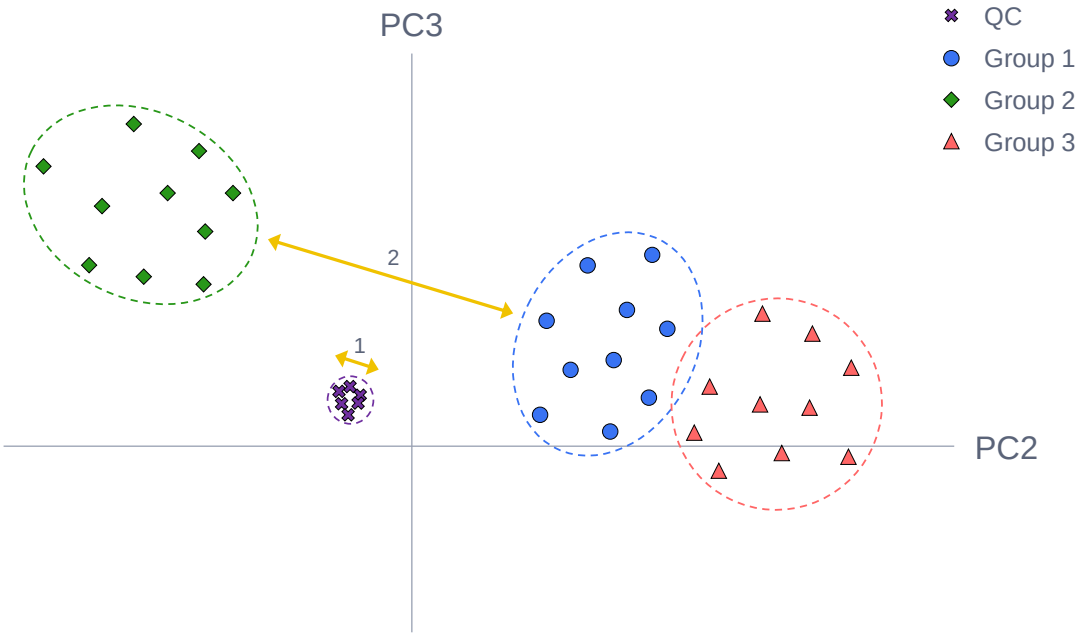

Figure 2.12: Diagram representing separation in a PCA scores plot. Arrow 1 indicates instrumental drift, Arrow 2 indicates separation of two groups

In an ideal plot, represented in Figure 2.12, all the quality control samples would be in the exact same position as they are repeat injections from the same vial. Any deviations are usually a sign of instrumental drift within the analytical run. Practically, this can be extremely difficult to achieve as there is always some element of drift within an analytical run, so having the quality control samples tightly clustered is acceptable. In Figure 2.12, Arrow 1 demonstrates the instrumental drift seen among the QC samples. Arrow 2 represents the separation between Group 1 and Group 2. If Arrow 2 is larger than Arrow 1, then it can be stated that the separation between the two sample groups is caused by chemical differences, and not by instrumental instability. Group 1 and Group 3 are not separated at a distance larger than Arrow 1, and therefore can not be differentiated from each other based on chemical composition as it could be caused by instrumental drift. However, it can be

stated that the samples from the same group do show a pattern and have clustered together, and due to the fact the samples are randomised prior to injection, this clustering can most likely be attributed to chemical composition.

The principal component that is responsible for the separation between sample groups can be used to find the markers that cause the separation; the higher the loading value, the more responsible for the separation between sample groups. In Figure 2.12, PC2 represents the most separation between sample groups, and so could be used to find the markers most responsible for this separation. In some data sets it is not possible to use this method to find the most significant markers between sample types because the principal component analysis plot is unsuccessful in separating the sample groups. In these situations, other statistical tests can be used to determine the most significant markers.

2.6 Identification of markers

The identification of markers that appear to be significantly different between sample types is widely acknowledged as a major issue in metabonomics [83]. There is a limited availability of authentic chemical standards for many metabolites, which makes confirmatory identification difficult, and is an area that requires crucial development [95]. Within metabonomic literature, specific levels of identification have been reported, and these have been summarised as guidelines with the aim to standardise the approach to the identification of markers in untargeted analyses [96]. These guidelines consist of four levels; identified compounds, tentatively identified compounds, tentatively identified classes of compounds, and unknown compounds. Identified compounds must have a minimum of two matching independent variables to a chemical standard, for example, retention time and mass spectrum. Tentatively identified compounds and classes of compounds do not use chemical standards, but

are based on similarities in mass spectra found on public databases. Unknown identifications are unidentified but can still be differentiated based on the mass spectra [96].

The methods used for identification throughout this research are based on these published guidelines, using a three step approach. The first is a very preliminary identification obtained as part of the *XCMS Online* data processing method, where the marker can be searched for on the METLIN database to find likely identifications. A manual search of the *m/z* value on this database can also be carried out. This preliminary identification can give an idea of the kind of compound the marker could be.

The second step is a tentative identification, as per the published guidelines previously described, which does not involve the use of a chemical standard, so it can be verified as a very likely but not confirmed identification. This includes gaining an accurate *m/z* value for the marker in question in order to match this feature to molecular formulae. Time-of-flight instruments have high mass resolution and mass accuracy, therefore the number of potential molecular formulae matches are reduced. *MassHunter Qualitative Analysis* is able to predict the formula of a compound from the mass spectrum based on monoisotopic mass, isotope abundances, and spacing between isotope peaks [97]. This feature also gives a score showing how likely this formula matches the experimental data. The formulae can then be searched for on METLIN, and the mass spectrum for the unknown marker can be compared to the mass spectrum on the database. If the spectra match, a tentative identification can be made. This is very useful in situations where a chemical standard can not be purchased.

The third step is a confirmed identification, again following the guidelines previously described, which relies on the availability of a chemical standard. In such cases,

MS/MS analysis in product ion scan mode can be carried out on the chemical standard and a QC sample containing the potential marker. The mass spectra can then be compared and the similarities or differences in the fragmentation pattern indicate whether or not the identification can be confirmed. The retention time of the compound in the chemical standard and in the QC sample can also be compared to confirm the chromatographic properties are the same, and a spiked QC sample with the chemical standard can further confirm the matching retention time.

Chapter 3

Using metabonomic profiling to differentiate between normally slaughtered and dead on arrival poultry meat *

The aim of this experiment was to investigate the potential of using metabonomic profiling to differentiate between normally slaughtered and dead on arrival chicken. It strives to show that the workflow used within this study is capable of reducing large and complex datasets to a small number of significant markers. An identification of these markers can then be attempted, to provide a direction for larger studies in developing a targeted assay for this type of food fraud.

* The work presented in this chapter has been published [98]: K. L. Sidwick, A. E. Johnson, C. D. Adam, L. Pereira, D. F. Thompson, "Use of liquid chromatography quadrupole time-of-flight mass spectrometry and metabonomic profiling to differentiate between normally slaughtered and dead on arrival poultry meat," *Analytical Chemistry*, vol. 89, pp. 12131-12136.

3.1 Introduction

Legislation in the United Kingdom states that "whole poultry bodies where animals are dead on arrival at the slaughterhouse" must be stained with a colouring agent in order to distinguish it as a product not fit for human consumption [99]. Despite this legal obligation to remove dead on arrival poultry, it can be tempting for companies to allow these birds to continue into the food chain to prevent any loss of profit, especially since there would not be any visual difference in the final chicken products.

A recent study carried out by the Food Standards Agency [100] found that 1.35 million chickens and 21,500 other poultry birds were dead on arrival to the slaughterhouse, either dying during transport or while waiting for slaughter. This study was conducted over a 15 month period between 2016 and 2017, and it also discovered 680,000 birds had bruising or fractures, 278,000 had a respiratory disease, and 376,000 were in an emaciated state. These figures indicate how many birds can be potentially removed from the food chain in a year, producing a large amount of waste and a decrease in potential profit. In the UK in 2016, over 1 billion chickens were slaughtered [101], resulting in a value of £1.76 billion [102], so even though the percentage of birds that are dead on arrival is extremely small, it could equate to approximately £2.3 million in lost revenue.

The difference between dead on arrival (DOA) and normally slaughtered chicken is very subtle, with the only difference being the manner in which they died and the time of death; chickens originating from the same batch would be the same age and breed, have been fed the same diet, and been transported in the same environment.

DOA poultry die whilst being transported to the slaughterhouse. During this journey, they are subjected to a range of stressors including vibration, motion, lack of food and water, heat, and noise [103], so it is reasonable to assume there could be a variety of different ways in which these chickens could die. Research has shown the manners in which these chickens could die include suffocation, injury, congestive heart failure, heart and circulation disorders [104], lung congestion, and nephropathy accompanied by dehydration [105]. This means that there could be many differences in metabolic content amongst the dead on arrival birds, as there is such a wide range of ways in which they could have died. This could add variation to the results as there would be a greater diversity in the DOA birds compared to the normally slaughtered birds. On the other hand, the changes may be so subtle, the only metabolic differences between all birds would be caused by general biological variation, making a discrimination

between DOA and normally slaughtered chickens extremely difficult. The way in which chickens are normally slaughtered involves the rapid bleeding of the bird for no less than 90 seconds. The bird is first stunned, usually by gas or electrical stunning, and must remain unconscious until death. The only exception to this is during a religious slaughter, by the Jewish method for Shechita food or by the Muslim method for Halal food, where no stunning is required prior to death. In this case, the bird is killed by the severance of both carotid arteries with a hand-held knife. During this research, the normally slaughtered chickens were slaughtered using Halal methods. These differences in how the two subsets of chickens died may cause a change in the metabolic content, and therefore a marker could be used to detect this kind of fraud.

Regarding the difference in time since death, there is a significant amount of research that tackles the issues in calculating post-mortem interval, especially in humans for forensic purposes [106]. However, this mainly involves physical changes to the body, such as rigor mortis, or the use of insects to determine the post-mortem interval. It is sensible to assume there are many biochemical changes that occur in all body tissues after death, mainly due to the lack of oxygen, and so a change from aerobic respiration to anaerobic respiration is to be expected [107]. The biochemical profiles of body tissue and fluids after death can give an insight into the metabolic changes occurring during the decomposition process, and these changes in metabolic content can aid in the determination of time since death. Research has found that there are many metabolites in blood that are known to change in concentration after death; for example, glucose, lactic acid and hypoxanthine all increase [108], so these types of compounds and the associated pathways could be important in determining post-mortem interval. However, when blood is not available, the tissue could contain additional important metabolites, that could then aid in the discrimination between normally slaughtered and dead on arrival chickens. This is important as the tissue is the final product in chicken manufacturing, and by this point the blood for that specific chicken would not be available, and so tissue is most appropriate to use when

developing an authentication test. Little has been done to specifically target the tissue and how the metabolites change after death.

At present, there are no methods to detect if a chicken product was dead before reaching the slaughterhouse. Only the paperwork associated with the chicken products and labels are used to assess the authenticity of the product. With the use of metabonomic methods, markers could be found to determine whether the product was in fact dead on arrival to the slaughterhouse and should not be in the food chain. The difference in metabolic content between different sample types is complex; metabolites within the samples could be present in one sample type and not the other, or there could be a difference in concentration. After death, some molecules will increase in concentration and some will decrease, depending on the mechanisms within specific metabolic pathways. The generation of one metabolite could involve the use of another metabolite, thus increasing one and decreasing another. Not only could this aid in the elimination of dead on arrival meat in the food chain, but it could also be a starting point for the development of similar assays that could target other problem areas within the food industry.

3.2 Experimental method

3.2.1 Materials

Methanol, dichloromethane and formic acid were purchased from Fisher Scientific (Loughborough, UK), and acetonitrile was purchased from VWR (East Grinstead, UK). Ultrapure water (18.2 MΩ) was purified using an in-house Milli-Q system from Elga (High Wycombe, UK). ESI-L low concentration tuning mix and API-TOF reference mass solution were purchased from Agilent Technologies (California, USA). Chemical standard for D-sphingosine was purchased from Sigma-Aldrich (UK).

3.2.2 Sample collection and storage

Chicken samples were collected from a certified poultry processor. Five DOA chickens and ten normally slaughtered chickens were obtained from the slaughterhouse on the day of slaughter. The number of DOA animals chosen was limited by the number of animals that were lost in transit on the day of collection. All chickens originated from the same farm, were the same age and breed, and had been fed the same diet. The tissue type selected for this study was based on what was available on the day of collection, as well as the consideration of what would be available during a fraud investigation. Blood samples were not obtained as collection of this sample would be unlikely during such an investigation. The muscle, heart and liver tissue was removed from each carcass and placed in individual polythene bags. All samples were immediately transported to Keele University in a refrigerated van held at 4°C, and stored at -80°C prior to extraction.

3.2.3 Metabolite extraction

Metabolite extraction was carried out on the muscle, heart and liver tissue; a section of breast tissue was used for the muscle, part of the myocardium from the ventricular wall was used for the heart, and a section of liver tissue from the edge of the right lobe was used for the liver. A small portion of each sample was homogenised using surgical scissors and approximately 100 mg was placed into an Eppendorf tube. To avoid carryover, the scissors were thoroughly cleaned with methanol between each sample. Methanol/H_2O (1:1) was added (1 mL per 100 mg of sample), then the sample was sonicated for 10 minutes and centrifuged at 16,100 rcf for 20 minutes. The supernatant was then moved to a glass vial and retained as the aqueous (AQ) extract. The tissue pellet was broken up using a clean pipette tip, and dichloromethane/methanol (3:1) was added (1 mL per 100 mg of sample). The sample was sonicated for 10 minutes and centrifuged at 16,100 rcf for 20 minutes, and 1 mL of the supernatant was then moved to a glass vial and allowed to evaporate overnight, then resuspended in 1 mL of methanol. After briefly vortexing the sample, it was retained as the organic (OR) extract. Both the aqueous and organic extracts were stored at -25°C prior to analysis.

3.3 Instrumental set-up

3.3.1 Analytical considerations

Quality control samples were made for each analytical run, consisting of an equal aliquot of every sample within each run. At the start of each analytical run, 10 QC samples were injected at a volume of 10 μL, then 20 QC samples at an injection volume of 3 μL were injected to condition the column. All non-QC samples were randomised to eliminate any issues arising from instrumental drift.

3.3.2 Chromatographic parameters

Chromatographic separation of extracts was performed with a Thermo Scientific Hypersil GOLD aQ column (100 mm x 2.1 mm, particle size of 1.9 μm) using an Agilent 1260 Binary Pump HPLC. The column was maintained at 40°C and the injection volume was 3 μL. The flow rate of the mobile phase was 0.3 mL/min and consisted of 0.1% formic acid (solvent A) and acetonitrile with 0.1% formic acid (solvent B). The chromatographic gradient method for positive ionisation mode can be seen in Table 3.1, and Table 3.2 for negative ionisation mode. A needle wash method was included after every injection, consisting of 100 μL from 3 separate vials of methanol each used in a specific order, with 3 washes per vial, to reduce any potential carryover.

Table 3.1: Solvent gradient method used for the analysis of organic extracts from dead on arrival and normally slaughtered chickens in positive ionisation mode

Time (mins)	Solvent A (%)	Solvent B (%)
0	95	5
2	95	5
3	47.5	52.5
30	0	100
40	0	100
41	95	5
50	95	5

Table 3.2: Solvent gradient method used for the analysis of organic extracts from dead on arrival and normally slaughtered chickens in negative ionisation mode

Time (mins)	Solvent A (%)	Solvent B (%)
0	95	5
2	95	5
3	40	60
13	35	65
25	20	80
28	0	100
35	0	100
45	95	5
50	95	5

3.3.3 Q-TOF parameters

An Agilent Technologies 6530 Accurate Mass Q-TOF LC/MS was used for the analysis. An electrospray ionisation source was used, and the parameters were set as shown in Table 3.3. The reference mass solution was continually run through the analysis, and used purine (121.0509 *m/z*) and hexakis (1H, 1H, 3H-tetrafluoropropoxy)phosphazine (922.0098 *m/z*) for positive ionisation mode, and ammonium trifluoroacetate (112.9856 *m/z*) for negative ionisation mode, as internal reference masses to ensure mass accuracy. The data was collected in profile mode.

Table 3.3: Q-TOF parameters used in this experiment

Parameter	Setting
Drying gas temperature	320°C
Drying gas flow rate	11 L/min
Capillary voltage	4000 V
Fragmentor voltage	125 V
Skimmer voltage	65 V
Mass range	100-1000 *m/z*

3.4 Data pre-processing

The data was pre-processed using *XCMS Online*. The parameters for the method used on this online platform were set to the default settings specifically designed by *XCMS Online* for analyses carried out with HPLC and ESI-QTOF-MS instruments, and were as shown in Table 3.4. This software also carried out normalisation of the raw data using the median fold change method. A feature table was produced, which included a list of m/z values and their median retention times, the peak areas for these features in each sample, the coefficient of variance calculated from the quality control samples, and a p-value based on the statistical test carried out within the software.

Table 3.4: Parameter settings for *XCMS Online* used in this experiment

XCMS method	Parameter	Setting
Feature detection = CentWave	ppm	30
	min peak width (seconds)	10
	max peak width (seconds)	60
	mzdiff (m/z)	0.01
Retention time correction = Obiwarp	profStep (m/z)	0.5
Alignment	bw (seconds)	5
	minfrac	0.5
	mzwid	0.025

3.5 Statistical analysis

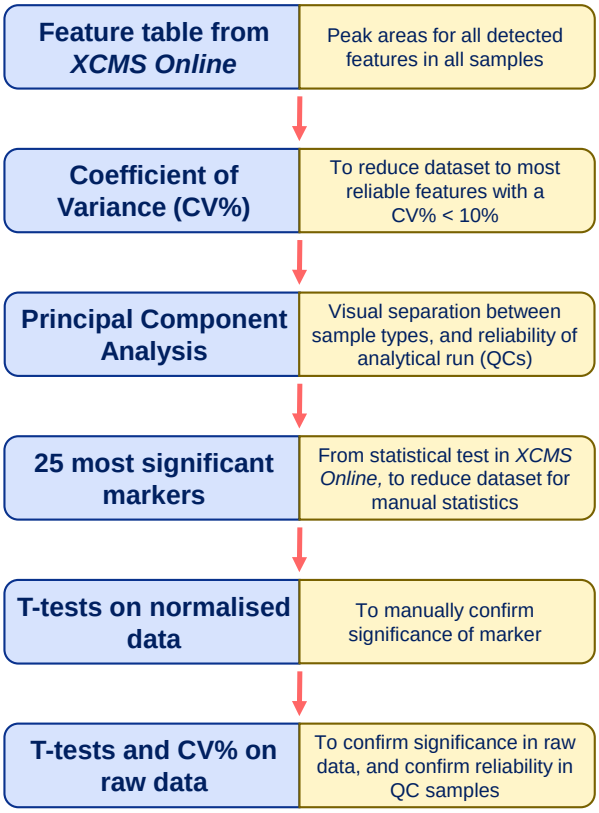

Figure 3.1: Statistical workflow for all datasets analysing extracts from normally slaughtered and DOA chickens

The statistical workflow used in this research is shown in Figure 3.1. The standard deviation, average, and coefficient of variance percentage were calculated using the peak areas of each feature in the QC samples throughout the analytical run. All features that had a CV% of more than 10% were removed, along with any features that had missing peak areas for some samples. A principal component analysis with standardisation was carried out using the Multivariate Analysis add-in for *Microsoft Excel 2010* [85], and a scores plot was produced in order to visualise any separation between normally slaughtered and DOA samples for each tissue type. The first six principal components were plotted in all combinations to find the components that best represented the separation of the sample types. The feature table was ordered

based on the p-value generated by *XCMS Online*, and the 25 most significantly different markers for each tissue type (muscle, heart and liver) were analysed further with a t-test using *Microsoft Excel 2010*, in order to verify their significance. The t-tests were carried out with a confidence level of 95%, giving an α value of 0.05, and assuming unequal variance. If the p-value was less than the α value, it indicated the abundance of that marker in the two sample groups was statistically different.

The raw data was then analysed in *Masshunter Qualitative Analysis* (Agilent Technologies) to produce extracted ion chromatograms (EICs) for the markers that were confirmed to be significantly different. T-tests were carried out on the peak areas of the EICs, as well as CV% of the QC samples. This process ensured the markers were significant before normalising the data in the pre-processing step. Any features that were found to not be significantly different or had a CV% of more than 30% were removed. This additional step in the methodology ensured the final markers were robust and reliable, with the intention of being able to confidently use these markers to detect this subtle type of fraud.

3.6 Identification of markers

The integrated METLIN search in the *XCMS Online* processing gave an indication of the potential identification to the most robust markers, and the potential molecular formulae predicted by *MassHunter Qualitative Analysis* were used to search the METLIN database manually. A tentative identification was made based on the comparison of the mass spectra of the sample and the mass spectra on the METLIN database (if available). An identification was confirmed with the use of a chemical standard, which was analysed in MS/MS mode. All parameters were the same as described previously in Table 3.3. The MS/MS parameters were set to a mass range of 25 - 350 *m/z*. The targeted analysis was set to the specific *m/z* of the chemical

standard (300.2893 *m/z*), and the retention time of the unknown marker in the sample (13.3 minutes). This produced a chromatogram that only showed peaks for this ion at this retention time. A collision energy of 10, 20 and 40 V was used in this analysis. The MS spectra were compared for the standard and the sample to confirm the identity of the marker. A sample was also spiked with the standard and analysed on an LC/MS in order to compare the chromatographic properties.

3.7 Repeatability on different instruments

With these types of studies, there are several different ways the datasets can be processed and statistically analysed after instrumental analysis. This can lead to differences in results that make it difficult to gain robust findings that can be replicated, especially when only a few markers are analysed in detail, based on specific parameters to reduce the dataset. There can be many variables affecting the instrumentation, so the data collected from two different instruments can be extremely different, especially if analysed on different days. In addition to this, the two instruments may have different mass analysers, so the time it takes for compounds to reach the detector varies based on the workings of these mass analysers. This, coupled with the differences in data processing and statistical analysis, can lead to a set of very different markers at the end of the process, especially when only the top 25 significantly different markers are analysed in detail. The aim of this work was to compare the findings from data collected from two different instruments that have been processed and statistically analysed differently.

The muscle extracts were therefore also analysed in positive ionisation mode on a Q Exactive Plus coupled to an UltiMate quaternary LC system at Thermo Fisher Scientific in Runcorn. Chromatographic separation of extracts was performed with a Thermo Scientific Hypersil GOLD aQ column (100 mm x 2.1 mm, particle size of 1.9

μm). The column was maintained at 40°C and the injection volume was 3 μL. The flow rate of the mobile phase was 0.3 mL/min and consisted of 0.1% formic acid (solvent A) and acetonitrile with 0.1% formic acid (solvent B). The solvent gradient was optimised for this instrumental set-up, and was as shown in Table 3.5. The parameters for the ESI source were set as shown in Table 3.6, which were the default settings.

Table 3.5: Solvent gradient method used for the analysis of muscle extracts from dead on arrival and normally slaughtered chickens in positive ionisation mode on LC coupled with a Q Exactive Plus

Time (mins)	Solvent A (%)	Solvent B (%)
0	95	5
2	95	5
3	35	65
13	35	65
25	20	80
28	0	100
35	0	100
45	95	5
50	95	5

Table 3.6: MS parameters on Q Exactive Plus

Parameter	Setting
Auxillary gas temperature	350°C
Auxillary gas flow	10 a.u.
Spray voltage	3015 V
Skimmer voltage	15 V
Mass range	100-1500 m/z

3.8 Results and discussion

3.8.1 Column conditioning

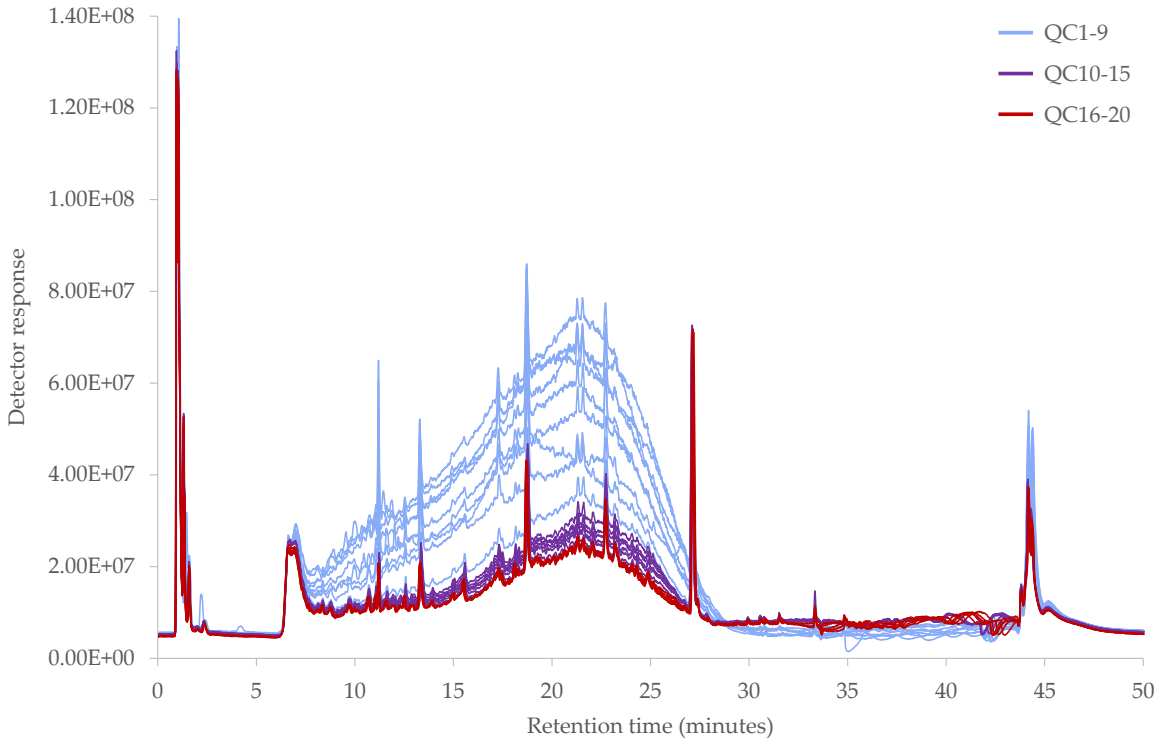

Figure 3.2: Total ion chromatograms of QC samples of muscle extracts from dead on arrival and normally slaughtered chickens, showing gradual conditioning of column

During preliminary studies, it became apparent that the chromatograms within the analytical run had some substantial drift during the QC samples that were injected at the beginning of the run to condition the column. The optimum conditioning sequence was tested by running QC samples at the beginning of the run until the chromatograms overlaid each other with minimal drift. Figure 3.2 shows that injections QC1-9 have an increased baseline between 7.5 and 30 minutes, which then gradually decreases as the number of repeat injections increases. QC10-15 are less erratic, however there are still deviations in the baseline. It is not until the last 5 injections (QC16-20) that the baseline becomes stable and the chromatograms are reproducible.

The optimum conditioning sequence was found to be 10 QC samples at a high volume (20 μL) using a shorter method, followed by 20 QC samples at the same volume and using the same method as the samples within the analytical run. This procedure was found to be efficient in stabilising the instrument, causing reproducibility in the chromatograms produced by the samples.

3.8.2 Aqueous extracts

Using the equipment described previously, it was not possible to create satisfactory chromatographic separation for the aqueous extracts that would ensure meaningful statistical analysis to take place. Therefore no further work on these extracts was undertaken.

3.8.3 Muscle tissue organic extracts

3.8.3.1 Quality control

Positive ionisation mode

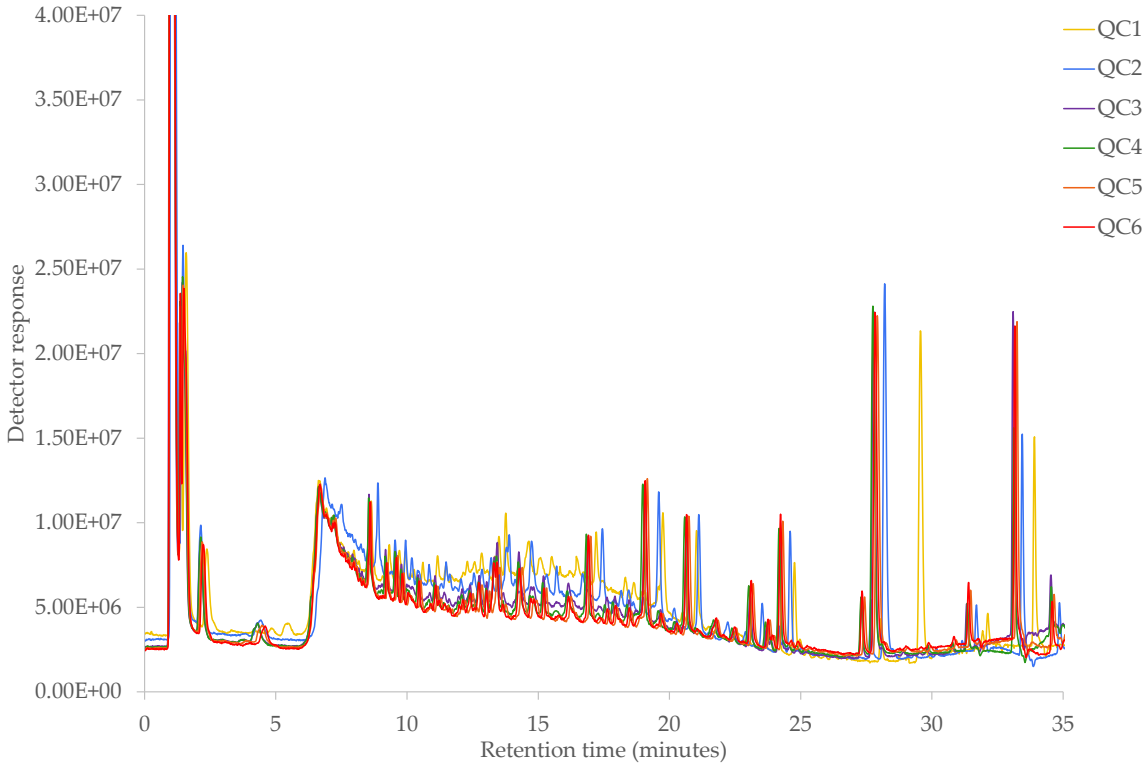

Figure 3.3: Total ion chromatograms of QC samples throughout analytical run for muscle tissue extracts in positive ionisation mode

Figure 3.3 shows that there was some instability in two of the QC samples run during this analysis; QC1 in particular has a large amount of retention time drift towards the end of the chromatogram, with a peak at 29.5 minutes where the same peak in the other QC samples is at 27.5 minutes. The data processing method is able to accommodate for this kind of retention time drift, and the samples are injected in a random order so all samples feel the effect of any instrumental variation during the run. This kind of retention time drift was most likely caused by the column not being entirely conditioned, and so future analytical runs included additional QC injections before the samples, despite significantly increasing the analysis time.

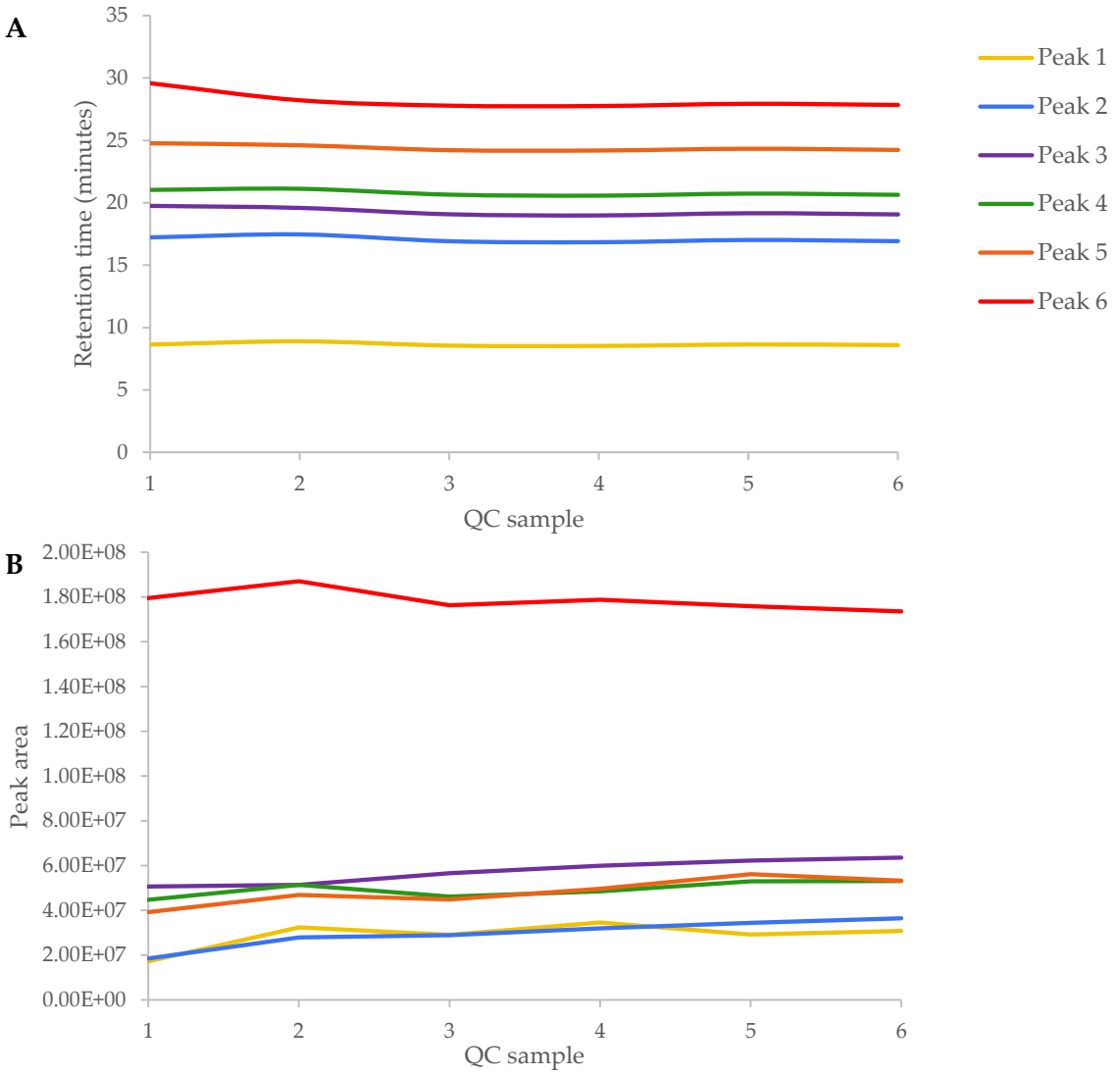

Figure 3.4: Variability of retention time (A) and peak area (B) of 6 peaks in QC samples throughout the analytical run for muscle tissue extracts in positive ionisation mode

To monitor the stability of the instrument throughout the analysis, six peaks in the total ion chromatogram were selected at differing retention times and peak intensities. Figure 3.4 shows the retention time variability and the peak area variability of these six peaks in all QC samples during this analytical run.

Table 3.7: Variability of retention time and peak area of 6 peaks in chromatograms of QC samples during the analysis of muscle tissue extracts in positive ionisation mode

	Retention time (minutes)								
Peak	QC1	QC2	QC3	QC4	QC5	QC6	SD	Average	CV%
1	8.64	8.89	8.56	8.54	8.65	8.60	0.13	8.65	1.48
2	17.22	17.46	16.91	16.83	17.01	16.92	0.24	17.06	1.39
3	19.76	19.60	19.09	18.99	19.17	19.07	0.32	19.28	1.66
4	21.04	21.13	20.66	20.58	20.75	20.65	0.23	20.80	1.09
5	24.78	24.61	24.21	24.19	24.33	24.24	0.24	24.39	1.00
6	29.57	28.21	27.78	27.75	27.93	27.84	0.70	28.18	2.49
	Peak area								
Peak	QC1	QC2	QC3	QC4	QC5	QC6	SD	Average	CV%
1	17197840	32339864	29111355	34485954	29236672	30820700	6063267	28865398	21.01
2	18419820	27828790	28843738	31908700	34376239	36415756	6376463	29632174	21.52
3	50573562	51412965	56633056	59937423	62169393	63572537	5483013	57383156	9.56
4	44642292	51334009	46203277	48487131	52932074	53080112	3561863	49446483	7.20
5	39178779	46937645	44836277	49646033	56217625	53285991	6105662	48350392	12.63
6	179488196	187028150	176373987	178811867	175917446	173552660	4678972	178528718	2.62

The retention time variation was between 1.00 and 2.49%, with the higher value calculated from the peak at 29.5 minutes in QC1 that was previously mentioned to have quite substantially drifted in retention time. The peak area variation was between 2.62 and 21.52%, and the highest values at 21.01 and 21.52% are calculated from two peaks that had a low abundance in QC1 and 2, further indicating that the column may not have been completely conditioned prior to injecting the samples. However, with all CV% for the peak areas under 30%, it can be concluded that the instrument was stable throughout this analytical run.

Negative ionisation

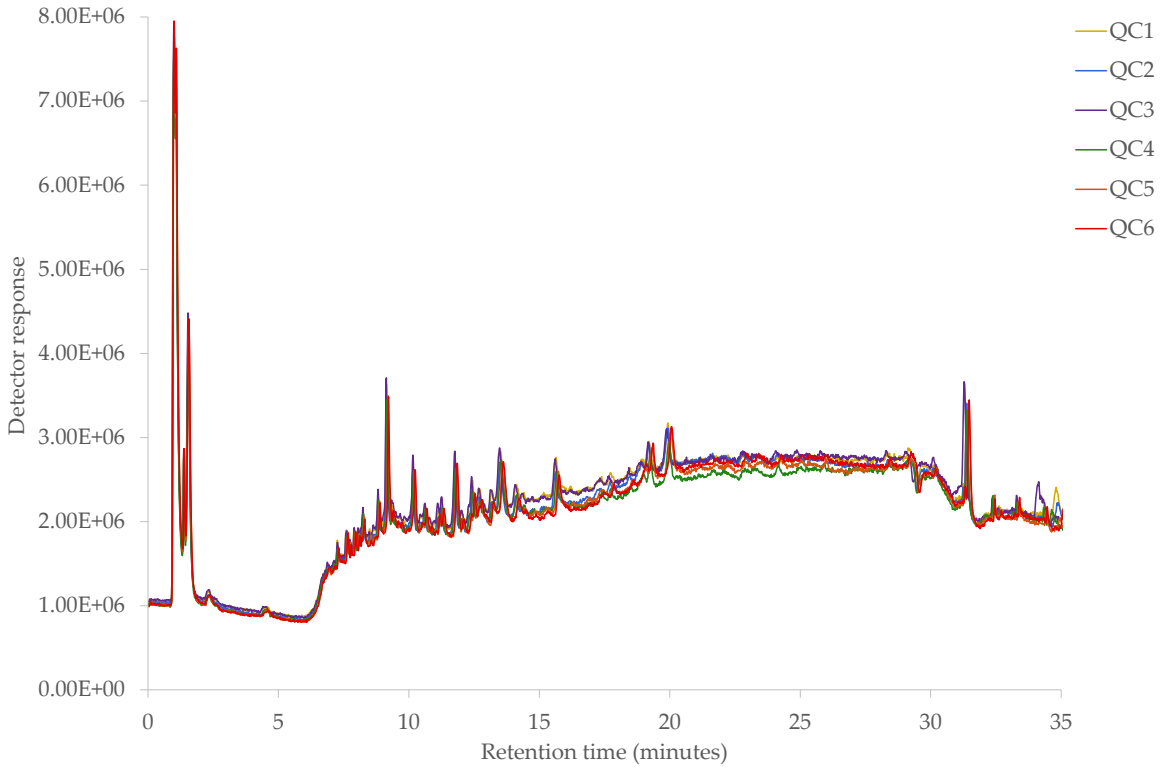

Figure 3.5: Total ion chromatograms of QC samples throughout analytical run for muscle tissue extracts in negative ionisation mode

Figure 3.5 shows the QC samples throughout this analytical run, and they appear to be mostly stable. QC1 and 3 did have some baseline drift, but the retention times do not appear shifted.

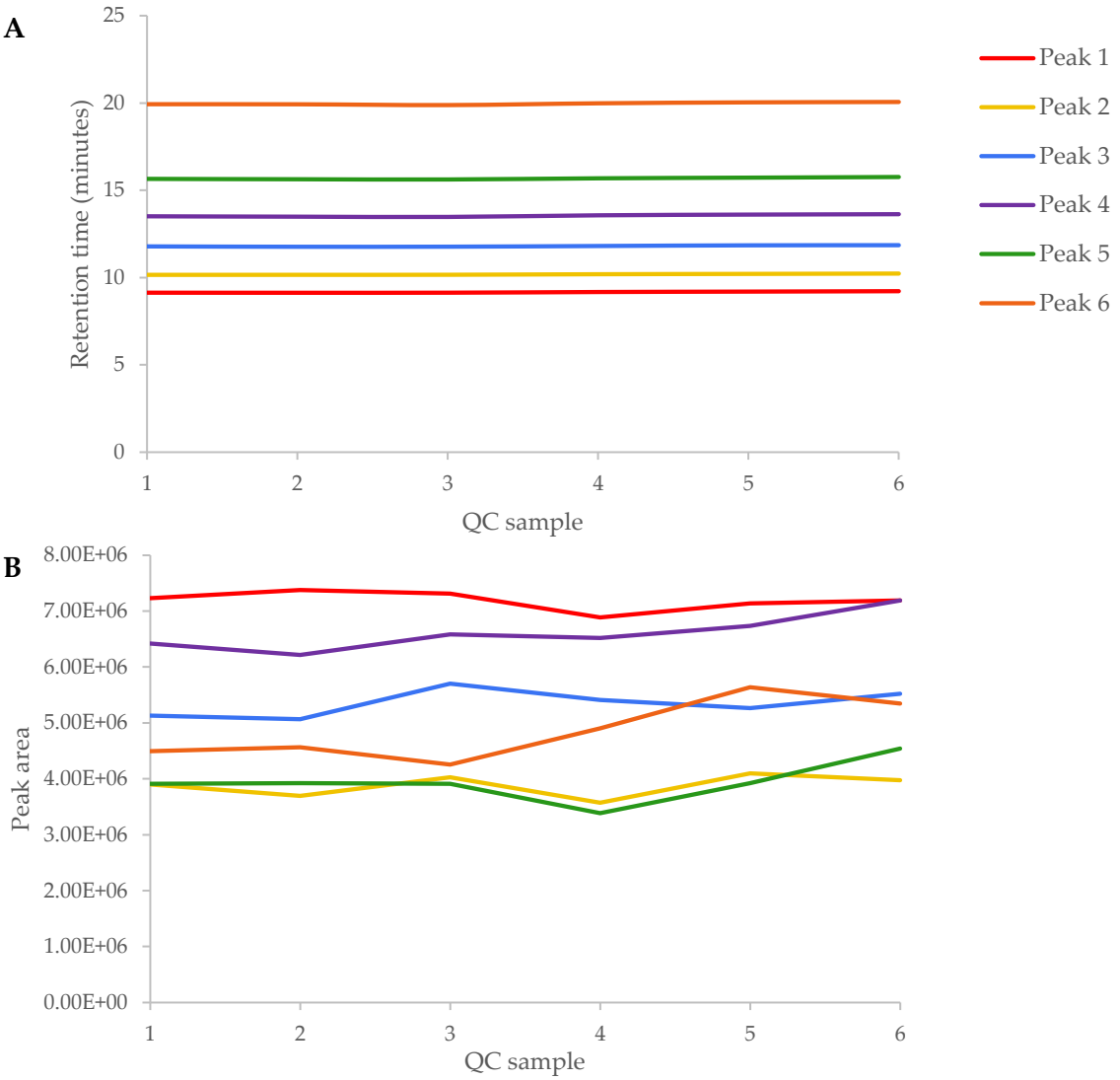

Figure 3.6: Variability of retention time (A) and peak area (B) of 6 peaks in QC samples throughout analytical run for muscle tissue extracts in negative ionisation mode

Figure 3.6 illustrates the variability of the retention time and peak area of six peaks throughout the analytical run in negative ionisation mode. The retention time was very stable with minimal drift, and the peak areas did contain some variability, particularly in peak 6, however it was within an acceptable amount of variability.

Table 3.8: Variability of retention time and peak area of 6 peaks in chromatograms of QC samples during the analysis of muscle tissue extracts in negative ionisation mode

	Retention time (minutes)								
Peak	QC1	QC2	QC3	QC4	QC5	QC6	SD	Average	CV%
1	9.14	9.14	9.14	9.18	9.20	9.22	0.04	9.17	0.39
2	10.15	10.15	10.16	10.19	10.21	10.24	0.04	10.18	0.36
3	11.78	11.761	11.77	11.80	11.84	11.85	0.04	11.80	0.31
4	13.51	13.49	13.48	13.56	13.60	13.62	0.06	13.54	0.45
5	15.65	15.63	15.62	15.69	15.72	15.76	0.06	15.68	0.37
6	19.93	19.93	19.88	19.99	20.04	20.06	0.07	19.97	0.35
	Peak area								
Peak	QC1	QC2	QC3	QC4	QC5	QC6	SD	Average	CV%
1	7230566	7373970	7313162	6885643	7138983	7188021	170812	7188391	2.38
2	3898530	3695071	4027611	3573273	4098152	3972045	203193	3877447	5.24
3	5127767	5067027	5702507	5412826	5262487	5520089	242590	5348784	4.54
4	6417111	6214879	6581020	6517158	6734598	7191457	333587	6609371	5.05
5	3913036	3923720	3911520	3387441	3923306	4541921	365912	3933491	9.30
6	4491817	4563657	4252627	4899908	5636614	5343526	534914	4864692	11.00

The retention time variability was minimal, with CV% values between 0.31 and 0.45%, and the peak area variability was between 2.38 and 11.00%. Therefore, the instrument was stable throughout this analytical run.

3.8.3.2 Metabolic fingerprinting

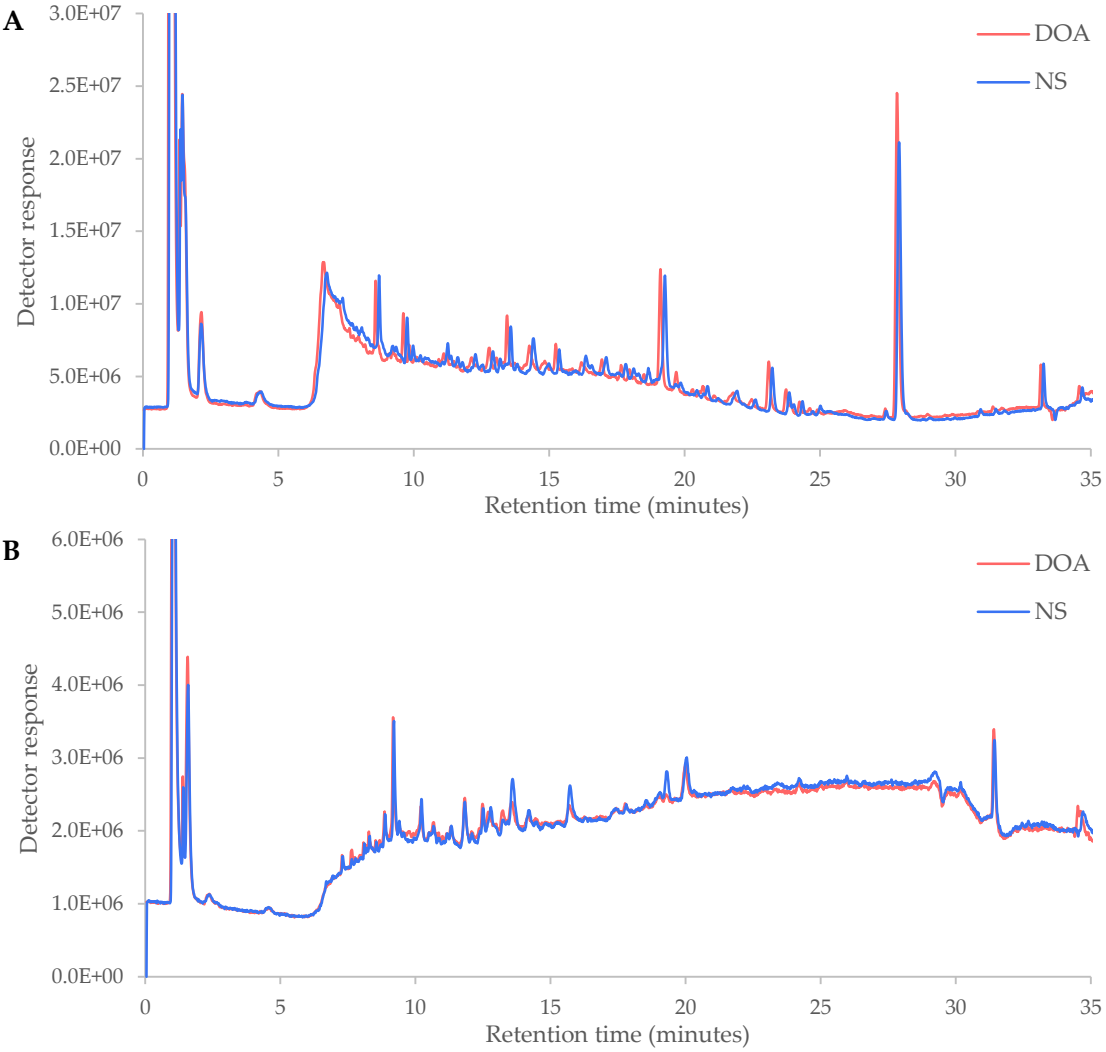

Figure 3.7: Example total ion chromatograms in (A) positive and (B) negative ionisation mode of muscle tissue extracts from normally slaughtered and DOA chickens

The total ion chromatograms (TICs) from the muscle tissue extracts showed a similar peak pattern in the normally slaughtered and the DOA chickens in both positive and negative mode (Figure 3.7). There is a slight discrepancy in the retention time of the overlaid chromatograms for positive ionisation, however this is accommodated for in the data processing. There does not appear to be any peaks that are present in the TIC for one sample type and not the other, but there are slight differences in the intensities of some of the peaks. In particular, in the positive ionisation mode, the peak at 28 minutes has a higher detector response in the DOA sample compared to

the normally slaughtered. In negative ionisation mode, the peak at 7.5 minutes has a higher intensity in the DOA sample, and the peaks at 14, 15.5 and 19.5 minutes all have a higher abundance in the normally slaughtered sample.

3.8.3.3 Multivariate statistics

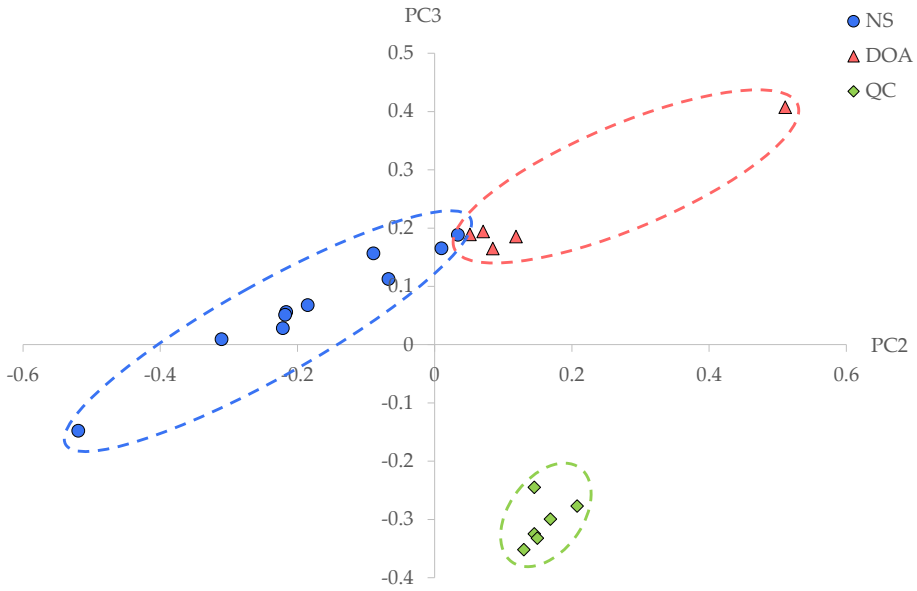

Figure 3.8: Principal component analysis scores plot of PC2 (0.163%) and PC3 (0.079%) for muscle tissue extracts in positive ionisation mode. PCA was carried out using markers with a p-value of < 0.05 and CV<10%

The principal component analysis plot for the muscle tissue extracts analysed in positive ionisation mode (Figure 3.8) shows the QC samples tightly clustered, and even though there is a slight overlap between the normally slaughtered and the DOA samples, this plot shows some separation between the two sample types. The sample data points are spread across the plot, implying there may have been some instrumental instability during this analytical run, however this pattern of data points is unlikely to be caused by this as the samples were randomised before injection.

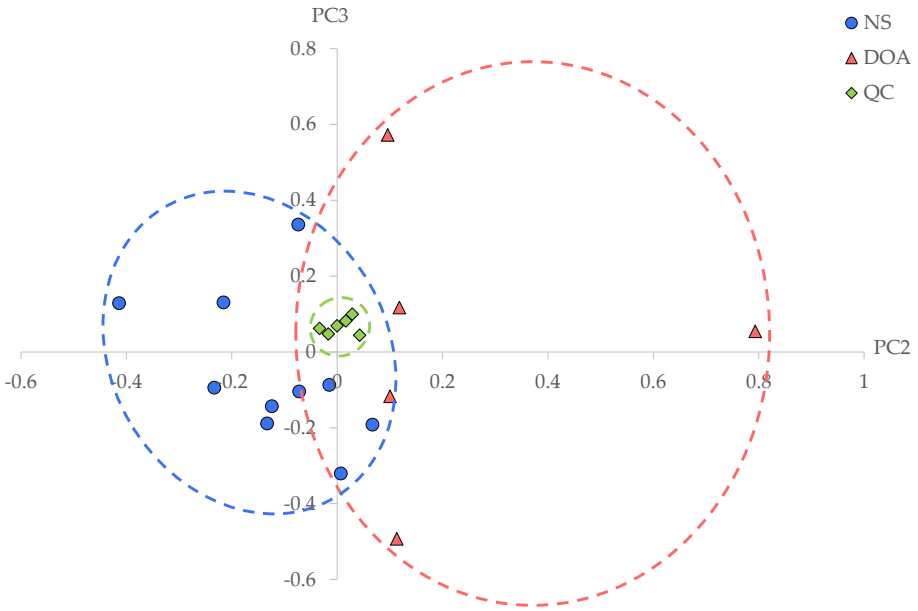

Figure 3.9: Principal component analysis scores plot of PC2 (1.182%) and PC3 (0.144%) for muscle organic extracts in negative ionisation mode. PCA was carried out using markers with a p-value of < 0.05 and CV<10%

The PCA plot for muscle tissue extracts in negative ionisation mode (Figure 3.9) shows the DOA samples grouped on the right and the normally slaughtered samples grouped on the left. The groupings for the two sample types overlap, so this multivariate technique is not appropriate to differentiate between normally slaughtered and DOA chicken muscle tissue.

3.8.3.4 Significant markers

The number of features detected in the muscle extracts found through *XCMS Online* was 9087 in positive ionisation mode and 2800 in negative ionisation mode. After removing all features with a CV% of more than 10% and a p-value of more than 0.05, 203 markers and 124 markers were remaining respectively. These markers were significantly different between the two sample types, and were reliable throughout the analytical run.

After taking the top 25 markers that had the lowest p-value from the statistical test in *XCMS Online*, Table 3.9 shows the markers that proved to be the most robust and

significantly different between normally slaughtered and DOA chickens. These markers were significantly different based on the *XCMS Online* statistical analysis, as well as in the t-tests of the peak areas in the raw data. All markers have a CV% of less than 10% in the normalised data and 30% in the raw data, indicating they were stable throughout the analytical run and were not affected by instrumental drift.

Table 3.9: Summary of remaining compounds from top 25 markers that were significantly different between normally slaughtered and dead on arrival chickens in muscle tissue extracts, in order of significance based on p-value from *XCMS Online*. Asterisk indicates markers were upregulated in the dead on arrival samples

Polarity	*m/z*	Retention time median (mins)	P-value from t-test (XCMS)	CV % (XCMS)	P-value from t-test (EICs)	CV % (EICs)
+	216.1944*	7.78	1.63E-03	6.62	2.45E-04	3.57
	130.1570	6.47	2.98E-03	6.04	4.73E-03	8.34
	708.1774*	1.02	5.71E-03	9.56	4.46E-02	6.73
	178.5856*	1.01	6.11E-03	5.65	4.01E-03	4.89
	300.2893	12.37	9.48E-03	6.61	1.47E-02	7.08
	421.2538	19.09	9.82E-03	6.95	2.76E-02	15.55
	509.2041*	1.49	1.43E-02	9.55	9.19E-03	5.67
-	371.1599*	1.05	5.58E-03	3.70	1.99E-03	27.03
	297.2461*	11.78	3.02E-02	4.85	3.06E-02	27.15
	180.0669*	1.12	3.72E-02	2.23	4.09E-02	3.79

In the muscle extracts, there was a mix of upregulated and downregulated markers in the DOA samples compared to the normally slaughtered samples. This shows the complexity of the metabolic processes that occur after death, and how the time since death can cause significant changes on metabolite concentrations. In the DOA samples, the time since death is longer than in the normally slaughtered samples, and so therefore the concentration of molecules will have changed more, whether it be increasing or decreasing, depending on the metabolic pathway in action.

3.8.3.5 Marker identification

The identification method within the *XCMS Online* process gave a potential indication to the identity of a few of the compounds. Markers with an m/z of 421.2538 and 509.2041 could be peptides, the marker with an m/z of 180.0669 could be L-tyrosine, and the marker with an m/z of 300.2893 could be sphingosine.

Tentative identification

The marker with an m/z of 300.2897 at 12.37 minutes gave a predicted formula of $C_{18}H_{37}NO_2$ with a likelihood score of 98.91%. The METLIN database suggested this molecule could be sphingosine, and the mass spectrum from the experimental data matched the mass spectrum on the database, making this a tentative identification.

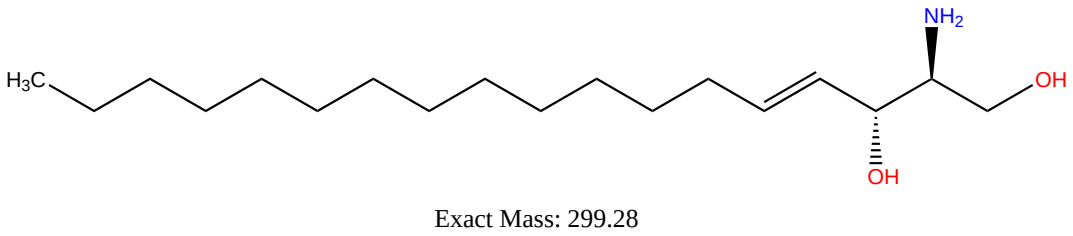

Figure 3.10: Molecular structure of sphingosine

Confirmed identification

After running a muscle tissue extract sample and the sphingosine chemical standard in MS/MS mode at a collision energy of 10 V, 20 V, and 40 V, the mass spectra were compared.

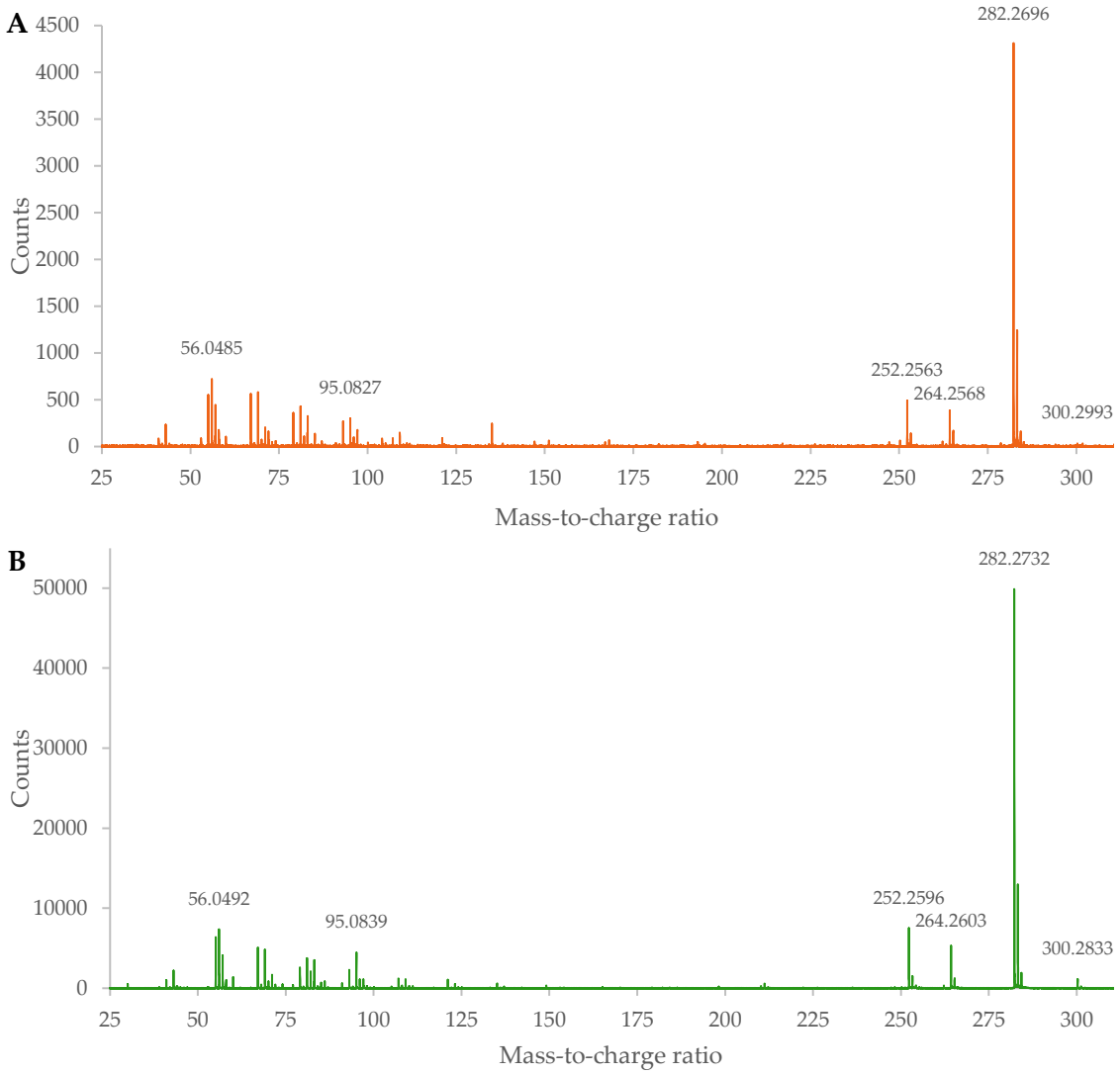

Figure 3.11: Mass spectra from MS/MS analysis of a muscle tissue extract sample (A) and the sphingosine chemical standard (B) at a collision energy of 10 V

With a collision energy of 10 V (Fig. 3.11), it can be seen that the fragmentation pattern in the muscle extract spectrum matches the fragmentation pattern in the sphingosine spectrum. Both spectra show fragment peaks at 282 m/z, caused by the loss of one water molecule, 264 m/z, caused by the loss of two water molecules, and 252 m/z, caused by the loss of one water molecule and a formaldehyde molecule.

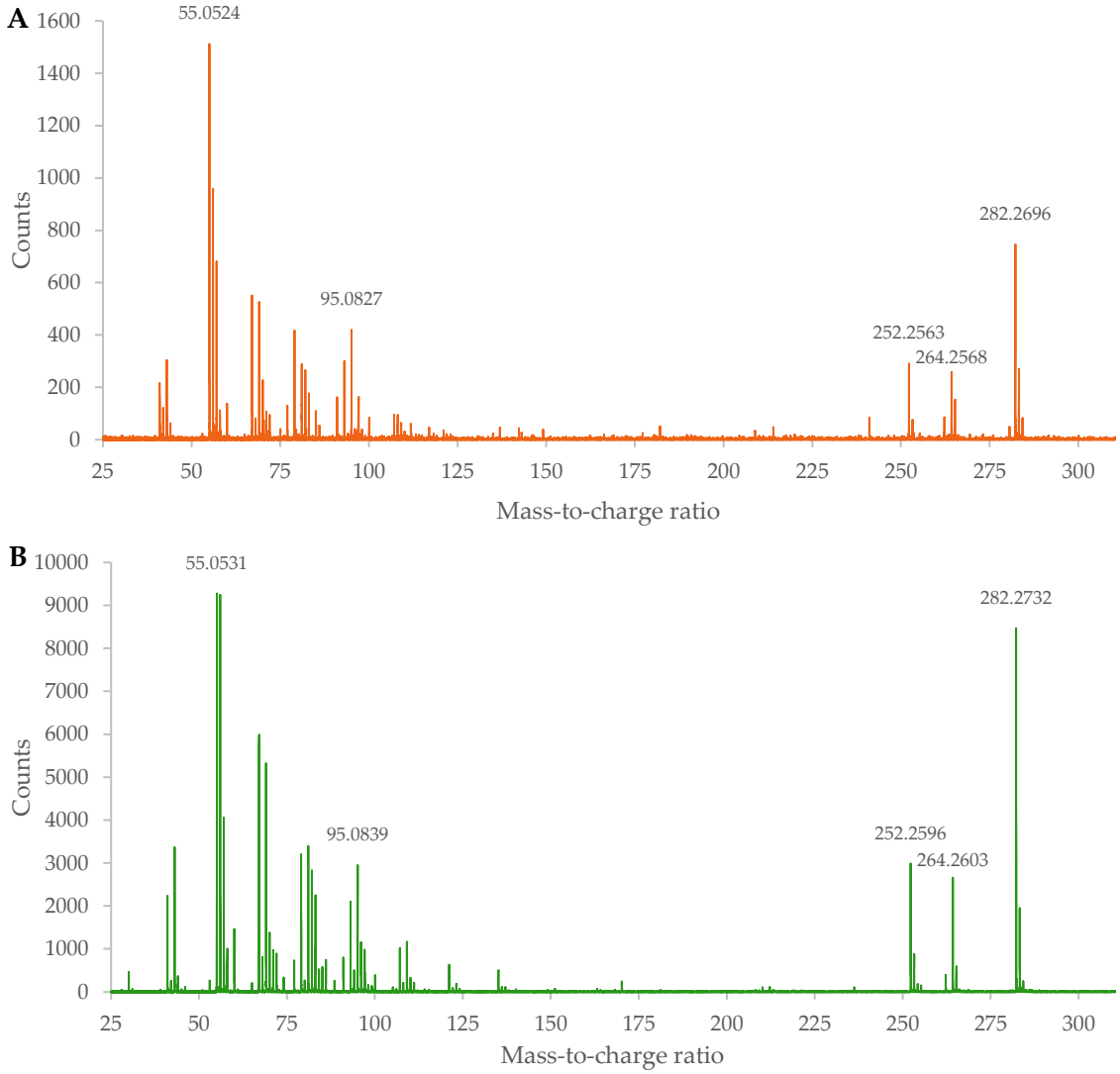

Figure 3.12: Mass spectra from MS/MS analysis of a muscle tissue extract sample (A) and the sphingosine chemical standard (B) at a collision energy of 20 V

The two spectra also match with a collision energy of 20 V (Fig. 3.12); the most prominent peaks at 55 *m/z*, caused by an alkyl group, and 282 *m/z*, caused by the loss of one water molecule, are consistent in both the muscle extract and the sphingosine chemical standard spectra, with the smaller peaks also the same.

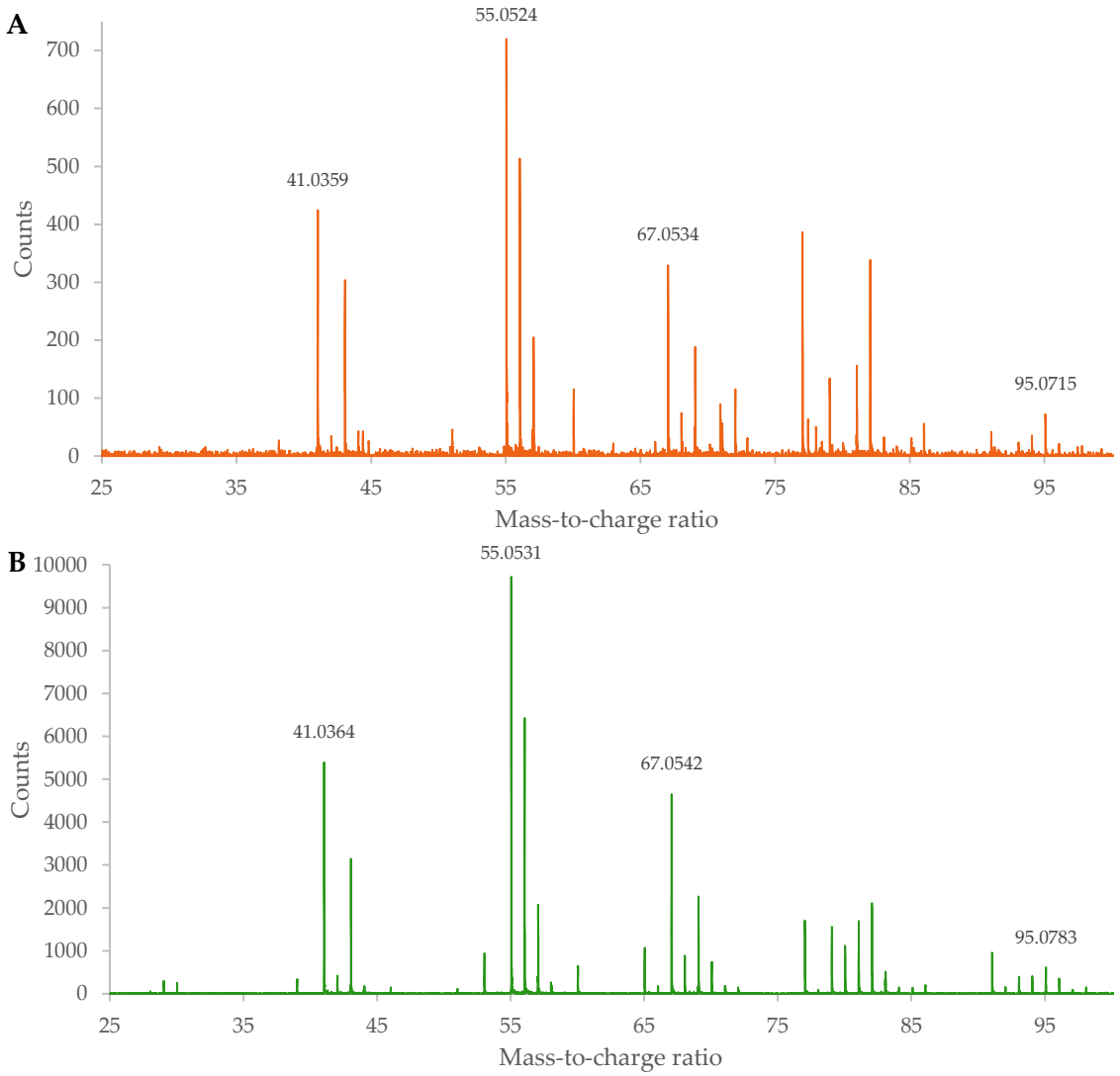

Figure 3.13: Mass spectra from MS/MS analysis of a muscle tissue extract sample (A) and the sphingosine chemical standard (B) at a collision energy of 40 V

Finally, when a collision energy of 40 V was used, the fragmentation patterns in the two mass spectra match; there are several peaks in the muscle tissue extract sample that match peaks in the sphingosine standard sample, specifically at 41, 55, 67 and 95 *m/z*, all caused by alkyl groups. There are some additional peaks in the muscle tissue extract that are at a higher abundance than in the sphingosine standard, however this is expected as the sample contained many components that may have co-eluted with sphingosine, whereas the sphingosine standard was pure.

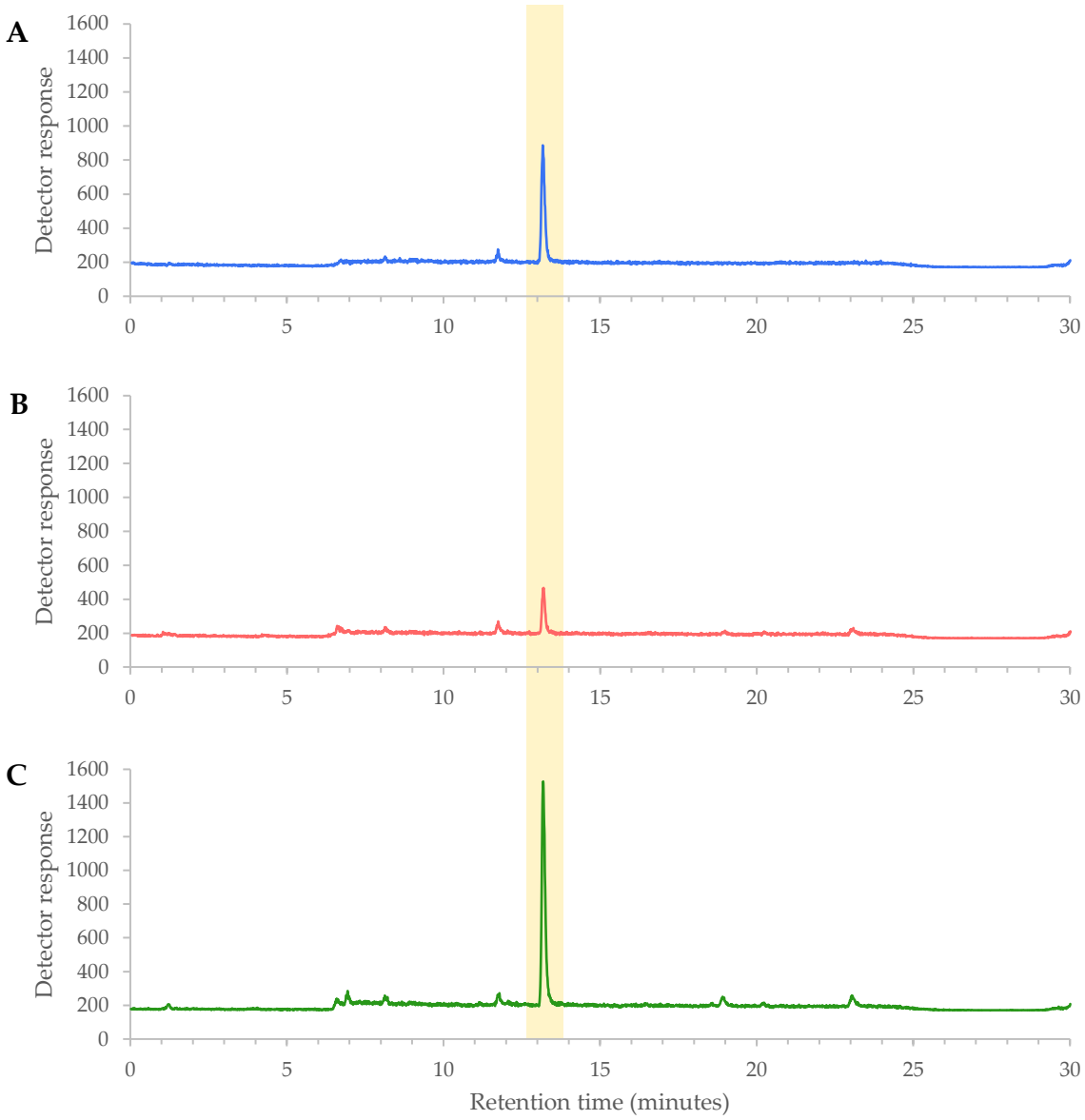

Figure 3.14: Total ion chromatograms comparing retention time for (A) sphingosine standard, (B) muscle extract sample, (C) muscle extract sample with internal standard of sphingosine

The sphingosine standard, a muscle extract sample, and a muscle extract sample with a sphingosine internal standard were all analysed on an HPLC-MS in selected ion monitoring (SIM) mode, using a specific m/z of 300.3. The chromatograms, as shown in Figure 3.14, indicate a main peak at a retention time of 13.2 minutes in all chromatograms. The top chromatogram shows the sphingosine standard, which confirmed the retention time for sphingosine at these chromatographic conditions. The middle chromatogram shows a muscle tissue extract from a normally slaughtered chicken, showing the same peak at 13.2 minutes at a smaller intensity. Finally, the

bottom chromatogram shows the same muscle tissue extract with an internal standard of sphingosine. This chromatogram shows a single peak at 13.2 minutes, and there are not two peaks for the sphingosine standard and the unknown marker in the muscle tissue extract. All of these three peaks align at the exact same retention time, indicating the unknown marker in the muscle extract is either a molecule with the same molecular mass and same chromatographic properties as sphingosine, or it is sphingosine. Taking the tentative identification, the MS/MS analysis, and chromatographic properties into account, the identification of this marker can be confirmed.

Sphingosine is a sphingolipid found endogenously in cells, and is the backbone to many sphingolipids, including ceramide. These sphingolipids are involved in a variety of cell signalling and pathological functions, specifically in the process of apoptosis [109, 110], and stress responses [111]. Sphingosine synthesis begins with the condensation of serine and palmitoyl CoA, producing 3-ketodihydrosphingosine. This is then reduced to dihydrosphingosine and acylated to dihydroceramide. Ceramide is then formed through a dehydrogenation reaction, and finally deacylated to form sphingosine. This pathway can be seen in Figure 3.15.

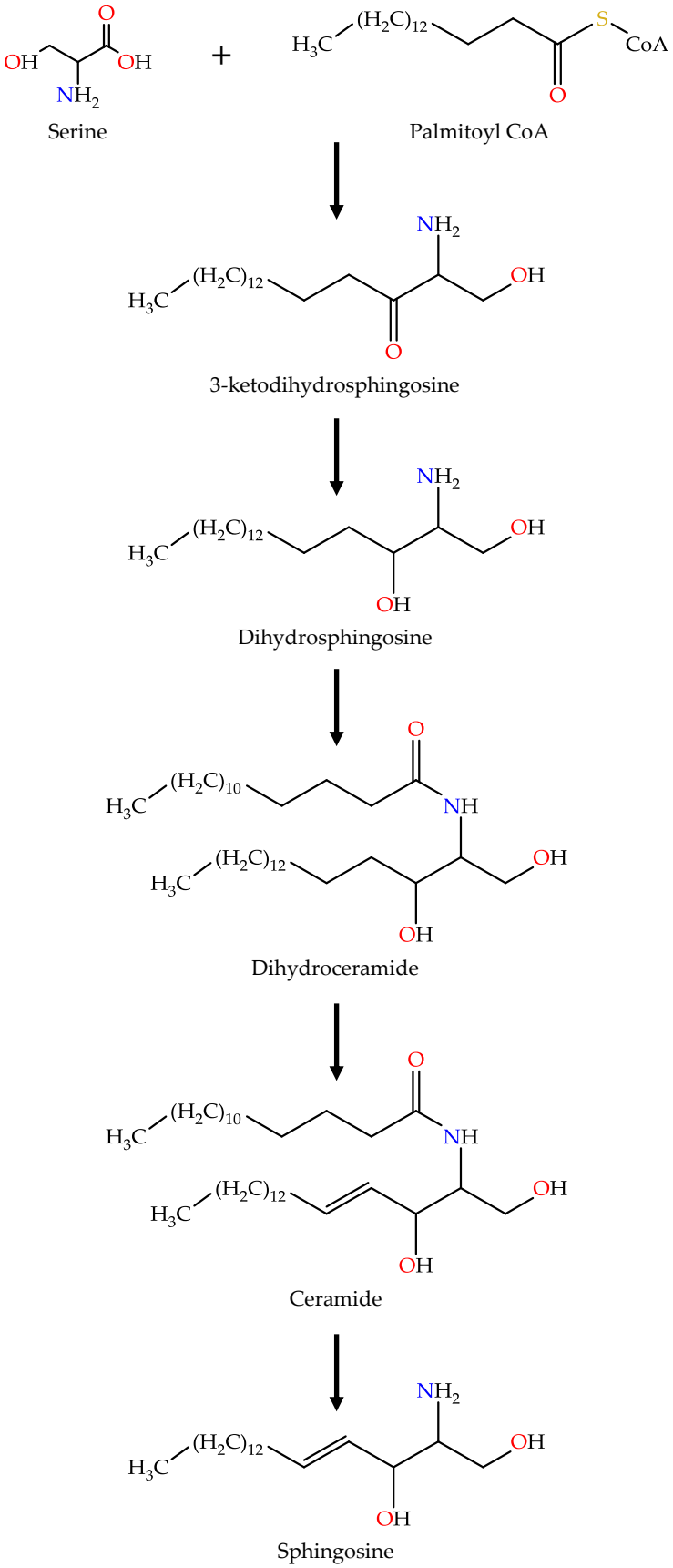

Figure 3.15: Metabolic pathway of sphingosine (created from information in Maceyka and Spiegel [112], and Gault et al. [113])

The regulation of sphingosine and ceramide is very important in maintaining functional levels of sphingolipids within an organism. As shown in Figure 3.16, sphingosine can either be phosphorylated to sphingosine-1-phosphate, which is key in the generation of glycerolipids, and then irreversibly degraded to phosphoethanolamine and hexadecenal. It can also be recycled back to ceramide following the reutilisation pathway, maintaining sphingolipid homeostasis [112] .

It has been found that ceramide production is induced by stress stimuli including hypoxia [114]. It is therefore possible that the presence of sphingosine in the chicken muscle is a result of the breakdown of ceramide, which accumulated in the muscle during the transport and slaughter of the chicken where there may have been a deficiency in oxygen reaching the muscle tissue. This marker was found to be upregulated in the normally slaughtered chicken muscle tissue compared to the DOA chicken muscle tissue, which could be because the DOA chickens have been dead for longer so the sphingosine was recycled back to ceramide in the time between death and sampling, or it has continued to form sphingosine-1-phosphate, and further broken down to hexadecenal and phosphoethanolamine [113].

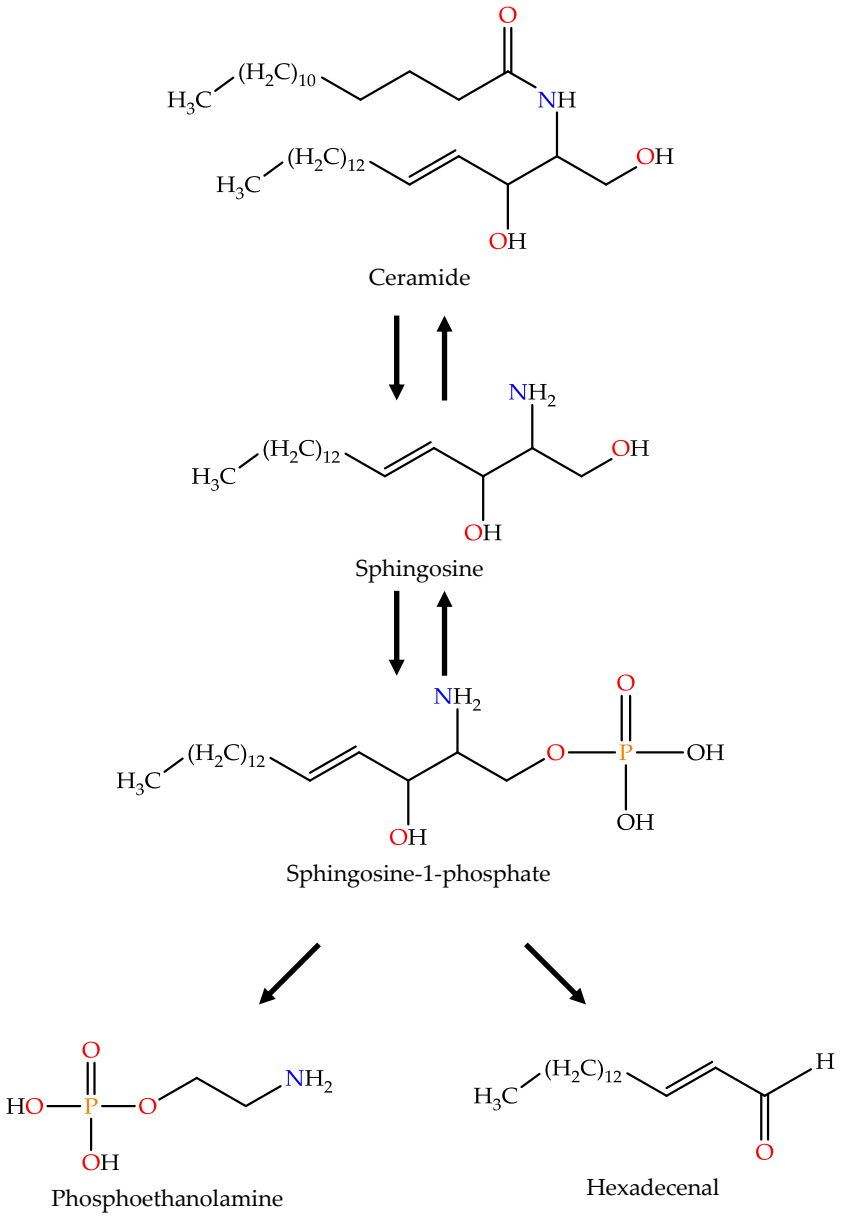

Figure 3.16: The breakdown pathways of sphingosine (created from information in Maceyka and Spiegel [112], and Gault et al. [113])

3.8.4 Liver tissue extracts

3.8.4.1 Quality control

Positive ionisation

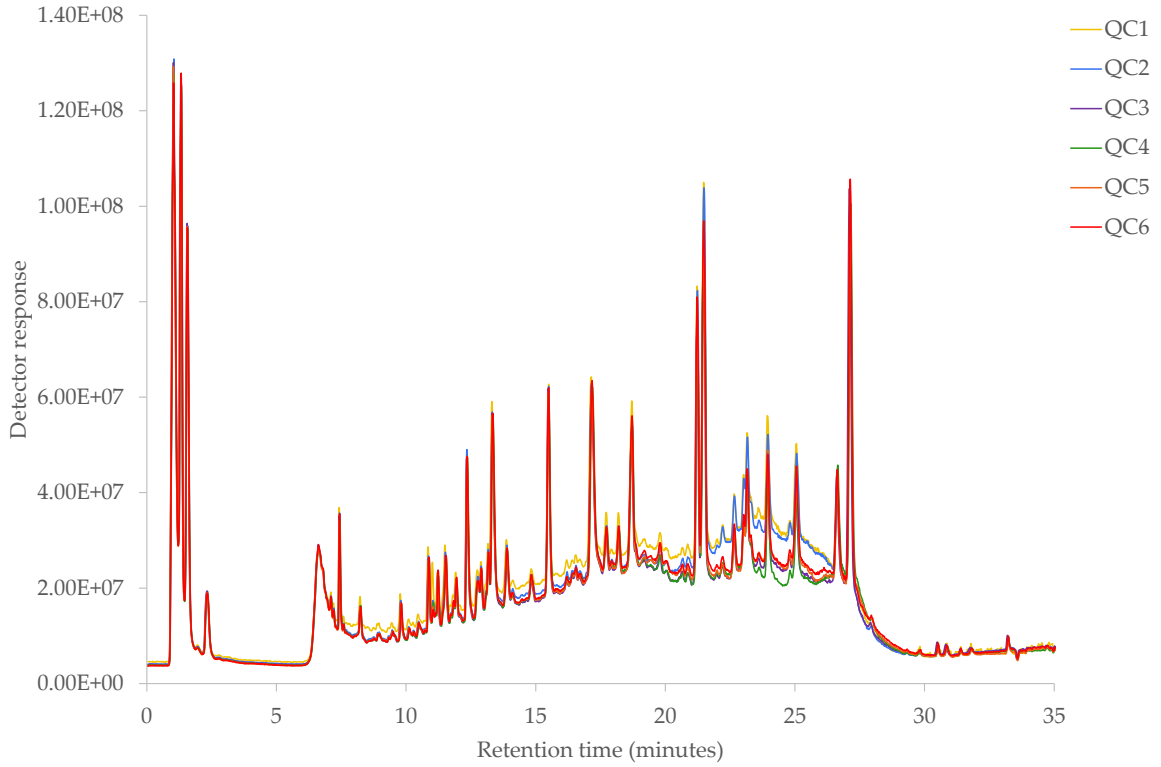

Figure 3.17: Total ion chromatograms of QC samples throughout analytical run for liver tissue extracts in positive ionisation mode

The chromatograms for the QC samples injected throughout the analysis of the liver tissue extracts in positive ionisation mode appear to be reproducible. QC1 and 2 both have slight baseline drift, particularly during the part of the solvent gradient that consists of 100% acetonitrile, however this did not affect the retention time or peak area variability.

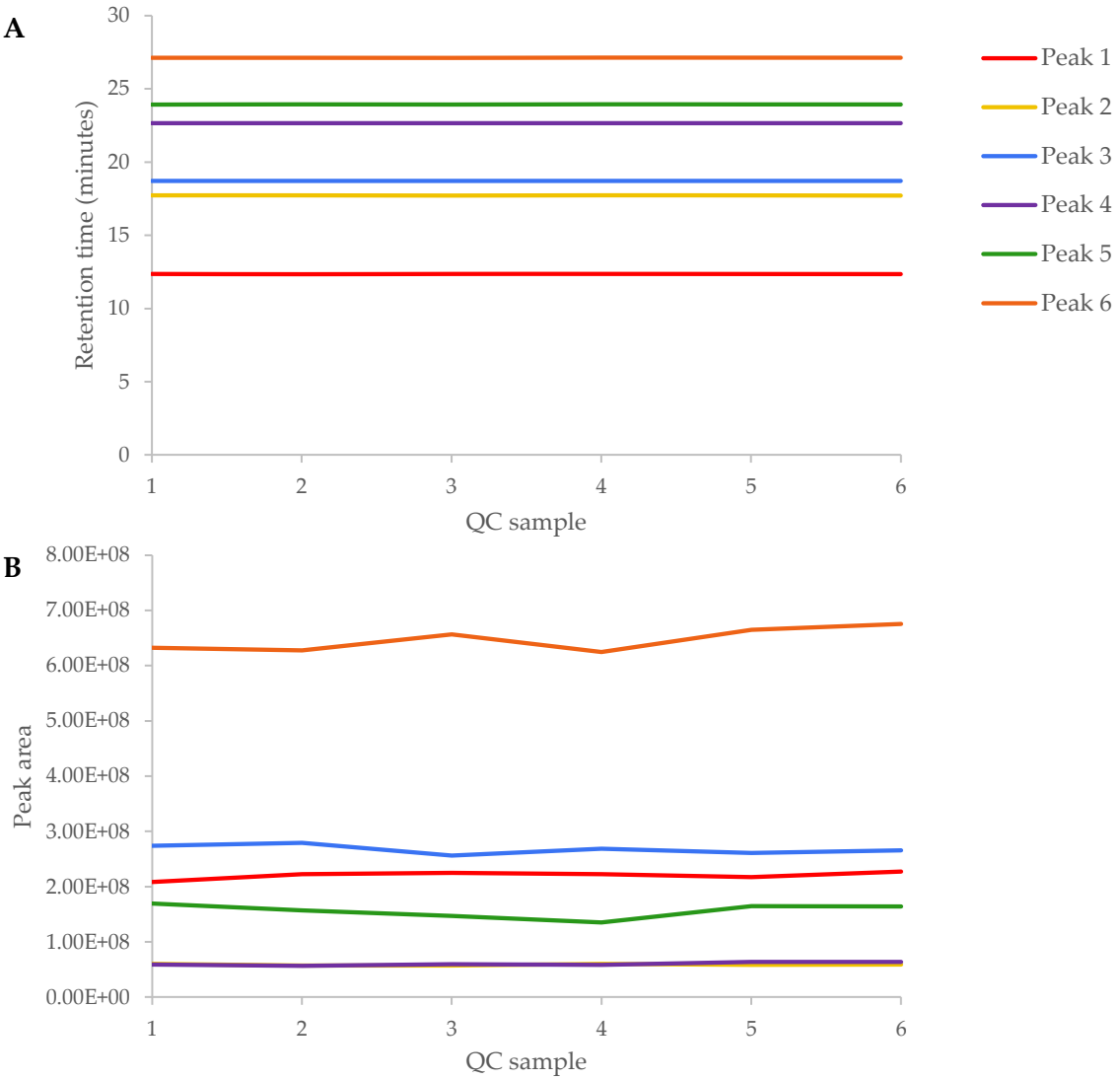

Figure 3.18: Variability of retention time (A) and peak area (B) of 6 peaks in QC samples throughout analytical run for liver tissue extracts in positive ionisation mode

Six peaks were selected to monitor the stability of the instrument during the analytical run, and the variability in retention time for each of these peaks in all QC samples was very minimal, and the peak area variability was low (Figure 3.18).

Table 3.10: Variability of retention time and peak area of 6 peaks in chromatograms of QC samples during the analysis of liver tissue extracts in positive ionisation mode

	Retention time (minutes)								
Peak	QC1	QC2	QC3	QC4	QC5	QC6	SD	Average	CV%
1	12.35	12.33	12.35	12.35	12.35	12.34	0.01	12.35	0.06
2	17.73	17.73	17.71	17.73	17.72	17.71	0.01	17.72	0.05
3	18.71	18.71	18.71	18.71	18.70	18.71	0.00	18.71	0.02
4	22.66	22.66	22.66	22.66	22.65	22.65	0.00	22.65	0.02
5	23.93	23.95	23.93	23.95	23.95	23.94	0.01	23.94	0.04
6	27.12	27.12	27.11	27.14	27.13	27.13	0.01	27.13	0.04
	Peak area								
Peak	QC1	QC2	QC3	QC4	QC5	QC6	SD	Average	CV%
1	208237889	222373901	224848713	222176405	217207775	227249237	6809503	220348987	3.09
2	59997668	57389830	56891868	59911561	58196760	58986232	1292993	58562320	2.21
3	273684502	279168223	256097863	268719604	260635687	265321542	8455083	267271237	3.16
4	58879870	56482854	59414616	58419011	63823202	63776867	3008092	60132737	5.00
5	169403984	157118872	147111814	134816921	164531950	163900197	12990138	156147290	8.32
6	632421710	627806736	656217259	624337515	664995180	675492446	21517488	646878474	3.33

The retention time variability for the six peaks was extremely low, with the CV% ranging from 0.02 to 0.06%, showing the retention time for each peak was very reproducible throughout the analytical run. The peak area variability was between 2.21 and 8.32%. This statistical analysis demonstrates the instrument was stable for the duration of this run and contained minimal drift effects, if any.

Negative ionisation

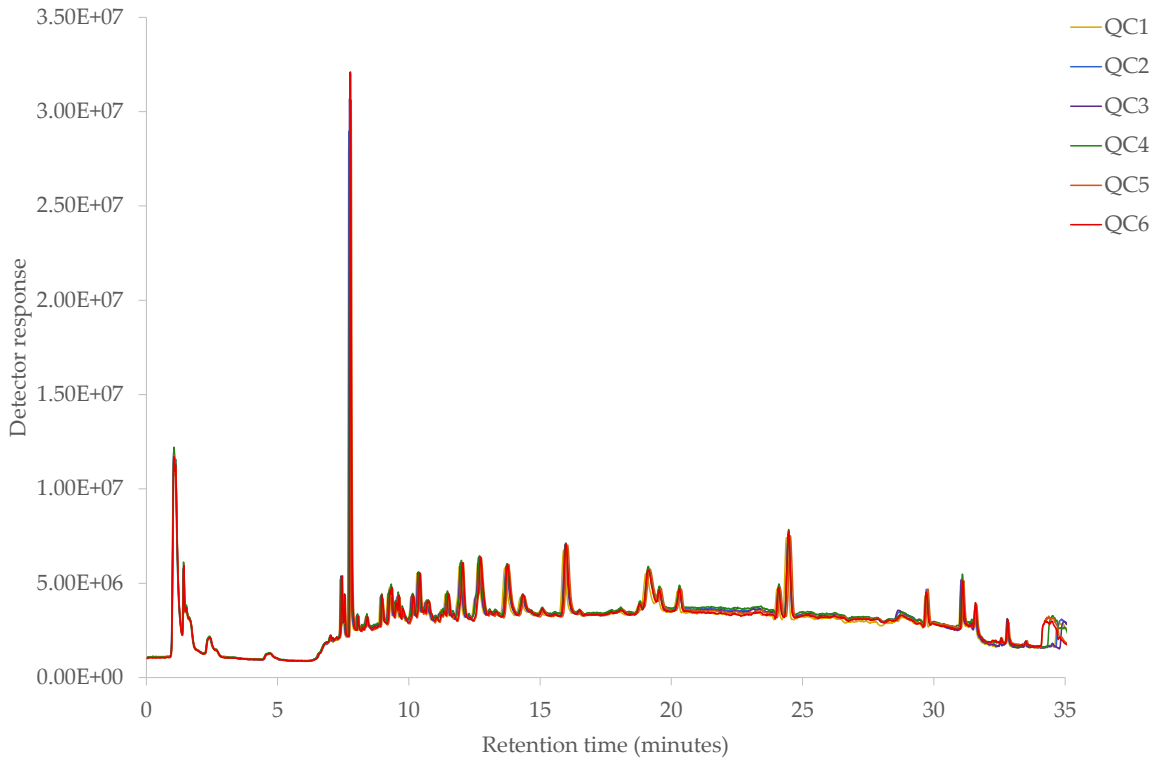

Figure 3.19: Total ion chromatograms of QC samples throughout analytical run for liver tissue extracts in negative ionisation mode

Figure 3.19 show the chromatograms for the QC samples run throughout the analysis, and all chromatograms are reproducible with extremely minimal drift. The only area of variability is at 34 minutes, but this does not look like an actual peak and may just be irregularity during the decrease of acetonitrile in the solvent gradient.

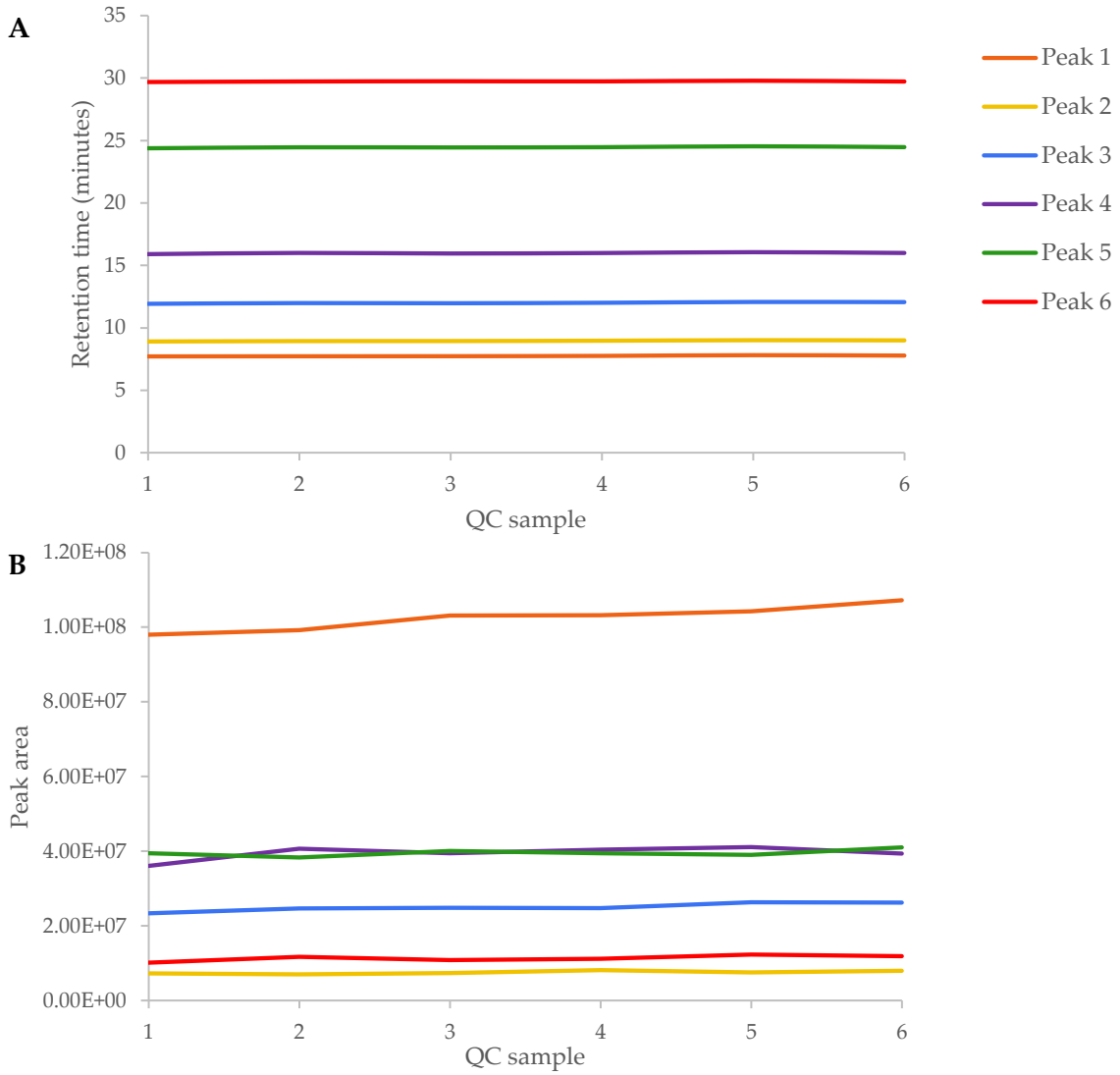

Figure 3.20: Variability of retention time (A) and peak area (B) of 6 peaks in QC samples throughout analytical run for liver tissue extracts in negative ionisation mode

The variability in retention time and peak area is demonstrated in Figure 3.20, which shows the consistency in retention time for all six peaks in each QC throughout the analytical run. The peak area also appears stable, with one peak increasing slightly over the course of the analysis.

Table 3.11: Variability of retention time and peak area of 6 peaks in chromatograms of QC samples during the analysis of liver tissue extracts in negative ionisation mode

	Retention time (minutes)								
Peak	QC1	QC2	QC3	QC4	QC5	QC6	SD	Average	CV%
1	7.72	7.73	7.74	7.76	7.81	7.78	0.03	7.75	0.42
2	8.92	8.94	8.945	8.97	9.00	8.99	0.03	8.96	0.36
3	11.92	11.98	11.97	12.01	12.07	12.06	0.06	12.00	0.49
4	15.90	16.00	15.95	15.99	16.06	15.99	0.05	15.98	0.33
5	24.39	24.46	24.45	24.47	24.54	24.48	0.05	24.46	0.20
6	29.68	29.72	29.74	29.73	29.78	29.72	0.03	29.73	0.11
	Peak area								
Peak	QC1	QC2	QC3	QC4	QC5	QC6	SD	Average	CV%
1	97980615	99209288	103168307	103240228	104260029	107230703	3397768	102514862	3.31
2	7281736	7021155	7342462	8109400	7558830	8002929	427275	7552752	5.66
3	23412628	24675874	24880103	24782431	26311934	26223442	1085433	25047735	4.33
4	36102188	40653615	39494326	40434290	41101107	39380509	1806771	39527673	4.57
5	39428903	38291612	40113677	39421673	39010152	41035842	941442	39550310	2.38
6	10136012	11758637	10886687	11169244	12292073	11884825	782496	11354580	6.89

The variability in retention time was between 0.11 and 0.49%, showing very good stability throughout the analysis, and the peak area variability was between 2.38 and 6.89%. These values confirm the instrument was stable throughout this analytical run.

3.8.4.2 Metabolic fingerprinting

The overlaid chromatograms for the liver organic extracts (Fig. 3.21) show the normally slaughtered and the DOA chickens had very similar metabolic contents, but the majority of peaks are at a higher intensity in the dead on arrival chickens compared to the normally slaughtered. This could be attributed to the difference in time since death between the two sample types, and so any metabolic pathways that are activated after death had been occurring for longer in the DOA samples.

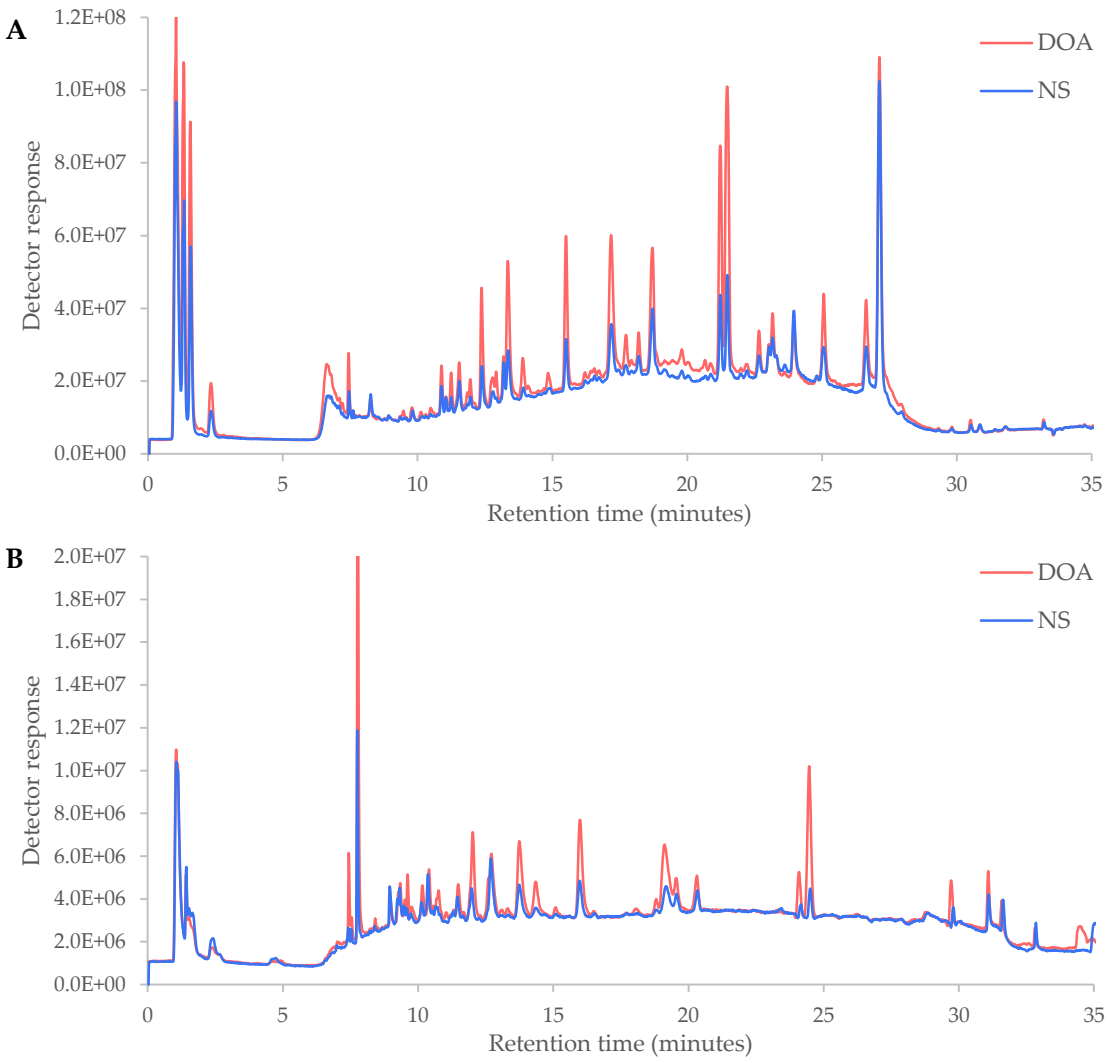

Figure 3.21: Example total ion chromatograms in (A) positive and (B) negative ionisation mode of liver tissue extracts from normally slaughtered and DOA chickens

There are some peaks that do not follow this trend in both ionisation modes. In positive ionisation mode, the peaks at 8 and 24.5 minutes have the same intensities in both sample types, and in the negative ionisation mode, the peaks at 9, 32 and 33 minutes also have the same intensities in both sample types. There are more peaks in the chromatograms for positive ionisation compared to negative ionisation, indicating that the positive ionisation mode may prove to be more useful during these global metabolic approaches as there are more features in these analyses, increasing the chance of finding useful markers, making it a good starting point in an untargeted analysis study.

3.8.4.3 Multivariate statistics

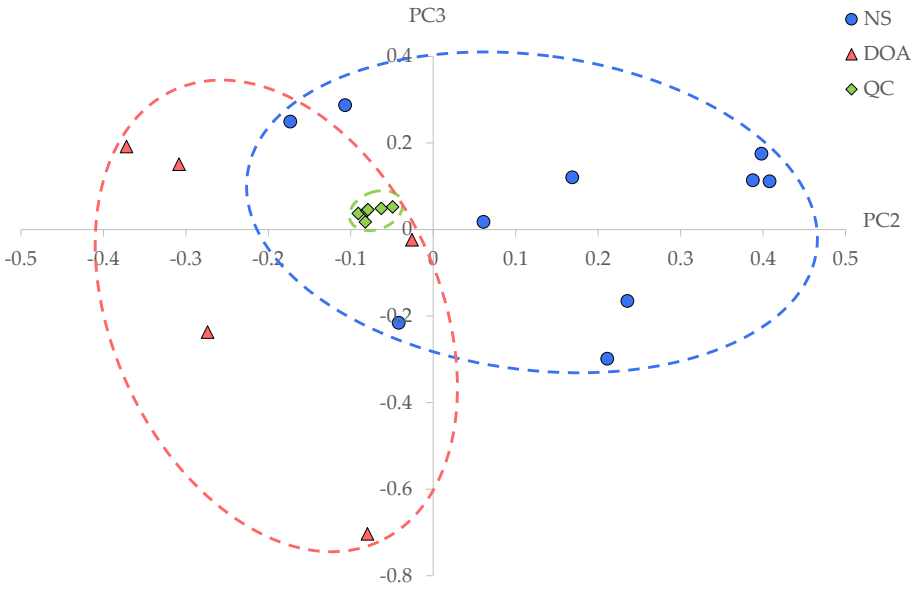

Figure 3.22: Principal component analysis scores plot of PC2 (3.808%) and PC3 (0.230%) for liver organic extracts in positive ionisation mode. PCA was carried out using markers with a p-value of < 0.05 and CV<10%

The spatial positioning of the data in the PCA plot for the significantly different markers with a CV% of less than 10% (Figure 3.22) is quite spread out, but the two groups can be seen, despite some overlap. This plot is not sufficient to identify if a piece of liver tissue is from a DOA chicken or a normally slaughtered chicken, but does show promise in markers being found that are statistically significantly different. The quality control samples are tightly clustered in the middle of the plot, showing stability within the analytical run. This is the same for the significantly different markers found in the negative ionisation mode, shown in Figure 3.23.

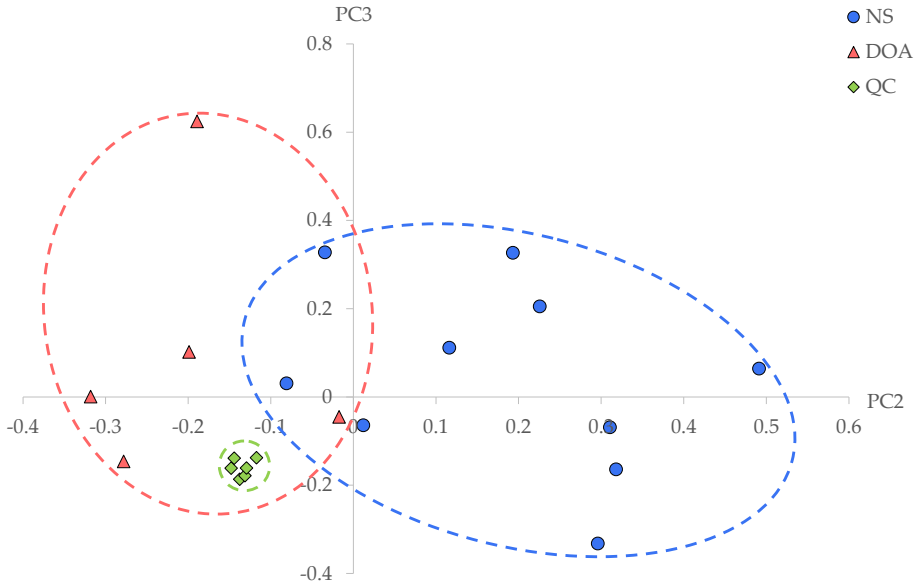

Figure 3.23: Principal component analysis scores plot of PC2 (2.629%) and PC3 (0.422%) for liver organic extracts in negative ionisation mode. PCA was carried out using markers with a p-value of < 0.05 and CV<10%

3.8.4.4 Significant markers

The number of features detected in the liver extracts found through *XCMS Online* was 14910 in positive ionisation mode and 5079 in negative ionisation mode. After removing all features with a CV% of more than 10% and a p-value of more than 0.05, 633 markers and 488 markers were remaining respectively. These markers were significantly different between the two sample types, and stable in the QC samples.

After taking the top 25 markers that had the lowest p-value from the statistical test in *XCMS Online*, Table 3.12 shows the markers that proved to be the most robust and significantly different between normally slaughtered and DOA chickens. These markers were significantly different based on the *XCMS Online* statistical analysis, as well as in the t-tests of the peak areas in the raw data. All markers have a CV% of less than 10% in the normalised data and 30% in the raw data, indicating they were stable throughout the analytical run and were not affected by instrumental drift.

Table 3.12: Summary of remaining compounds from top 25 markers that were significantly different between normally slaughtered and dead on arrival chickens in liver tissue extracts, in order of significance based on p-value from *XCMS Online*. Asterisk indicates markers were upregulated in the dead on arrival samples

Polarity	*m/z*	Retention time median (mins)	P-value from t-test (XCMS)	CV % (XCMS)	P-value from t-test (EICs)	CV % (EICs)
+	548.2953*	14.11	1.94E-05	9.41	1.71E-03	22.41
	524.3002*	11.92	1.11E-03	6.97	2.62E-04	6.93
	282.6343*	14.11	1.34E-03	3.41	3.53E-03	8.36
	526.3129*	14.11	1.59E-03	0.78	3.02E-03	1.58
	508.3065*	14.11	3.20E-03	3.54	2.84E-02	24.17
	291.6224*	14.11	3.92E-03	5.05	5.28E-04	29.87
	312.1370*	14.11	5.11E-03	9.32	8.35E-05	9.45
	498.2808*	11.39	8.00E-03	0.45	1.53E-02	0.88
	106.0501	1.03	1.40E-02	1.54	4.19E-02	1.33
	333.2389*	15.24	2.31E-02	5.38	2.36E-02	8.93
-	485.2729*	13.33	5.97E-03	1.08	3.49E-03	28.83
	614.2536*	14.30	1.93E-02	5.27	4.97E-03	10.63
	319.2214*	11.23	3.61E-02	2.79	4.18E-02	29.57
	296.2258*	11.02	3.69E-02	5.27	4.40E-03	26.76

All but one of the markers were found to be at a higher abundance in the DOA samples compared to the normally slaughtered samples.

3.8.4.5 Marker identification

No markers were able to be identified within the liver extracts. Only the top 25 significantly different markers were analysed and so despite there not being a successful identification within these markers, there may be other markers that are still significantly different that could be identified, however further research would be required.

3.8.5 Heart tissue extracts

3.8.5.1 Quality control

Positive ionisation

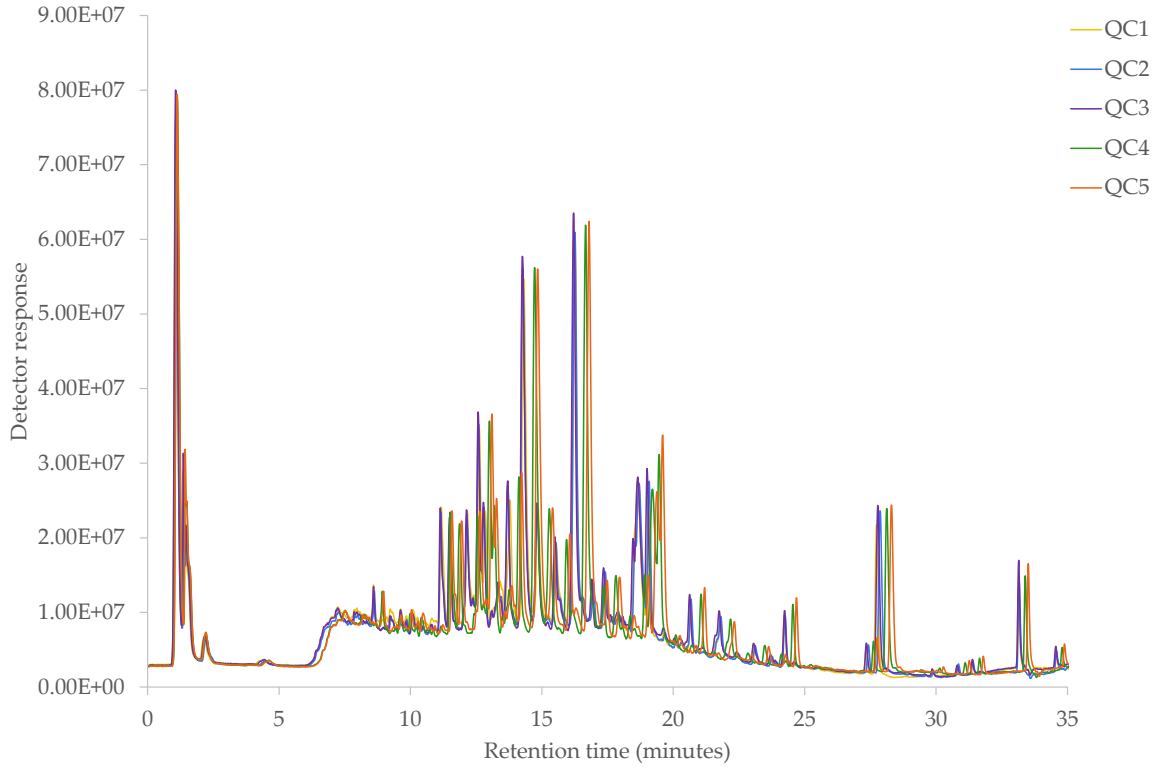

Figure 3.24: Total ion chromatograms of QC samples throughout analytical run for heart tissue extracts in positive ionisation mode

Figure 3.24 shows there was some instrumental drift during the analytical run; in particular, all peaks in QC4 and 5 have shifted to the right of the chromatogram, and the compounds within the sample have been retained for longer on the column. The first peaks at 2 minutes have the same retention time in all QC samples, and it is after this point that the retention time drift begins, therefore it was not an error in the injection of these samples. These are the last QC samples injected in the analytical run, and so it could have been a change in pressure in the system, or ambient temperature, that caused this retention time drift. Nonetheless, this was corrected during the data processing, and was still within the recommended threshold of variability.

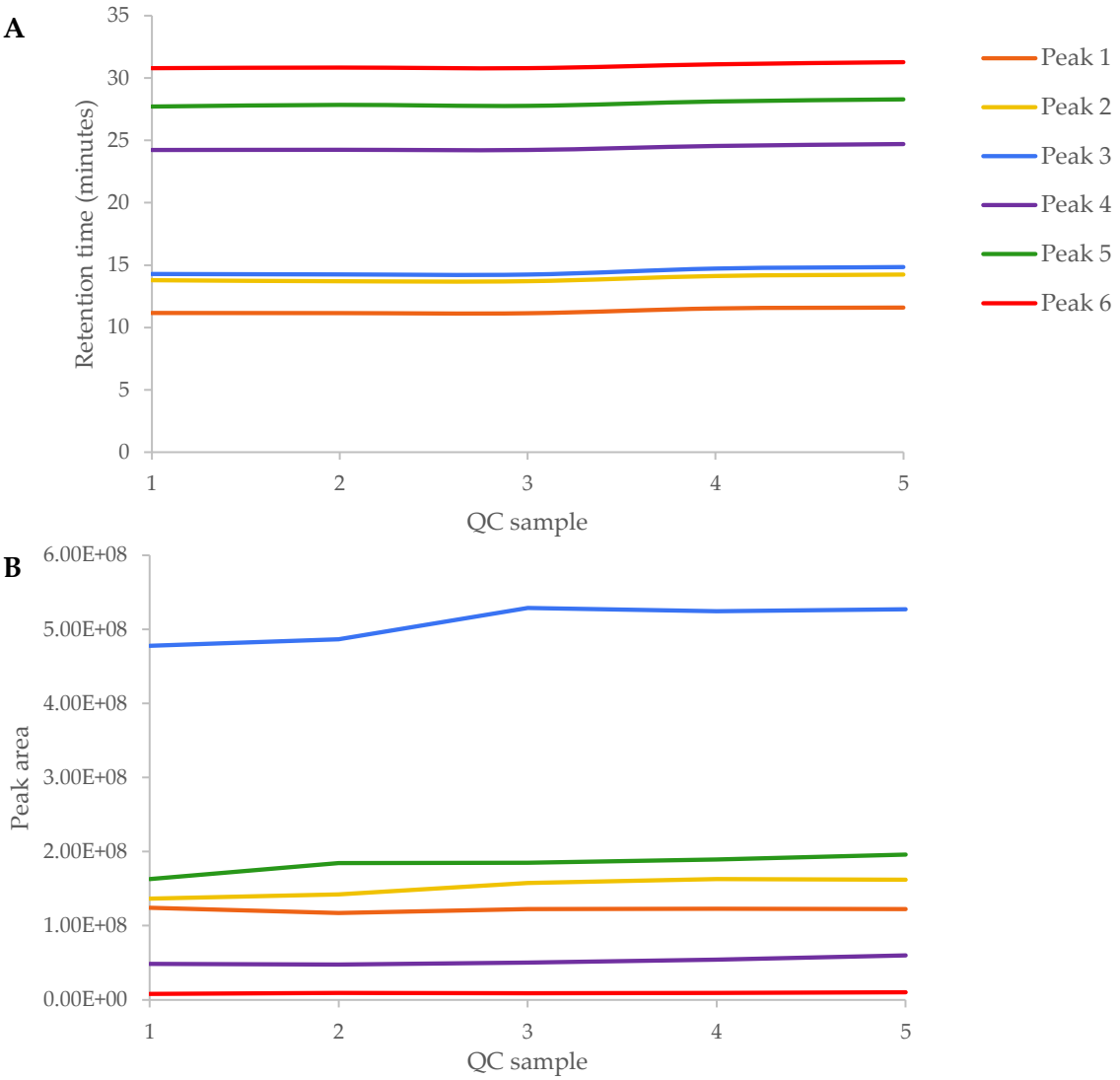

Figure 3.25: Variability of retention time (A) and peak area (B) of 6 peaks in QC samples throughout analytical run for heart tissue extracts in positive ionisation mode

The retention time and peak area variability are illustrated in Figure 3.25. The slight change in retention time in QC4 and 5 can be seen in the retention time variability plot, but overall the retention times appear stable throughout the analysis. The peak areas also show stability during the run.

Table 3.13: Variability of retention time and peak area of 6 peaks in chromatograms of QC samples during the analysis of heart tissue extracts in positive ionisation mode

	Retention time (minutes)							
Peak	QC1	QC2	QC3	QC4	QC5	SD	Average	CV%
1	11.15	11.14	11.13	11.51	11.58	0.23	11.30	2.00
2	13.78	13.70	13.70	14.12	14.24	0.25	13.91	1.83
3	14.30	14.26	14.25	14.72	14.84	0.28	14.47	1.95
4	24.22	24.24	24.22	24.54	24.70	0.22	24.38	0.91
5	27.72	27.85	27.78	28.13	28.30	0.25	27.96	0.88
6	30.79	30.84	30.80	31.10	31.27	0.21	30.96	0.69
	Peak area							
Peak	QC1	QC2	QC3	QC4	QC5	SD	Average	CV%
1	123946828	116890494	122522554	122671594	122252548	2742998	121656804	2.25
2	136306217	142042100	157724065	162730220	162033349	12184883	152167190	8.01
3	477596852	486225114	528783372	524159355	527063802	24759177	508765699	4.87
4	48422156	47658537	50088337	54300646	59743674	5013783	52042670	9.63
5	162849434	184569712	184923791	189478792	195929293	12448273	183550204	6.78
6	7869388	9252853	8765728	9420359	10250809	876898	9111827	9.62

The variability in retention time was between 0.69 and 2.00%, and the peak area variability was between 2.25 and 9.63%. These values indicate that the instrument was stable throughout the analytical run.

Negative ionisation

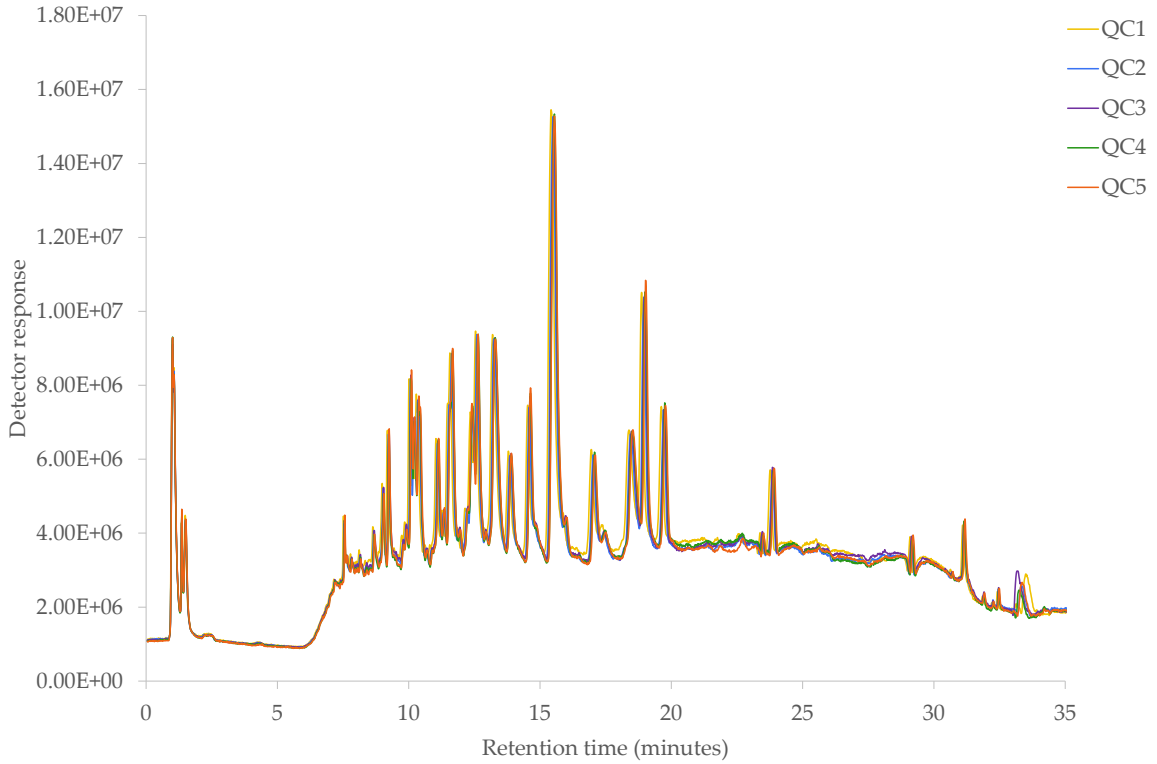

Figure 3.26: Total ion chromatograms of QC samples throughout analytical run for heart tissue extracts in negative ionisation mode

Overall, the stability of the QC samples throughout this analytical run was consistent, with all chromatograms overlaying each other. There were some fluctuations along the baseline, however these were minimal.

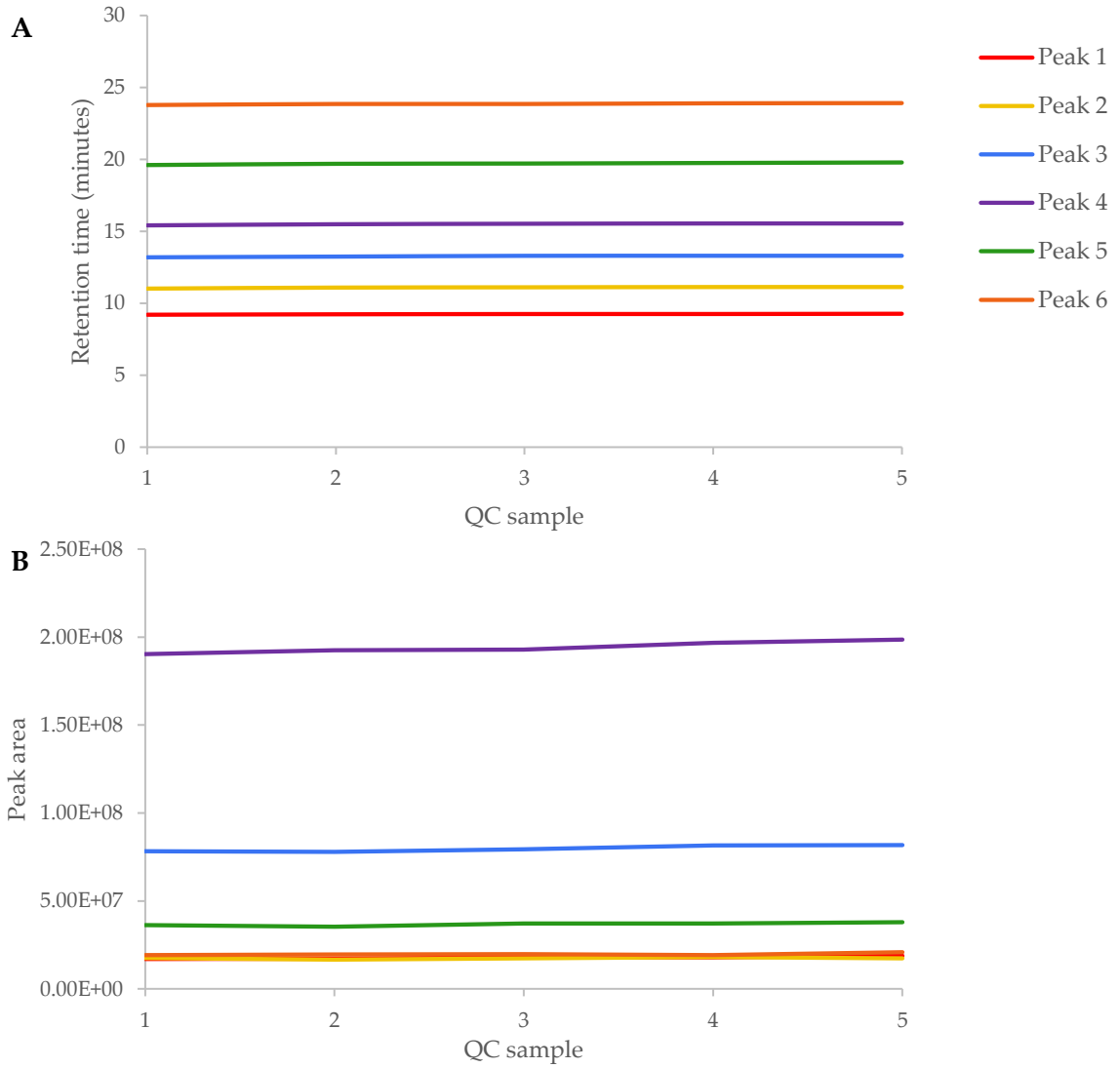

Figure 3.27: Variability of retention time (A) and peak area (B) of 6 peaks in QC samples throughout analytical run for heart tissue extracts in negative ionisation mode

The variability in retention time and peak area in six selected peaks within the total ion chromatograms of the QC samples are illustrated in Figure 3.27, and both appear to be stable throughout the analytical run.

Table 3.14: Variability of retention time and peak area of 6 peaks in chromatograms of QC samples during the analysis of heart tissue extracts in negative ionisation mode

	Retention time (minutes)							
Peak	QC1	QC2	QC3	QC4	QC5	SD	Average	CV%
1	9.20	9.23	9.24	9.25	9.26	0.03	9.23	0.28
2	11.03	11.10	11.12	11.14	11.14	0.04	11.11	0.40
3	13.20	13.24	13.29	13.30	13.30	0.05	13.26	0.34
4	15.42	15.50	15.53	15.55	15.55	0.06	15.51	0.36
5	19.62	19.70	19.72	19.75	19.79	0.06	19.71	0.32
6	23.77	23.85	23.85	23.90	23.92	0.06	23.86	0.25
	Peak area							
Peak	QC1	QC2	QC3	QC4	QC5	SD	Average	CV%
1	17080827	17163500	17876338	17952157	18880445	727710	17790653	4.09
2	17480140	16547806	17273227	18128199	17283138	564829	17342502	3.26
3	78260413	77904246	79297863	81620958	81670102	1803980	79750716	2.26
4	190407978	192514042	192966340	196654441	198610909	3324886	194230742	1.71
5	36267337	35258292	37227262	37226649	37985234	1052343	36792955	2.86
6	19197094	19509976	19782536	19236646	20779800	647397	19701210	3.29

The variability in retention time was between 0.25 and 0.40%, and the peak area variability was between 1.71 and 4.09%. These values indicate that the instrument remained stable throughout this analysis.

3.8.5.2 Metabolic fingerprinting

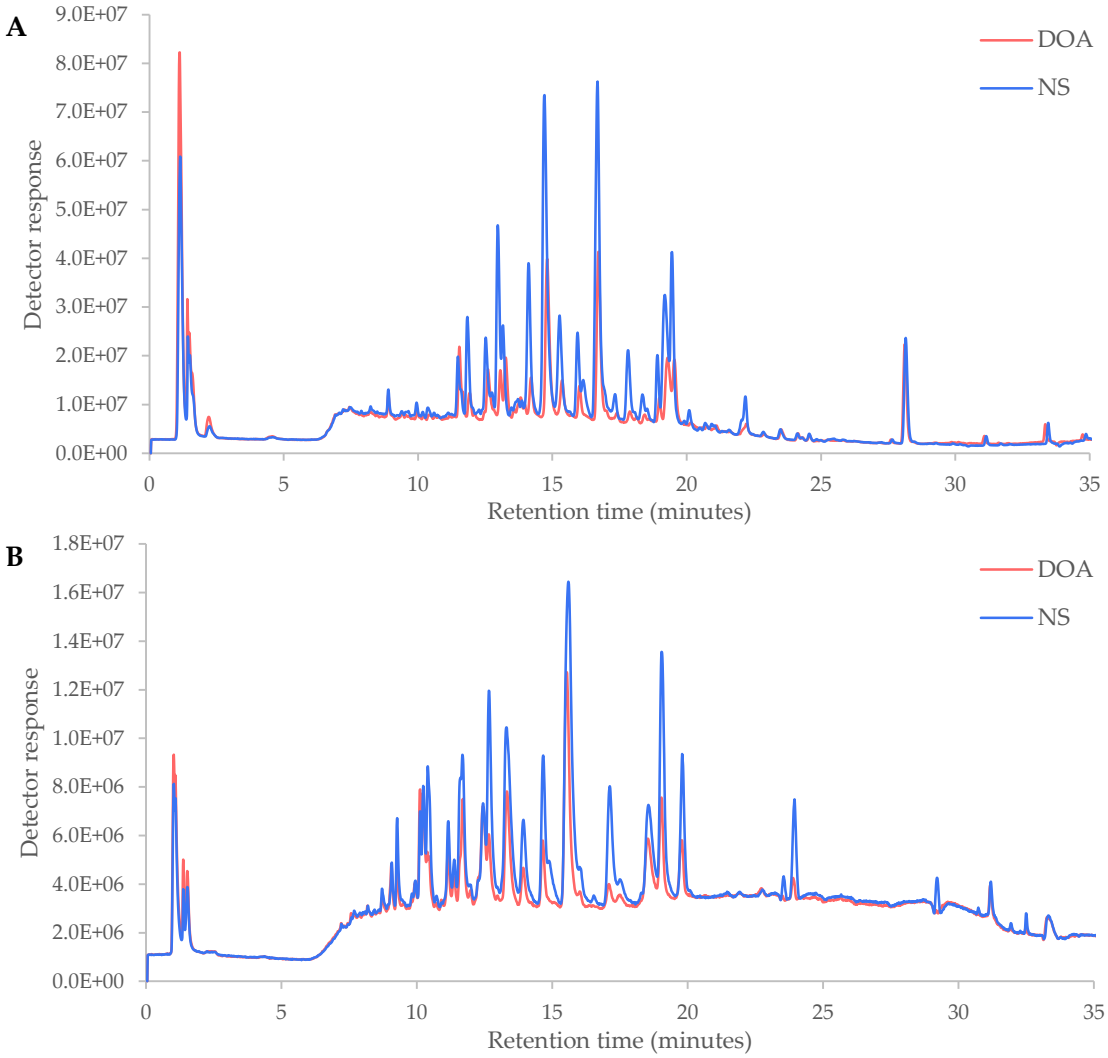

Figure 3.28: Example total ion chromatograms in (A) positive and (B) negative ionisation mode of heart tissue extracts from normally slaughtered and DOA chickens

The chromatograms for the heart tissue extracts (Fig. 3.28) show many peaks are at a higher intensity in the normally slaughtered compared to the DOA chickens. This is opposite to the liver extracts, where the peaks are at a higher intensity in the DOA extracts. This may indicate that the metabolites present in the heart muscle are decreasing after death, and so are downregulated in the DOA samples as these have a longer post-mortem interval than the normally slaughtered samples. There are some peaks that do not follow this trend; in positive ionisation mode, the peak at 11.5 minutes has a higher abundance in the DOA sample, and in the negative ionisation

mode, the peak at around 10 minutes also has a higher intensity in the DOA sample. Additionally, the peaks at the beginning of the chromatogram in both ionisation modes all have a higher abundance in the DOA sample, which are very polar compounds that are the least retained by the column and therefore elute rapidly.

3.8.5.3 Multivariate statistics

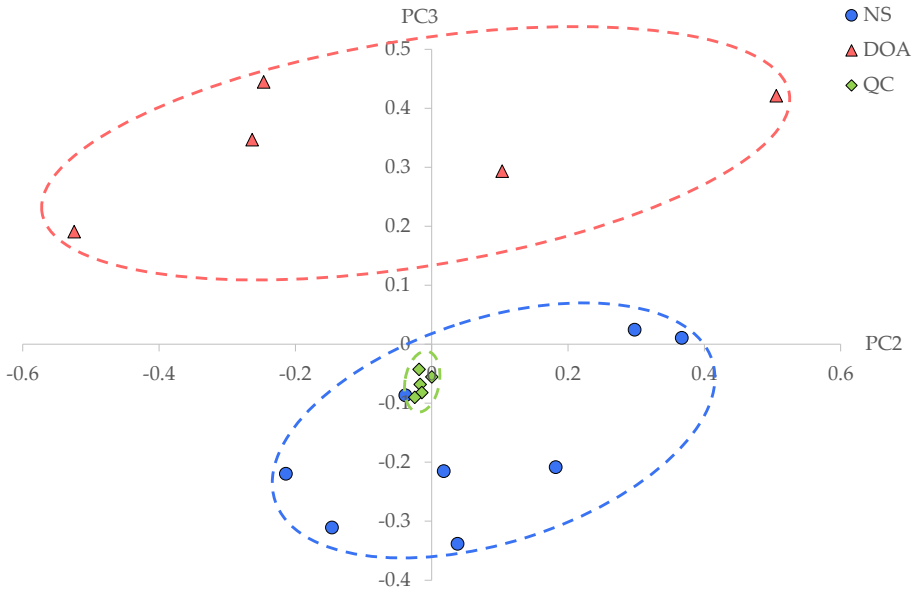

Figure 3.29: Principal component analysis scores plot of PC2 (0.493%) and PC3 (0.382%) for heart tissue extracts in positive ionisation mode. PCA was carried out using markers with a p-value of < 0.05 and CV<10%

The PCA plot (Figure 3.29) was constructed by using only the significantly different markers found by *XCMS Online* at a p-value of 0.05, with a CV% of less than 10%. Looking at the PCA plot, the QC samples are tightly clustered, showing good precision within the data, and the distance between the normally slaughtered samples and the DOA samples is greater than the spread within the QC samples, showing that the difference is caused by the difference in metabolic content in the samples and not by instrumental drift.

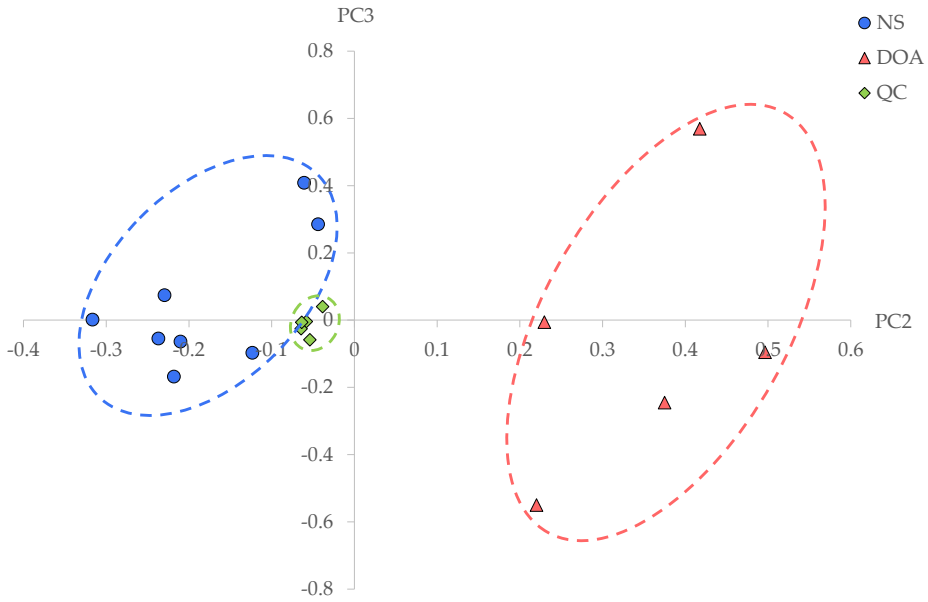

Figure 3.30: Principal component analysis scores plot of PC2 (0.811%) and PC3 (0.348%) for heart tissue extracts in negative ionisation mode. PCA was carried out using markers with a p-value of < 0.05 and CV<10%

The PCA plots for the negatively charged markers (Figure 3.30) showed greater separation than the positively charged markers. The separation between the two sample types is greater than the spread within the QC samples.

Taking these multivariate analysis results into account, it can be concluded that untargeted analysis of extracts taken from slaughtered chicken hearts, with the use of these multivariate techniques, has the potential of being used as a preliminary test to differentiate between normally slaughtered and DOA chickens, without the need for detecting specific compounds. Due to the small sample size in this study, this conclusion can not be definite, however if these results were to be replicated in a larger study it would increase the usefulness of this multivariate technique in discriminating between normally slaughtered and DOA chickens.

3.8.5.4 Significant markers

The number of features detected in the heart tissue extracts found through *XCMS Online* was 10919 in positive ionisation mode and 4278 in negative ionisation mode. After removing all features with a CV% of more than 10% and a p-value of more than 0.05, 842 markers and 729 markers were remaining respectively. These markers were significantly different between the two sample types, and were stable in the QC samples throughout the analytical run.

After taking the top 25 markers that had the lowest p-value from the statistical test in *XCMS Online*, Table 3.15 show the markers that proved to be the most robust and significantly different between normally slaughtered and DOA chickens. These markers were significantly different based on the *XCMS Online* statistical analysis, as well as in the t-tests of the peak areas in the raw data. All markers have a CV% of less than 10% in the normalised data and 30% in the raw data, indicating they were stable throughout the analytical run and were not affected by instrumental drift. All markers in this table were found at a lower concentration in the DOA samples compared to the normally slaughtered, which coincides with the findings from the peak patterns in the chromatograms.

Table 3.15: Summary of remaining compounds from top 25 markers that were significantly different between normally slaughtered and dead on arrival chickens in heart tissue extracts, in order of significance based on p-value from *XCMS Online*

Polarity	*m/z*	Retention time median (mins)	P-value from t-test (XCMS)	CV % (XCMS)	P-value from t-test (EICs)	CV % (EICs)
	261.6288	17.83	1.44E-07	2.89	2.60E-06	4.40
	282.1428	17.83	2.74E-07	8.44	6.31E-03	21.34
	467.3261	14.74	4.66E-07	2.72	5.15E-05	25.26
	268.1302	14.16	5.46E-07	8.79	9.18E-03	29.28
	270.1278	16.67	7.35E-07	4.22	6.65E-04	11.08
	238.6263	14.16	8.88E-07	5.34	1.62E-03	7.51
	747.9430	16.68	8.90E-07	9.91	1.41E-03	25.79
+	216.0630	16.68	1.04E-06	4.82	1.84E-04	11.03
	482.3266	16.68	2.25E-06	0.66	1.34E-05	4.52
	988.1003	16.68	6.61E-06	6.24	2.41E-05	11.40
	741.9572	16.68	1.51E-05	4.00	5.66E-05	6.95
	539.2375	14.18	2.23E-05	8.74	2.41E-04	28.34
	290.1398	16.68	2.51E-05	4.96	6.99E-05	5.12
	982.6152	16.68	6.03E-05	7.27	7.96E-06	25.04
	501.8004	16.67	6.48E-05	4.47	9.13E-04	24.88
	521.2542	12.65	3.90E-08	1.89	1.12E-02	20.24
	980.5186	12.65	4.29E-08	4.22	5.66E-09	4.31
	963.5288	12.65	4.36E-08	2.52	1.94E-08	6.31
	504.2655	12.65	8.20E-08	1.84	5.51E-05	3.22
	522.2672	17.08	1.56E-07	3.19	3.17E-04	6.62
	462.2929	13.96	2.05E-07	4.34	2.25E-05	3.14
	895.5412	12.65	3.13E-07	2.18	2.04E-06	4.09
	988.6422	15.93	3.24E-07	6.19	1.14E-04	25.70
	617.2718	17.08	3.54E-07	3.90	1.26E-04	6.46
	436.2792	12.65	5.69E-07	1.98	8.01E-04	2.65
	572.2515	12.65	6.06E-07	3.32	9.59E-03	29.00
-	925.5891	13.23	6.92E-07	4.93	1.74E-06	6.07
	549.2846	17.08	8.83E-07	3.36	8.75E-04	10.58
	494.2358	12.66	9.13E-07	5.62	9.44E-04	1.84
	462.2937	13.23	1.21E-06	2.18	2.43E-05	2.30
	600.2811	17.08	1.43E-06	3.58	3.77E-03	1.14
	959.6218	13.28	1.78E-06	2.44	9.93E-06	23.50
	482.3097	15.54	1.97E-06	1.99	3.82E-02	1.38
	947.5698	13.21	4.16E-06	4.39	8.26E-08	6.81
	961.6116	15.54	5.31E-06	1.22	6.35E-03	21.51
	668.2685	17.09	1.29E-05	2.38	6.47E-06	1.99
	965.6203	15.54	3.59E-05	3.73	9.45E-04	21.09
	999.5758	13.43	7.24E-05	9.11	8.28E-05	11.04

3.8.5.5 Marker identification

No markers were able to be identified in the heart extracts. Only the top 25 significantly different markers were analysed and so despite there not being a successful identification within these markers, there may be other markers that are still significantly different that could be identified with further analysis.

3.8.6 Targeted approach

Based on previous research, a number of metabolites have been found to change in blood after death. As an additional step to the analysis, metabolites that have been found to be a marker of interest in post-mortem studies were searched for within the raw data. In particular, the m/z (M+H) for hypoxanthine, uric acid, lactic acid, adrenaline and creatinine were attempted to be extracted from the chromatograms for all extracts. The only marker that appeared to be present in any of the tissue types was hypoxanthine, however this was poorly retained by the column and eluted quickly. Therefore, this marker would not be useful in this type of analysis and would be better suited to other chromatographic conditions, such as with the use of a HILIC (hydrophilic interaction chromatography) column, or gas chromatography, which is a technique more suited to analysing volatile compounds.

3.8.7 Repeatability on different instruments

3.8.7.1 Multivariate statistics

In order to directly compare the separation of groups in a principal component analysis scores plot, both sets of data needed to be processed in the same way. The Q Exactive Plus data was processed using *XMCS Online* with the same parameters as the Q-TOF data, as stated in Table 3.4. This allowed PCA scores plots to be carried out on the peak areas of the significantly different markers with a CV% of less than 10% for each sample. The differences in group separation between analytical runs on different instruments could then be visualised.

The PCA plot for the muscle tissue extracts analysed on the Q Exactive Plus (Figure 3.31 B) is very different to the PCA plot for the samples analysed on the Q-TOF (Figure 3.31 A). Firstly, the quality control samples are more tightly clustered in the data analysed on the Q Exactive Plus, implying the analytical run had less instrumental drift and more stability. However, the spread of the normally slaughtered samples is wider in this plot. The differences observed highlight the weaknesses of PCA scores plots; it is very useful when presenting the differences between sample types in a visual way, however, it is difficult to use as a method to differentiate between the sample types when the differences are extremely small, especially when analysed on different instruments on different days.

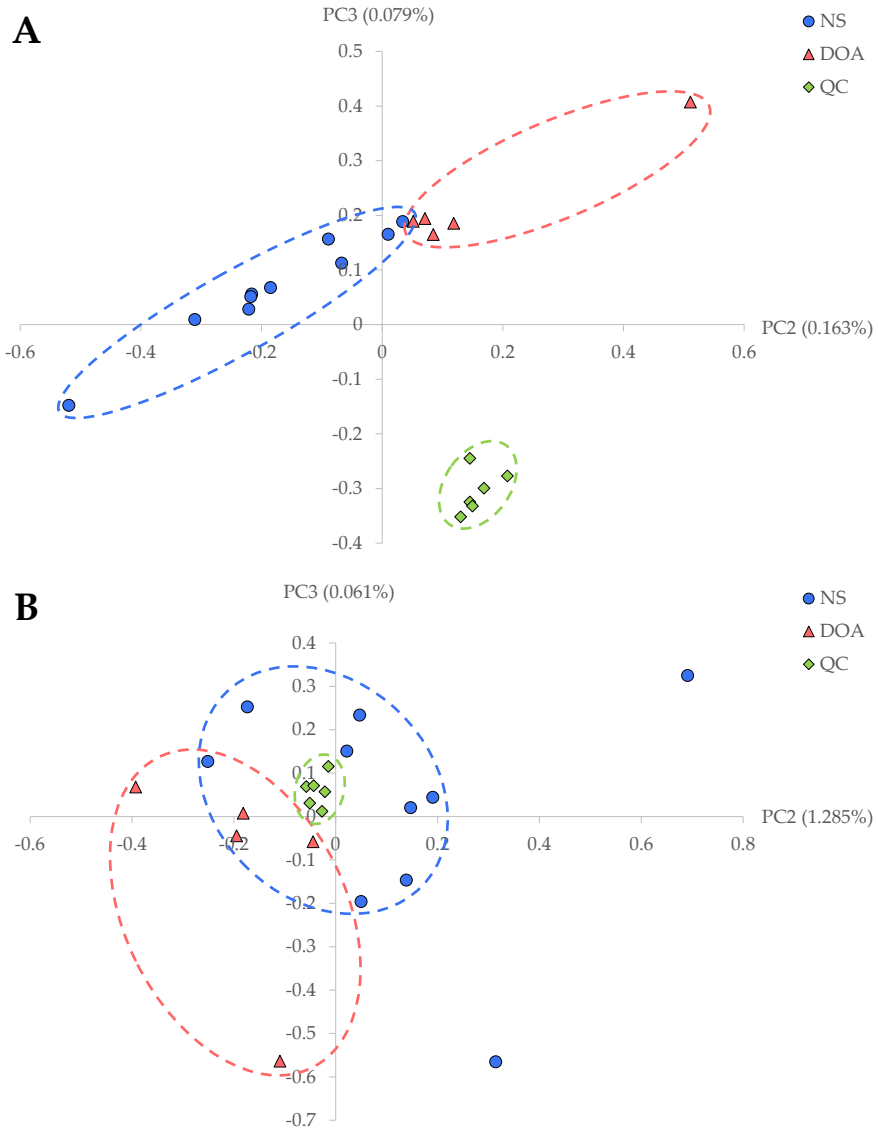

Figure 3.31: Principal component analysis scores plots of PC2 and PC3 for muscle tissue extracts in positive ionisation mode, using A) an Agilent Technologies 6530 Accurate Mass Q-TOF LC/MS, and B) a Thermo Fisher Q Exactive Plus. PCA was carried out using markers that were significantly different with a p-value of < 0.05 and a CV $< 10\%$

3.8.7.2 Marker identification

The data obtained from the Q Exactive Plus was analysed using *Compound Discoverer*. The workflows for the two data sets were very different and so it is difficult to directly compare them thoroughly. *Compound Discoverer* created a volcano plot that showed the significantly different markers at specific p-values and markers that increased or decreased by a specific fold change. This allowed only the most interesting markers to be further analysed for potential identification.

In the muscle extracts, only 4 markers were found to be significant at a p-value of less than 0.05 and different by a fold change of 0.5. Due to the unknown specifics of the statistical tests used within the *Compound Discoverer* software, manual t-tests were carried out to confirm the significance of these 4 markers; only 2 were confirmed as significant. All four markers could be found in the Agilent Q-TOF feature table, and so the two datasets were compared (Table 3.16). Of the two markers confirmed to be significantly different in the Q Exactive Plus data, one of these was not found to be significantly different in the Q-TOF data. The other compound was significant in both datasets and had a CV% of less than 10%. Interestingly, this compound had an *m/z* of 300.2892, and the identification based on database searches within the *Compound Discoverer* software found this marker to be sphingosine. This compound is the same compound that was successfully identified in the Q-TOF dataset, shown in Section 3.8.3.5.

Table 3.16: Comparison of significantly different markers in muscle tissue extracts analysed on an Agilent Q-TOF and a Thermo Q Exactive Plus. P-value calculated from manual t-test on normalised peak areas

m/z	Retention time median (mins)	P-value (QE Plus)	P-value (Q-TOF)	CV% (QE Plus)	CV% (Q-TOF)
522.3554	8.25	0.153	0.303	9.39	44.73
300.2892	6.93	<0.001	0.010	1.57	6.61
298.0967	3.95	0.031	0.462	2.52	58.75
466.3286	10.57	0.071	0.237	4.63	5.79

The difference in results when using two different instruments with different workflows demonstrates how varied untargeted analyses can be, and how the discovery of markers for diagnostic purposes largely depends on the techniques used in initial investigations. The fact that the only marker that was significantly different between DOA and normally slaughtered chicken muscle in both analyses was sphingosine shows the reliability and robustness of this marker.

3.9 Conclusion

This work has shown that it is possible to use established metabonomic profiling methods to differentiate between animals that have died in transit and those that were subjected to the normal slaughter process. This approach has also shown that it is possible to generate a large dataset of metabolites that can be statistically analysed to determine potential markers that could be useful for the detection of this type of fraud.

The liquid chromatography-mass spectrometry techniques used in this work have shown to produce reliable data, through the use of quality control samples injected throughout the analytical run. In all analyses, the QC samples had minimal retention time and peak area variability, and have proved to be a beneficial way in ensuring the data is reliable for continued statistical analysis.

This untargeted approach on the analysis of muscle, liver and heart tissue extracts obtained metabolic profiles that could be used to detect features within the samples. Overall, the use of positive ionisation mode on the Q-TOF obtained more features than in negative ionisation mode, and the liver appeared to contain the most features overall. Despite this, the heart had the most remaining features by the end of the statistical analysis, with 37 out of 50 features being significantly different between the two sample types (p-value < 0.05) and stable throughout the analysis (CV% $< 30\%$ in QC samples in the raw data), compared to the liver, which had 14 out of 50 features, and the muscle, which had 10 out of 50 features. The muscle tissue had the fewest features detected in the chromatograms, however the muscle was the only tissue type that was able to provide a marker that could be identified successfully.

In the muscle tissue, a marker was identified as sphingosine, and the intensity of this marker was found to be downregulated in the dead on arrival chickens compared to

the normally slaughtered chickens. It was postulated that the presence of sphingosine is likely due to the accumulation of ceramide during the transport and slaughter, and the breakdown of this compound to sphingosine. The difference in concentration of sphingosine between DOA and normally slaughtered chickens could be attributed to the difference in time of death. Due to the number of samples available for this study, it is clear that further work is required to validate this marker for this purpose. However, this work highlights the potential of this approach to provide markers that could be used in targeted assays to detect fraud of this nature.

Due to the time consuming data analysis methodologies involved in this research, only the top 25 significantly different compounds were analysed in detail, including confirmation of significance, statistical testing of the raw data, and attempted identification. This means that there was only one successful identification made within this work. In future work, more significantly different markers would be analysed in detail in order to gain more identifications of the markers that contribute to the differences between normally slaughtered and DOA chickens.

To evaluate the variability between instruments, the extracts were analysed on two separate systems and processed in different ways. Very few markers were found to be significant in the Q Exactive data, but sphingosine was among these. This demonstrates the robustness of this marker; the fact that it was the single marker found in both methods in this small study increases the potential usefulness of this compound as a marker for detecting dead on arrival meat in the human food market.

Overall, the analytical techniques and workflows used within this research was able to discriminate between DOA and normally slaughtered chickens, and successfully identify a statistically significantly different marker as sphingosine. It has shown that these techniques are suitable for detecting very subtle differences in food matrices that can be exploited in future initial untargeted analyses.

Chapter 4

The effect of freezing duration and freeze-thaw cycling on the metabolic profile of meat

The aims of this experiment were to determine how the metabolic profile of meat changes depending on the duration of frozen storage, and the number of freeze-thaw cycles the meat product has undergone, using liquid chromatography-mass spectrometry and untargeted metabonomic techniques.

4.1 Introduction

Consumers rely on the information provided on labels of products in order to make an educated choice when purchasing, however these details can be falsified to benefit the manufacturer. Within the meat industry, it can be expensive to dispose goods that have not been sold before the end of their shelf life, so it can be tempting to freeze products and claim they have never been frozen, or alter the date of freezing to make the duration of frozen storage appear shorter. The Fresh Meat (Hygiene and Inspection) Regulations 1995 [115] states that all meat must be "stamped before freezing so as to indicate the month and year in which it is frozen or a label is attached to it after freezing indicating this." Council Regulation (EC) No 1234/2007 [116] states that poultry meat can only be marketed as either fresh, frozen, or quick-frozen. Fresh refers to meat that has been kept between -2°C and 4°C and not been stiffened by the cooling process and frozen refers to meat that must be frozen as soon as possible within the constraints of normal slaughtering procedures

and is kept at a temperature no higher than -12°C at any time. Quick-frozen refers to meat that is kept at a temperature no higher than -18°C at any time. It is therefore essential that techniques are available to combat the mislabelling of fresh or frozen meat products.

Not only is there legislation regarding the action of freezing meat, but there are also regulations to control multiple freeze-thaw cycles of meat products. Regulations (EC) No 853/2004 [117] states that "minced meat, meat preparations and MSM (mechanically separated meat) must not be re-frozen after thawing." This legislation dictates that any meat that has been frozen, thawed, and then re-frozen is illegal, and therefore it is important to develop techniques that can not only detect if a meat product has been previously frozen, but also whether it has undergone multiple freeze-thaw cycles, due to risk of bacterial growth.

At present, many consumers make the decision to purchase fresh meat instead of frozen meat due to the sensory and nutritional benefits of the product, despite the cost of fresh meat being significantly higher than frozen meat [118]. This creates a target for retailers to fraudulently mislabel their frozen-thawed meat products as fresh, for economic benefit. There is no visual difference between fresh and thawed chicken, so the customer could be deceived into purchasing thawed chicken at the higher price. Some research has been conducted on meat quality after freezing in beef, lamb and chicken meat [118–122]. The physico-chemical changes in chicken meat have been investigated in meat that has undergone multiple freeze-thaw cycles compared to fresh chicken, with lipid and protein oxidation increasing after 4 freeze-thaw cycles [122], and the use of impedance measurements has been able to discriminate between fresh and frozen-thawed meat [118]. Spectroscopic methods have also been successful in differentiating between fresh and frozen-thawed chicken meat [121], and an inter-laboratory experiment was successful in using the presence of a mitochondrial enzyme called β-hydroxyacyl-CoA-dehydrogenase (HADH) to

determine if a piece of chicken had been previously frozen [123]. This research can differentiate between fresh and frozen, but can not determine the length of frozen storage. Also, little research has been carried out using liquid chromatography-mass spectrometry in order to monitor the change in metabolic content that may occur during multiple freeze-thaw cycles. The application of this technique would be beneficial in initial untargeted analyses due to the holistic nature of this type of analysis.

Meat quality is affected by protein and lipid oxidation [124, 125]. The length of time a poultry product has been frozen for affects the quality of the meat. Many studies have found that protein and lipid oxidation occurs during the freezing process [126, 127]. This not only causes a decrease in the quality of the meat, but may also have a negative impact on the health of the consumer [128]. Oxidative stress is known to be an issue resulting in disease such as cancer and atherosclerosis. It is caused by an imbalance of oxidants and antioxidants that can result in damage to cells. Reactive oxygen species (ROS) is the active form of oxygen and is required for a number of functions within a biological system [129], however the amount of ROS must be controlled before a chain reaction is initiated, resulting in cell death and tissue damage. Antioxidants can neutralise ROS to stop oxidative effects, with defence mechanisms activating when ROS activity becomes excessive. These antioxidants can be endogenous, such as glutathione, or introduced through the diet, such as vitamin C and E [129]. However, it is important to note that too many antioxidants can cause a disruption in the normal functions ROS are involved with, which is why oxidative stress occurs when there is an imbalance of these two mechanisms. Specific biomarkers of oxidative stress have been found in chronic diseases; specifically cardiovascular diseases and cancer. These biomarkers are difficult to detect due to their short half life, but the by-products of oxidative stress can be used to indicate excessive ROS production; specifically malonaldehyde [129]. Interestingly, this molecule has been found to increase in concentration after frozen

storage [130], as well as after a series of freeze-thaw cycles [122] due to lipid and protein oxidation. This indicates that oxidative stress continues after death and is not prevented even during the freezing process. If this is the case, then it is in the public's best interest to be aware of any adverse effects that frozen meat could have to their health.

Lipid oxidation is one of the main contributors to the deterioration of muscle food, and it has been found that chicken is more susceptible to lipid oxidation due to a high poly-unsaturated fatty acid content [127]. Oxidation of lipids is considered to be the most important mechanism of lipid oxidation within meat products, and it consists of initiation, which is the formation of unstable free radicals, propagation, which is the chain reaction of free alkyl radicals and peroxy radicals, and termination, which is the formation of nonradical products and ends the chain reaction [131].

Lipid oxidation favours unsaturated fatty acids due to the presence of double carbon bonds that are vulnerable to being attacked by free radicals. Pre-slaughter, lipid oxidation is usually controlled by antioxidants that donate electrons to free radicals in order to stabilise them and prevent continued oxidation. Post-slaughter, meat undergoes a variety of complex biochemical changes, including the destruction of cell membranes, and many biological functions cease to occur, such as circulation of nutrients, aerobic metabolism, and the preventative antioxidant enzyme system [132]. Oxidation can no longer be controlled and autoxidation occurs, leading to complete break down of the phospholipid membranes, which are mostly made up of phosphatidylcholines. These degrade into fatty acids, which are further oxidised by free radicals.

4.2 Experimental procedures

4.2.1 Materials

Acetonitrile (HPLC grade), methanol (HPLC grade) and dichloromethane (analytical grade) were purchased from VWR (East Grinstead, UK), and ultra pure water (18.2 MΩ) was purified using an in-house Milli-Q system from Elga (High Wycombe, UK). Formic acid (laboratory reagent grade) was purchased from Fisher Scientific (Loughborough, UK). ESI-L low concentration tuning mix and API-TOF reference mass solution were purchased from Agilent Technologies (California, USA).

4.2.2 Sample collection and storage

Chicken breasts, lamb shoulders and lamb livers were obtained from a local butcher. Each tissue type was cut into equal sized portions approximately 2 cm by 2 cm, stored in individual polythene bags, and frozen in a domestic freezer that had been set to the recommended 'medium' temperature setting. Measurements were taken over 24 hours and 72 hours to ascertain the exact temperature and any fluctuations.

4.2.3 Sampling

4.2.3.1 Freezing duration

Metabolites were extracted from a fresh sample from each tissue type on the day of collection, to determine the metabolic content of meat that had not been previously frozen. A sample from each tissue type was then removed from the freezer at 1, 2, 3, 4, 6, 8, and 10 weeks, (1, 2, 3, 4, 6, 7, and 10 weeks for chicken muscle tissue) and allowed to defrost at 4°C for 24 hours. Six replicate extracts were obtained.

4.2.3.2 Number of freeze-thaw cycles

Six freeze-thaw cycles (FT1-6) were investigated with six replicates for each cycle. To ensure all samples were frozen for the same amount of time, all samples were stored in the freezer for a total of 6 weeks. Over the 6 weeks, the samples were removed, as shown in Table 4.1, and stored at 4°C for 24 hours, after which they were returned to the freezer. After 6 weeks, all samples were removed, allowed to thaw at 4°C for 24 hours, and then metabolite extraction was carried out. This was conducted with chicken muscle and lamb liver tissue.

Table 4.1: Sample preparation for freeze-thaw samples

Week	Samples removed from freezer
1	FT6
2	FT6, FT5
3	FT6, FT5, FT4
4	FT6, FT5, FT4, FT3
5	FT6, FT5, FT4, FT3, FT2
6	All samples

4.2.4 Metabolite extraction

Approximately 500 mg of each portion of meat was homogenised with small surgical scissors, and approximately 110 mg was placed into an Eppendorf tube. Methanol/H_2O (1:1) was added (1 mL per 100 mg of sample), then the sample was sonicated for 15 minutes and centrifuged at 16100 rcf for 20 minutes. The supernatant was then moved to a glass vial and retained as the aqueous (AQ) extract. The tissue pellet was broken up using a clean pipette tip, and dichloromethane/methanol (3:1) was added (1 mL per 100 mg of sample). The sample was sonicated for 15 minutes and centrifuged at 16100 rcf for 20 minutes, and 1 mL of the supernatant was then moved to a glass vial and allowed to evaporate overnight, then resuspended in 1 mL of methanol. This was retained as the organic (OR) extract. Both the aqueous and organic extracts were stored at -25°C prior to analysis.

4.2.5 Stability of freezer temperature

The freezer was set to the recommended 'medium' temperature setting, however as it was a domestic freezer, there was no digital display with the exact temperature. The temperature within the freezer was monitored using a temperature probe, which logged the temperature every minute. The temperature measurements were recorded over a 24 hour period, to monitor any temperature fluctuations, and the average temperature measurements from each hour over a 72 hour period were recorded, to monitor any overall fluctuations over multiple days.

4.3 Instrumental set-up

4.3.1 Analytical considerations

Quality control samples were made for each analytical run, consisting of an equal aliquot of every sample within each run. At the start of each analytical run, 10 QC samples were injected at a volume of 10 μL, then 20 QC samples at an injection volume of 3 μL were injected to condition the column. All non-QC samples were randomised to eliminate any issues arising from instrumental drift.

4.3.2 Chromatographic parameters

Chromatographic separation of the extracts was performed with a Thermo Scientific Hypersil GOLD aQ column (100 mm x 2.1 mm, particle size of 1.9 μm) using an Agilent 1260 Binary Pump HPLC. The column was maintained at 40°C and the injection volume was 3 μL. The flow rate of the mobile phase was 0.3 mL/min and consisted of 0.1% formic acid (solvent A) and acetonitrile with 0.1% formic acid (solvent B). The chromatographic gradient method can be seen in Table 4.2. A needle wash method was included after every injection, consisting of 3 separate vials of methanol, each used in a specific order, with 3 washes per vial. The column was flushed with 100% organic solvent after each run to reduce any potential carryover.

Table 4.2: Solvent gradient method used for the analysis of organic extracts from all sample types

Time (mins)	Solvent A (%)	Solvent B (%)
0	95	5
2	95	5
3	47.5	52.5
30	0	100
40	0	100
41	95	5
50	95	5

4.3.3 Q-TOF parameters

For the analysis, an Agilent Technologies 6530 Accurate Mass Q-TOF was used with an electrospray ionisation source, and the parameters were set as shown in Table 4.3. The reference mass solution was continually run through the analysis, and used purine (121.0509 *m/z*) and hexakis (1H, 1H, 3H-tetrafluoropropoxy)phosphazine (922.0098 *m/z*) in positive ionisation mode as internal reference masses to ensure mass accuracy. The data was collected in both profile and centroid mode.

Table 4.3: Q-TOF parameters used in this experiment

Parameter	Setting
Drying gas temperature	320°C
Drying gas flow rate	11 L/min
Capillary voltage	4000 V
Fragmentor voltage	125 V
Skimmer voltage	65 V
Mass range	100-1000 *m/z*

4.4 Data pre-processing

The data was pre-processed using *XCMS Online*. The parameters for the method used on this online platform were set to the default settings specifically designed by *XCMS Online* for analyses carried out with HPLC and ESI-QTOF-MS instruments, and were as shown in Table 4.4. This software also carried out normalisation of the raw data using the median fold change method. A feature table was produced, which included a list of *m/z* values and their median retention times, and the peak areas for these features in each sample.

Table 4.4: Parameter settings for *XCMS Online* used in this experiment

XCMS method	Parameter	Setting
Feature detection = CentWave	ppm	30
	min peak width (seconds)	10
	max peak width (seconds)	60
	mzdiff (*m/z*)	0.01
Retention time correction = Obiwarp	profStep (*m/z*)	0.5
Alignment	bw (seconds)	5
	minfrac	0.5
	mzwid	0.025

4.5 Statistical analysis

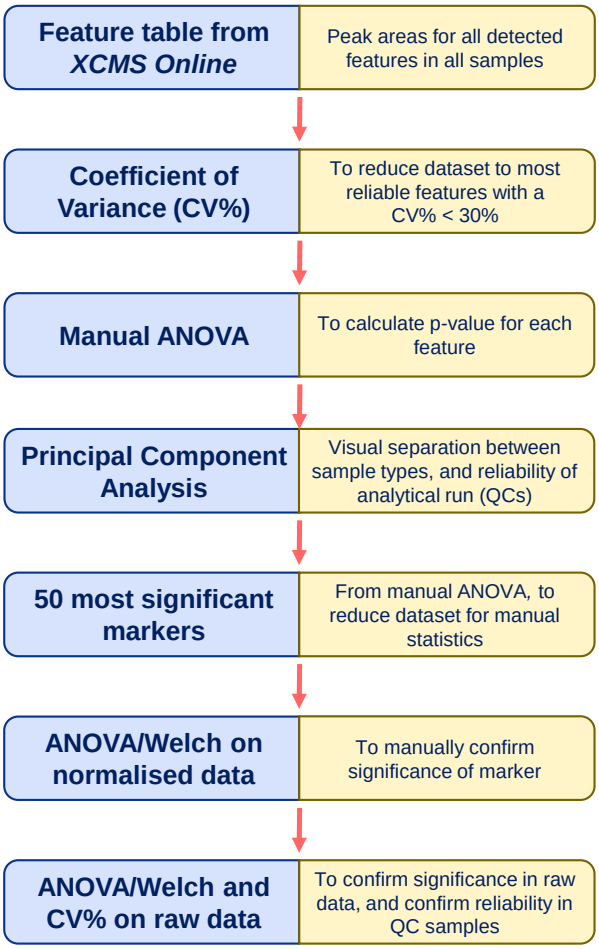

Figure 4.1: Statistical workflow for all datasets analysing extracts from tissue stored in the freezer for different lengths of time, and from tissue that has undergone different numbers of freeze-thaw cycles

The standard deviation, average, and coefficient of variance percentage were calculated using the peak areas of each feature in the QC samples throughout the analytical run. All features that had a CV% of more than 30% were removed. A manual ANOVA test in *Microsoft Excel* was carried out on the peak areas of each sample in order to get a p-value for each feature. A principal component analysis with standardisation was carried out on all features with a p-value < 0.05 using the Multivariate Analysis add-in for *Microsoft Excel 2010* [85], and a scores plot was produced in order to visualise any separation between sample types. The first six

principal components were plotted in all combinations to find the components that best represented the separation of the sample types. The feature table was ordered based on the p-value in the manual ANOVA test, and the 50 most significantly different markers were analysed in *SPSS*, in order to verify their significance. Either ANOVA or Welch tests were performed, depending on the homogeneity of variance value for each marker. The tests were carried out with a confidence level of 95%, giving an α value of 0.05. If the p-value was less than the α value, it indicated the abundance of that marker was statistically different between sample groups.

The raw data was then analysed in *Masshunter Qualitative Analysis* (Agilent Technologies) to produce extracted ion chromatograms (EICs) for the markers that were confirmed to be significantly different. Using *SPSS*, ANOVA or Welch tests were carried out on the peak areas of the EICs. The CV% of the QC samples was also calculated. This process ensured the markers were significant even before normalising the data in the pre-processing step. Any markers that were found to not be significantly different or had a CV% of more than 30% in the QC samples were removed. This additional step in the methodology ensured the final markers were robust and reliable, with the intention of being able to confidently use these markers as an indicator of frozen storage length or number of freeze-thaw cycles.

It is important to note that these analyses generate vast datasets that detect many features within a chromatogram. After the removal of unstable features (CV% $>$ 30%) and not significantly different features (p-value $>$ 0.05), there are still many features remaining. Due to the nature of the workflow and the extensive manual statistics each feature undergoes, only the top 50 most significantly different features are investigated in the raw data and attempted to be identified. This means there is a strong likelihood of many other markers that were not in the top 50 that could prove to be useful as an indicator for the number of freeze-thaw cycles meat has undergone, however further research would be required.

This statistical analysis was then repeated with fewer sample types in order to gain a deeper insight into the markers that may be significantly changing during specific times of the frozen storage process. The time periods were; Week 1 to Week 10, to examine samples that have been previously frozen only; Week 4 to Week 10, to examine the later stages of the freezing process; and Fresh to Week 4, to examine the initial stages of the freezing process. During this, only the top 10 most significantly different markers were statistically analysed through the full workflow.

4.6 Identification of markers

The potential formulae predicted by *MassHunter Qualitative Analysis* were used to search the METLIN database manually. A tentative identification was made based on the comparison of the mass spectrum of the sample and mass spectra of compounds with the same formula on the METLIN database, if available. If a tentative identification could not be made, an idea of the class of compound could be determined based on the predicted formulae matching to a number of similar compounds on the METLIN database.

4.7 Results and discussion

4.7.1 Stability of freezer temperature

The temperature change over 24 hours can be seen in Figure 4.2A. There was a fluctuation in temperature every 9 minutes, from approximately -20.5°C to -24.5°C, which is quite a large range, however it is well below the -18°C recommendation [133], and these fluctuations were consistent throughout this time period. The average temperature of each hour can be seen in Figure 4.2B. This average ranged from -22.41°C to -22.92°C, showing stability in the temperature of the freezer.

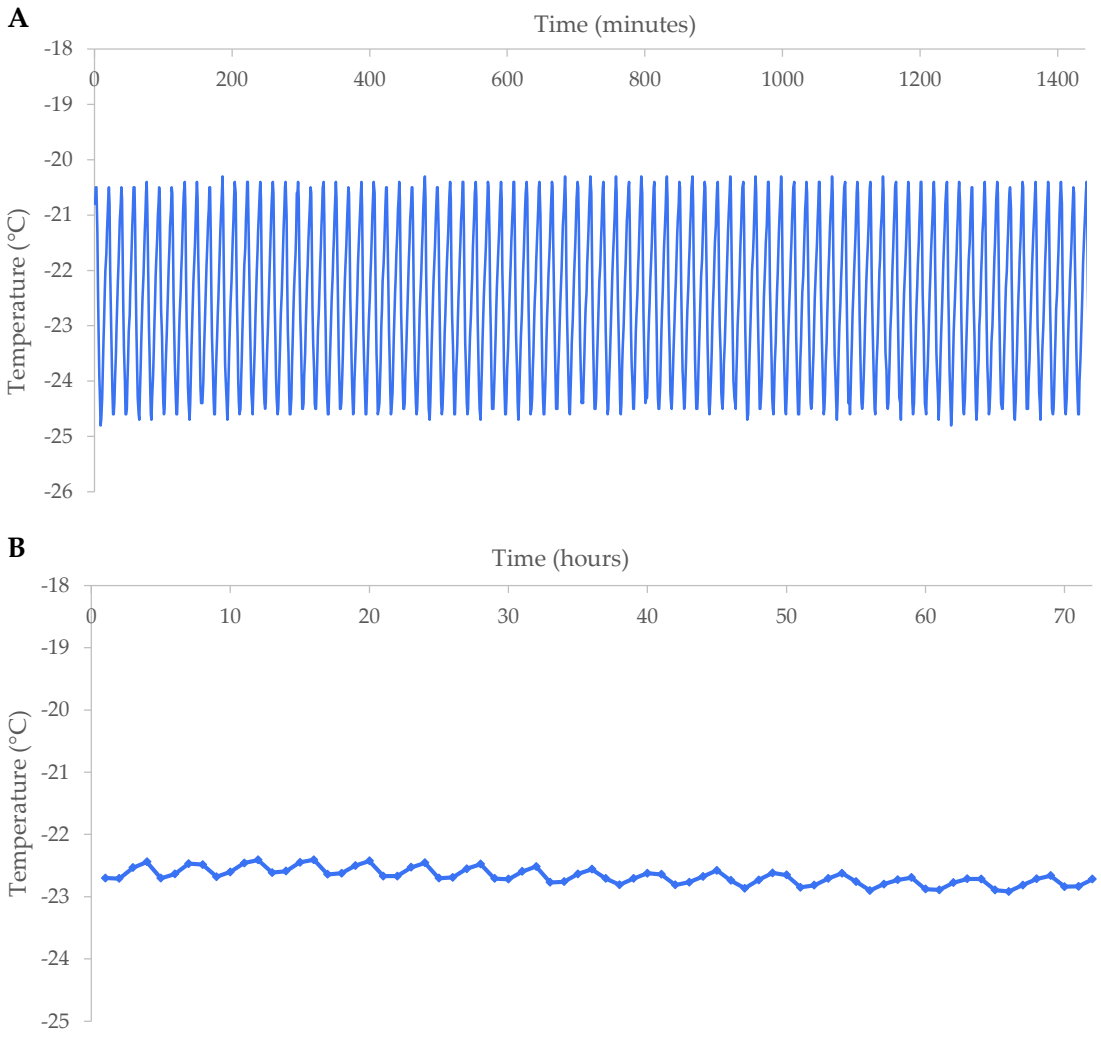

Figure 4.2: Change in temperature of freezer; A) Recorded temperature at intervals of one minute over 24 hours, B) Recorded hourly average temperature over 72 hours

4.7.2 Freezing duration of chicken muscle tissue

4.7.2.1 Quality control

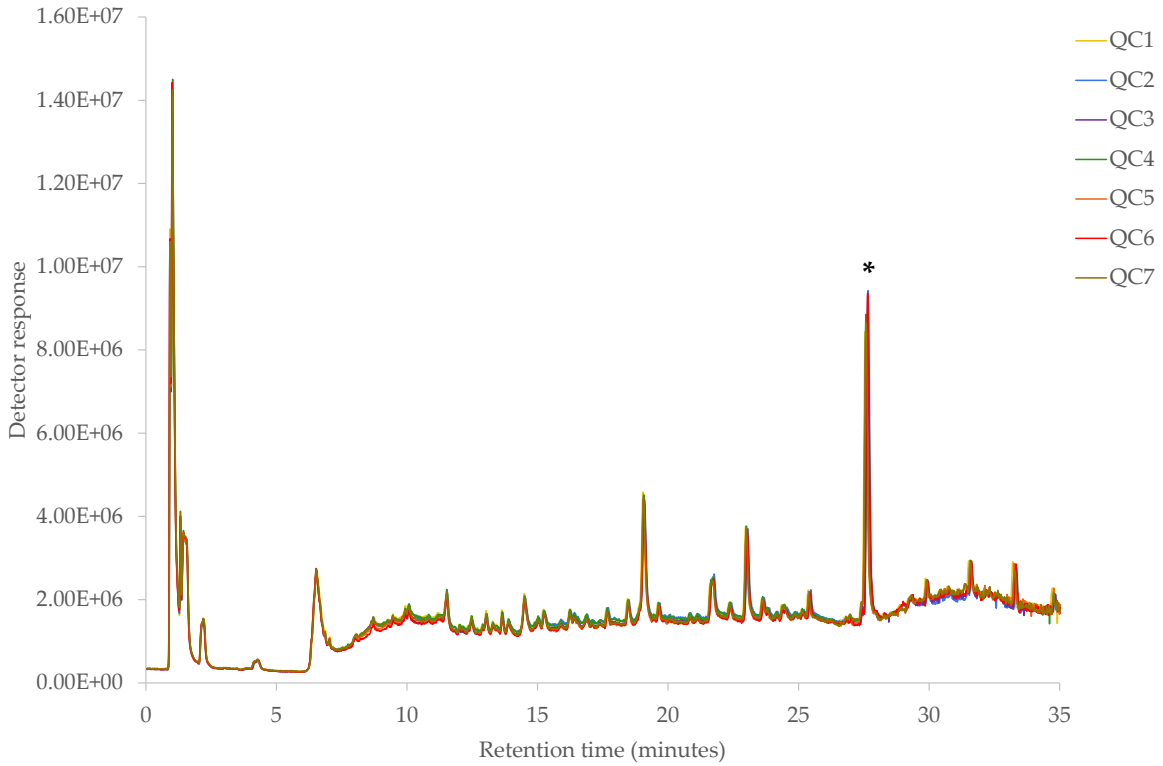

Figure 4.3: Total ion chromatograms of QC samples throughout analytical run for extracts from chicken muscle tissue frozen for different lengths of time

The QC samples run during this analysis created reproducible chromatograms (Figure 4.3) with no visible retention time variability. There are slight differences in peak intensity, specifically in the peak at 27.5 minutes (indicated with an asterisk), where QC2 and 6 have a higher peak intensity than the other QC samples, however this is only a small difference.

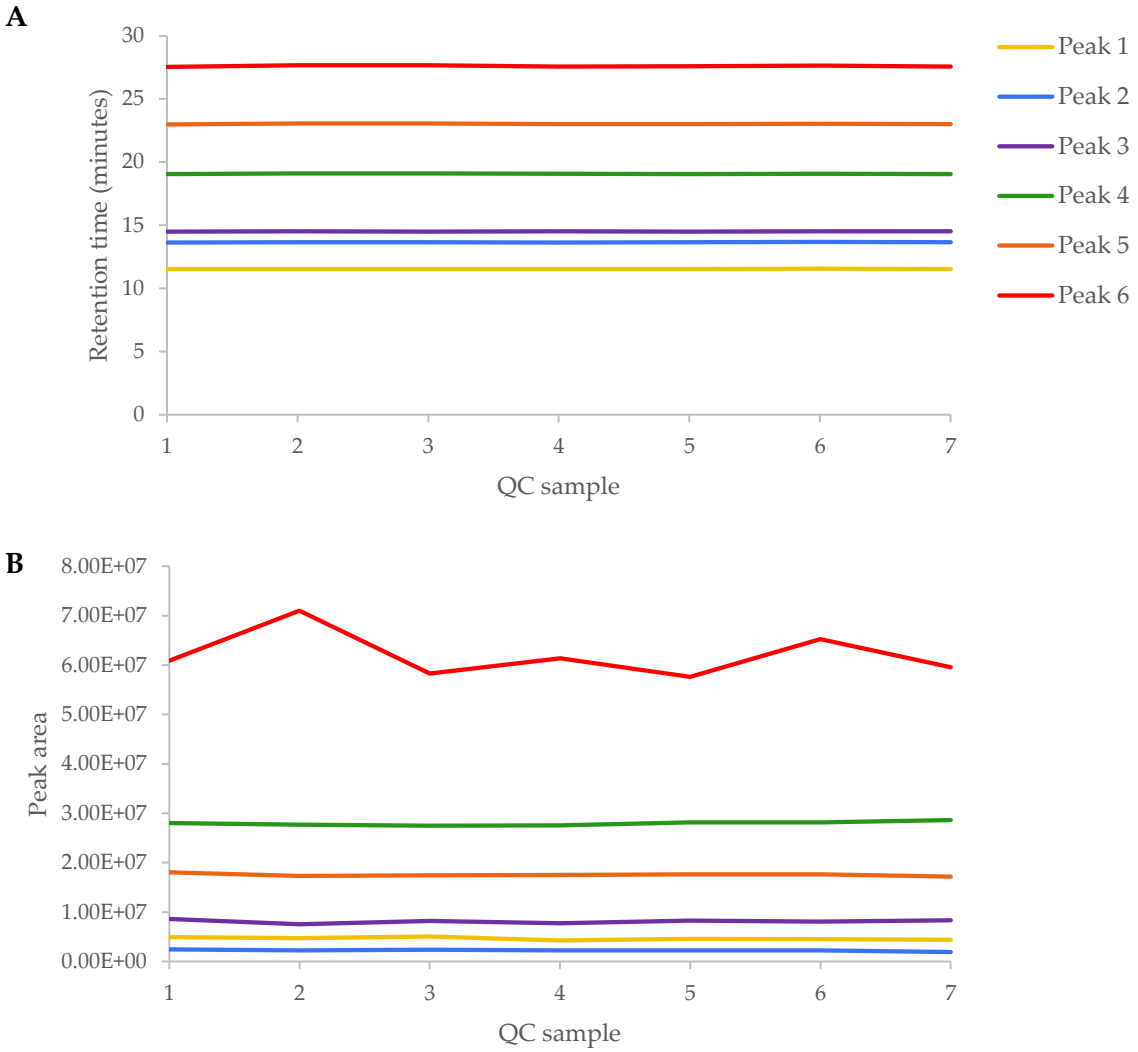

Figure 4.4: Variability of retention time (A) and peak area (B) of 6 peaks in QC samples throughout analytical run for extracts from chicken muscle tissue frozen for different lengths of time

Figure 4.4 show the retention time and peak area of six peaks in the QC sample chromatograms. The retention time appears very stable in all six peaks, and the peak area is stable in the majority of these peaks, with slight variation in Peak 6, which is the peak previously mentioned that had a visible difference in intensity in the total ion chromatogram.

Table 4.5: Variability of retention time and peak area of 6 peaks in chromatograms of QC samples during the analysis of extracts from chicken muscle tissue frozen for different lengths of time

	Retention time (minutes)									
Peak	QC1	QC2	QC3	QC4	QC5	QC6	QC7	SD	Average	CV%
1	11.52	11.54	11.52	11.52	11.53	11.55	11.52	0.01	11.53	0.11
2	13.63	13.66	13.66	13.64	13.66	13.67	13.65	0.01	13.65	0.10
3	14.49	14.52	14.50	14.51	14.50	14.52	14.51	0.01	14.51	0.08
4	19.04	19.10	19.10	19.07	19.06	19.09	19.05	0.02	19.07	0.13
5	22.97	23.05	23.05	23.00	23.01	23.04	23.00	0.03	23.02	0.13
6	27.55	27.66	27.66	27.58	27.60	27.65	27.58	0.04	27.61	0.16
	Peak area									
Peak	QC1	QC2	QC3	QC4	QC5	QC6	QC7	SD	Average	CV%
1	4954447	4706746	5078072	4246364	4581845	4537112	4399248	294968	4643405	6.35
2	2426735	2267751	2415083	2274630	2266419	2221512	1910226	171166	2254622	7.59
3	8626433	7543431	8211082	7719404	8294026	8066633	8345162	374466	8115167	4.61
4	28046948	27672017	27460030	27558745	28140666	28163534	28628703	412786	27952949	1.48
5	18037318	17280711	17463745	17535140	17651075	17677756	17155561	288513	17543044	1.64
6	60891655	71021212	58256494	61385302	57587193	65229808	59563634	4705355	61990757	7.59

The retention time variability was between 0.08 and 0.16%, which indicates a very accurate and reproducible set of data was obtained, and the peak area variability was between 1.48 and 7.59%, again demonstrating that the instrument was stable throughout this analysis.

4.7.2.2 Metabolic fingerprinting

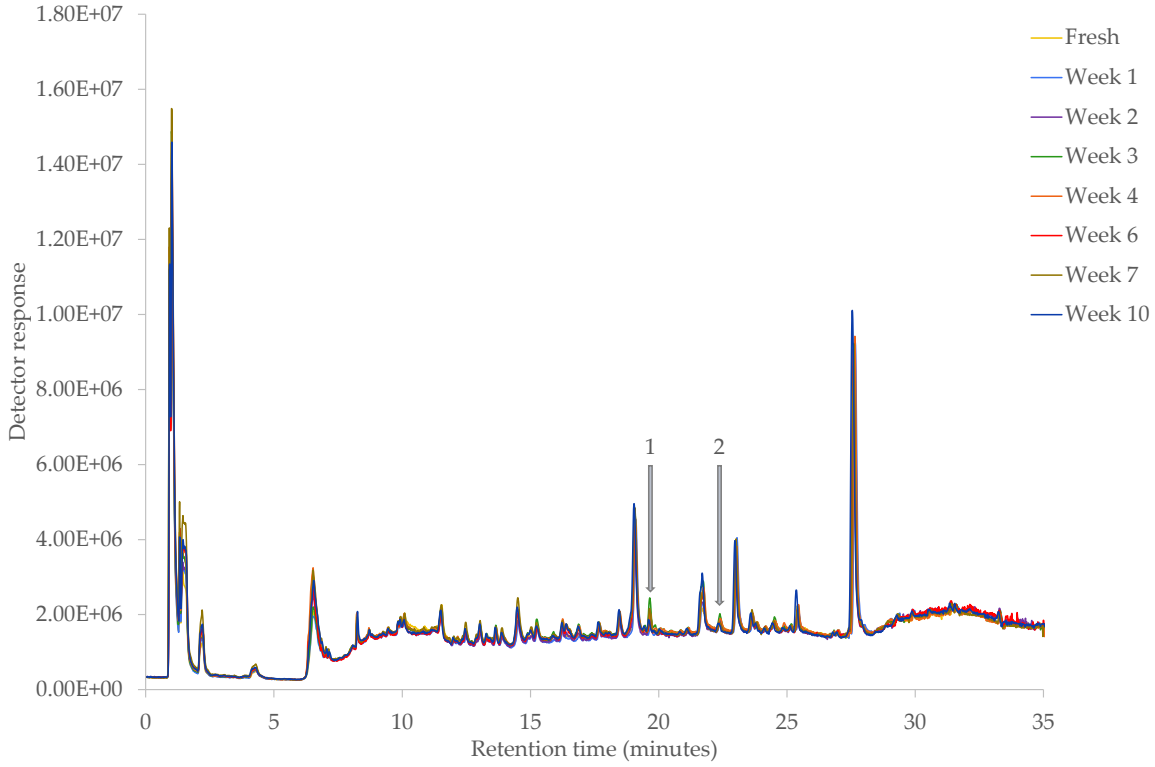

Figure 4.5: Example total ion chromatograms of extracts from chicken muscle tissue frozen for different lengths of time

The chromatograms in Figure 4.5 show that the Week 10 samples generally have a higher intensity for most peaks compared to chicken that had been frozen for less time. The peaks at 19.5 (peak 1) and 22.5 (peak 2) minutes have a higher intensity in the Week 3 sample, and the Week 7 sample has a higher intensity in the peaks between 10 and 15 minutes.

4.7.2.3 Multivariate statistics

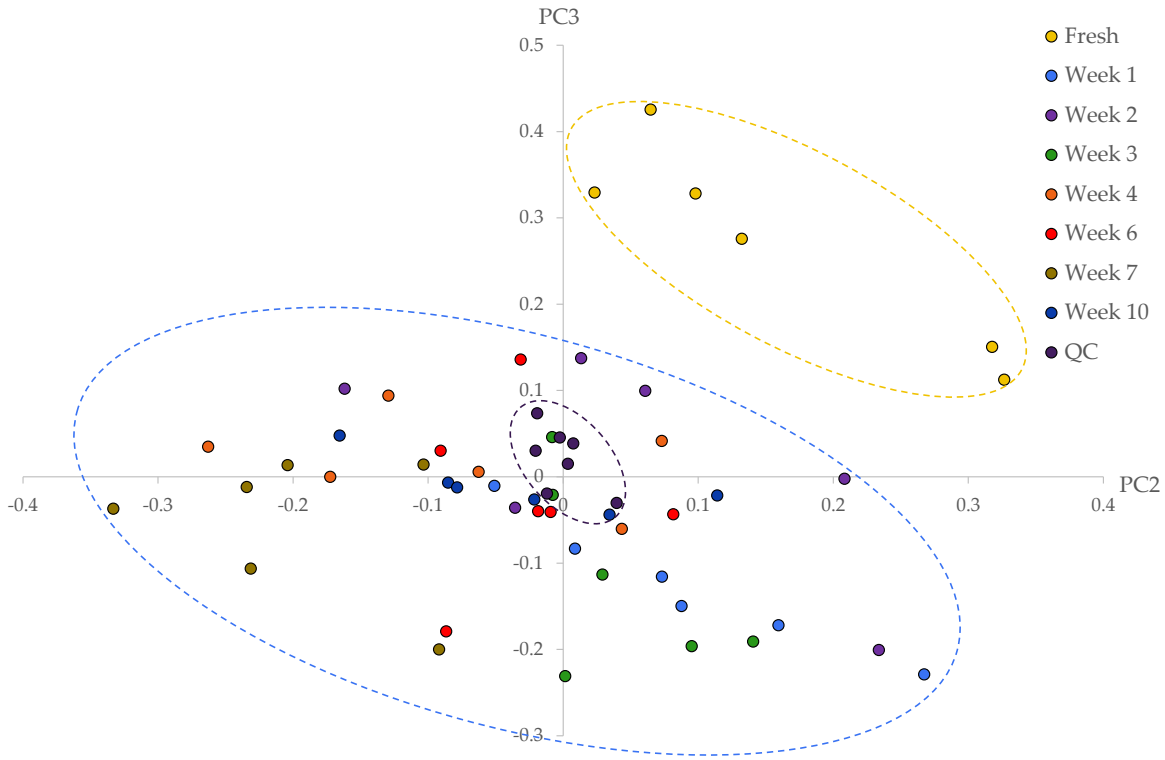

Figure 4.6: Principal component analysis scores plot of PC2 (0.625%) and PC3 (0.108%) for extracts from chicken muscle tissue frozen for different lengths of time. PCA was carried out using markers with a p-value of < 0.05 and CV $< 10\%$

The PCA plot in Figure 4.6 shows the quality control samples are tightly clustered, indicating the analytical run was stable and there was minimal instrumental drift. All sample types overlap so it is difficult to see the groupings for each freezing length sample group, however the fresh samples are separated from the frozen samples. This implies that the metabolic profile was significantly different between fresh chicken and chicken that had been frozen. At this point, it is not evident that the freezing duration had a significant effect on the metabolic content.

4.7.2.4 Significant markers

The following tables include the remaining markers from the most significantly different markers in each case after statistical analysis and confirmation with the raw data. Table 4.6 shows the most robust markers found in the top 50 significantly different markers in the chicken muscle that were statistically different from Fresh to Week 10 throughout the whole time period. All markers had a very strong significance with a p-value of less than 0.001 in the normalised and raw data. All markers were stable throughout the analytical run, with all CV% values from the QC samples less than 30%, and the majority less than 10%. The trends of these markers varied; some markers increased and some decreased, while a few had a more erratic trend.

Table 4.6: Summary of remaining compounds from top 50 markers that were significantly different among **Fresh** to **Week 10** chicken muscle tissue samples, in order of significance from manual ANOVA.
Marker trend: ↓ = decreased, ↑ = increased, ↕ = increased then decreased, * = random

m/z	Retention time median (mins)	P-value from ANOVA/Welch (XCMS)	CV% (XCMS)	P-value from ANOVA/Welch (EICs)	CV% (EICs)
↓ 339.0960	7.62	<0.001	13.23	<0.001	21.63
↓ 361.3306	21.12	<0.001	4.99	<0.001	10.61
↑ 197.1194	16.41	<0.001	9.61	<0.001	10.56
↓ 471.3646	20.32	<0.001	6.65	<0.001	5.97
↑ 361.2730	16.18	<0.001	8.38	<0.001	4.87
↑ 337.2735	16.41	<0.001	2.49	<0.001	2.79
↓ 397.3263	23.18	<0.001	10.81	<0.001	9.31
↑ 265.2513	18.91	<0.001	10.85	<0.001	9.42
↓ 347.3149	19.04	<0.001	3.49	<0.001	4.41
↓ 364.3404	19.18	<0.001	4.91	<0.001	11.27
* 126.0204	1.05	<0.001	3.50	<0.001	13.50
↓ 485.3805	22.33	<0.001	5.54	<0.001	18.69
↑ 381.2994	17.52	<0.001	4.14	<0.001	8.73
↑ 205.1054	16.41	<0.001	9.47	<0.001	9.11
↑ 584.8932	16.41	<0.001	18.14	<0.001	15.84
↑ 379.2812	18.91	<0.001	6.93	<0.001	7.63
↓ 596.5090	24.09	<0.001	9.58	<0.001	8.27
↑ 405.2993	16.77	<0.001	5.33	<0.001	8.31
↑ 576.9056	16.41	<0.001	19.66	<0.001	24.08
↑ 358.3025	18.91	<0.001	5.01	<0.001	3.63
↓ 331.3155	23.79	<0.001	4.91	<0.001	9.41
↑ 353.2703	14.55	<0.001	6.59	<0.001	5.98
↓ 464.3134	14.40	<0.001	2.01	<0.001	1.96
↓ 309.1283	7.59	<0.001	15.17	<0.001	26.90
↑ 245.2252	16.41	<0.001	6.67	<0.001	6.38
↓ 583.4944	23.06	<0.001	6.57	<0.001	20.48
↕ 462.2973	12.54	<0.001	3.35	<0.001	1.77
↕ 374.3255	19.45	<0.001	4.94	<0.001	7.62
↓ 510.4354	20.03	<0.001	6.51	<0.001	8.09
↕ 315.2879	21.14	<0.001	4.79	<0.001	4.48
* 373.1705	0.94	<0.001	16.41	<0.001	6.46
↑ 459.8101	18.90	<0.001	13.42	<0.001	25.34
↑ 339.2890	18.91	<0.001	2.41	<0.001	3.07
↓ 626.5195	22.15	<0.001	7.72	<0.001	7.05
↓ 598.4873	18.90	<0.001	7.17	<0.001	7.94
↓ 325.2707	19.63	<0.001	9.36	<0.001	13.28

Table 4.6 continued: Summary of remaining compounds from top 50 markers that were significantly different among **Fresh** to **Week 10** chicken muscle tissue samples, in order of significance from manual ANOVA.
Marker trend: ↓ = decreased

m/z	Retention time median (mins)	P-value from ANOVA/Welch (XCMS)	CV% (XCMS)	P-value from ANOVA/Welch (EICs)	CV% (EICs)
↓ 477.4124	23.86	<0.001	7.17	<0.001	14.63
↓ 964.5481	6.80	<0.001	9.28	<0.001	29.95
↓ 524.4497	22.02	<0.001	9.86	<0.001	12.54
↓ 684.5616	24.37	<0.001	5.17	<0.001	5.25
↓ 568.4775	20.62	<0.001	6.09	<0.001	6.80

In order to gain a more thorough idea of how the metabolic content changes during specific stages of the freezing process, additional investigations were carried out on differences from Week 1 to Week 10, Week 4 to Week 10, and Fresh to Week 4, where the top 10 markers were analysed. Looking at the metabolic differences of samples at Week 1 to Week 10 (Table 4.7), most of the markers increased over the freezing time, with two decreasing, and one having an erratic trend. Interestingly, the retention time for three of the increasing markers was the same, so these compounds could be of a similar class of compound.

Table 4.7: Summary of remaining compounds from top 10 markers that were significantly different among **Week 1** to **Week 10** chicken muscle tissue samples, in order of significance from manual ANOVA.
Marker trend: ↓ = decreased, ↑ = increased, * = random

m/z	Retention time median (mins)	P-value from ANOVA/Welch (XCMS)	CV% (XCMS)	P-value from ANOVA/Welch (EICs)	CV% (EICs)
↑ 197.1194	16.41	<0.001	9.61	<0.001	10.56
↑ 361.2730	16.18	<0.001	8.38	<0.001	4.87
* 126.0204	1.05	<0.001	3.50	<0.001	13.50
↑ 263.2361	16.41	<0.001	3.78	<0.001	4.36
↓ 471.3647	19.91	<0.001	4.07	<0.001	4.96
↓ 373.1705	0.94	<0.001	16.41	<0.001	6.46
↑ 337.2735	16.41	<0.001	2.49	<0.001	2.79

Table 4.8 shows the markers that were significantly different among the chicken that had been frozen for 4 to 10 weeks. All of these markers showed a very erratic trend and so therefore would not be suitable as markers to determine the duration of freeze length for a piece of chicken muscle.

Table 4.8: Summary of remaining compounds from top 10 markers that were significantly different among **Week 4** and **Week 10** chicken muscle tissue samples, in order of significance from manual ANOVA.
Marker trend: * = random

m/z	Retention time median (mins)	P-value from ANOVA/Welch (XCMS)	CV% (XCMS)	P-value from ANOVA/Welch (EICs)	CV% (EICs)
* 126.0204	1.05	<0.001	3.50	<0.001	13.50
* 333.1534	16.90	<0.001	11.22	<0.001	16.01
* 605.6707	6.55	<0.001	17.60	<0.001	26.70
* 161.0912	1.07	<0.001	3.00	<0.001	9.34
* 258.1080	1.03	<0.001	2.36	<0.001	11.80
* 584.8932	16.41	<0.001	18.14	0.005	15.84
* 659.0319	6.61	<0.001	6.83	<0.001	7.53
* 442.3508	14.50	<0.001	9.67	<0.001	13.63

When examining the differences from Fresh to Week 4 (Table 4.9), all markers were very stable within the analytical run, and all were highly significant. These markers mostly followed a trend where the fresh samples were the most different to the other samples, potentially giving markers that could be used to determine whether chicken has been previously frozen. These markers were either increasing or decreasing during the freezing process.

Table 4.9: Summary of remaining compounds from top 10 markers that were significantly different among **Fresh** and **Week 4** chicken muscle tissue sample, in order of significance from manual ANOVA.
Marker trend: ↓ = decreased, ↑ = increased

m/z	Retention time median (mins)	P-value from ANOVA/Welch (XCMS)	CV% (XCMS)	P-value from ANOVA/Welch (EICs)	CV% (EICs)
↓ 361.3306	21.12	<0.001	4.99	<0.001	10.61
↓ 339.0960	7.62	<0.001	13.23	<0.001	21.63
↑ 390.8911	6.37	<0.001	15.13	<0.001	20.71
↓ 347.3149	19.04	<0.001	3.49	<0.001	4.41
↑ 263.2361	16.41	<0.001	3.78	<0.001	4.36
↓ 471.3646	20.32	<0.001	6.65	<0.001	5.97
↑ 355.2840	16.41	<0.001	2.93	<0.001	1.40
↑ 339.2890	18.91	<0.001	2.41	<0.001	3.07

4.7.2.5 Tentative identifications

Most markers generated a formula in the *Masshunter* software, however when searching for these formulae on available databases, very few gave a potential identification. Three markers found to be significantly different among all freezing lengths including fresh chicken samples with an m/z of 358.3025, 379.2812 and 405.2993 at retention times of 18.91 minutes for the first two markers and 16.77 minutes for the latter, all gave a likely formula that matched to monoglycerides. These markers increased from Fresh to Week 3, then became more erratic but generally still increased, with all markers following a very similar trend (Figure 4.7).

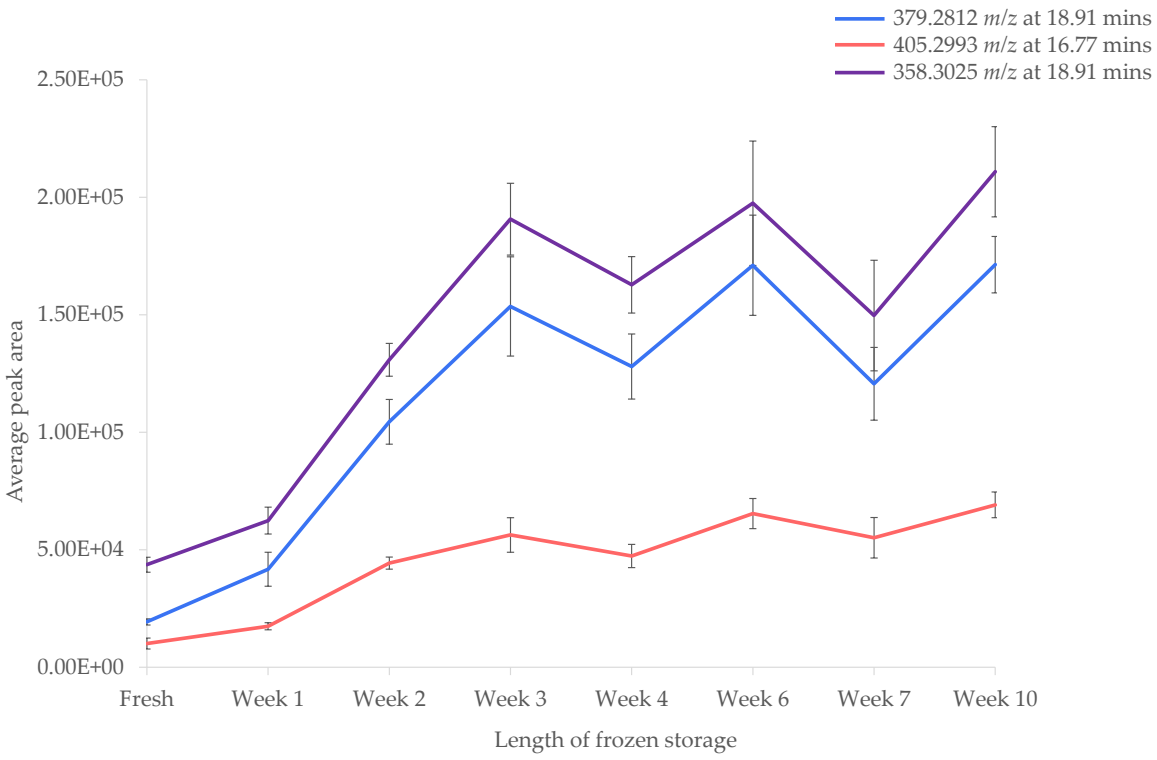

Figure 4.7: Trends of the three markers with formulae that matched monoglycerides that were significantly different among all extracts from chicken muscle tissue frozen for different lengths of time, including fresh chicken. Error bars correspond to ± 1 standard deviation

Two of these markers were able to be tentatively identified by comparing the mass spectrum of the sample with available mass spectra on the METLIN database. The marker with an m/z of 379.2812 at a retention time of 18.91 minutes gave a likely formula of $C_{21}H_{40}O_4$ with a M+Na adduct. This formula matched that of

MG(18:1(9Z)/0:0/0:0) on the METLIN database, and after further analysis of the available mass spectrum at 0 V collision energy, it can be seen that this mass spectrum matches the mass spectrum of this peak in the sample. In Figure 4.8, the M+Na peak can be seen in the top mass spectrum. The M+H peak at 357.2998 *m/z* can be seen in both spectra, as well as the two fragments at 339.2898 *m/z*, which is due to loss of water, and 265.2519 *m/z*, which is caused by hydrolysis in the ester bond. Due to these mass spectra matching, this marker can be tentatively identified as the monoglyceride, MG(18:1(9Z)/0:0/0:0).

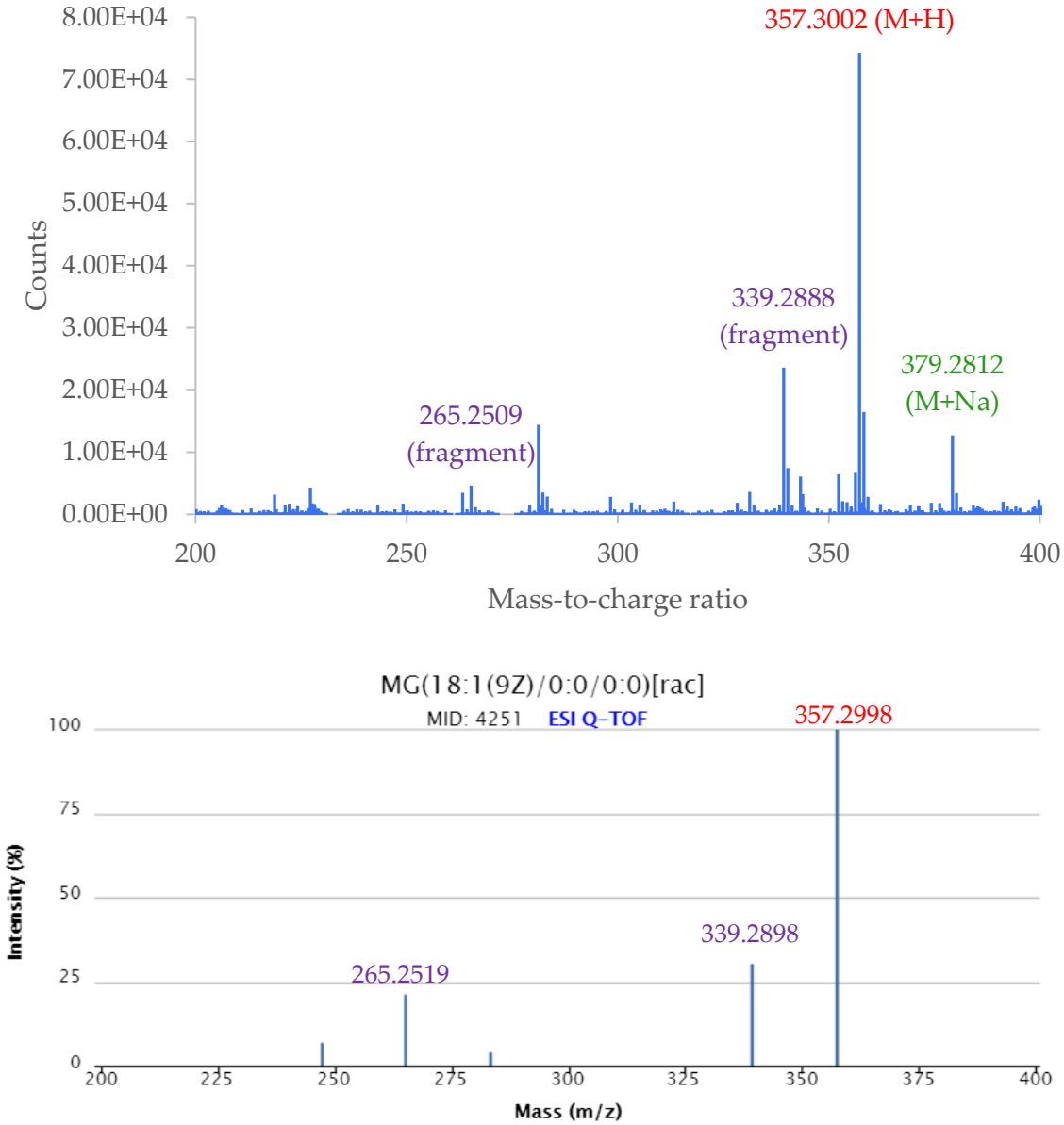

Figure 4.8: Mass spectrum of marker 379.2812 *m/z* at a retention time of 18.91 minutes in QC sample (top) compared to the mass spectrum of MG(18:1(9Z)/0:0/0:0) found on METLIN (bottom)

The marker with an *m/z* of 358.3025 also at the retention time of 18.91 minutes again gave a likely formula of $C_{21}H_{40}O_4$. After looking at the mass spectrum for this extracted ion chromatogram, this is an isotopic peak of the M+H peak at 357.2984 *m/z* previously tentatively identified as the monoglyceride MG(18:1(9Z)/0:0/0:0). It is interesting that the isotopic peak was the significant feature and not the M+H peak, however, only the top 50 features were analysed, so the M+H peak may just not be as significant as the isotopic peak. After searching for the M+H peak in the

feature table, it appeared that this feature is indeed statistically different among samples from Fresh to Week 10, with a highly significant p-value of less than 0.001.

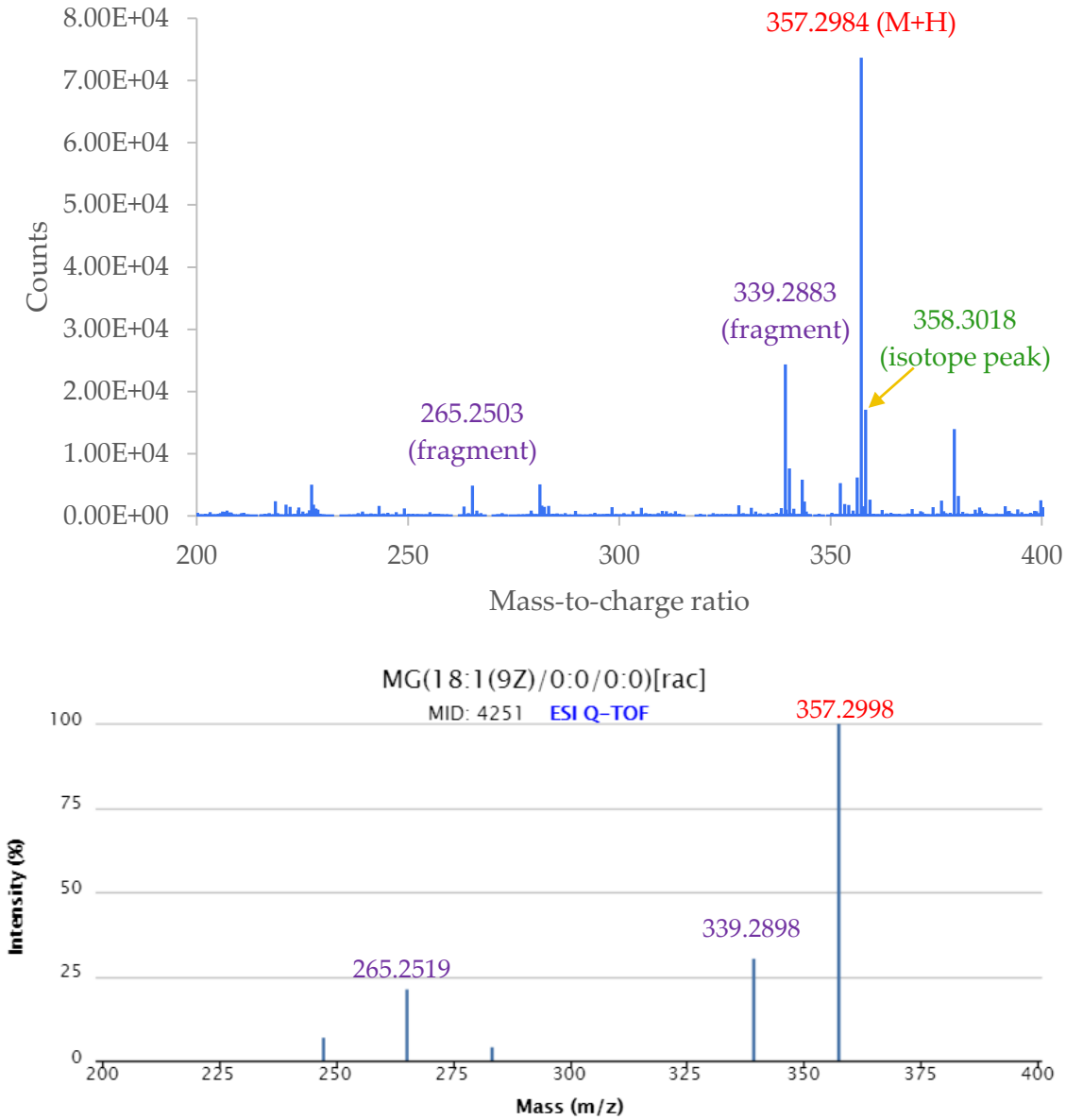

Figure 4.9: Mass spectrum of marker 358.3025 *m/z* at a retention time of 18.91 minutes in QC sample (top) compared to the mass spectrum of MG(18:1(9Z)/0:0/0:0) found on METLIN (bottom)

MG(18:1(9Z)/0:0/0:0) is a monoglyceride, or monoacylglycerol, consisting of glycerol and one fatty acid. It is involved in the glycerolipid metabolism pathway, where monoacylglycerol is converted to diacylglycerol, then triacylglycerol, which acts as storage for fatty acids that can be released for energy when required. Lipolysis is the

reverse of this, where monoacylglycerol is formed through the break down of triacylglycerol in order to release fatty acids for energy. This is catalysed by the enzyme lipase, and usually only partially hydrolyses triacylglycerols due to a preference in hydrolysing fatty acids that are bonded to the first carbon in the glycerol molecule. This causes an accumulation of monoacylglycerols and fatty acids [134]. This catabolism of triacylglycerol explains the accumulation of monoacylglycerol in this work, and is supported by other research, where monoacylglycerol content was found to increase during frozen storage [135]. The fact that the monoacylglycerol concentration increased even when the meat was frozen shows that degradation still occurs, which is the opposite of the desired effect of preserving the quality of the meat.

4.7.3 Freezing duration of lamb muscle tissue

4.7.3.1 Quality control

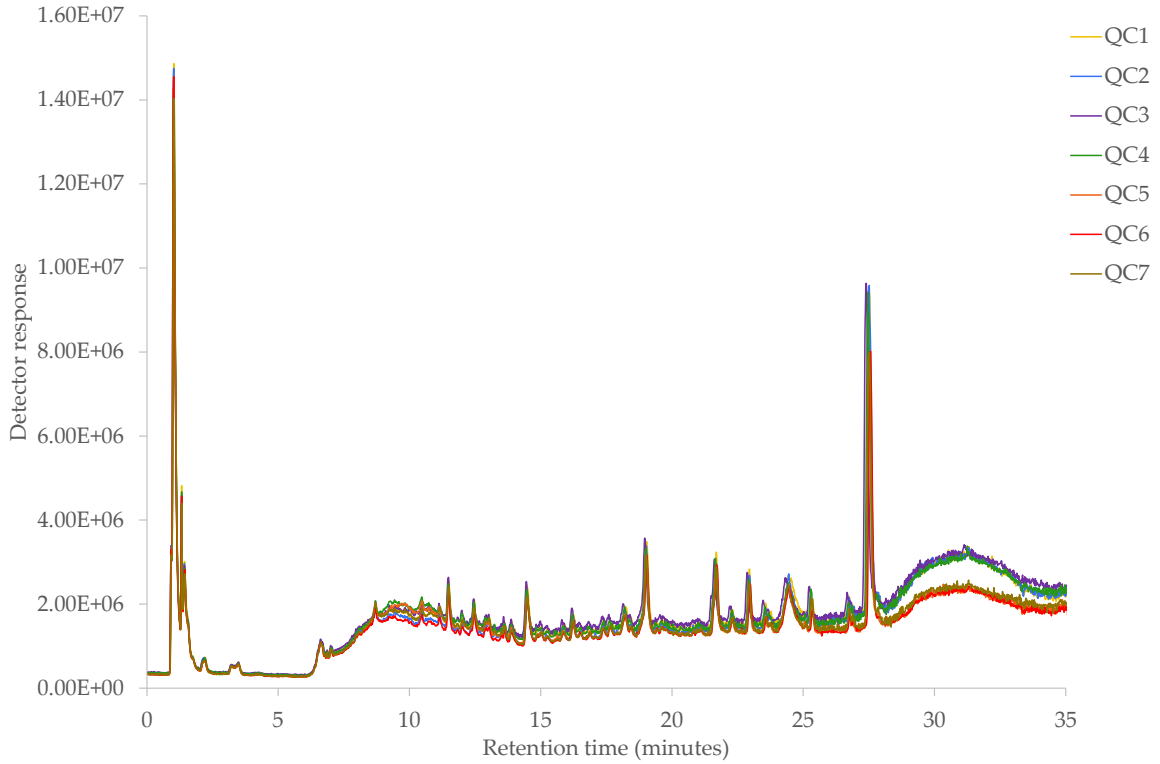

Figure 4.10: Total ion chromatograms of QC samples throughout analytical run for extracts from lamb muscle tissue frozen for different lengths of time

The chromatograms for the QC samples throughout this analytical run (Figure 4.10) show all peaks aligned at the same retention time. One observation is that the baseline appears unstable, particularly in QC5, 6 and 7 towards the end of the chromatogram. After examining the pressure curves of these samples, it could be seen that the pressure was consistent in all quality control samples. This unstable baseline may have been due to a change in temperature during this part of the analytical run, as these were run towards the end.

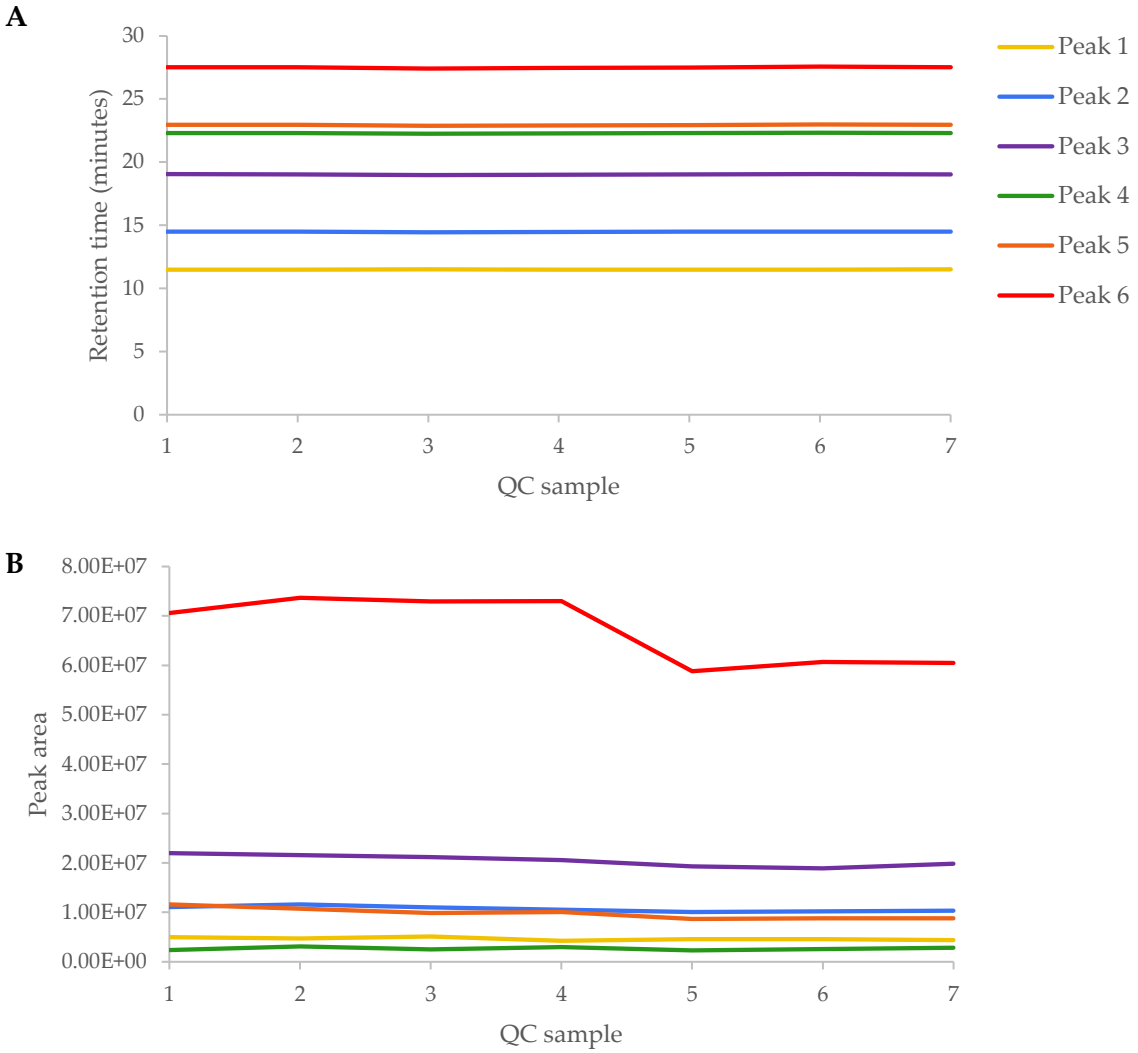

Figure 4.11: Variability of retention time (A) and peak area (B) of 6 peaks in QC samples throughout analytical run for extracts from lamb muscle tissue frozen for different lengths of time

Figure 4.11 illustrates the retention time and peak area differences for six of the peaks in the QC samples. The retention time appears to have been very stable throughout the analysis, and the peak area looks stable for 5 of the peaks, however there were some variations in the peak at 27.5 minutes, which was where the baseline had some variability and so could have been caused by this.

Table 4.10: Variability of retention time and peak area of 6 peaks in chromatograms of QC samples during the analysis of extracts from lamb muscle tissue frozen for different lengths of time

	Retention time (minutes)									
Peak	QC1	QC2	QC3	QC4	QC5	QC6	QC7	SD	Average	CV%
1	11.49	11.48	11.50	11.47	11.49	11.49	11.50	0.01	11.49	0.09
2	14.48	14.48	14.45	14.46	14.48	14.50	14.49	0.02	14.48	0.12
3	19.04	19.03	18.96	19.01	19.03	19.04	19.02	0.03	19.02	0.15
4	22.29	22.31	22.25	22.27	22.29	22.33	22.30	0.03	22.29	0.12
5	22.96	22.96	22.88	22.90	22.94	22.97	22.95	0.03	22.94	0.15
6	27.52	27.52	27.41	27.47	27.50	27.57	27.51	0.05	27.50	0.18
	Peak area									
Peak	QC1	QC2	QC3	QC4	QC5	QC6	QC7	SD	Average	CV%
1	6706350	6578408	6374637	5914869	4958489	5744786	5681502	609941	5994149	10.18
2	11055657	11590023	11018914	10509493	10075236	10158395	10303930	561561	10673093	5.26
3	21971162	21548452	21201250	20600304	19327693	18896752	19825346	1166395	20481566	5.69
4	2365694	3083305	2476785	2944418	2312069	2565408	2855395	302326	2657582	11.38
5	11582579	10730788	9822762	10084032	8650383	8804970	8773266	1117122	9778397	11.42
6	70597846	73673631	72892574	72971632	58811142	60645451	60442235	6808741	67147787	10.14

The retention time variability was between 0.09 and 0.18%, showing strong stability and reproducibility in this analytical run. The peak area variability was between 5.26 and 11.42%, which confirms the stability of the instrument during this analysis.

4.7.3.2 Metabolic fingerprinting

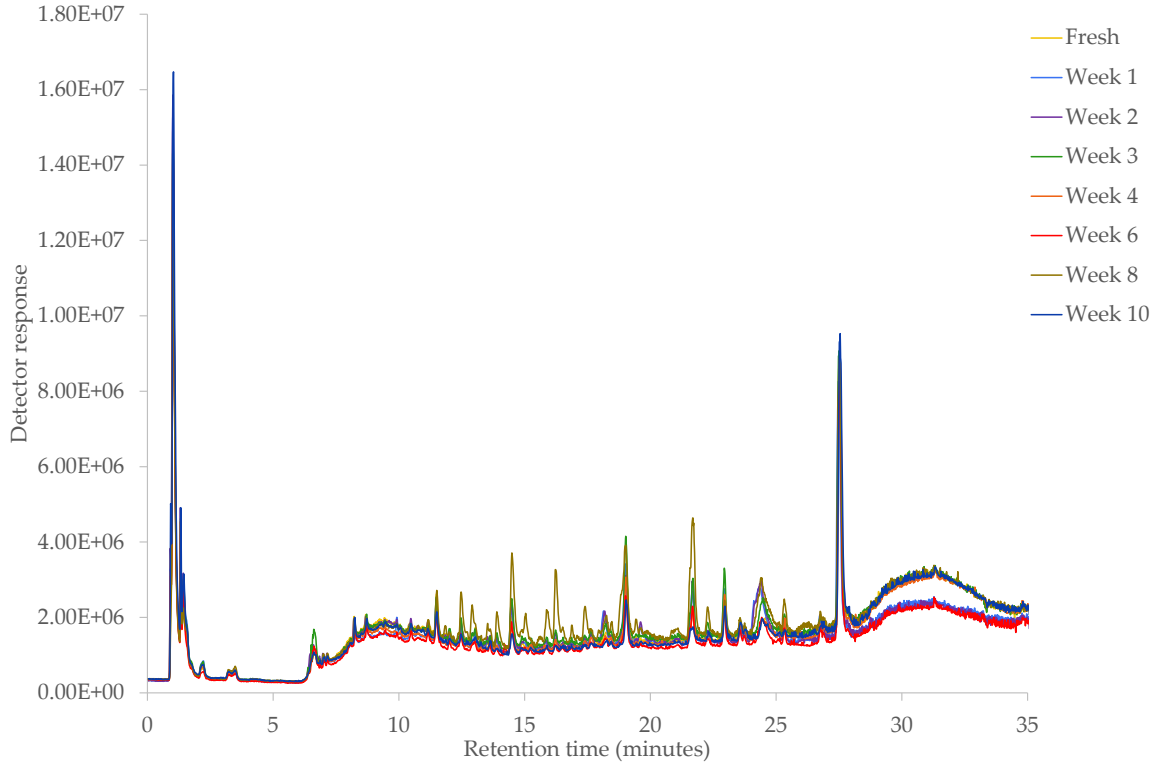

Figure 4.12: Example total ion chromatograms of extracts from lamb muscle tissue frozen for different lengths of time

In Figure 4.12, the baseline becomes irregular towards the end of the chromatograms, which is the same as seen previously in the QC samples for this analytical run. The samples that have a lower baseline are the samples that were run later in the analysis, in between QC5, 6 and 7, so it is a gradual change in baseline over the time of the analysis. This did not affect the reliability of this dataset though, as shown in the statistical analysis of the QC samples. Week 8 has a noticeably higher peak intensity for many of the peaks, and this could have been caused by this piece of lamb having a different chemical composition, potentially a higher fat content. In general, Week 10 has a lower intensity than all other samples, and Week 3 samples have a higher intensity in some peaks. However, it does appear that the baseline is not the same for all samples, and so the intensity observed in these chromatograms is only qualitative, and the integrated peak areas will give a more accurate indication of the differences in these sample types.

4.7.3.3 Multivariate statistics

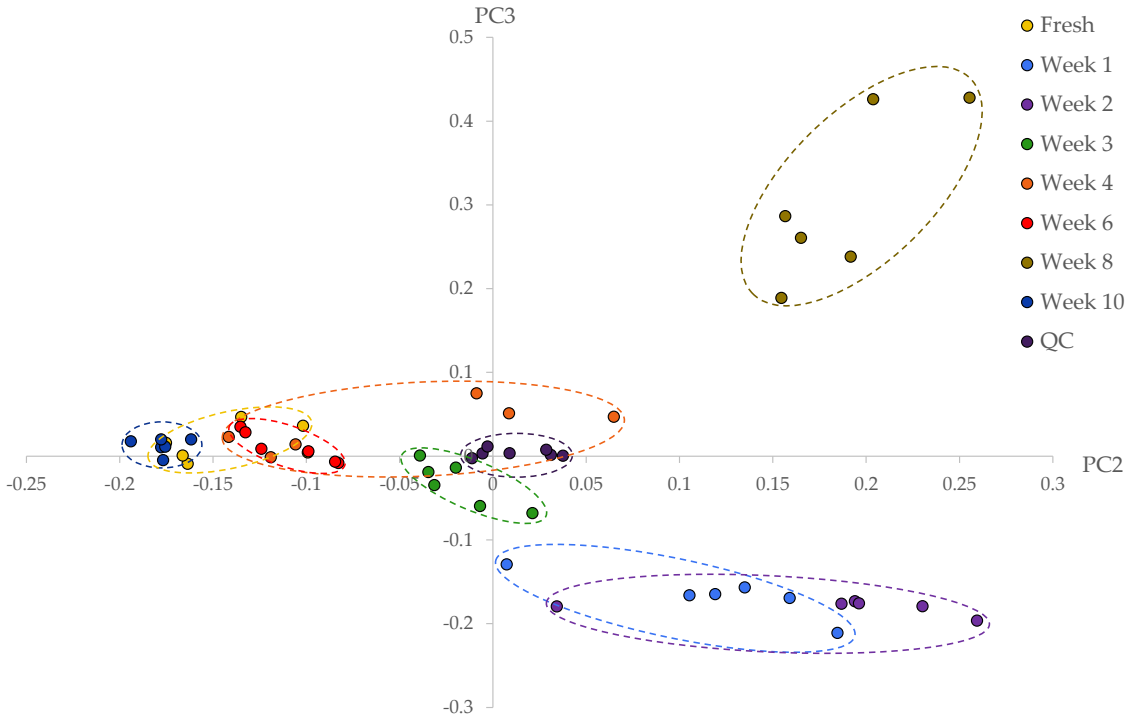

Figure 4.13: Principal component analysis scores plot of PC2 (1.715%) and PC3 (0.537%) for extracts from lamb muscle tissue frozen for different lengths of time. PCA was carried out using markers with a p-value of < 0.05 and CV $< 10\%$

In Figure 4.13, the QC samples are tightly clustered showing stability within the run. The Week 1 and Week 2 freeze length sample groups are separated from the others, while the rest generally overlap each other. Interestingly, the Fresh samples are not separated in the PCA plot but are in the same overlapped area as the Week 3-10 freeze length samples. However the most separated group in this PCA plot is the Week 8 samples that are clustered in the top right. After further analysis of the data, it appears all the significantly different markers were either higher or lower at Week 8 compared to all other freezing lengths. Whilst this could be a possibility in lamb tissue, it is more likely that the piece of lamb used for this freeze length contained a higher fat content and so was different to the pieces of lamb used in the other freeze lengths. This would explain why the metabolic content was vastly different in this freeze length and potentially skewed the results. It is for this reason that further analysis was carried out without including Week 8 data.

After removing Week 8 samples from the principal component analysis, the PCA plot (Fig. 4.14) shows more overlap of sample types than the previous PCA plot, and the QC samples are less tightly clustered. The first PCA plot (Fig. 4.13) shows more separation in sample types because the Week 8 samples are very different to the other sample types, and so therefore the principal component analysis accentuated this separation, causing the other sample types to be more tightly clustered. Once Week 8 samples are removed (Fig. 4.14), the difference in the sample types is considerably less, causing more overlap in the data, and the QC samples to be more spread due to the lack of difference. In Figure 4.14, Fresh and Week 10 samples overlap, and Week 1 and Week 2 are on the other side of the plot, which is unexpected.

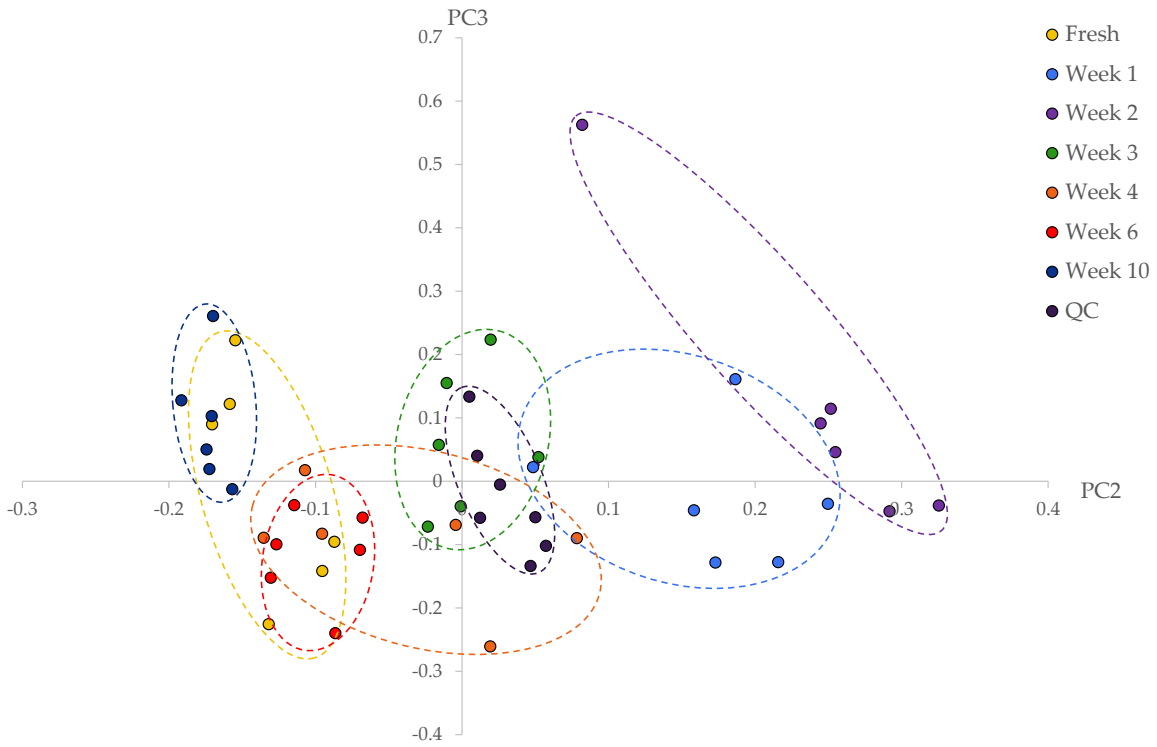

Figure 4.14: Principal component analysis scores plot of PC2 (1.589%) and PC3 (0.231%) for extracts from lamb muscle tissue frozen for different lengths of time with the removal of Week 8. PCA was carried out using markers with a p-value of < 0.05 and CV$<$ 10%

4.7.3.4 Significant markers

The following tables include the remaining markers from the most significantly different markers in each case after statistical analysis and confirmation with the raw data. The markers in Table 4.11 were all highly significant with a CV% of these markers in the QC samples all below 30% in both the normalised and raw data. The trends of these markers varied; some increased or decreased specifically at Week 10, some increased at Week 1 and Week 2 and then decreased, and others had an erratic trend.

Table 4.11: Summary of remaining compounds from top 50 markers that were significantly different among **Fresh** to **Week 10** lamb muscle tissue samples, excluding Week 8, in order of significance from manual ANOVA.
Marker trend: ↓ = decreased, ↑ = increased, ↷ = increased Week 4 then decreased, ↷ = increased Week 1 and 2 then decreased, * = random

m/z	Retention time median (mins)	P-value from ANOVA/Welch (XCMS)	CV% (XCMS)	P-value from ANOVA/Welch (EICs)	CV% (EICs)
↑ 343.0547	15.00	<0.001	8.60	<0.001	8.20
↑ 134.0710	7.10	<0.001	19.92	<0.001	22.67
↑ 300.2887	23.04	<0.001	5.19	<0.001	8.78
↷ 323.2571	18.98	<0.001	5.38	<0.001	12.02
↷ 351.2889	22.21	<0.001	5.91	<0.001	8.40
↓ 652.4518	20.10	<0.001	4.08	<0.001	21.98
↷ 400.3420	18.11	<0.001	2.39	<0.001	2.59
↓ 556.4405	13.47	<0.001	7.08	<0.001	6.64
↓ 657.4881	14.30	<0.001	6.45	<0.001	5.60
↓ 512.4143	13.51	<0.001	8.70	<0.001	7.47
↷ 428.3736	24.30	<0.001	3.63	<0.001	3.79
* 319.2626	23.04	<0.001	4.62	<0.001	7.27
* 317.2472	20.90	<0.001	5.16	<0.001	8.97
↷ 440.3713	21.43	<0.001	20.84	<0.001	7.47
↓ 468.3869	13.55	<0.001	11.02	<0.001	9.17
↷ 414.3569	20.93	<0.001	4.16	<0.001	2.92
↓ 600.4670	13.45	<0.001	8.60	<0.001	6.16
↓ 613.4627	14.36	<0.001	7.08	<0.001	25.14
↷ 349.7267	6.73	<0.001	10.18	<0.001	13.93
↷ 426.3576	18.87	<0.001	2.18	<0.001	4.17
↷ 366.3102	17.64	<0.001	8.15	<0.001	5.21
↓ 235.1309	10.40	<0.001	18.05	<0.001	20.79
↷ 345.2780	23.55	<0.001	6.32	<0.001	9.16
↷ 501.2800	10.76	<0.001	5.06	<0.001	4.78

Further analysis of the overall feature table allowed additional insight into markers that were different during various points of the freezing period. Table 4.12 includes markers that were statistically different from Week 1 to Week 10, and so could be used as indicators to determine the length of time a meat product has been frozen for. Two of these markers, 342.0547 and 134.0710 *m/z*, were also found to be different in Fresh to Week 10 samples, and these markers have a higher concentration in Week 10 compared to all other weeks. The other two markers increased at Week 3 and

Week 4, then began to decrease, indicating that these markers may be of a similar class of compound.

Table 4.12: Summary of remaining compounds from top 10 markers that were significantly different among **Week 1** to **Week 10** lamb muscle tissue samples, excluding Week 8, in order of significance from manual ANOVA.
Marker trend: ↑ = increased Week 10, ↷ = increased then decreased

m/z	Retention time median (mins)	P-value from ANOVA/Welch (XCMS)	CV% (XCMS)	P-value from ANOVA/Welch (EICs)	CV% (EICs)
↑ 343.0547	15.00	<0.001	8.60	<0.001	8.20
↑ 134.0710	7.10	<0.001	19.92	<0.001	22.67
↷ 351.2889	22.21	<0.001	5.91	<0.001	8.40
↷ 323.2571	18.98	<0.001	5.38	<0.001	12.02

The markers found to be significantly different between Week 4 and Week 10 are shown in Table 4.13, and the same two markers as previously discussed, 342.0547 and 134.0710 *m/z*, are present. This is expected as the trend for these markers was an increase at Week 10.

Table 4.13: Summary of remaining compounds from top 10 markers that were significantly different among **Week 4** to **Week 10** lamb muscle tissue samples, excluding Week 8, in order of significance from manual ANOVA.
Marker trend: ↓ = decreased, ↑ = increased

m/z	Retention time median (mins)	P-value from ANOVA/Welch (XCMS)	CV% (XCMS)	P-value from ANOVA/Welch (EICs)	CV% (EICs)
↑ 343.0547	15.00	<0.001	8.60	<0.001	8.20
↑ 134.0710	7.10	<0.001	19.92	<0.001	22.67
↓ 556.4405	13.47	<0.001	7.08	<0.001	6.64
↓ 468.3869	13.55	<0.001	11.02	<0.001	9.17

Nine out of the ten markers investigated that were significantly different between Fresh and Week 4 were confirmed to be significant in the normalised data as well as the raw data. These markers could prove useful in determining the difference between fresh meat products, and products that have been previously frozen. The trends

indicate that some markers increase at Week 1 and Week 2, and so these markers could also aid in estimating the length of time a meat product has been frozen for.

Table 4.14: Summary of remaining compounds from top 10 markers that were significantly different among **Fresh** to **Week 4** lamb muscle tissue samples, in order of significance from manual ANOVA.
Marker trend: ↓ = decreased, ↑ = increased, ↷ = increased Week 1 and 2 then decreased, * = random

m/z	Retention time median (mins)	P-value from ANOVA/Welch (XCMS)	CV% (XCMS)	P-value from ANOVA/Welch (EICs)	CV% (EICs)
↑ 323.2571	18.98	<0.001	5.38	<0.001	12.02
↑ 351.2889	22.21	<0.001	5.91	<0.001	8.20
* 317.2472	20.90	<0.001	5.16	<0.001	8.97
* 319.2626	23.04	<0.001	4.62	<0.001	7.27
↷ 258.2772	14.14	<0.001	14.24	<0.001	23.01
↷ 345.2780	23.55	<0.001	6.32	<0.001	9.16
↷ 400.3420	18.11	<0.001	2.39	<0.001	2.59
↓ 652.4518	20.10	<0.001	4.08	<0.001	21.98
↷ 349.7267	6.73	<0.001	10.18	<0.001	13.93

4.7.3.5 Tentative identifications

As before, most markers generated a likely formula in the *Masshunter* software, however when searching for these formulae on available databases, very few gave a potential identification. There were three markers with predicted formulae that matched acyl carnitines, which are fatty acids attached to carnitine through an ester bond. The trends for these three markers, as shown in Figure 4.15, are all very similar, increasing at Week 1 and Week 2, then decreasing from Week 3 to Week 10.

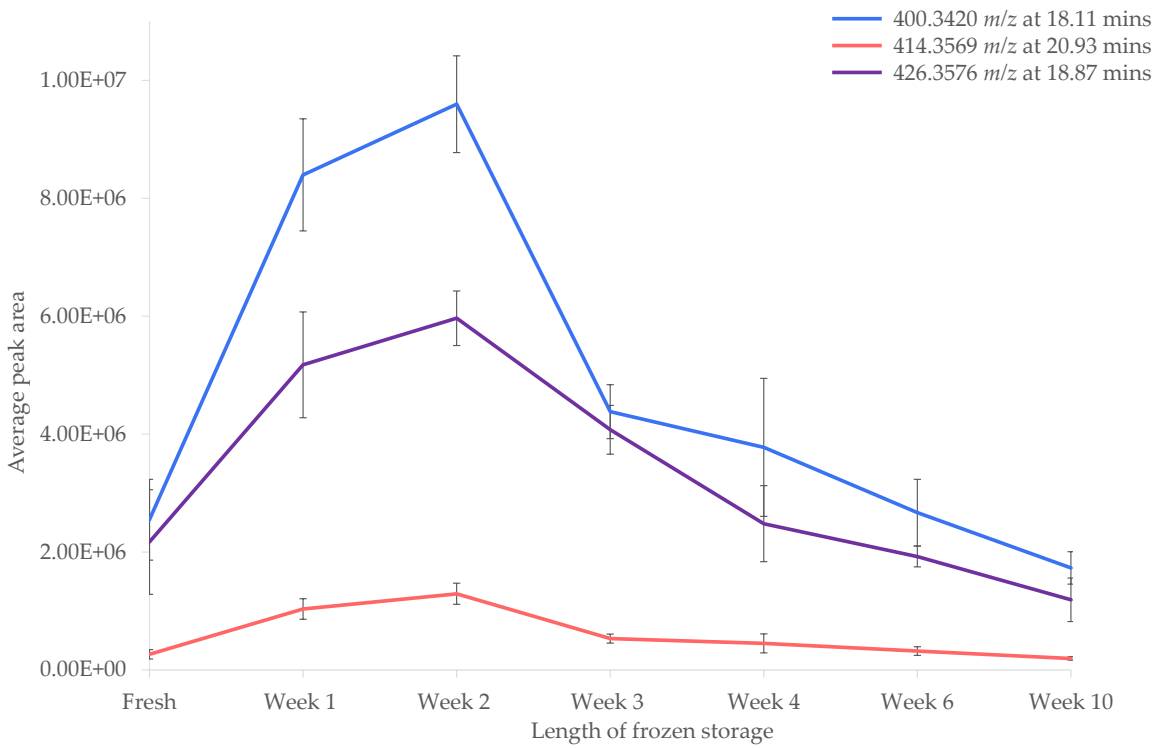

Figure 4.15: Trends of three markers tentatively identified as acyl carnitines that were significantly different among all extracts from lamb muscle tissue frozen for different lengths of time, including Fresh, excluding Week 8 samples. Error bars correspond to ± 1 standard deviation

The marker 400.3420 m/z at a retention time of 18.11 minutes could be tentatively identified as palmitoyl-L-carnitine, with the mass spectrum for this peak in the sample matching the mass spectrum for this compound on the METLIN database, as seen in Figure 4.16. The other two compounds could not be tentatively identified as the mass spectra were not available at 0 V collision energy, however the marker

414.3569 m/z at 20.93 minutes had the same predicted formula as heptadecanoyl carnitine, and the marker 426.3576 m/z had the same predicted formula as vaccenyl carnitine or elaidic carnitine, and as these markers follow a similar trend to palmitoyl-L-carnitine, it can be assumed these markers could also be acyl carnitines.

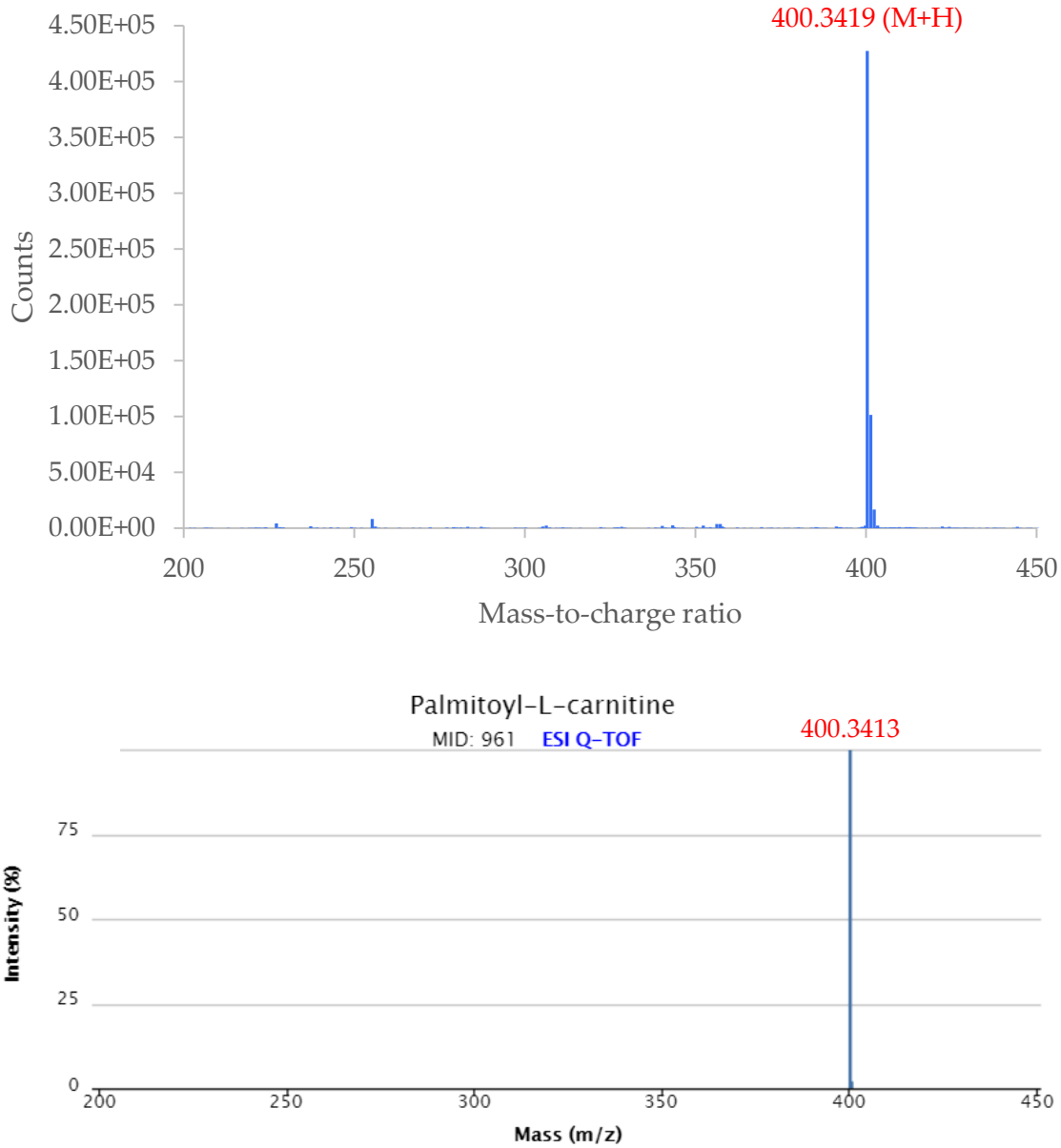

Figure 4.16: Mass spectrum of marker 400.3420 m/z at a retention time of 18.11 minutes in QC sample (top) compared to the mass spectrum of palmitoyl-L-carnitine found on METLIN (bottom)

Acyl carnitines are an intermediate in fatty acid degradation. Acyl-CoA is generated by a thioester bond forming between the carboxyl group of a fatty acid and the thiol

group of coenzyme A (CoA), which requires ATP and generates adenosine monophosphate (AMP) and 2 phosphate groups. This occurs in the cytosol of the cell, but lipid oxidation occurs in the mitochondrial matrix, so the activated fatty acid is transported to the mitochondrion. The acyl CoA is able to pass through the outer membrane, but must be converted to acyl carnitine through transesterification before being able to pass through the inner membrane into the matrix. This is known as the carnitine shuttle pathway. This is catalysed by the enzyme carnitine palmitoyltransferase (CPT-I). Once the acyl carnitine is in the matrix, the acyl group is transferred from the carnitine to mitochondrial CoA forming acyl CoA again, catalysed by a second carnitine palmitoyltransferase (CPT-II). This is then oxidised by a repeated sequence of reactions, each reaction cleaving two carbon units from the fatty acid, and this process is known as β-oxidation. Each reaction is made up of four individual reactions, beginning with the acyl-CoA being oxidised to unsaturated acyl-CoA. This is then hydrated to produce β-hydroxylacyl-CoA, then oxidised forming β-ketoacyl-CoA. Cleavage then occurs, requiring a CoA molecule, producing acetyl-CoA and an acyl-CoA that has two less carbons than the original molecule. These four reactions continue until the fatty acid can no longer be cleaved. The acetyl-CoA produced enters the citric acid cycle to generate energy [136].

Immediately after death, several biological changes happen; specifically, circulation stops, causing a decrease in oxygen concentration, anaerobic respiration to occur and the citric acid cycle to stop [107]. This causes pyruvate to convert to lactic acid, which oxidises nicotinamide adenine dinucleotide, NADH to NAD+, which is then used in generating ATP from glucose [136]. The generation of lactic acid causes a decrease in the pH of the tissue, causing denaturation of proteins. In addition to this, lipids undergo autoxidation, where free radicals attack fatty acids and phospholipids, destroying cell membranes.

Palmitoyl carnitine, as well as the other two acyl carnitines, were found to increase at

Week 1 and Week 2 of frozen storage, and then decrease after this point. Using the knowledge previously discussed, there are a number of reasons why this trend was observed. The increase could be caused by the continuation of palmitoyl carnitine generation through the normal processes as described previously, while NADH and ATP still remained in the tissue. The decrease could have been caused by the lack of palmitic acid due to fatty acid stores becoming depleted through lipid autoxidation breaking down remaining fatty acids in the tissue, and so palmitoyl carnitine stopped being generated, and existing palmitoyl carnitine depleted as it continued through β-oxidation. Another reason for this decrease could be all pyruvate had been converted to lactic acid, no longer generating any more NAD+, which is required for glycolysis, and so ATP stores became depleted and palmitic acid and CoA could no longer create palmitoyl-CoA and then palmitoyl carnitine. This decrease could also have been observed due to the decrease in pH causing the denaturation of the enzymes involved in the carnitine shuttle pathway. During the decomposition process, the increase in free radicals through lipid oxidation prevents all metabolic pathways from continuing, and causes cell death, which is potentially the most likely cause of the decrease in palmitoyl carnitine and the other acyl carnitines after Week 2.

Another variable to consider is the generation of carnitine. Carnitine is an amino acid, synthesised from lysine and methionine [137]. Without the generation of carnitine, the transport of palmitoyl-CoA from the cytosol to the mitochondria can not occur, meaning that fatty acid β-oxidation to acetyl-CoA can not happen. This could play a role in the increase in concentration of palmitoyl carnitine initially at Week 1 and 2, where there were still enough amino acids to generate carnitine, however the store of lysine and methionine depleted, and so carnitine stores depleted also, causing a decrease in the generation of palmitoyl carnitine.

The marker 319.2626 m/z at 23.04 minutes can be tentatively identified as arachidonic acid methyl ester, due to the mass spectrum of this peak in the sample

matching the mass spectrum of this compound on the METLIN database (Figure 4.17). This marker had a random trend (Figure 4.18), and did not have a specific pattern correlating to the length of frozen storage, so despite it not necessarily being a useful marker for determining the length of time meat has been frozen for, it does illustrate the complexity of the metabolic processes that occur after death, even when frozen.

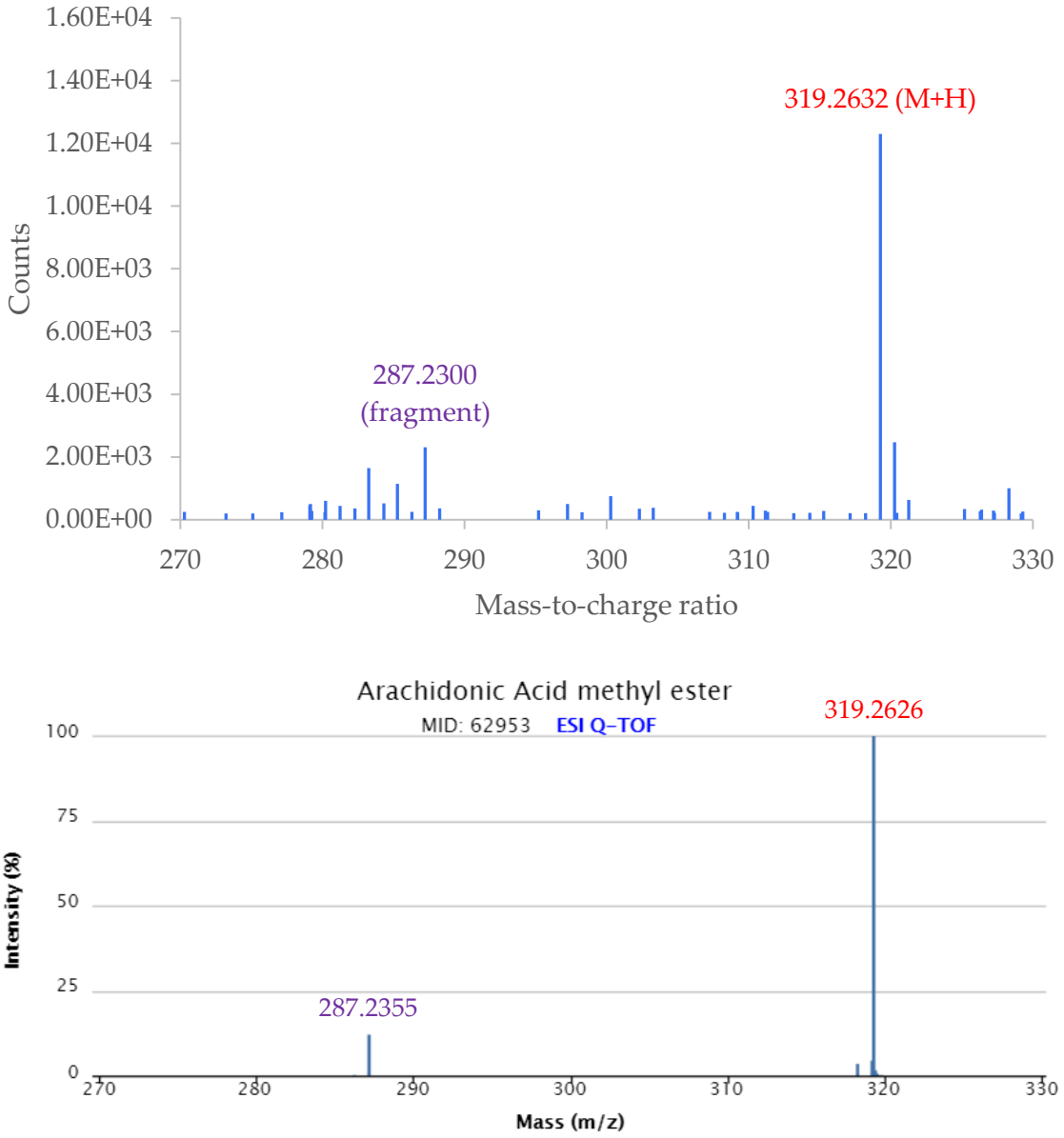

Figure 4.17: Mass spectrum of marker 319.2626 m/z at a retention time of 23.04 minutes in QC sample (top) compared to the mass spectrum of arachidonic acid methyl ester found on METLIN (bottom)

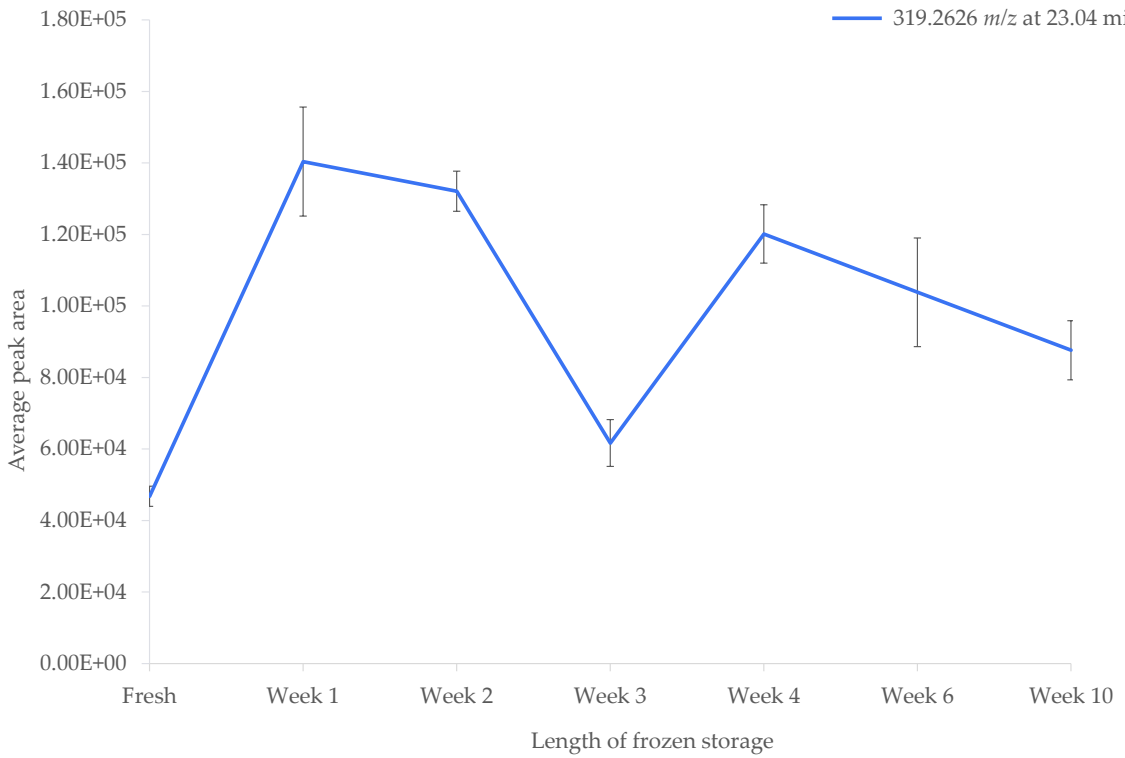

Figure 4.18: Trend of one marker tentatively identified as arachidonic acid that was significantly different among all extracts from lamb muscle tissue frozen for different lengths of time including Fresh, excluding Week 8 samples. Error bars correspond to ± 1 standard deviation

4.7.4 Freezing duration of lamb liver tissue

4.7.4.1 Quality control

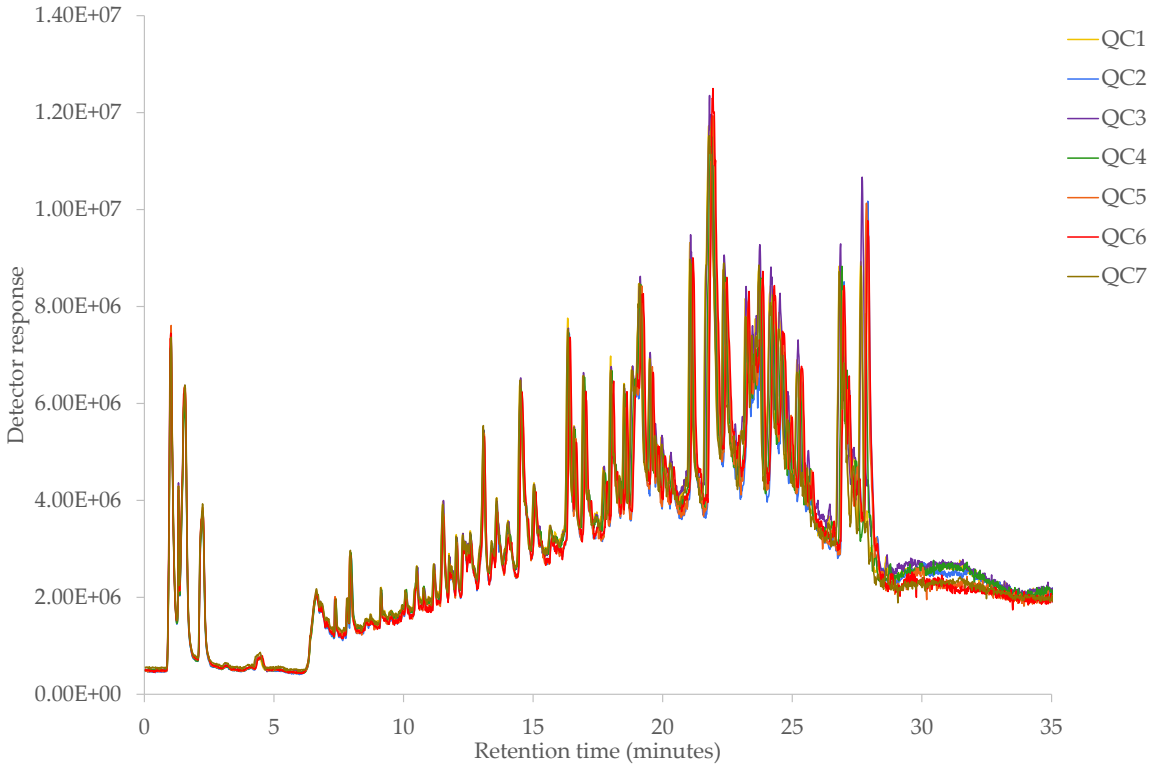

Figure 4.19: Total ion chromatograms of QC samples throughout analytical run for extracts from lamb liver tissue frozen for different lengths of time

The chromatograms for the QC samples throughout this analytical run appear to have very good reproducibility in the first 17.5 minutes of the analysis, and then the second part of the chromatograms include some baseline drift, as well as slight retention time deviation. In particular, QC3 appears to have a higher peak intensity and baseline in this second half of the chromatogram. It is also very noticeable that there are many more peaks present in these chromatograms compared to the chromatograms for chicken and lamb muscle tissue, indicating the liver tissue contains a more complex chemical composition.

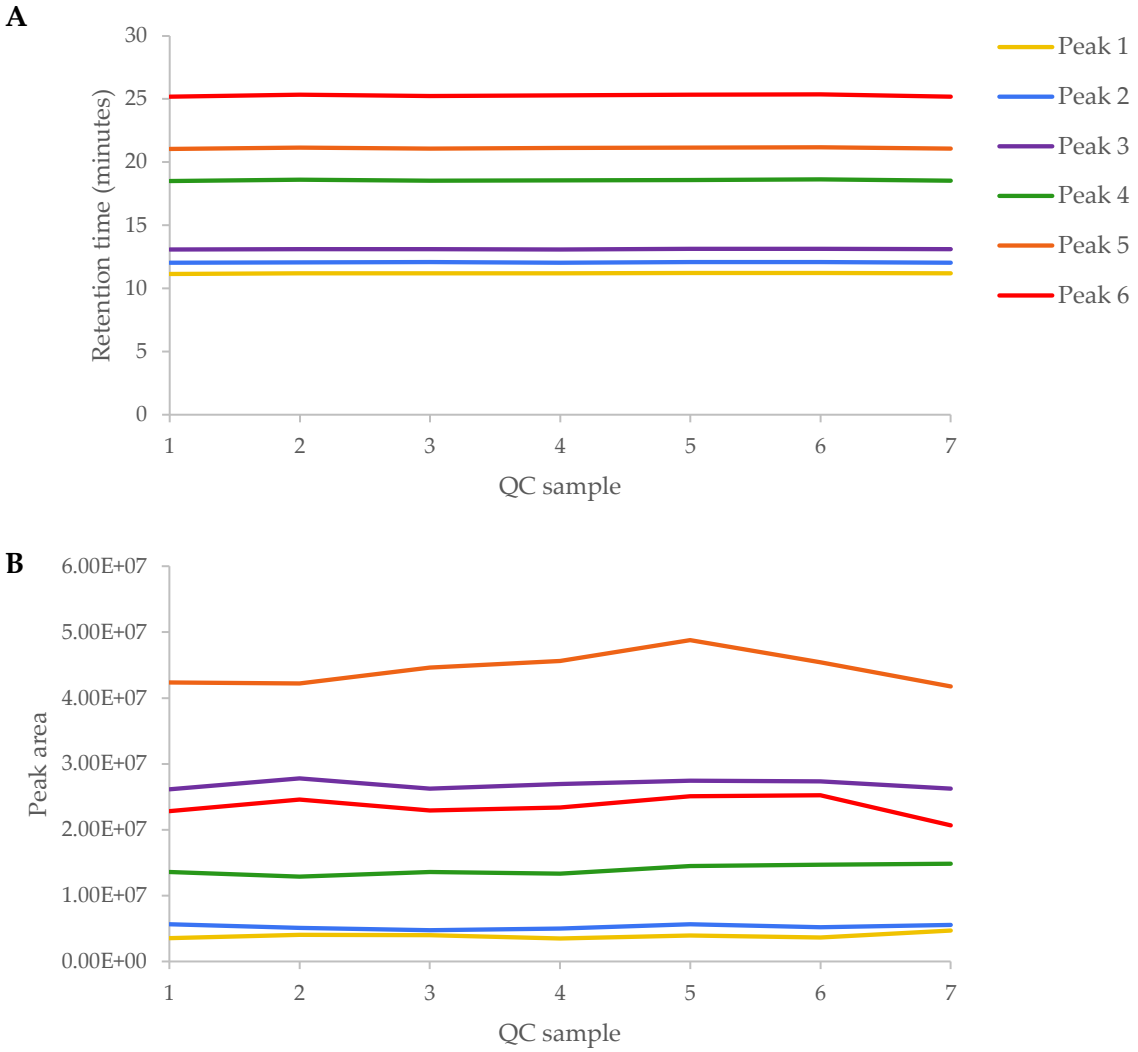

Figure 4.20: Variability of retention time (A) and peak area (B) of 6 peaks in QC samples throughout analytical run for extracts from lamb liver tissue frozen for different lengths of time

Figure 4.20 shows that the retention time is consistent within the QC samples for six peaks, and the peak area is mostly consistent with some slight variability, particularly in peak 5.

Table 4.15: Variability of retention time and peak area of 6 peaks in chromatograms of QC samples during the analysis of extracts from lamb liver tissue frozen for different lengths of time

	Retention time (minutes)									
Peak	QC1	QC2	QC3	QC4	QC5	QC6	QC7	SD	Average	CV%
1	11.14	11.19	11.19	11.18	11.21	11.21	11.18	0.02	11.19	0.21
2	12.04	12.05	12.07	12.04	12.07	12.08	12.04	0.02	12.06	0.14
3	13.08	13.10	13.10	13.08	13.12	13.12	13.09	0.02	13.10	0.13
4	18.51	18.61	18.53	18.56	18.59	18.63	18.53	0.05	18.57	0.24
5	21.04	21.16	21.08	21.11	21.16	21.17	21.07	0.05	21.11	0.24
6	25.17	25.34	25.23	25.29	25.34	25.36	25.18	0.08	25.27	0.31
	Peak area									
Peak	QC1	QC2	QC3	QC4	QC5	QC6	QC7	SD	Average	CV%
1	3534314	4041132	4004108	3509926	3947523	3638078	4718983	419716	3913438	10.73
2	5631703	5104981	4772634	5007204	5643433	5215964	5551880	340617	5275400	6.46
3	26125250	27796557	26223474	26958385	27467996	27338718	26229317	686341	26877100	2.55
4	13604563	12873031	13609978	13348103	14498208	14672492	14838697	748709	13920725	5.38
5	42375979	42226801	44603615	45617960	48787400	45427816	41781369	2500240	44402991	5.63
6	22838862	24560973	22920005	23361817	25076763	25252842	20683510	1602295	23527825	6.81

The retention time variability was between 0.13 and 0.31%, and the peak area variability was between 2.55 and 10.73%, which both indicate that the analytical run was stable throughout this analysis.

4.7.4.2 Metabolic fingerprinting

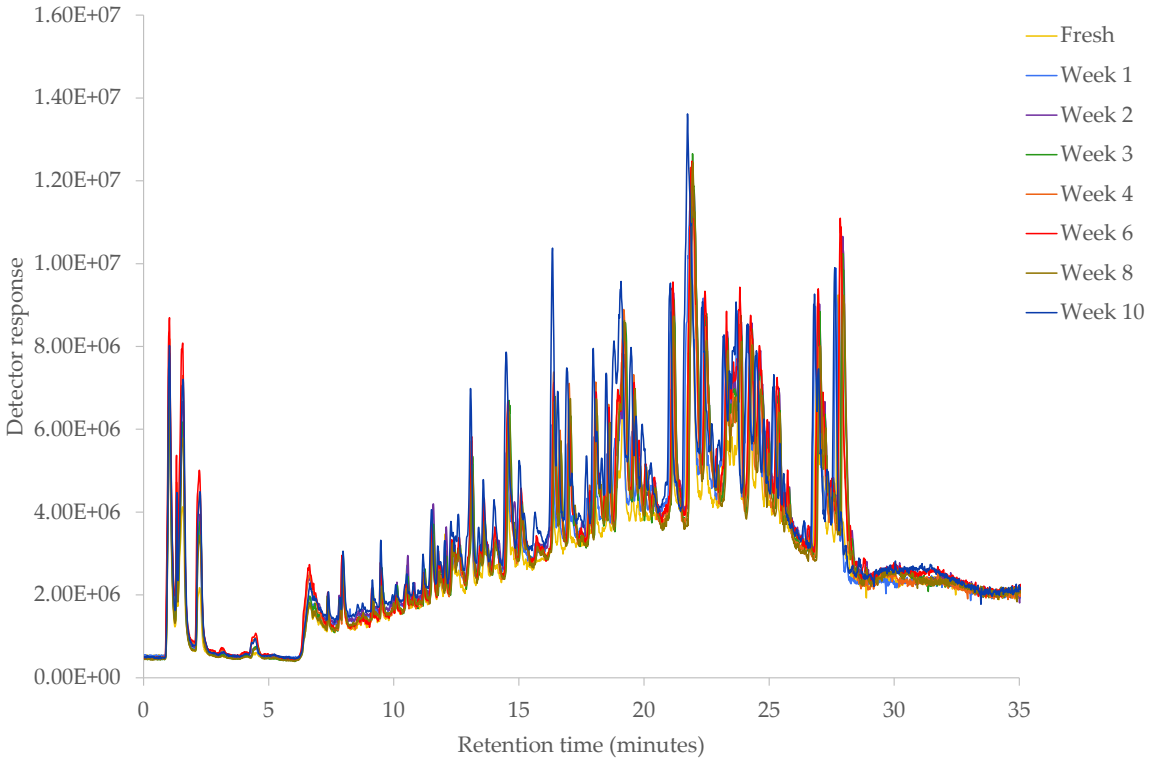

Figure 4.21: Example total ion chromatograms of extracts from lamb liver tissue frozen for different lengths of time

The chromatograms for the liver samples (Figure 4.21) appear to all have similar metabolic profiles based on the peak pattern. It does, however, show differences in the intensities of these peaks. In particular, Week 10 has a higher intensity for the majority of peaks through the chromatogram, and Fresh has a lower intensity, and this is also seen in the baseline. There is a slight retention time drift, which was expected as it was also seen in the QC sample chromatograms.

4.7.4.3 Multivariate statistics

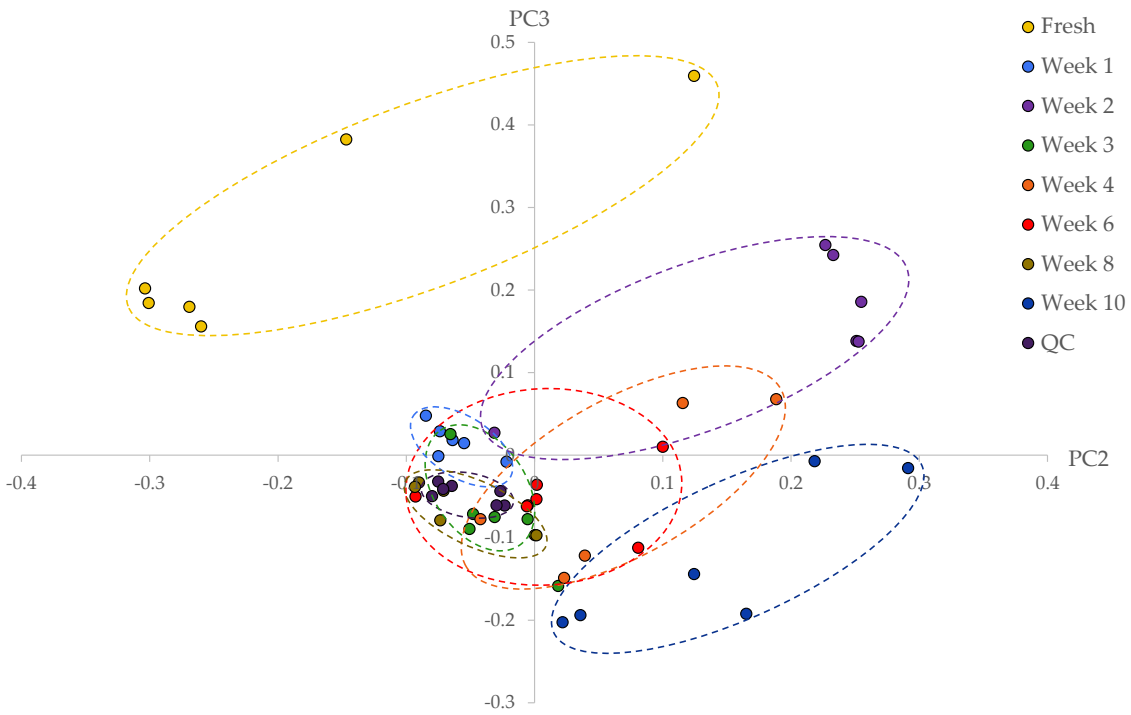

Figure 4.22: Principal component analysis scores plot of PC2 (2.762%) and PC3 (1.183%) for extracts from lamb liver tissue frozen for different lengths of time. PCA was carried out using markers with a p-value of < 0.05 and CV $< 10\%$

The PCA plot for the liver extracts show there is a distinct separation between the fresh samples and the rest of the freezing length sample types. It can also be seen that the Fresh, Week 1, and Week 10 samples are all separated from each other, indicating that the metabolic profile is different enough between these sample types to be separated in this unsupervised method. Many of the sample types have a large spread within each grouping, demonstrating the diversity of the chemical composition between replicate samples with the same frozen storage period. The QC samples are tightly clustered showing stability within the analytical run.

4.7.4.4 Significant markers

The following tables include the remaining markers from the most significantly different markers in each case after statistical analysis and confirmation with the raw data. Table 4.16 contains the markers that were highly significant from Fresh to Week 10 samples. These markers all had a CV% in the QC samples of less than 30% in both normalised and raw data, with the majority of markers having less than 10%, indicating these are very robust and stable within the QC samples. The trends for these markers varied substantially, with only a few markers producing an increasing or decreasing trend over the frozen storage time period.

Table 4.16: Summary of remaining compounds from top 50 markers that were significantly different among **Fresh** to **Week 10** lamb liver tissue samples, in order of significance from manual ANOVA.
Marker trend: ↓ = decreased, ↑ = increased, ↷ = increased Week 1 and 2 then decreased, ↳ = increased Fresh then decreased, ⇂ = increased Week 10, ↓ = decreased Week 10

m/z	Retention time median (mins)	P-value from ANOVA/Welch (XCMS)	CV% (XCMS)	P-value from ANOVA/Welch (EICs)	CV% (EICs)
↳ 316.2462	9.12	<0.001	8.74	<0.001	8.55
↳ 344.2755	11.08	<0.001	5.46	<0.001	8.17
↓ 283.6320	12.08	<0.001	2.50	<0.001	3.42
↷ 311.2572	18.48	<0.001	1.91	<0.001	2.99
↷ 514.2596	9.27	<0.001	5.07	<0.001	20.03
↳ 361.2683	9.99	<0.001	7.34	<0.001	8.30
↷ 516.2738	9.97	<0.001	4.65	<0.001	20.87
⇂ 465.1164	9.62	<0.001	11.26	<0.001	26.24
↷ 307.2625	21.02	<0.001	3.80	<0.001	4.66
↓ 270.6250	11.56	<0.001	2.91	<0.001	3.79
↳ 218.1382	1.76	<0.001	4.32	<0.001	2.94
↑ 307.2263	14.80	<0.001	1.65	<0.001	3.79
↷ 348.2500	14.80	<0.001	4.35	<0.001	9.49
↳ 603.2987	9.98	<0.001	6.77	<0.001	10.38
↷ 332.2319	14.92	<0.001	3.84	<0.001	7.55
↳ 359.2540	9.32	<0.001	9.97	<0.001	12.18
↷ 600.3302	10.63	<0.001	2.82	<0.001	3.78
↷ 289.2156	14.80	<0.001	2.15	<0.001	7.80
↷ 217.1582	14.78	<0.001	6.63	<0.001	9.66
↷ 383.3290	25.63	<0.001	18.33	<0.001	16.60
↓ 522.2594	10.55	<0.001	5.19	<0.001	8.33
↑ 203.1783	19.23	<0.001	7.94	<0.001	14.51
↳ 339.2867	10.96	<0.001	6.54	<0.001	6.54
↷ 257.1925	14.80	<0.001	5.65	<0.001	11.48
↓ 547.2851	12.07	<0.001	8.18	<0.001	10.38
↑ 329.2474	18.08	<0.001	4.29	<0.001	3.61
↑ 657.4868	18.08	<0.001	6.13	<0.001	7.23
↓ 657.4870	14.37	<0.001	5.65	<0.001	5.27
↷ 349.2348	16.21	<0.001	7.17	<0.001	8.62
↑ 259.6320	14.05	<0.001	1.40	<0.001	3.63
⇂ 343.0553	15.15	<0.001	9.47	<0.001	17.80
↓ 524.2779	11.56	<0.001	7.02	<0.001	7.60

Table 4.16 continued: Summary of remaining compounds from top 50 markers that were significantly different among **Fresh** to **Week 10** lamb liver tissue samples, in order of significance from manual ANOVA.
Marker trend: ↓ = decreased, ↑ = increased, ↷ = increased Week 1 and 2 then decreased, ↳ = increased Fresh then decreased, ⇂ = increased Week 10, ↓ = decreased Week 10

m/z	Retention time median (mins)	P-value from ANOVA/Welch (XCMS)	CV% (XCMS)	P-value from ANOVA/Welch (EICs)	CV% (EICs)
↳ 629.3117	10.36	<0.001	11.48	<0.001	16.17
↑ 305.2467	18.29	<0.001	4.96	<0.001	10.12
↑ 440.2786	11.81	<0.001	6.55	<0.001	9.85
↷ 155.1064	13.92	<0.001	3.45	<0.001	4.93

Table 4.17 shows the markers that were significantly different from Week 1 to Week 10 frozen storage period. The majority of these markers were at a higher concentration at Week 1 and Week 2, and then the concentration decreased rapidly and remained relatively consistent for the rest of the frozen storage duration.

Table 4.17: Summary of remaining compounds from top 10 markers that were significantly different among **Week 1** to **Week 10** lamb liver tissue samples, in order of significance from manual ANOVA.
Marker trend: ↷ = increased Week 1 and 2 then decreased, ⇂ = increased Week 10

m/z	Retention time median (mins)	P-value from ANOVA/Welch (XCMS)	CV% (XCMS)	P-value from ANOVA/Welch (EICs)	CV% (EICs)
↷ 311.2572	18.48	<0.001	1.91	<0.001	2.99
↷ 514.2596	9.27	<0.001	5.07	<0.001	20.03
↷ 275.1994	14.80	<0.001	6.06	<0.001	9.72
↷ 383.3290	25.63	<0.001	18.33	<0.001	16.60
⇂ 465.1164	9.62	<0.001	11.26	<0.001	26.24
↷ 348.2500	14.80	<0.001	4.35	<0.001	9.49
↷ 313.2173	14.95	<0.001	4.63	<0.001	7.49

Table 4.18 shows the markers that were significantly different from Week 4 to Week 10, and these markers were fairly consistent in Week 4, Week 6 and Week 8 samples, and it was Week 10 samples that had either a significant increase or decrease in concentration. This could have been caused by a number of reasons, however these

trends do not aid in understanding the overall metabolic changes during the frozen storage time period.

Table 4.18: Summary of remaining compounds from top 10 markers that were significantly different among **Week 4** to **Week 10** lamb liver tissue samples, in order of significance from manual ANOVA.
Marker trend: ⇀ = increased Week 10, ↓ = decreased Week 10

m/z	Retention time median (mins)	P-value from ANOVA/Welch (XCMS)	CV% (XCMS)	P-value from ANOVA/Welch (EICs)	CV% (EICs)
↓ 314.3039	11.80	<0.001	3.43	<0.001	5.33
⇀ 657.4870	14.37	<0.001	5.65	<0.001	5.27
⇀ 465.1164	9.62	<0.001	11.26	<0.001	26.24
↓ 512.4130	13.57	<0.001	6.62	<0.001	9.40
↓ 556.4394	13.54	<0.001	7.31	<0.001	8.26

The markers that were significantly different from Fresh to Week 4 samples (Table 4.19) mostly appeared to have an increase in concentration in the Fresh samples, and all frozen samples were very low in concentration, with no significant differences in frozen storage time. Marker 283.6320 *m/z* at 12.08 minutes decreased over the frozen storage period, and marker 259.6320 *m/z* at 14.05 minutes increased over the frozen storage period. Both of these markers were also significant in the analysis of Fresh to Week 10, however on observation of these trends, it can be seen that the concentration changes from Fresh to Week 4, and then becomes fairly stable after this point. Therefore, these markers could have the potential in being useful during the early frozen storage period of up to 4 weeks, but then may not be able to determine the longer frozen storage durations.

Table 4.19: Summary of remaining compounds from top 10 markers that were significantly different among **Fresh** to **Week 4** lamb liver tissue samples, in order of significance from manual ANOVA.
Marker trend: ↓ = decreased, ↑ = increased, ↷ = increased Week 1 and 2 then decreased, ↳ = increased Fresh then decreased

m/z	Retention time median (mins)	P-value from ANOVA/Welch (XCMS)	CV% (XCMS)	P-value from ANOVA/Welch (EICs)	CV% (EICs)
↳ 316.2462	9.12	<0.001	8.74	<0.001	8.55
↳ 344.2755	11.08	<0.001	5.46	<0.001	8.17
↓ 283.6320	12.08	<0.001	2.50	<0.001	3.42
↳ 361.2683	9.99	<0.001	7.34	<0.001	8.30
↑ 259.6320	14.05	<0.001	1.40	<0.001	3.63
↷ 275.1994	14.80	<0.001	6.06	<0.001	9.72
↳ 218.1382	1.76	<0.001	4.32	<0.001	2.94
↳ 359.2540	9.32	<0.001	9.97	<0.001	12.18
↷ 311.2572	18.48	<0.001	1.91	<0.001	2.99

4.7.4.5 Tentative identifications

Due to the availability of MS spectra on the METLIN database, no markers were able to be tentatively identified in the liver extracts.

4.7.5 Number of freeze-thaw cycles - Chicken muscle

4.7.5.1 Quality control

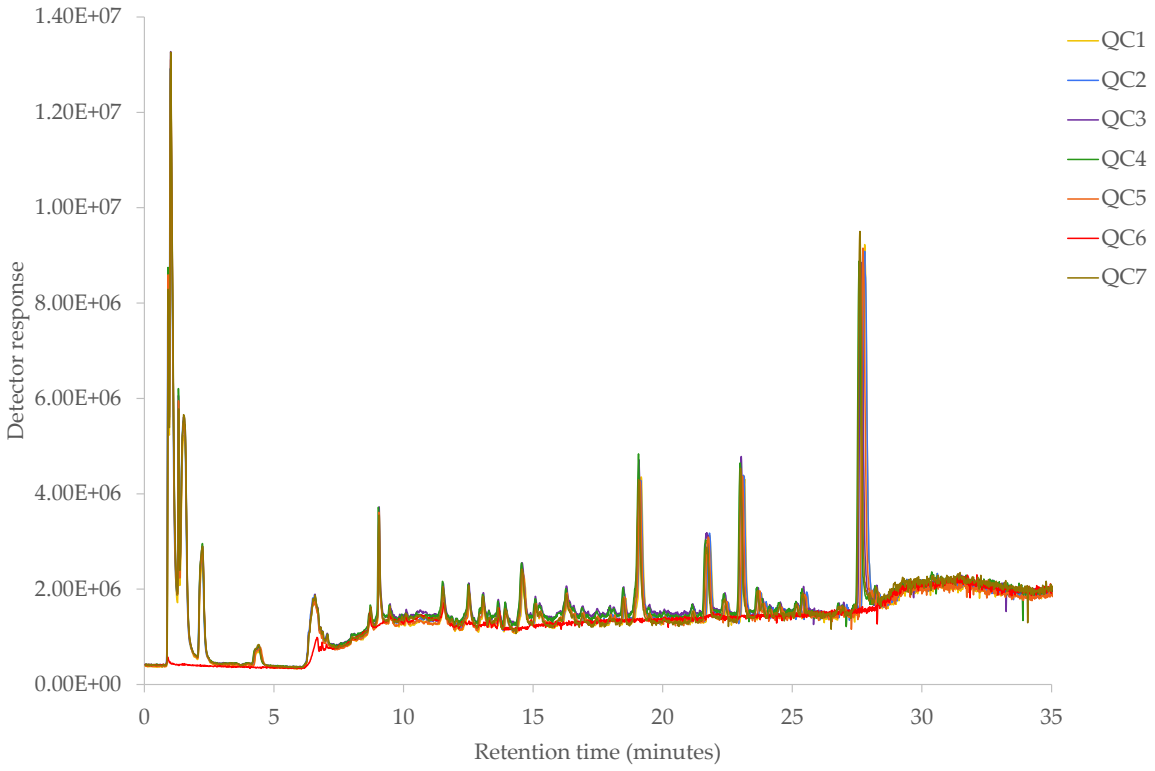

Figure 4.23: Total ion chromatograms of QC samples throughout analytical run for extracts from chicken muscle tissue that has undergone multiple freeze-thaw cycles

As shown in Figure 4.23, QC6 did not inject correctly during this analysis, as it is very obviously completely different to the other QC samples. Many peaks are missing, and so it would appear that no sample was actually injected. Therefore, it was appropriate to remove this from any further analysis. The remaining QC samples appear to be very stable in retention time and peak intensity, illustrated by the reproducible chromatograms.

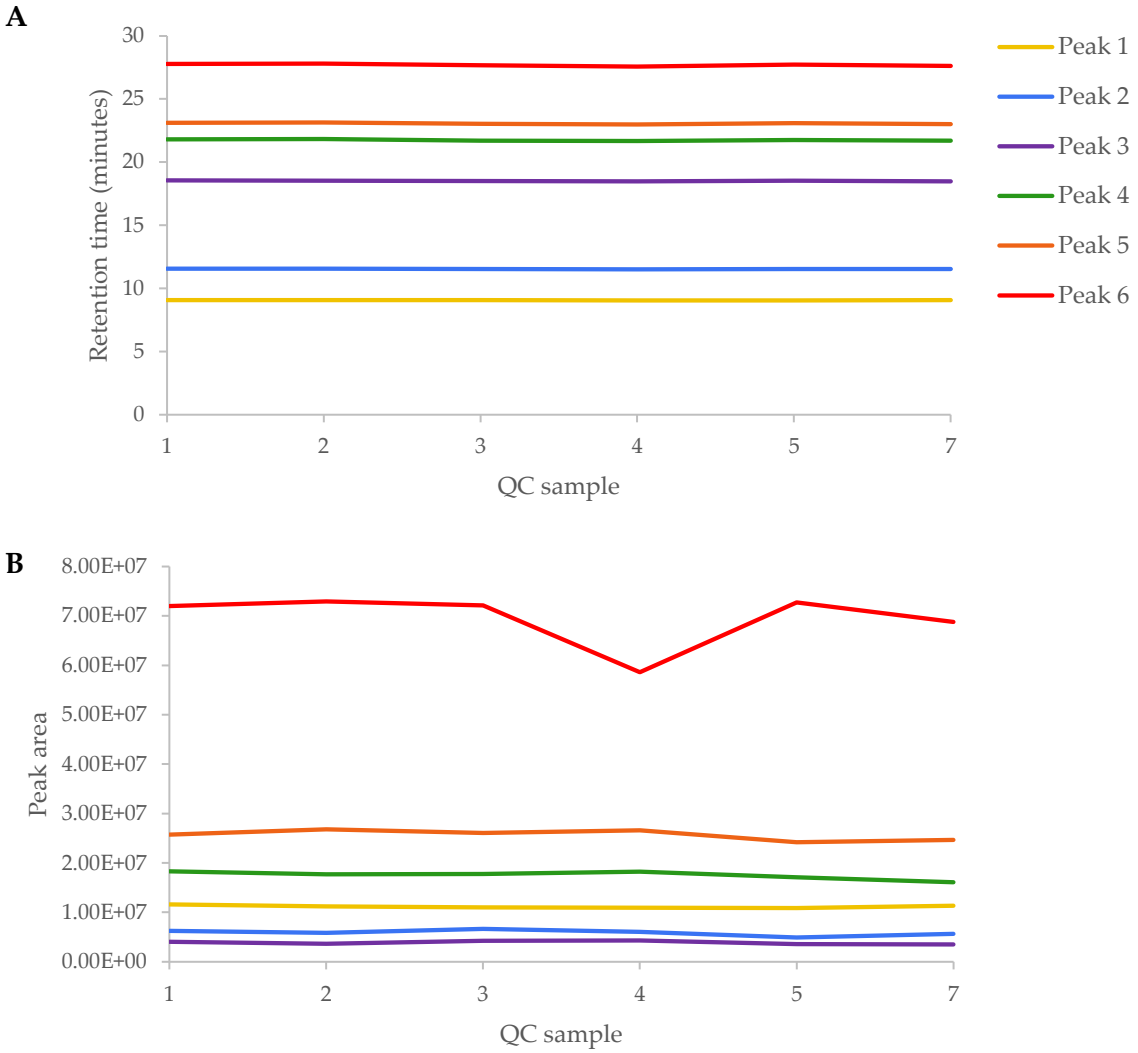

Figure 4.24: Variability of retention time (A) and peak area (B) of 6 peaks in QC samples throughout analytical run for extracts from chicken muscle tissue that has undergone multiple freeze-thaw cycles

After manually integrating six peaks within the QC samples, it can be seen in Figure 4.24 that the retention time is very stable in all peaks, and the peak area is mostly consistent, apart from peak 6, where QC4 had a lower peak area than the other QC samples.

Table 4.20: Variability of retention time and peak area of 6 peaks in chromatograms of QC samples during the analysis of extracts from chicken muscle tissue that has undergone multiple freeze-thaw cycles

	Retention time (minutes)								
Peak	QC1	QC2	QC3	QC4	QC5	QC7	SD	Average	CV%
1	9.06	9.06	9.07	9.04	9.05	9.06	0.01	9.06	0.11
2	11.56	11.55	11.54	11.51	11.54	11.52	0.02	11.54	0.16
3	18.56	18.53	18.51	18.47	18.52	18.48	0.03	18.51	0.18
4	21.80	21.82	21.71	21.66	21.76	21.69	0.06	21.74	0.29
5	23.12	23.13	23.04	22.99	23.08	23.00	0.06	23.06	0.26
6	27.79	27.80	27.66	27.58	27.73	27.61	0.09	27.70	0.33
	Peak area								
Peak	QC1	QC2	QC3	QC4	QC5	QC7	SD	Average	CV%
1	11621122	11174036	10997619	10912281	10847981	11349185	294331	11150371	2.64
2	6251637	5862572	6644637	6049506	4918481	5668213	586342	5899174	9.94
3	4015101	3642992	4213916	4271064	3571042	3474581	345626	3864783	8.94
4	18288399	17661652	17754791	18222890	17088164	16109738	816701	17520939	4.66
5	25718584	26796784	26051497	26604065	24214612	24680006	1038067	25677591	4.04
6	71974236	72905753	72147101	58579594	72746886	68791243	5568205	69524136	8.01

The retention time variability was between 0.11 and 0.33%, and the peak area variability was between 2.64 and 9.94%. These values confirm that the instrument was stable throughout this analytical run, and the data obtained was reliable.

4.7.5.2 Metabolic fingerprinting

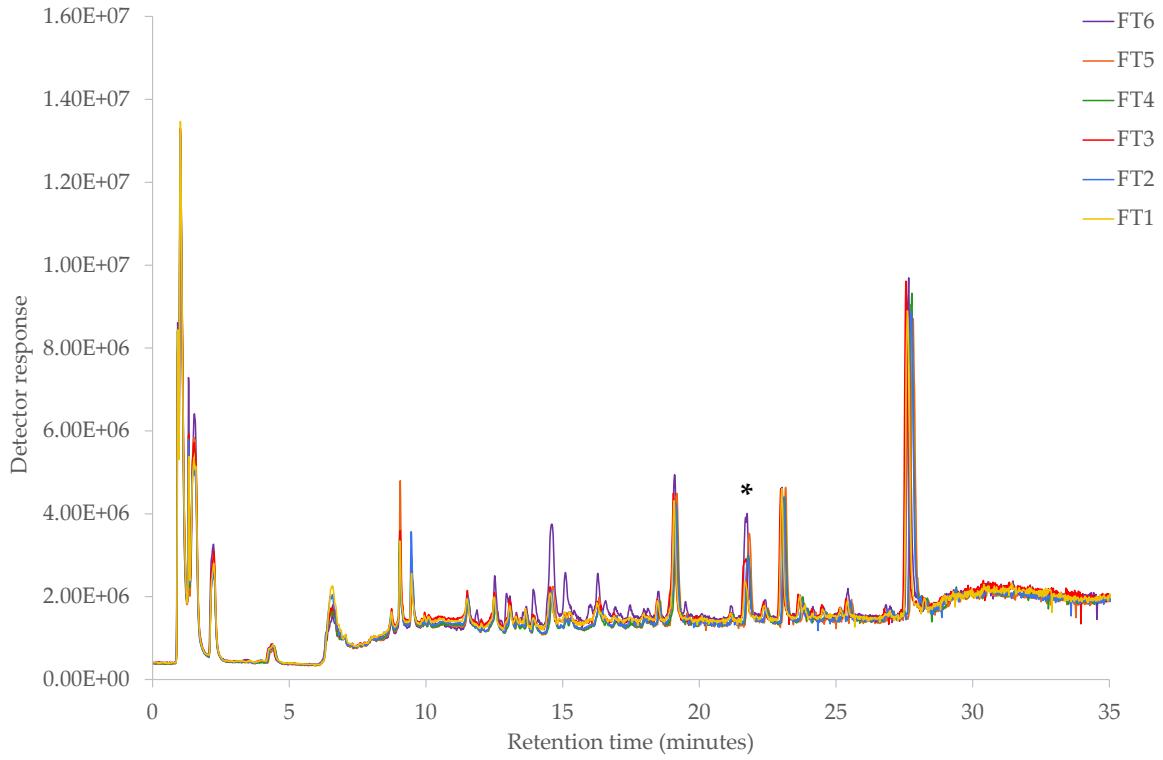

Figure 4.25: Example total ion chromatograms for chicken muscle tissue that has undergone multiple freeze-thaw cycles

The chromatograms for each sample type (number of freeze-thaw cycles 1-6, FT1-FT6) can be seen in Figure 4.25. Each chromatogram for the different number of freeze-thaw cycles shows a very similar peak pattern, with slight differences in abundance. Between 12 minutes and 23 minutes, the chromatograms for FT1-5 are all very similar, but FT6 has the highest intensity, indicating that the ions responsible for these peaks increase from FT5 to FT6. The peak at 22 minutes (indicated with an asterisk) has a decreasing intensity from FT6 down to FT1.

4.7.5.3 Multivariate statistics

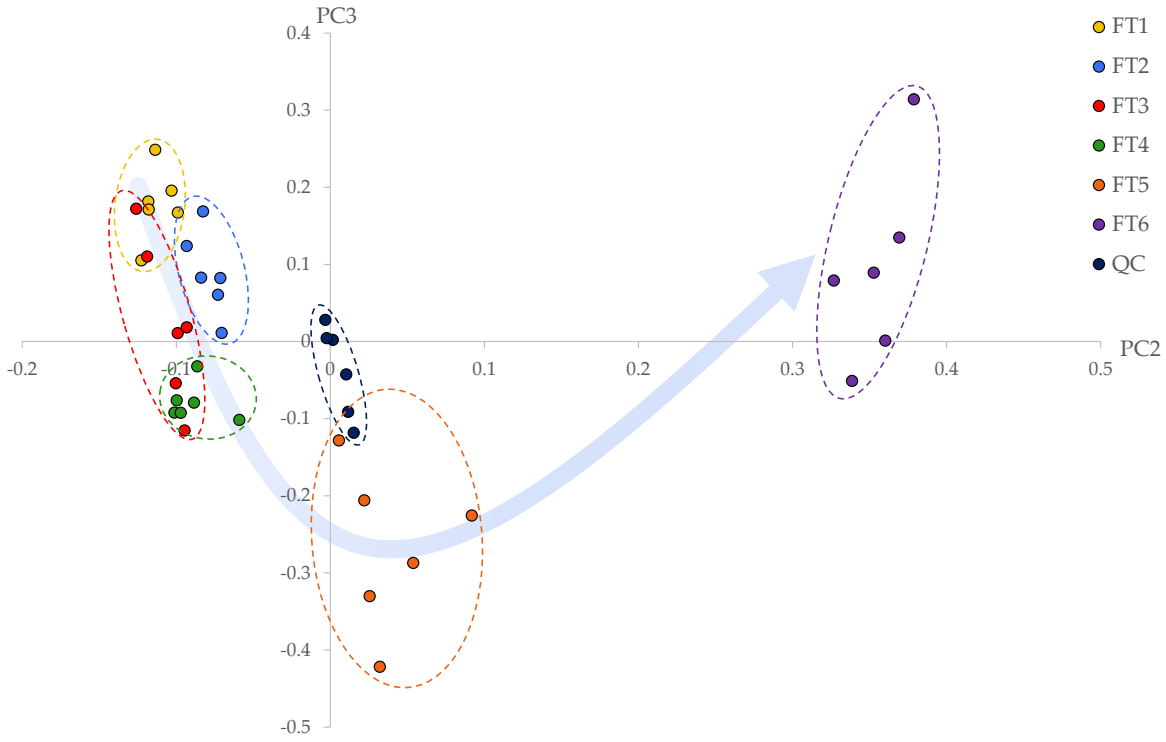

Figure 4.26: Principal component analysis scores plot of PC2 (1.345%) and PC3 (0.097%) for extracts from chicken muscle tissue that has undergone multiple freeze-thaw cycles. PCA was carried out using markers with a p-value of < 0.05 and CV $< 10\%$

The PCA plot (Fig. 4.26) shows very good separation between the different sample types. The first 4 freeze-thaw cycles are gathered in the same area, with some individual separation particularly between FT1 and FT4, and FT5 samples are separated from these. FT6 samples are completely separated from all other sample types. The FT1 samples are in the left of the plot, and as the number of freeze-thaw cycles increases, the groups move across the plot, shown by the blue arrow. The groups appear to be slightly elongated in the direction of the y-axis (PC3), and this can also be seen in the QC samples. This is most likely showing the slight instrument variability within the analytical run. The QC samples are gathered together, and the separation between sample types is across the x-axis, PC2, and so not affected by instrumental variability.

4.7.5.4 Significant markers

The markers found in the chicken mostly increased in abundance the more freeze-thaw cycles the chicken had undergone. Some markers decreased instead, however these markers were not retained on the column, so are very polar and would be better suited to being analysed using a column with a different stationary phase.

Table 4.21: Summary of remaining compounds from top 50 markers that were significantly different among all chicken muscle tissue samples that have undergone multiple freeze-thaw cycles, in order of significance from manual ANOVA. Arrow indicates marker increased or decreased the more freeze-thaw cycles the chicken had undergone

m/z	Retention time median (mins)	P-value from ANOVA/Welch (XCMS)	CV% (XCMS)	P-value from ANOVA/Welch (EICs)	CV% (EICs)
↓ 175.1171	0.98	<0.001	0.85	<0.001	2.78
↑ 103.1226	0.93	<0.001	5.58	<0.001	11.22
↑ 365.3500	13.92	<0.001	11.88	<0.001	7.35
↑ 409.2702	17.27	<0.001	11.23	<0.001	19.97
↑ 480.3441	16.01	<0.001	2.09	<0.001	1.41
↑ 131.1275	0.94	<0.001	2.02	<0.001	3.09
↑ 506.3595	16.56	<0.001	3.09	<0.001	2.08
↑ 508.3754	16.98	<0.001	2.54	<0.001	1.70
↓ 269.0889	1.08	<0.001	4.04	<0.001	4.53
↑ 395.3714	17.07	<0.001	13.23	<0.001	19.83
↑ 281.2468	19.51	<0.001	2.89	<0.001	4.64
↑ 775.9876	14.58	<0.001	12.27	<0.001	12.93
↑ 174.1107	6.75	<0.001	15.67	<0.001	19.69
↑ 341.3483	15.73	<0.001	9.90	<0.001	20.32
↑ 75.0445	21.17	<0.001	4.68	<0.001	7.10
↑ 482.3551	16.57	<0.001	3.57	<0.001	2.26
↑ 537.5222	21.17	<0.001	8.96	<0.001	11.22
↑ 265.2518	14.65	<0.001	4.05	<0.001	5.00
↑ 369.3561	16.23	<0.001	25.32	<0.001	18.08
↑ 464.3133	14.45	<0.001	3.28	<0.001	2.43
↑ 509.3458	16.57	<0.001	5.00	<0.001	5.73
↑ 93.0549	21.72	<0.001	4.09	<0.001	5.83
↑ 290.2028	1.36	<0.001	6.47	<0.001	18.45
↓ 564.1231	1.46	<0.001	5.35	<0.001	7.12
↑ 105.0687	3.45	<0.001	11.52	<0.001	5.68
↑ 345.3351	25.91	<0.001	7.45	<0.001	6.42
↓ 306.1880	1.03	<0.001	8.15	<0.001	19.96
↑ 337.2701	19.03	<0.001	3.68	<0.001	9.23
↑ 401.2060	1.79	<0.001	2.89	<0.001	6.24
↑ 295.2621	24.49	<0.001	6.14	<0.001	26.88
↑ 524.3619	15.11	<0.001	2.43	<0.001	7.89
↑ 561.4870	19.50	<0.001	4.93	<0.001	4.55
↓ 292.1963	1.03	<0.001	7.12	<0.001	5.18
↑ 297.2769	19.03	<0.001	1.82	<0.001	3.38
↑ 482.3237	15.63	<0.001	4.14	<0.001	3.08

4.7.5.5 Tentative identifications

Table 4.22 shows the possible formula and likelihood score for the markers that were able to generate a formula in *Masshunter Qualitative Analysis*. It also shows the trend of these markers, with most of them increasing the more freeze-thaw cycles the chicken meat had undergone.

Table 4.22: Predicted formulae and possible identifications of significantly different compounds in extracts from chicken muscle tissue samples that have undergone 1-6 freeze-thaw cycles. Arrow indicates trend of marker, and asterisk indicates marker was found to be an isotopic peak

m/z	Retention time median (mins)	Possible formula	Adduct	Likelihood score (%)	Potential METLIN identification
↓ 175.1171	0.98	$C_4H_{16}N_4O_2$	M+Na	78.33	
↑ 103.1226	0.93	$C_5H_{14}N_2$	M+H	80.02	
↑ 480.3441	16.01	$C_{23}H_{48}N_5O_2P$	M+Na	83.31	
↑ 506.3595	16.56	$C_{23}H_{48}ClN_7O_3$	M+H	86.77	
↑ 508.3754	16.98	$C_{26}H_{54}NO_6P$	M+H	96.40	phosphatidylcholines
↓ 269.0889	1.08	$C_{13}H_{14}N_2O_3$	M+Na	91.78	
↑ 281.2468	19.51	$C_{18}H_{32}O_2$	M+H	76.04	linoleic acid/linoelaidic acid
↑ 341.3483	15.73	$C_{11}H_{33}N_9OS$	M+H	85.88	
↑ 75.0445	21.17	$C_3H_6O_2$	M+H	79.75	propionic acid/lactaldehyde
↑ 482.3551	16.57	$C_{24}H_{49}N_3O_5$	M+Na	99.34	
↑ 265.2518	14.65	$C_{18}H_{32}O$	M+H	81.13	
↑ 464.3133	14.45	$C_{23}H_{46}NO_6P$	M+H	96.96	
↑ 509.3458	16.57	$C_{21}H_{46}ClN_9O_3$	M+H	84.63	
↑ 345.3351	25.91	$C_{21}H_{44}O_3$	M+H	93.43	monoglycerides
↑ 337.2701	19.03	$C_{11}H_{33}N_{10}P$	M+H	82.86	
* 524.3619	15.11	$C_{26}H_{52}NO_7P$	M+H	99.21	phosphatidylcholines
↑ 561.4870	19.50	$C_{35}H_{62}N_4$	M+Na	85.39	
↑ 482.3237	15.63	$C_{23}H_{48}NO_7P$	M+H	99.00	glycerophospholipids

Due to the nature of these compounds, the majority of the markers could not be tentatively identified through comparison with mass spectra on the METLIN database as the mass spectra were not available at 0 V collision energy. The general class of compound could be assumed if most of the compounds in each search were of a particular group of compound. After searching the METLIN database, markers 482.3237 *m/z* at 15.63 minutes, 508.3754 *m/z* at 16.98 minutes, and 524.3619 *m/z* at

15.11 minutes are all most likely glycerophosolipids.

The trend for markers 524.3619 m/z and 508.3754 m/z can be seen in Figure 4.27, and both of these markers had predicted formulae that matched phosphatidylcholines.

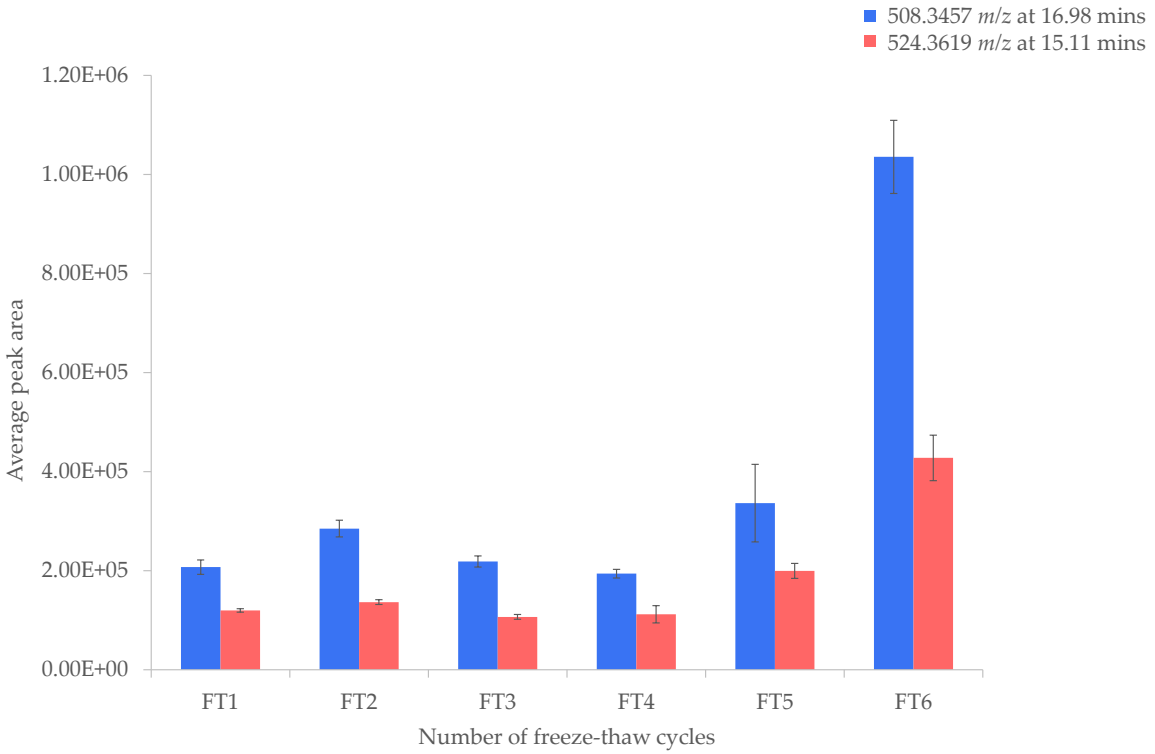

Figure 4.27: Trends of two markers with formulae that matched phosphatidylcholines that were significantly different among all chicken muscle tissue samples that have undergone multiple freeze-thaw cycles. Error bars correspond to ± 1 standard deviation

The marker 281.2468 m/z at a retention time of 19.51 minutes gave a likely formula of $C_{18}H_{32}O_2$, with a likelihood score of 76.04 %. This matched to many compounds on the METLIN database, however when comparing the mass spectrum with that of linoleic acid and linoelaidic acid (Figure 4.28), all spectra have a peak at 281.25 m/z, which was the M+H peak, and a fragment peak at 263.24 m/z, which was caused by the loss of water. Therefore, this marker could be tentatively identified as either linoleic acid, or its isomer linoelaidic acid. Despite this tentative identification, the likelihood of this marker having the same formula as linoleic acid or linoelaidic acid was not very high, so this marker could be another molecule with a different formula that fragments in a similar way, as the loss of a water molecule is a common fragmentation.

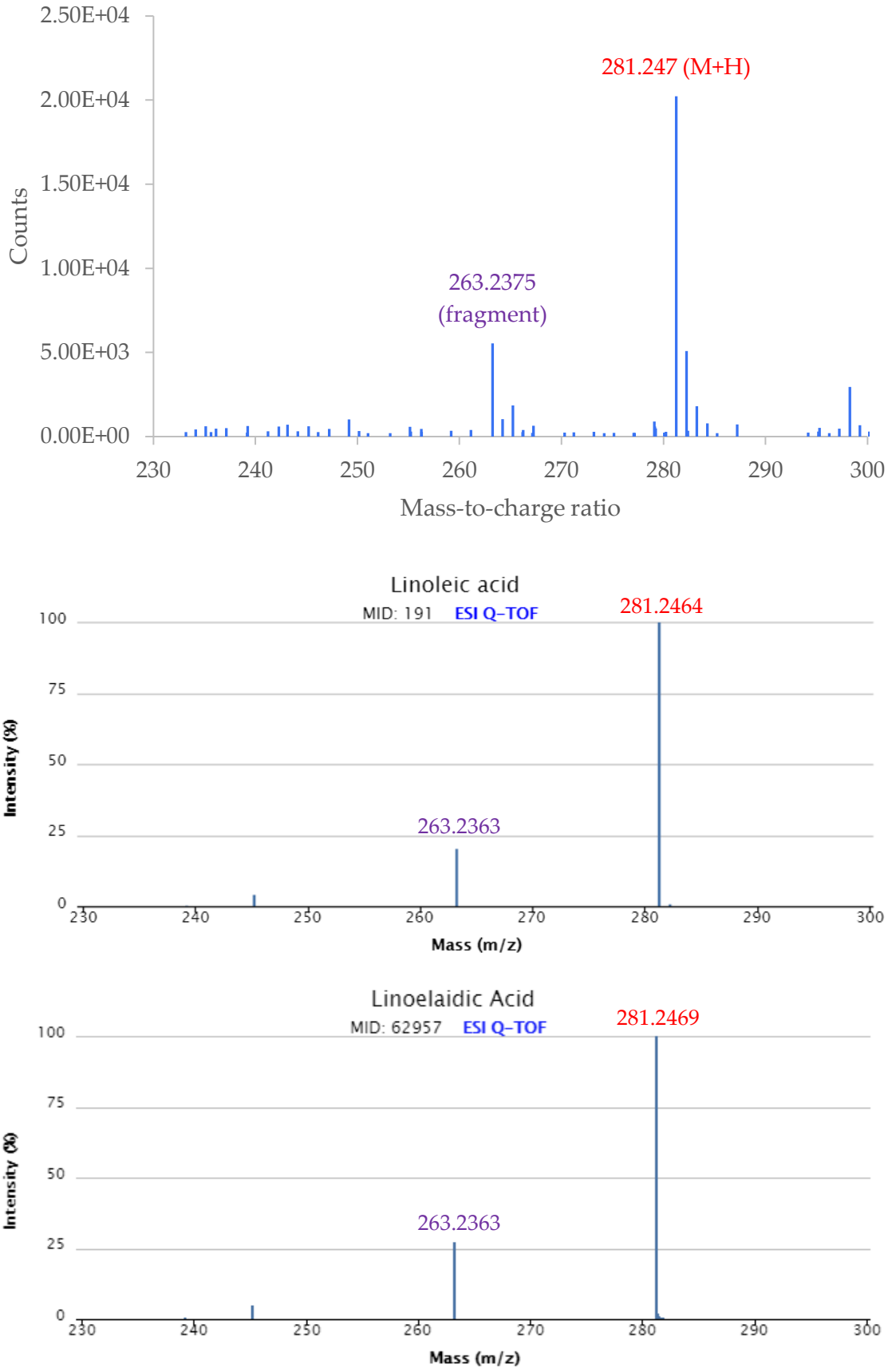

Figure 4.28: Mass spectrum of marker 281.2468 m/z at a retention time of 19.51 minutes in QC sample (top) compared to the mass spectra of linoleic acid (middle) and linoelaidic acid (bottom) found on METLIN

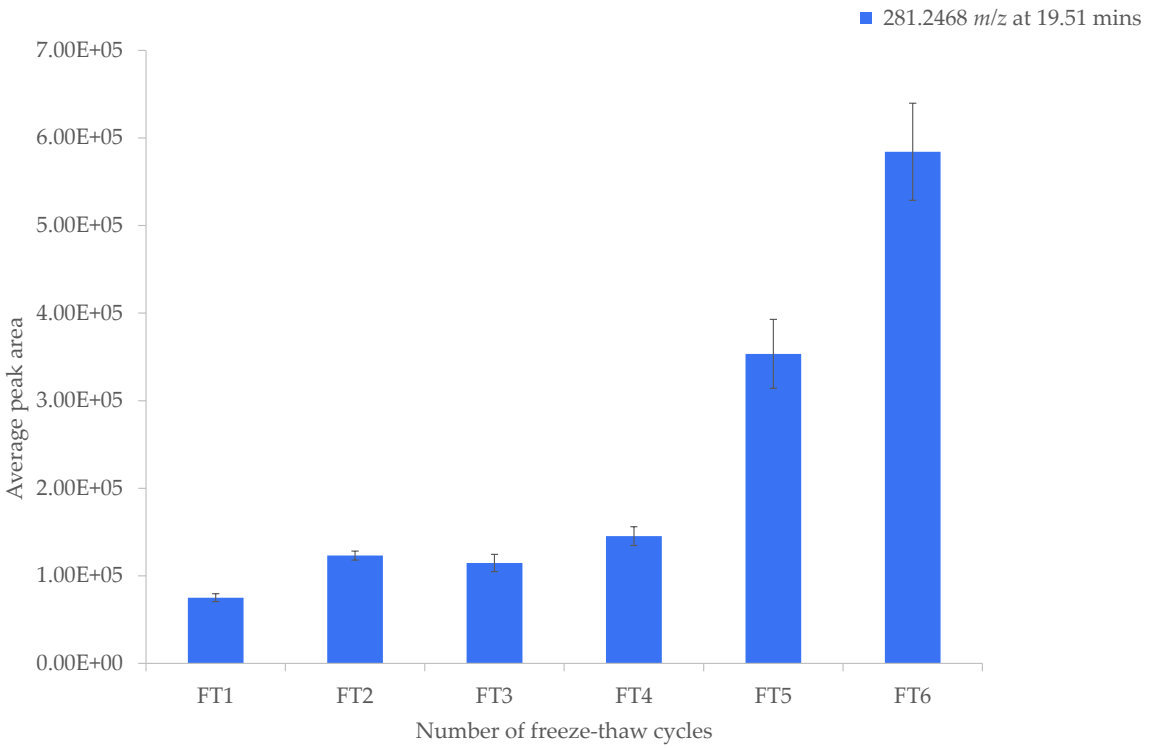

Figure 4.29: Trend of one marker tentatively identified as linoleic acid or linoelaidic acid that was significantly different among all chicken muscle tissue samples that have undergone multiple freeze-thaw cycles. Error bars correspond to ± 1 standard deviation

Linoleic acid is a polyunsaturated fatty acid that is involved in the production of arachidonic acid, which in turn produces eicosanoids. Linoleic acid also contributes to cell membrane structure. The trend of this marker (Figure 4.29) showed an increase as the number of freeze-thaw cycles increased. The degradation that occurs after death involves the breakdown of cell membranes, as previously discussed, and so it is therefore expected that linoleic acid or linoelaidic acid would increase as the phospholipid bilayer of the cell membrane is destroyed, as this releases fatty acids. If this marker is linoelaidic acid, which is a trans fatty acid and the isomer of linoleic acid, then this could be a cause for concern for the consumers' health. Trans fatty acids have been shown to cause cardiovascular disease [138], and the FDA state that trans fatty acids must be included on the label of products to inform the consumer. Therefore, it would be important to try and identify this marker in further research to assess if there are health implications associated with frozen-thawed meat.

4.7.6 Number of freeze-thaw cycles - Lamb liver

4.7.6.1 Quality control

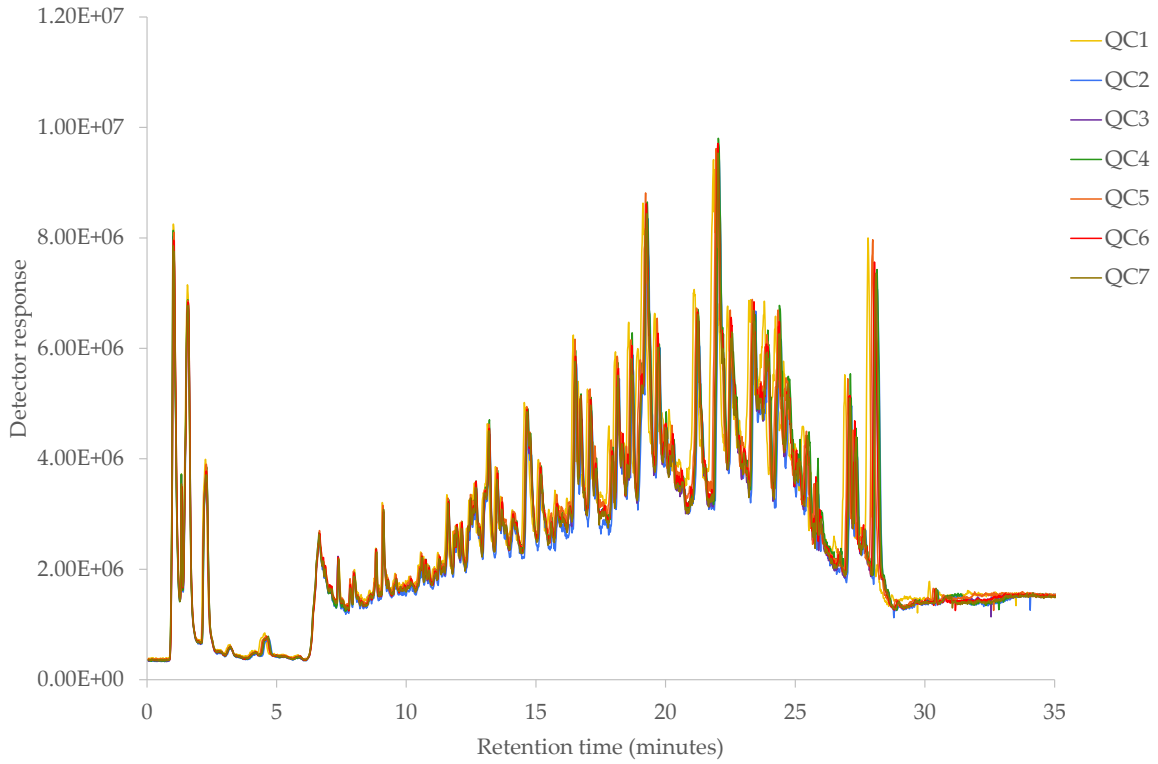

Figure 4.30: Total ion chromatograms of QC samples throughout analytical run for extracts from lamb liver tissue that has undergone multiple freeze-thaw cycles

Figure 4.30 shows overlaid chromatograms of the QC samples injected during this analytical run. These samples appear to be very replicable, with only slight retention time variation in QC1 compared to the other samples. The baseline looks stable throughout the analysis.

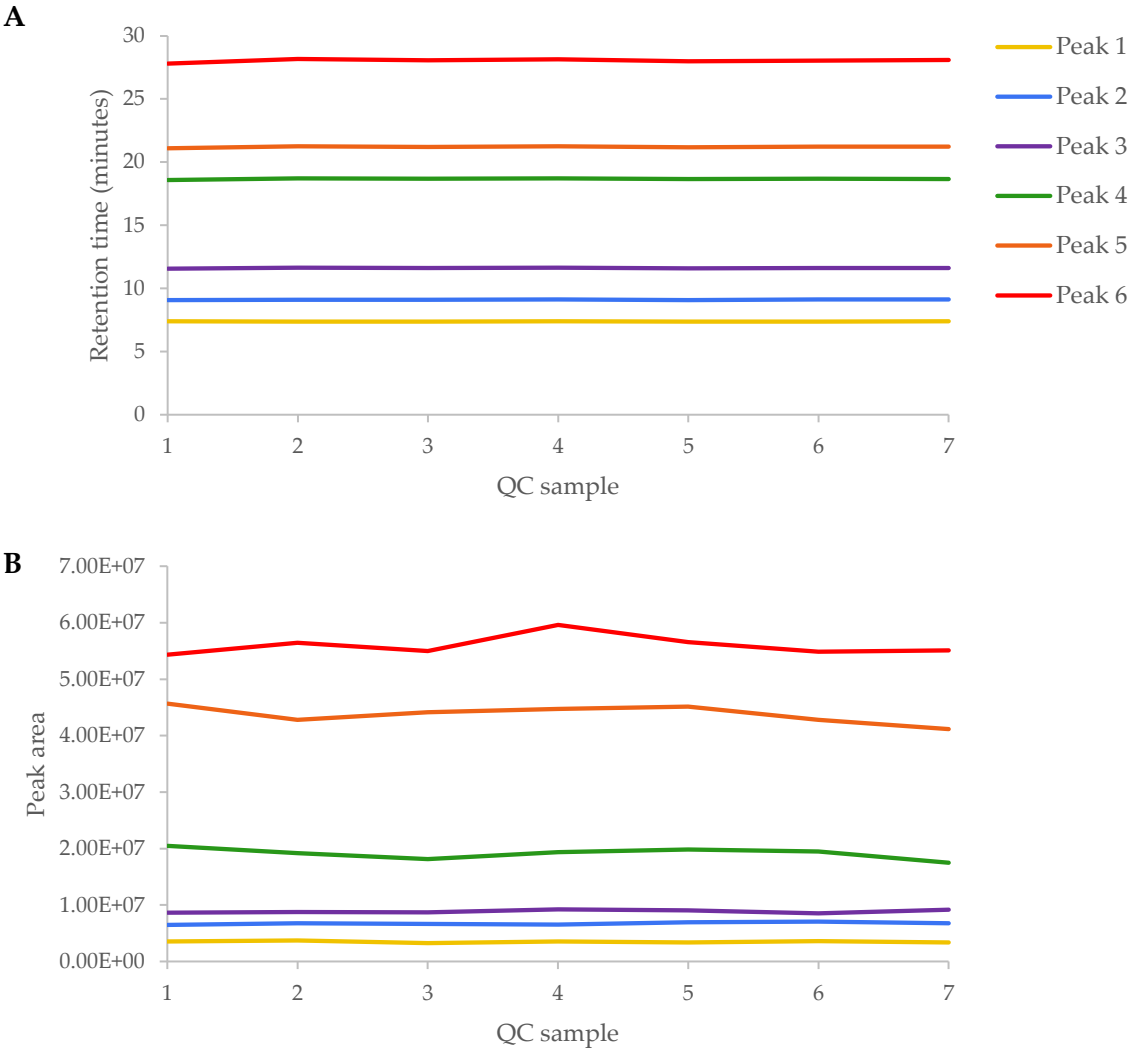

Figure 4.31: Variability of retention time (A) and peak area (B) of 6 peaks in QC samples throughout analytical run for extracts from lamb liver tissue that has undergone multiple freeze-thaw cycles

After six peaks were selected from the chromatograms for the QC samples, Figure 4.31 illustrates the stability of the retention time and the peak area. It can be seen that all six peaks are stable in retention time and peak area in the QC samples.

Table 4.23: Variability of retention time and peak area of 6 peaks in chromatograms of QC samples during the analysis of extracts from lamb liver tissue that has undergone multiple freeze-thaw cycles

	Retention time (minutes)									
Peak	QC1	QC2	QC3	QC4	QC5	QC6	QC7	SD	Average	CV%
1	7.40	7.36	7.36	7.38	7.36	7.37	7.38	0.01	7.37	0.20
2	9.08	9.10	9.10	9.12	9.08	9.11	9.12	0.02	9.10	0.18
3	11.57	11.64	11.62	11.63	11.59	11.62	11.61	0.02	11.61	0.21
4	18.58	18.72	18.69	18.71	18.65	18.68	18.67	0.05	18.67	0.25
5	21.10	21.26	21.21	21.25	21.17	21.22	21.23	0.06	21.21	0.26
6	27.81	28.16	28.07	28.15	27.98	28.04	28.10	0.12	28.04	0.43
	Peak area									
Peak	QC1	QC2	QC3	QC4	QC5	QC6	QC7	SD	Average	CV%
1	3574228	3708073	3262714	3542251	3382035	3595878	3373114	155755	3491185	4.46
2	6462373	6770731	6667240	6545422	6920318	7042512	6766406	202442	6739286	3.00
3	8653838	8785081	8726388	9202886	9034916	8544282	9180142	262885	8875362	2.96
4	20475735	19179053	18147363	19385829	19863323	19462456	17472104	1019846	19140838	5.33
5	45688377	42793587	44119769	44711041	45139183	42821341	41145775	1597002	43774153	3.65
6	54326761	56465912	55008691	59604636	56560684	54852402	55098479	1799815	55988224	3.21

The retention time variability was between 0.18 and 0.43% and the peak area variability was between 2.96 and 5.33%. These values confirm that the instrument was stable throughout, and the data collected from this analytical run was reliable.

4.7.6.2 Metabolic fingerprinting

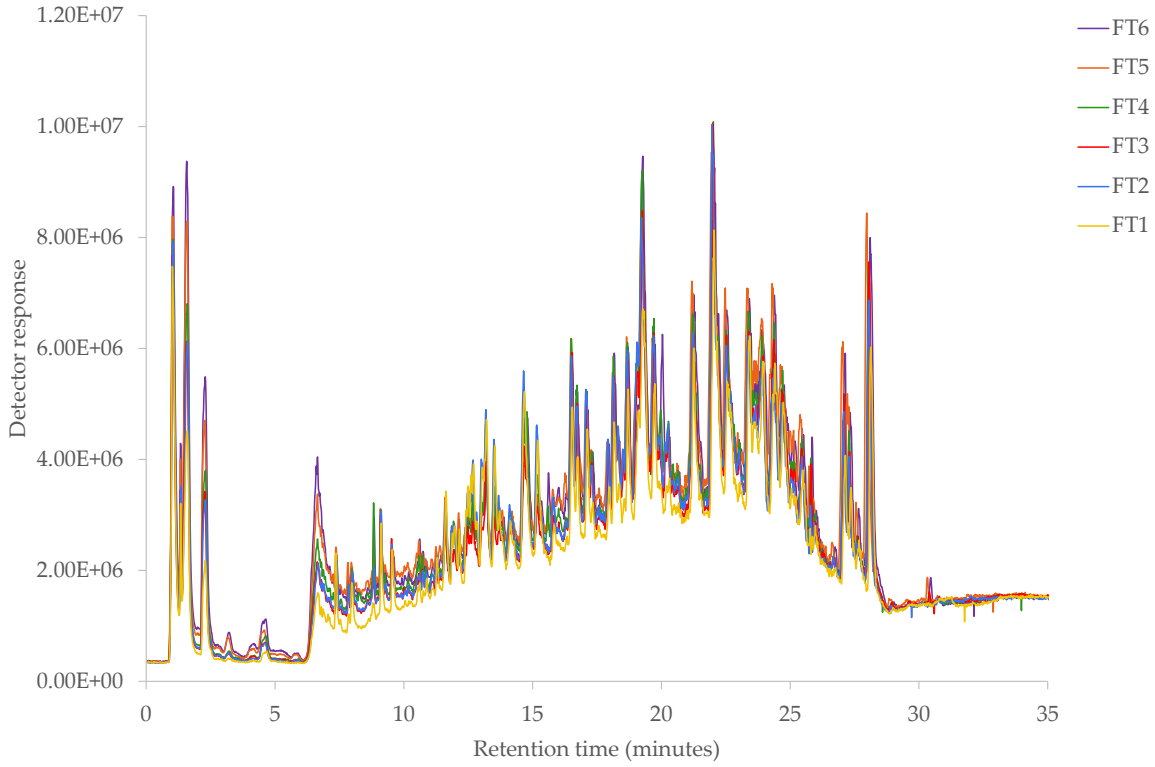

Figure 4.32: Example total ion chromatograms for extracts from lamb liver tissue that has undergone multiple freeze-thaw cycles

The overlaid chromatograms for the lamb liver extracts in Figure 4.32 contain many peaks, showing the metabolic profile of liver tissue is quite complex. On observation, the number of freeze-thaw cycles does appear to have had an effect on the abundance of some of these peaks. The first ten minutes of the chromatogram visibly shows the abundance of the peaks increasing as the number of freeze-thaw cycles increases, specifically at 2, 3, 4.5 and 7 minutes. In general, the total ion count appears to increase as the number of freeze-thaw cycles increases, and this can be seen by the elevated baseline. Between 11 minutes and 15 minutes, the FT1 and FT2 samples appear to have the highest abundance for most peaks, and then from 15 minutes onwards, the majority of the peaks have the highest abundance in the FT5 and FT6 samples, especially in the peaks at around 19 minutes and 28 minutes.

4.7.6.3 Multivariate statistics

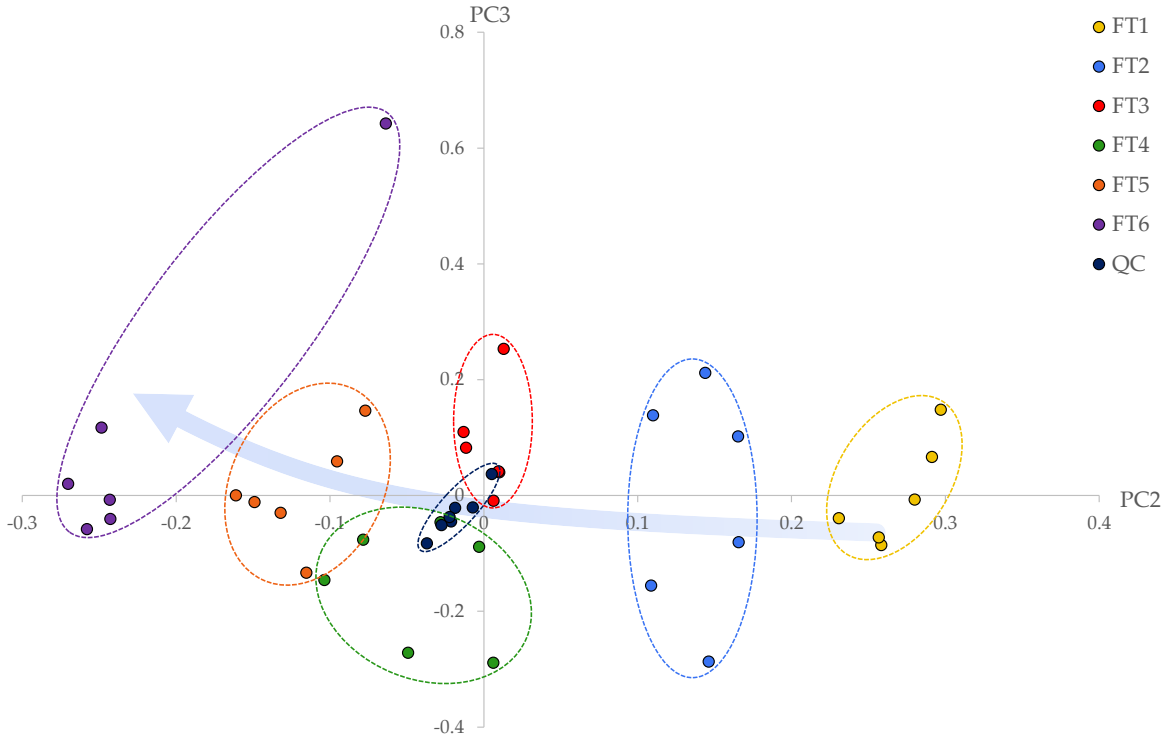

Figure 4.33: Principal component analysis scores plot of PC2 (2.748%) and PC3 (0.377%) for extracts from lamb liver tissue that has undergone multiple freeze-thaw cycles. PCA was carried out using markers with a p-value of < 0.05 and CV $< 10\%$

The PCA plot for the liver samples that have undergone a different number of freeze-thaw cycles (Figure 4.33) shows each sample type grouped together. The FT1 samples in yellow are clustered on the right hand side of the plot, with the FT2 samples clustered next in blue. The groupings go across the plot along the x-axis, increasing in the number of freeze-thaw cycles, ending with the FT6 samples on the left in purple. This trend, shown by the blue arrow, shows that it could be determined whether meat has undergone multiple freeze-thaw cycles based purely on the overall metabolic profile using multivariate statistics, however this trend would need further research. Again, the QC samples are tightly grouped, and the separation between FT1 and FT2 and the rest of the sample types is greater than the spread within the QC samples, showing any differences are caused by metabolic differences and not by instrumental instability or drift.

4.7.6.4 Significant markers

The markers found to be significantly different between all samples of liver that had undergone 1-6 freeze-thaw cycles are shown in Table 4.24. The majority of markers decreased as the number of freeze-thaw cycles increased, which is different to what was observed in the chicken muscle samples.

Table 4.24: Summary of remaining compounds from top 50 markers that were significantly different among all lamb liver tissue samples that have undergone multiple freeze-thaw cycles, in order of significance from manual ANOVA. Arrow indicates marker increased or decreased the more freeze-thaw cycles the liver had undergone

m/z	Retention time median (mins)	P-value from ANOVA/Welch (XCMS)	CV% (XCMS)	P-value from ANOVA/Welch (EICs)	CV% (EICs)
↓ 303.6476	12.40	<0.001	4.84	<0.001	5.13
↓ 272.6665	14.62	<0.001	8.50	<0.001	15.92
↓ 219.0261	0.98	<0.001	3.71	<0.001	4.13
↓ 279.6475	12.60	<0.001	5.25	<0.001	5.11
↑ 598.4156	12.28	<0.001	4.89	<0.001	4.95
↓ 291.6458	12.49	<0.001	4.24	<0.001	4.76
↓ 278.6395	11.30	<0.001	5.69	<0.001	12.61
↓ 568.3398	12.40	<0.001	1.05	<0.001	1.47
↑ 430.2981	15.36	<0.001	1.27	<0.001	1.57
↓ 258.6241	11.63	<0.001	7.16	<0.001	19.68
↓ 280.6568	14.62	<0.001	3.14	<0.001	6.06
↓ 528.8234	14.65	<0.001	8.56	<0.001	11.29
↓ 621.3068	10.02	<0.001	9.25	<0.001	18.92
↓ 564.3072	11.27	<0.001	5.77	<0.001	8.81
↓ 570.3557	13.14	<0.001	1.26	<0.001	1.20
↓ 541.3321	14.62	<0.001	9.23	<0.001	6.12
↓ 271.6574	12.60	<0.001	7.56	<0.001	11.83
↑ 86.09642	0.93	<0.001	7.24	<0.001	4.41
↑ 428.2826	13.36	<0.001	2.38	<0.001	9.83
↓ 344.1299	1.38	<0.001	14.02	<0.001	12.64
↓ 476.2773	10.56	<0.001	1.36	<0.001	3.68
↓ 355.2851	17.56	<0.001	9.69	<0.001	3.30
↓ 572.3705	14.77	<0.001	1.60	<0.001	2.20
↑ 389.3512	14.19	<0.001	2.71	<0.001	4.45
↕ 277.1799	10.75	<0.001	2.13	<0.001	1.86
↑ 452.2827	13.43	<0.001	2.03	<0.001	3.83
↓ 520.3400	12.60	<0.001	1.44	<0.001	1.51

Table 4.24 continued: Summary of remaining compounds from top 50 markers that were significantly different among all lamb liver tissue samples that have undergone multiple freeze-thaw cycles. Arrow indicates marker increased or decreased the more freeze-thaw cycles the liver had undergone

m/z	Retention time median (mins)	P-value from ANOVA/Welch (XCMS)	CV% (XCMS)	P-value from ANOVA/Welch (EICs)	CV% (EICs)
↓ 546.3548	13.61	<0.001	1.72	<0.001	1.93
↓ 537.1601	1.48	<0.001	3.47	<0.001	4.39
↓ 296.6669	13.13	<0.001	16.53	<0.001	27.56
↓ 544.3397	12.49	<0.001	1.00	<0.001	1.34
↓ 148.0024	1.00	<0.001	8.92	<0.001	8.57
↓ 403.2822	16.00	<0.001	5.22	<0.001	10.54
↓ 304.6555	13.52	<0.001	20.72	<0.001	6.91
↓ 478.2927	11.63	<0.001	0.97	<0.001	1.49
↓ 283.6319	12.15	<0.001	5.35	<0.001	5.62
↓ 337.2725	11.62	<0.001	9.20	<0.001	12.62
↓ 539.8161	12.59	<0.001	7.25	<0.001	11.22
↓ 518.3236	11.29	<0.001	1.07	<0.001	6.60
↓ 581.3101	10.99	<0.001	4.07	<0.001	21.17
↓ 575.1223	1.48	<0.001	14.78	<0.001	12.08
↓ 587.8177	12.69	<0.001	12.52	<0.001	9.82
↓ 500.2763	12.02	<0.001	2.97	<0.001	7.71
↓ 123.0520	1.31	<0.001	4.27	<0.001	22.54

4.7.6.5 Tentative identifications

Table 4.25 shows the possible formulae and likelihood score for the markers that were able to generate a formula in *Masshunter Qualitative Analysis*. It also shows the trend of these markers, with most of them decreasing the more freeze-thaw cycles the lamb liver tissue had undergone. No markers were tentatively identified due to the availability of the mass spectra on the METLIN database.

Table 4.25: Predicted formulae and possible identifications of significantly different markers of significantly different compounds in extracts from lamb liver tissue samples that have undergone 1-6 freeze-thaw cycles. Arrow indicates trend of marker

m/z	Retention time median (mins)	Possible formula	Adduct	Likelihood score (%)	Potential METLIN identification
↓ 219.0261	0.98	$C_6H_7ClN_4O_3$	M+H	87.67	
↓ 279.6475	12.60	$C_{31}H_{45}NO_4P_2$	M+2H+2	97.87	
↑ 598.4156	12.28	$C_{34}H_{55}N_5O_2S$	M+H	86.68	
↓ 291.6458	12.49	$C_{30}H_{45}N_5P_2$	M+2Na+2	89.05	
↓ 278.6395	11.30	$C_{23}H_{50}N_3O_3PS_2$	M+2Na+2	84.31	
↓ 568.3398	12.40	$C_{30}H_{50}NO_7P$	M+H	99.18	phosphatidylcholine
↑ 430.2981	15.36	$C_{23}H_{43}NO_4S$	M+H	98.02	
↓ 280.6568	14.62	$C_{26}H_{46}N_3O_8P$	M+2H+2	86.99	
↓ 528.8234	14.65	$C_{25}H_{53}ClN_3PS_2$	M+H	88.62	
↓ 621.3068	10.02	$C_{14}H_{42}N_{18}O_6P_2$	M+H	93.46	
↓ 570.3557	13.14	$C_{30}H_{52}NO_7P$	M+H	99.30	lysophosphatidylcholine
↑ 86.09642	0.93	$C_5H_{11}N$	M+H	87.14	piperidine
↓ 344.1299	1.38	$C_{22}H_{17}NO_3$	M+H	80.85	
↓ 476.2773	10.56	$C_{23}H_{45}N_3OS_3$	M+H	86.90	
↓ 355.2851	17.56	$C_{17}H_{40}N_4S$	M+Na	76.93	
↓ 572.3705	14.77	$C_{33}H_{45}N_7O_2$	M+H	76.24	
↑ 389.3512	14.19	$C_{23}H_{46}N_2O$	M+Na	76.62	
↓ 277.1799	10.75	$C_{17}H_{24}O_3$	M+H	99.72	
↓ 520.3400	12.60	$C_{26}H_{50}NO_7P$	M+H	97.31	phosphatidylcholine
↓ 546.3548	13.61	$C_{28}H_{52}NO_7P$	M+H	96.48	phosphatidylcholine
↓ 537.1601	1.48	$C_{21}H_{28}N_{10}P_2S$	M+Na	90.51	
↓ 296.6669	13.13	$C_{24}H_{51}N_9P_2S$	M+2H+2	86.04	
↓ 544.3397	12.49	$C_{28}H_{50}NO_7P$	M+H	98.26	phosphatidylcholine
↓ 148.0024	1.00	$C_4H_7N_5$	M+Na	87.20	
↓ 478.2927	11.63	$C_{23}H_{47}N_3OS_3$	M+H	82.54	
↓ 283.6319	12.15	$C_{24}H_{35}N_7O_9$	M+2H+2	90.18	four amino acid chain
↓ 337.2725	11.62	$C_{17}H_{37}NS_2$	M+NH_4	83.35	
↓ 518.3236	11.29	$C_{27}H_{52}NO_2PS_2$	M+H	89.56	
↓ 575.1223	1.48	$C_{27}H_{28}N_4O_3S_3$	M+Na	79.80	
↓ 500.2763	12.02	$C_{28}H_{46}Cl_2NP$	M+H	81.12	

Despite not achieving a tentative identification for any of these markers, some molecular formulae did match specific classes of compounds. Markers with an *m/z* of 520.3400, 544.3397, 546.3548 and 568.3398 all had predicted formulae that matched phosphatidylcholine compounds. All of these markers decreased as the number of

freeze-thaw cycles increased, as seen in Figure 4.34, which is different to the chicken muscle samples. This trend could have been found because phosphatidylcholine contributes to cell membranes, and so as these break down, phosphatidylcholine continues to break down into glycerophosphocholine, releasing fatty acids. The difference in trends could be caused by a difference in the rate of metabolism in the two tissue types.

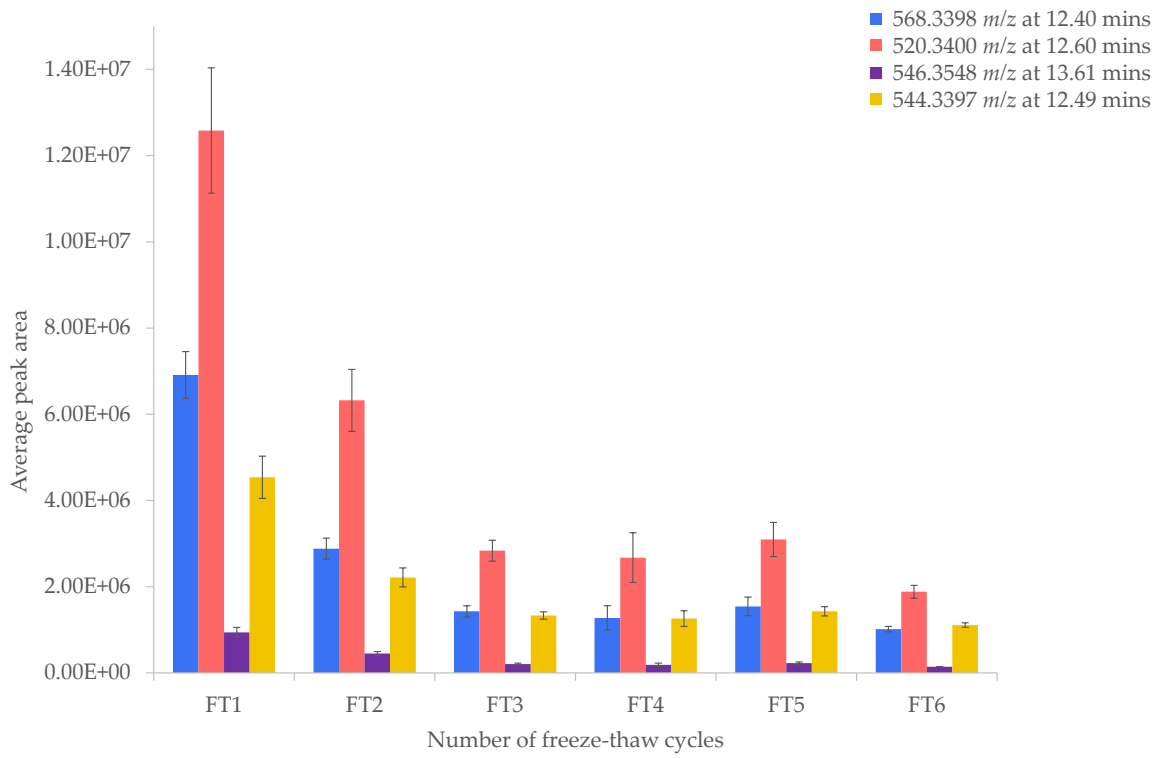

Figure 4.34: Trends of four markers with formulae that matched phosphatidylcholines that were significantly different among all lamb liver tissue samples that have undergone multiple freeze-thaw cycles. Error bars correspond to ± 1 standard deviation

4.8 Conclusions

The data gathered in this work has shown to be reproducible and reliable, and this was confirmed through the use of quality control samples injected throughout each analytical run. In all analyses, the QC samples had minimal retention time and peak area variability, and the implementation of QC samples proved to be a successful way to monitor the reliability of the data obtained.

The multivariate statistics employed in this research was most successful when investigating freeze-thaw cycling, where all groups were separated from each other in both the chicken muscle and lamb liver extract analyses. Consequently, this technique could be used to determine whether meat has previously undergone a freeze-thaw cycle, and potentially how many.

The statistical approaches used in this research were able to find markers that were significantly different in each analysis, however due to the nature of the statistical tests, the trends of these markers sometimes appeared quite random and did not prove to be of interest. Ideally, a statistical test to discover the markers that have an increasing or decreasing trend as the frozen storage time period increased would have been more beneficial, however this is not possible to do with such a large dataset and would have required manual statistics for each individual marker prior to any reduction of the size of the dataset. For the purpose of this untargeted analysis, ANOVA was suitable to detect markers that were significantly different overall, and despite meaning this detected a large number of markers that were not suitable to determine the frozen storage time period due to the erratic trends, it did find a small number of markers that could be further investigated for this purpose.

When investigating the length of frozen storage time, it was clear from the chromatograms that the lamb liver tissue samples contained the most number of

small molecules, and the chicken muscle tissue and lamb muscle tissue contained a similar amount to each other. The multivariate statistics showed some group separation, however there was a lot of overlapping sample types in all datasets. Nevertheless, it was able to separate the fresh samples from the frozen samples in the chicken muscle dataset and the lamb liver tissue dataset.

In the experiment involving multiple freeze-thaw cycles, it was found that both chicken muscle and lamb liver change in metabolic content depending on how many freeze-thaw cycles they have undergone. Specifically, as the number of freeze-thaw cycles increased, the majority of markers in the chicken increased, and the majority of markers in the liver decreased. This could be caused by a difference in the rate of degradation in these tissue types. Specifically, both the chicken muscle and the lamb liver extracts showed changes in the concentration of phosphatidylcholines, however the trends for these compounds were different in the two tissue types. The chicken muscle had increasing concentrations of these compounds, and the lamb liver had decreasing concentrations. The liver tissue could be degrading more rapidly than the chicken muscle tissue, causing phosphatidylcholine to already be decreasing as it converts to glycerophosphocholine and fatty acids. The chicken muscle could be degrading slower and still releasing phosphatidylcholines during cell degradation, which was observed in the increasing trend in this experiment. Further investigations would be needed in order to better understand the complex nature of the degradation processes in the soft tissues after death, and how this could affect the nutritional value of meat. In particular, monitoring the metabolic changes in different tissue types from the same animal could help to discern the differences in the rate of degradation.

Investigating the effect of freeze-thaw cycling in chicken muscle tissue obtained a marker that was tentatively identified as either linoleic acid or linoelaidic acid. Further research would be required to confirm which fatty acid this marker was,

especially due to the vast amount of evidence proving that linoelaidic acid could have severe health implications for the consumer.

This untargeted study has shown that the metabolic profile does change depending on the length of frozen storage time as well as the number of freeze-thaw cycles, and that these techniques could be developed in order to specifically determine these parameters and assist in detecting subtle frauds that involve the mislabelling of meat products. Additional investigations would be needed in order to identify specific markers, or the technique could be adapted to focus specifically on the lipid profile as this class of compound appeared to be of most interest in this study. This experiment investigated the frozen storage time and number of freeze-thaw cycles using tissue from one animal at a time, however a repeated study with different animals of the same species could provide a deeper insight into whether the changes in metabolic profile can still be observed despite differences in metabolic profile due to biovariability.

Chapter 5

The detection of adulterated meat products with other meat species

This work investigated the difference in metabolic content between species and how this can aid in the detection of adulterated meat products. Different percentages of adulterant meat were investigated, as well as the adulteration of minced beef of different fat contents, and whether the detection of adulterant meat is affected by the meat being cooked or raw.

5.1 Introduction

The United Kingdom has a clear law on the labelling of meat products; in The Meat Products (Hygiene) Regulations 1994, it states that all meat products must be labelled with the "species of meat used in the manufacture of the product". The substitution of meat products for financial gain is not only an economic issue, but also a problem for religious communities and people with allergies. Additionally, consumers have the right to make an informed decision on their purchases.

Within the Muslim and other religious communities, certain food is prohibited under strict dietary laws laid out in religious texts, specifically any product derived from pigs [139]. Pork meat is readily available and inexpensive, and is ideal to use when adulterating or substituting high-price meat items, which is especially easy with minced meat products as the original cut of meat is no longer visible [140]. These consumers must be able to have confidence in the meat products they purchase, and

due to mislabelling, robust methodologies for authenticating meat products must be developed.

There is a vast array of techniques targeting the issue of adulterating meat products with other meat species, the largest being protein- and DNA-based techniques. Enzyme-linked immunosorbent assay (ELISA) has been implemented for the detection of meat substitution with different species and with different tissue types [59]. The discrimination between pork, beef, lamb and poultry was achieved with the use of ELISA, however due to the multiple variables associated with processed food products, such as fat content, processing temperatures, and muscle origin, the level of detection may be different from one product to another [22]. Another ELISA technique has been developed to detect porcine skeletal muscle in raw, cooked and autoclaved samples, and is able to specifically discriminate porcine skeletal muscle from cardiac muscle, smooth muscle, blood, and organs [141]. Protein-based techniques have proven to be fast with limited sample preparation, and useful in developing rapid on-site testing. Nevertheless, these techniques are not suitable for reliable and robust testing of processed meat products, where the manufacturing of these products involves subjecting the meat to high temperatures. This causes the denaturation of the proteins, making these techniques unsuitable. DNA techniques are more advantageous than protein-based techniques when analysing processed meat products that have undergone heating processes as the short fragments of DNA are still able to be obtained. There are many different methods that can use DNA in order to determine the species of a meat product, including polymerase chain reaction (PCR) based methods, restriction fragment length polymorphism (RFLP) assays, real-time PCR, and random amplified polymorphic DNA (RAPD) PCR [142]. DNA hybridisation techniques have been used in the past for the identification of meat products, however this is a complicated and insufficient method. PCR is more time efficient, and has been utilised in distinguishing between beef, pork, chicken, lamb, goat, and horse [143]. A quick

multiplex PCR method has been created that was able to identify six meats at the same time, and investigated the effect of cooking on the results, however the primer selection is more critical in multiplex PCR studies compared to conventional PCR assays. Also, this study only investigated cooking at temperatures up to 120°C and showed the PCR products were considerably more faded on the gel electrophoresis results. Meat is usually cooked at much higher temperatures than this, indicating this method would not be very useful for detecting different meat species in meat products once cooked. RFLP has been successfully used to identify 10 salmon species, where a length of DNA was exploited that is still intact after processing, which could be useful in detecting adulteration of processed salmon products [144]. Several real-time PCR techniques have been successful in detecting different meat species in meat products, in particular with the use of the EvaGreen dye and a TaqMan fluorescent probe. The detection of low levels of horse meat in beef products was achieved with EvaGreen fluorescent dye [145]. In China, there has been an increase in meat fraud where mutton meat has been substituted with meat from rodents. The TaqMan probe has been successfully utilised to detect small traces of rodent meat down to 0.1% in a mutton meat mixture, showing how sensitive this technique is [146]. Despite all this valuable and reliable research, DNA can still degrade substantially during the processing of the meat product, and can become undetectable [147], as well as the data-mining being difficult to carry out after analysis [148]. Techniques that do not involve the collection of DNA would be more universally applicable to all types of meat products.

Spectroscopic methods have been investigated for these types of frauds. Ultraviolet-visible, near infrared and mid-infrared spectroscopy have been used to detect turkey meat in minced beef, and it was found that a combination of these techniques was most suitable for preliminary testing of suspected adulterated meat products [149]. The application of Fourier transform infrared spectroscopy to the detection of rat meat in beef meatballs has been carried out, proving this technique is

beneficial in finding this fraudulent activity [150]. This technique has also been successful in determining the presence of pork fat in meatballs, which is an extremely important issue within religious communities [151]. These studies also showed the importance of coupling techniques with advanced chemometrics in order to visually interpret the results with the intention of creating a predictive model for unknown samples. Another spectroscopic technique that has been successful in discriminating horsemeat from beef is Raman spectroscopy, where PCA analysis proved to be appropriate to illustrate the difference in the percentage of horsemeat [152]. Spectroscopic techniques have many advantages; they are non-destructive, require minimal sample preparation, and are quick. However, they do not allow for the potential of identifying the compounds that cause the differences.

There has been limited research in the use of liquid chromatography-mass spectrometry for detecting adulteration of meat products.

5.2 Experimental procedures

5.2.1 Materials

Acetonitrile (HPLC grade), methanol (HPLC grade) and dichloromethane (analytical grade) was purchased from VWR (East Grinstead, UK), and ultra-pure water (18.2 MΩ) was purified using an in-house Milli-Q system from Elga (High Wycombe, UK). Formic acid (laboratory grade) was purchased from Fisher Scientific (Loughborough, UK). ESI-L low concentration tuning mix and API-TOF reference mass solution were purchased from Agilent Technologies (California, USA).

5.2.2 Sample collection

Minced beef, pork, lamb and turkey products were purchased from the national retail outlet, Sainsbury's, and immediately stored at 4°C before processing the following day. Two types of minced beef were purchased based on the fat content; 5% and 20%. Only one type of minced pork, lamb and turkey were used (10%, 10% and 7% fat content respectively) to keep variability to a minimum.

5.2.3 Sample preparation

The minced meat was accurately weighed to produce two sets of 9 meatballs for each type of adulterant meat; one set to analyse raw, and one set to analyse after cooking. Each meatball had a different percentage of adulterant meat, as shown in Table 5.1. From this point on, the meatballs will be referred to based on the percentage of adulterant meat, except for meatballs with 100% beef. Extraction was carried out on one set of meatballs immediately after sample preparation. The other set of meatballs were cooked on the same day as preparation at 200°C for 20 minutes, allowed to cool, and then stored at 4°C. The extraction was carried out the day after cooking.

Table 5.1: Sample preparation for adulterated meatballs

Meatball	Fat content in beef	Beef %	Adulterant meat %
1	5%	100	0
2		90	10
3		75	25
4		50	50
5	20%	100	0
6		90	10
7		75	25
8		50	50
9	n/a	0	100

5.2.4 Metabolite extraction

A small section from the middle of each meatball was homogenised with surgical scissors, and approximately 110 mg was placed into an Eppendorf tube. Methanol/H_2O (1:1) was added (1 mL per 100 mg of sample), then the sample was sonicated for 10 minutes and centrifuged at 16100 rcf for 20 minutes. The supernatant was then moved to a glass vial and retained as the aqueous (AQ) extract. The tissue pellet was broken up using a clean pipette tip, and dichloromethane/methanol (3:1) was added (1 mL per 100 mg of sample). The sample was sonicated for 10 minutes and centrifuged at 16100 rcf for 20 minutes, and 1 mL of the supernatant was then moved to a glass vial and allowed to evaporate overnight, then resuspended in 1 mL of methanol. This was retained as the organic (OR) extract. This two-part metabolite extraction was carried out 3 times to get replicate samples. Both the aqueous and organic extracts were stored at -25°C prior to analysis.

5.3 Instrumental set-up

5.3.1 Analytical considerations

Quality control samples were made for each analytical run, consisting of an equal aliquot of every sample within each run. At the start of each analytical run, 10 QC samples were injected at a volume of 10 μL, then 20 QC samples at an injection volume of 3 μL were injected to condition the column. All non-QC samples were randomised to eliminate any issues arising from instrumental drift.

5.3.2 Chromatographic parameters

Chromatographic separation of the extracts was performed with a Thermo Scientific Hypersil GOLD aQ column (100 mm x 2.1 mm, particle size of 1.9 μm) using an Agilent 1260 Binary Pump HPLC. The column was maintained at 40°C and the injection volume was 3 μL. The flow rate of the mobile phase was 0.3 mL/min and consisted of 0.1% formic acid (solvent A) and acetonitrile with 0.1% formic acid (solvent B). The chromatographic gradient method can be seen in Table 5.2. A needle wash method was included after every injection, consisting of 3 separate vials of methanol, each used in a specific order, with 3 washes per vial. The column was flushed with 100% organic solvent after each run to reduce any potential carryover.

Table 5.2: Solvent gradient method used for analysis of organic extracts from all sample types

Time (mins)	Solvent A (%)	Solvent B (%)
0	95	5
2	95	5
3	47.5	52.5
30	0	100
40	0	100
41	95	5
50	95	5

5.3.3 Q-TOF parameters

For the analysis, an Agilent Technologies 6530 Accurate Mass Q-TOF was used with an electrospray ionisation source, and the parameters were set as shown in Table 5.3. The reference mass solution was continually run through the analysis, and used purine (121.0509 *m/z*) and hexakis (1H, 1H, 3H-tetrafluoropropoxy)phosphazine (922.0098 *m/z*) in positive ionisation mode as internal reference masses to ensure mass accuracy. The data was collected in both profile and centroid mode.

Table 5.3: Q-TOF parameters used in this experiment

Parameter	Setting
Drying gas temperature	320°C
Drying gas flow rate	11 L/min
Capillary voltage	4000 V
Fragmentor voltage	125 V
Skimmer voltage	65 V
Mass range	100-1000 *m/z*

5.4 Data pre-processing

The data was pre-processed using *XCMS Online*. The parameters for the method used on this online platform were set to the default settings specifically designed by *XCMS Online* for analyses carried out with HPLC and ESI-QTOF-MS instruments, and were as shown in Table 5.4. This software also carried out normalisation of the raw data using the median fold change method. A feature table was produced, which included a list of *m/z* values and their median retention times, and the peak areas for these features in each sample.

Table 5.4: Parameter settings for *XCMS Online* used in this experiment

XCMS method	Parameter	Setting
Feature detection = CentWave	ppm	30
	min peak width (seconds)	10
	max peak width (seconds)	60
	mzdiff (*m/z*)	0.01
Retention time correction = Obiwarp	profStep (*m/z*)	0.5
Alignment	bw (seconds)	5
	minfrac	0.5
	mzwid	0.025

5.5 Statistical analysis

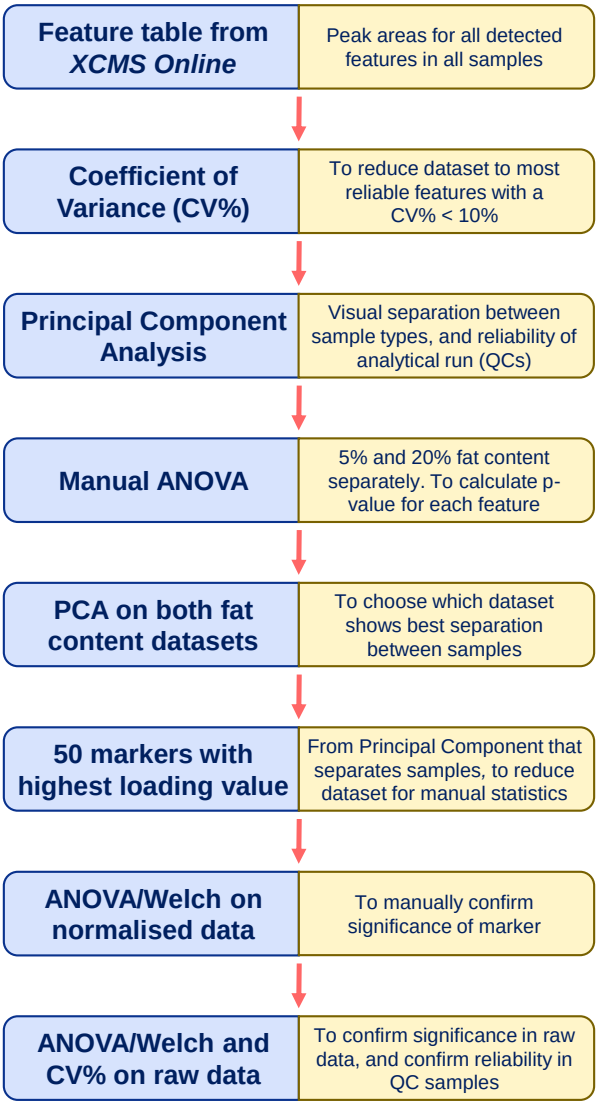

Figure 5.1: Statistical workflow for all datasets analysing extracts from beef samples adulterated with other meat species

The standard deviation, average, and coefficient of variance percentage were calculated using the peak areas of each feature in the QC samples throughout the analytical run. All features that had a CV% of more than 10% were removed. A principal component analysis with standardisation was carried out using the Multivariate Analysis add-in for *Microsoft Excel 2010* [85], and a scores plot was produced in order to visualise any separation between sample types, and to gain an

understanding of the comparison of beef with different fat contents. The first six principal components were plotted in all combinations to find the components that best represented the separation of the sample types. Focussing on each fat content dataset separately (5% fat content and 20% fat content), a manual ANOVA test in *Microsoft Excel* was carried out on the peak areas of each sample in order to get a p-value for each feature. After removing all features that were not significantly different, additional principal component analyses with standardisation were carried out, and scores plots were created for each beef fat content type separately, to ascertain whether 5% or 20% fat content in beef showed the most difference among adulterated beef samples. The dataset that showed the best separation was the single dataset used for the rest of the analysis. The principal component that represented the separation between sample types was used to find the top 50 markers that were most responsible for this separation, based on the loading values. These were analysed in *SPSS*, in order to verify their significance, where either ANOVA or Welch tests were performed, depending on the homogeneity of variance value for each marker. The tests were carried out with a confidence level of 95%, giving an α value of 0.05. If the p-value was less than the α value, it indicated the abundance of that marker in the sample groups was statistically different.

The raw data was then analysed in *Masshunter Qualitative Analysis* (Agilent Technologies) to produce extracted ion chromatograms (EICs) for the markers that were confirmed to be significantly different. ANOVA or Welch tests in *SPSS* were carried out on the peak areas of the EICs, as well as CV% of the QC samples. This process ensured the markers were significant even before normalising the data in the pre-processing step. Any markers that were found to not be significantly different or had a CV% in the QC samples of more than 30% were removed. This additional step in the methodology ensured the final markers were robust and reliable, with the intention of being able to confidently use these markers as an indicator of adulterated beef products with pork, lamb or turkey.

5.6 Identification of markers

The potential formulae predicted by *MassHunter Qualitative Analysis* were used to search the METLIN database manually. A tentative identification was made based on the comparison of the mass spectrum of the sample and mass spectra of compounds with the same formulae on the METLIN database, if available. If a tentative identification could not be made, an idea of the class of compound could be determined based on the predicted formulae matching to a number of similar compounds on the METLIN database.

5.7 Results and discussion

5.7.1 Raw minced beef adulterated with minced pork

5.7.1.1 Quality control

Both the raw and cooked samples were analysed in the same analytical run, and so the quality control sample analysis applies to both datasets.

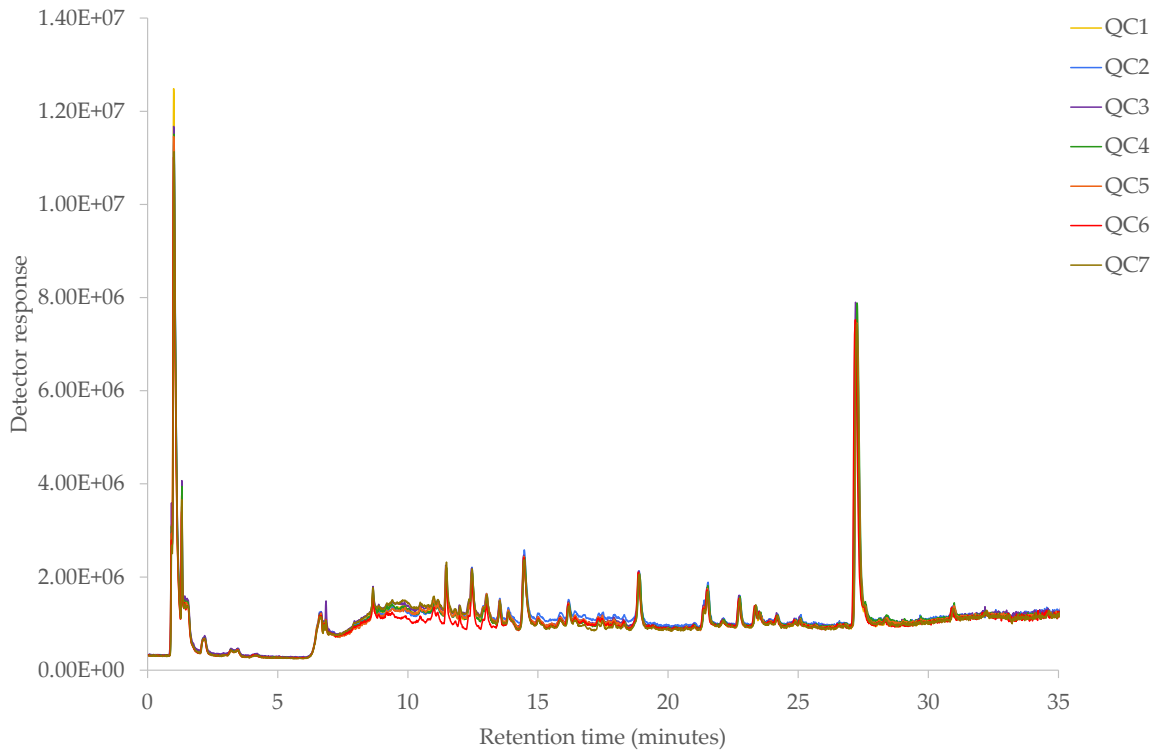

Figure 5.2: Total ion chromatograms of QC samples throughout analytical run for extracts from minced beef adulterated with minced pork

The quality control samples that were injected throughout the analytical run appeared mostly stable when overlaid (Figure 5.2). There is some slight baseline variation from 7 to 20 minutes, however the samples were randomised so this effect will be minimised on the dataset as a whole.

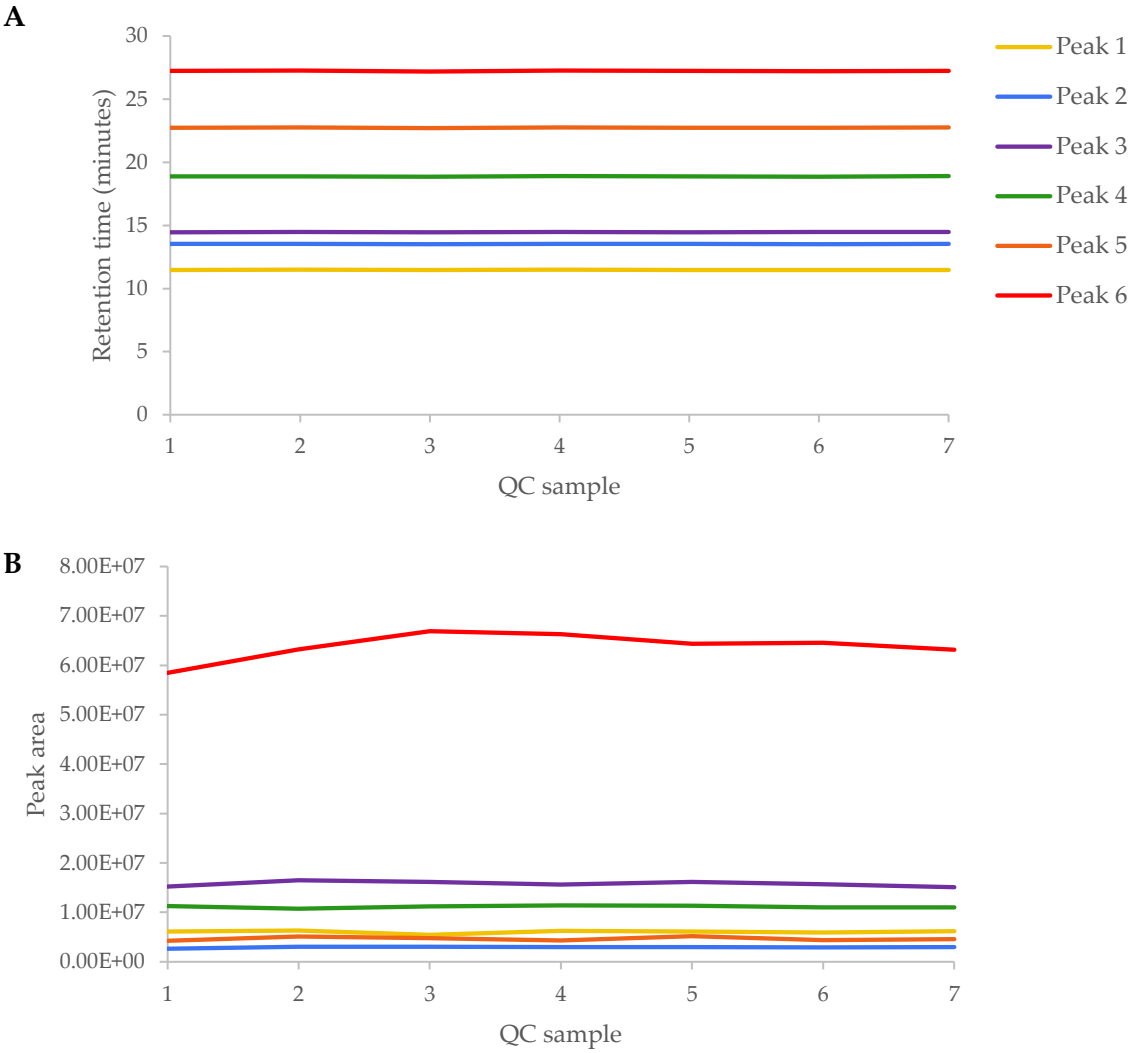

Figure 5.3: Variability of retention time (A) and peak area (B) of 6 peaks in QC samples throughout analytical run for extracts from minced beef adulterated with minced pork

Throughout the chromatograms, 6 peaks were selected at varying retention times and peak intensities to assess the stability of the analytical run. Figure 5.3 shows that the retention time was very stable in the QC samples for all peaks, and the peak areas showed minimal variation.

Table 5.5: Variability of retention time and peak area of 6 peaks in chromatograms of QC samples during the analysis of extracts from minced beef adulterated with minced pork

	Retention time (minutes)									
Peak	QC1	QC2	QC3	QC4	QC5	QC6	QC7	SD	Average	CV%
1	11.46	11.49	11.46	11.49	11.48	11.48	11.48	0.01	11.48	0.11
2	13.54	13.53	13.51	13.54	13.53	13.52	13.54	0.01	13.53	0.09
3	14.46	14.47	14.46	14.49	14.46	14.47	14.47	0.01	14.47	0.07
4	18.89	18.89	18.87	18.90	18.88	18.86	18.90	0.02	18.88	0.08
5	22.74	22.75	22.72	22.77	22.74	22.73	22.75	0.02	22.74	0.07
6	27.24	27.26	27.20	27.26	27.25	27.21	27.24	0.02	27.24	0.09
	Peak area									
Peak	QC1	QC2	QC3	QC4	QC5	QC6	QC7	SD	Average	CV%
1	6082269	6294988	5422940	6251566	6136383	5898173	6176703	300106	6037575	4.97
2	2592657	3046076	2994572	2961451	2960833	2882351	2980394	151103	2916905	5.18
3	15217770	16514430	16162572	15636824	16152800	15661459	15093215	523926	15777010	3.32
4	11250096	10697096	11206374	11418835	11303260	10985421	11011782	243512	11124695	2.19
5	4240450	5124344	4740405	4265987	5200444	4393094	4544781	393319	4644215	8.47
6	58459373	63235499	66900768	66282751	64358133	64573694	63153126	2766751	63851906	4.33

After statistical analysis, it can be seen in Table 5.5 that all 6 peaks had a very small CV% from the retention times of each peak in all QC samples, indicating the retention time variability was minimal. The peak area variability was also small, with all CV% values less than 10%. Due to these results, it can be confirmed that this analytical run was stable throughout, and all data collected was reliable.

5.7.1.2 Metabolic profiling

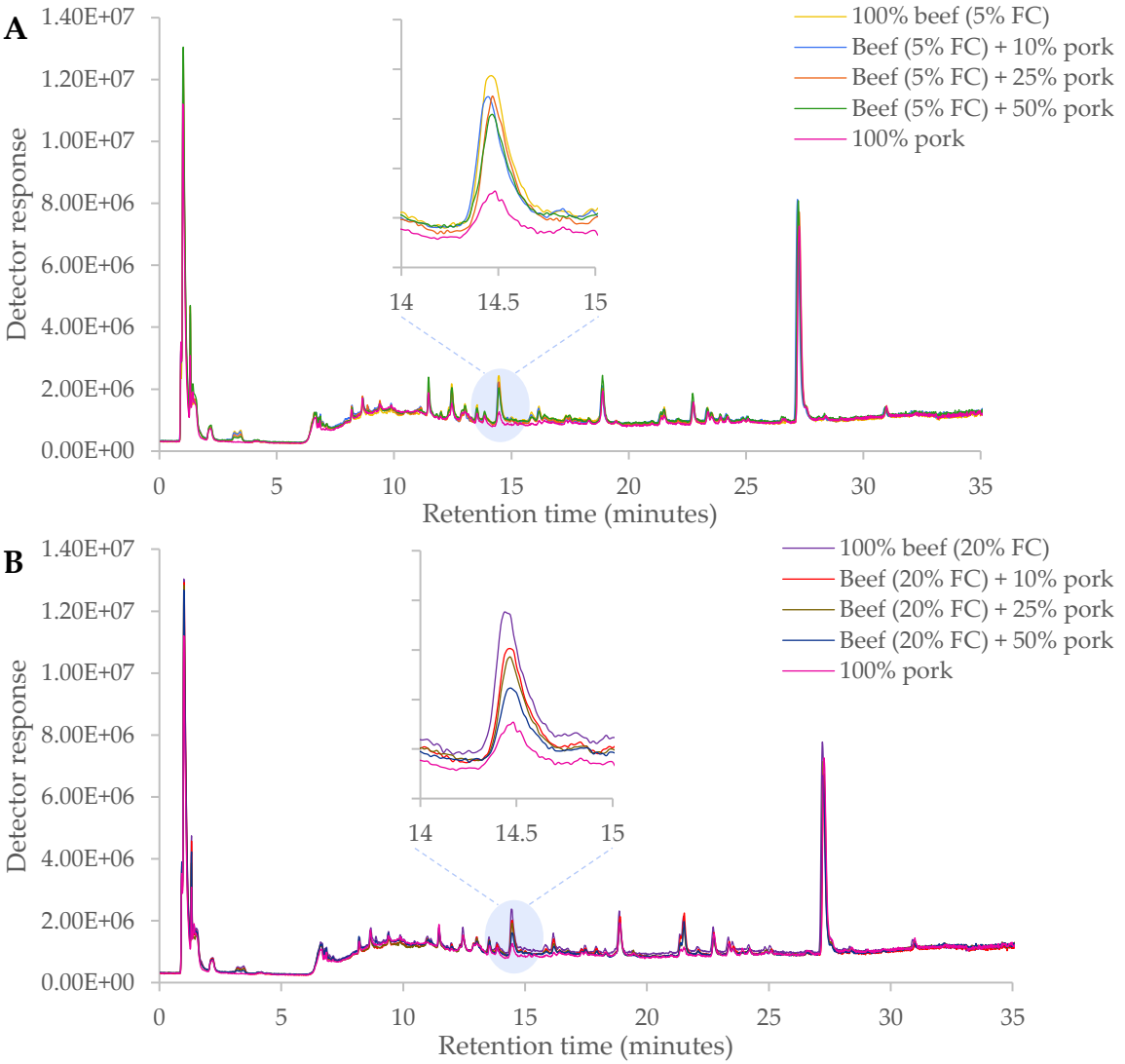

Figure 5.4: Example total ion chromatograms of extracts from raw minced beef adulterated with different percentages of minced pork. A) Beef with 5% fat content, B) Beef with 20% fat content

Looking at the overlaid chromatograms for beef with 5% fat content in Figure 5.4A, the peak pattern appears very similar in all sample types, however there are some differences in peak intensities. Specifically, the peak at 14.5 minutes has a higher intensity in the 100% beef sample and other samples containing adulterant pork meat, and the 100% pork sample has the lowest intensity. Similarly, there are two small unresolved peaks at around 3 minutes that have a noticeably higher intensity in the 100% beef sample, and gradually decreases as the beef percentage decreases, with

the 100% pork sample having no peak present. Figure 5.4B shows the overlaid chromatograms for beef with 20% fat content, and these show noticeable differences in percentage of adulterant pork. The peak at 19 minutes has the highest intensity in the 100% beef sample, and the lowest intensity in the 100% pork sample, and the peaks at 14.5, 16.5 and 22 minutes have a decreasing trend from 100% beef down to 100% pork. Comparing the chromatograms obtained from 5% and 20% fat content in beef, both follow a very similar peak pattern, however beef with 20% fat content has a larger peak at 22 minutes compared to beef with 5% fat content, and this peak is one that shows a difference in intensity for the different percentages of adulterant pork. The compounds that are eluting in this peak could prove useful in detecting adulterations in beef with a high fat content, but may not be as useful in beef with a lower fat content.

5.7.1.3 Multivariate statistics

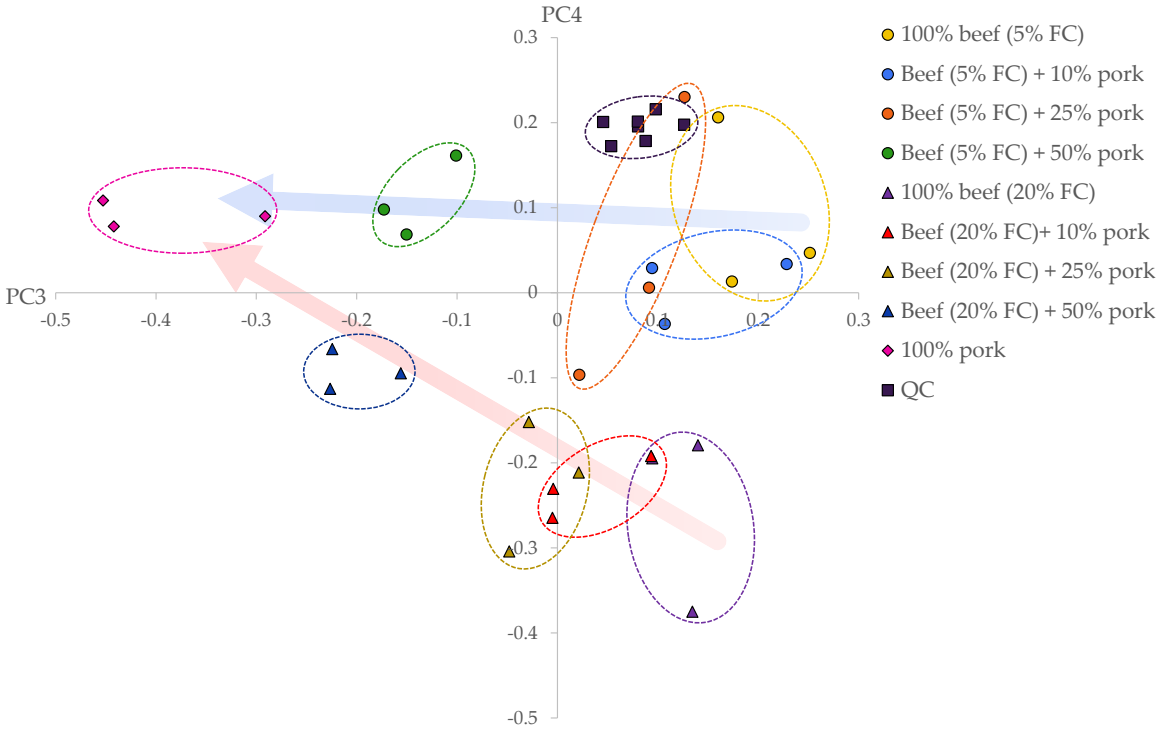

Figure 5.5: Principal component analysis scores plot of PC3 (0.446%) and PC4 (0.138%) for extracts from raw minced beef with 5% and 20% fat content adulterated with different percentages of minced pork. PCA was carried out using all features detected with a CV < 10%

Figure 5.5 shows the samples that were adulterated with different percentages of pork, with the 100% pork samples clustered individually on the left of the plot. It can be seen that for both percentages of fat content, the 100% minced beef and the beef adulterated with 10% and 25% pork were not separated from each other, however the minced beef adulterated with 50% pork were clustered individually for both the minced beef with 5% fat content, and with 20% fat content. The trend of the sample groups moved from the right of the plot to the left as the percentage of adulterant meat increased, as shown by the blue and red arrows. The two minced beef products with 5% and 20% fat content could also be differentiated from each other regardless of the amount of adulteration, illustrating that even the subtle difference of fat content in the same type of meat caused separation in the PCA plot. However, it is important to note that this disparity may not be caused just by fat

content, but could also be due to the manufacturing processes, as these samples originated from different meat products. The quality control samples are tightly clustered, showing the analytical run was stable throughout. This plot indicates there may be a number of markers that differ in concentration between beef and pork.

Manual ANOVA tests were carried out on both datasets individually; beef with 5% fat content, and 20% fat content. PCAs were carried out on significant markers with a CV% in the QC samples of less than 10% to determine which percentage of fat content in beef was most suitable for finding markers that indicate the presence of adulterant meat. It was found that minced beef with a 20% fat content gave the best separation in the PCA scores plot between beef and the meatballs with varying percentages of adulteration. Figure 5.6 shows this separation, with the differences most represented along the x-axis (PC2). The trend of these groups is represented by the blue arrow. This principal component was used to find the top markers that were the most responsible for the differences, based on the loading values.

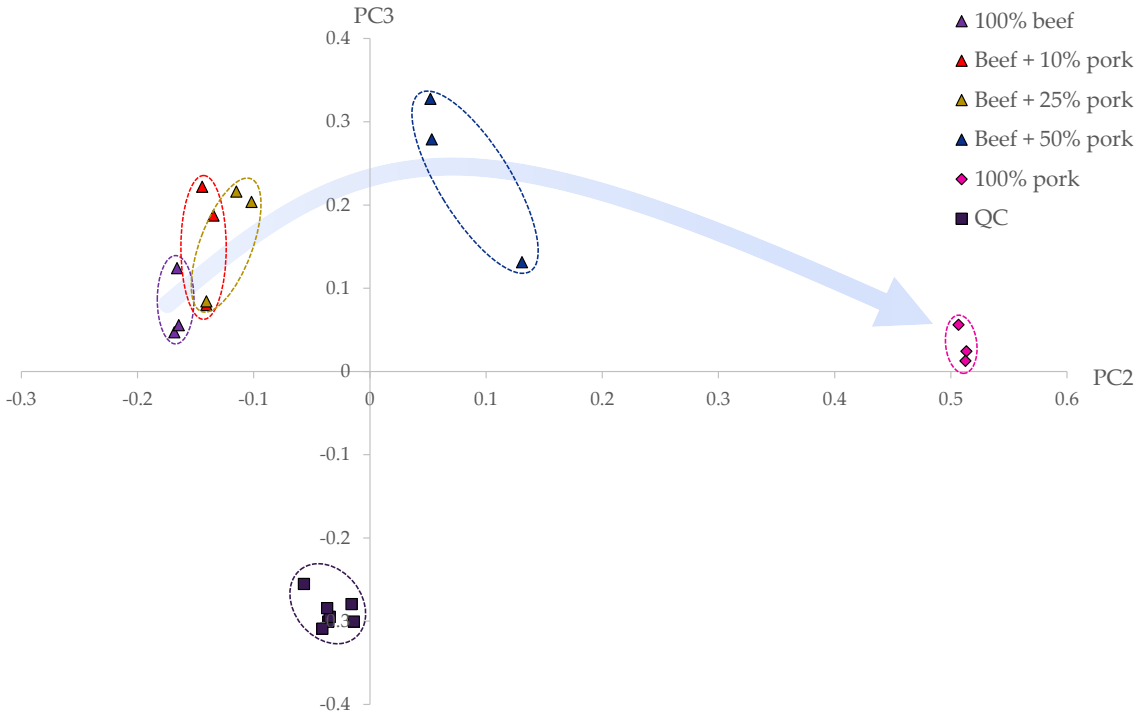

Figure 5.6: Principal component analysis scores plot of PC2 (5.746%) and PC3 (1.492%) for extracts from raw minced beef with 20% fat content adulterated with different percentages of minced pork. PCA was carried out using all markers with a CV $< 10\%$ and a p-value of < 0.05

5.7.1.4 Significant markers

Table 5.6: Summary of compounds that contribute the most to the differences among all extracts from raw minced beef with a 20% fat content that has been adulterated with different percentages of pork, including 100% beef and 100% pork, using PC2.
FC = fat content. Red values indicate p-value > 0.05.
Marker trend: ↓ = decreased, ↑ = increased, * = random or consistent

m/z	Retention time median (mins)	P-value from ANOVA/Welch (XCMS)		CV% (XCMS)	P-value from ANOVA/Welch (EICs)		CV% (EICs)
		5% FC	20% FC		5% FC	20% FC	
↑ 502.2930	11.49	<0.001	0.016	3.96	<0.001	0.007	3.16
↑ 269.0860	1.44	<0.001	<0.001	4.68	<0.001	<0.001	4.44
↑ 482.3550	16.40	0.029	0.002	2.58	0.021	0.006	4.54
↓ 496.3399	14.48	0.001	<0.001	1.32	0.001	<0.001	2.81
* 438.2977	13.87	0.020	0.001	2.03	0.054	0.001	1.63
↑ 249.1457	1.04	<0.001	<0.001	8.24	<0.001	<0.001	5.84
↑ 295.2621	23.90	<0.001	0.003	5.07	<0.001	0.003	4.89
↑ 464.3130	14.38	<0.001	<0.001	1.79	<0.001	<0.001	2.61
↑ 229.1456	1.09	0.001	<0.001	3.57	0.001	0.001	4.74
* 524.3717	18.81	0.092	0.021	3.69	0.008	0.018	5.67
* 466.3289	17.33	0.528	0.001	6.71	0.489	<0.001	7.51
↑ 297.2778	26.54	<0.001	0.001	4.81	0.001	0.005	5.65
↑ 271.2620	26.64	0.001	0.017	6.78	0.001	0.034	6.08
↑ 116.0628	1.06	0.001	0.003	5.15	<0.001	<0.001	4.53
↑ 258.1014	1.06	<0.001	<0.001	5.11	0.001	<0.001	5.03
↑ 265.0711	0.95	0.004	<0.001	6.97	0.014	0.007	7.63
↑ 508.3753	16.85	<0.001	0.002	2.49	<0.001	0.001	3.96
↑ 530.3237	13.30	<0.001	0.005	3.64	<0.001	0.004	2.94
↓ 147.0690	1.08	<0.001	<0.001	7.35	<0.001	<0.001	7.83
↑ 241.1513	1.51	0.045	0.045	8.45	0.139	0.027	7.53
↓ 544.3394	12.36	<0.001	<0.001	2.67	<0.001	0.003	2.82
* 583.3238	13.06	0.002	0.011	2.54	0.004	0.004	1.94
↑ 440.3116	13.98	0.012	<0.001	1.16	0.038	0.001	1.90
↑ 220.1169	2.37	<0.001	<0.001	5.03	<0.001	<0.001	5.28
↑ 319.2624	22.96	<0.001	0.001	5.13	<0.001	0.002	6.39
↑ 389.1661	0.96	0.003	0.008	9.12	0.006	<0.001	16.28
↑ 466.3266	14.43	<0.001	<0.001	2.94	<0.001	<0.001	5.67
↑ 452.3130	15.49	0.004	<0.001	2.71	0.006	0.006	4.79
↑ 300.2885	13.26	<0.001	0.007	5.79	<0.001	0.002	5.07
* 269.2477	23.17	0.001	0.003	7.06	<0.001	0.002	8.07
* 211.2045	17.48	0.008	0.008	6.03	0.009	<0.001	6.43
↑ 144.0932	1.06	0.051	0.014	4.41	0.013	0.009	4.65

Table 5.6 shows markers that were significantly different among all adulterant meat samples using beef with a fat content of 20% in both normalised and raw data. Nearly all of these markers were also significantly different in samples made using beef with a fat content of 5%, however a few markers appear to only be significant in the samples made using beef with 20% fat content. This shows that there could be markers that would only be useful in beef samples containing a higher fat content.

5.7.1.5 Tentative identification

Table 5.7: Compounds that were significantly different and tentatively identified in extracts from raw minced beef (20% fat content) adulterated with minced pork based on comparison of mass spectra on METLIN

m/z	Retention time median (mins)	Possible formula	Likelihood score (%)	Tentative identification
496.3399	14.48	$C_{24}H_{50}NO_7P$	99.70	PC(16:0/0:0)
295.2621	23.90	$C_{19}H_{34}O_2$	91.64	linoleic acid methyl ester
271.2620	26.64	$C_{17}H_{34}O_2$	85.26	palmitic acid methyl ester
300.2885	13.26	$C_{18}H_{37}NO_2$	85.82	sphingosine

Four markers were tentatively identified, as shown in Table 5.7 (see Appendix A for mass spectra comparisons). Some of these tentative identifications are quite hesitant because the intensity of the peaks in the mass spectrum are low and so become lost in the noise. Therefore, the tentative identifications are less confident than in previous experiments and are only used as a guide to the potential identification, and it is known that more research would be required in order to fully tentatively identify them.

Two of these markers exhibited an interesting trend relating to the increase in adulterant pork. Figure 5.7 shows the trend of marker 271.2620 *m/z* that was tentatively identified as palmitic acid methyl ester, and Figure 5.8 shows the trend for marker 295.2621 *m/z* that was tentatively identified as linoleic acid methyl ester.

Both of these markers increase as the percentage of adulterant pork increases. These markers were found through the statistical analysis of the beef with 20% fat content samples, however the trends are actually more prominent in the beef with 5% fat content, so these markers could have potential in detecting adulterant pork regardless of fat content percentage. Both of these markers are types of fatty acid methyl esters, however despite the fact these can be found endogenously due to endogenous methanol, it is unlikely these compounds were naturally present in the meat samples. It is more likely these methyl esters were formed during the extraction process, potentially when sonicating. Other results on the METLIN database that matched the predicted formulae, but did not have available mass spectra, were types of fatty acids, and so these markers are still likely to be of this class of compound. Interestingly, previous research found that linoleic acid was higher in pork meat compared to beef meat, however palmitic acid was found to be higher in beef compared to pork [153], which is different to what was observed in this experiment. From this analysis, it could be that pork meat has a higher fatty acid concentration compared to beef meat, if these tentative identifications were to be confirmed.

If these markers are indeed fatty acids, it is interesting that the beef with a fat content of 5% had a higher concentration of these markers compared to beef with a 20% fat content; it would be expected to be the other way round with a higher concentration in the beef with a higher fat content. This could be because the lower fat content beef has an abundance of free fatty acids, which are components in triglycerides, whereas the higher fat content contains fully formed triglycerides.

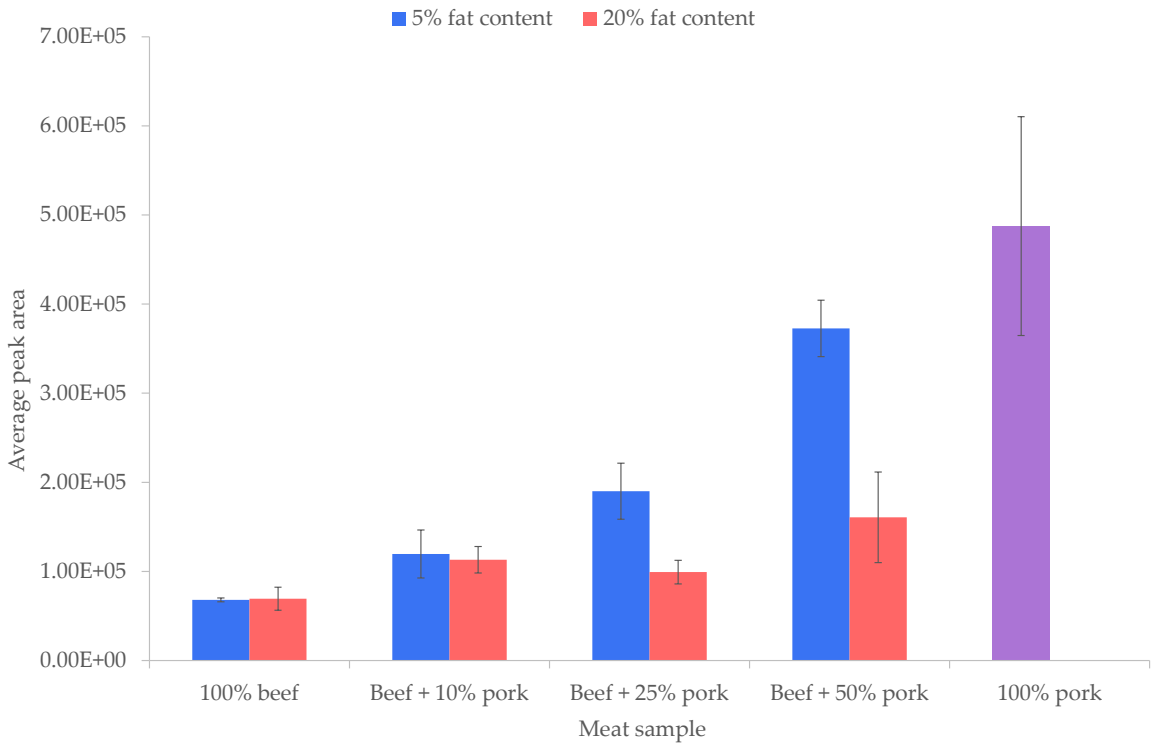

Figure 5.7: Trend of marker tentatively identified as palmitic acid methyl ester that was significantly different among all raw minced beef (20% fat content) adulterated with minced pork samples. Error bars correspond to ± 1 standard deviation

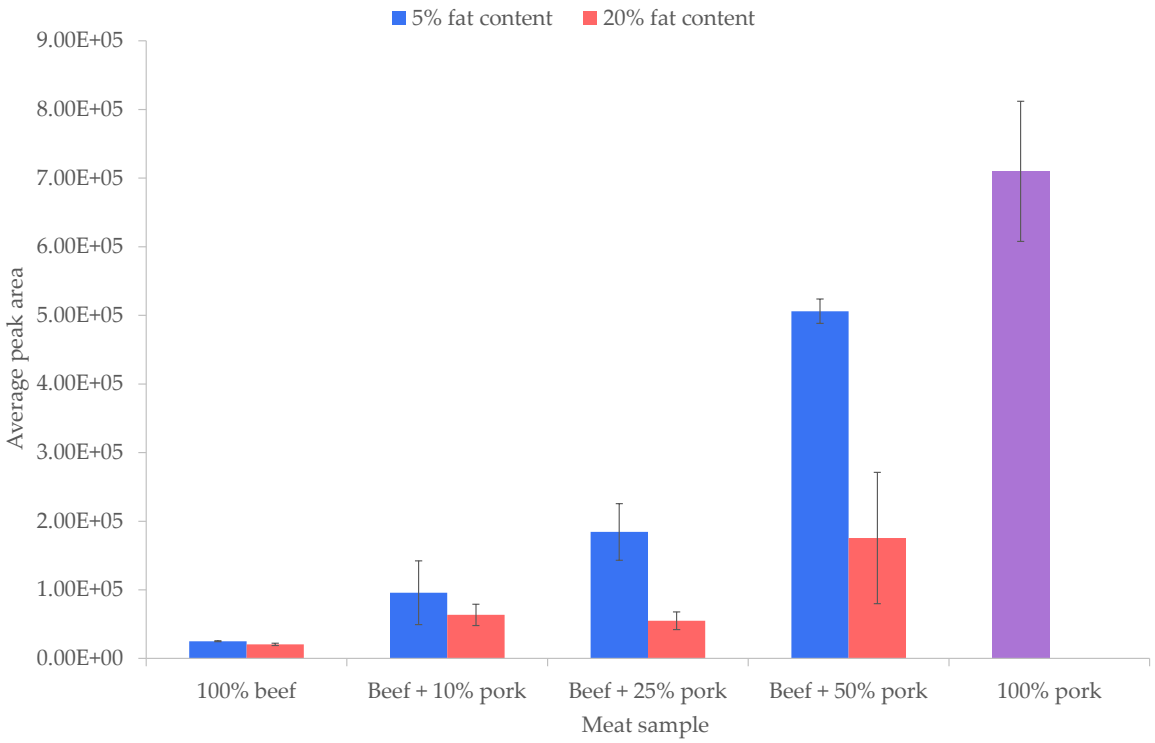

Figure 5.8: Trend of marker tentatively identified as linoleic acid methyl ester that was significantly different among all raw minced beef (20% fat content) adulterated with minced pork samples. Error bars correspond to ± 1 standard deviation

5.7.2 Raw minced beef adulterated with minced lamb

5.7.2.1 Quality control

Both the raw and cooked samples were analysed in the same analytical run, and so the quality control analysis applies to both datasets.

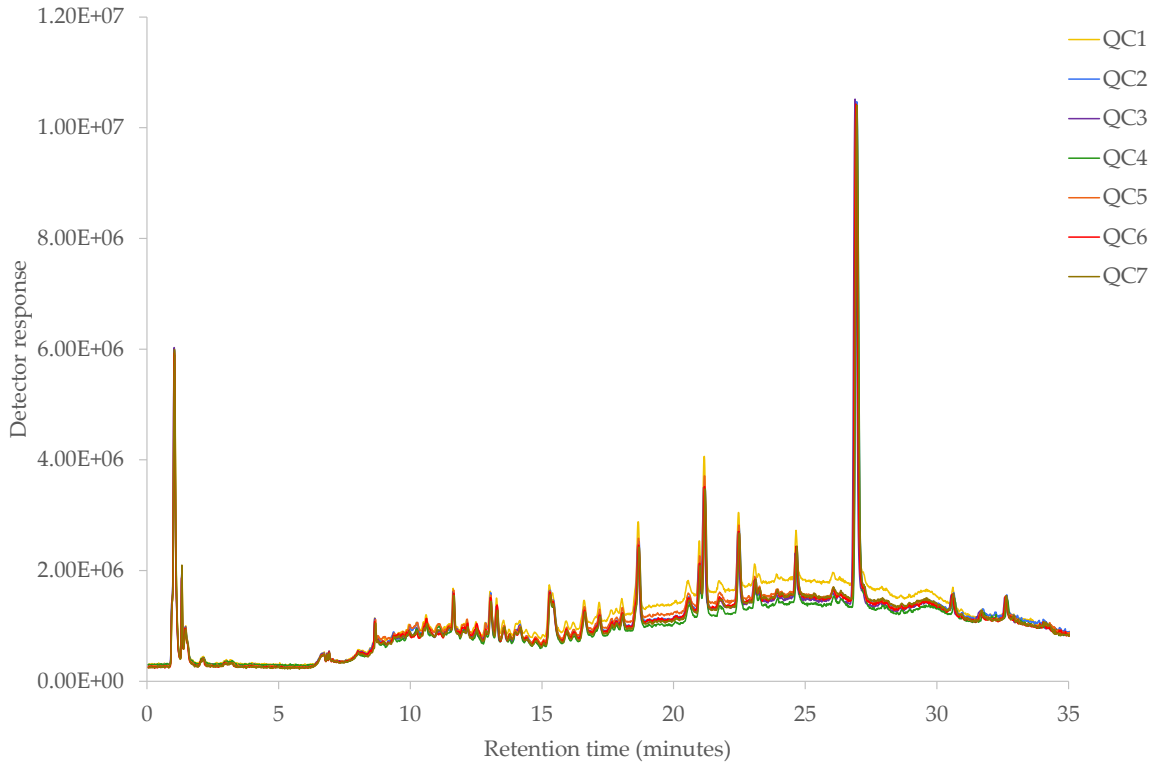

Figure 5.9: Total ion chromatograms of QC samples throughout analytical run for extracts from minced beef adulterated with minced lamb

The overlaid chromatograms of the QC samples injected throughout this analytical run (Figure 5.9) show that overall the chromatograms are reproducible. QC1 does have a slightly raised baseline, but this was the last QC in the series of injections at the beginning of the run to condition the system. Once samples were injected after this point, it appears the QC injections throughout the analytical run have stabilised at a lower baseline. This shows the importance of assessing the stability through the use of QC injections to highlight any stability issues, and to statistically determine whether these issues are enough to cause the collection of unreliable data.

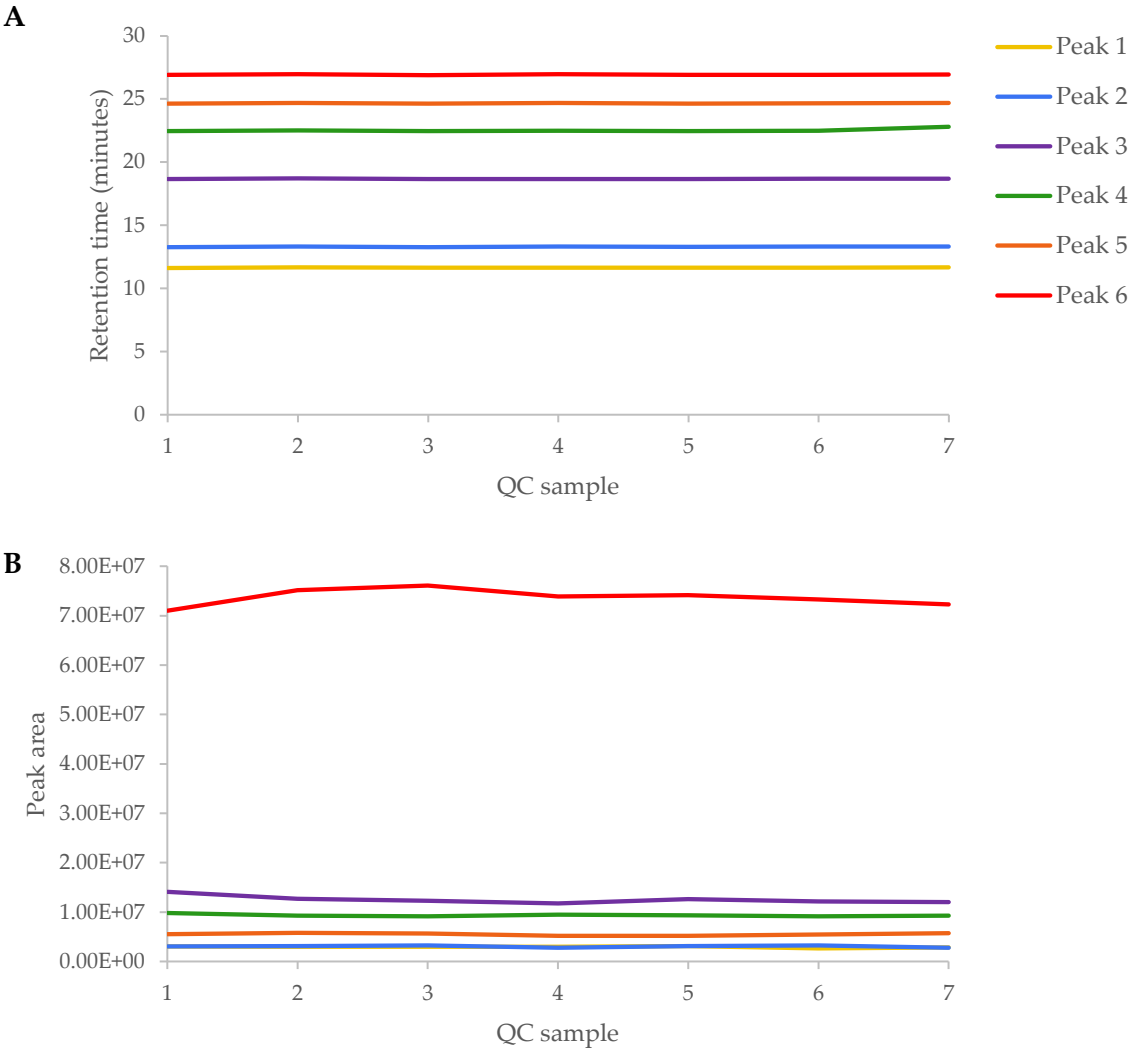

Figure 5.10: Variability of retention time (A) and peak area (B) of 6 peaks in QC samples throughout analytical run for extracts from minced beef adulterated with minced lamb

The retention time and peak area variability were investigated in 6 peaks throughout the analytical run. Figure 5.10 shows the trends of these peaks, and it can be seen that both the retention time and peak area were stable.

Table 5.8: Variability of retention time and peak area of 6 peaks in chromatograms of QC samples during the analysis of extracts from minced beef adulterated with minced lamb

	Retention time (minutes)									
Peak	QC1	QC2	QC3	QC4	QC5	QC6	QC7	SD	Average	CV%
1	11.62	11.65	11.63	11.64	11.64	11.64	11.65	0.01	11.64	0.09
2	13.26	13.30	13.27	13.30	13.28	13.30	13.31	0.02	13.29	0.14
3	18.65	18.70	18.65	18.67	18.66	18.68	18.69	0.02	18.67	0.10
4	22.45	22.50	22.45	22.49	22.47	22.48	22.79	0.12	22.52	0.54
5	24.64	24.69	24.62	24.68	24.64	24.65	24.68	0.03	24.66	0.11
6	26.91	26.96	26.89	26.97	26.92	26.92	26.95	0.03	26.93	0.11
	Peak area									
Peak	QC1	QC2	QC3	QC4	QC5	QC6	QC7	SD	Average	CV%
1	3069696	3008824	2972546	3017575	3114801	2673084	2859565	149587	2959442	5.05
2	3056191	3107593	3271047	2786084	3118023	3254734	2787615	198795	3054470	6.51
3	14100498	12680553	12299849	11722579	12658328	12179554	12043100	771393	12526352	6.16
4	9780929	9258806	9133170	9447785	9313918	9165848	9308310	218823	9344109	2.34
5	5532453	5778638	5674395	5211159	5223354	5459740	5731082	231781	5515832	4.20
6	71027454	75170221	76106754	73862790	74179437	73283490	72295146	1707819	73703613	2.32

The retention time variability was between 0.09 and 0.54%, and the peak area variability was between 2.32 and 6.51%. These values confirm that the analytical run was stable throughout and collected reliable data.

5.7.2.2 Metabolic profiling

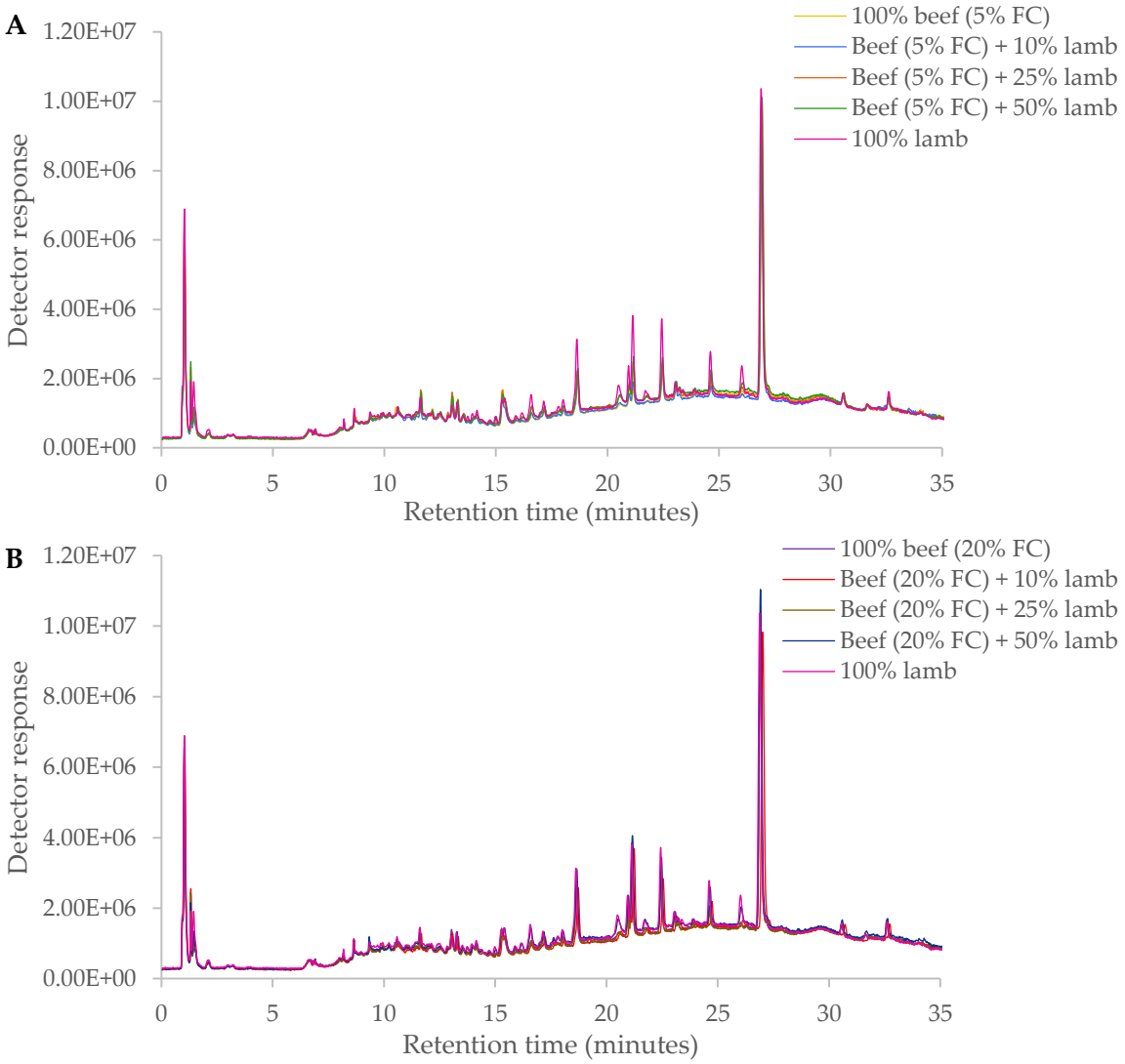

Figure 5.11: Example total ion chromatograms of extracts from raw minced beef adulterated with different percentages of minced lamb. A) Beef with 5% fat content, B) Beef with 20% fat content

The chromatograms in 5.11A (beef with 5% fat content) have several peak intensity differences; peaks between 16 and 27.5 minutes all have a higher intensity in the 100% lamb samples. The chromatograms in 5.11B (beef with 20% fat content) show the beef with 50% lamb samples and 100% lamb samples have the highest intensity in the peaks after 15 minutes. The two unresolved peaks at 3 minutes that were seen to have intensity differences in the beef adulterated with pork samples do not appear to be different in these beef adulterated with lamb samples.

5.7.2.3 Multivariate statistics

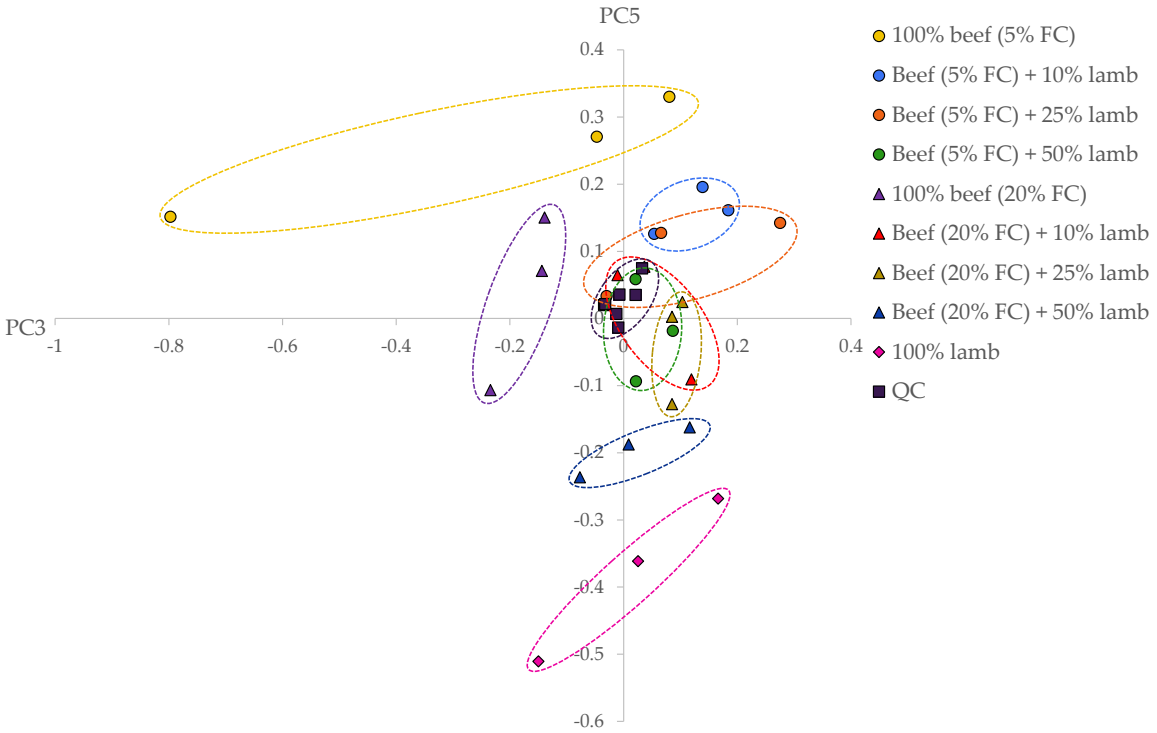

Figure 5.12: Principal component analysis scores plot of PC3 (0.310%) and PC5 (0.154%) for extracts from raw minced beef with 5% and 20% fat content adulterated with different percentages of minced lamb. PCA was carried out using all features detected with a CV $< 10\%$

The PCA plot for raw beef adulterated with varying percentages of lamb (Figure 5.12) shows some separation between the 100% beef at differing fat contents (5% and 20%), and 100% lamb. There is a lot of overlap between all other samples, but both 100% beef samples are separated from all samples of beef adulterated with lamb. This PCA plot analysed all features that had a CV% of less than 10%, without any prior filtering through the use of a p-value from a statistical test. The separation seen shows that the overall metabolic profile of these samples are different enough to be seen without focussing purely on statistically significant markers.

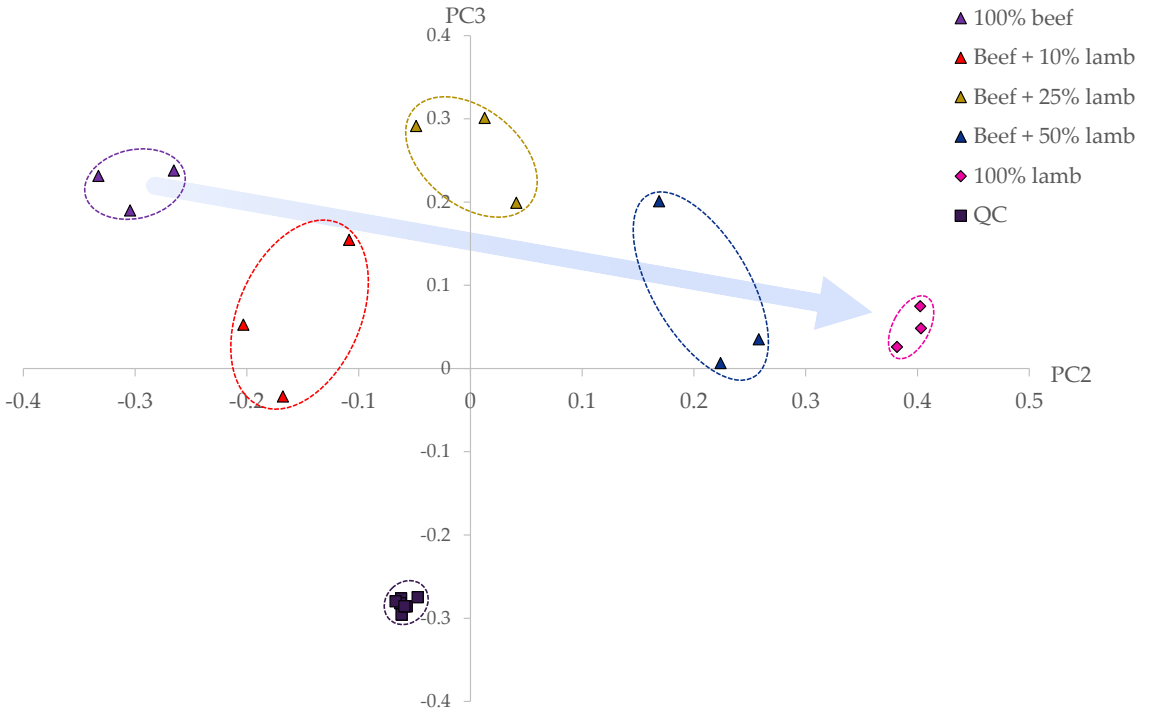

Figure 5.13: Principal component analysis scores plot of PC2 (3.927%) and PC3 (1.149%) for extracts from raw minced beef with 20% fat content adulterated with different percentages of minced lamb. PCA was carried out using all markers with a CV $< 10\%$ and p-value of < 0.05

After statistical analysis of the beef with 5% fat content samples, and the beef with 20% fat content samples, the best separation in the principal component analysis scores plots could be seen with markers that were significantly different in the beef with 20% fat content samples. The PCA plot in Figure 5.13 shows separation between all sample types, and the quality control samples are tightly clustered. The difference between each sample set is greater than the spread of the individual QC samples, so these differences can be attributed to the metabolic content of each sample type, and are not caused by any instrumental instability during the analytical run. The separation of these sample groups lies along the x-axis, starting with the 100% beef samples on the left of the plot, and gradually moving across as the percentage of adulterant lamb increases, as shown by the blue arrow. Therefore, PC2 was used to find the markers most responsible for this separation, based on the loading values.

5.7.2.4 Significant markers

Table 5.9: Summary of compounds that contribute the most to the differences among all extracts from raw minced beef with a 20% fat content that has been adulterated with different percentages of lamb, including 100% beef and 100% lamb, using PC2. All markers increased as the percentage of adulterant lamb increased. FC = fat content.

m/z	Retention time median (mins)	P-value from ANOVA/Welch (XCMS)		CV% (XCMS)	P-value from ANOVA/Welch (EICs)		CV% (EICs)
		5% FC	20% FC		5% FC	20% FC	
428.3735	20.60	<0.001	<0.001	2.71	<0.001	<0.001	3.30
482.3244	16.65	<0.001	<0.001	1.22	<0.001	<0.001	1.50
269.0860	1.45	<0.001	<0.001	1.05	<0.001	<0.001	2.16
297.2787	26.09	<0.001	<0.001	2.43	<0.001	<0.001	2.80
537.1673	1.45	<0.001	<0.001	2.23	<0.001	<0.001	2.87
466.3291	17.88	<0.001	<0.001	1.75	<0.001	<0.001	2.37
456.4045	26.30	<0.001	<0.001	2.21	<0.001	0.001	2.87
400.3421	16.27	<0.001	<0.001	2.50	<0.001	<0.001	3.53
438.2980	14.21	<0.001	<0.001	1.36	<0.001	<0.001	2.13
241.1286	0.97	<0.001	<0.001	8.46	<0.001	0.001	9.60
271.2626	26.16	<0.001	0.001	2.39	0.003	0.002	2.53
295.2629	23.47	<0.001	<0.001	4.02	<0.001	0.001	3.82
524.3710	20.66	<0.001	<0.001	3.30	<0.001	<0.001	2.33
293.2471	21.23	<0.001	0.001	3.09	0.002	0.002	3.67
480.3448	17.10	0.002	0.001	1.46	0.002	0.002	1.89
480.3088	14.28	<0.001	<0.001	0.99	<0.001	<0.001	3.02
312.2898	26.16	<0.001	0.001	2.83	0.004	0.002	3.64
303.2317	16.20	<0.001	<0.001	1.21	<0.001	<0.001	2.35
464.3132	15.23	<0.001	<0.001	2.38	<0.001	<0.001	2.99
279.2314	16.55	<0.001	<0.001	2.68	0.002	<0.001	3.21
500.2773	10.63	0.007	0.001	7.58	0.002	<0.001	4.15
496.3403	15.47	0.006	0.002	0.71	0.038	0.003	1.75
372.3107	12.90	<0.001	<0.001	3.05	<0.001	<0.001	2.46
426.3574	17.43	<0.001	<0.001	3.86	<0.001	<0.001	4.85
329.2479	17.57	<0.001	<0.001	4.43	<0.001	<0.001	5.14
317.2477	20.45	0.006	0.003	6.37	0.010	0.005	7.26
454.3884	21.61	<0.001	<0.001	2.42	<0.001	<0.001	6.43
414.3574	18.33	<0.001	<0.001	3.10	<0.001	<0.001	3.81
508.3759	23.54	0.001	<0.001	8.44	0.001	<0.001	3.52
305.2474	18.06	0.039	0.001	2.36	0.019	0.001	2.54
963.6401	16.65	<0.001	<0.001	2.65	<0.001	<0.001	3.02
319.2630	22.52	<0.001	0.002	4.64	<0.001	0.003	6.76
262.1635	1.73	<0.001	<0.001	4.65	<0.001	<0.001	2.90

Table 5.9 continued: Summary of compounds that contribute the most to the differences within among all extracts from raw minced beef with a 20% fat content that has been adulterated with different percentages of lamb, including 100% beef and 100% lamb, using PC2. All markers increased as the percentage of adulterant lamb increased. FC = fat content.

m/z	Retention time median (mins)	P-value from ANOVA/Welch (XCMS)		CV% (XCMS)	P-value from ANOVA/Welch (EICs)		CV% (EICs)
		5% FC	20% FC		5% FC	20% FC	
267.2680	24.71	<0.001	<0.001	3.77	<0.001	<0.001	4.00
444.3676	15.94	0.005	<0.001	8.46	<0.001	<0.001	4.14
454.3886	20.82	<0.001	<0.001	1.68	<0.001	<0.001	3.16
370.2954	11.37	<0.001	<0.001	3.06	<0.001	<0.001	5.78
284.0968	1.46	<0.001	0.001	7.14	<0.001	<0.001	5.72
212.1018	0.96	<0.001	<0.001	5.61	<0.001	<0.001	6.86
299.2937	29.29	<0.001	0.006	7.16	0.006	0.006	4.64
526.2934	11.60	<0.001	<0.001	4.54	0.001	<0.001	4.98
452.3133	15.92	<0.001	<0.001	1.44	<0.001	<0.001	6.48
575.1243	1.06	0.014	<0.001	4.78	<0.001	<0.001	5.09
307.2630	20.38	<0.001	<0.001	6.40	<0.001	<0.001	6.12

The markers in Table 5.9 were all found using principal component 2 from the PCA plot in Figure 5.13. All of these markers were very robust in the QC samples, with a CV% of less than 10% in the normalised data obtained through *XCMS* and the raw data from the extracted ion chromatograms. Markers were confirmed to be significant in the raw data in the beef with 20% fat content samples, and the beef with 5% fat content. The trends of these markers all increased as the percentage of adulterant lamb increased.

5.7.2.5 Tentative identification

Table 5.10: Compounds that were significantly different and tentatively identified in extracts from raw minced beef (20% fat content) adulterated with minced lamb based on comparison of mass spectra on METLIN

m/z	Retention time median (mins)	Possible formula	Likelihood score (%)	Tentative identification
400.3421	16.27	$C_{23}H_{45}NO_4$	99.58	palmitoyl-L-carnitine
271.2626	26.16	$C_{17}H_{34}O_2$	96.83	palmitic acid methyl ester
524.3710	20.66	$C_{26}H_{54}NO_7P$	99.67	platelet activating factor (PAF) C-16
303.2317	16.20	$C_{20}H_{30}O_2$	97.33	eicosapentanoic acid
496.3403	15.47	$C_{24}H_{50}NO_7P$	99.46	PC(16:0/0:0)
372.3107	12.90	$C_{21}H_{41}NO_4$	98.36	myristoylcarnitine
305.2474	18.06	$C_{20}H_{32}O_2$	99.39	arachidonic acid

Seven markers were tentatively identified in these samples, as shown in Table 5.10. Each formula matched a compound on the METLIN database that had an available mass spectrum, and these can be seen in Appendix B. Again, these tentative identifications must be treated with caution due to the lack of fragmentation at 0 V collision energy, and the lack of available mass spectra for many compounds with the same formula on METLIN. However, they can give an insight into the potential type of compound that these markers may be.

All of these markers increased in concentration as the percentage of adulterant lamb increased. Two of these compounds were tentatively identified as palmitoyl carnitine and myristoyl carnitine, which are acyl carnitines involved in the β-oxidation of fatty acids generating acetyl-CoA for the citric acid cycle, and have been previously discussed in Chapter 4, Section 4.7.3.5.

Both of these acyl carnitines increase in concentration as the percentage of lamb increases (Figure 5.14 and 5.15), showing that lamb muscle has a higher concentration of these carnitines compared to beef muscle. It has been found that lamb muscle

contains over three times the amount of carnitine than beef muscle [154], and so this explains the increasing trend of acyl carnitines observed in this research. Generally, the beef with a fat content of 20% has a higher amount of these markers compared to beef with a fat content of 5%, except for myristoyl carnitine in beef with 25% lamb.

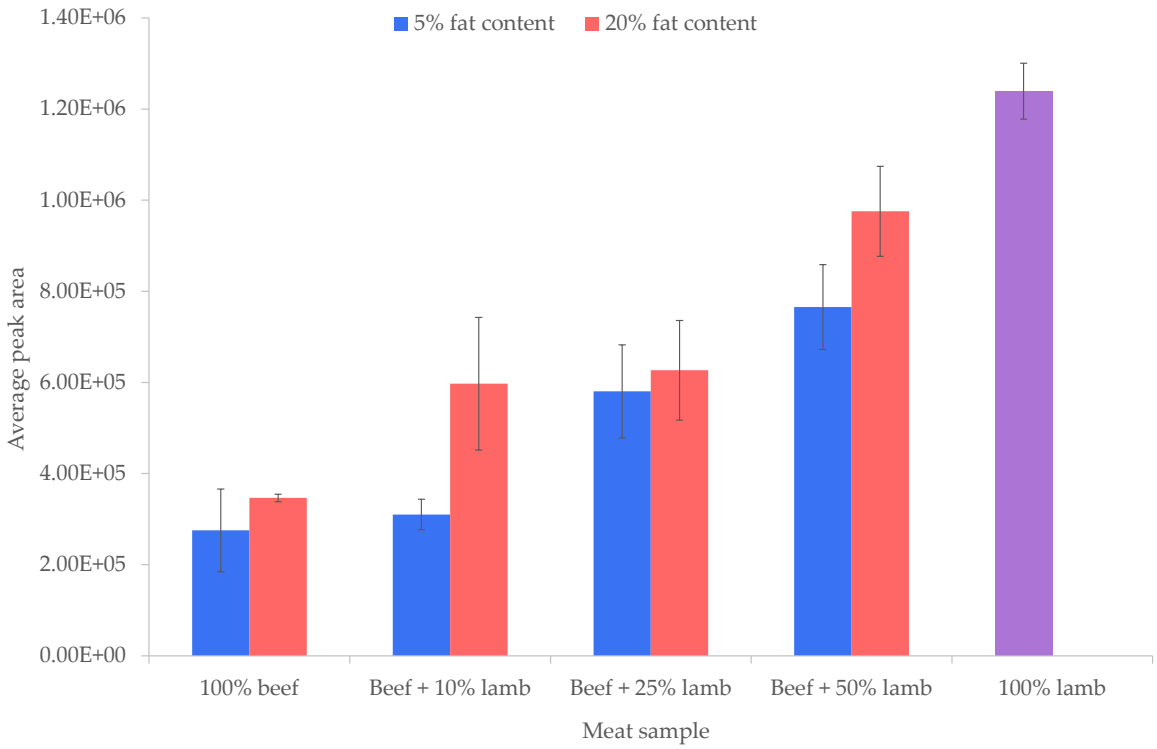

Figure 5.14: Trend of marker tentatively identified as palmitoyl carnitine that was significantly different among all raw minced beef (20% fat content) adulterated with minced lamb samples. Error bars correspond to ± 1 standard deviation

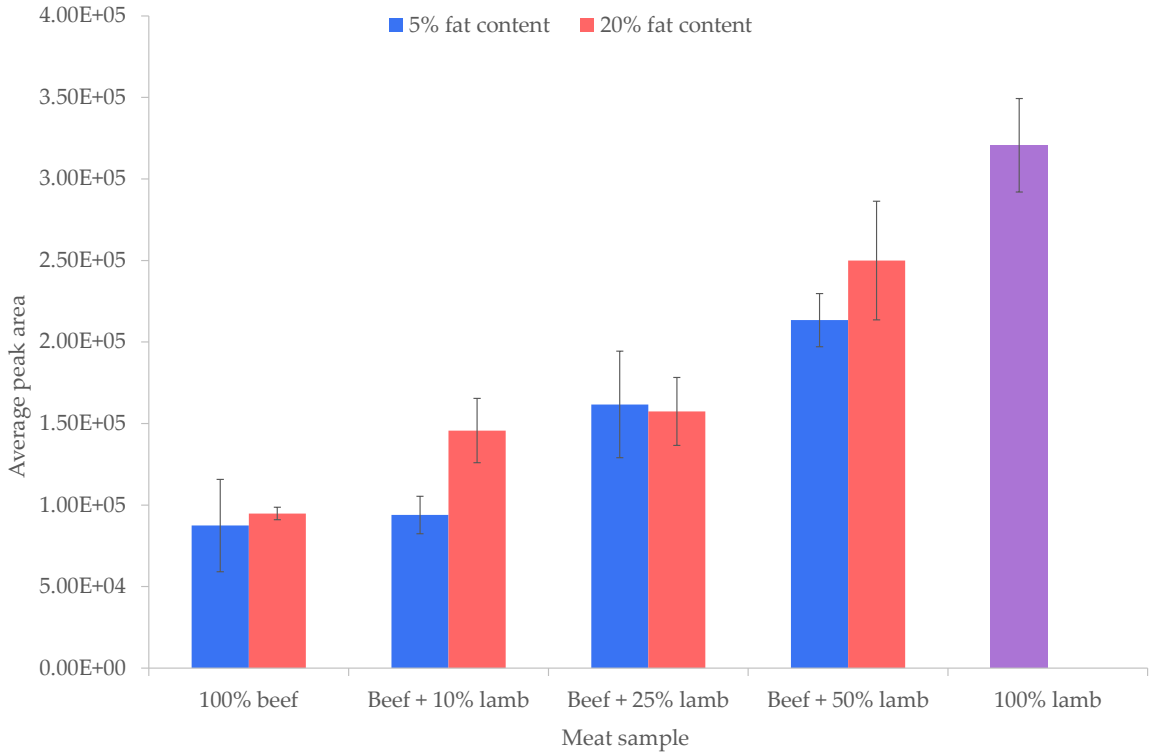

Figure 5.15: Trend of marker tentatively identified as myristoyl carnitine that was significantly different among all raw minced beef (20% fat content) adulterated with minced lamb samples. Error bars correspond to ± 1 standard deviation

5.7.3 Raw minced beef adulterated with minced turkey

5.7.3.1 Quality control

Both the raw and cooked samples were analysed in the same analytical run, and so the quality control analysis applies to both datasets.

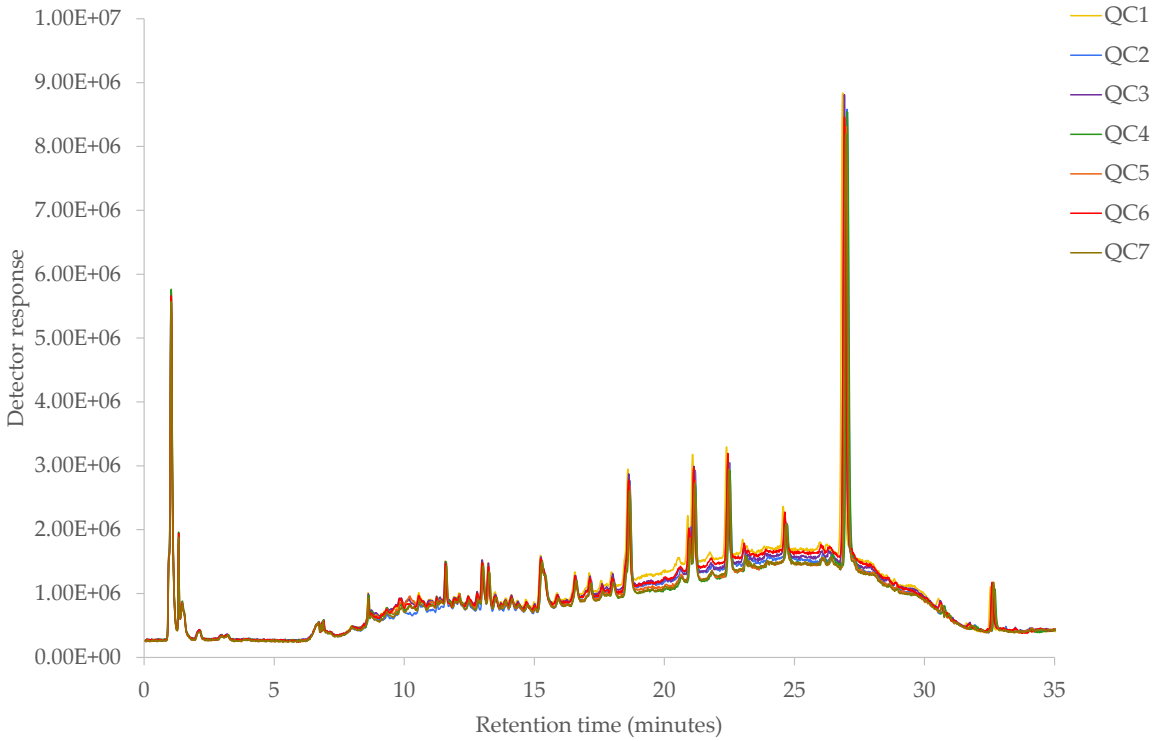

Figure 5.16: Total ion chromatograms of QC samples throughout analytical run for extracts from minced beef adulterated with minced turkey

Figure 5.16 shows the overlaid chromatograms for the QC samples injected throughout this analytical run. The chromatograms appear to be reproducible, and there is minimal retention time variation observed. There is some baseline variation between 17 and 27 minutes, and so further statistical analysis is required to assess the reliability of the data from this run.

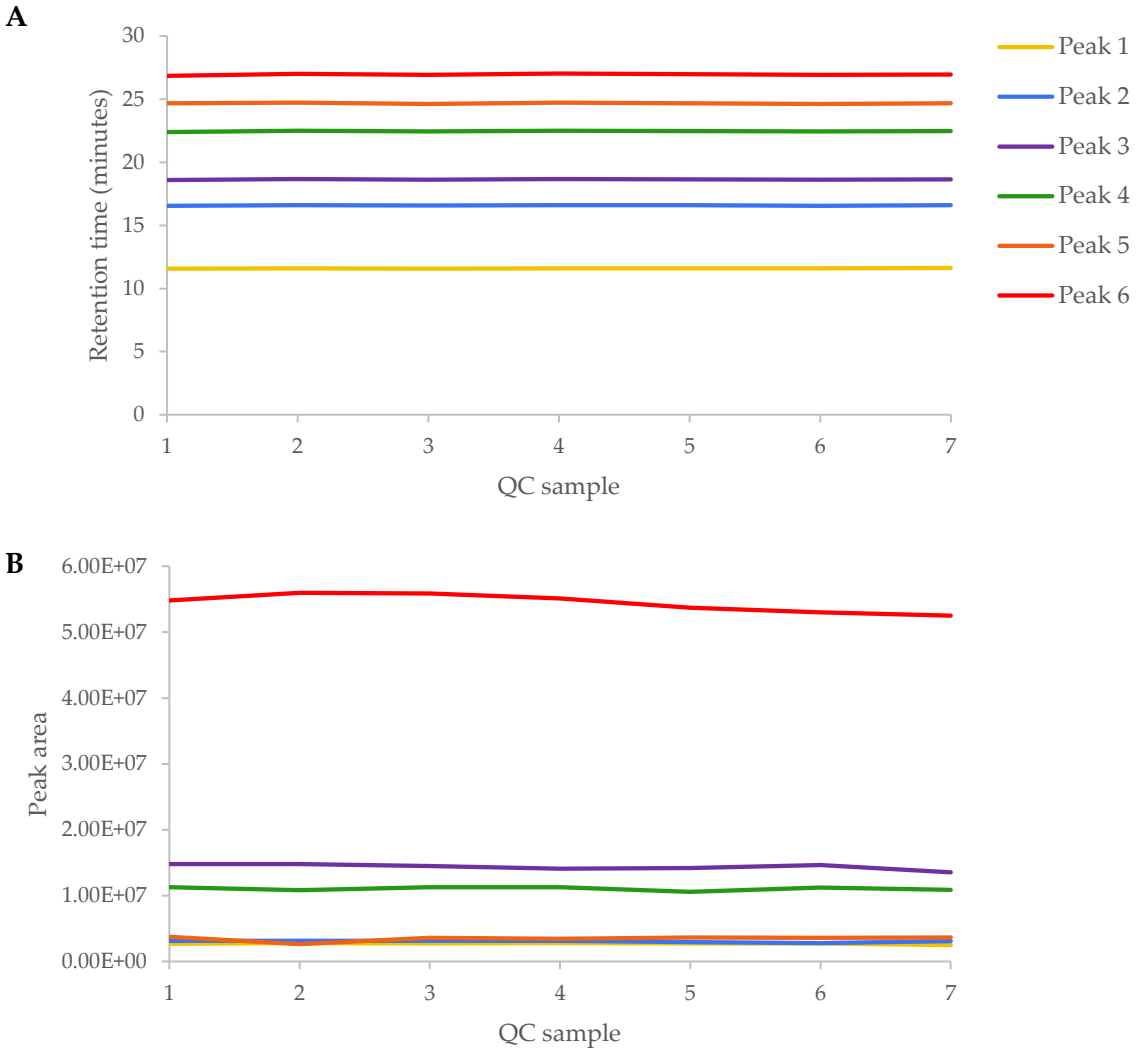

Figure 5.17: Variability of retention time (A) and peak area (B) of 6 peaks in QC samples throughout analytical run for extracts from minced beef adulterated with minced turkey

Peaks were selected from a range of retention times and peak intensities to further determine the stability of this analytical run. Figure 5.17 shows that the retention time and peak areas were stable in all QC samples for these 6 peaks.

Table 5.11: Variability of retention time and peak area of 6 peaks in chromatograms of QC samples during the analysis of extracts from minced beef adulterated with minced turkey

	Retention time (minutes)									
Peak	QC1	QC2	QC3	QC4	QC5	QC6	QC7	SD	Average	CV%
1	11.58	11.61	11.57	11.60	11.61	11.59	11.62	0.02	11.60	0.16
2	16.56	16.61	16.58	16.60	16.60	16.56	16.60	0.02	16.59	0.12
3	18.60	18.68	18.62	18.67	18.66	18.62	18.65	0.03	18.64	0.16
4	22.40	22.51	22.44	22.50	22.48	22.44	22.47	0.04	22.46	0.17
5	24.67	24.72	24.63	24.72	24.68	24.63	24.68	0.04	24.68	0.15
6	26.86	27.02	26.92	27.03	26.99	26.92	26.96	0.06	26.96	0.23
	Peak area									
Peak	QC1	QC2	QC3	QC4	QC5	QC6	QC7	SD	Average	CV%
1	2673734	2783074	2755159	2807911	2718131	2738113	2513540	98046	2712809	3.61
2	3131375	3142839	3150036	3136273	2954563	2789635	3082419	135673	3055306	4.44
3	14773344	14777063	14482896	14111684	14211750	14636569	13526130	450068	14359919	3.13
4	11280303	10839161	11290124	11297110	10598814	11203509	10856401	283077	11052203	2.56
5	3749450	2662162	3609691	3425631	3654287	3615344	3662704	374891	3482753	10.76
6	54833114	55967285	55880510	55099823	53715259	53004236	52508605	1373184	54429833	2.52

The retention time variability was between 0.12 and 0.23%, and the peak area variability was between 2.52 and 10.76%, showing the data was very reproducible. These values confirm that this analytical run was stable and obtained reliable data.

5.7.3.2 Metabolic profiling

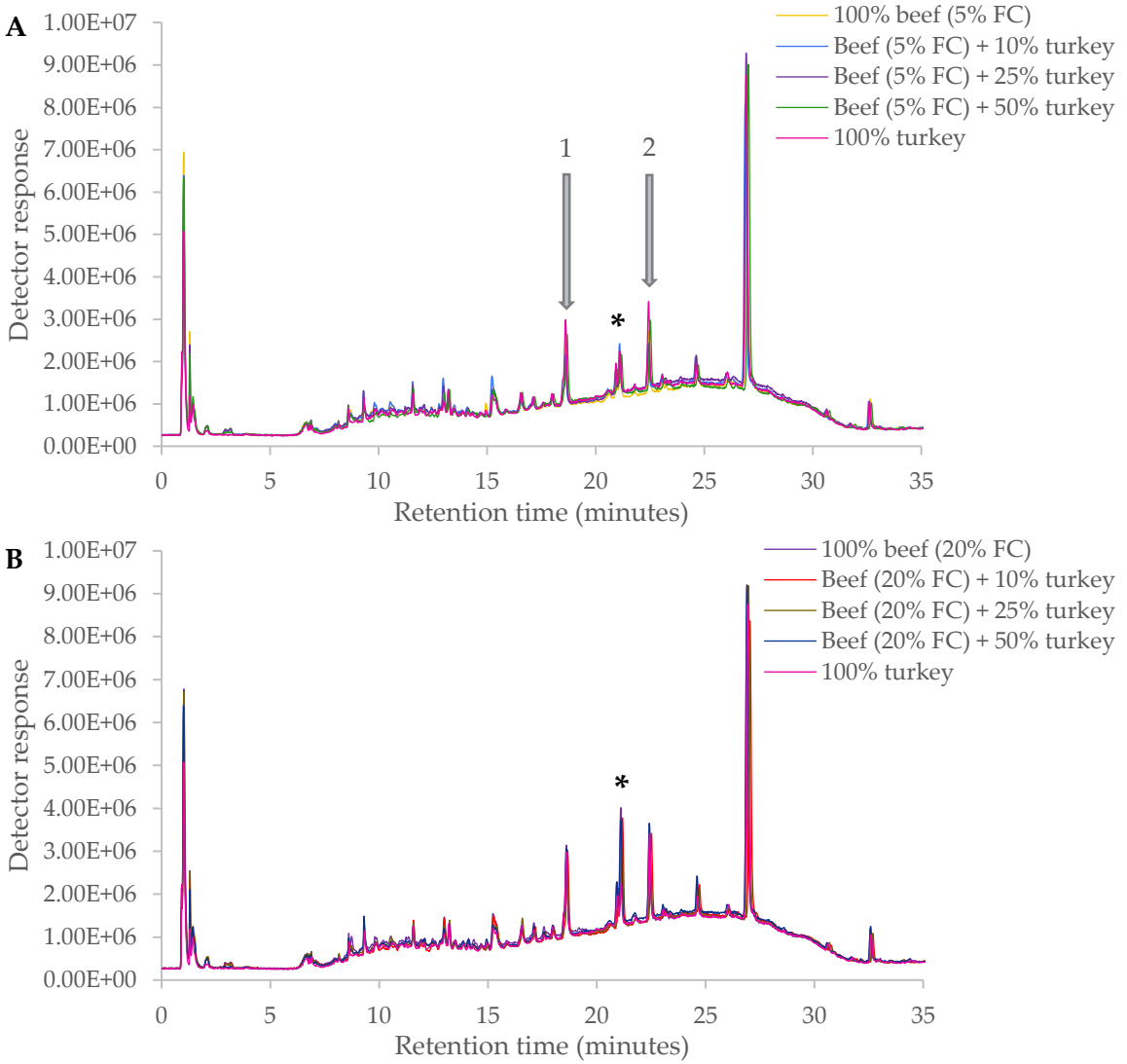

Figure 5.18: Example total ion chromatograms of extracts from raw minced beef adulterated with different percentages of minced turkey. A) Beef with 5% fat content, B) Beef with 20% fat content

The chromatograms in Figure 5.18 do not show many differences in peak pattern, only subtle differences in peak intensity. In the chromatograms for beef with a fat content of 5% (A), two peaks at 18.5 (peak 1) and 22.5 minutes (peak 2) have the highest intensity in the 100% turkey samples. The peaks at the beginning of the chromatograms that are attributed to the non-retained polar compounds in the samples all show a higher intensity in the 100% beef and a lower intensity in the 100% turkey. In particular, the two unresolved peaks at 3 minutes that have been

seen previously to be different in adulterated pork samples but not in adulterated lamb samples, do show a difference in these adulterated turkey samples. The chromatograms from beef with a fat content of 20% (B) show very similar characteristics to beef with a fat content of 5% (A), however there is one difference between chromatograms A and B at around 21 minutes (indicated by the asterisks), where the beef with a fat content of 20% has a higher abundance than in beef with a fat content of 5%. This difference may be caused by lipids that are at a higher concentration in the beef with a higher fat content.

5.7.3.3 Multivariate statistics

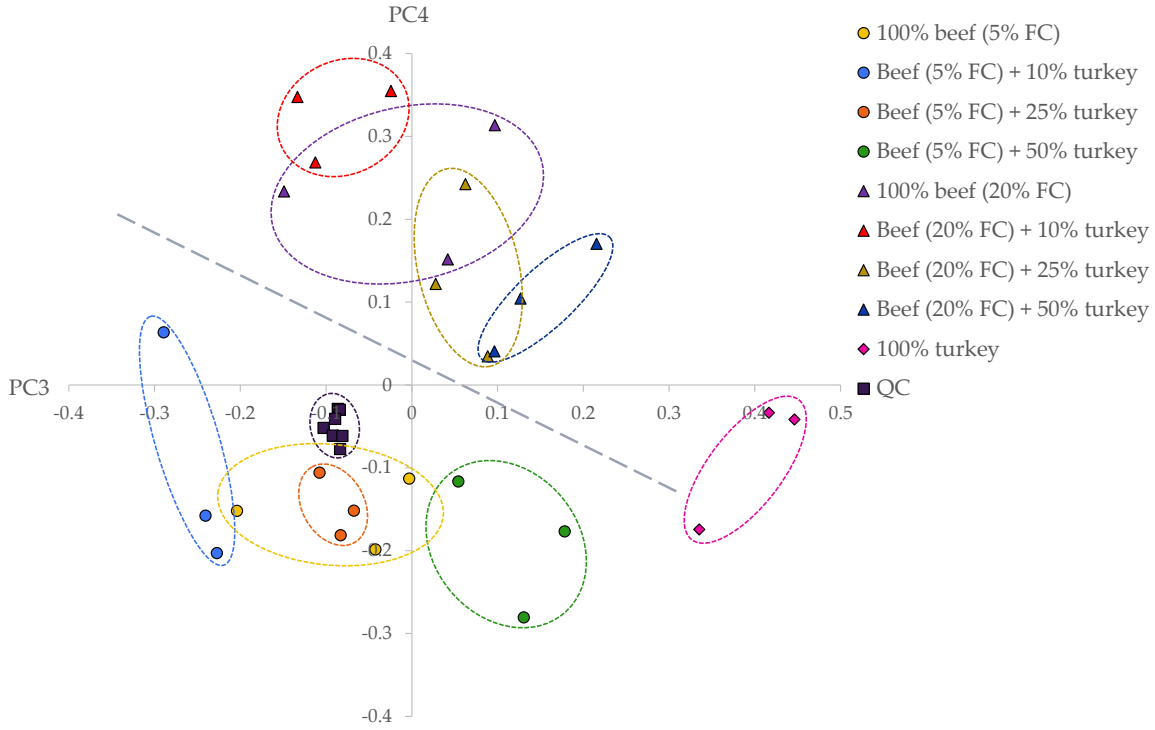

Figure 5.19: Principal component analysis scores plot of PC3 (0.407%) and PC4 (0.159%) for extracts from raw minced beef with 5% and 20% fat content adulterated with different percentages of minced turkey. PCA was carried out using all features detected with a CV $< 10\%$. Dotted line shows separation of beef with a fat content of 5% and beef with a fat content of 20% sample groups

All features in the raw beef adulterated with turkey with a CV% in the QC samples of less than 10% were analysed using principal component analysis and a scores plot

was produced (Figure 5.20), and each sample set is clearly distinguishable. The two types of beef with differing fat content are clearly separated, as shown by the grey dotted line; the top part of the plot contains the beef with a fat content of 20%, and the lower part of the plot contains the beef with a fat content of 5%. Both 100% beef samples of both fat content percentages and the 100% turkey samples are separated from each other.

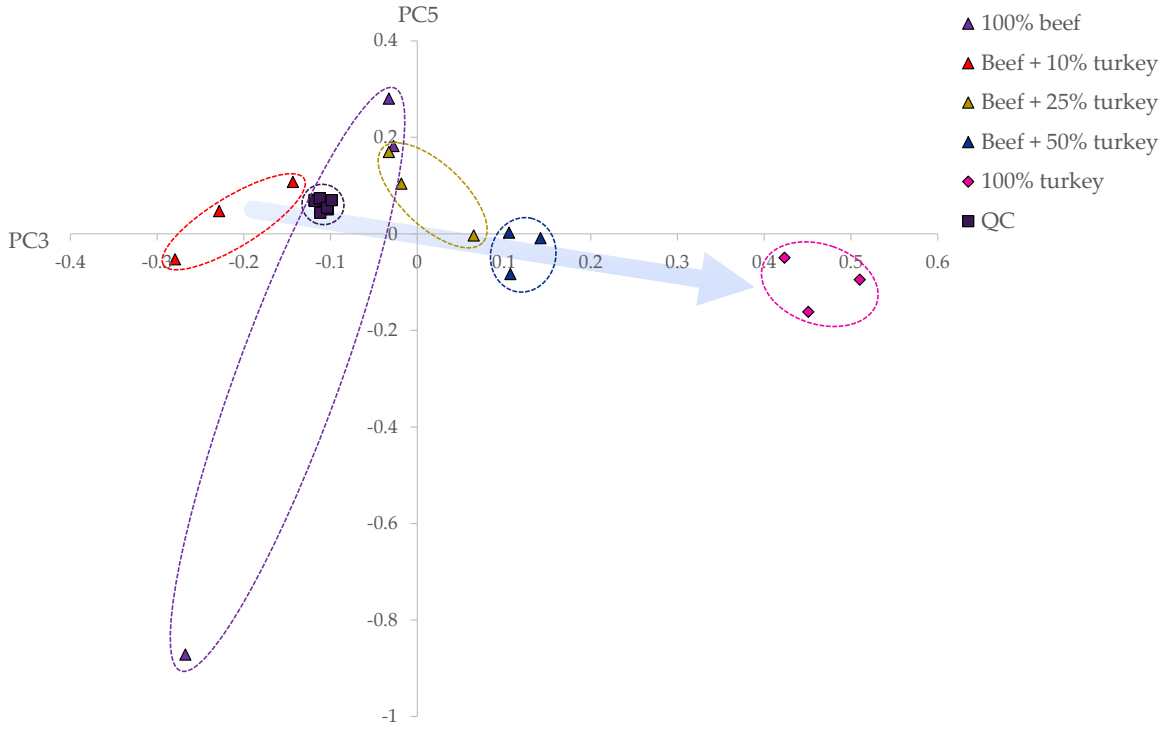

Figure 5.20: Principal component analysis scores plot of PC3 (0.444%) and PC5 (0.029%) for extracts from raw minced beef with 20% fat content adulterated with different percentages of minced turkey. PCA was carried out using all markers with a CV $< 10\%$ and p-value of < 0.05

The sample groups show an overall trend, represented by the blue arrow. Despite there being a large variation in the 100% beef samples, there is separation between sample types along the x-axis, representing PC3. Therefore, PC3 was used to determine the markers that were most responsible for this separation, based on the loading values.

5.7.3.4 Significant markers

Table 5.12: Summary of compounds that contribute the most to the differences among all extracts from raw minced beef with a 20% fat content that has been adulterated with different percentages of turkey, including 100% beef and 100% turkey, using PC3. FC = fat content. Red values indicate p-value > 0.05. Marker trend: ↑ = increased, * = random or consistent

m/z	Retention time median (mins)	P-value from ANOVA/Welch (XCMS)		CV% (XCMS)	P-value from ANOVA/Welch (EICs)		CV% (EICs)
		5% FC	20% FC		5% FC	20% FC	
↑ 241.1298	0.96	<0.001	<0.001	1.52	<0.001	<0.001	4.44
* 482.3241	16.61	0.001	<0.001	1.16	0.001	<0.001	1.45
* 338.3422	26.99	0.223	0.022	2.40	0.513	0.020	3.10
↑ 249.1557	1.05	0.002	0.003	1.87	<0.001	<0.001	2.46
↑ 520.5080	36.54	0.002	0.002	4.51	0.001	0.001	5.13
↑ 454.2925	13.26	<0.001	<0.001	2.59	<0.001	<0.001	3.43
↑ 281.2474	18.52	0.002	<0.001	2.75	<0.001	<0.001	3.10
↑ 271.2629	26.14	0.003	0.003	4.23	0.003	0.003	5.26
↑ 530.3235	13.47	<0.001	<0.001	2.62	<0.001	<0.001	3.72
↑ 212.1028	0.95	<0.001	<0.001	4.55	<0.001	<0.001	1.87
↑ 524.3706	20.62	<0.001	0.002	1.91	<0.001	0.021	2.22
↑ 295.2628	23.42	0.001	0.005	2.29	0.001	0.005	4.03
↑ 502.2928	11.61	0.004	0.001	2.01	0.003	<0.001	2.22
↑ 560.5007	36.56	0.003	<0.001	6.63	0.003	<0.001	5.86
↑ 300.2893	12.44	<0.001	<0.001	3.91	<0.001	<0.001	7.14
↑ 141.5820	0.95	<0.001	<0.001	7.80	<0.001	<0.001	7.20
↑ 340.3568	31.83	0.485	0.036	9.68	0.622	0.047	10.01
↑ 537.1650	1.45	0.001	0.001	4.12	0.004	0.001	4.57
↑ 572.3705	15.35	0.005	0.001	2.10	0.004	0.001	2.43
↑ 279.2314	16.50	<0.001	<0.001	2.38	<0.001	0.001	3.00
↑ 305.2475	18.02	0.006	<0.001	4.68	0.010	<0.001	3.57
↑ 528.3101	12.77	<0.001	<0.001	2.51	<0.001	<0.001	4.67
↑ 526.2928	11.55	<0.001	<0.001	1.66	0.001	<0.001	4.09
↑ 298.2740	18.51	0.002	<0.001	3.15	<0.001	<0.001	3.01
↑ 464.3128	14.67	0.002	0.003	2.63	0.002	0.007	3.43
↑ 263.1117	0.95	<0.001	0.001	7.49	<0.001	0.001	7.71
↑ 496.3392	14.74	0.011	<0.001	2.75	0.003	0.002	3.19
↑ 372.1985	1.05	<0.001	0.001	6.16	<0.001	<0.001	6.75
↑ 640.4995	33.11	<0.001	<0.001	7.57	<0.001	<0.001	11.61
* 580.3609	18.60	0.030	0.003	2.66	0.027	0.001	3.17
↑ 302.3047	13.22	<0.001	<0.001	3.95	<0.001	<0.001	7.33
* 336.3258	23.96	0.068	0.035	3.24	0.123	0.036	3.08
↑ 431.3517	29.93	0.013	0.003	9.13	0.014	0.003	10.75

Table 5.12 shows there were a number of markers that remained from the top 50 markers with the highest loading values in PC3 after statistical analysis was carried out on the raw data. Most of the markers had an increasing trend, however the beef with 50% turkey sample showed a slight decrease before increasing again for 100% turkey. This could be caused by the crude nature in which the meatballs were formed prior to extraction.

5.7.3.5 Tentative identification

Table 5.13: Compounds that were significantly different and tentatively identified in extracts from raw minced beef (20% fat content) adulterated with minced turkey based on comparison of mass spectra on METLIN

m/z	Retention time median (mins)	Possible formula	Likelihood score (%)	Tentative identification
338.3422	26.99	$C_{22}H_{43}NO$	99.17	13Z-docosenamide
271.2629	26.14	$C_{17}H_{34}O_2$	95.32	palmitic acid methyl ester
524.3706	20.62	$C_{26}H_{54}O_7P$	99.00	PAF C-16
300.2893	12.44	$C_{18}H_{37}NO_2$	96.32	sphingosine
305.2475	18.02	$C_{20}H_{32}O_2$	99.56	arachidonic acid
298.2740	18.51	$C_{18}H_{35}NO_2$	94.58	3-ketosphingosine

Some markers were successfully tentatively identified by matching the mass spectrum to available mass spectra on METLIN, and are shown in Appendix C. Two of these markers were tentatively identified as sphingosine and 3-ketosphingosine, which are both sphingolipids. The increasing trends observed as the percentage of turkey increases (Figure 5.21 and 5.22) indicates that turkey meat contains a higher concentration of sphingolipids than beef.

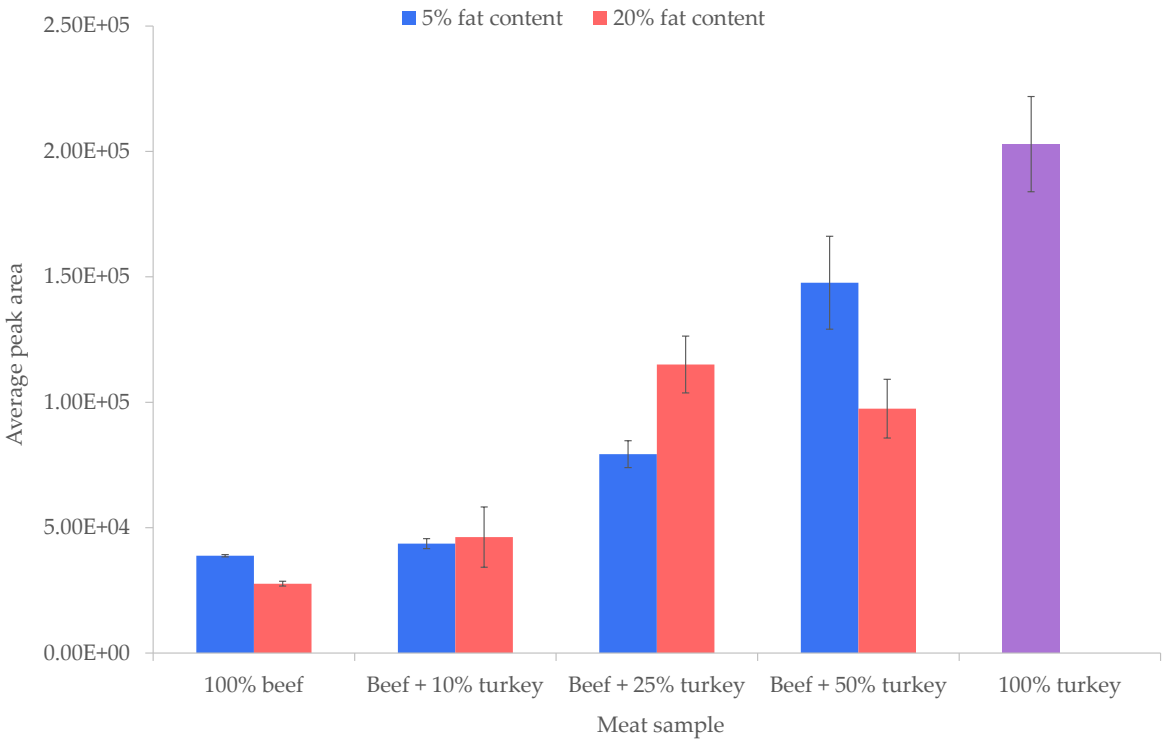

Figure 5.21: Trend of marker tentatively identified as sphingosine that was significantly different among all raw minced beef (20% fat content) adulterated with minced turkey samples. Error bars correspond to ± 1 standard deviation

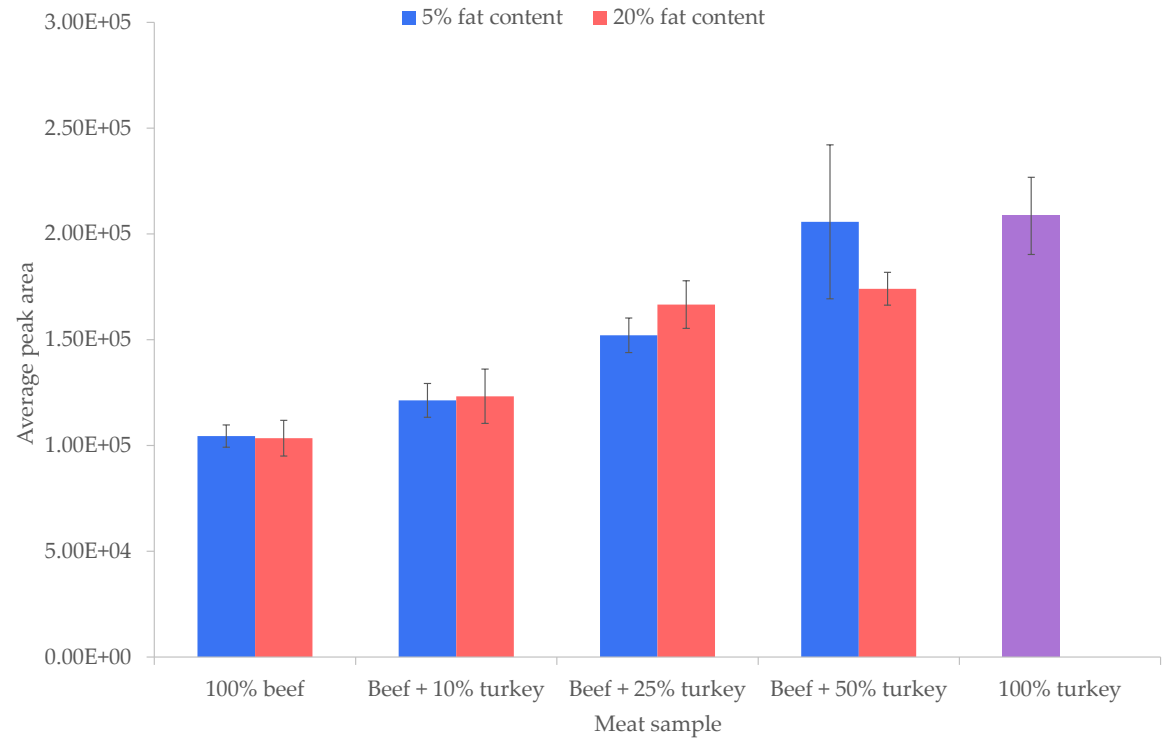

Figure 5.22: Trend of marker tentatively identified as 3-ketosphingosine that was significantly different among all raw minced beef (20% fat content) adulterated with minced turkey samples. Error bars correspond to ± 1 standard deviation

5.7.4 Cooked minced beef adulterated with minced pork

5.7.4.1 Metabolic profiling

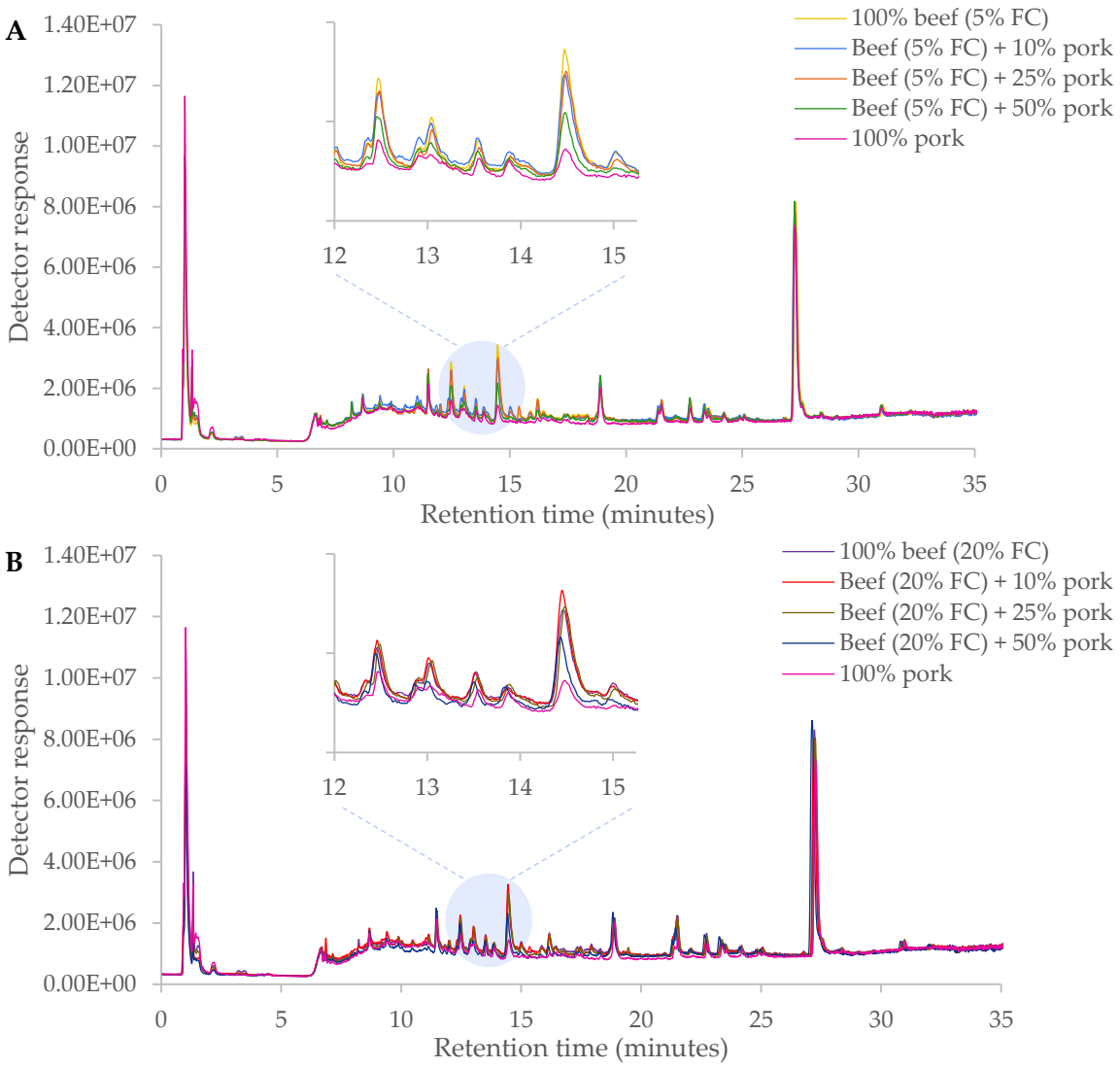

Figure 5.23: Example total ion chromatograms of extracts from cooked minced beef adulterated with different percentages of minced pork. A) Beef with 5% fat content, B) Beef with 20% fat content

The chromatograms for cooked beef adulterated with pork (Figure 5.23) show similar peak patterns, with differences in peak intensity for each sample type. Specifically, the peaks between 12.5 and 16 minutes show a higher intensity in the chromatograms for 100% beef samples, and gradually decrease as the percentage of adulterant pork increases. The peaks in the chromatograms for 100% pork samples have a very low abundance, with some peaks not present, such as the peaks at 8 and 15.5 minutes.

5.7.4.2 Multivariate statistics

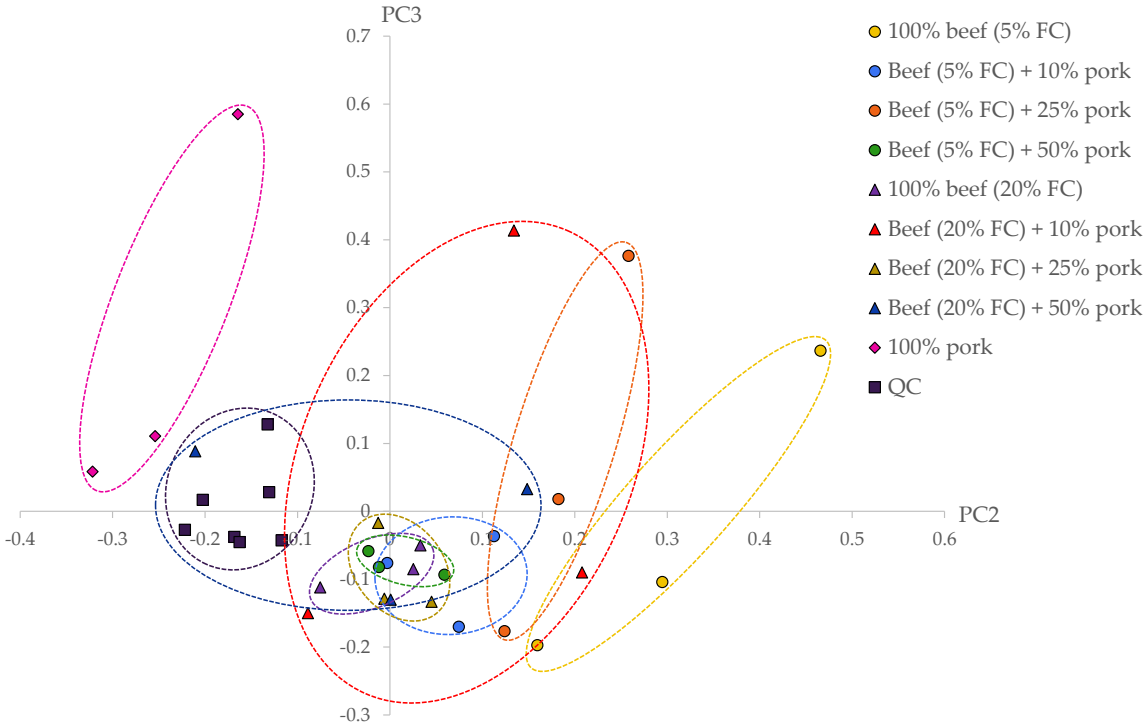

Figure 5.24: Principal component analysis scores plot of PC2 (1.021%) and PC3 (0.692%) for extracts from cooked minced beef with 5% and 20% fat content adulterated with different percentages of minced pork. PCA was carried out using all features detected with a CV $< 10\%$

The cooked samples for beef adulterated with pork produced a PCA plot that had most of the sample types overlapping. Despite only using features with a CV% in the QC samples of less than 10%, the QC samples are not very tightly clustered, implying there was some instability within the analytical run, although this was not seen in the QC analysis. However, there is no trend in the spatial placement of the QC samples, and so there does not appear to have been any gradual drift during the analytical run. This spread of data points may be because the separation between the sample types was extremely small, and so the multivariate statistical technique found all samples to be very similar, thus decreasing the overall spread of data points, emphasising the subtle differences. The 100% pork samples are separated from the other samples, but no differences can be seen between the two types of beef with differing fat contents.

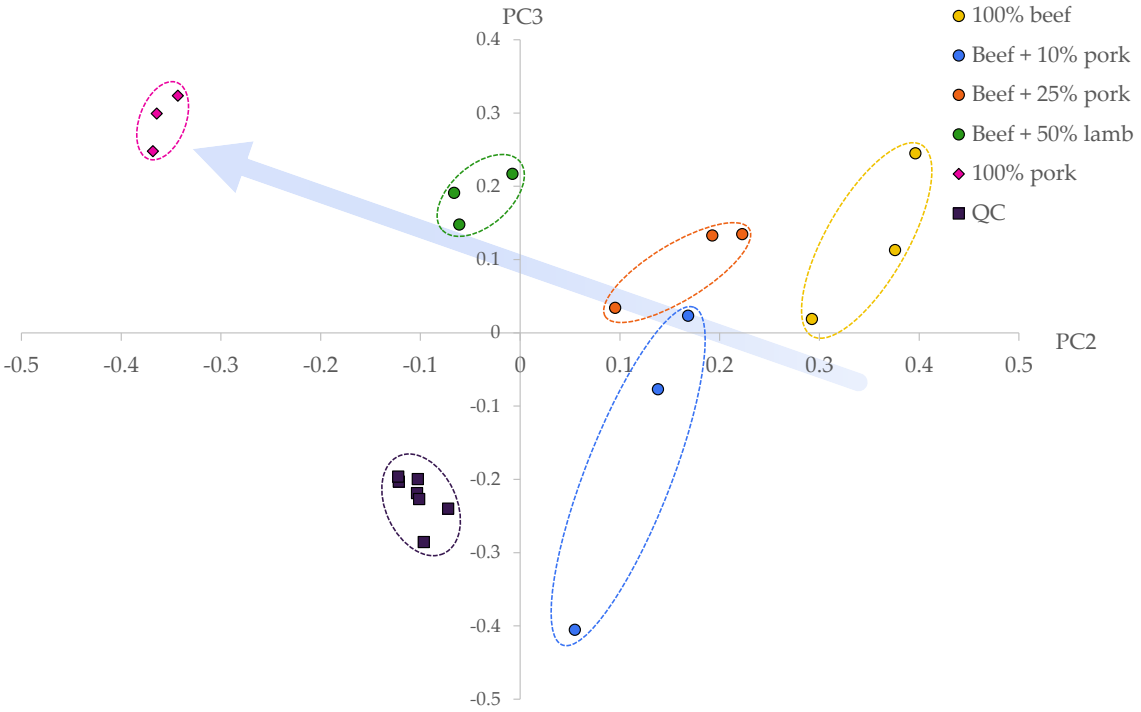

Figure 5.25: Principal component analysis scores plot of PC2 (4.325%) and PC3 (0.403%) for extracts from cooked minced beef with 5% fat content adulterated with different percentages of minced pork. PCA was carried out using all markers with a CV< 10% and p-value of < 0.05

Individual principal component analyses were carried out on the samples with each fat content in the beef, to assess which showed the largest difference among samples with differing percentages of adulterant pork. This was found to be in beef with a 5% fat content, and the separation between sample types can be seen in Figure 5.25. The trend of the sample groups goes from the right side of the plot to the left as the percentage of adulterant meat increases, as shown by the blue arrow. The QC samples are tightly clustered, confirming that there was minimal drift in the analytical run, and the separation of the sample types can be attributed to PC2 on the x-axis.

5.7.4.3 Significant markers

Table 5.14: Summary of compounds that contribute the most to the differences among all extracts from cooked minced beef with a 5% fat content that has been adulterated with different percentages of pork, including 100% beef and 100% pork, using PC2. FC = fat content. Red values indicate p-value > 0.05. Marker trend: ↓ = decreased, * = random or consistent

m/z	Retention time median (mins)	P-value from ANOVA/Welch (XCMS)		CV% (XCMS)	P-value from ANOVA/Welch (EICs)		CV% (EICs)
		5% FC	20% FC		5% FC	20% FC	
↓ 522.3561	14.47	<0.001	<0.001	2.07	<0.001	0.001	2.63
↓ 520.3404	12.48	<0.001	0.425	2.70	<0.001	0.318	3.07
↓ 162.1039	1.03	<0.001	<0.001	5.60	0.001	<0.001	5.48
↓ 482.3248	16.18	<0.001	<0.001	2.39	<0.001	<0.001	2.50
* 496.3401	14.48	0.004	0.069	1.21	0.002	0.040	2.81
↓ 480.3085	13.04	0.001	0.005	2.56	0.001	0.008	2.44
↓ 160.1254	1.08	<0.001	<0.001	6.94	<0.001	<0.001	6.71
↓ 478.2932	11.48	0.010	0.065	3.81	0.010	0.187	3.10
↓ 480.3445	15.86	<0.001	<0.001	2.10	<0.001	<0.001	3.19
↓ 544.3395	12.36	<0.001	0.006	2.48	<0.001	0.027	3.12
* 204.1157	1.08	0.003	0.019	4.67	0.011	0.061	7.17
↓ 546.3550	13.49	<0.001	0.003	2.33	<0.001	0.006	5.07
↓ 310.3100	23.34	0.030	0.055	7.93	0.008	0.014	8.21
↓ 205.1425	8.24	<0.001	<0.001	8.45	<0.001	0.001	8.11
↓ 570.3551	13.02	<0.001	<0.001	2.78	<0.001	0.001	3.25
↓ 400.3414	17.92	<0.001	<0.001	3.46	<0.001	<0.001	4.27
↓ 528.3088	12.00	<0.001	0.005	3.12	<0.001	0.006	3.62
↓ 518.3237	11.18	<0.001	0.001	2.88	<0.001	0.002	3.29
↓ 583.3238	13.06	<0.001	0.300	2.40	<0.001	0.231	2.33
↓ 504.3088	12.33	<0.001	0.093	3.72	<0.001	0.011	2.80
↓ 508.3393	12.92	<0.001	0.001	2.47	<0.001	<0.001	2.92
↓ 87.04437	8.24	<0.001	0.003	5.97	<0.001	<0.001	4.68
↓ 494.3237	11.63	<0.001	0.001	2.53	<0.001	0.002	2.98
↓ 327.0081	9.44	<0.001	0.011	4.19	<0.001	0.010	3.65
↓ 552.3284	44.78	<0.001	0.450	9.09	<0.001	0.229	11.03
↓ 550.3505	16.44	<0.001	<0.001	6.76	<0.001	<0.001	7.21
↓ 578.3810	18.12	<0.001	0.015	6.95	<0.001	0.010	5.80
↓ 580.3621	18.20	<0.001	0.243	3.86	<0.001	0.097	6.18
↓ 542.3235	11.15	<0.001	<0.001	4.86	<0.001	<0.001	3.98
↓ 552.3286	9.35	0.003	0.139	4.69	0.001	0.074	3.76
↓ 429.3758	23.61	<0.001	<0.001	8.29	<0.001	<0.001	7.09
↓ 500.2768	10.50	<0.001	0.001	3.56	<0.001	0.001	3.64
* 336.3254	24.19	0.004	0.027	8.39	0.010	0.105	7.99

Table 5.14 continued: Summary of compounds that contribute the most to the difference among all percentages of cooked pork adulteration in beef with 5% fat content, including 100% beef and 100% pork, using PC2. Arrows indicate marker decreased the higher percentage of adulterant pork. FC = fat content. Red values indicate p-value > 0.05

m/z	Retention time median (mins)	P-value from ANOVA/Welch (XCMS)		CV% (XCMS)	P-value from ANOVA/Welch (EICs)		CV% (EICs)
		5% FC	20% FC		5% FC	20% FC	
↓ 426.3569	18.68	<0.001	<0.001	4.77	<0.001	<0.001	4.93
↓ 465.3429	11.02	0.003	0.027	8.71	0.002	0.029	7.90
↓ 606.4121	20.47	<0.001	0.006	9.58	<0.001	0.023	7.18
↓ 454.3878	23.88	<0.001	<0.001	5.62	<0.001	<0.001	7.52
↓ 650.4384	22.11	0.021	0.406	6.07	0.007	0.547	9.15
↓ 548.3385	14.05	<0.001	0.325	6.71	<0.001	0.011	7.74
↓ 526.3137	14.64	<0.001	0.007	2.12	<0.001	0.006	1.49
↓ 594.3757	16.74	<0.001	0.125	4.35	<0.001	0.012	5.28
↓ 153.0385	1.34	<0.001	<0.001	5.20	<0.001	<0.001	3.39
↓ 372.3108	13.75	<0.001	<0.001	5.81	<0.001	<0.001	5.40
↓ 510.3913	22.47	0.002	0.227	3.76	<0.001	0.298	3.15
↓ 508.3753	20.88	<0.001	<0.001	4.02	<0.001	<0.001	3.14
↓ 259.1896	12.89	0.025	0.439	6.39	0.020	0.415	6.43

The majority of the top 50 markers with the highest loading values in PC2 remained after confirming CV% in the QC samples and significance in raw data. A large amount of these markers were not found to be significantly different in samples consisting of beef with a 20% fat content, however these markers were specifically found by using the PCA plot generated from the analysis of the beef with 5% fat content. All markers had a very low CV% in the QC samples of below 12%, which is extremely robust in an untargeted metabonomic study. Despite not showing a gradual trend as the percentage of adulterant meat increased, the majority of these markers were found to be at a lower concentration in the 100% pork samples compared to all other sample types, which is the opposite of what was observed in raw beef adulterated with pork. This is most likely caused by the workflow and the use of a principal component to find markers of interest, as the largest separation in this case could be caused by markers with a lower concentration in the 100% pork samples, and so the workflow would only highlight markers with this trend.

5.7.4.4 Tentative identification

Table 5.15: Compounds that were significantly different and tentatively identified in extracts from cooked minced beef (5% fat content) adulterated with minced pork based on comparison of mass spectra on METLIN

m/z	Retention time median (mins)	Possible formula	Likelihood score (%)	Tentative identification
496.3401	14.48	$C_{24}H_{50}NO_7P$	99.70	PC(16:0/0:0)
400.3414	17.92	$C_{23}H_{45}NO_4$	91.49	palmitoyl carnitine
372.3108	13.75	$C_{21}H_{41}NO_4$	97.85	myristoyl carnitine

Three markers were tentatively identified, and their matching mass spectra can be seen in Appendix D. Two of these markers were tentatively identified as acyl carnitines, and these both had a decreasing trend as the percentage of adulterant pork increased (Figure 5.26 and 5.27). These tentative identifications were not made in the raw beef with pork samples. The very low abundance of these acyl carnitines in the 100% pork samples could imply that acyl carnitines are more susceptible to degradation during the cooking process in pork than in beef. The samples containing varying percentages of pork do not follow the gradual decreasing trend, but this could be caused by the sampling process, where the small samples taken from each homogenised meat sample did not actually contain the expected percentage of adulterant meat. Despite this, the 50% pork samples do show a decreased abundance that falls in between the 100% beef and 100% pork concentration, indicating there is an acyl carnitine concentration difference in beef and pork once cooked.

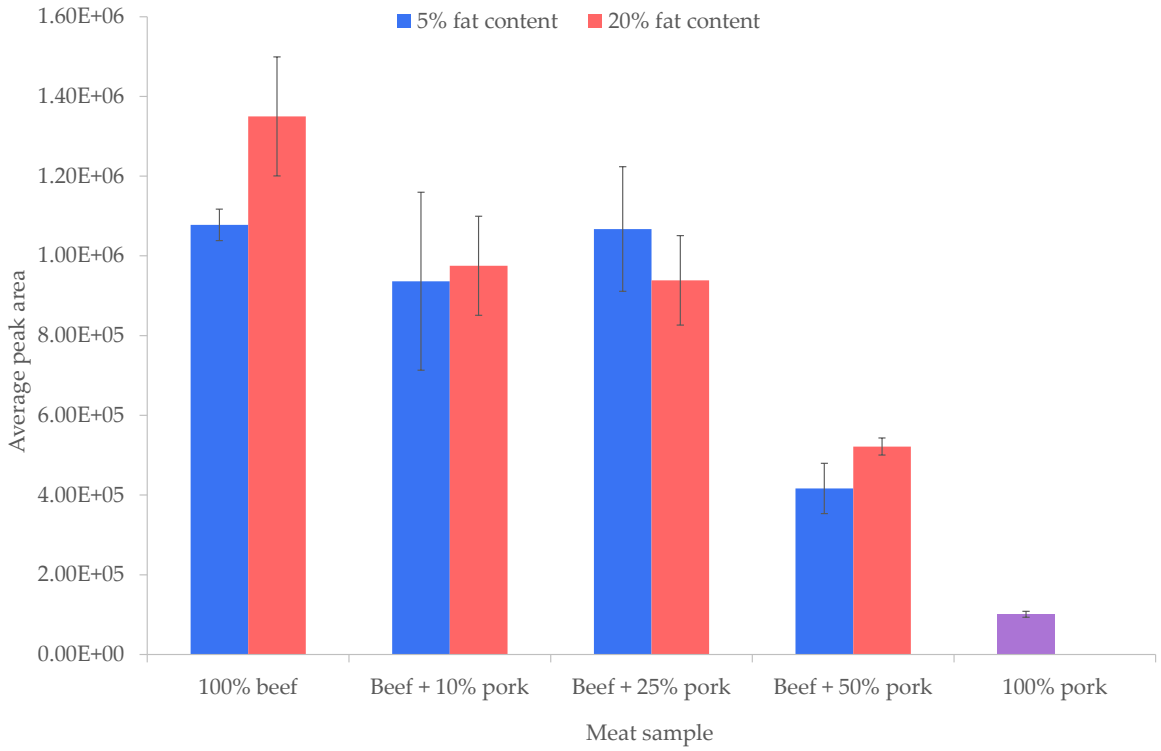

Figure 5.26: Trend of marker tentatively identified as palmitoyl carnitine that was significantly different among all cooked minced beef (5% fat content) adulterated with minced pork samples. Error bars correspond to ± 1 standard deviation

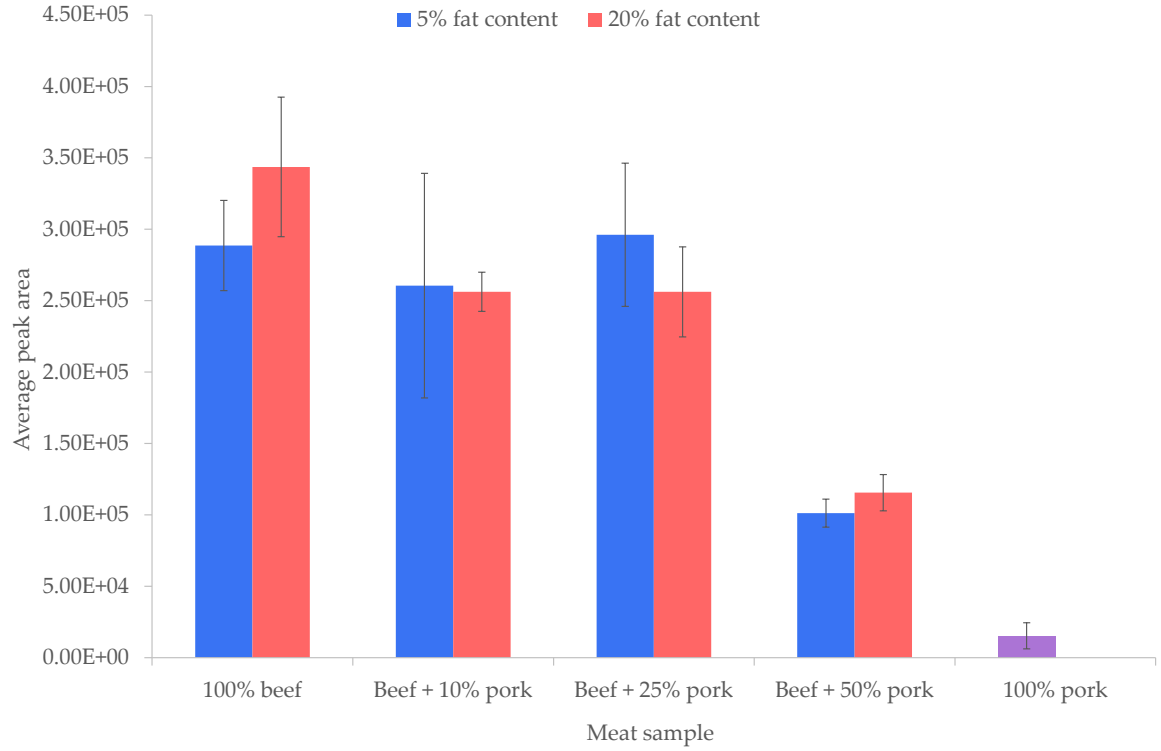

Figure 5.27: Trend of marker tentatively identified as myristoyl carnitine that was significantly different among all cooked minced beef (5% fat content) adulterated with minced pork samples. Error bars correspond to ± 1 standard deviation

5.7.5 Cooked minced beef adulterated with minced lamb

5.7.5.1 Metabolic profiling

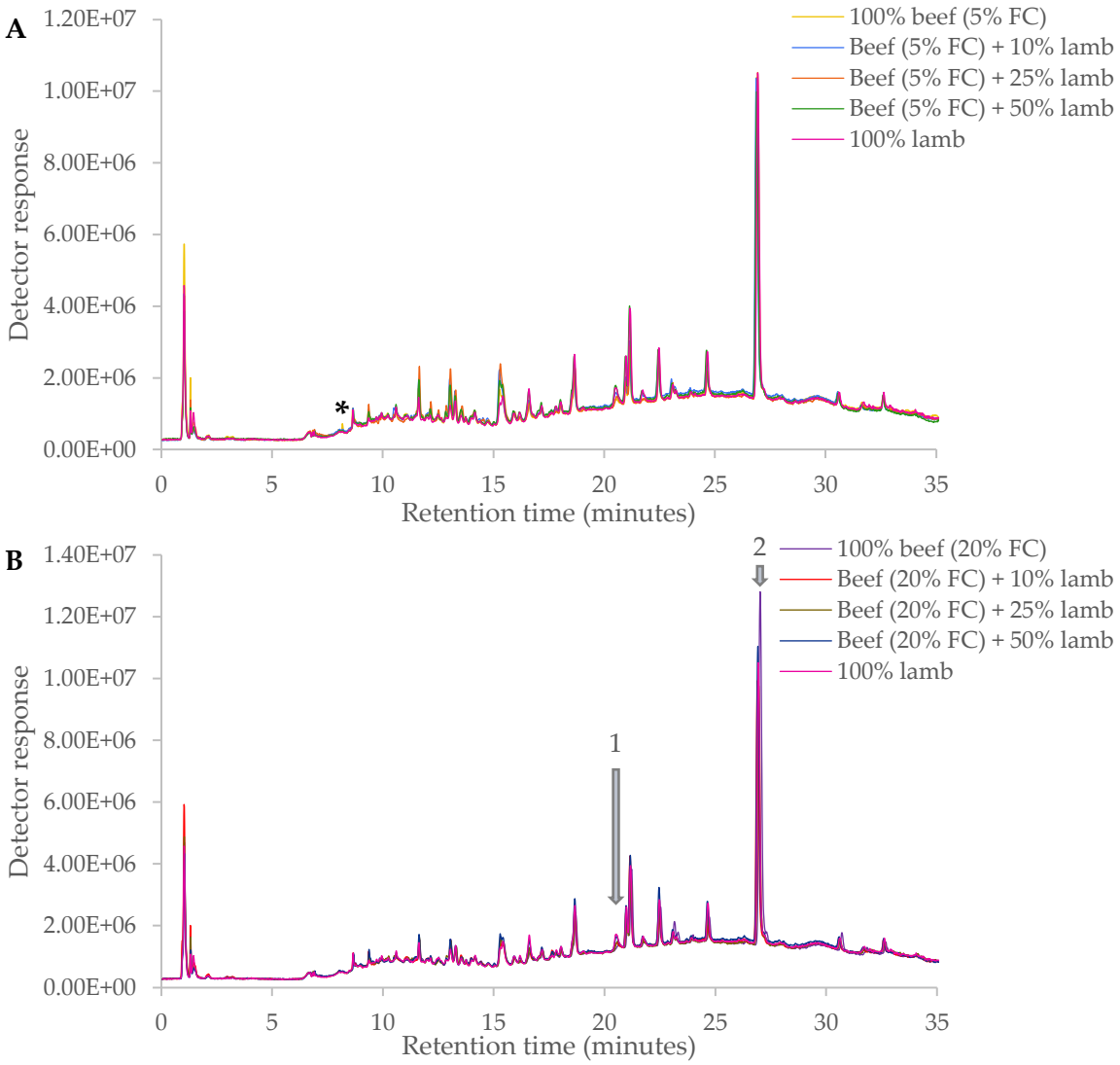

Figure 5.28: Example total ion chromatograms of extracts from cooked minced beef adulterated with different percentages of minced lamb. A) Beef with 5% fat content, B) Beef with 20% fat content

Several peaks in the chromatogram for beef with a fat content of 5% (Figure 5.28A) show a difference in abundance as the percentage of adulterant lamb changes, particularly for the peaks between 11 and 15.5 minutes. The peaks between 16 and 22.5 minutes all show a slightly higher abundance in the 100% lamb samples, however in the early part of the chromatogram (up to 15.5 minutes), the 100% lamb samples have a lower intensity than all other sample types. The chromatograms for the 100%

beef sample shows a peak at 8 minutes (indicated with an asterisk) that is not present in any other samples. The chromatograms for beef with a fat content of 20% (Figure 5.28B) have a higher peak intensity in the beef with 50% lamb for many of the peaks, however the peak at 20.5 minutes (peak 1) has a decreasing peak intensity from 100% lamb down to 100% beef. The peak at 27 minutes (peak 2) has the highest peak intensity in the 100% beef sample.

5.7.5.2 Multivariate statistics

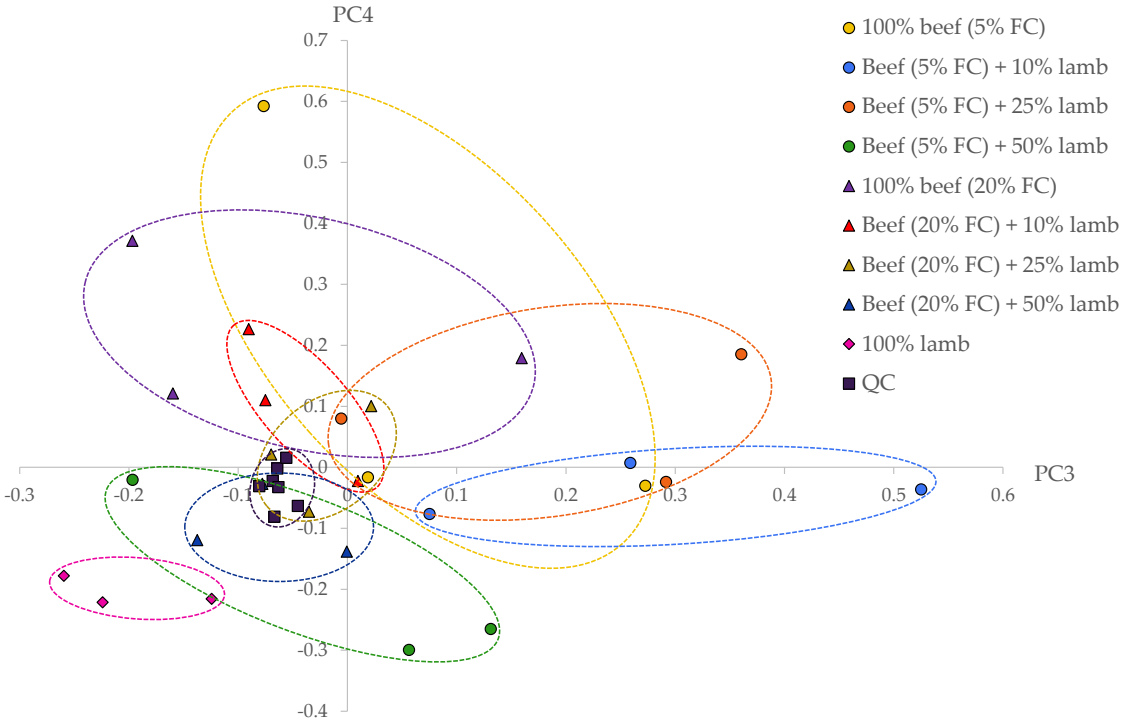

Figure 5.29: Principal component analysis scores plot of PC3 (0.338%) and PC4 (0.282%) for extracts from cooked minced beef with 5% and 20% fat content adulterated with different percentages of minced lamb. PCA was carried out using all features detected with a CV < 10%

The cooked beef with adulterated lamb produced a PCA plot with many overlapping data points. The QC samples are clustered, but all other sample types are spread across the plot. The sample groups for beef with a fat content of 5% show greater spread within each sample type than beef with a fat content of 20%. The 100% lamb samples are clustered on the left hand side of the plot, but are overlapped slightly by beef with a fat content of 5% with 50% lamb.

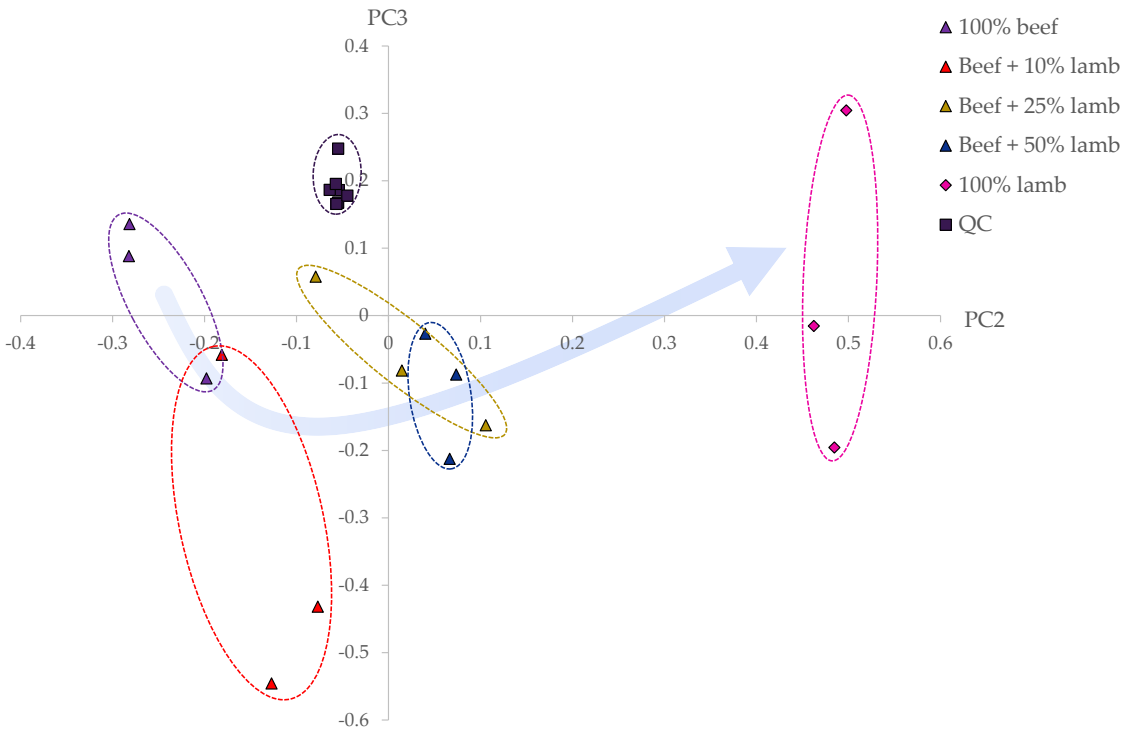

Figure 5.30: Principal component analysis scores plot of PC2 (3.959%) and PC3 (0.251%) for extracts from cooked minced beef with 20% fat content adulterated with different percentages of minced lamb. PCA was carried out using all markers with a CV $<$ 10% and p-value of $<$ 0.05

Features found to be significant in beef with a fat content of 20% proved to show the best separation of sample types during principal component analysis. Figure 5.30 shows separation between all sample types. Looking at the blue arrow, which shows the trend of the sample groups, the 100% beef samples appear on the left of the plot, and the percentage of adulterant meat increases across the x-axis (PC2), with the 100% lamb samples on the right side of the plot. There is some overlap of the adulterated samples, but that could be caused by the variation attained during the sampling process. The QC samples are clustered together, confirming the analytical run was stable throughout.

5.7.5.3 Significant markers

Table 5.16: Summary of compounds that contribute the most to the differences among all extracts from cooked minced beef with a 20% fat content that has been adulterated with different percentages of lamb, including 100% beef and 100% lamb, using PC2. All markers increased the higher percentage of adulterant lamb. FC = fat content. Red values indicate p-value > 0.05

m/z	Retention time median (mins)	P-value from ANOVA/Welch (XCMS)		CV% (XCMS)	P-value from ANOVA/Welch (EICs)		CV% (EICs)
		5% FC	20% FC		5% FC	20% FC	
428.3737	20.51	0.001	<0.001	2.76	0.145	<0.001	3.22
482.3246	16.58	0.042	0.007	1.51	0.065	0.014	1.47
466.3291	17.81	0.005	0.005	1.98	0.010	0.007	2.37
269.0849	1.45	<0.001	<0.001	1.34	<0.001	0.005	2.06
456.4045	26.21	0.072	0.010	2.27	0.093	0.003	2.87
400.3422	16.20	<0.001	<0.001	2.55	0.001	0.001	3.53
267.2680	24.61	<0.001	0.001	4.06	0.001	0.004	4.00
480.3085	13.74	0.195	0.024	1.35	0.149	0.030	1.68
279.2315	16.48	<0.001	<0.001	3.00	<0.001	0.001	2.79
241.1286	0.97	<0.001	<0.001	8.32	<0.001	<0.001	9.60
303.2317	16.14	0.003	0.001	1.32	<0.001	0.004	2.15
537.1663	1.45	<0.001	<0.001	2.21	<0.001	<0.001	2.87
305.2474	17.99	0.061	0.003	2.58	0.024	0.020	2.54
464.3132	15.17	0.001	0.001	2.45	0.006	0.016	2.99
500.2773	10.60	0.282	0.001	7.29	0.242	0.016	4.15
329.2479	17.51	0.003	0.003	4.66	<0.001	0.006	5.14
464.3132	14.65	0.013	0.023	3.40	0.004	0.018	2.43
426.3576	17.36	0.006	0.001	4.11	0.007	<0.001	4.85
454.3885	21.54	0.014	<0.001	2.58	0.022	0.001	3.81
963.6399	16.58	0.064	0.022	2.90	0.081	0.028	3.02
372.3108	12.85	0.011	0.001	3.00	0.014	0.001	2.75
357.3001	18.50	0.002	0.008	2.90	0.038	0.039	6.92
414.3574	18.25	0.001	0.001	3.45	0.002	0.002	3.81
452.3132	15.85	0.015	0.032	1.33	0.007	0.044	6.47
444.3676	15.86	0.004	0.001	8.32	0.001	<0.001	4.14
526.2931	11.57	0.037	0.009	4.83	0.051	0.015	5.38
307.2629	20.31	0.003	0.001	6.61	0.005	0.005	6.20
253.2520	22.82	<0.001	0.015	4.37	0.001	0.010	5.76
414.3571	17.62	<0.001	<0.001	6.56	0.001	<0.001	6.07
370.2956	11.34	<0.001	0.006	3.10	0.028	0.028	5.79
398.3266	13.66	0.009	0.025	5.03	0.009	0.041	6.77
322.2739	18.50	0.038	0.017	4.54	0.092	0.045	4.50

Table 5.16 continued: Summary of compounds that contribute the most to the differences within all percentages of lamb adulteration in beef with 20% fat content, including 100% beef and 100% lamb, in cooked meatball samples, using PC2. All markers increased the higher percentage of adulterant lamb. FC = fat content. Red values indicate p-value > 0.05

m/z	Retention time median (mins)	P-value from ANOVA/Welch (XCMS)		CV% (XCMS)	P-value from ANOVA/Welch (EICs)		CV% (EICs)
		5% FC	20% FC		5% FC	20% FC	
468.3109	14.80	0.004	0.003	3.29	0.009	0.010	5.23
317.3044	21.12	0.005	<0.001	5.09	0.006	0.006	4.53
212.1018	0.97	<0.001	<0.001	5.36	0.002	0.014	6.86
296.0657	1.00	0.007	0.032	6.74	0.004	0.022	10.15

All markers in Table 5.16 proved to be significantly different in the beef with 20% fat content samples in the normalised data and in the raw data, as well as showing reliability in the QC samples with a CV% of less than 11%. Most of these markers were also significantly different in the beef with 5% fat content samples, however some had a p-value of more than 0.05, and so would not be suitable markers to use to detect adulteration in beef products with a lower fat content. All of these markers showed an increasing trend as the percentage of adulterant lamb increased, with the majority showing a gradual trend in the adulterated samples.

5.7.5.4 Tentative identification

Table 5.17: Compounds that were significantly different and tentatively identified in extracts from cooked minced beef (20% fat content) adulterated with minced lamb based on comparison of mass spectra on METLIN

m/z	Retention time median (mins)	Possible formula	Likelihood score (%)	Tentative identification
400.3422	16.20	$C_{23}H_{45}NO_4$	99.58	palmitoyl carnitine
305.2474	17.99	$C_{20}H_{32}O_2$	99.93	arachidonic acid
372.3108	12.85	$C_{21}H_{41}NO_4$	98.36	myristoyl carnitine

Three markers were tentatively identified as acyl carnitines and arachidonic acid (Table 5.17), and the matching mass spectra to standards on the METLIN database can be seen in Appendix E. All of these compounds have been seen in this research previously, and they all follow a similar increasing trend as the percentage of adulterant lamb increases. In particular, the acyl carnitines have a low concentration in the beef samples, and this concentration gradually increases, with a higher concentration in the 100% lamb samples, as seen in Figures 5.31 and 5.32.

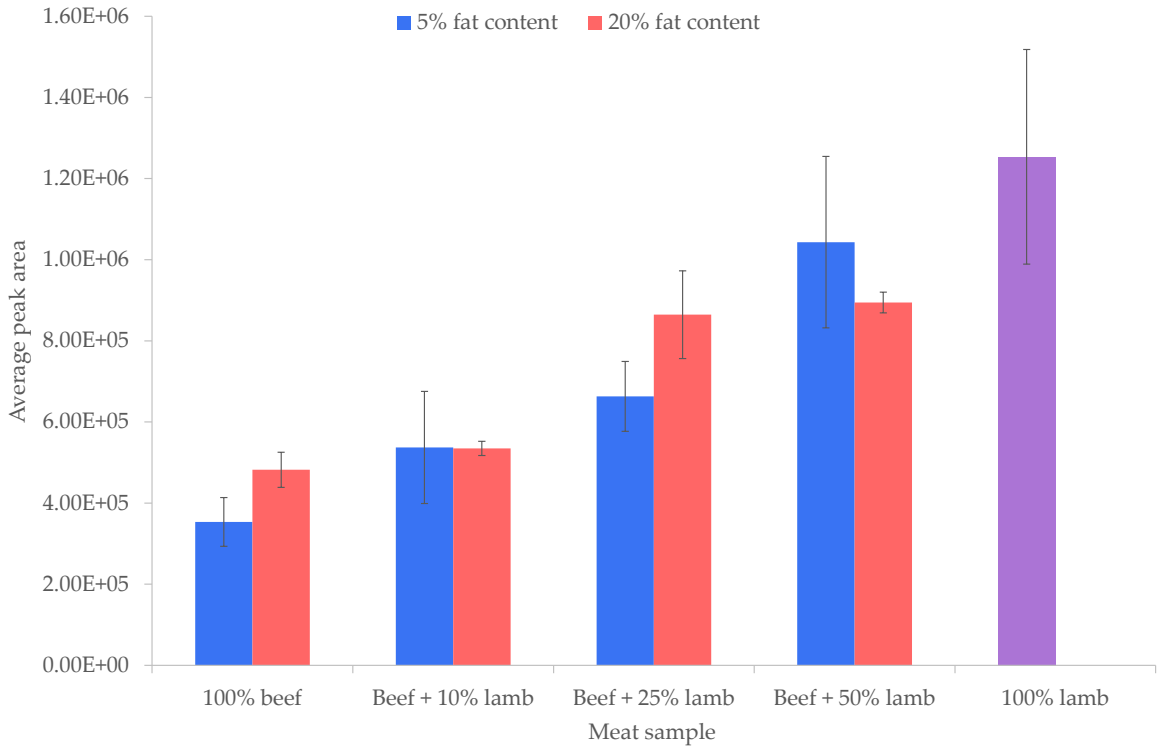

Figure 5.31: Trend of marker tentatively identified as palmitoyl carnitine that was significantly different among all cooked minced beef (20% fat content) adulterated with minced lamb samples. Error bars correspond to ± 1 standard deviation

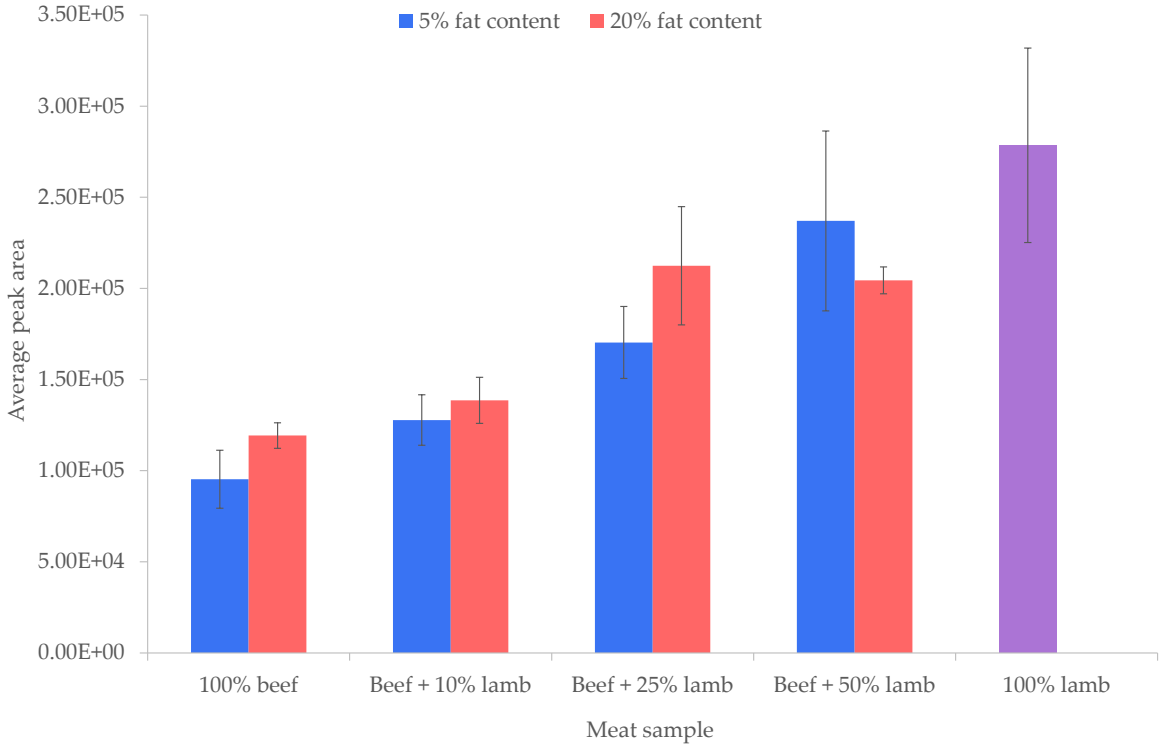

Figure 5.32: Trend of marker tentatively identified as myristoyl carnitine that was significantly different among all cooked minced beef (20% fat content) adulterated with minced lamb samples. Error bars correspond to ± 1 standard deviation

5.7.6 Cooked minced beef adulterated with minced turkey

After initial observations, it was clear that one repeat sample from the beef with a fat content of 5% adulterated with 10% turkey did not inject correctly. Therefore, this sample was removed from any further statistical analysis, so this sample group only has two samples.

5.7.6.1 Metabolic profiling

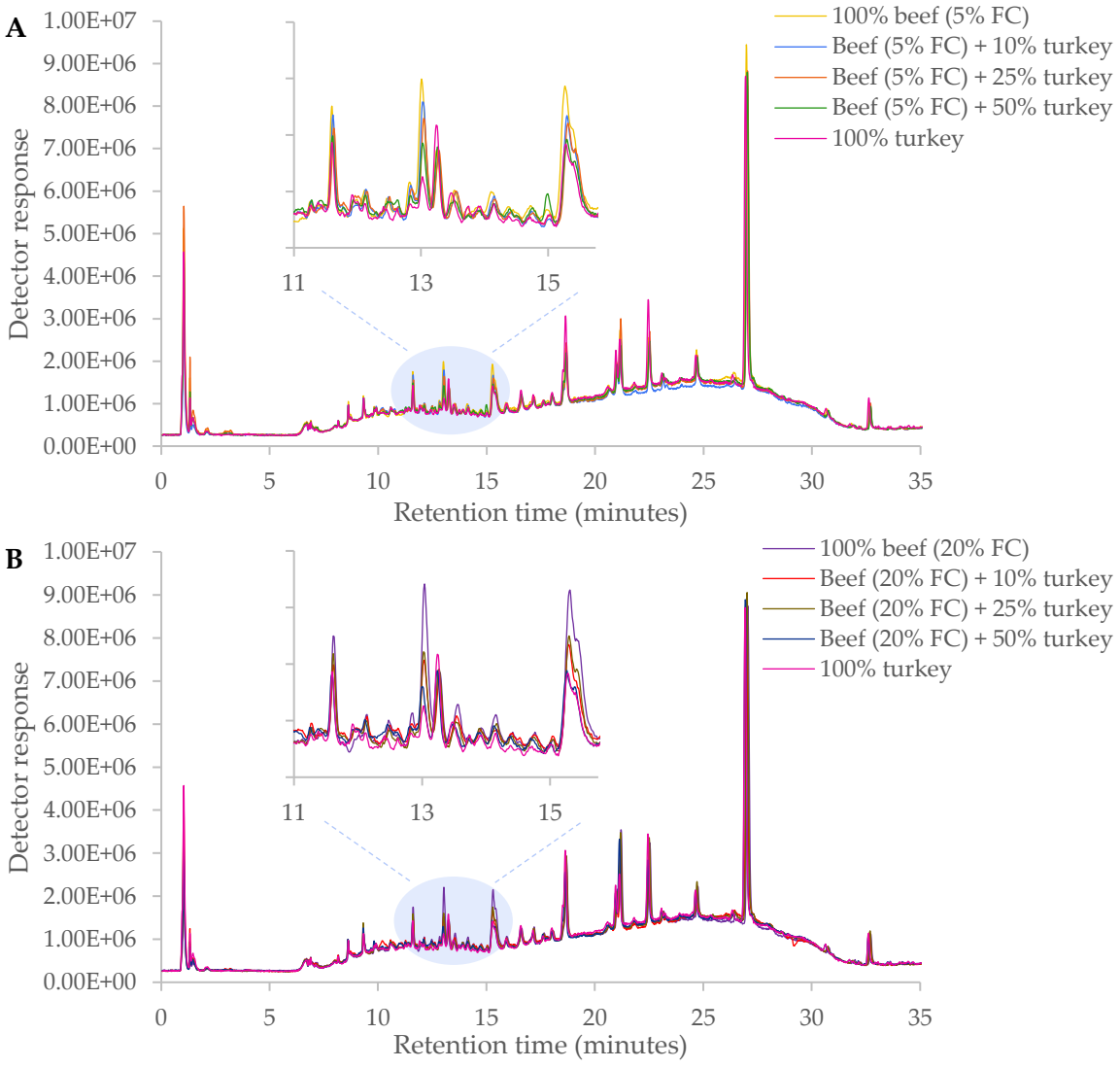

Figure 5.33: Example total ion chromatograms of extracts from cooked minced beef adulterated with different percentages of minced turkey. A) Beef with 5% fat content, B) Beef with 20% fat content

There are slight differences in the intensity of some peaks in the chromatograms for cooked beef with a fat content of 5% adulterated with turkey (Figure 5.33A). This is especially apparent in the peaks eluting before 2 minutes. These peaks correspond to the highly polar compounds that are not retained on the stationary phase. The small peaks at 3 minutes do not appear to be present in the 100% turkey samples, so this could be attributed to compounds that are only present in the beef. Generally, the 100% turkey samples have the lowest abundance in all peaks that show a difference between sample types, apart from the peaks at 19 and 22.5 minutes where it has the highest intensity. Peaks at 11.5, 13 and 15.5 minutes all show a decreasing intensity as the percentage of adulterant turkey increases. This is similar in beef with a fat content of 20% (B), where the peaks at 11.5, 13 and 15.5 minutes all have a higher intensity in 100% beef.

5.7.6.2 Multivariate statistics

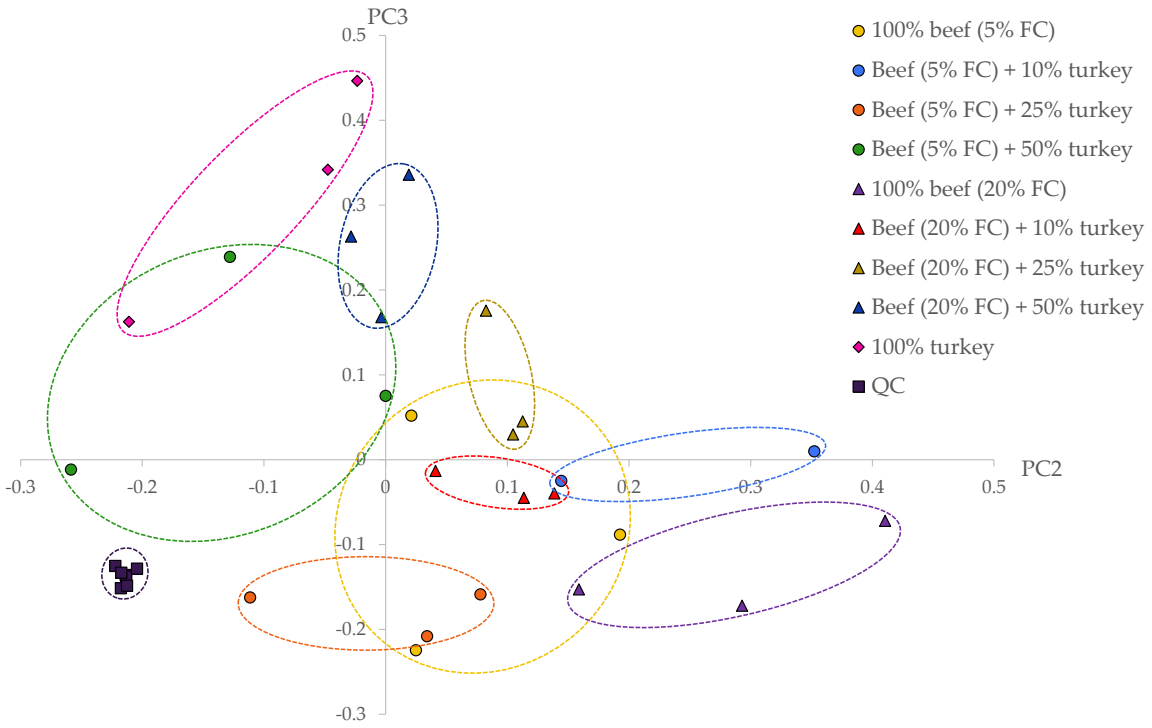

Figure 5.34: Principal component analysis scores plot of PC2 (0.935%) and PC3 (0.437%) for extracts from cooked minced beef with 5% and 20% fat content adulterated with different percentages of minced turkey. PCA was carried out using all features detected with a CV $< 10\%$

Some sample types have a large spread in the PCA plot (Figure 5.34), however there is a definite pattern in the spatial placement for the sample types. Specifically, the 100% beef with a fat content of 20% is in the bottom right quadrant of the plot, and as the plot moves diagonally across to the 100% turkey samples in the top left quadrant, the other beef samples with varying percentages of adulterant meat can be seen. Particularly in the beef with a fat content of 20%, the placement of the groups diagonally across is in the order of percentage of adulterant turkey. This indicates there was a trend in the metabolites that caused this separation.

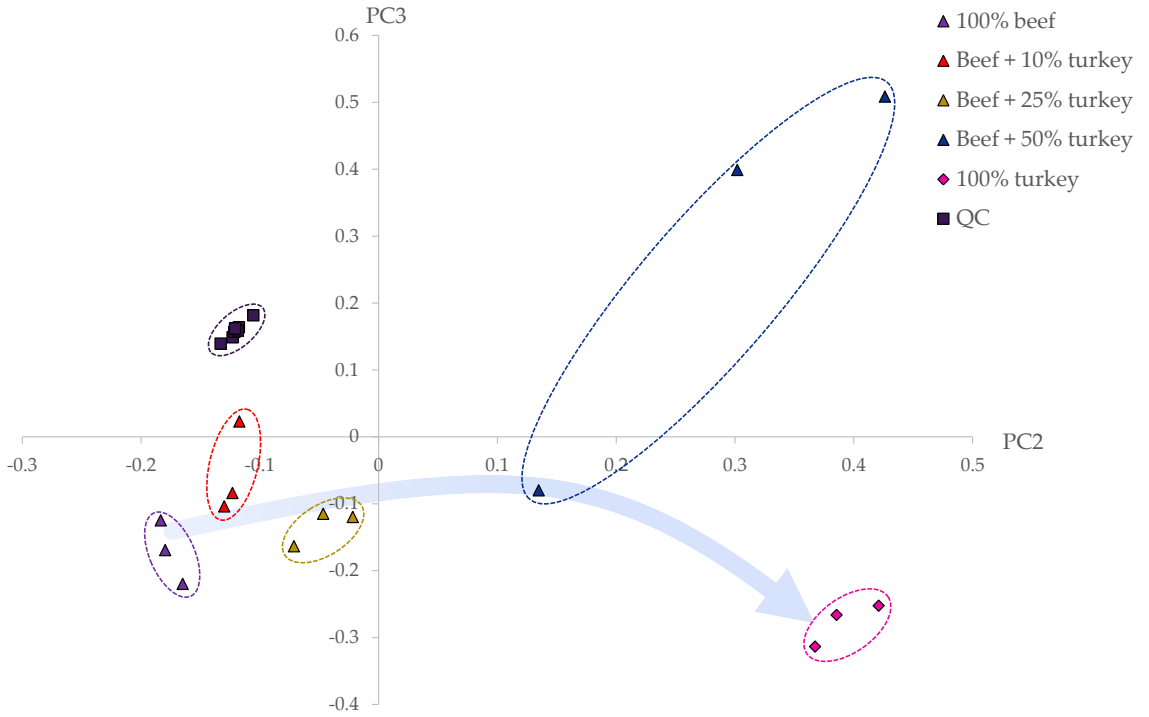

Figure 5.35: Principal component analysis scores plot of PC2 (3.352%) and PC3 (1.768%) for extracts from cooked minced beef with 20% fat content adulterated with different percentages of minced turkey. PCA was carried out using all markers with a CV $<$ 10% and p-value of $<$ 0.05

Figure 5.35 shows all samples are separated, and the QC samples are tightly clustered. The separation of these sample groups, represented by the blue arrow, is along the x-axis, with the 100% beef samples on the left and moving to the 100% turkey samples on the right, indicating that PC2 is responsible for the separation. The beef with 50% turkey has a large spread within the group, which could be due to a larger difference in the 3 replicates taken from the original meat sample, implying there may have been an issue in the homogenisation process when producing this adulterated meatball.

5.7.6.3 Significant markers

Table 5.18: Summary of compounds that contribute the most to the differences among all extracts from cooked minced beef with a 20% fat content that has been adulterated with different percentages of turkey, including 100% beef and 100% turkey, using PC2. FC = fat content. Red values indicate p-value > 0.05.
Marker trend: ↓ = decreased, ↑ = increased, * = random or consistent

m/z	Retention time median (mins)	P-value from ANOVA/Welch (XCMS)		CV% (XCMS)	P-value from ANOVA/Welch (EICs)		CV% (EICs)
		5% FC	20% FC		5% FC	20% FC	
* 482.3241	16.60	0.015	0.006	1.17	0.003	0.017	1.45
↑ 524.3707	20.63	0.006	0.006	1.97	<0.001	0.031	2.22
↑ 241.1297	0.98	0.364	<0.001	1.53	0.013	<0.001	4.44
↑ 454.2926	13.24	<0.001	<0.001	2.58	<0.001	<0.001	3.42
↑ 401.3412	26.42	<0.001	<0.001	4.32	<0.001	<0.001	4.47
↑ 530.3235	13.47	<0.001	0.001	2.66	<0.001	0.001	3.72
↓ 522.3551	15.93	0.010	<0.001	0.68	0.001	<0.001	1.52
↑ 502.2924	11.94	0.002	<0.001	2.73	<0.001	<0.001	2.45
↑ 520.5081	36.58	<0.001	<0.001	4.47	<0.001	<0.001	5.12
* 283.2632	21.17	0.115	0.010	2.40	0.058	0.016	2.47
↓ 496.3399	15.43	0.002	0.002	1.78	<0.001	0.005	1.70
↑ 305.2474	18.01	0.045	0.001	4.72	0.076	0.003	4.08
↑ 279.2314	16.50	<0.001	0.002	2.38	<0.001	<0.001	3.00
↑ 572.3706	15.34	0.005	<0.001	2.16	0.004	<0.001	2.43
↑ 596.3558	16.97	0.001	<0.001	2.58	0.001	<0.001	3.14
↑ 300.2892	12.43	<0.001	<0.001	3.90	<0.001	<0.001	7.14
↑ 298.2738	18.53	<0.001	<0.001	3.11	<0.001	<0.001	3.34
↑ 560.5005	36.58	0.013	0.007	6.66	0.012	0.005	5.88
↑ 212.1027	0.96	0.005	<0.001	4.54	0.007	<0.001	6.04
↑ 528.3108	12.77	<0.001	<0.001	2.36	<0.001	<0.001	5.44
↑ 121.5703	0.96	0.003	<0.001	6.16	0.008	<0.001	6.53
↑ 367.3355	24.53	<0.001	<0.001	5.56	<0.001	0.001	5.72
↑ 526.2928	11.54	<0.001	<0.001	1.57	<0.001	<0.001	4.09
↑ 385.3456	30.84	0.002	0.021	8.72	0.001	0.044	9.29
↑ 322.2739	18.53	0.010	<0.001	6.04	<0.001	<0.001	4.42
↑ 367.3352	25.43	<0.001	0.001	6.12	<0.001	0.002	7.22
↑ 580.3610	18.61	0.414	0.011	2.66	0.333	0.017	3.17
↓ 478.2923	12.01	0.003	0.001	3.18	<0.001	0.003	4.71
↑ 163.9777	1.01	0.050	<0.001	1.92	0.001	0.001	2.85
↑ 652.3858	17.07	0.001	<0.001	9.56	<0.001	<0.001	6.88

The markers shown in Table 5.18 were all significantly different in beef with a fat content of 20% among all adulterated beef samples, in both the normalised data and the raw data. Only a few markers were found to not be significantly different in the beef with a fat content of 5%, indicating these markers may not be robust enough to detect adulteration as these were only significant in the beef with a higher fat content. Many markers showed an increasing trend as the percentage of adulterant turkey increased, however a few markers showed a decreasing trend. All other markers showed one sample type to be higher than the others that did not correlate with the percentage of adulterant meat.

5.7.6.4 Tentative identifications

Table 5.19: Compounds that were significantly different and tentatively identified in extracts from cooked minced beef (20% fat content) adulterated with minced turkey based on comparison of mass spectra on METLIN

m/z	Retention time median (mins)	Possible formula	Likelihood score (%)	Tentative identification
524.3707	20.63	$C_{26}H_{54}NO_7P$	99.00	PAF C-16
401.3412	26.42	$C_{27}H_{44}O_2$	98.72	7-ketocholesterol
496.3399	15.43	$C_{24}H_{50}NO_7P$	99.75	PC(16:0/0:0)
305.2474	18.01	$C_{20}H_{32}O_2$	99.56	arachidonic acid
298.2738	18.53	$C_{18}H_{35}NO_2$	94.58	3-ketosphingosine

Five markers were tentatively identified, as shown in Table 5.19, and the matching mass spectra to the compounds on the METLIN database can be seen in Appendix F. The marker 401.3412 *m/z* was tentatively identified as 7-ketocholesterol, which is an oxidised form of cholesterol. Cholesterol contains one double bond, causing it to be vulnerable to oxidation [155], which occurs during the biochemical changes after death, and produces many oxidation products, one of which is 7-ketocholesterol. This marker was found to have a higher abundance in the 100% turkey samples compared to all other sample types, however this was not a gradual trend (Figure 5.36).

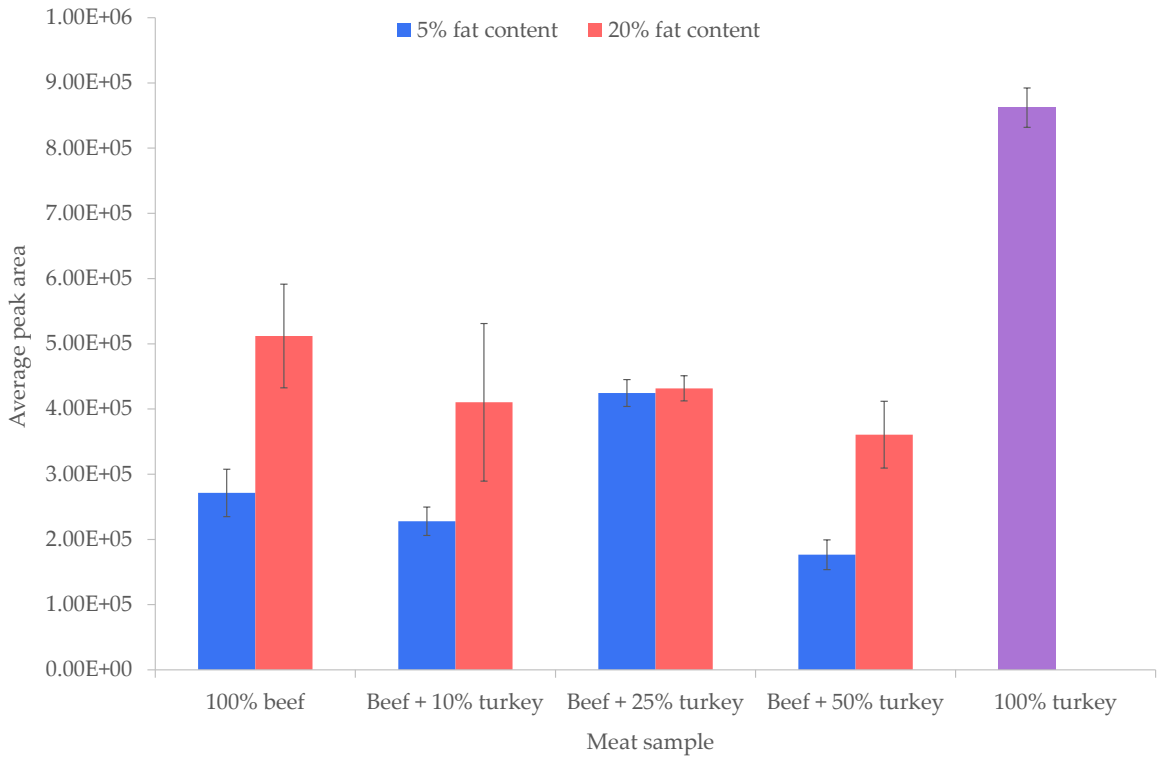

Figure 5.36: Trend of marker tentatively identified as 7-ketocholesterol that was significantly different among all cooked minced beef (20% fat content) adulterated with minced turkey samples. Error bars correspond to ± 1 standard deviation

Marker 496.3399 m/z was tentatively identified as PC(16:0/0:0), which has previously been identified in raw beef adulterated with pork and with lamb, and cooked beef adulterated with pork. This was one of the few markers in the remaining top 50 markers in Table 5.18 that had a gradual decreasing trend as the percentage of turkey increased (Figure 5.37). PC(16:0/0:0) is a type of phospholipid, specifically a phosphatidylcholine, and these compounds contribute heavily to the structure of cell membranes.

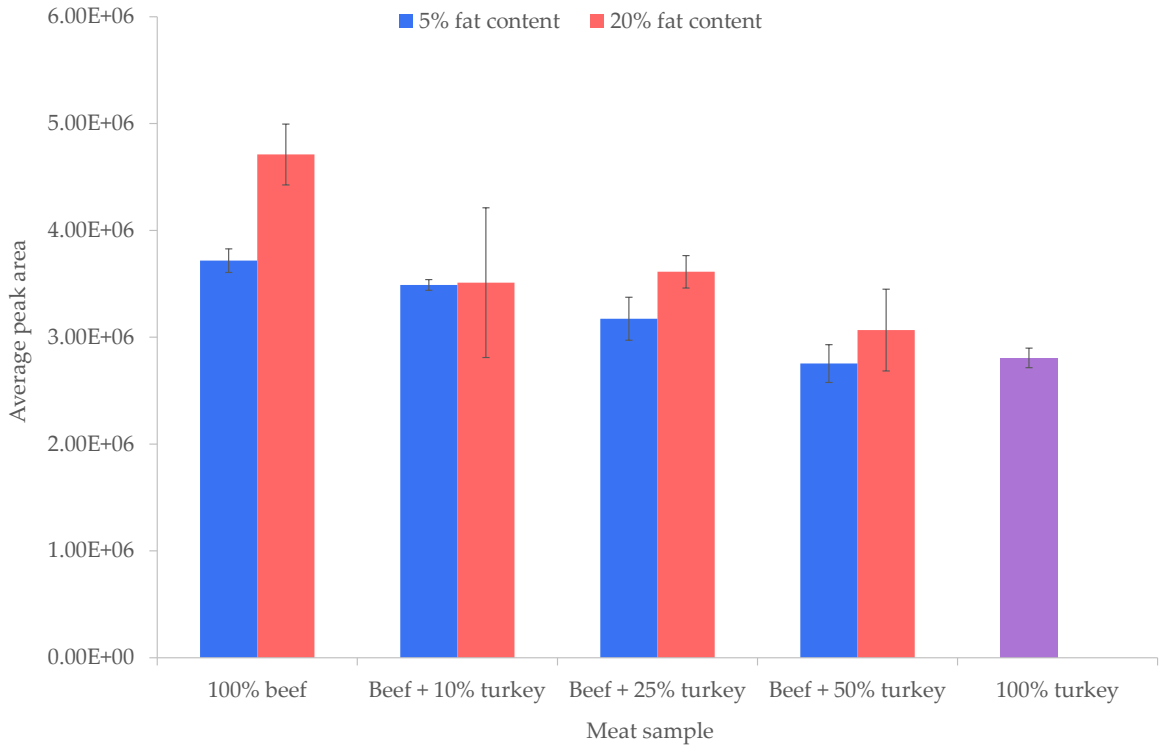

Figure 5.37: Trend of marker tentatively identified as PC(16:0/0:0) that was significantly different among all cooked minced beef (20% fat content) adulterated with minced turkey samples. Error bars correspond to ± 1 standard deviation

5.7.7 Comparison between raw and cooked

The process of cooking can cause a variety of changes to the meat, including an increase in oxidation products. Cooked meat is more susceptible to oxidation than raw meat due to the phospholipid membrane structure breaking down during the heating process [156]. It is important to investigate whether compounds would only be suitable to use as a marker for adulteration when the meat is specifically either raw or cooked, or whether it could be used regardless of the cooked state of the meat product.

The markers that were tentatively identified in each dataset (raw and cooked) were searched for in the other dataset to see if that marker was significant in both raw and cooked meat samples. Table 5.20 shows this comparison, with the p-values for all datasets. Looking at the tentative identifications made in the pork samples, linoleic acid methyl ester, sphingosine, palmitoyl carnitine and myristoyl carnitine were all significantly different regardless of fat content percentage and whether it was raw or cooked. With further targeted research, these markers could be used to detect the adulteration of beef products with pork, which would be particularly important to some religious communities. Palmitic acid methyl ester was not found at all in the cooked samples, indicating that this compound degrades during the cooking process.

A marker in the raw lamb samples was tentatively identified as PC(16:0/0:0), which was only significantly different in the raw beef samples, and not detected at all in the cooked samples, therefore would most likely not be suitable as a marker for the adulteration with lamb after cooking. Palmitoyl carnitine, myristoyl carnitine and eicosapentanoic acid were found to be significantly different in all datasets, so could be useful in detecting the adulteration of beef products with lamb, regardless of fat content or cooking status.

Finally, the turkey samples had two tentative identifications, docosenamide and

palmitic acid methyl ester, that were not detected in the cooked samples. Palmitic acid methyl ester was also found in the pork samples, and was also not detected after cooking, supporting the theory that this compound may degrade during the cooking process. This compound, however, was found in both raw and cooked lamb samples, but the significance after cooking was only slight, indicating this compound would not be suitable in cooked meat samples. PC(16:0/0:0) was also tentatively identified in the pork and lamb samples, and in each case, the significance of this marker decreased after cooking, except for in the turkey samples. All other tentative identifications made with the turkey samples were significantly different in all datasets, and so could be used as markers to detect adulteration of beef products with turkey meat in the future.

Table 5.20: Comparison of tentative identifications made during analysis of raw and cooked minced beef adulterated with each different meat species.
[a] = tentatively identified in raw dataset, [b] = tentatively identified in cooked dataset, ND = not detected. Asterisk indicates dataset used in finding most significant markers in either raw or cooked. FC = fat content. Red values indicate p-value > 0.05

Pork

m/z	Retention time median (mins)	Tentative identification	P-value from raw datasets		P-value from cooked datasets	
			5% FC	20% FC*	5% FC*	20% FC
496.3399	14.48	PC(16:0/0:0)[ab]	0.001	<0.001	0.004	0.069
295.2621	23.90	linoleic acid methyl ester[a]	<0.001	0.003	<0.001	<0.001
271.2620	26.64	palmitic acid methyl ester[a]	0.001	0.017	ND	ND
300.2885	13.26	sphingosine[a]	<0.001	0.007	0.020	0.003
400.3414	17.92	palmitoyl carnitine[b1]	0.001	<0.001	<0.001	<0.001
372.3108	13.75	myristoyl carnitine[b]	<0.001	<0.001	<0.001	<0.001

Lamb

m/z	Retention time median (mins)	Tentative identification	P-value from raw datasets		P-value from cooked datasets	
			5% FC	20% FC*	5% FC	20% FC*
400.3421	16.27	palmitoyl carnitine[ab1]	<0.001	<0.001	<0.001	<0.001
372.3107	12.90	myristoyl carnitine[ab]	<0.001	<0.001	0.011	0.001
305.2474	18.06	arachidonic acid[ab]	0.039	0.001	0.061	0.003
271.2626	26.16	palmitic acid methyl ester[a]	<0.001	0.001	0.046	0.111
524.3710	20.66	PAF C-16[a]	<0.001	<0.001	0.005	0.094
303.2317	16.20	eicosapentanoic acid[a]	<0.001	<0.001	<0.001	<0.001
496.3403	15.47	PC(16:0/0:0)[a]	0.006	0.002	ND	ND

Turkey

m/z	Retention time median (mins)	Tentative identification	P-value from raw datasets		P-value from cooked datasets	
			5% FC	20% FC*	5% FC	20% FC*
524.3706	20.62	PAF C-16[ab]	<0.001	0.002	0.006	0.006
305.2475	18.02	arachidonic acid[ab]	0.006	<0.001	0.045	0.001
298.2740	18.51	3-ketosphingosine[ab]	0.002	<0.001	<0.001	<0.001
338.3422	26.99	docosenamide[a]	0.223	0.022	ND	ND
271.2629	26.14	palmitic acid methyl ester[a]	0.003	0.003	ND	ND
300.2893	12.44	sphingosine[a]	<0.001	<0.001	<0.001	<0.001
401.3412	26.42	7-ketocholesterol[b]	<0.001	0.001	<0.001	<0.001
496.3399	15.43	PC(16:0/0:0)[b]	0.010	0.002	0.002	0.002

[1]These were tentatively identified as palmitoyl carnitine, however these markers may have been isomers of this compound.

5.8 Conclusion

The quality control throughout this research has proved that the data obtained was reliable and robust. The retention time and peak area variability was minimal in all analytical runs throughout this study.

This work was a preliminary investigation into detecting features that were significantly different between beef and other species of meat, with the intention of finding markers that could be used in the future to detect adulteration of beef products with pork, lamb or turkey. It also aimed to investigate the impact that the cooking status had on detecting the adulteration of beef products. Now this has been achieved, future work would involve refining the meatball preparation in order to get a more accurate percentage of adulteration. Additional to this, more percentages of adulterant meat would need to be investigated, which would also aid in the assessment of the limit of detection for each meat type, and whether these techniques would be applicable to detect trace amounts of adulterant meat in the human food chain.

The production of the adulterated meatballs in this research was quite crude; each meatball was homogenised by hand. However, only a small portion from that sample was used for metabolite extraction, and these portions would most likely not have included the exact percentages of beef and adulterant meat as desired. Whilst this means that some of the results may not be accurate, this is most representative of how these products would be sampled in a food control setting. Ideally, it would have been more beneficial to use the whole meatball in the metabolite extraction to get a better understanding of the difference in metabolite content in differing percentages of adulterant meat, however with the use of the 100% beef and 100% adulterant meat samples, a difference in metabolite content could be determined, and it is only the samples in the middle of these extremes with varying percentages of adulterant meat

that could be slightly inaccurate. Any markers that proved to have a gradual trend as the percentage of adulterant meat increased has great potential in being utilised as a marker for the detection of that species of adulterant meat.

Only three replicates of each meatball sample were analysed due to the restriction on the number of samples in an analytical run and the overall duration of time. Further work would be necessary to include more replicates, which could help in using multivariate statistics to detect adulterant meat in a beef product.

The multivariate statistics proved to be most successful in separating datasets in the beef with a fat content of 20% analyses, except for cooked beef adulterated with pork. This may be because the adulterant meat all had a fat content of 10% and less, and so the differences seen between the beef and adulterant meat could be attributed to the difference in lipid concentration, and this was shown by the majority of the tentatively identified compounds being lipids. In particular, the raw beef with a fat content of 20% adulterated with lamb meat showed very good separation between the sample types in the PCA plot.

The metabolic differences in this experiment could have been caused by the difference in species, however it could also be caused by the pre-slaughter conditions of these animals. For example, in Chapter 3, it was found that sphingosine had a lower concentration in dead on arrival chicken compared to normally slaughtered chicken, which could be attributed to the difference in time since death. The markers found in this study could be post-mortem interval indicators and not actually species indicators. Nevertheless, the markers were chosen based on the contribution to the separation in PCA plots, and so it would be expected that the largest difference between each sample would be caused by the difference in species, and not by the more subtle difference of pre-slaughter conditions and postmortem interval.

Regarding the tentative identifications made throughout this experiment, it is vital to take caution with these identities as they can not be confirmed without the use of a suitable standard. It provides invaluable insight into the possible identity of the compound in question, however many compounds on the METLIN database do not have available mass spectra at 0 V collision energy to compare to. Therefore, the marker could be one of these compounds that do not have the mass spectrum available for comparison. Coelution can cause a loss of visualisation of the fragments of a parent ion, especially if the marker is at a low concentration and the parent ion peak is at a low intensity in the mass spectrum. This creates an issue when making a comparison with mass spectra on the database, as some of the fragments may be hidden by base level noise or coeluting compounds at this retention time. Some compounds also do not fragment at 0 V collision energy, and so the identity of the marker could be one of several compounds with the same accurate mass.

Overall, the results presented here demonstrate the potential of these techniques to identify markers that could be utilised for the detection of adulterated processed meat products. It also shows that adulteration can still be detected regardless of whether the meat product is raw or cooked. The markers of particular interest within these results are those that could be used to detect adulteration in both raw and cooked meat products.

Chapter 6

The effect of spoilage on the metabolic profile of meat

The aim of this experiment was to investigate the change in the small molecule profile in meat during the time since slaughter when stored in different temperature controlled conditions over a period of 20 days. It specifically looked at the spoilage profile of chicken muscle tissue stored at room temperature and in the fridge at 4° C.

6.1 Introduction

Meat spoilage can be described as an ecological problem that includes changes in the low molecular compounds within the product during the proliferation of bacteria [157]. The condition of the meat is usually assessed by the consumer, and any discolouration, strong odours, or change in surface texture of the meat product would constitute the meat as unacceptable for consumption. There are three main mechanisms that contribute to the spoilage of meat and produce these characteristics; microbial activity, lipid oxidation, and autolytic enzymatic spoilage [158]. The *Pseudomonas* species of bacteria has been found to be the main bacteria involved in spoilage when stored aerobically, where these bacteria remove all glucose and lactate present in the meat and start to metabolise amino acids into ammonia [157]. This bacteria, along with other microorganisms, are the main cause for the strong odours of spoiled food, as they cause degradation of organic substances that release volatile organic compounds, such as acetone, toluene, and ethyl-benzene [159]. Lipid oxidation involves reactive oxygen species attacking double bonds within unsaturated

fatty acids, causing the degradation of lipids vital to the structure within cells, such as phospholipids in cell membranes. The degradation products are aldehydes, ketones and alcohols, which also contribute to the discolouration and bad odours of spoiled meat [131]. Autolytic enzymatic spoilage is the breakdown of complex compounds; for example, the degradation of polypeptides results in the changes in flavour and texture sometimes associated with the ageing of beef. This process takes place in all types of tissue, however the rate at which it occurs varies between tissue types; it is slower in striated tissue such as muscle than in glandular tissue such as the liver, due to the structure of the tissue [158]. All these chemical changes occur postmortem, and can be affected by the conditions at slaughter, contamination during handling and transport, and the temperature during storage.

Previous research has used a variety of techniques to deduce the spoilage status of food items. A metabolic profiling approach with the use of gas chromatography time-of-flight mass spectrometry has been successful in detecting markers that change in the first week of spoilage in bread, egg, and cucumber [160]. The multivariate statistics employed in this study showed separation between most time points in each food type. Enzymatic assays have been utilised to measure microbial products, which found a reduction of glucose, an increase in lactate, and an increase in pH in spoiled cooked meat [161], caused by the activity of lactic acid bacteria, which also contributes to the discolouration and strong odours. Proton transfer reaction mass spectrometry has detected volatile organic compounds to assess the amount of bacteria present on beef and pork, and found that many volatile compounds increase over the storage period of meat [162].

Spectroscopic techniques have also been shown to be able to determine the spoilage status of meat, specifically beef, pork and chicken. Fourier transform infrared spectroscopy has been used to measure the number of bacteria on meat to determine the spoilage status of beef [163] and pork [164]. Spoilage in beef has also been

investigated with the use of Raman spectroscopy and chemometrics [165]. Infrared spectroscopy has been successful in determining the spoilage status of chicken breast tissue, where absorbance between 3000-2800 cm^{-1} decreases during the first 5 days of storage. This wavelength is attributed to fatty acids of lipids and phospholipids [166]. These findings comply with the understanding that lipid oxidation is one of the fundamental mechanisms that occur during the spoilage process.

Some studies have been conducted in order to investigate the spoilage of meat using high performance liquid chromatography. Specifically, HPLC with an ultra-violet detector has been applied to identifying the spoilage status of minced beef [167]. This study found that there is promise in the use of HPLC to determine the presence of certain markers within a meat sample, however, further validation is required. The retention times of peaks to known standards were compared, but with the combination of mass spectrometry, an accurate mass of the ions producing these peaks would enable a more accurate estimation of the identity of the molecule and potential marker for the spoilage of meat. HPLC has also been used to measure the concentration of free amino acids in chicken breast tissue, which was found to increase gradually over an 8 day storage period [168].

All of this research only investigated the early stages of the spoilage process, so it would be useful to allow the time period to extend further than 14 days. Also, despite some studies using HPLC, it was used as a targeted assay, and an approach involving the untargeted analysis of all small molecules has not been explored. Using HPLC coupled with mass spectrometry would also increase the potential in identifying markers that could determine the spoilage status of meat. This could help verify the shelf-life, which may have been manipulated to avoid losing revenue from the disposal of meat products, and therefore prevent the consumption of spoiled meat.

6.2 Experimental procedures

6.2.1 Materials

Acetonitrile (HPLC grade), methanol (HPLC grade) and dichloromethane (analytical grade) were purchased from VWR (East Grinstead, UK), and ultra pure water (18.2 MΩ) was purified using an in-house Milli-Q system from Elga (High Wycombe, UK). Formic acid (laboratory reagent grade) was purchased from Fisher Scientific (Loughborough, UK). ESI-L low concentration tuning mix and API-TOF reference mass solution were purchased from Agilent Technologies (California, USA).

6.2.2 Sample collection and storage

Chicken muscle was obtained from a local butchers and stored at 4°C prior to extraction, which was carried out on the same day. Equal portions of chicken tissue were placed into individual weighing boats and covered in parafilm. The samples were then stored either in the fridge at 4°C or at room temperature. Extractions were carried out every day for 8 days, then every other day until day 20.

6.2.3 Metabolite extraction

External and internal extracts were taken from each chicken portion in order to investigate the difference in metabolite profile based on sampling location. For the external extract, the top surface of each portion of chicken was removed with smaller surgical scissors, homogenised, and three separate pieces were weighed (approximately 100 mg) into Eppendorf tubes. This was then repeated with a small section of chicken from the centre of the portion to gain the internal extracts. Methanol/H_2O (1:1) was added (1 mL per 100 mg of sample), then the sample was sonicated for 10 minutes and centrifuged at 16100 rcf for 20 minutes. The supernatant was then moved to a

glass vial and retained as the aqueous (AQ) extract. The tissue pellet was broken up using a clean pipette tip, and dichloromethane/methanol (3:1) was added (1 mL per 100 mg of sample). The sample was sonicated for 10 minutes and centrifuged at 16100 rcf for 20 minutes, and 1 mL of the supernatant was then moved to a glass vial and allowed to evaporate overnight, then resuspended in 1 mL of methanol. This was retained as the organic (OR) extract. The three external and three internal extracts from each chicken portion were stored at -25°C prior to analysis.

6.3 Instrumental set-up

6.3.1 Analytical considerations

Quality control samples were made for each analytical run, consisting of an equal aliquot of every sample within each run. At the start of each analytical run, 10 QC samples were injected at a volume of 10 μL, then 20 QC samples at an injection volume of 3 μL were injected to condition the column. All non-QC samples were randomised to eliminate any issues arising from instrumental drift.

6.3.2 Chromatographic parameters

Chromatographic separation of extracts was performed with a Thermo Scientific Hypersil GOLD aQ column (100 mm x 2.1 mm, particle size of 1.9 μm) using an Agilent 1260 Binary Pump HPLC. The column was maintained at 40°C and the injection volume was 3 μL. The flow rate of the mobile phase was 0.3 mL/min and consisted of 0.1% formic acid (solvent A) and acetonitrile with 0.1% formic acid (solvent B). The chromatographic gradient method can be seen in Table 6.1. A needle wash method was included after every injection, consisting of 3 separate vials of methanol, each used in a specific order, with 3 washes per vial. The column was flushed with 100% organic solvent after each run to reduce any potential carryover.

Table 6.1: Solvent gradient method used in this experiment

Time (mins)	Solvent A (%)	Solvent B (%)
0	95	5
2	95	5
3	47.5	52.5
30	0	100
40	0	100
41	95	5
50	95	5

6.3.3 Q-TOF parameters

For the analysis, an Agilent Technologies 6530 Accurate Mass Q-TOF was used with an electrospray ionisation source, and the parameters were set as shown in Table 6.2. The reference mass solution was continually run through the analysis, and used purine (121.0509 *m/z*) and hexakis (1H, 1H, 3H-tetrafluoropropoxy)phosphazine (922.0098 *m/z*) in positive ionisation mode as internal reference masses to ensure mass accuracy. The data was collected in both profile and centroid mode.

Table 6.2: Q-TOF parameters used in this experiment

Parameter	Setting
Drying gas temperature	320°C
Drying gas flow rate	11 L/min
Capillary voltage	4000 V
Fragmentor voltage	125 V
Skimmer voltage	65 V
Mass range	100-1000 *m/z*

6.4 Data pre-processing

The data was pre-processed using *XCMS Online*. The parameters for the method used on this online platform were set to the default settings specifically designed by *XCMS Online* for analyses carried out with HPLC and ESI-QTOF-MS instruments, and were as shown in Table 6.3. This software also carried out normalisation of the raw data using the median fold change method. A feature table was produced, which included a list of *m/z* values and their median retention times, and the peak areas for these features in each sample.

Table 6.3: Parameter settings for *XCMS Online* used in this experiment

XCMS method	Parameter	Setting
Feature detection = CentWave	ppm	30
	min peak width (seconds)	10
	max peak width (seconds)	60
	mzdiff (*m/z*)	0.01
Retention time correction = Obiwarp	profStep (*m/z*)	0.5
Alignment	bw (seconds)	5
	minfrac	0.5
	mzwid	0.025

6.5 Statistical analysis

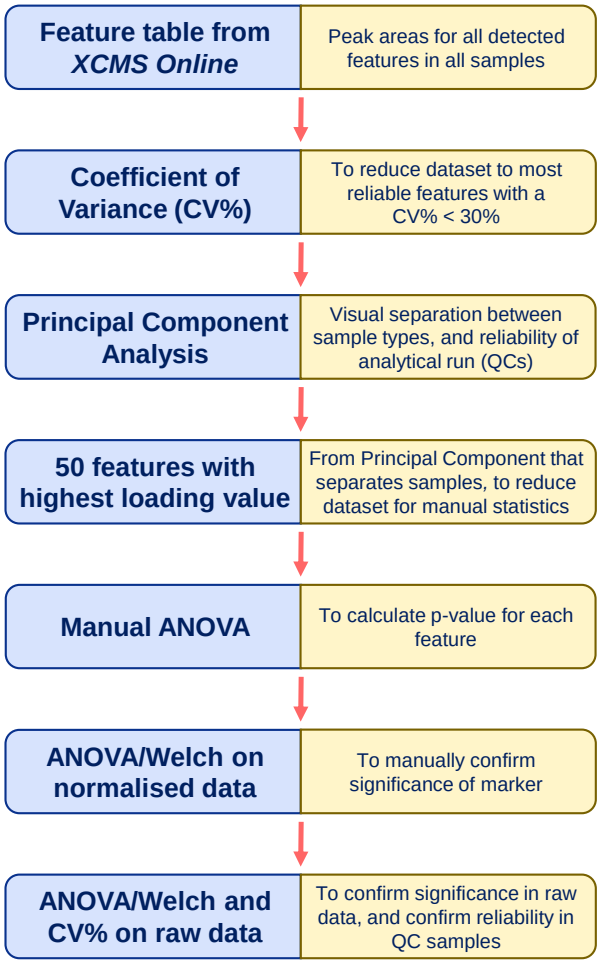

Figure 6.1: Statistical workflow for all datasets analysing the spoilage status of chicken muscle tissue

The standard deviation, average, and coefficient of variance percentage were calculated using the peak areas of each feature of the QC samples throughout the analytical run, and all features that had a CV% in the QC samples of more than 30% were removed. A principal component analysis with standardisation was carried out using the Multivariate Analysis add-in for *Microsoft Excel 2010* [85], and a scores plot was produced in order to visualise any separation between sample types. The first six principal components were plotted in all combinations to find the components that best represented the separation of the sample types. The principal component that represented the separation between sample types was used to find the top 50 features

most responsible for this separation, based on the loading values. A manual ANOVA test in *Microsoft Excel* was carried out on the peak areas of each sample in order to get a p-value for each feature. These were then analysed in *SPSS* in order to verify their significance, where either ANOVA or Welch tests were performed, depending on the homogeneity of variance value for each marker. The tests were carried out with a confidence level of 95%, giving an α value of 0.05. If the p-value was less than the α value, it indicated the abundance of that marker in the sample groups was statistically different.

The raw data was then analysed in *Masshunter Qualitative Analysis* (Agilent Technologies) to produce extracted ion chromatograms (EICs) for the markers that were confirmed to be significantly different. ANOVA or Welch tests in *SPSS* were carried out on the peak areas of the EICs, as well as CV% of the QC samples. This process ensured the markers were significant even before normalising the data in the pre-processing step. Any markers that were found to not be significantly different or had a CV% in the QC samples of more than 30% were removed. This additional step in the methodology ensured the final markers were robust and reliable, with the intention of being able to confidently use these markers as an indicator of shelf-life.

6.6 Identification of markers

The potential formulae predicted by *MassHunter Qualitative Analysis* were used to search the METLIN database manually. A tentative identification was made based on the comparison of the mass spectrum of the sample and mass spectra of compounds with the same formula on the METLIN database, if available. If a tentative identification could not be made, an idea of the class of compound could be determined based on the predicted formulae matching to a number of similar compounds on the METLIN database.

6.7 Results and discussion

6.7.1 Spoilage of chicken at room temperature

6.7.1.1 Quality control

In order to investigate the spoilage profile of chicken muscle tissue at room temperature, the external extracts were used. These were run in the same analytical run as the internal extracts, and therefore the quality control data is applicable for both the spoilage profile and the comparison between external and internal extracts of chicken muscle tissue at room temperature.

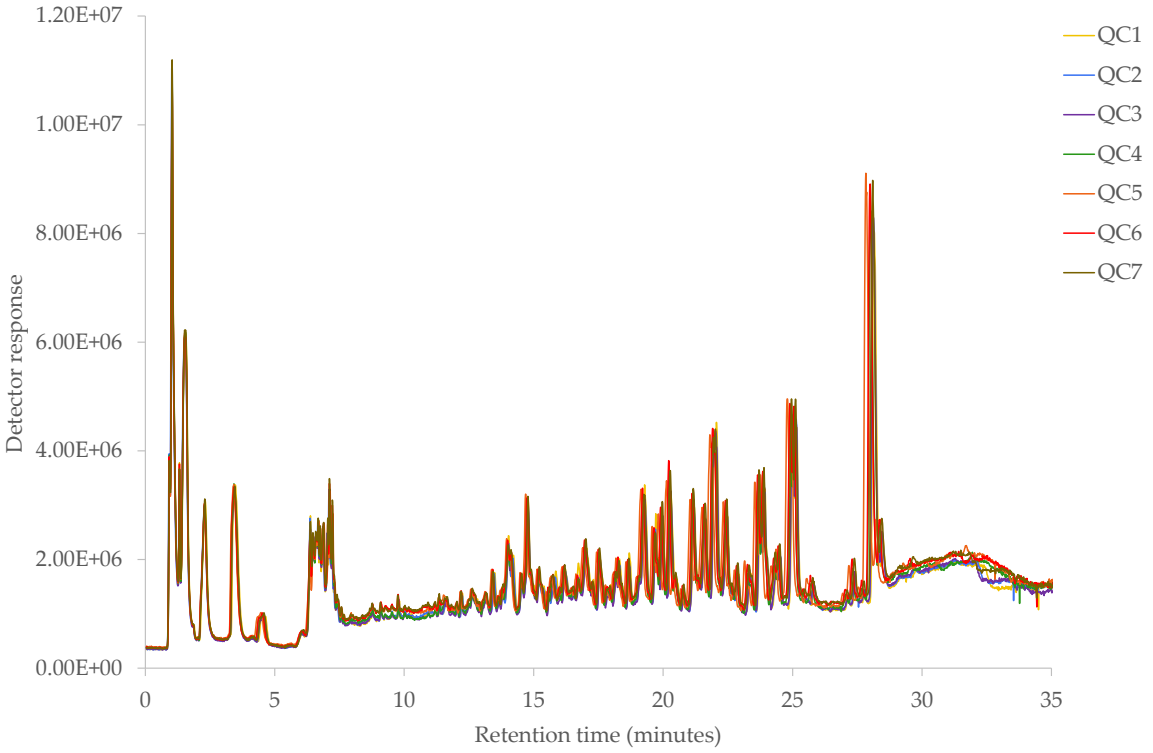

Figure 6.2: Total ion chromatograms of QC samples throughout analytical run for extracts from chicken muscle tissue stored at room temperature for different lengths of time

The chromatograms of the quality control samples in the external and internal extracts of chicken muscle tissue stored at room temperature (Figure 6.2) show some slight retention time variation, particularly in QC5, 6 and 7. However, this is only very subtle and the following statistical analysis will aid in the verification of the reliability of the data collected in this analytical run.

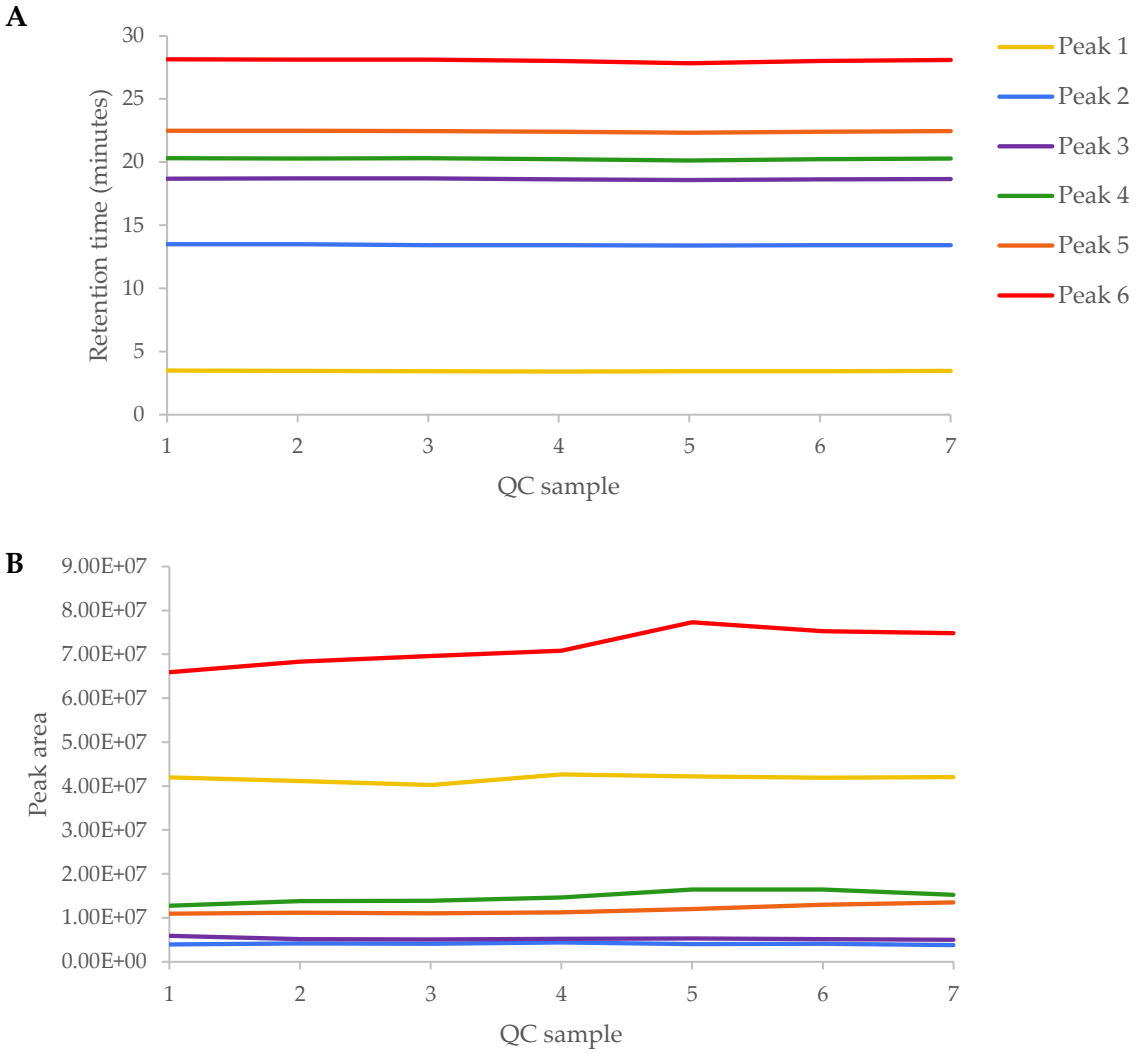

Figure 6.3: Variability of retention time (A) and peak area (B) of 6 peaks in QC samples throughout analytical run for extracts from chicken muscle tissue stored at room temperature for different lengths of time

Several peaks were selected throughout the chromatogram at varying peak intensities for additional statistical analysis in order to ascertain whether the data obtained was reliable. Figure 6.3 shows that the retention time was very stable throughout the analytical run, and the peak area was also mostly stable, despite the peak area increasing slightly in QC5, 6 and 7 in Peak 6.

Table 6.4: Variability of retention time and peak area of 6 peaks in chromatograms of QC samples during the analysis of extracts from chicken muscle tissue stored at room temperature for different lengths of time

	Retention time (minutes)									
Peak	QC1	QC2	QC3	QC4	QC5	QC6	QC7	SD	Average	CV%
1	3.36	3.37	3.39	3.39	3.40	3.37	3.40	0.02	3.38	0.47
2	13.31	13.33	13.32	13.33	13.32	13.30	13.32	0.01	13.32	0.08
3	18.45	18.47	18.48	18.47	18.48	18.44	18.48	0.02	18.47	0.09
4	22.96	22.98	23.01	22.98	23.01	22.93	23.01	0.03	22.98	0.13
5	23.61	23.63	23.66	23.65	23.66	23.60	23.65	0.02	23.64	0.10
6	27.56	27.60	27.64	27.61	27.66	27.55	27.63	0.04	27.61	0.15
	Peak area									
Peak	QC1	QC2	QC3	QC4	QC5	QC6	QC7	SD	Average	CV%
1	41756528	39629134	37802048	42593500	42058430	42765385	39988711	1846336	40941962	4.51
2	3038861	2825876	2861479	3193174	3139363	3098134	3028505	137410	3026485	4.54
3	4507725	4472819	4162206	4945693	4632566	4418223	4413489	239755	4507532	5.32
4	4694474	4503556	4720156	5532707	5030721	4862198	5053363	334853	4913882	6.81
5	7782129	7456931	7995639	8161053	7884796	8138054	8254553	273927	7953308	3.44
6	64308953	62268867	63259511	59892569	62657293	65740527	65735563	2078117	63409040	3.28

The retention time variability was between 0.08 and 0.47%, and the peak area variability was between 3.28 and 6.81%, which indicates that the data obtained in this analytical run was reliable.

6.7.1.2 Metabolic profiling

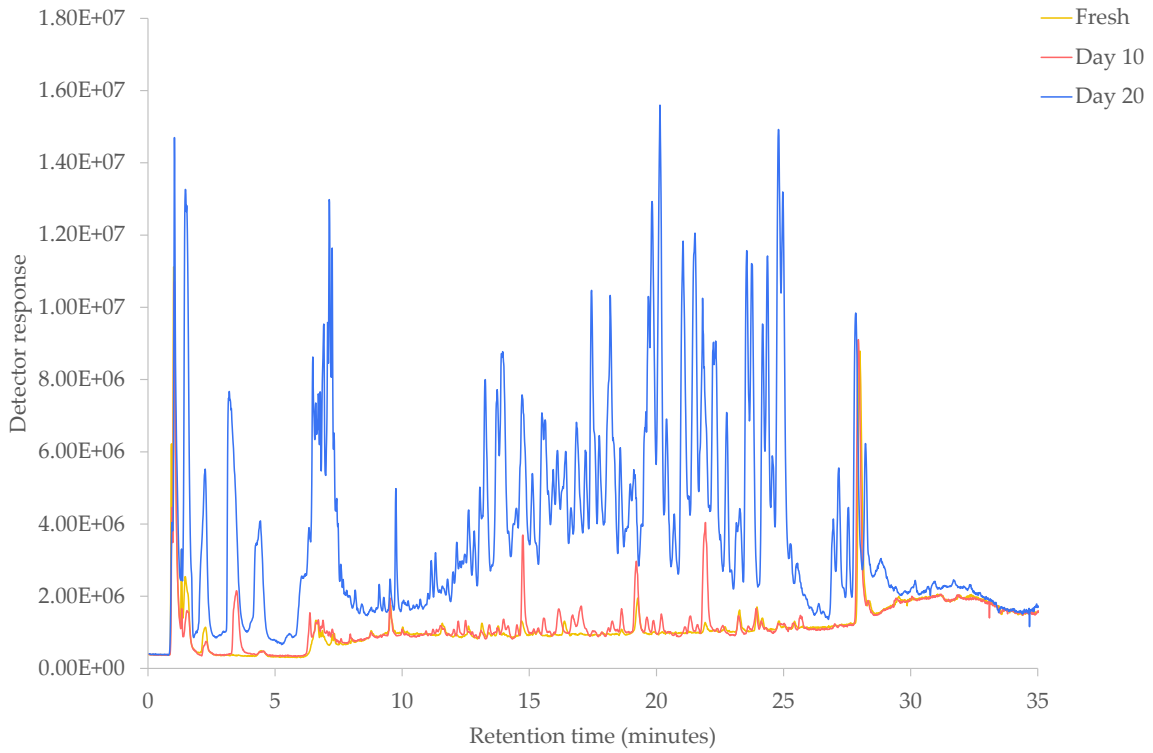

Figure 6.4: Example total ion chromatograms for extracts from chicken muscle tissue stored at room temperature for different lengths of time

The chromatograms for each time point during the spoilage of chicken muscle tissue at room temperature showed a dramatic increase in most peaks from Fresh to Day 20. These differences can be seen in Figure 6.4 where Fresh, Day 10 and Day 20 are compared. The chromatogram for the fresh samples (yellow) has a low detector response, the Day 10 samples (red) contain more peaks and at a higher intensity, and the Day 20 samples (blue) contain many more peaks within the chromatogram at a much larger intensity. A peak at 3 minutes in the chromatograms for Day 10 and Day 20 samples is not present in the Fresh samples, potentially representing a compound or group of co-eluting compounds that are a product of the spoilage process. The Fresh sample chromatogram has a stable baseline throughout the analysis, however this baseline increases in the Day 20 samples, indicating there are many ions beneath the baseline contributing to this chromatogram. It is obvious from the chromatograms that the metabolic profile changes a lot through the spoilage process.

6.7.1.3 Multivariate statistics

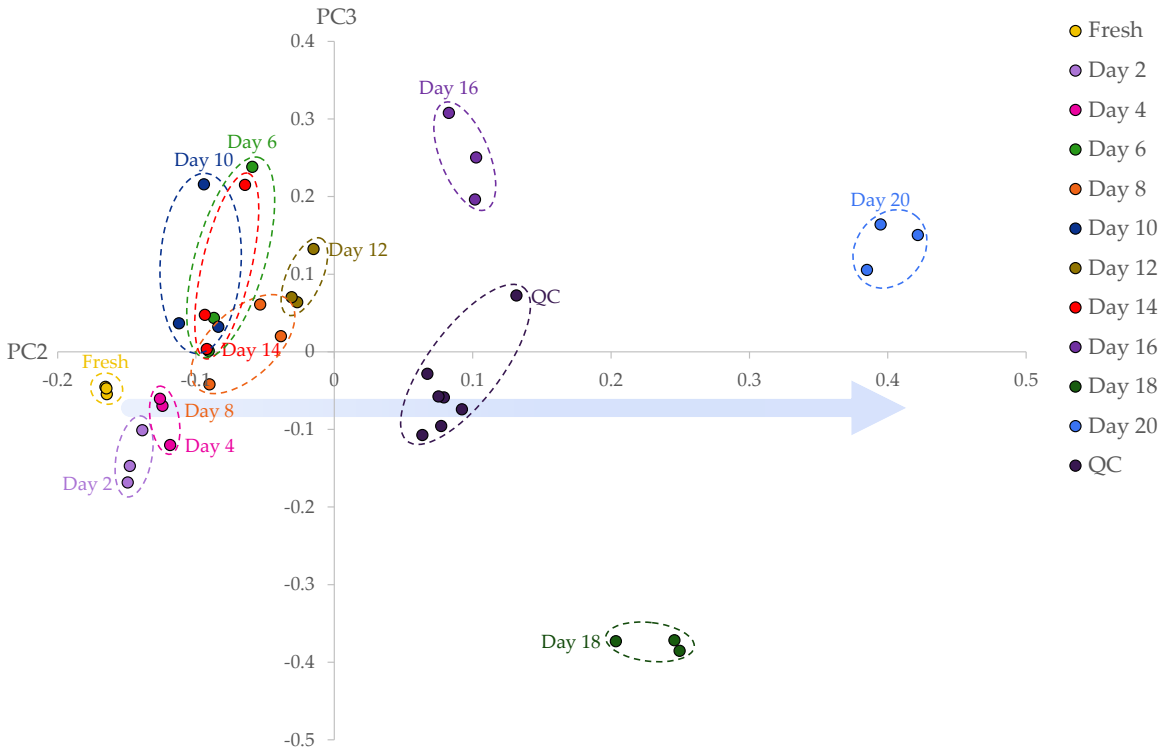

Figure 6.5: Principal component analysis scores plot of PC2 (7.192%) and PC3 (1.980%) for extracts from chicken muscle tissue stored at room temperature for different lengths of time. PCA was carried out using all features detected with a CV < 30%

The PCA plot for all features with a CV% in the QC samples of less than 30% is shown in Figure 6.5. There is a lot of overlapping in Day 6 to Day 14 samples, however the other sample types are all separated from each other. The QC samples are quite spread out, but they still form an individual group separate from the other sample types. The trend of the sample groups across the plot is interesting as the Fresh sample group is on the left side, and as the storage time increases, the sample groups move to the right side, represented by the blue arrow. Day 12 sample group appears to be further along the trend line than Day 14 sample group, indicating there may be some sample groups that do not follow this gradual trend across the plot.

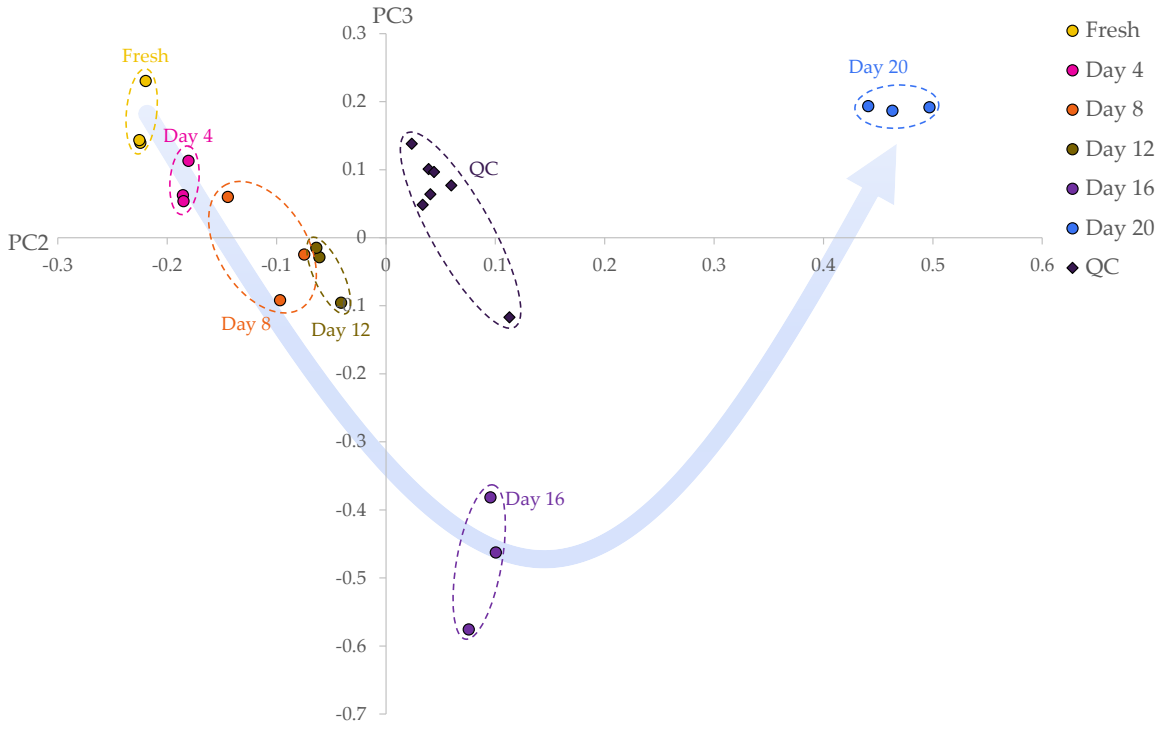

Figure 6.6: Principal component analysis scores plot of PC2 (8.337%) and PC3 (1.532%) for extracts from chicken muscle tissue stored at room temperature for different lengths of time, specifically showing time points from every 4 days. PCA was carried out using all features detected with a CV $< 30\%$

In order to illustrate this trend further, sample groups from every 4 days instead of every 2 are shown in Figure 6.6. In both of these PCA plots, the general separation is along the x-axis, so principal component 2 would be suitable to use to find features that are most responsible for the separation between the sample groups. After comparing the features that were in the top 100 based on the loading values for PC2, it was seen that the majority of the features were the same, and so to avoid any unnecessary removal of features, the PCA in Figure 6.5 was used to find the features that were most responsible for the differences between groups. The 50 features with the highest loading values were statistically analysed with a manual ANOVA test to see whether these features were significantly different, and further statistically analysed to investigate whether these markers were robust and still significantly different in the raw data.

6.7.1.4 Significant markers

The markers that were stable in the normalised data as well as the raw data are shown in Table 6.5. All markers were reliable in the normalised data with a CV% in the QC samples of less than 12.24%, and in the raw data with a CV% of less than 15.75%. All markers were highly significant with a p-value of 0.001 and below, in both normalised and raw data.

The trends of these markers were generally increasing in abundance over the spoilage time period, however many markers showed quite an erratic trend where the marker decreased at Day 10, 14, and 18, but increased at Day 12, 16 and 20, which was also seen in the intensities of the peaks in the total ion chromatograms. This could have been caused by the experimental set-up, where some of the samples may not have spoiled as quickly as others due to being more firmly covered by the parafilm.

Table 6.5: Summary of compounds that contribute the most to the differences among all extracts from chicken muscle tissue stored at room temperature for different lengths of time, using PC2.
Marker trend: ↑ = increased, ↗ = erratically increased, * = other

m/z	Retention time median (mins)	P-value from ANOVA/Welch (XCMS)	CV% (XCMS)	P-value from ANOVA/Welch (EICs)	CV% (EICs)
* 352.3573	25.03	<0.001	3.27	<0.001	5.93
* 326.3415	24.87	<0.001	3.42	<0.001	5.43
↗ 338.3416	23.81	<0.001	4.69	<0.001	6.71
↗ 312.3259	23.61	<0.001	5.25	<0.001	7.10
* 105.0699	3.24	<0.001	2.16	<0.001	2.75
↗ 282.2789	19.88	<0.001	4.01	<0.001	5.81
* 350.3415	22.40	<0.001	4.84	<0.001	6.40
↑ 130.1217	7.11	<0.001	9.11	<0.001	12.13
↗ 256.2631	20.21	<0.001	3.10	<0.001	4.84
* 341.3522	15.67	<0.001	4.20	<0.001	2.77
* 354.3724	28.31	<0.001	6.02	<0.001	7.40
↑ 360.3255	24.24	<0.001	5.99	<0.001	7.22
↗ 505.3746	13.98	<0.001	2.27	<0.001	1.47
↑ 324.3254	21.55	<0.001	6.23	<0.001	7.89
↑ 402.3360	20.18	<0.001	1.90	<0.001	2.87
↑ 376.3200	19.75	<0.001	2.16	<0.001	3.47
↗ 336.3258	21.11	<0.001	5.73	<0.001	6.87
↗ 340.3568	27.26	<0.001	8.44	<0.001	10.08
↑ 164.1065	7.26	<0.001	12.24	<0.001	15.75
↗ 396.3468	21.58	<0.001	4.33	<0.001	4.63
* 367.3677	16.54	<0.001	6.66	<0.001	4.30
↑ 201.1950	7.15	<0.001	5.93	<0.001	4.36
↑ 384.3254	22.28	<0.001	3.86	0.001	4.50
↗ 430.3311	21.48	<0.001	5.14	<0.001	5.30
* 144.0798	6.33	<0.001	2.90	<0.001	6.59
↗ 479.3587	13.29	<0.001	3.21	<0.001	1.39
↗ 434.3373	14.81	<0.001	2.81	<0.001	1.01
↗ 116.1064	6.01	<0.001	7.80	<0.001	9.22
↗ 404.3158	21.08	<0.001	5.23	<0.001	5.59
* 327.3363	14.91	<0.001	4.83	<0.001	2.61
* 374.3410	22.00	<0.001	4.81	<0.001	3.84
↗ 145.1334	1.07	<0.001	4.59	<0.001	2.84
↗ 310.3097	20.19	<0.001	7.70	<0.001	9.86
↑ 187.1775	6.86	<0.001	2.54	<0.001	1.19
↑ 413.3547	29.01	<0.001	10.58	<0.001	7.80

Table 6.5 continued: Summary of compounds that contribute the most to the differences among all extracts from chicken muscle tissue stored at room temperature for different lengths of time, using PC2.
Marker trend: ↑ = increased, ↗ = erratically increased, * = other

m/z	Retention time median (mins)	P-value from ANOVA/Welch (XCMS)	CV% (XCMS)	P-value from ANOVA/Welch (EICs)	CV% (EICs)
↑ 280.2626	17.51	<0.001	5.37	<0.001	6.74
↑ 336.3254	21.59	<0.001	5.97	<0.001	7.67
↗ 187.1432	3.23	<0.001	4.54	<0.001	3.41
↑ 235.1793	7.22	<0.001	4.46	<0.001	1.82
↗ 394.3313	19.07	<0.001	3.27	<0.001	3.93
↑ 188.0695	4.44	<0.001	2.30	<0.001	4.27
↑ 400.3220	18.25	<0.001	2.40	<0.001	4.59

6.7.1.5 Tentative identifications

Table 6.6: Compounds that were significantly different and tentatively identified in extracts from chicken muscle tissue stored at room temperature for different lengths of time based on comparison of mass spectra on METLIN

m/z	Retention time median (mins)	Possible formula	Likelihood score (%)	Tentative identification
338.3416	23.81	$C_{22}H_{43}NO$	99.61	N-cyclohexanecarbonylpentadecylamine
256.2631	20.21	$C_{16}H_{33}NO$	99.08	palmitic amide
324.3254	21.55	$C_{21}H_{41}NO$	98.88	N-cyclohexanecarbonyltetradecylamine
310.3097	20.19	$C_{20}H_{39}NO$	98.62	oleoyl ethyl amide

Four markers were tentatively identified as amines and amides, and the matching mass spectra can be seen in Appendix G. These compounds did not fragment with a collision energy of 0 V, and so there was only a single peak to match to the available mass spectra on the METLIN database. However, all compounds had a high likelihood score for the possible formulae based on the isotopic ratios of the chromatographic peak in the raw data, and each search on the METLIN database presented less than 3 results, all of a similar type of compound.

All markers showed an overall increasing trend over the course of the storage period. Meat undergoes many chemical changes during the spoilage process, and one mechanism for this is through protein degradation [158]. Therefore, the increasing trends observed in these markers tentatively identified as amines and amides were most likely caused by the autolysis of proteins and amino acids.

6.7.2 Spoilage of chicken at room temperature - external and internal sample collection

The location at which a sample is collected from can be very important. The rate of spoilage could be dramatically increased on the exterior of a piece of meat compared to the interior. The difference in metabolic content in external and internal extracts of chicken muscle tissue stored at room temperature is discussed in this section.

6.7.2.1 Metabolic profiling

Figure 6.7 shows the differences between external and internal sample collection extracts at Fresh, Day 12 and Day 20 of the spoilage profile at room temperature. There did not appear to be much difference in the peak pattern in the chromatograms for Fresh samples, but the Day 12 and Day 20 samples both had a lower intensity in the internal extracts compared to the external extracts. This is what would be expected as the external area of the chicken is more available to bacteria and so would spoil more rapidly than the internal parts of the chicken.

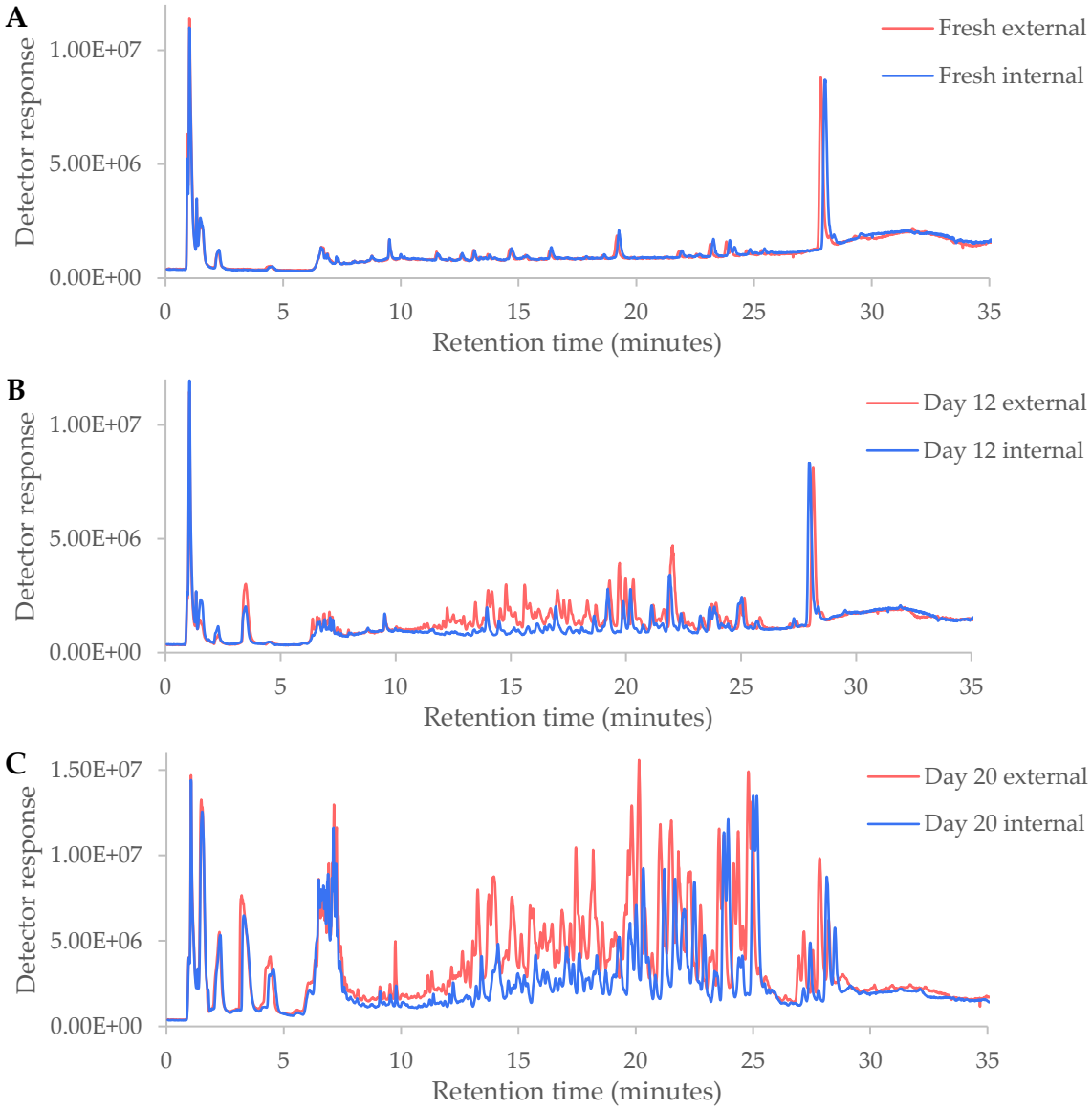

Figure 6.7: Example total ion chromatograms for extracts of chicken muscle tissue stored at room temperature for different lengths of time, comparing external and internal extracts. A) Fresh, B) Day 12, C) Day 20

6.7.2.2 Multivariate statistics

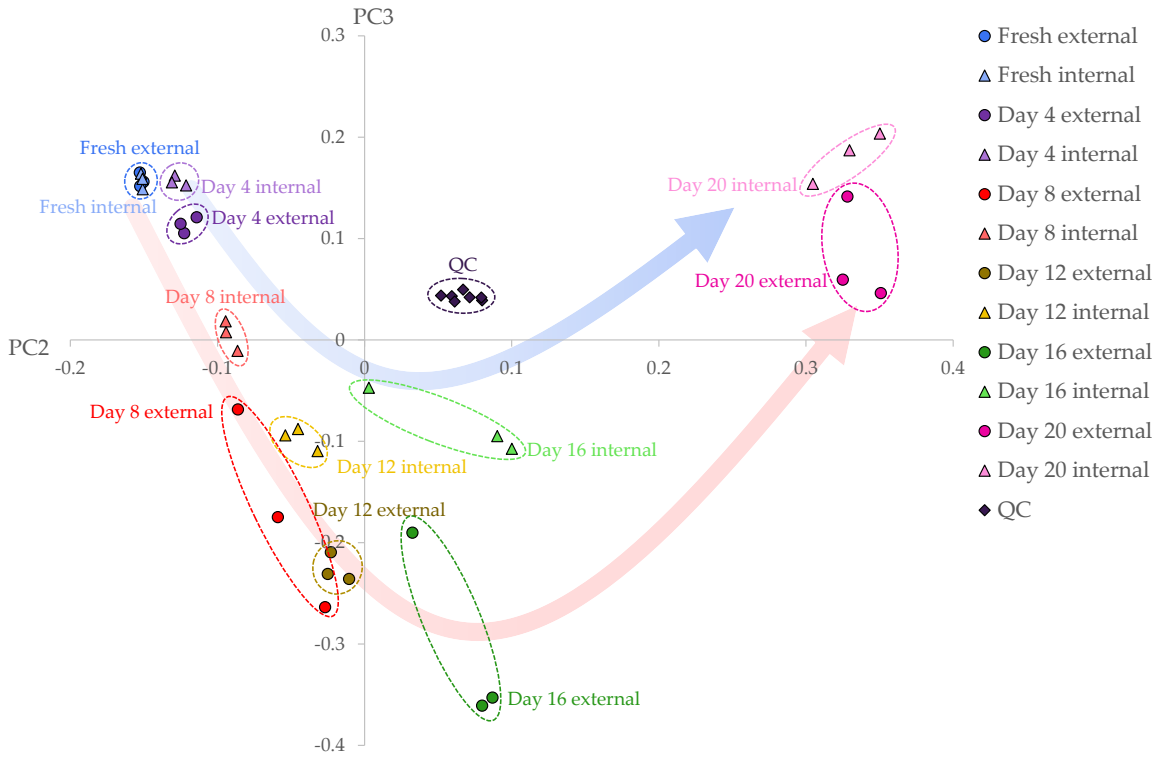

Figure 6.8: Principal component analysis scores plot of PC2 (12.994%) and PC3 (2.387%) for external and internal extracts from chicken muscle tissue stored at room temperature for different lengths of time. PCA was carried out using all features detected with a CV< 30%

The PCA plot in Figure 6.8 shows most sample types grouped individually. The spread of the groups starts on the left side of the plot with the Fresh external and internal samples that were not separated. The different time points then move gradually across the plot, with each time point having two separate groups; one for external extracts, respresented by the red arrow, and one for internal extracts, represented by the blue arrow. This pattern of distribution indicates the changes in metabolic content increase the longer a piece of chicken is spoiled for. The quality control samples are tightly clustered in the middle of the plot showing instrument stability during the analytical run.

During the spoilage process, it is expected that the surface of the meat will spoil at a faster rate than the inside of the meat, as this is more accessible to bacteria. After a

certain amount of time, the spoilage process becomes so great that the tissue degrades substantially, meaning it is difficult to differentiate between an external and internal extract when collecting the sample, which could explain why the difference between Day 20 external and internal samples is smaller than other time points.

The difference between the external and internal extracts is most represented by principal component 3 on the y-axis, however the separation of the groups at different time points is mostly along the x-axis representing principal component 2, therefore the 50 features with the highest loading values in this component were statistically analysed with a manual ANOVA test to see whether these features were significantly different, and further statistically analysed to investigate whether these markers would be robust enough for the determination of the storage time of chicken muscle tissue.

6.7.2.3 Significant markers

The remaining markers from the 50 features with the highest loading values that were found to be significantly different in the normalised and raw data are shown in Table 6.7. All markers were reliable in the quality control samples in the normalised data with a CV% of less than 12.34%, and in the raw data with a CV% of less than 15.75%. All markers were significantly different with a p-value of 0.001 and below.

The trends of these markers mostly increased as the storage time increased. The difference between external and internal extracts could be seen in all markers, however some markers were at a higher concentration in the external extracts, and others were higher in the internal extracts.

Table 6.7: Summary of compounds that contribute the most to the differences among all external and internal extracts from chicken muscle tissue stored at room temperature for different lengths of time, using PC2.
Marker trend: ↑ = increased, ↑ = increased at Day 20, ↷ = increased then decreased, * = random

m/z	Retention time median (mins)	P-value from ANOVA/Welch (XCMS)	CV% (XCMS)	P-value from ANOVA/Welch (EICs)	CV% (EICs)
↑ 352.3574	25.03	<0.001	3.38	<0.001	5.96
↑ 338.3417	23.81	<0.001	4.78	<0.001	6.69
↑ 326.3416	24.87	<0.001	3.53	<0.001	5.42
↑ 312.3260	23.63	<0.001	5.36	<0.001	7.10
* 122.0964	3.26	<0.001	3.69	<0.001	1.59
↑ 282.2790	19.88	<0.001	4.13	<0.001	5.81
↑ 130.1219	7.11	<0.001	9.20	<0.001	12.08
↑ 350.3416	22.40	<0.001	4.93	<0.001	6.40
↑ 386.3414	24.42	<0.001	5.60	<0.001	5.74
↷ 256.2632	20.21	<0.001	3.23	<0.001	4.84
↑ 354.3727	28.31	<0.001	6.06	<0.001	7.41
↑ 350.3415	22.84	<0.001	6.35	<0.001	8.43
* 341.3522	15.64	<0.001	4.12	<0.001	2.77
↷ 336.3260	21.11	<0.001	5.82	<0.001	6.89
* 105.0699	3.25	<0.001	2.09	<0.001	2.75
↑ 340.3570	27.26	<0.001	8.52	<0.001	10.08
↑ 324.3255	21.56	<0.001	6.31	<0.001	7.89
* 505.3741	14.03	<0.001	2.21	<0.001	1.48
↑ 360.3256	24.25	<0.001	6.08	<0.001	7.27
↑ 201.1950	7.16	<0.001	5.85	<0.001	4.36
↑ 116.1066	6.03	<0.001	7.86	<0.001	9.25
↑ 164.1065	7.26	<0.001	12.34	<0.001	15.75
↑ 336.3255	21.59	<0.001	6.06	<0.001	7.67
↑ 310.3098	20.19	<0.001	7.80	<0.001	9.83
↑ 376.3200	19.75	<0.001	2.28	<0.001	3.47
↑ 402.3360	20.18	<0.001	1.98	<0.001	2.87
* 367.3677	16.54	<0.001	6.56	<0.001	4.30
* 479.3587	13.29	<0.001	3.13	<0.001	1.39
↑ 413.3546	29.01	<0.001	10.38	<0.001	8.18
* 396.3468	21.58	<0.001	4.38	<0.001	4.63
↑ 187.1776	6.87	<0.001	2.52	<0.001	1.19
* 327.3363	14.89	<0.001	4.75	<0.001	2.61
* 370.3332	21.16	<0.001	5.30	<0.001	8.16
↑ 430.3311	21.47	<0.001	5.17	<0.001	5.30

Table 6.7 continued: Summary of compounds that contribute the most to the differences among all external and internal extracts from chicken muscle tissue stored at room temperature for different lengths of time, using PC2.
Marker trend: ↑ = increased, ↑ = increased at Day 20, ↷ = increased then decreased, * = random

m/z	Retention time median (mins)	P-value from ANOVA/Welch (XCMS)	CV% (XCMS)	P-value from ANOVA/Welch (EICs)	CV% (EICs)
↑ 384.3255	22.28	<0.001	3.58	<0.001	4.55
* 434.3374	14.78	<0.001	2.79	<0.001	1.04
↑ 374.3414	22.00	<0.001	4.85	<0.001	3.84
↑ 187.1432	3.28	<0.001	4.42	<0.001	3.41
↑ 404.3158	21.08	<0.001	5.28	<0.001	5.59
* 480.3449	16.15	<0.001	3.36	<0.001	0.55
↑ 280.2625	17.53	<0.001	5.47	<0.001	6.74
↑ 235.1792	7.23	<0.001	4.38	<0.001	1.82
* 138.0911	1.50	<0.001	6.57	<0.001	3.79
↑ 188.0695	4.47	<0.001	2.24	<0.001	4.27
* 491.3588	13.76	<0.001	2.98	0.001	1.69
* 283.2630	21.94	<0.001	6.51	<0.001	3.32
↑ 400.3208	18.25	<0.001	2.45	<0.001	4.07

6.7.2.4 Tentative identifications

Table 6.8: Compounds that were significantly different and tentatively identified in external and internal extracts from chicken muscle tissue stored at room temperature for different lengths of time based on comparison of mass spectra on METLIN

m/z	Retention time median (mins)	Possible formula	Likelihood score (%)	Tentative identification
338.3417	23.81	$C_{22}H_{43}NO$	99.61	N-cyclohexanecarbonylpentadecylamine
256.2632	20.21	$C_{16}H_{33}NO$	99.08	palmitic amide
324.3255	21.56	$C_{21}H_{41}NO$	98.88	N-cyclohexanecarbonyltetradecylamine
310.3098	20.19	$C_{20}H_{39}NO$	98.62	oleoyl ethyl amide
138.0911	1.50	$C_8H_{11}NO$	96.57	tyramine
283.2630	21.94	$C_{18}H_{34}O_2$	99.71	oleic acid

There were several markers that were tentatively identified in this dataset, some of which were also tentatively identified in the room temperature spoilage profile dataset, specifically markers 338.3417, 256.2632, 324.3255, and 310.3098 *m/z*. These matching mass spectra can be seen in Appendix G. The marker with an *m/z* of 338.3417, tentatively identified as N-cyclohexanecarbonylpentadecylamine, had a very gradual increasing trend as the storage time increased. The marker with an *m/z* of 256.2632 was tentatively identified as palmitic amide, and this compound gradually increased to Day 16, and then decreased at Day 20. Markers with an *m/z* of 324.3255, tentatively identified as N-cyclohexanecarbonyltetradecylamine, and 310.3098, tentatively identified as oleoyl ethyl amide, both had a trend that gradually increased then dramatically increased at Day 20. The marker that was tentatively identified as tyramine with an *m/z* value of 138.0911 had a slightly more random trend, where the concentration increased at Day 4, then decreased, until it increased again at Day 20. This marker did not show much of a difference in concentration between the external and internal extracts.

The marker with an m/z of 283.2630 was tentatively identified as oleic acid, and the mass spectrum for this marker in the QC sample had many fragments that matched the reference mass spectrum for oleic acid on the METLIN database, as seen in Appendix G.6, making this a strong tentative identification. The concentration for this marker gradually increased and then decreased, as seen in Figure 6.9. Oleic acid is an unsaturated fatty acid that naturally occurs in animal fat. During the spoilage process, lipid oxidation occurs, which can target the double bonds in phopholipids within cell membranes. This releases fatty acids, which explains the initial increase of this marker during the first 8 days. Fatty acids continue to breakdown through this oxidation process, which explains the decrease of this marker after Day 8. This marker was at a higher concentration in the external extracts than in the internal extracts during the overall increase, and it decreased more rapidly in the external extracts than in the internal extracts. This demonstrates the difference in the rate of spoilage between the external and internal areas of the chicken muscle tissue sample.

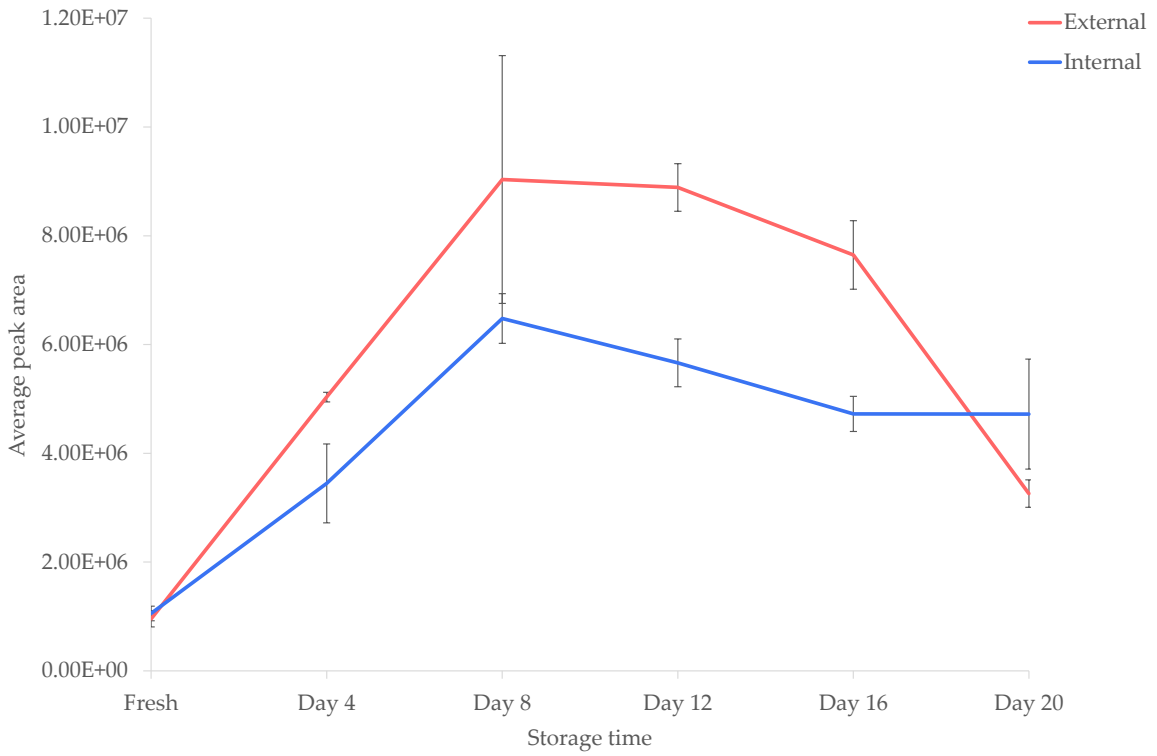

Figure 6.9: Trend of marker tentatively identified as oleic acid that was significantly different among all chicken muscle tissue samples stored at room temperature for different lengths of time. Error bars correspond to ± 1 standard deviation

6.7.3 Spoilage of chicken at 4°C

6.7.3.1 Quality control

In order to investigate the spoilage profile of chicken muscle tissue at 4°C, the external extracts were used. These were run in the same analytical run as the internal extracts, and so therefore the quality control data is applicable for both the spoilage profile and the comparison between external and internal extracts of chicken muscle tissue at 4°C.

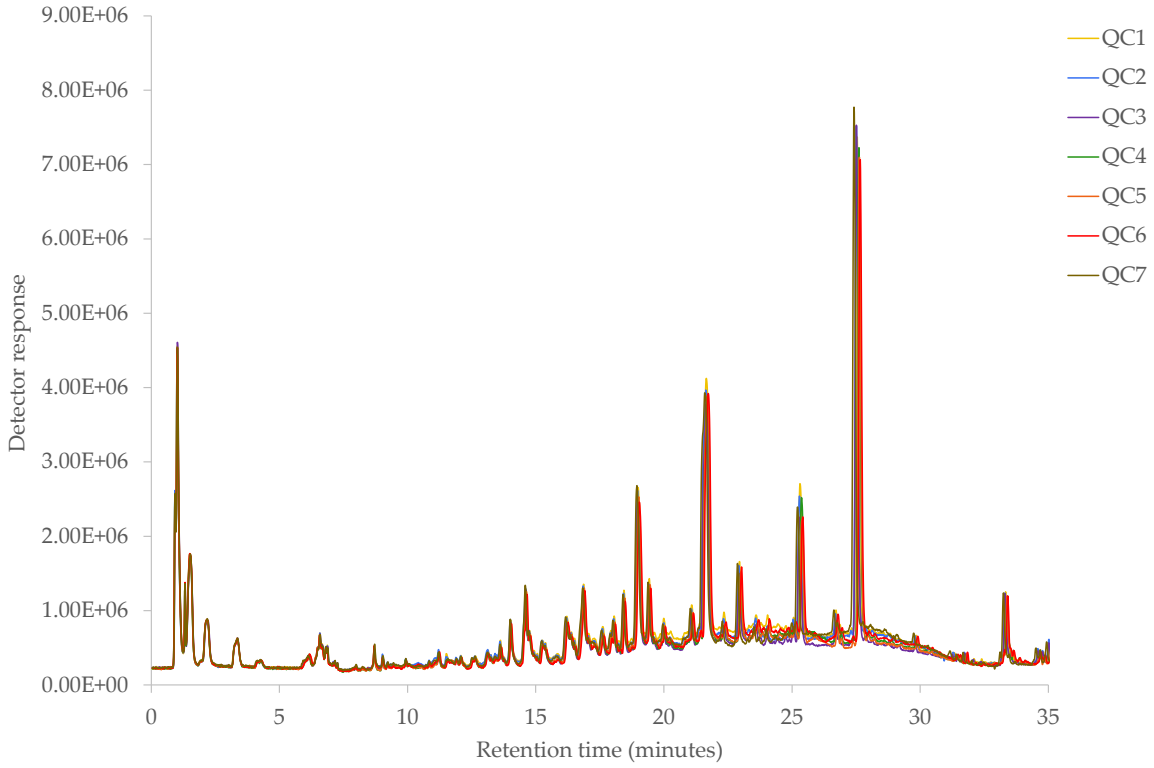

Figure 6.10: Total ion chromatograms of QC samples throughout analytical run for extracts from chicken muscle tissue stored at 4°C

The QC samples shown in Figure 6.10 are all consistent with minimal retention time drift. The baseline also shows minimal differences.

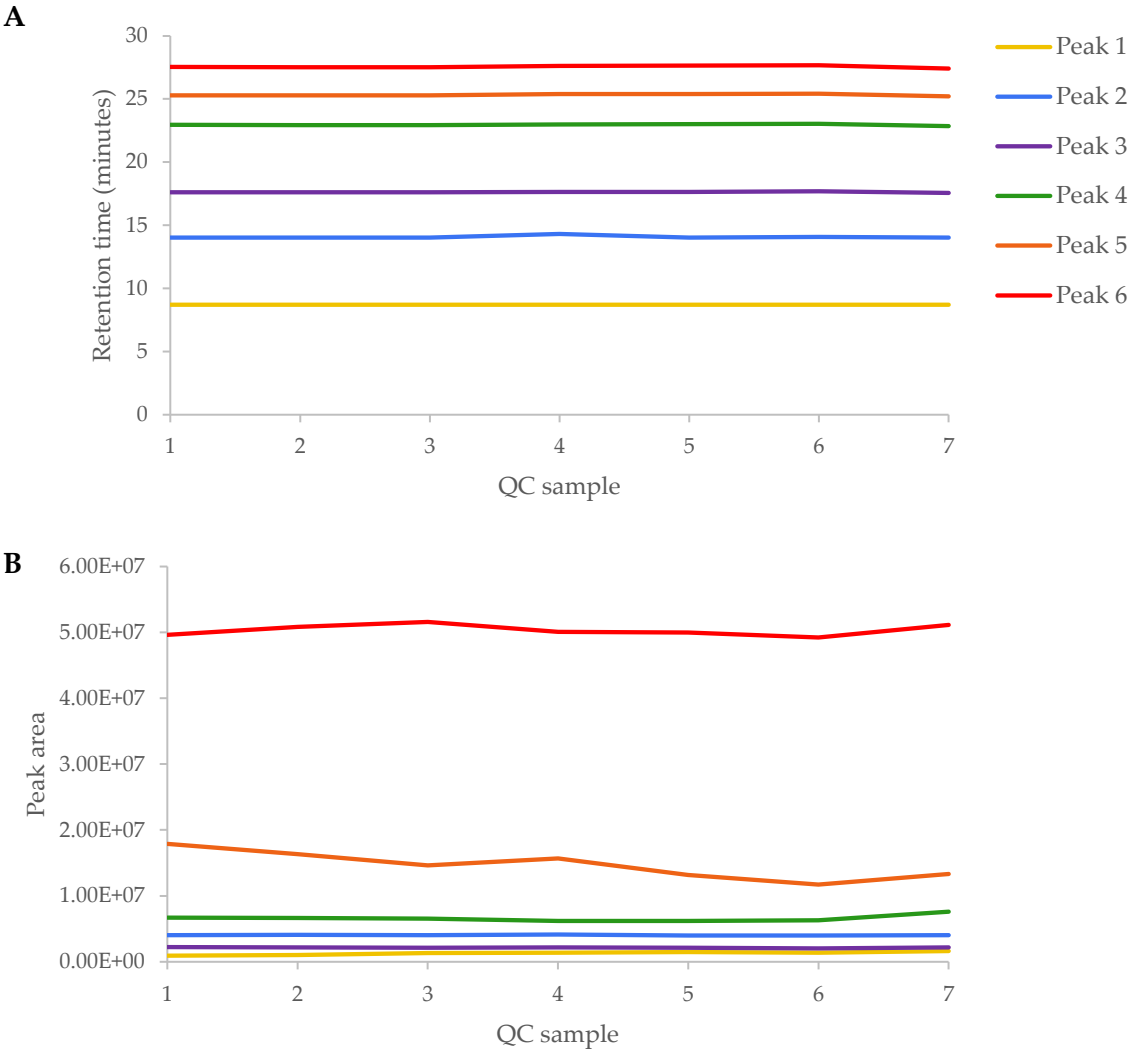

Figure 6.11: Variability of retention time (A) and peak area (B) of 6 peaks in QC samples throughout analytical run for extracts from chicken muscle tissue stored at 4°C

Analysing 6 peaks within the QC samples, the retention time is very stable in all peaks throughout the analytical run, and the peak area of most of these peaks remains constant in all QC samples. Peak 5 shows a slightly decreasing peak area throughout the 7 QC samples, and so further statistical analysis is required to assess the reliability of the data from this run.

Table 6.9: Variability of retention time and peak area of 6 peaks in chromatograms of QC samples during the analysis of extracts from chicken muscle tissue stored at 4°C

	Retention time (minutes)									
Peak	QC1	QC2	QC3	QC4	QC5	QC6	QC7	SD	Average	CV%
1	8.70	8.71	8.70	8.71	8.71	8.70	8.71	0.01	8.71	0.06
2	14.02	14.02	14.02	14.30	14.03	14.06	14.01	0.10	14.07	0.74
3	17.61	17.62	17.60	17.63	17.63	17.68	17.57	0.03	17.62	0.19
4	22.95	22.93	22.93	22.99	23.01	23.03	22.86	0.06	22.96	0.25
5	25.30	25.30	25.29	25.38	25.4	25.42	25.20	0.08	25.33	0.30
6	27.54	27.52	27.51	27.62	27.64	27.66	27.41	0.09	27.56	0.32
	Peak area									
Peak	QC1	QC2	QC3	QC4	QC5	QC6	QC7	SD	Average	CV%
1	922618	1007436	1308501	1354543	1465202	1387078	1620568	247834	1295135	19.14
2	4019585	4070291	4012717	4140406	3995509	3954424	4005537	60140	4028353	1.49
3	2197409	2168149	2144265	2185517	2132216	2041083	2149833	51492	2145496	2.40
4	6680318	6637009	6543257	6200057	6209219	6293571	7601977	486722	6595058	7.38
5	17896464	16324211	14637768	15652370	13188480	11716502	13338293	2113586	14679155	14.40
6	49645730	50834001	51598082	50060745	49960779	49196977	51108642	859053	50343565	1.71

The retention time variability was between 0.06 and 0.74%, and the peak area variability was between 1.49 and 19.14%, which despite being high, is still below the threshold of 30% and so confirms that the data obtained in this analytical run was reliable.

6.7.3.2 Metabolic profiling

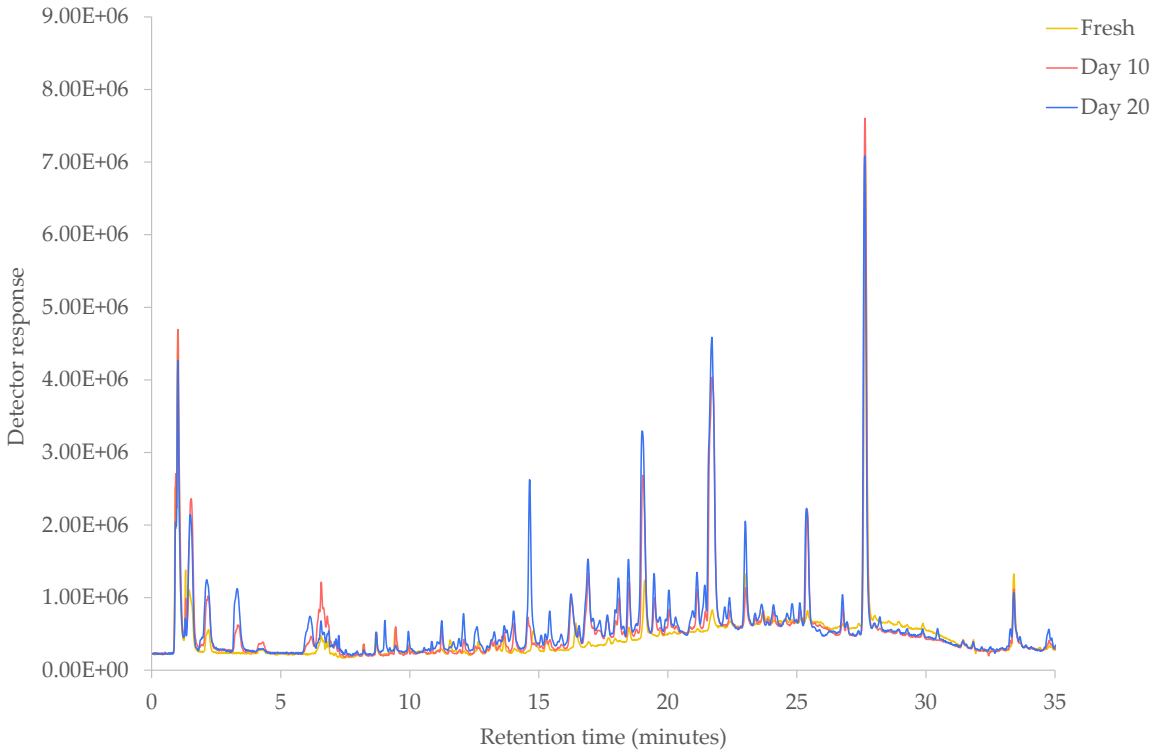

Figure 6.12: Example total ion chromatograms for extracts from chicken muscle tissue stored at 4°C for different lengths of time

The differences within the chromatograms during spoilage at 4°C (Figure 6.12) are not as obvious as in the chicken spoiled at room temperature, which is expected as the room temperature chicken would have spoiled quicker than that kept at 4°C. It can still be seen that the intensity of the peaks increase during the spoilage process, with the chromatograms for the Day 20 sample showing the greatest peak intensities.

6.7.3.3 Multivariate statistics

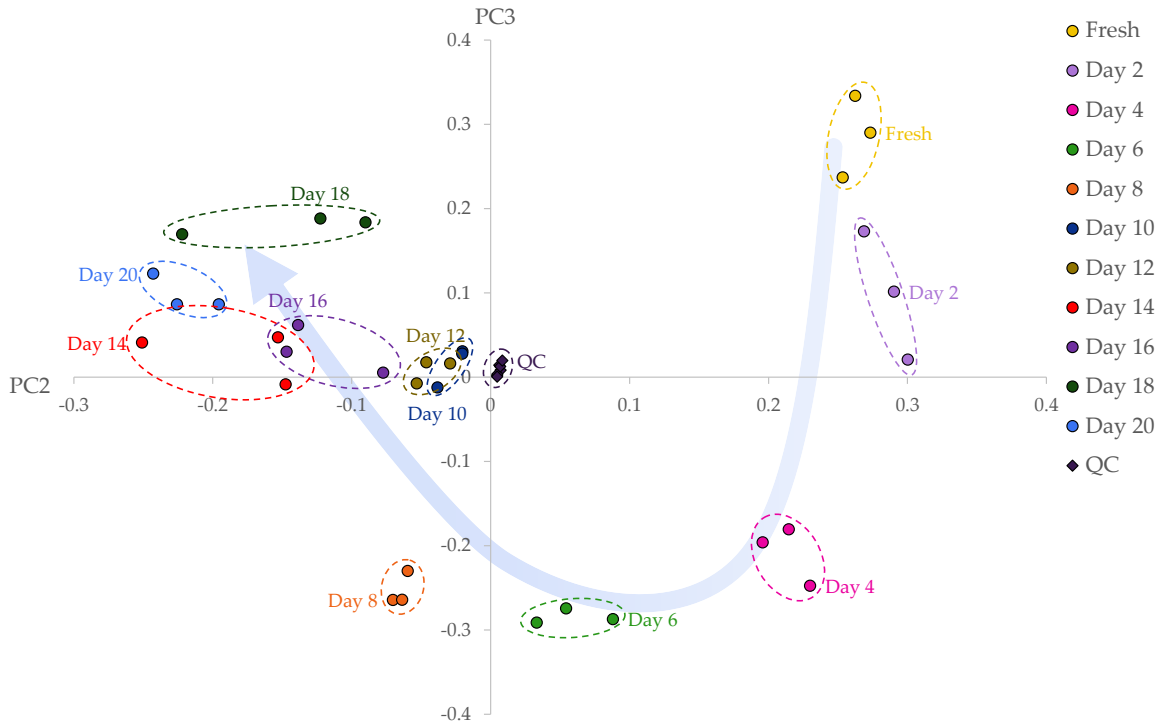

Figure 6.13: Principal component analysis scores plot of PC2 (4.105%) and PC3 (1.397%) for extracts from chicken muscle tissue stored at 4°C for different lengths of time. PCA was carried out using all features detected with a CV < 30%

The PCA plot for chicken spoiled at 4°C (Figure 6.13) shows the beginning of the spoilage profile as very separate groups; Fresh, Day 2, Day 4, Day 6, and Day 8 are all separated from each other and the rest of the time points. For the remaining time points, there were less distinct groups, with a lot of overlap, which could have been caused by the severity of the spoilage at these time points. The general trend of these sample groups is represented by the blue arrow, where the Fresh sample group is on the right, and the groups follow in chronological order up until the Day 10 sample group, which is where the overlapping of groups begins. It can be seen that the quality control samples are tightly clustered in the middle of the plot, showing the analytical run was stable throughout. The separation of these sample groups is in the direction of the x-axis, so principal component 2 was used to find the 50 features with the highest loading values.

6.7.3.4 Significant markers

The remaining markers from the 50 features with the highest loading values can be seen in Table 6.10. All of these markers were reliable throughout the analytical run, with a CV% in the QC samples of less than 25.10% in the normalised data, and 18.70% in the raw data. All markers were significantly different in both the normalised and raw data, with a p-value of 0.032 and below, with the majority of markers having a p-value of less than 0.001.

The trend of these markers generally decreased as the storage time increased, with some markers increasing at Day 4 or Day 6 and then decreasing.

Table 6.10: Summary of compounds that contribute the most to the differences among all extracts from chicken muscle tissue stored at 4°C for different lengths of time, using PC2. Marker trend: ↓ = decreased, ↷ = increased then decreased

m/z	Retention time median (mins)	P-value from ANOVA/Welch (XCMS)	CV% (XCMS)	P-value from ANOVA/Welch (EICs)	CV% (EICs)
↓ 132.0771	1.03	<0.001	3.35	<0.001	1.20
↷ 496.3391	14.83	<0.001	0.80	<0.001	1.00
↓ 338.3424	27.68	<0.001	3.04	0.032	3.86
↷ 522.3546	15.35	<0.001	1.34	<0.001	0.83
↷ 524.3703	19.38	<0.001	1.17	<0.001	1.44
↷ 482.3257	16.46	<0.001	2.25	<0.001	1.64
↷ 137.0458	1.32	<0.001	4.23	<0.001	6.63
↓ 241.1295	0.94	<0.001	4.01	<0.001	4.02
↷ 520.3390	13.13	<0.001	1.80	<0.001	0.93
↓ 269.0888	1.42	<0.001	5.76	<0.001	1.40
↓ 663.4541	33.43	<0.001	2.80	<0.001	3.95
↓ 123.0555	1.30	<0.001	15.08	0.001	2.41
↷ 583.3235	13.48	<0.001	1.86	<0.001	2.55
↷ 150.0586	1.28	<0.001	24.58	<0.001	6.64
↷ 526.3132	15.02	<0.001	3.14	0.001	1.90
↷ 273.0845	1.29	<0.001	2.00	<0.001	2.20
↷ 636.5556	35.14	<0.001	25.10	<0.001	18.70
↓ 182.0809	1.38	<0.001	8.45	<0.001	3.05
↷ 357.2999	18.98	<0.001	6.55	<0.001	3.56
↷ 610.5398	35.42	<0.001	24.19	<0.001	10.40
↷ 638.5712	36.96	<0.001	4.64	<0.001	4.05
↓ 480.3085	13.14	<0.001	6.48	0.001	6.40
↷ 612.5556	37.42	<0.001	13.18	<0.001	12.59
↓ 327.0076	9.47	<0.001	2.52	<0.001	3.16
↓ 502.2917	11.60	<0.001	7.83	<0.001	9.22
↷ 355.2844	16.92	<0.001	3.52	<0.001	2.94
↓ 212.1029	0.94	<0.001	2.44	<0.001	1.73
↓ 162.1117	1.01	<0.001	2.46	<0.001	1.96
↷ 438.2976	14.07	<0.001	2.65	<0.001	1.95
↷ 478.2920	11.98	0.001	2.45	0.019	2.10
↓ 204.1232	1.31	<0.001	4.58	<0.001	4.71
↓ 268.2454	22.12	<0.001	5.92	<0.001	2.84
↷ 178.0725	1.31	<0.001	12.13	<0.001	11.62
↷ 494.3230	12.23	<0.001	3.69	<0.001	8.29
↓ 279.0851	0.96	<0.001	4.46	<0.001	4.22

6.7.3.5 Tentative identifications

Several markers were tentatively identified from the remaining markers that were significantly different in both the normalised and raw data. Each marker gave a predicted formula that matched compounds on the METLIN database, and the mass spectra comparisons can be seen in Appendix H.

Table 6.11: Compounds that were significantly different and tentatively identified in extracts from chicken muscle tissue stored at 4°C for different lengths of time based on comparison of mass spectra on METLIN

m/z	Retention time median (mins)	Possible formula	Likelihood score (%)	Tentative identification
132.0771	1.03	$C_4H_9N_3O_2$	99.79	creatine
338.3424	27.68	$C_{22}H_{43}NO$	98.61	13Z-docosenamide
137.0458	1.32	$C_5H_4N_4O$	99.50	hypoxanthine
182.0809	1.38	$C_9H_{11}NO_3$	97.16	tyrosine

The marker with an *m/z* of 132.0771 was tentatively identified as creatine, which is an organic acid involved in the recycling of ATP. The trend of this marker can be seen in Figure 6.14; this compound decreased as the spoilage time increased. Past research contradicts this finding, and found that creatine increased as the storage time increased in beef that was stored at 4°C in air [169]. This contradiction could be explained by the difference in species of the muscle tissue investigated, as the tissue used in the research presented here was chicken, not beef. The biochemistry of muscle tissue from different animals varies substantially, and the protein and lipid concentration differs [25], so the metabolic changes of compounds such as creatine could differ during the spoilage process.

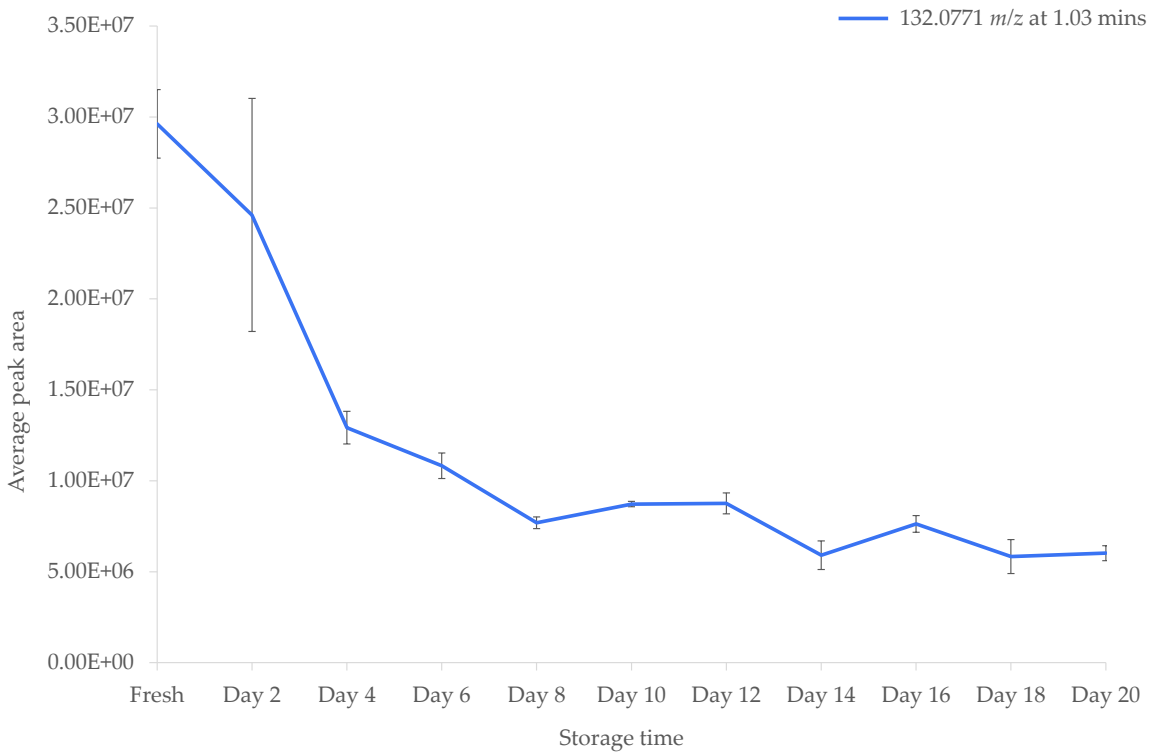

Figure 6.14: Trend of marker tentatively identified as creatine that was significantly different among all chicken muscle tissue samples stored at 4°C for different lengths of time. Error bars correspond to ± 1 standard deviation

The experimental storage of the meat samples also differed in these two experiments; in this research, each time point was sampled from a different piece of muscle tissue, whereas in the study carried out by Ercolini et al. [169], each time point was sampled from the same piece of muscle. This could have an effect on the spoilage process, as uncovering the muscle tissue every time a sample is taken provides an opportunity for bacteria to enter the sample environment and change the spoilage process, compared to if the sample is taken from a different piece of muscle tissue each time, like in this research.

The marker with an m/z of 137.0458 was tentatively identified as hypoxanthine, based on the mass spectrum containing the same single peak in the available mass spectrum on the METLIN database. This marker showed a trend that increased at Day 2 and then decreased over the course of the storage period, as seen in Figure 6.15. Hypoxanthine is involved in the purine catabolism pathway, with the end

product being uric acid [108], and has been shown to have a higher concentration in the blood after death [107]. The decreasing trend found in this research would be expected if the sample was taken while the muscle was still within the body of the animal, as the hypoxanthine increases in the blood and therefore decreases in the muscle. However, this research was carried out with muscle that had been removed from the animal, and so the increase in concentration at Day 2 may be the catabolism of purine, and then the continued decreasing concentration of this marker may be caused by the catabolism of hypoxanthine to uric acid.

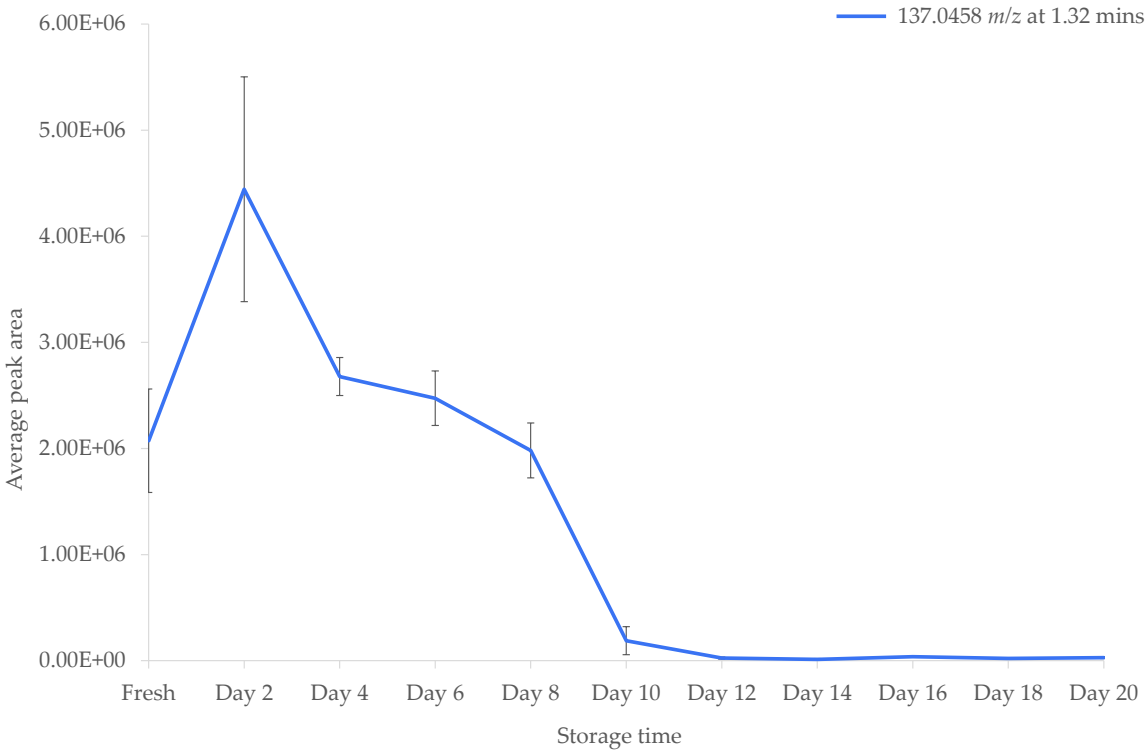

Figure 6.15: Trend of marker tentatively identified as hypoxanthine that was significantly different among all chicken muscle tissue samples stored at 4°C for different lengths of time. Error bars correspond to ± 1 standard deviation

Another marker with an m/z of 182.0809 was tentatively identified as tyrosine, which is an amino acid. The mass spectrum for this compound matched the available mass spectrum for tyrosine on the METLIN database, however the spectral peaks are low in intensity compared to other peaks in the mass spectrum for this chromatographic peak. As this chromatographic peak is at the very beginning of the chromatogram at

1.38 minutes, it is likely there were many polar compounds that co-eluted within this peak, which leads to other spectral peaks that can distract from the peaks of interest.

This marker showed a decreasing trend over the course of the storage period, as shown in Figure 6.16. This contradicts the findings in other research, where the concentration of tyrosine significantly increased during the storage period of buffalo meat in refrigerated conditions [170], and free amino acids were found to increase in chicken muscle tissue stored aerobically at 4°C [168]. The specific increase of tyrosine was seen in a study that used a different species of animal than in this research, and so the metabolic changes during the spoilage process may differ in content and in rate between different species. The increase in amino acids was seen in chicken breast muscle tissue, which is the same sample type as in this research, however the samples were collected directly from the processing plant on the day of slaughter, and were only sampled for a duration of 8 days. In this current research, the chicken muscle was collected from a local butcher and examined over a period of 20 days. It is known that bacteria, in particular the *Pseudomonas* species, catabolise many substrates within the meat during the spoilage process, starting with glucose, then lactate and pyruvate, and ending with amino acids [157]. Therefore, the decreasing trend observed in this research could be because the chicken muscle tissue was further along the spoilage process than in the study by Alexandrakis et al. [168], and so the bacteria had consumed all the previous substrates and had begun to catabolise amino acids.

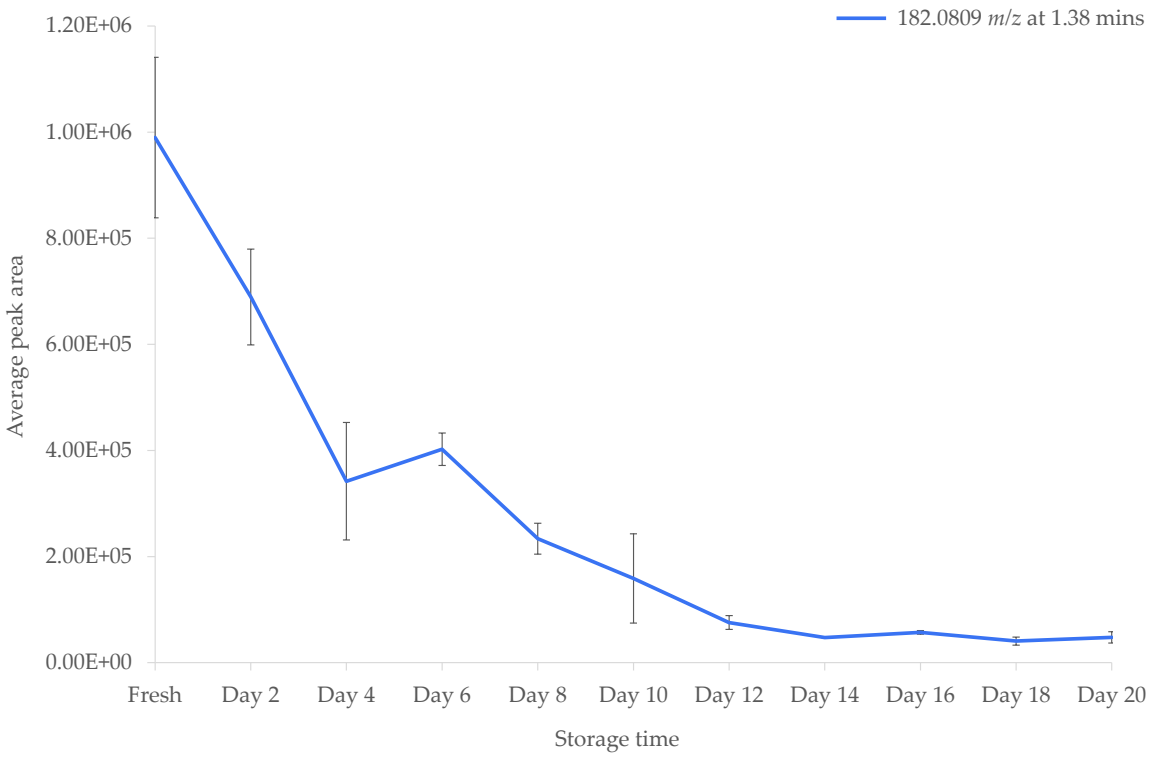

Figure 6.16: Trend of marker tentatively identified as tyrosine that was significantly different among all chicken muscle tissue samples stored at 4°C for different lengths of time. Error bars correspond to ± 1 standard deviation

6.7.4 Spoilage of chicken at 4°C - external and internal sample collection

6.7.4.1 Metabolic profiling

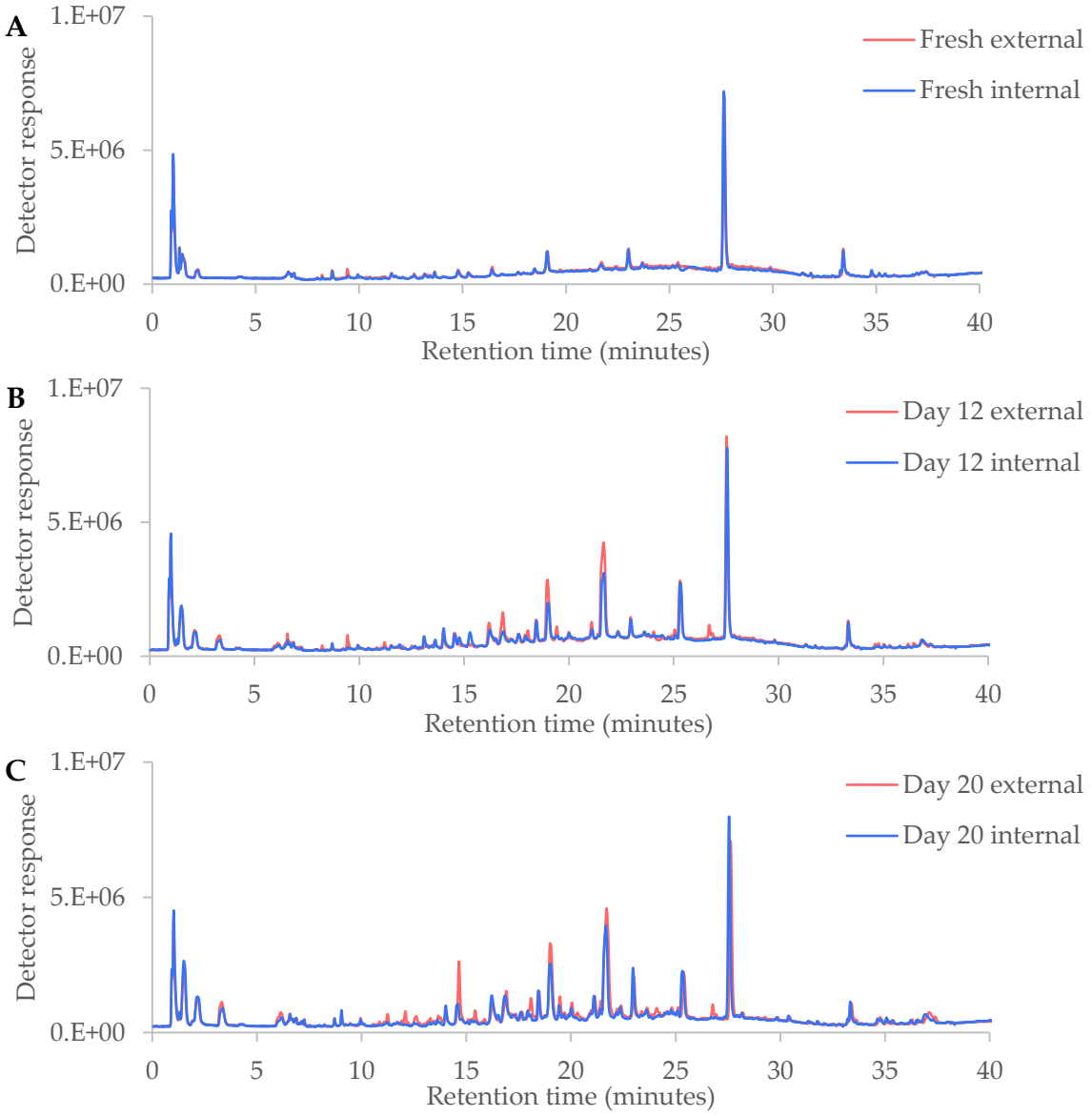

Figure 6.17: Example total ion chromatograms for extracts from chicken muscle tissue stored at 4°C for different lengths of time, comparing external and internal sample collection. A) Fresh, B) Day 12, C) Day 20

The differences between external and internal sample collection extracts in the chicken stored at 4°C are less obvious in the chromatograms (Figure 6.17) compared to chicken stored at room temperature. The Fresh samples do not show any difference

between the external and internal sample collection extracts except for a peak at 9.5 minutes. There is a difference between the two sample types at Day 12 and Day 20, with the external extracts showing a higher intensity in many of the peaks. Purely based on the observation of the chromatograms, it can be seen that the external and internal extracts vary in the rate of spoilage during the storage time.

6.7.4.2 Multivariate statistics

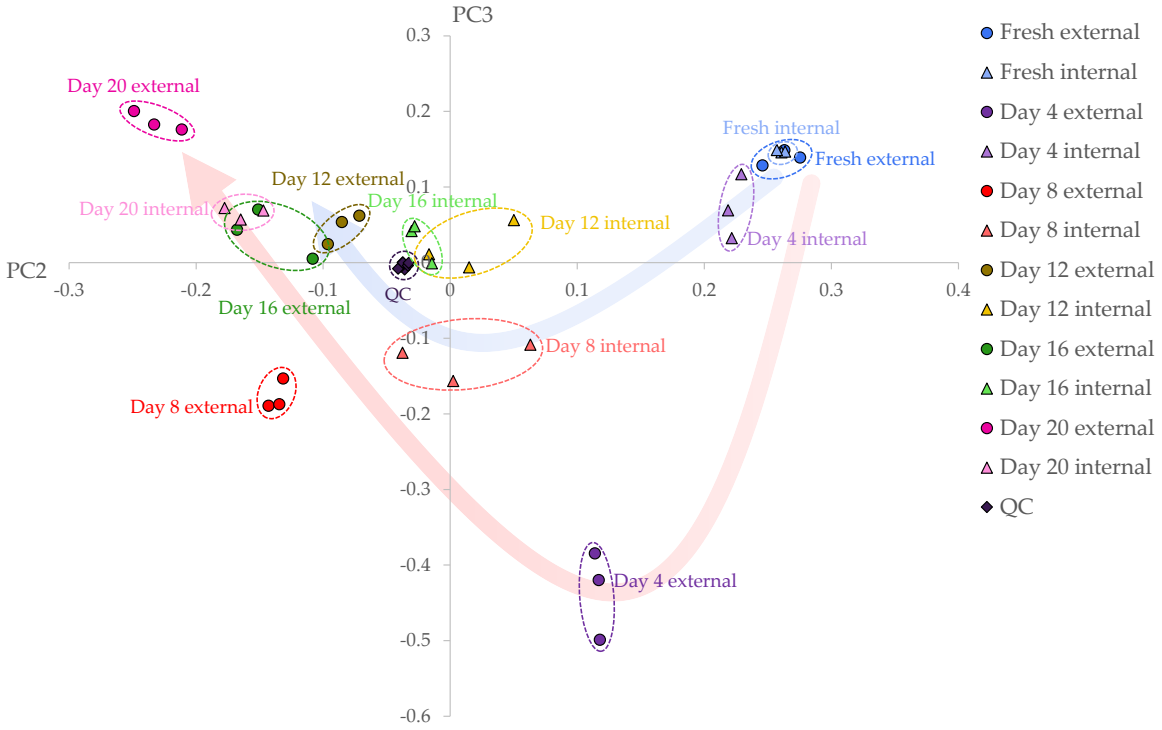

Figure 6.18: Principal component analysis scores plot of PC2 (4.019%) and PC3 (1.146%) for external and internal extracts from chicken muscle tissue stored at 4°C for different lengths of time. PCA was carried out using all features detected with a CV < 30%

Figure 6.18 shows the samples for external and internal collection points from chicken spoiled at 4°C are well separated from each other at every time point except for Fresh. The indistinct groupings at the Fresh time point would likely be due to not enough time elapsing for the spoilage process to have a difference externally compared to internally in the chicken muscle tissue sample. All other time points have had a length of time to allow for the spoilage process to continue externally while the internal part of the chicken spoils at a slower rate as it is protected from bacterial activity. Both the external and internal extract groups follow a similar trend, with the Fresh samples on the right and moving down and then up in the direction of the x-axis to the left side of the plot. This is represented by the red arrow for the external extracts and the blue arrow for the internal extracts. The QC samples are very tightly clustered in the middle of the plot, confirming the reliability of this data.

6.7.4.3 Significant markers

The remaining markers from the 50 features with the highest loading values are shown in Table 6.12. All markers were reliable within the QC samples throughout the analytical run, with a CV% of less than 24.88% in the normalised data, and 18.79% in the raw data. All markers were highly significant with a p-value of 0.016 and below.

The trend of the markers were mostly decreasing, with some showing a slight increase at Day 4 before decreasing. Most of the markers were at a higher concentration in the internal extracts compared to the external extracts, indicating these markers were decreasing at a quicker rate in the external extracts. This is interesting to observe as in the chromatograms, the intensity for many peaks were higher in the external extracts. It may be that the markers that most contribute to the separation of sample types in the PCA analysis are not the compounds that produce these higher intensity peaks in the total ion chromatogram, and may even be hidden under the baseline. This demonstrates an advantage of the workflow implemented in this work, as the subtle and lower intensity compounds can still be investigated despite potentially not being observed in the total ion chromatograms.

Table 6.12: Summary of compounds that contribute the most to the differences among all external and internal extracts from chicken muscle tissue stored at 4°C for different lengths of time, using PC2.
Marker trend: ↓ = decreased, ↷ = increased at Day 4 then decreased

m/z	Retention time median (mins)	P-value from ANOVA/Welch (XCMS)	CV% (XCMS)	P-value from ANOVA/Welch (EICs)	CV% (EICs)
↓ 132.0772	1.04	<0.001	4.40	<0.001	1.20
↓ 338.3424	27.57	<0.001	2.74	0.016	3.86
↷ 496.3391	14.78	<0.001	1.53	<0.001	1.00
↷ 482.3250	16.42	<0.001	3.09	<0.001	1.73
↷ 522.3546	15.29	<0.001	2.31	<0.001	0.83
↓ 241.1296	0.95	<0.001	4.22	<0.001	4.02
↷ 137.0460	1.32	<0.001	5.17	<0.001	6.63
↓ 269.0888	1.44	<0.001	5.37	<0.001	1.40
↷ 524.3703	19.32	<0.001	1.24	<0.001	1.44
↓ 663.4540	33.36	<0.001	1.77	<0.001	3.95
↷ 520.3390	13.10	<0.001	2.73	<0.001	0.93
↓ 204.1232	1.06	<0.001	2.22	<0.001	3.13
↷ 116.0711	1.04	<0.001	4.03	<0.001	3.91
↓ 263.1472	1.04	<0.001	1.18	<0.001	2.04
↓ 182.0810	1.39	<0.001	8.55	<0.001	2.96
↷ 150.0586	1.29	<0.001	24.88	<0.001	6.64
↓ 480.3081	13.16	<0.001	6.83	<0.001	5.74
↓ 340.2531	6.62	<0.001	2.21	0.015	5.37
↓ 502.2918	11.59	<0.001	8.62	<0.001	9.22
↓ 114.0649	0.95	<0.001	21.19	<0.001	7.93
↓ 227.1141	0.94	<0.001	3.64	<0.001	13.40
↓ 426.3567	18.64	0.004	3.95	0.001	1.77
↷ 583.3235	13.44	<0.001	1.11	0.001	2.55
↓ 162.1117	1.02	<0.001	3.48	<0.001	1.96
↷ 273.0846	1.31	<0.001	2.46	<0.001	2.20
↓ 212.1029	0.94	<0.001	3.41	<0.001	1.73
↷ 617.5110	37.31	<0.001	19.26	<0.001	18.79
↓ 400.1579	1.06	<0.001	12.78	<0.001	4.93
↓ 610.1837	33.21	<0.001	19.66	<0.001	18.76
↓ 684.2021	34.73	<0.001	6.24	<0.001	5.57
↓ 453.3382	6.80	<0.001	3.94	<0.001	5.59
↓ 478.2923	11.59	<0.001	5.79	<0.001	4.69

6.7.4.4 Tentative identifications

Table 6.13: Compounds that were significantly different and tentatively identified in external and internal extracts from chicken muscle tissue stored at 4°C for different lengths of time based on comparison of mass spectra on METLIN

m/z	Retention time median (mins)	Possible formula	Likelihood score (%)	Tentative identification
132.0772	1.04	$C_4H_9N_3O_2$	99.79	creatine
338.3424	27.57	$C_{22}H_{43}NO$	98.61	13Z-docosenamide
137.0460	1.32	$C_5H_4N_4O$	99.50	hypoxanthine

There were three markers that were tentatively identified, and these markers were also tentatively identified in the 4°C spoilage profile dataset. The matching mass spectra can be seen in Appendix H. Interestingly, creatine and 13Z-docosenamide were found at a higher concentration in the internal extracts compared to the external extracts, showing there is a difference in concentration of significant markers based on the location in which the sample is taken from the muscle tissue. The marker tentatively identified as hypoxanthine showed a similar trend in the internal extracts to in the external extracts as demonstrated previously, however the increase at Day 4 was higher.

These trends, along with the majority of the other significantly different markers that were not tentatively identified, show the concentration for the markers were lower in the external extracts compared to the internal extracts and therefore decreased quicker than in the internal extracts. This shows the changes that occur in chicken muscle tissue during the spoilage process at 4°C occurs at a faster rate in the external extracts compared to the internal extracts.

6.7.5 Comparison of spoilage of chicken at room temperature and 4°C

6.7.5.1 Quality control

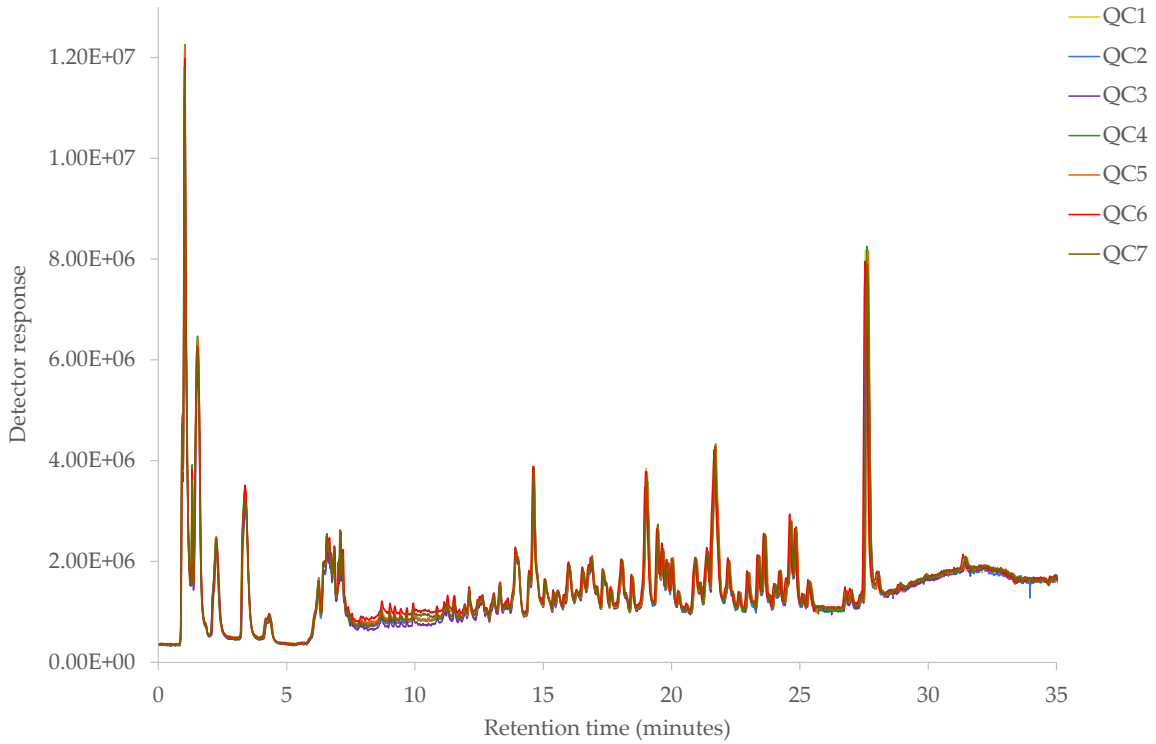

Figure 6.19: Total ion chromatograms of QC samples throughout analytical run for extracts from chicken muscle tissue stored at room temperature and 4°C

The chromatograms for the quality control samples in this dataset are shown in Figure 6.19, and it can be seen that the chromatograms are very reproducible with no retention time drift. The only area of baseline variation is between 7.5 and 12 minutes, and this is only slight.

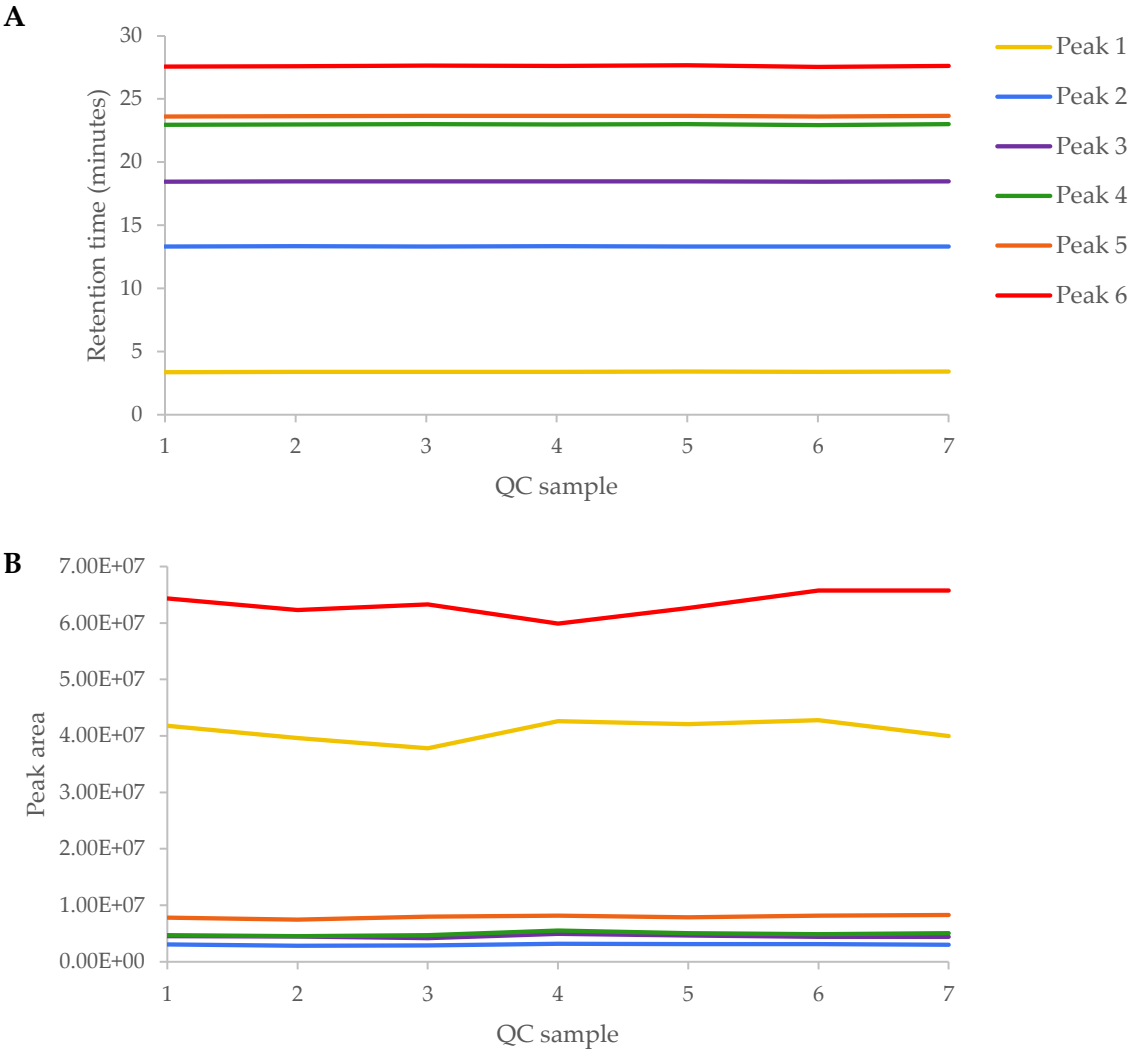

Figure 6.20: Variability of retention time (A) and peak area (B) of 6 peaks in QC samples throughout analytical run for extracts from chicken muscle tissue stored at room temperature and 4°C

The 6 peaks chosen to carry out further analysis on proved to have a very stable retention time in all QC samples, and the peak areas for these peaks remain constant throughout the analytical run, as seen in Figure 6.20.

Table 6.14: Variability of retention time and peak area of 6 peaks in chromatograms of QC samples during the analysis of extracts from chicken muscle tissue stored at room temperature and 4°C

	Retention time (minutes)									
Peak	QC1	QC2	QC3	QC4	QC5	QC6	QC7	SD	Average	CV%
1	3.36	3.37	3.39	3.39	3.40	3.37	3.40	0.02	3.38	0.47
2	13.31	13.33	13.32	13.33	13.32	13.30	13.32	0.01	13.32	0.08
3	18.45	18.47	18.48	18.47	18.48	18.44	18.48	0.02	18.47	0.09
4	22.96	22.98	23.01	22.98	23.01	22.93	23.01	0.03	22.98	0.13
5	23.61	23.63	23.66	23.65	23.66	23.60	23.65	0.02	23.64	0.10
6	27.56	27.60	27.64	27.61	27.66	27.55	27.63	0.04	27.61	0.15
	Peak area									
Peak	QC1	QC2	QC3	QC4	QC5	QC6	QC7	SD	Average	CV%
1	41756528	39629134	37802048	42593500	42058430	42765385	39988711	1846336	40941962	4.51
2	3038861	2825876	2861479	3193174	3139363	3098134	3028505	137410	3026485	4.54
3	4507725	4472819	4162206	4945693	4632566	4418223	4413489	239755	4507532	5.32
4	4694474	4503556	4720156	5532707	5030721	4862198	5053363	334853	4913882	6.81
5	7782129	7456931	7995639	8161053	7884796	8138054	8254553	273927	7953308	3.44
6	64308953	62268867	63259511	59892569	62657293	65740527	65735563	2078117	63409040	3.28

The retention time variability was between 0.08 and 0.47%, and the peak area variability was between 3.28 and 6.81%, which shows that the retention time and peak area was extremely reproducible during this analytical run, and the data obtained was reliable.

6.7.5.2 Metabolic profiling

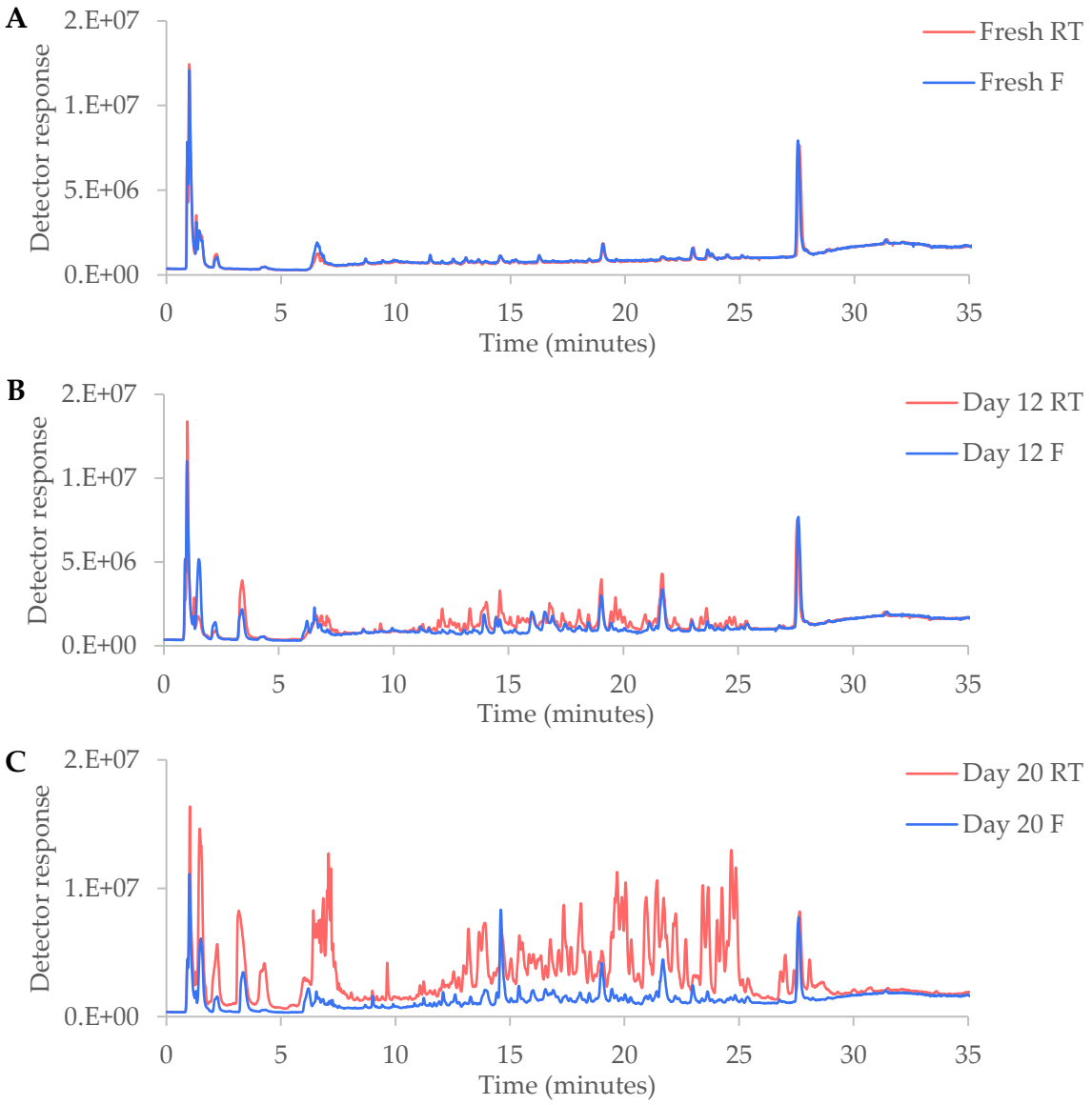

Figure 6.21: Example total ion chromatograms for extracts from chicken muscle tissue stored at room temperature (RT) and 4°C (F) for different lengths of time. A) Fresh, B) Day 12, C) Day 20

When comparing the two different storage temperatures (Figure 6.21), it can be seen that there is not much difference in the Fresh samples except for a slight discrepancy in the intensity of the peak at 6 minutes. However, at Day 12 and Day 20, there is a very obvious difference in the chromatograms for room temperature and 4°C. The room temperature extracts showed a greater intensity on the chromatograms for nearly all peaks. This is expected as the chicken would degrade more rapidly at a

higher temperature as this is more ideal for bacterial activity. The peak at 27.5 minutes remains fairly consistent in intensity at all three time points in both room temperature and 4°C samples. The rate of spoilage can very clearly be seen in these chromatograms, with the chicken muscle tissue spoiling more rapidly at room temperature than compared to at 4°C.

6.7.5.3 Multivariate statistics

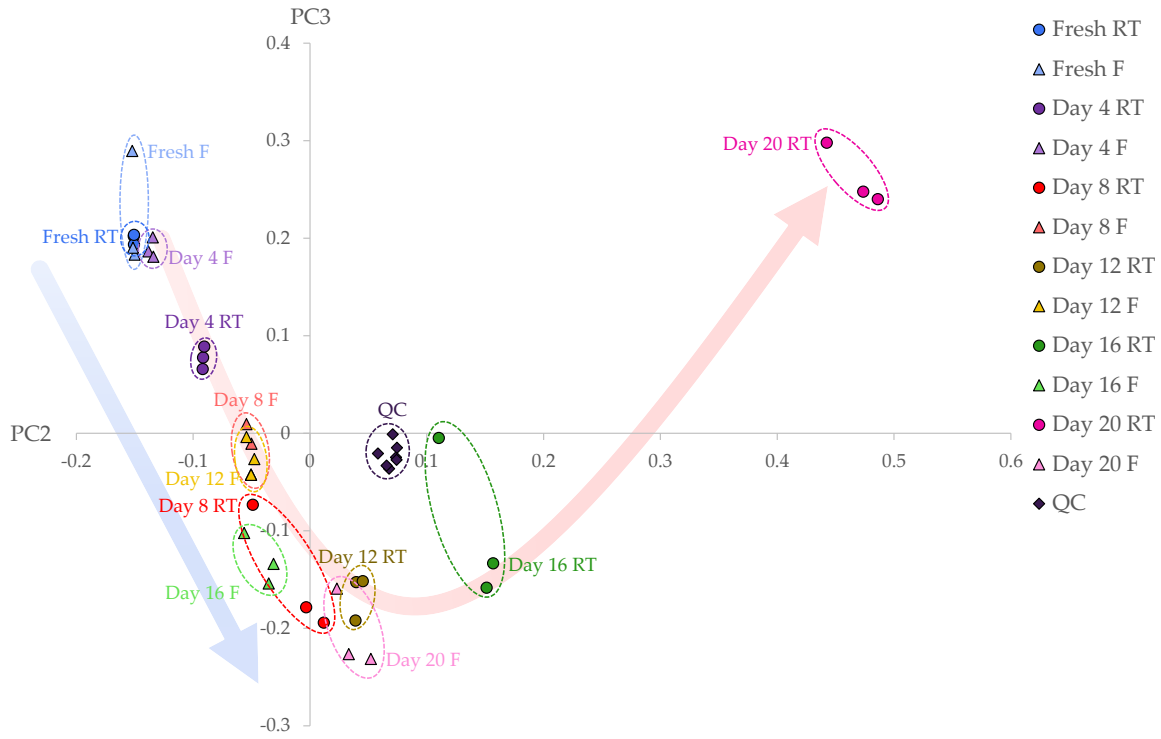

Figure 6.22: Principal component analysis scores plot of PC2 (5.967%) and PC3 (1.248%) for extracts from chicken muscle tissue stored at room temperature (RT) and 4°C (F) for different lengths of time. PCA was carried out using all features detected with a CV < 30%

The PCA plot in Figure 6.22 shows the differences in the spoilage process between room temperature and at 4°C. There is greater separation between each time point in chicken stored at room temperature compared to the time points during spoilage at 4°C. It is clear to see that there is indeed a difference at each time point between room temperature and 4°C, with the differences becoming greater as the spoilage time increases. The trend of these sample types moves in the direction of the x-axis, representing PC2. The room temperature samples move down then up from left to right, shown by the red arrow. The 4°C samples follows a similar trend to the beginning of the room temperature samples, but only moves down, from left to right, and does not continue upwards, shown by the blue arrow. The quality control samples are tightly clustered in the middle of the plot, showing the analytical run was stable throughout with minimal instrumental drift.

6.7.5.4 Significant markers

The remaining markers from the 50 features with the highest loading values are shown in Table 6.15. All markers were reliable in the QC samples throughout the analytical run, with a CV% of less than 10.05% in the normalised data, and 11.27% in the raw data. All markers were highly significant in both the normalised data and raw data, with a p-value of less than 0.003.

The trends for these markers mostly increased as the storage time increased, with some markers having an erratic trend that would therefore not be very useful in determining the shelf-life of chicken meat. All markers that gradually increased were at a higher concentration in the room temperature samples compared to the 4°C samples.

Table 6.15: Summary of compounds that contribute the most to the differences among all extracts from chicken muscle tissue stored at room temperature and 4°C for different lengths of time, using PC2.
Marker trend: ↑ = increased, *↑ = RT erratic and 4°C increased, ↑↓ = RT decreased, 4°C increased, * = random

m/z	Retention time median (mins)	P-value from ANOVA/Welch (XCMS)	CV% (XCMS)	P-value from ANOVA/Welch (EICs)	CV% (EICs)
↑ 352.3572	24.89	<0.001	3.19	<0.001	3.44
↑ 326.3412	24.69	<0.001	3.33	<0.001	3.98
↑ 338.3415	23.66	<0.001	3.80	<0.001	2.93
↑ 312.3258	23.43	<0.001	3.34	<0.001	3.75
↑ 282.2786	19.70	<0.001	3.25	<0.001	2.30
*↑ 105.0694	3.21	<0.001	1.66	<0.001	4.00
↑ 256.2630	19.90	<0.001	3.51	<0.001	2.95
↑ 130.1214	7.07	<0.001	8.90	<0.001	11.27
↑ 386.3411	24.28	<0.001	1.56	<0.001	2.94
*↑ 505.3742	13.95	<0.001	2.91	<0.001	1.52
*↑ 341.3521	15.58	<0.001	2.77	<0.001	2.25
↑ 350.3413	22.27	<0.001	3.43	<0.001	4.06
↑ 360.3255	24.07	<0.001	2.50	<0.001	3.26
↑ 396.3469	21.46	<0.001	3.21	<0.001	1.37
*↑ 434.3374	14.79	<0.001	3.15	<0.001	2.17
*↑ 145.1333	1.06	<0.001	3.59	<0.001	3.10
↑ 402.3360	20.07	<0.001	2.77	<0.001	1.72
*↑ 367.3678	16.42	<0.001	3.39	<0.001	3.64
*↑ 479.3585	13.29	<0.001	3.02	<0.001	1.55
↑ 336.3257	20.99	<0.001	3.69	<0.001	4.53
↑ 324.3254	21.43	<0.001	10.05	<0.001	4.96
↑ 384.3255	22.16	<0.001	2.14	0.002	2.63
↑ 376.3197	19.60	<0.001	2.79	<0.001	1.66
↑ 340.3565	27.05	<0.001	5.14	<0.001	6.82
↑ 430.3312	21.35	<0.001	3.64	<0.001	2.58
↑ 201.1946	7.11	<0.001	2.30	<0.001	3.68
↑ 354.3719	28.10	<0.001	3.99	<0.001	5.53
↑ 370.3318	21.02	<0.001	3.38	<0.001	2.28
↑ 164.1065	7.21	<0.001	9.04	<0.001	9.93
↑ 404.3157	20.94	<0.001	4.26	<0.001	1.81
↑ 116.1063	5.98	<0.001	7.40	<0.001	7.22
↑ 280.2623	17.36	0.001	4.13	0.003	3.02
*↑ 327.3362	14.93	<0.001	3.01	<0.001	1.76
↑ 413.3544	28.67	<0.001	2.69	<0.001	3.69
↑ 187.1426	3.22	<0.001	2.69	<0.001	4.37

Table 6.15 continued: Summary of compounds that contribute the most to the differences among all extracts from chicken muscle tissue stored at room temperature and 4°C for different lengths of time, using PC2.
Trends: ↑ = increased, *↑ = RT erratic and 4°C increased, ↑↓ = RT decreased, 4°C increased, * = random

m/z	Retention time median (mins)	P-value from ANOVA/Welch (XCMS)	CV% (XCMS)	P-value from ANOVA/Welch (EICs)	CV% (EICs)
↑ 310.3098	20.08	<0.001	4.10	<0.001	5.09
↑ 187.1776	6.83	<0.001	3.56	<0.001	4.51
↑ 284.2941	24.58	<0.001	3.08	<0.001	2.79
* 86.0970	1.50	<0.001	3.52	<0.001	6.58
*↑ 394.3313	18.99	<0.001	3.01	<0.001	1.49
↑ 491.3587	13.68	<0.001	2.61	<0.001	2.02
* 283.2632	14.65	<0.001	3.85	0.001	3.91
↑↓ 118.0867	1.04	<0.001	6.22	<0.001	4.64
*↑ 408.3216	13.85	<0.001	3.03	<0.001	1.96
↑ 382.3309	18.06	<0.001	3.68	<0.001	2.08
↑ 374.3410	21.88	<0.001	3.66	<0.001	1.72
↑ 235.1790	7.18	<0.001	3.10	<0.001	5.01

6.7.5.5 Tentative identifications

Table 6.16: Compounds that were significantly different and tentatively identified in extracts from chicken muscle tissue stored at room temperature and 4°C for different lengths of time based on comparison of mass spectra on METLIN

m/z	Retention time median (mins)	Possible formula	Likelihood score (%)	Tentative identification
132.1020	1.50	$C_6H_{13}NO_2$	99.99	leucine
256.2630	19.90	$C_{16}H_{33}NO$	99.00	palmitic amide
324.3254	21.43	$C_{21}H_{41}NO$	98.49	N-cyclohexanecarbonyltetradecylamine
310.3098	20.08	$C_{20}H_{39}NO$	98.49	oleoyl ethyl amide
284.2941	24.58	$C_{18}H_{37}NO$	98.42	stearamide
283.2632	14.65	$C_{18}H_{34}O_2$	99.14	oleic acid
118.0867	1.04	$C_5H_{11}NO_2$	98.88	N-methyl-α-aminoisobutyric acid

Several markers were tentatively identified, that were significantly different among all extracts from chicken muscle tissue stored at room temperature and at 4°C, in the top 50 markers based on the loading values of the PCA. The matching mass spectra can be seen in Appendix I.

Many of these markers have been identified in previous datasets, indicating these markers show potential in being used as an indicator of shelf-life regardless of storage temperature. These include palmitic amide, N-cyclohexanecarbonyltetradecylamine, oleoyl ethyl amide and oleic acid, all of which were found in the external and internal extract comparison of chicken muscle tissue stored at room temperature. The first three of these markers showed an increasing trend over the storage period, and were at a higher concentration in the chicken muscle tissue stored at room temperature compared to at 4°C. This is to be expected as the rate of spoilage is faster at higher temperatures.

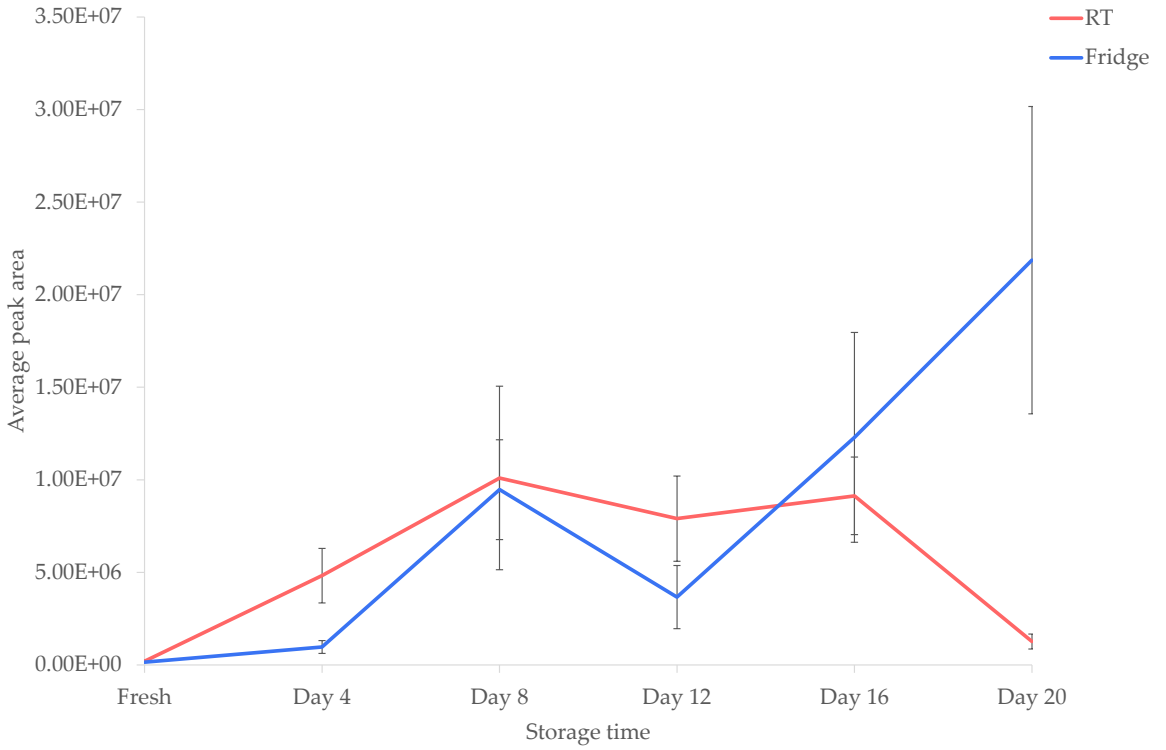

Figure 6.23: Trend of marker tentatively identified as oleic acid that was significantly different among all chicken muscle tissue samples stored at room temperature and 4°C for different lengths of time. Error bars correspond to ± 1 standard deviation

Oleic acid showed a difference in trend between the two temperature conditions, as shown in Figure 6.23. The chicken muscle tissue stored at 4°C showed an overall increase in concentration of oleic acid, however in the chicken muscle tissue stored at room temperature, this marker increased and then decreased. These differing trends could be caused by the rate of spoilage at each of these temperature conditions; meat spoils faster at higher temperatures and so the chicken muscle tissue at room temperature may be further along in the spoilage process where fatty acids like oleic acid have begun to degrade.

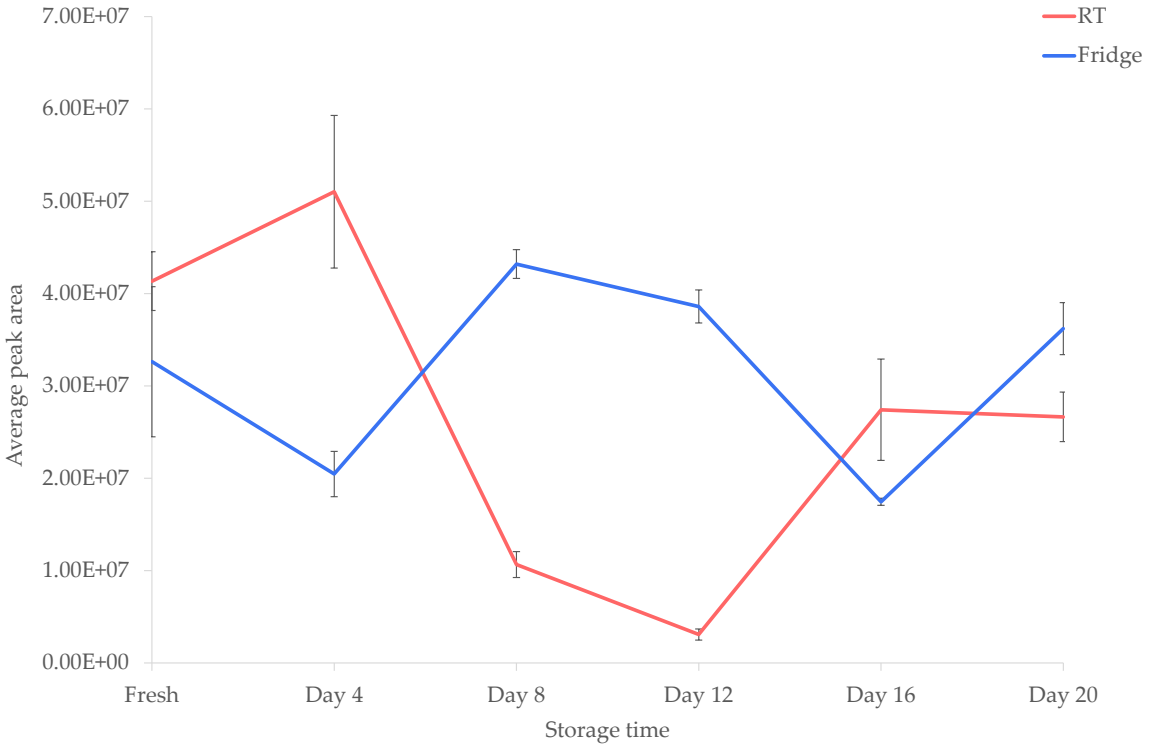

Figure 6.24: Trend of marker tentatively identified as leucine that was significantly different among all chicken muscle tissue samples stored at room temperature and 4°C for different lengths of time. Error bars correspond to ± 1 standard deviation

Markers with an m/z of 132.1020, 284.2941 and 118.0867 have not been previously tentatively identified within this research. The marker that was tentatively identified as leucine had a very interesting trend over the course of the spoilage process, which was very different in the two temperature conditions, as seen in Figure 6.24. In the chicken muscle tissue stored at room temperature, the marker increased at Day 4, then decreased at Day 8 and Day 12, then increased again at Day 16 and maintained concentration up to Day 20. In the chicken muscle tissue stored at 4°C, it was nearly the opposite of what was observed at room temperature; the marker decreased at Day 4, then increased at Day 8 and Day 12, then decreased at Day 16, and increased at Day 20.

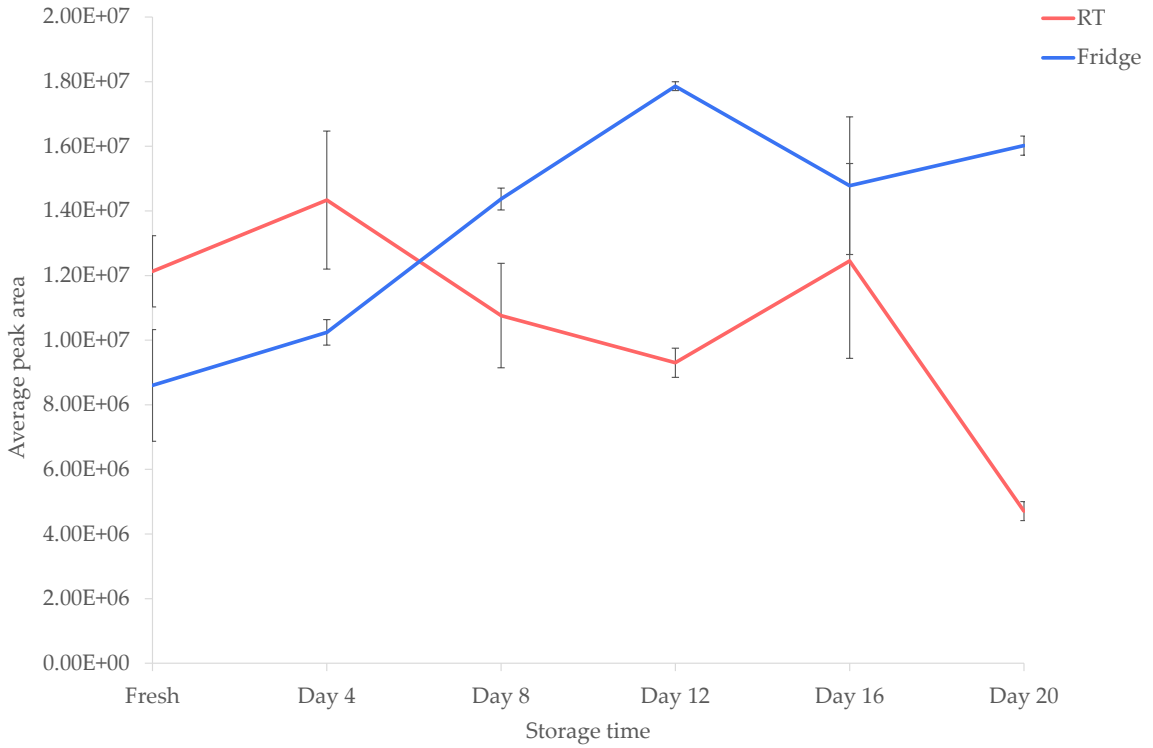

Figure 6.25: Trend of marker tentatively identified as N-methyl-α-aminoisobutyric acid that was significantly different among all chicken muscle tissue samples stored at room temperature and 4°C for different lengths of time. Error bars correspond to ± 1 standard deviation

The marker that was tentatively identified as N-methyl-α-aminoisobutyric acid also showed an interesting trend (Figure 6.25). The concentration increased at Day 4 in both storage temperatures, then at room temperature it decreased until Day 12, while at 4°C it decreased. At Day 16, the marker increased at room temperature but decreased at 4°C, and then finally the marker increased at Day 20 at 4°C and decreased at room temperature. Despite both of these markers showing trends that appear inversely correlated to each other at the two different temperature conditions, this could be caused by the rate of spoilage at each temperature, as previously explained. Both of these compounds are amino acids, which are known to be produced when proteins deteriorate during the biochemical changes that occur postmortem [158]. The trends observed for these markers indicate the mechanisms involved in the spoilage process are very complex. It is imperative to thoroughly understand the mechanisms of markers that are selected for shelf-life determination, as any marker with a complicated trend may cause confusion in the analysis.

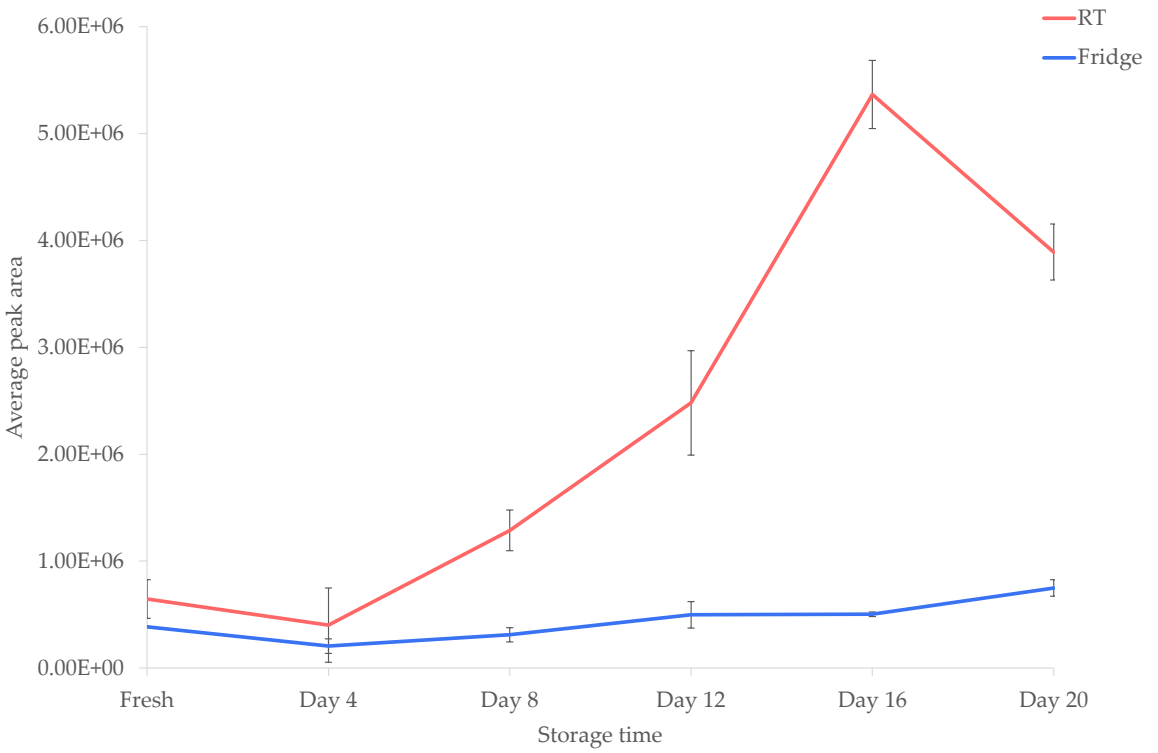

Figure 6.26: Trend of marker tentatively identified as stearamide that was significantly different among all chicken muscle tissue samples stored at room temperature and 4°C for different lengths of time. Error bars correspond to ± 1 standard deviation

The marker with an m/z of 284.2941 was tentatively identified as stearamide, which is an organic acid mostly found in cell membranes. This marker gradually increased in both temperature conditions, however at room temperature the increase was up to Day 16 of the storage period, and then the marker decreased at Day 20. As previously described, cell membranes degrade postmortem due to lipid oxidation, and so the increase in this marker could be caused by this membrane degradation. The decrease at Day 20 in the chicken muscle tissue stored at room temperature could be due to the quicker degradation process at this temperature compared to that at 4°C, where the stearamide has begun to degrade.

6.7.6 Conclusions

Each analytical dataset collected in this work showed reliability in the quality control samples with minimal retention time drift and peak area variability, confirming the data was robust.

Many factors affect the rate of spoilage, however the chicken muscle tissue used in this study was obtained from the same chicken and stored in the same manner prior to being placed in the experimental storage conditions. Therefore, factors that affect the spoilage rate during the handling, transport and storage prior to obtaining the chicken muscle would have been the same for all samples.

When looking at the difference between the external and internal extracts from spoiled meat, the Fresh samples and Day 20 samples showed the least separation in the PCA plots in this research. Fresh samples would not have had the time to spoil and so the difference in metabolic profile in the external and internal extracts would be minimal. The Day 20 samples were extremely spoiled, and so the sampling of the external and internal tissue was difficult to achieve as the consistency had reduced from a solid chicken sample to more of a liquid. This meant that the external and internal samples were difficult to physically separate.

The trends for the markers varied quite a bit between each dataset; the chicken muscle tissue that was stored in the fridge showed markers that decreased, whereas markers in other datasets increased. This is most likely caused by the data mining workflow. Markers are ranked based on their loading value in the principal component that most represented the separation of the groups in the PCA. If the PCA found the biggest difference between the samples to be based on markers that mostly decreased, then these markers would have the highest loading value. As only the top 50 markers were statistically analysed thoroughly, it is possible for only one type of trend to be observed. Using statistical tests to rank the markers is difficult

when investigating a time-based issue, as if one marker is especially different at one specific time point, the p-value from the ANOVA would be very low. Therefore, the top most significant markers may include many that have one specific time point different to the others, instead of finding the markers that gradually increase or decrease over time. This workflow has proven to find markers that are significantly different over the course of the storage period, however more work would be necessary to detect markers that either gradually increase or decrease in each dataset.

Another reason for the increasing trends of markers found in chicken stored at room temperature and the decreasing trend of markers found in chicken stored in the fridge could be because of the difference in rate of spoilage at these two temperatures. Markers that were changing the most and therefore contributing to the separation of the sample types on the PCA scores plots were the increasing ones in the room temperature analyses, and the decreasing ones in the fridge analyses. As the chicken samples would spoil at a faster rate at the higher temperature, the room temperature samples would undergo the same level of degradation as the fridge samples, but at a faster rate and so earlier in the spoilage time period.

Throughout this research, the majority of the markers that were tentatively identified were amides, amino acids and fatty acids. This is in agreement with the literature where it is known that biochemical changes that occur after death mostly affect proteins and lipids due to oxidation.

Future work would include multiple meat samples at each time point, rather than a single meat sample with replicate extracts, in order to get an average spoilage profile throughout the time period. However, this would increase the number of samples involved in the investigation, and would require the development of a shorter chromatographic method to reduce the overall length of the analytical run, or fewer time points would be able to be investigated.

Chapter 7

Conclusions and future work

7.1 Conclusions

This work aimed to address the issues within the food industry, specifically in meat products that are vulnerable to subtle and complex types of fraud. Current methods rely on the information on labels of products, which can be easily manipulated. This research aimed to develop a data processing and statistical workflow, with robust quality control protocols, suitable for untargeted metabonomic studies. This would enhance the understanding of the chemical composition of meat samples, and potentially find markers that could be used to detect fraudulent activities.

The investigation into the detection of dead on arrival chicken in the human food chain found markers that were significantly different in muscle, liver and heart tissue extracts. This research was able to use multivariate statistics to discriminate between DOA and normally slaughtered chicken, which was most successful with heart tissue. A marker in the muscle tissue was identified as sphingosine, and this was found at a lower concentration in the DOA samples. This marker showed potential in being useful in detecting DOA chicken products in the human food chain. A comparison between instruments was made, specifically using an LC coupled with an Agilent Technologies Q-TOF MS and an LC coupled with a Thermo Fisher Scientific Q Exactive Plus. More markers were found to be significantly different when using the Agilent instrument, however one marker was found to be significantly different when using both instruments. This marker was sphingosine, increasing the potential this marker has for being utilised in a targeted assay. The comparison of instruments also showed the methods implemented in this study were robust and transferable.

Multivariate statistics showed great promise in determining the number of freeze-thaw cycles that chicken muscle tissue and lamb liver tissue had undergone. For both tissue types, the PCA showed separation between sample types, and so could be a useful technique in determining if meat has previously been frozen, and potentially how many times. This multivariate technique was also able to differentiate between fresh and frozen chicken tissue and lamb liver tissue when investigating the length of frozen storage. A number of tentative identifications were made in the chicken and lamb tissue during the length of frozen storage experiment. Monoglycerides were found to increase in the chicken muscle tissue, which could be caused by the break down of triglycerides. Acyl carnitines were found to decrease in the lamb muscle tissue, which are compounds involved in the degradation of fatty acids and are integral to the transport of fatty acids across cell membranes. This shows these metabolic pathways could be involved in the changes that occur during frozen storage, and should be investigated further. When investigating the number of freeze-thaw cycles, no tentative identifications were made, however the likely class of compound was able to be determined for several markers. Phosphatidylcholines were found to increase in chicken muscle tissue as the number of freeze-thaw cycles increased, and this same class of compound was found to decrease in the lamb liver tissue. Further research is necessary to understand the complex changes in soft tissue after death, which would further explain the difference in the trend of these compounds between the two tissue types.

The detection of pork, lamb and turkey in minced beef products was achieved in this research. The results demonstrated the potential of using these techniques to identify markers that could discover adulteration in processed meat products. In particular, the adulterated samples made with minced beef with a fat content of 20% showed the best separation on the PCA scores plot, compared to beef with a fat content of 5%. This could indicate that the detection of adulterant meat in meat products could be influenced by the fat content. It was also found that adulteration could be detected

regardless of whether the meat product was raw or cooked. Within this work, the markers of most interest were those that were significantly different in both raw and cooked meat. These markers proved to not be affected by the heating process, and therefore could be more suitable for detecting adulterated meat products that have undergone processing methods.

The last area of the meat industry that was investigated in this work was the metabolic changes that occur during the spoilage of chicken breast tissue. The findings of this research would be beneficial in detecting the shelf-life of chicken meat, especially since the shelf-life date can be vulnerable to manipulation. The differences in metabolic content were very obvious from the start; the TICs showed many differences in peak patterns during the 20 day spoilage period. The principal component analyses showed separation in the majority of sample types without the removal of features that were not statistically significantly different. The majority of the markers that were tentatively identified in this work were amides, amino acids and fatty acids. This is in accordance with previous literature that states the biochemical changes that occur after death mostly involve the oxidation of proteins and lipids.

Overall, this research successfully developed a data processing and statistical workflow that is able to interpret vast metabonomic datasets obtained through liquid chromatography quadrupole time-of-flight mass spectrometry, and reduce the number of features detected down to a manageable number of significantly different markers. The use of quality control samples ensured the data was screened for robustness prior to further statistical analysis for the detection of potential markers. This research has shown the significant possibility to be used in the approach to combat food fraud, and has deepened the understanding of the chemical composition of meat during different storage conditions, and in different species. The identification of sphingosine as a marker for dead on arrival chicken has proved the success of these techniques,

and how they could greatly benefit the development of targeted assays for the detection of food fraud in the future.

7.2 Future work

7.2.1 Analytical considerations

The experimental design throughout this research has shown to produce reliable and robust data. There are, however, a number of factors that should be considered for future work.

The organic extracts were the focus of the analyses within this research, and these were obtained from a two-step metabolite extraction that also produced aqueous extracts. Due to the available instrument time, the aqueous extracts were not successfully analysed, despite some method development on these samples. Further time spent on developing a chromatographic method could enable these aqueous samples to be analysed, with the potential of discovering more markers of interest.

Only one type of chromatographic column was used throughout this work, which was selected as it was the most suitable type of column for initial untargeted analyses. The experiments presented in this work could be repeated using multiple columns with stationary phases of different chemical properties, which would allow for a greater marker coverage. In this work, only positive ionisation was used to detect compounds, except for in the investigation of dead on arrival chicken in Chapter 3. Analysing the extracts in negative ionisation mode in addition to positive would further increase the number of compounds detected. Furthermore, investigating alternative metabolite extraction methods could provide a complementary approach to the current extraction process, and increase the number of metabolites analysed.

Prior to the metabolite extraction, tissue samples were homogenised by hand with small surgical scissors. This was sufficient for small samples weighing approximately 100 mg, however in parts of this research it would have been more beneficial to take a more holistic approach and homogenise the whole sample. For example, in the experiment with adulterated meat, the ability to homogenise the whole meatball would ensure the percentage of adulterant meat was accurate in the tissue sample used in the metabolite extraction.

Throughout this research, only one marker was identified and confirmed with a chemical standard. Despite many other markers being tentatively identified, the confirmation of these identifications could not be carried out during this project. It is a known issue within metabonomic research that the identification of markers is an extremely difficult challenge. Many compounds are not available to purchase as a standard, and many significant features are not able to provide a predicted formula and therefore it is difficult to know which standard to buy even if it is available. It is essential that this problem is addressed within the metabonomic research area, especially for untargeted studies that aim to gain an overall global approach and are not looking for specific compounds.

7.2.2 Continuation of research

This research was successful in identifying sphingosine as a marker for dead on arrival chicken muscle. This experiment, however, had a very small sample size. A larger scale study involving a targeted approach for the detection of sphingosine in chicken muscle would aid in the validation of this compound as a marker for dead on arrival meat. This targeted approach could also search for compounds that are known to be involved in the same metabolic pathway as sphingosine, to see if the concentration of these compounds also differ between normally slaughtered and dead on arrival chicken meat. Sphingosine is known to be involved in the stress response, and so

searching for other compounds that are known to be involved in this stress response could provide additional markers for this kind of subtle fraud.

The length of frozen storage was investigated using chicken muscle, lamb muscle and lamb liver tissue. It would be interesting to see if the trends observed in this research were the same in other species and types of tissue. A greater sample size for each of these meat samples would also confirm the significance of the markers detected in these preliminary studies. Furthermore, the U.S. Food and Drug Administration give guidance on the recommended length of time certain food products should be stored in the freezer to maintain quality. There are differences in storage times based on whether the food is cooked or not prior to being stored in the freezer. It would be interesting to conduct experiments to investigate the differences between raw and cooked meat during frozen storage. It would also be beneficial to extend the frozen storage duration from 10 weeks to up to 12 months, as the recommended frozen storage time for some meat products is 12 months.

The adulteration of beef products with undeclared horsemeat has been a major concern in recent years, and therefore repeating this experiment with horsemeat as the adulterant would help combat this fraud. The application of DNA-based techniques enabled the discovery of the large scale adulteration of beef products in 2013, however the techniques within this research may provide a quicker and more cost effective method of ensuring the meat industry remains safe and is not subjected to more adulteration issues. The meatballs in this adulteration experiment were formed manually by accurately weighing out the minced meat and mixing together by hand, to create meatballs with the required percentage of adulterant meat. However, the sample for extraction was a very small portion of approximately 110 mg that may not have contained the accurate percentage of adulterant meat. Homogenising the whole meatball and acquiring the sample for extraction from this would ensure the data was representative of the expected percentage of adulteration.

An additional experiment that could aid in the detection of illegal adulteration in the food industry would involve the adulteration of processed meat products with the same species of meat. EU legislation [117] states that when minced meat products are prepared, only skeletal muscle must be used, and must not include mechanically separated meat (MSM), or any bone fragments or skin. MSM is any meat that is removed from bones after boning, with the use of mechanical instruments, that modifies the muscle fibre structure. Two studies could be conducted in order to investigate adulteration of minced beef that is illegal according to this legislation; the adulteration of minced beef with non-skeletal beef tissue, such as liver or kidney tissue, and the adulteration of minced beef with MSM. These types of adulteration are a lot more subtle than adulterating with different species of meat, and this research would ascertain the benefits these techniques have for food fraud issues with a higher level of complexity.

The investigation into the metabolic content of spoiled meat focussed on chicken muscle tissue. This experiment used small portions of chicken breast that had been allowed to spoil at different temperatures. In a real-life setting, it would be more likely for a whole chicken breast to be stored before consuming, and so this experiment would be useful to repeat with whole chicken breasts. Chicken meat has a shorter spoilage time than other meat products, and is more readily available so was useful in this initial untargeted analysis, however the spoilage status and shelf-life of meat is very much dependent on the species of meat in question. Therefore, it would be necessary to repeat this experiment with other species of meat, such as beef or pork, in order to get specific spoilage profiles of these meat types.

7.2.3 Future areas of interest

The acquisition of suitable samples to investigate the slaughter method proved to be very difficult due to the ethical and moral issues associated with certain slaughter processes. Creating a partnership with food authorities and processing plants was unsuccessful during the time this research was carried out. Gaining the confidence of a processing plant would enable the investigation of the slaughter method so that specific frauds within this area of the meat industry could be investigated. In particular, the metabolic profile of halal and nonhalal meat products could be researched to aid in the authentication of these products that at present can only be checked based on the paperwork and labels. This would allow consumers to have confidence in their purchase choices, whether for religious or moral reasons.

Another area within the meat industry that could be examined using these techniques could be the ageing of beef. Beef products have a higher price associated with them based on the length of time they have been aged for. A method for authenticating this duration of ageing would combat against this kind of fraud.

These analytical techniques coupled with the data processing and statistical workflow have proven to be successful in differentiating between very similar sample groups, and discovering compounds that could be used as markers to detect fraud within the meat industry. The application of these techniques to other issues within the food industry will further show the usefulness of these methods.

References

[1] C. Elliott, "Elliott review into the integrity and assurance of food supply networks interim report," 2013.

[2] D. C. Moyer, J. W. DeVries, and J. Spink, "The economics of a food fraud incident - case studies and examples including melamine in wheat gluten," *Food Control*, vol. 71, pp. 358–364, 2017.

[3] M. Esteki, Z. Shahsavari, and J. Simal-Gandara, "Use of spectroscopic methods in combination with linear discriminant analysis for authentication of food products," *Food Control*, vol. 91, pp. 100–112, 2018.

[4] J. Moore, J. Spink, and M. Lipp, "Development and application of a database of food ingredient fraud and economically motivated adulteration from 1980-2010," *Journal of Food Science*, vol. 77, pp. 118–156, 2012.

[5] H. N. Lubis, N. F. Mohd-Naim, N. N. Alizul, and M. U. Ahmed, "From marker to food plate: Current trusted technology and innovations in halal food analysis," *Trends in Food Science & Technology*, vol. 58, pp. 55–68, 2016.

[6] J. Premanandh, "Horse meat scandal - a wake up call for regulatory authorities," *Food Control*, vol. 34, pp. 568–569, 2013.

[7] B. Bates, C. Roberts, H. Lepps, and L. Porter, "The Food & You Survey Wave 4." Combined report for England, Wales and Northern Ireland, 2014.

[8] R. Evershed and N. Temple, *Sorting the beef from the bull. The science of food fraud forensics*. London, UK: Bloomsbury Publishing Plc, 2016.

[9] Joint Research Centre for European Commission, *Monthly summary of articles of food fraud and adulteration*, 2018 (accessed July 20, 2018). https://ec.europa.eu/jrc/en/food-fraud-and-quality/monthly-summary-articles.

[10] E. Y. Y. Chan, S. M. Griffiths, and C. W. Chan, "Public-health risks of melamine in milk products," *The Lancet*, vol. 372, pp. 1444–1445, 2008.

[11] X. Pei, A. Tandon, A. Alldrick, L. Giorgi, W. Huang, and R. Yang, "The China melamine milk scandal and its implications for food safety," *Food Policy*, vol. 36, pp. 412–420, 2011.

[12] G. P. Danezis, A. S. Tsagkaris, F. Camin, V. Brusic, and C. A. Georgiou, "Food authentication: techniques, trends & emerging approaches," *Trends in Analytical Chemistry*, vol. 85, pp. 123–132, 2016.

[13] M. Woolfe and S. Primrose, "Food forensics: using DNA technology to combat misdescription and fraud," *TRENDS in Biotechnology*, vol. 22, pp. 222–226, 2004.

[14] R. Korte and J. Brockmeyer, "Novel mass spectrometry approaches in food proteomics," *Trends in Analytical Chemistry*, vol. 96, pp. 99–106, 2017.

[15] L. M. Reid, C. P. O'Donnell, and G. Downey, "Recent technological advances for the determination of food authenticity," *Trends in Food Science & Technology*, vol. 17, pp. 344–353, 2006.

[16] M. C. Díaz-García, J. M. Obón, M. R. Castella, J. Collado, and M. Alacid, "Quantification by UHPLC of total individual polyphenols in fruit juice," *Food Chemistry*, vol. 138, pp. 938–949, 2013.

[17] "Council Regulation (EEC) No 2081/92 of 14 July 1992 on the protection of geographical indications and designations of origin for agricultural products and foodstuffs."

[18] S. Kelly, K. Heaton, and J. Hoogewerff, "Tracing the geographical origin of food: The application of multi-element and multi-isotope analysis," *Trends in Food Science & Technology*, vol. 16, pp. 555–567, 2005.

[19] D. M. A. M. Luykx and S. M. van Ruth, "An overview of analytical methods for determining geographical origin of food products," *Food Chemistry*, vol. 107, pp. 897–911, 2008.

[20] A. Faberi, D. Compagnone, F. Fuselli, A. L. Mantia, M. Mascini, C. Montesano, R. Rocchi, and M. Sergi, "Italian cheeses discrimination by means of δ^{13}C and δ^{15}N isotopic ratio mass spectrometry," *Food Analytical Methods*, vol. 11, pp. 1467–1475, 2017.

[21] K. Ariyama, Y. Aoyama, A. Mochizuki, Y. Homura, M. Kadokura, and A. Yasui, "Determination of the geographical origin of onions between three main production areas in Japan and other countries by mineral composition," *Journal of Agricultural and Food Chemistry*, vol. 55, pp. 347–354, 2007.

[22] I. Giovannacci, C. Guizard, M. Carlier, V. Duval, J. L. Martin, and C. Demeulemester, "Species identification of meat products by ELISA," *International Journal of Food Science and Technology*, vol. 39, pp. 863–867, 2004.

[23] M. A. Sentandreu and E. Sentandreu, "Authenticity of meat products: Tools against fraud," *Food Research International*, vol. 60, pp. 19–29, 2014.

[24] R. B. Petronijević, B. Velebit, and T. Baltić, "Shedding light on food fraud: spectrophotometric and spectroscopic methods as a tool against economically motivated adulteration of food," *IOP Conference Series: Earth and Environmental Science*, vol. 85, pp. 1–6, 2017.

[25] H.-D. Belitz and W. Grosch, *Food Chemistry.* Heidelberg, Germany: Springer-Verlag Berlin Heidelberg New York, second ed., 1999.

[26] C. L. Stanfield and W. J. Germann, *Principles of human physiology.* San Francisco, USA: Pearson Benjamin Cummings, third ed., 2007.

[27] R. Warner, "Meat: Conversion of muscle to meat," in *The Encyclopedia of Food and Health* (B. Caballero, P. Finglas, and F. Toldrá, eds.), pp. 677–684, Academic Press.

[28] A. D'Alessandro and L. Zolla, "Meat science: From proteomics to integrated omics towards system biology," *Journal of Proteomics*, vol. 78, pp. 558–577, 2013.

[29] B. O. Alao, A. B. Falowo, A. Chulayo, and V. Muchenje, "The potential of animal by-products in food systems: Production, prospects and challenges," *Sustainability*, vol. 9, pp. 1–18, 2017.

[30] P. N. Seong, S. H. Cho, K. M. Park, G. H. Kang, B. Y. Park, S. S. Moon, and H. V. Ba, "Characterization of chicken by-products by mean of proximate and nutritional compositions," *Korean Journal for Food Science of Animal Resources*, vol. 2, pp. 179–188, 2015.

[31] P. C. Boisteanu, M. G. Usturoi, R. Lazar, and B. V. Avararei, "Changes of poultry meat chemical composition, in relationship with lighting schedule," *International Scholarly and Scientific Research & Innovation*, vol. 4, pp. 311–315, 2010.

[32] W. B. Dunn and D. I. Ellis, "Metabolomics: Current analytical platforms and methodologies," *Trends in Analytical Chemistry*, vol. 24, pp. 285–294, 2005.

[33] J. K. Nicholson, J. C. Lindon, and E. Holmes, "Metabonomics: understanding the metabolic responses of living systems to pathophysiological stimuli via multivariate statistical analysis of biological NMR spectroscopic data," *Xenobiotica*, vol. 29, pp. 1181–1189, 1999.

[34] J. C. Lindon, E. Holmes, and J. K. Nicholson, "So what's the deal with metabonomics," *Analytical Chemistry*, vol. 75, pp. 384–391, 2003.

[35] D. W. Cook and S. C. Rutan, "Chemometrics for the analysis of chromatographic data in metabolomics investigations," *Journal of Chemometrics*, vol. 28, pp. 681–687, 2014.

[36] J. K. Nicholson and J. C. Lindon, "Metabonomics," *Nature*, vol. 455, pp. 1054–1056, 2008.

[37] P. Masson, A. C. Alves, T. M. D. Ebbels, J. K. Nicholson, and E. J. Want, "Optimization and evaluation of metabolite extraction protocols for untargeted metabolic profiling of liver samples by UPLC-MS," *Analytical Chemistry*, vol. 82, pp. 7779–7786, 2010.

[38] S. P. Putri, Y. Nakayama, F. Matsuda, T. Uchikata, S. Kobayashi, A. Matsubara, and E. Fukusaki, "Current metabolomics: Practical applications," *Journal of Bioscience and Bioengineering*, vol. 115, pp. 579–589, 2013.

[39] C. Ke, Y. Hou, H. Zhang, L. Fan, T. Ge, B. Guo, F. Zhang, K. Yang, J. Wang, G. Loou, and K. Li, "Large-scale profiling of metabolic dysregulation in ovarian cancer," *International Journal of Cancer*, vol. 136, pp. 516–526, 2014.

[40] J. T. Brindle, H. Antti, E. Holmes, G. Tranter, J. K. Nicholson, H. W. L. Bethell, S. Clarke, P. M. Schofield, E. McKilligin, D. E. Mosedale, and D. J. Grainger, "Rapid and noninvasive diagnosis of the presence and severity of coronary heart disease using ^{1}H-NMR-based metabonomics," *Nature Medicine*, vol. 8, pp. 1439–1444, 2002.

[41] S. Rezzi, Z. Ramadan, L. B. Fay, and S. Kochlar, "Nutritional metabonomics: applications and perspectives," *Journal of Proteome Research*, vol. 6, pp. 513–525, 2006.

[42] D. Wishart, "Metabolomics: applications to food science and nutrition research," *Trends in Food Science and Technology*, vol. 19, pp. 482–493, 2008.

[43] J. G. Bundy, M. P. Davey, and M. R. Viant, "Environmental metabolomics: a critical review and future perspectives," *Metabolomics*, vol. 5, pp. 3–21, 2009.

[44] L. M. Samuelsson, L. Forlin, G. Karlsson, M. Adolfsson-Erici, and D. G. J. Larsson, "Using NMR metabolomics to identify responses of an environmental estrogen in blood plasma of fish," *Aquatic Toxicology*, vol. 78, pp. 341–349, 2006.

[45] C. Guy, F. Kaplan, J. Kopka, J. Selbig, and D. K. Hincha, "Metabolomics of temperature stress," *Physiologia Plantarum*, vol. 132, pp. 220–235, 2008.

[46] D. G. Robertson, M. D. Reily, R. E. Sigler, D. F. Wells, D. A. Paterson, and T. K. Braden, "Metabonomics: Evaluation of nuclear magnetic resonance (NMR) and pattern recognition technology for rapid *in vivo* screening of liver and kidney toxicants," *Toxicological Sciences*, vol. 57, pp. 326–337, 2000.

[47] W. Mattes, K. David, E. Fabian, J. Greenhaw, M. Herold, R. Looser, W. Mellert, S. Groeters, H. Marxfield, N. Moeller, G. Montoya-Parra, A. Prokoudine, B. van Ravenzwaay, V. Strauss, T. Walk, and H. Kamp, "Detection of hepatotoxicity potential with metabolite profiling (metabolomics) of rat plasma," *Toxicology Letters*, vol. 230, pp. 467–478, 2014.

[48] D. G. Robertson, "Metabonomics in toxicology: A review," *Toxicological Sciences*, vol. 85, pp. 809–822, 2005.

[49] J. K. Nicholson, M. J. Buckingham, and P. J. Sadler, "High resolution ^{1}H n.m.r. studies of vertebrate blood and plasma," *Biochemical Journal*, vol. 211, pp. 605–615, 1983.

[50] O. Beckonert, H. C. Keun, T. M. D. Ebbels, J. Bundy, E. Holmes, J. C. Lindon, and J. K. Nicholson, "Metabolic profiling, metabolomic and metabonomic procedures for NMR spectroscopy of urine, plasma, serum and tissue extracts," *Nature Protocols*, vol. 2, pp. 2692–2703, 2007.

[51] I. D. Wilson, R. Plumb, J. Granger, H. Major, R. Williams, and E. M. Lenz, "HPLC-MS-based methods for the study of metabonomics," *Journal of Chromatography*, vol. 817, pp. 67–76, 2005.

[52] X. Lu, X. Zhao, C. Bai, C. Zhao, G. Lu, and G. Xu, "LC-MS-based metabonomics analysis," *Journal of Chromatography*, vol. 866, pp. 64–76, 2008.

[53] S. Tyagi, Raghvendra, U. Singh, T. Kalra, and K. Munjal, "Applications of metabolomics - a systematic study of the unique chemical fingerprints: An overview," *International Journal of Pharmaceutical Sciences Review and Research*, vol. 3, pp. 83–86, 2010.

[54] J. M. Cevallos-Cevallos, J. I. Reyes-De-Corcuera, E. Etxeberria, M. D. Danyluk, and G. E. Rodrick, "Metabolomic analysis in food science: a review," *Trends in Food Science and Technology*, vol. 20, pp. 557–566, 2009.

[55] E. Cubero-Leon, R. Peñalver, and A. Maquet, "Review on metabolomics for food authentication," *Food Research International*, vol. 60, pp. 95–107, 2014.

[56] Z. Jandrić, D. Roberts, M. N. Rathor, A. Abrahim, M. Islam, and A. Cannavan, "Assessment of fruit juice authenticity using UPLC-QToF MS; a metabolomics approach," *Food Chemistry*, vol. 148, pp. 7–17, 2014.

[57] S. Esslinger, J. Reidl, and C. Fauhl-Hassek, "Potential and limitations of non-targeted fingerprinting for authentication of food in official control," *Food Research International*, vol. 60, pp. 189–204, 2014.

[58] R. Diaz, O. J. Pozo, J. V. Sancho, and F. Hernandez, "Metabolomic approaches for orange origin discrimination by ultra-high performance liquid chromatography coupled to quadrupole time-of-flight mass spectrometry," *Food Chemistry*, vol. 157, pp. 84–93, 2014.

[59] N. Z. Ballin, "Authentication of meat and meat products," *Meat Science*, vol. 86, pp. 577–587, 2010.

[60] Y. Jung, J. Lee, J. Kwon, K. S. Lee, D. H. Ryu, and G. S. Hwang, "Discrimination of the geographical origin of beef by ^{1}H NMR-based metabolomics," *Journal of Agricultural and Food Chemistry*, vol. 158, pp. 10458–10466, 2010.

[61] I. Suroweic, P. D. Fraser, R. Patel, J. Halket, and P. M. Bramley, "Metabolomic approach for the detection of mechanically recovered meat in food products," *Food Chemistry*, vol. 125, pp. 1468–1475, 2011.

[62] F. Rouessac and A. Rouessac, *Chemical analysis - Modern instrumentation methods and techniques*. Chichester, England: John Wiley & Sons Ltd., 2000.

[63] V. R. Meyer, *Practical high-performance liquid chromatography.* Chichester, England: John Wiley & Sons Ltd., 2010.

[64] S. Bayne and M. Carlin, *Forensic applications of high performance liquid chromatography.* Boca Raton, Florida: CRC Press, 2010.

[65] M. Wilm, "Principles of electrospray ionization," *Molecular and Cellular Proteomics*, vol. 10, pp. 1–7, 2011.

[66] S. Banerjee and S. Mazumdar, "Electrospray ionization mass spectrometry: a technique to access the information beyond the molecular weight of the analyte," *International Journal of Analytical Chemistry*, vol. 2012, pp. 1–40, 2012.

[67] C. S. Ho, C. W. K. Lam, M. H. M. Chan, R. C. K. Cheung, L. K. Law, L. C. W. Lit, K. F. Ng, M. W. M. Suen, and H. L. Tai, "Electrospray ionisation mass spectrometry: Principles and clinical applications," *The Clinical Biochemists Reviews*, vol. 24, pp. 3–12, 2003.

[68] E. de Hoffman and V. Stroobant, *Mass Spectrometry: Principles and Applications.* Chichester, England: John Wiley & Sons Ltd., third ed., 2007.

[69] A. Kruve and K. Kaupmees, "Adducts formation in ESI/MS by mobile phase additives," *Journal of the American Society for Mass Spectrometry*, vol. 28, pp. 887–894, 2017.

[70] R. A. Zubarev and A. Makarov, "Orbitrap mass spectrometry," *Analytical Chemistry*, vol. 85, pp. 5288–5296, 2013.

[71] Q. Hu, R. J. Noll, H. Li, A. Makarov, M. Hardman, and R. G. Cooks, "The orbitrap: a new mass spectrometer," *Journal of Mass Spectrometry*, vol. 40, pp. 430–443, 2005.

[72] R. H. Perry, R. G. Cooks, and R. J. Noll, "Orbitrap mass spectrometry: instrumentation, ion motion and applications," *Mass Spectrometry Reviews*, vol. 27, pp. 661–699, 2008.

[73] B. A. Mamyrin, "Time-of-flight mass spectrometry (concepts, achievements, and prospects)," *International Journal of Mass Spectrometry*, vol. 206, pp. 251–266, 2001.

[74] Thermo Fisher Scientific, "Thermo Fisher Scientific Q Exactive Plus Orbitrap LC-MS/MS System." Product Specification, 2016.

[75] E. J. Want, I. D. Wilson, H. Gika, G. Theodoridis, R. S. Plumb, J. Shockcor, E. Holmes, and J. K. Nicholson, "Global metabolite profiling procedures for urine using UPLC-MS," *Nature Protocols*, vol. 5, pp. 1005–1018, 2010.

[76] E. Zelena, W. B. Dun, D. Broadhurst, S. Francis-McIntyre, K. M. Carroll, P. Begley, S. O'Hagan, J. D. Knowles, A. Halsall, I. D. Wilson, and D. B. Kell, "Development of a robust and repeatable UPLC-MS method for the long-term metabolomic study of human serum," *Analytical Chemistry*, vol. 81, pp. 1357–1364, 2009.

[77] T. Sangster, H. Major, R. Plumb, A. J. Wilson, and I. D. Wilson, "A pragmatic and readily implemented quality control strategy for HPLC-MS and GC-MS-based metabonomic analysis," *Analyst*, vol. 131, pp. 1075–1078, 2006.

[78] E. J. Want, P. Masson, F. Michopoulos, I. D. Wilson, G. Theodoridis, R. S. Plumb, J. Shockcor, N. Loftus, E. Holmes, and J. K. Nicholson, "Global metabolic profiling of animal and human tissues via UPLC-MS," *Nature Protocols*, vol. 8, pp. 17–32, 2013.

[79] L. Lai, F. Michopoulos, H. Gika, G. Theodoridis, R. W. Wilkinson, R. Odedra, J. Wingate, R. Bonner, S. Tate, and I. D. Wilson, "Methodological considerations in the development of HPLC-MS methods for the analysis of rodent plasma for metabonomic studies," *Molecular Biosystems*, vol. 6, pp. 108–120, 2010.

[80] F. Michopoulos, L. Lai, H. Gika, G. Theodoridis, and I. Wilson, "UPLC-MS-based analysis of human plasma for metabonomics using solvent precipitation

or solid phase extraction," *Journal of Proteome Research*, vol. 8, pp. 2114–2121, 2009.

[81] X. Shen, X. Gong, Y. Cai, Y. Guo, J. Tu, H. Li, T. Zhang, J. Wang, F. Zue, and Z.-J. Zhu, "Normalization and integration of large-scale metabolomics data using support vector regression," *Metabolomics*, vol. 12, pp. 1–12, 2016.

[82] K. A. Veselkov, L. K. Vingara, P. Masson, S. L. Robinette, E. Want, J. V. Li, R. H. Barton, C. Boursier-Neyret, B. Walther, T. M. Ebbels, I. Pelczer, E. Holmes, J. C. Lindon, and J. K. Nicholson, "Optimized preprocessing of ultra-performance liquid chromatography/mass spectrometry urinary metabolic profiles for improved information recovery," *Analytical Chemistry*, vol. 83, pp. 5864–5872, 2011.

[83] H. P. Benton, J. Ivanisevic, N. G. Mahieu, M. E. Kurczy, C. H. Johnson, L. Franco, D. Rinehart, E. Valentine, H. Gowda, B. K. Ubhi, R. Tautenhahn, A. Gieschen, M. W. Fields, G. J. Patti, and G. Siuzdak, "Autonomous metabolomics for rapid metabolite identification in global profiling," *Analytical Chemistry*, vol. 87, pp. 884–891, 2015.

[84] R. Tautenhahn, G. J. Patti, D. Rinehart, and G. Suizdak, "XCMS online: A web-based platform to process untargeted metabolomic data," *Analytical Chemistry*, vol. 84, pp. 5035–5039, 2012.

[85] R. G. Brereton, *Chemometrics, Data Analysis for the Laboratory and Chemical Plant*. Chichester, England: John Wiley & Sons Ltd., 2003.

[86] C. Adam, *Essential Mathematics and Statistics for Forensic Science*. Chichester, England: John Wiley & Sons Ltd., 2010.

[87] R. Ennos, *Statistical and data handling skills in biology*. Harlow, England: Pearson Education Limited, third ed., 2012.

[88] S. L. R. Ellison, V. J. Barwick, and T. J. D. Farrant, *Practical Statistics for the Analytical Scientist: A Bench Guide*. Cambridge, England: The Royal Society of Chemistry, second ed., 2009.

[89] S.-L. Jan and G. Shieh, "Sample size determinations for Welch's test in one-way heteroscedastic ANOVA," *British Journal of Mathematical and Statistical Psychology*, vol. 67, pp. 72–93, 2014.

[90] G. A. Theodoridis, H. G. Gika, E. J. Want, and I. D. Wilson, "Liquid chromatography-mass spectrometry based global metabolite profiling: a review," *Analytica Chimica Acta*, vol. 711, pp. 7–16, 2012.

[91] S. D. Brown, S. T. Sum, and F. Despagne, "Chemometrics," *Analytical Chemistry*, vol. 68, pp. 21R–61R, 1996.

[92] R. G. Brereton, *Applied Chemometrics for Scientists*. Chichester, England: John Wiley & Sons Ltd., 2007.

[93] J. N. Miller and J. C. Miller, *Statistics and Chemometrics for Analytical Chemistry*. Harlow, England: Pearson Education Limited, sixth ed., 2010.

[94] F. Marini, *Chemometrics in Food Chemistry*. Oxford, UK: Elsevier, first ed., 2013.

[95] W. B. Dunn, D. I. Broadhurst, H. J. Atherton, R. Goodacre, and J. L. Griffin, "Systems level studies of mammalian metabolomes: the roles of mass spectrometry and nuclear magnetic resonance spectroscopy," *Chemical Society Reviews*, vol. 40, pp. 387–426, 2011.

[96] L. W. Sumner, A. Amberg, D. Barrett, M. H. Beale, R. Beger, C. A. Daykin, T. W.-M. Fan, O. Fiehn, R. Goodacre, J. L. Griffin, T. Hankemeier, N. Hardy, J. Harnly, R. Higashu, J. Kopka, A. N. Lane, J. C. Lindon, P. Marriott, A. W. Nicholls, M. D. Reily, J. J. Thaden, and M. R. Viant, "Proposed minimum reporting standards for chemical analysis: Chemical analysis working

group (CAWG) metabolomics standards initiative (MSI)," *Metabolomics*, vol. 3, pp. 211–221, 2007.

[97] T. R. Sana, J. C. Roark, X. Li, K. Waddell, and S. M. Fischer, "Molecular formula and METLIN personal metabolite database matching applied to the identification of compounds generated by LC/TOF-MS," *Journal of Biomolecular Techniques*, vol. 19, pp. 258–266, 2008.

[98] K. L. Sidwick, A. E. Johnson, C. D. Adam, L. Pereira, and D. F. Thompson, "Use of liquid chromatography quadrupole time-of-fight mass spectrometry and metabonomic profiling to differentiate between normally slaughtered and dead on arrival poultry meat," *Analytical Chemistry*, vol. 89, pp. 12131–12136, 2017.

[99] "Statutory instruments 2013, no. 2952. Public Health, England, The Animal By-Products (Enforcement) (England) Regulations." Part III, Paragraph 3b and 4, pp. 6.

[100] The Bureau of Investigative Journalism, "Why a million chickens are dying on the way to the abattoir." Available at https://www.gov.uk/government/statistics/agriculture-in-the-united-kingdom-2016.

[101] E&W Poultry Slaughterhouse Survey DAERA and RESAS, February 2018, "UK poultry slaughterings, weights and poultry meat production - monthly dataset." Available at https://www.gov.uk/government/statistics/poultry-and-poultry-meat-statistics.

[102] National Statistics, "Agriculture in the United Kingdom 2016." Available at https://www.gov.uk/government/statistics/agriculture-in-the-united-kingdom-2016.

[103] A. H. Nilipour and G. Melo, "Poultry in transit are a cause for concern," *World Poultry*, vol. 18, pp. 30–32, 2002.

[104] E. Nijdam, A. R. M. Zailan, J. H. H. van Eck, E. Decuypere, and J. A. Stegeman, "Pathological features in dead on arrival broilers with special reference to heart disorders," *Poultry Science*, vol. 85, pp. 1303–1308, 2006.

[105] V. P. Lund, N. C. Kyvsgaard, J. P. Christensen, and M. Bisgaard, "Pathological manifestations observed in dead-on-arrival broilers at a danish abattoir," *British Poultry Science*, vol. 54, pp. 430–440, 2013.

[106] J. Amendt, C. P. Campobasso, E. Gaudry, C. Reiter, H. N. LeBlanc, and M. J. R. Hall, "Best practice in forensic entomology - standards and guidelines," *International Journal of Legal Medicine*, vol. 121, pp. 90–104, 2007.

[107] A. Donaldson and I. Lamont, "Biochemistry changes that occur after death: potential markers for determining post-mortem interval," *PLoS ONE*, vol. 8, pp. 1–10, 2013.

[108] A. Donaldson and I. Lamont, "Estimation of post-mortem interval using biochemical markers," *Australian Journal of Forensic Sciences*, vol. 46, pp. 8–26, 2014.

[109] O. Cuvillier, "Sphingosine in apoptosis signaling," *Biochimica et Biophysica Acta*, vol. 1585, pp. 153–162, 2002.

[110] J. Woodcock, "Sphingosine and ceramide signalling in apoptosis," *IUBMB Life*, vol. 58, pp. 462–466, 2006.

[111] S. Spiegel and S. Milstien, "Sphingosine-1-phosphate: signaling inside and out," *FEBS letters*, vol. 476, pp. 55–57, 2000.

[112] M. Maceyka and S. Spiegel, "Sphingolipid metabolites in inflammatory disease," *Nature*, vol. 510, pp. 58–67, 2014.

[113] C. R. Gault, L. M. Obeid, and Y. A. Hannun, "An overview of sphingolipid metabolism: from synthesis to breakdown," *Advances in Experimental Medicine and Biology*, vol. 688, pp. 1–23, 2010.

[114] T. Levade, S. Malagarie-Cazenave, V. Gouazé, B. Ségui, C. Tardy, S. Betito, N. Andrieu-Abadie, and O. Cuvillier, "Ceramide in apoptosis: A revisited role," *Neurochemical Research*, vol. 27, pp. 601–607, 2002.

[115] "Statutory Instruments, No. 539. The Fresh Meat (Hygiene and Inspection) Regulations 1995." Schedule 15, Paragraph 1d, pp. 61.

[116] "Council Regulation (EC) No 1234/2007 of 22 October 2007 establishing a common organisation of agricultural markets and on specific provisions for certain agricultural products (Single CMO Regulations)." Annex XIV, Section B, Chapter III, pp. L99/111.

[117] "Regulation (EC) No 853/2004 of the European Parliament and of the Council of 29 April 2004 laying down specific hygiene rules for food of animal origin." Annex III, Section V, Chapter II, pp. L226/53.

[118] T. Chen, Y. Zhu, P. Wang, M. Han, R. Wei, X. Xu, and G. Zhou, "The use of the impedance measurements to distinguish between fresh and frozen-thawed chicken breast muscle," *Meat Science*, vol. 116, pp. 151–157, 2016.

[119] C. N. Aroeira, R. A. T. Filho, P. R. Fontes, L. A. M. Gomide, A. L. S. Ramos, M. M. Ladeira, and E. M. Ramos, "Freezing, thawing and aging effects on beef tenderness from *bos indicus* and *bos taurus* cattle," *Meat Science*, vol. 116, pp. 118–125, 2016.

[120] J. Choe, A. Stuart, and Y. H. B. Kim, "Effect of different aging temperatures prior to freezing on meat quality attributes of frozen/thawed lamb loins," *Meat Science*, vol. 116, pp. 158–164, 2016.

[121] T. Grunert, R. Stephan, M. Ehling-Schulz, and S. Johler, "Fourier transform infrared spectroscopy enables rapid differentiation of fresh and frozen/thawed chicken," *Food Control*, vol. 60, pp. 361–364, 2016.

[122] S. Ali, W. Zhang, N. Rajput, M. A. Khan, C. Li, and G. Zhou, "Effect of multiple freeze-thaw cycles on the quality of chicken breast meat," *Food Chemistry*, vol. 173, pp. 808–814, 2015.

[123] S. Elahi, P. Lawrence, J. Topping, S. Ellison, and M. Woolfe, "Poultry marketing controls - inter-laboratory validation of a method to detect previously frozen chicken breasts by determination of HADH activity," *Food Control*, vol. 68, pp. 186–191, 2016.

[124] M. N. Lund, M. Heinonen, C. P. Baron, and M. Estévez, "Protein oxidation in muscle foods: A review," *Molecular Nutrition & Food Research*, vol. 55, pp. 83–95, 2011.

[125] W. Zhang, S. Xiao, and D. U. Ahn, "Protein oxidation: Basic principles and implications for meat quality," *Critical Reviews in Food Science and Nutrition*, vol. 53, pp. 1191–1201, 2013.

[126] J. O. Igene, A. M. Pearson, R. A. Merkel, and T. H. Coleman, "Effect of frozen storage time, cooking and holding temperature upon extractable lipids and TBA values of beef and chicken," *Journal of Animal Science*, vol. 49, pp. 701–707, 1979.

[127] A. Soyer, B. Özalp, Ü. Dalmiş, and V. Bilgin, "Effects of freezing temperature and duration of frozen storage on lipid and protein oxidation in chicken meat," *Food Chemistry*, vol. 120, pp. 1025–1030, 2010.

[128] J. Kanner, "Dietary advanced lipid oxidation endproducts are risk factors to human health," *Molecular Nutrition and Food Research*, vol. 51, pp. 1094–1101, 2007.

[129] J. Preiser, "Oxidative stress," *Journal of Parenteral and Enteral Nutrition*, vol. 36, pp. 147–154, 2012.

[130] J. E. Pie, K. Spahis, and C. Seillan, "Cholesterol oxidation in meat products during cooking and frozen storage," *Journal of Agricultural and Food Chemistry*, vol. 39, pp. 250–254, 1991.

[131] J. H. Cheng, "Lipid oxidation in meat," *Journal of Nutrition and Food Sciences*, vol. 6, pp. 1–3, 2016.

[132] P. A. Morrissey, P. J. A. Sheehy, K. Galvin, J. P. Kerry, and D. J. Buckley, "Lipid stability in meat and meat products," *Meat Science*, vol. 49, pp. S73–S86, 1998.

[133] Food Standards Agency, "The Safe Catering Guide," 2015.

[134] M. I. Gurr and J. L. Harwood, *Lipid biochemistry.* London, UK: Chapman and Hall, fourth ed., 1991.

[135] S. I. El-Syiad and M. M. El-Ghazali, "Effect of frozen storage on lipid, phospholipid fractions and fatty acid composition of cobb chicken tissues," *Journal of Applied Animal Research*, vol. 2, pp. 47–56, 1992.

[136] M. K. Campbell and S. O. Farrell, *Biochemistry.* Stamford, Connecticut: Cengage Learning, eighth ed., 2015.

[137] J. L. Flanagan, P. A. Simmons, J. Vehige, M. D. P. Willcox, and Q. Garrett, "Role of carnitine in disease," *Nutrition and Metabolism*, vol. 7, pp. 1–14, 2010.

[138] D. Mozaffarian, M. B. Katan, A. Ascherio, M. J. Stampfer, and W. C. Willett, "Trans fatty acids and cardiovascular disease," *The New England Journal of Medicine*, vol. 354, pp. 1601–1613, 2006.

[139] K. Nakyinsige, Y. B. C. Man, and A. Q. Sazili, "Halal authenticity issues in meat and meat products," *Meat Science*, vol. 91, pp. 207–214, 2012.

[140] D. K. Trivedi, K. A. Hollywood, N. J. W. Rattray, H. Ward, D. K. Trivedi, J. Greenwood, D. I. Ellis, and R. Goodacre, "Meat, the metabolites: an integrated metabolite profiling and lipidomics approach for the detection of the adulteration of beef with pork," *Analyst*, vol. 141, pp. 2155–2164, 2016.

[141] L. Liu, F. C. Chen, J. L. Dorsey, and Y. H. P. Hsieh, "Sensitive monoclonal antibody-based sandwich ELISA for the detection of porcine skeletal meat in meat and feed products," *Journal of Food Science*, vol. 71, pp. M1–M6, 2006.

[142] A. Kumar, R. R. Kumar, B. D. Sharma, P. Gokulakrishnan, S. K. Mendiratta, and D. Sharma, "Identification of species origin of meat and meat products on the DNA basis: A review," *Critical Reviews in Food Science and Nutrition*, vol. 55, pp. 1340–1351, 2015.

[143] T. Matsunaga, K. Chikuni, R. Tanabe, S. Muroya, K. Shibata, J. Yamada, and Y. Shinmura, "A quick and simple method for the identification of meat species and meat products by PCR assay," *Meat Science*, vol. 51, pp. 143–148, 1999.

[144] V. J. Russell, G. L. Hold, S. E. Pryde, H. Rehbein, J. Quinteiro, M. Rey-Mendez, C. G. Sotelo, R. I. Pérez-Martin, A. T. Santos, and C. Rosa, "Use of restriction fragment length polymorphism to distinguish between salmon species," *Journal of Agriculture and Food Chemistry*, vol. 48, pp. 2184–2188, 2000.

[145] L. Meira, J. Costa, C. Villa, F. Ramos, M. B. P. P. Oliveira, and I. Mafra, "Evagreen real-time PCR to determine horse meat adulteration in processed foods," *LWT - Food Science and Technology*, vol. 75, pp. 408–416, 2017.

[146] X. Fang and C. Zhang, "Detection of adulterated murine components in meat products by TaqMan© real-time PCR," *Food Chemistry*, vol. 192, pp. 485–490, 2016.

[147] O. Abbas, M. Zadravec, V. Baeten, T. Mikuš, T. Lešic, A. Vulić, J. Prpić, L. Jemeršić, and J. Pleadin, "Analytical methods used for the authentication of food of animal origin," *Food Chemistry*, vol. 246, pp. 6–17, 2018.

[148] X. D. Pan, J. Chen, Q. Chen, B. F. Huang, and J. L. Han, "Authentication of pork in meat mixtures using PRM mass spectrometry of myosin peptides," *RSC Advances*, vol. 8, pp. 11157–11162, 2018.

[149] C. Alamprese, M. Casale, N. Sinelli, S. Lanteri, and E. Casiraghi, "Detection of minced beef adulteration with turkey meat by UV-vis, NIR and MIR spectroscopy," *LWT - Food Science and Technology*, vol. 53, pp. 225–232, 2013.

[150] H. Rahmania, Sudjadi, and A. Rohman, "The employment of FTIR spectroscopy in combination with chemometrics for analysis of rat meat in meatball formulation," *Meat Science*, vol. 100, pp. 301–305, 2015.

[151] E. Kurniawati, A. Rohman, and K. Triyana, "Analysis of lard in meatball broth using Fourier transform infrared spectroscopy and chemometrics," *Meat Science*, vol. 96, pp. 94–98, 2014.

[152] I. H. Boyaci, H. T. Temiz, R. S. Uysal, H. M. Velioğlu, R. J. Yadegari, and M. M. Rishkan, "A novel method for discrimination of beef and horsemeat using raman spectroscopy," *Food Chemistry*, vol. 148, pp. 37–41, 2014.

[153] M. Enser, K. Hallett, B. Hewitt, G. A. J. Fursey, and J. D. Wood, "Fatty acid content and composition of English beef, lamb and pork in retail," *Meat Science*, vol. 42, pp. 443–456, 1996.

[154] P. Williams, "Nutritional composition of red meat," *Nutrition and Dietetics*, vol. 64, pp. S113–119, 2007.

[155] G. Lercker and M. T. Rodriguez-Estrada, "Cholesterol oxidation: Presence of 7-ketocholesterol in different food products," *Journal of Food Composition and Analysis*, vol. 13, pp. 625–631, 2000.

[156] M. Du, K. C. Nam, and D. U. Ahn, "Cholesterol and lipid oxidation products in cooked meat as affected by raw-meat packaging and irradiation and by cooked-meat packaging and storage time," *Journal of Food Science*, vol. 66, pp. 1396–1401, 2001.

[157] G. J. E. Nychas, P. N. Skandamis, C. C. Tassou, and K. P. Koutsoumani, "Meat spoilage during distribution," *Meat Science*, vol. 78, pp. 77–89, 2008.

[158] D. Dave and A. E. Ghaly, "Meat spoilage mechanisms and preservation techniques: A critical review," *American Journal of Agricultural and Biological Sciences*, vol. 6, pp. 486–510, 2011.

[159] N. Phan, K. Kim, E. Jeon, U. Kim, J. R. Sohn, and S. K. Pandey, "Analysis of volatile organic compounds released during food decaying processes," *Environmental monitoring and assessment*, vol. 184, pp. 1683–1692, 2012.

[160] J. Cheng, R. Gao, H. Li, S. Wu, J. Fang, K. Ma, J. Yang, X. Yan, and F. Dong, "Evaluating potential markers of spoilage foods using a metabolic profiling approach," *Food Analytical Methods*, vol. 8, pp. 1141–1149, 2015.

[161] M. Mataragas, P. Skandamis, G. J. E. Nychas, and E. H. Drosinos, "Modeling and predicting spoilage of cooked, cured meat products by multivariate analysis," *Meat Science*, vol. 77, pp. 348–356, 2007.

[162] D. Mayr, R. Margesin, E. Klingsbichel, E. Hartungen, D. Jenewein, F. Schinner, and T. D. Märk, "Rapid detection of meat spoilage by measuring volatile organic compounds by using proton transfer reaction mass spectrometry," *Applied and Environmental Microbiology*, vol. 69, pp. 4697–4705, 2003.

[163] D. I. Ellis, D. Broadhurst, and R. Goodacre, "Rapid and quantitative detection of the microbial spoilage of beef by Fourier transform infrared spectroscopy and machine learning," *Analytica Chimica Acta*, vol. 514, pp. 193–201, 2004.

[164] O. Papadopoulou, E. Z. Panagou, C. C. Tassou, and G.-J. Nychas, "Contribution of Fourier transform infrared (FTIR) spectroscopy data on the quantitative determination of minced pork meat spoilage," *Food Research International*, vol. 44, pp. 3264–3271, 2011.

[165] A. A. Argyri, R. M. Jarvis, D. Wedge, Y. Xu, E. Z. Panagou, R. Goodacre, and G.-J. E. Nychas, "A comparison of Raman and FT-IR spectroscopy for the prediction of meat spoilage," *Food Control*, vol. 29, pp. 461–470, 2013.

[166] A. Sahar and É. Dufour, "Use of Fourier transform-infrared spectroscopy to predict spoilage bacteria on aerobically stored chicken breast fillets," *LWT - Food Science and Technology*, vol. 56, pp. 315–320, 2014.

[167] A. A. Argyri, A. I. Doulgeraki, V. A. Blana, E. Z. Panagou, and G. E. Nychas, "Potential of a simple HPLC-based approach for the identification of the spoilage status of minced beef stored at various temperatures and packaging systems," *International Journal of Food Microbiology*, vol. 150, pp. 25–33, 2011.

[168] D. Alexandrakis, N. P. Brunton, G. Downey, and A. G. Scannell, "Identification of spoilage marker metabolites in Irish chicken breast muscle using HPLC, GC-MS coupled with SPME and traditional chemical techniques," *Food and Biopress Technology*, vol. 5, pp. 1917–1923, 2012.

[169] D. Ercolini, I. Ferrocino, A. Nasi, M. Ngagijimana, P. Vernocchi, A. L. Storia, L. Laghi, G. Mauriello, M. E. Guerzoni, and F. Villani, "Monitoring of microbial metabolites and bacterial diversity in beef stored under different packaging conditions," *Applied and Environmental Microbiology*, vol. 77, pp. 7372–7381, 2011.

[170] V. Shukla, G. Kandeepan, and M. R. Vishnuraj, "Evaluation of shelf life of buffalo meat in aerobic cold storage using physicochemical parameters," *Buffalo Bulletin*, vol. 34, pp. 453–457, 2015.

Appendix A

Mass spectra comparisons for tentative identifications of markers in raw beef adulterated with pork

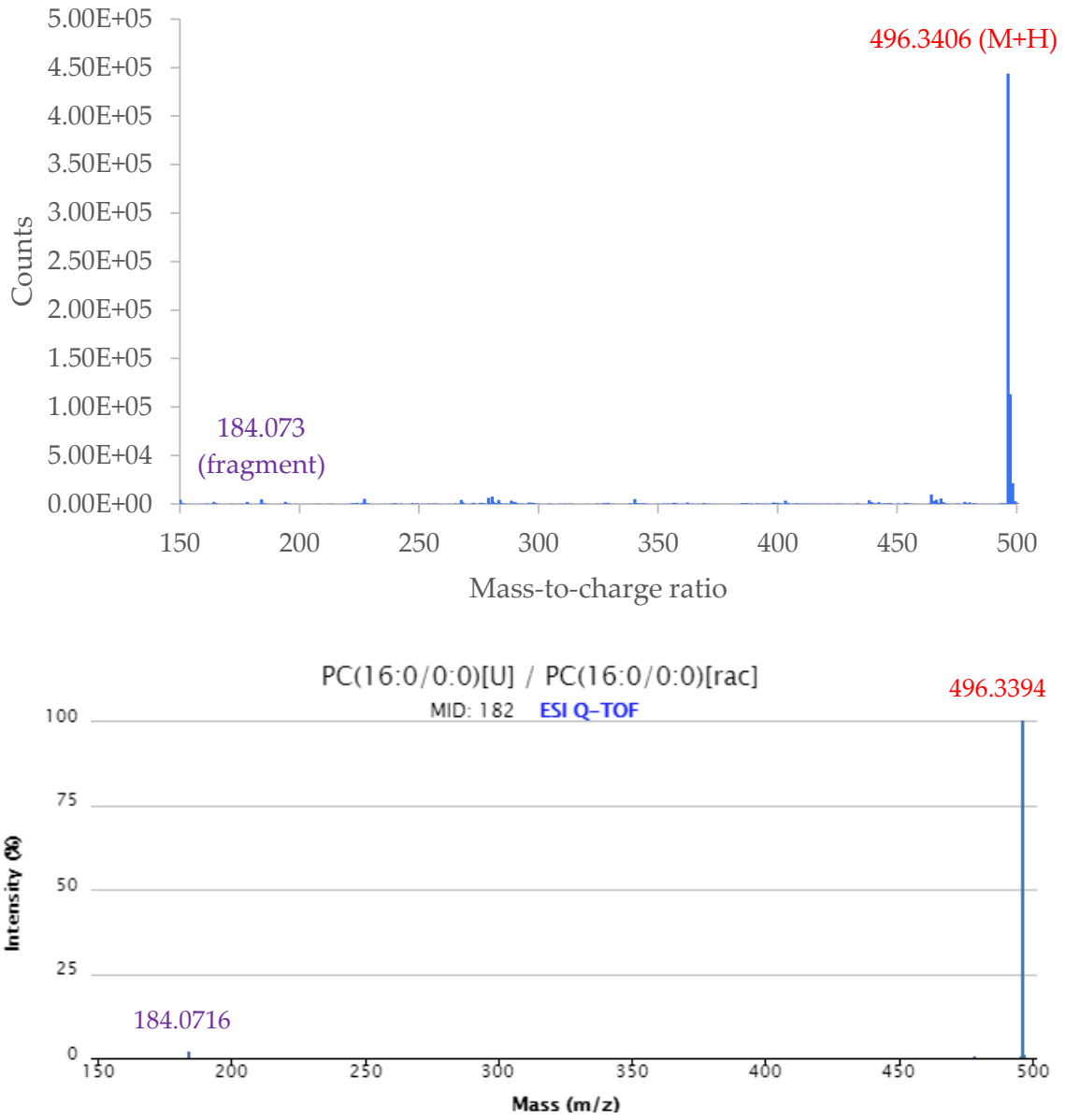

Figure A.1: Mass spectrum of marker 496.3399 m/z at a retention time of 14.48 minutes in QC sample (top) compared to the mass spectrum of PC(16:0/0:0) found on METLIN (bottom)

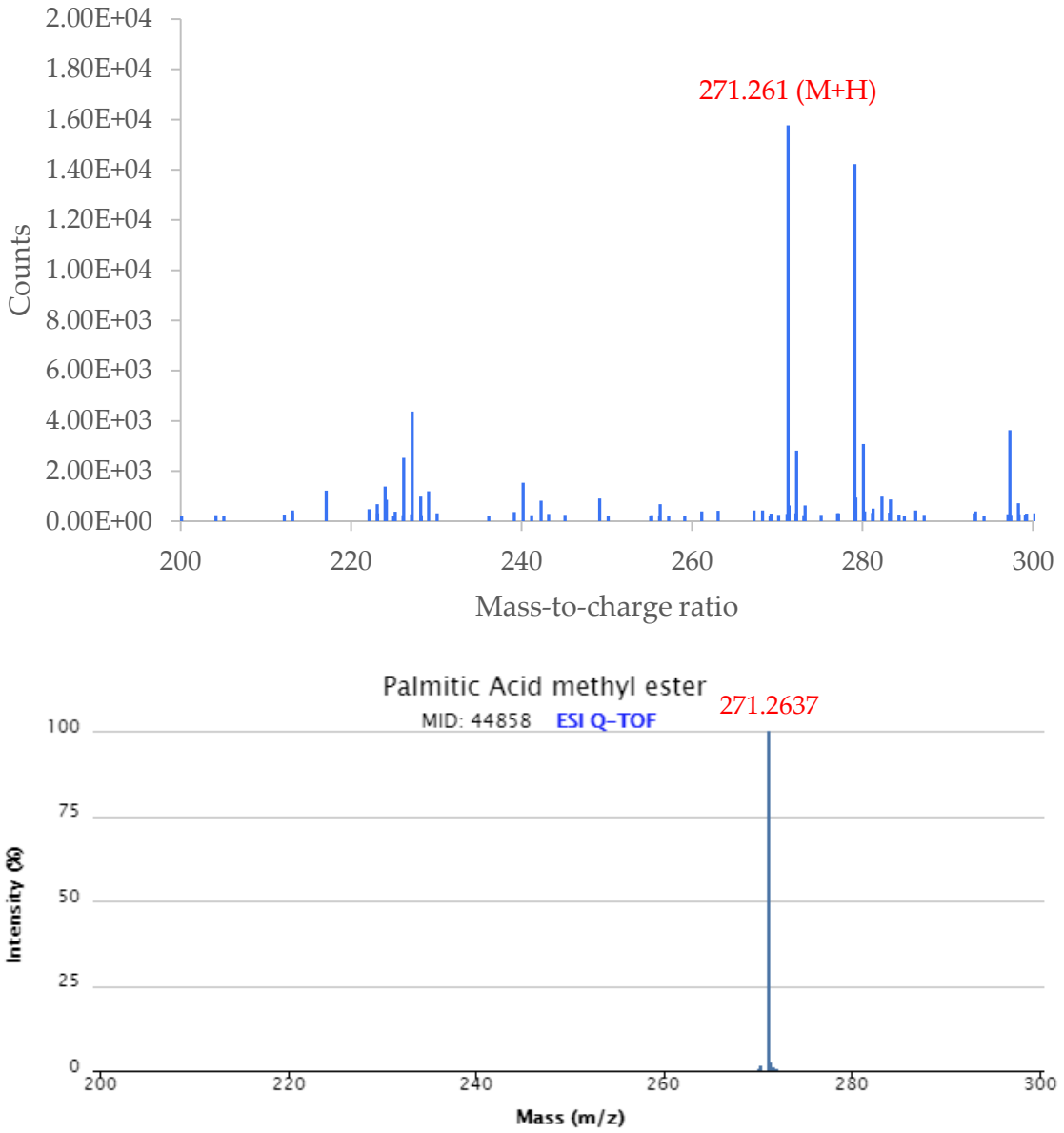

Figure A.2: Mass spectrum of marker 271.2620 m/z at a retention time of 26.64 minutes in QC sample (top) compared to the mass spectrum of palmitic acid methyl ester found on METLIN (bottom)

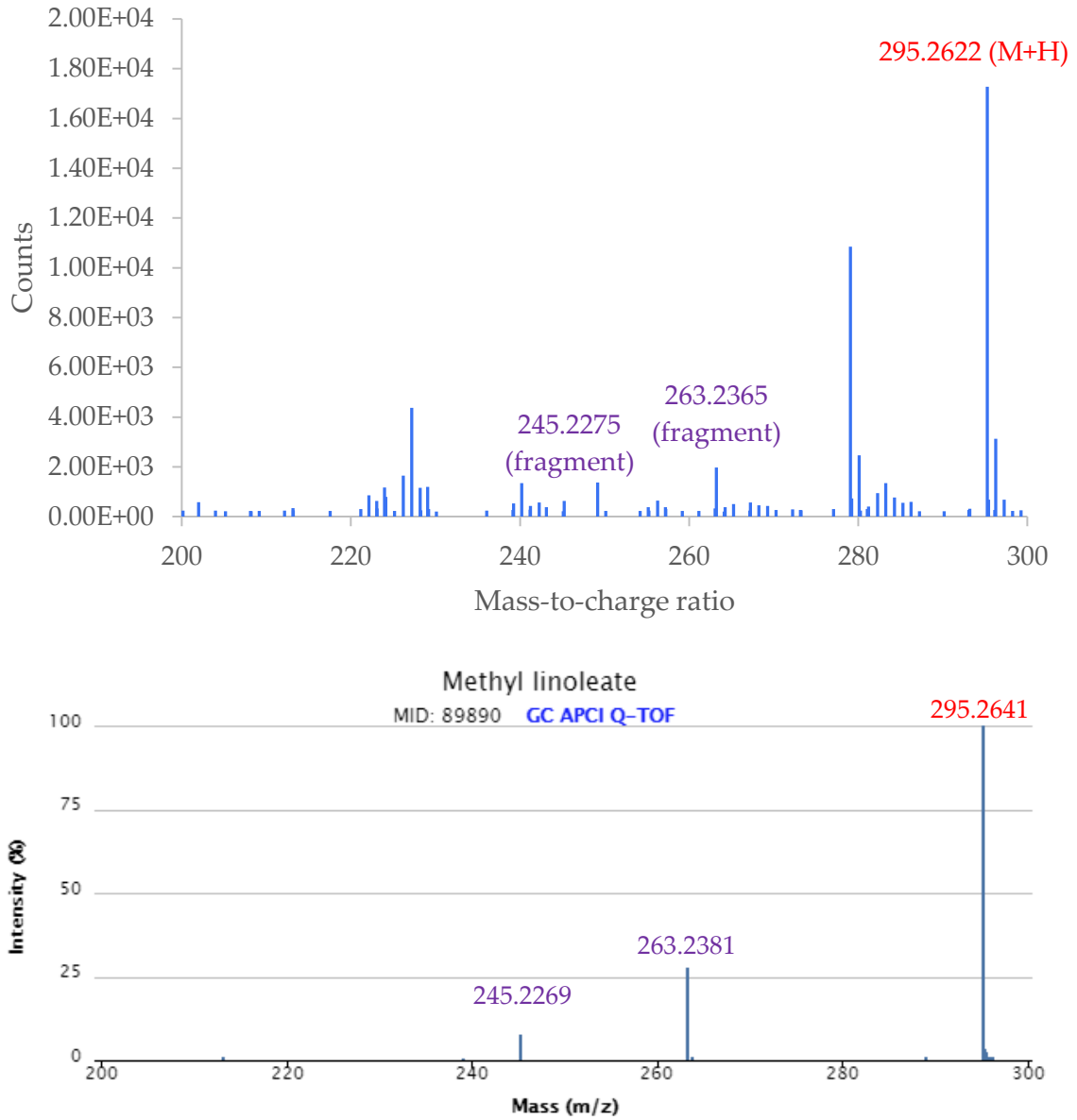

Figure A.3: Mass spectrum of marker 295.2621 m/z at a retention time of 23.90 minutes in QC sample (top) compared to the mass spectrum of linoleic acid methyl ester found on METLIN (bottom)

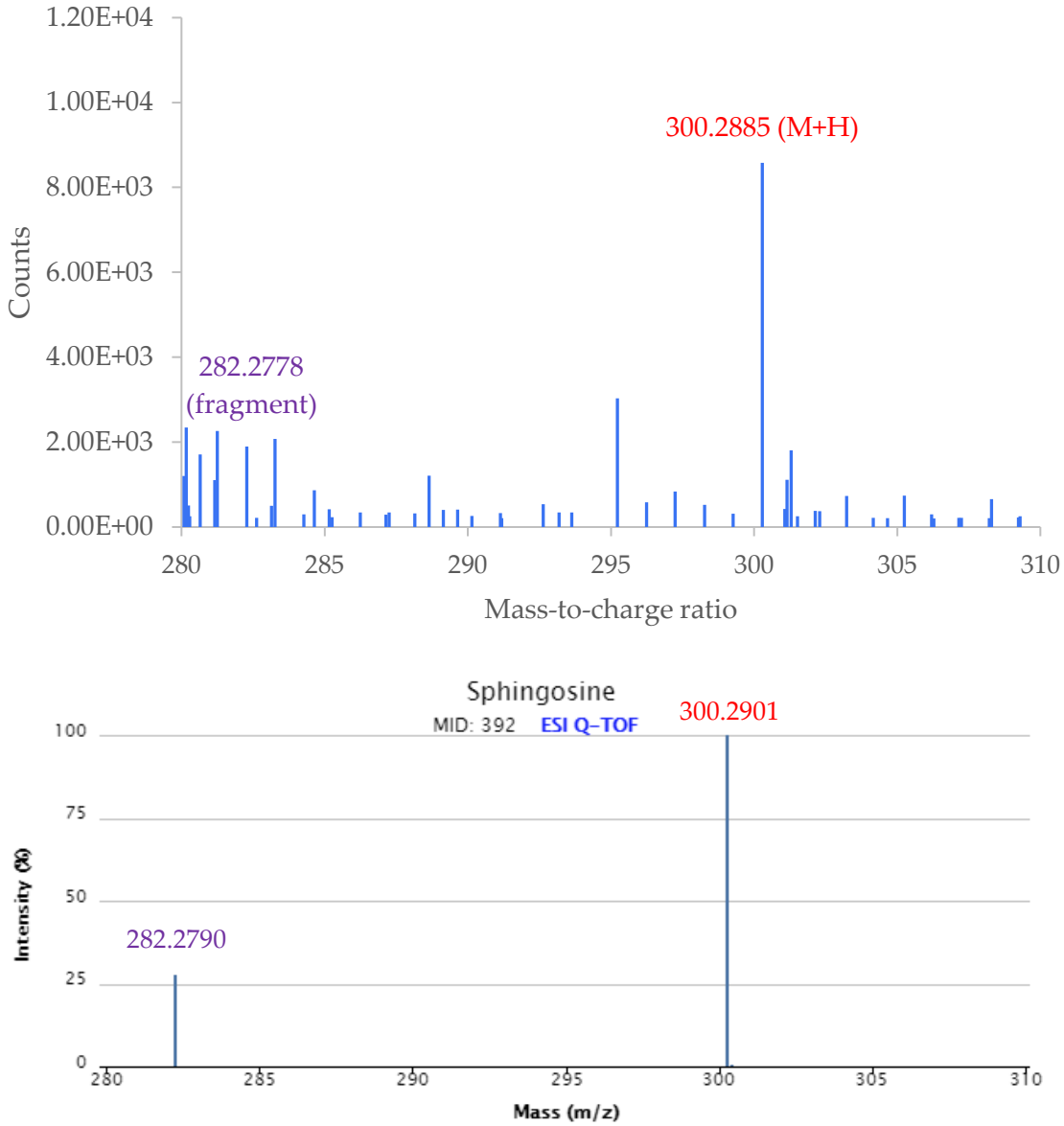

Figure A.4: Mass spectrum of marker 300.2885 m/z at a retention time of 13.26 minutes in QC sample (top) compared to the mass spectrum of sphingosine found on METLIN (bottom)

Appendix B

Mass spectra comparisons for tentative identifications of markers in raw beef adulterated with lamb

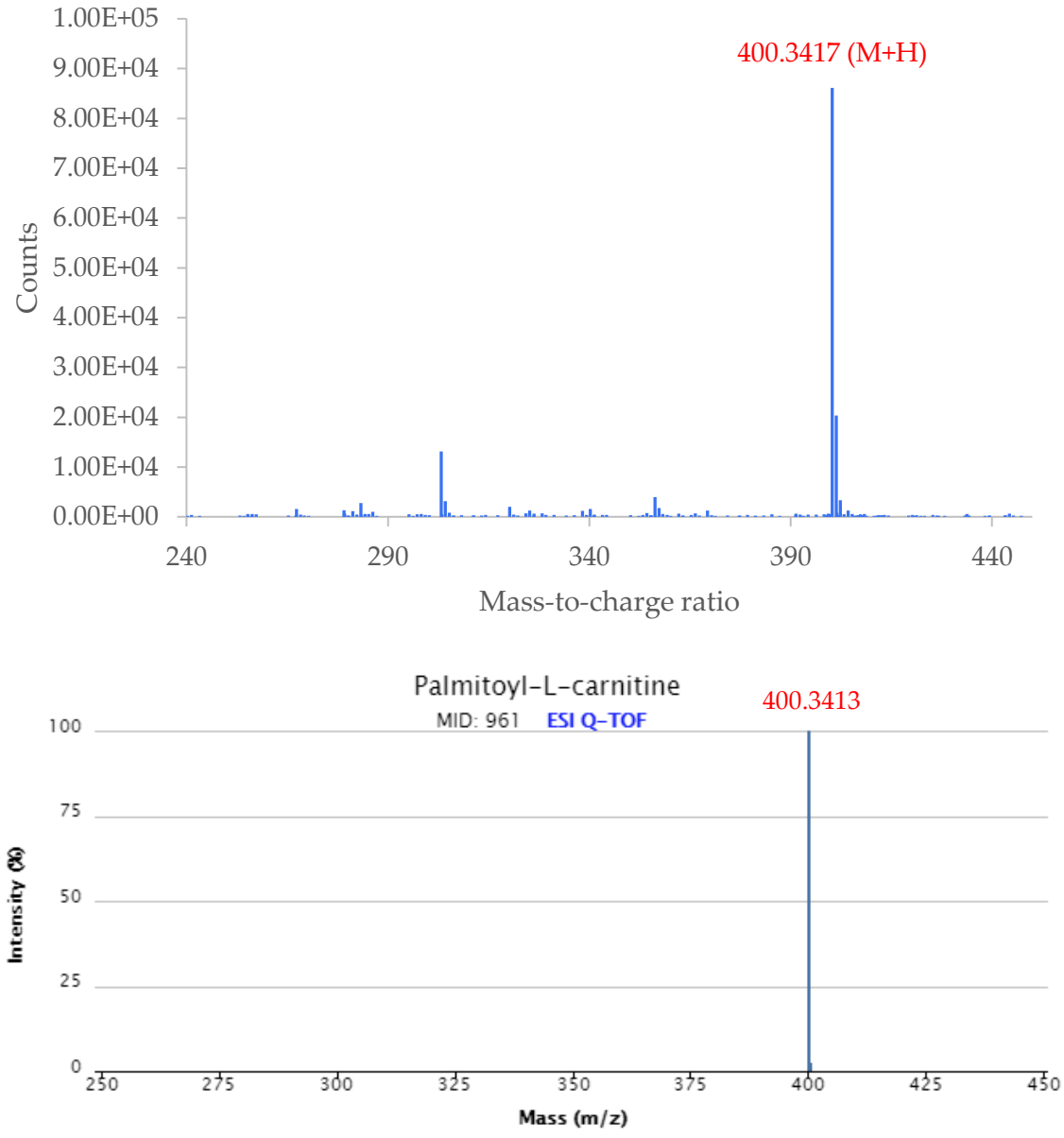

Figure B.1: Mass spectrum of marker 400.3421 m/z at a retention time of 16.27 minutes in QC sample (top) compared to the mass spectrum of palmitoyl carnitine found on METLIN (bottom)

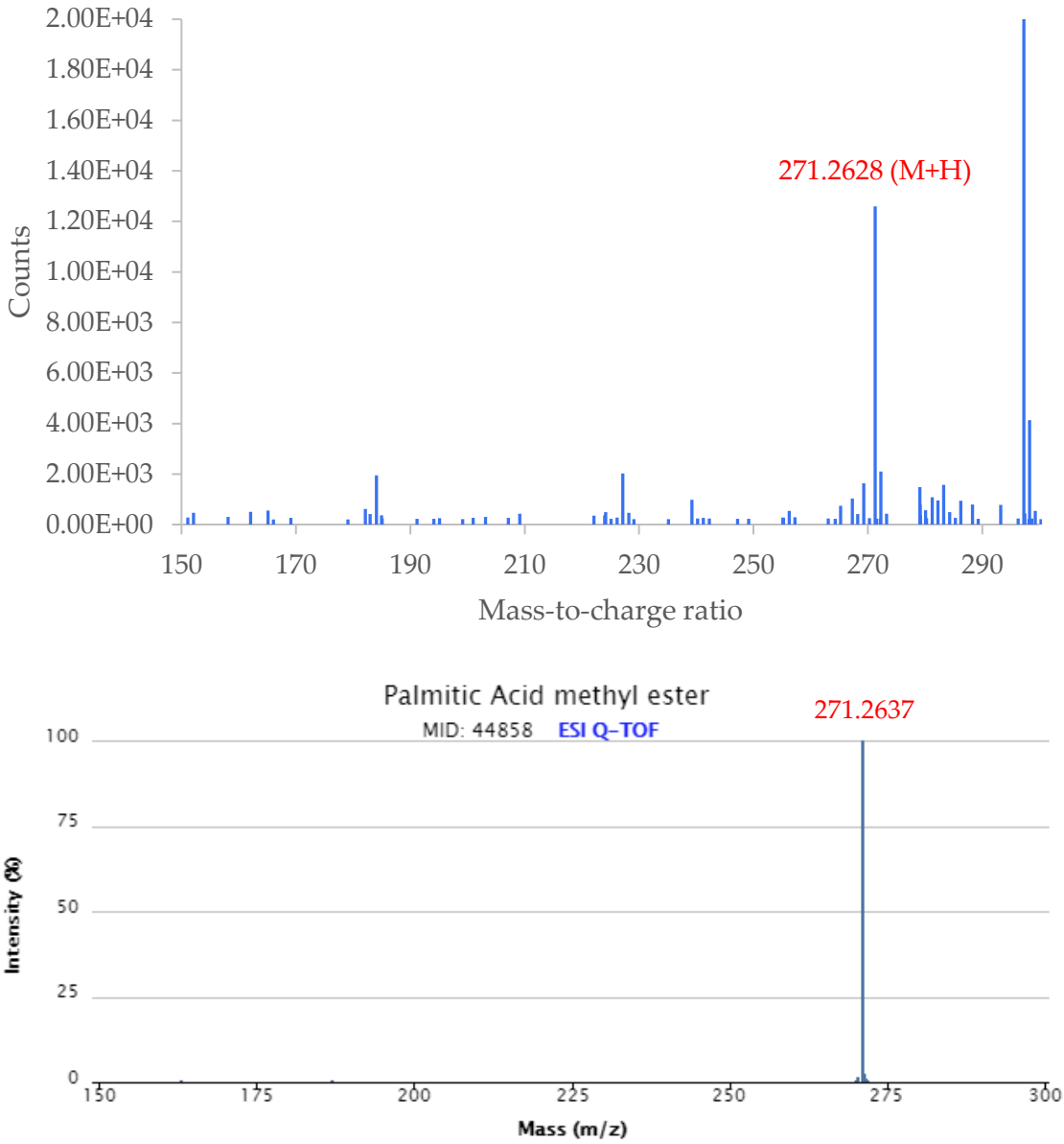

Figure B.2: Mass spectrum of marker 271.2626 m/z at a retention time of 26.16 minutes in QC sample (top) compared to the mass spectrum of palmitic acid methyl ester found on METLIN (bottom)

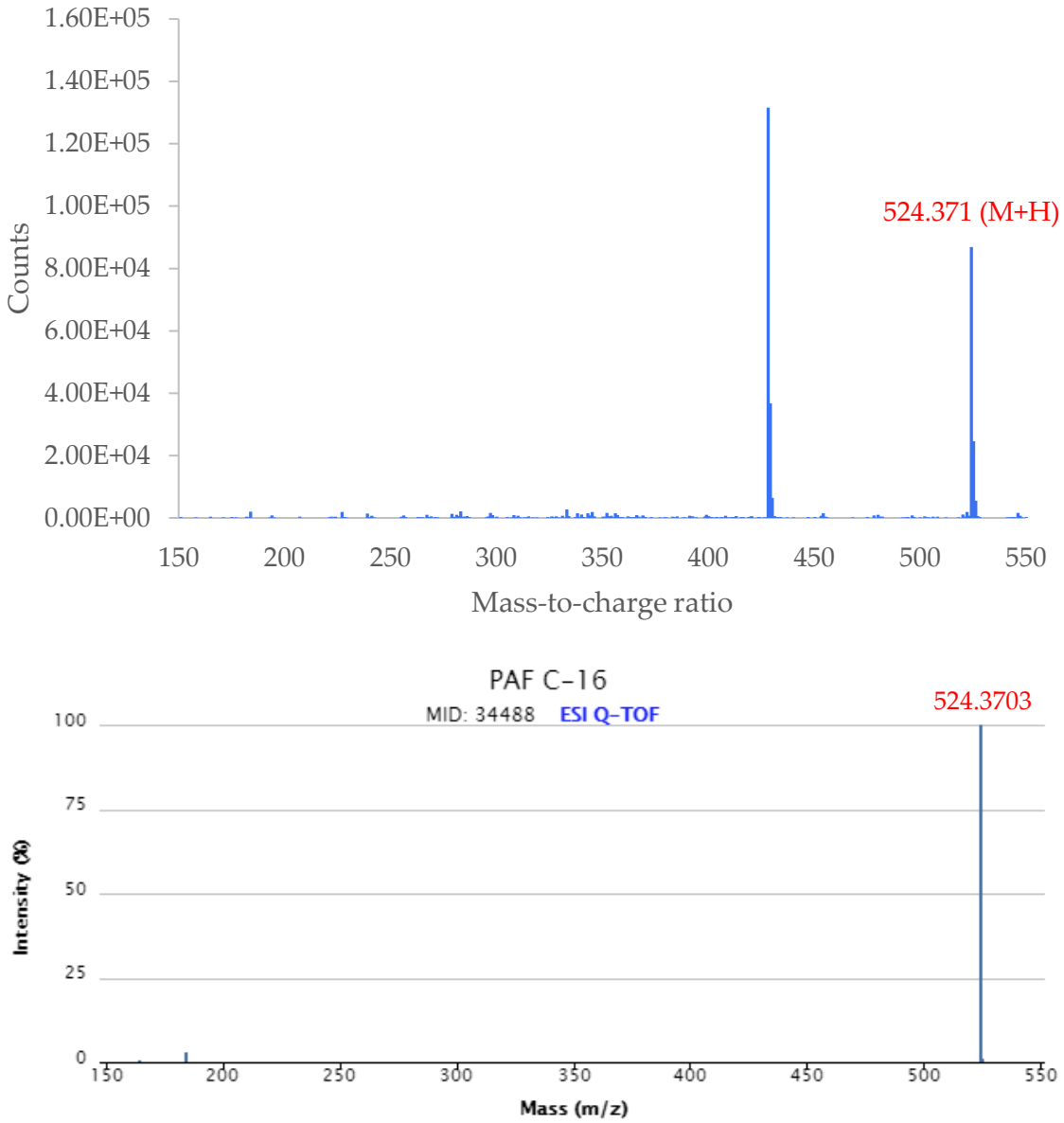

Figure B.3: Mass spectrum of marker 524.3710 m/z at a retention time of 20.66 minutes in QC sample (top) compared to the mass spectrum of PAF C-16 found on METLIN (bottom)

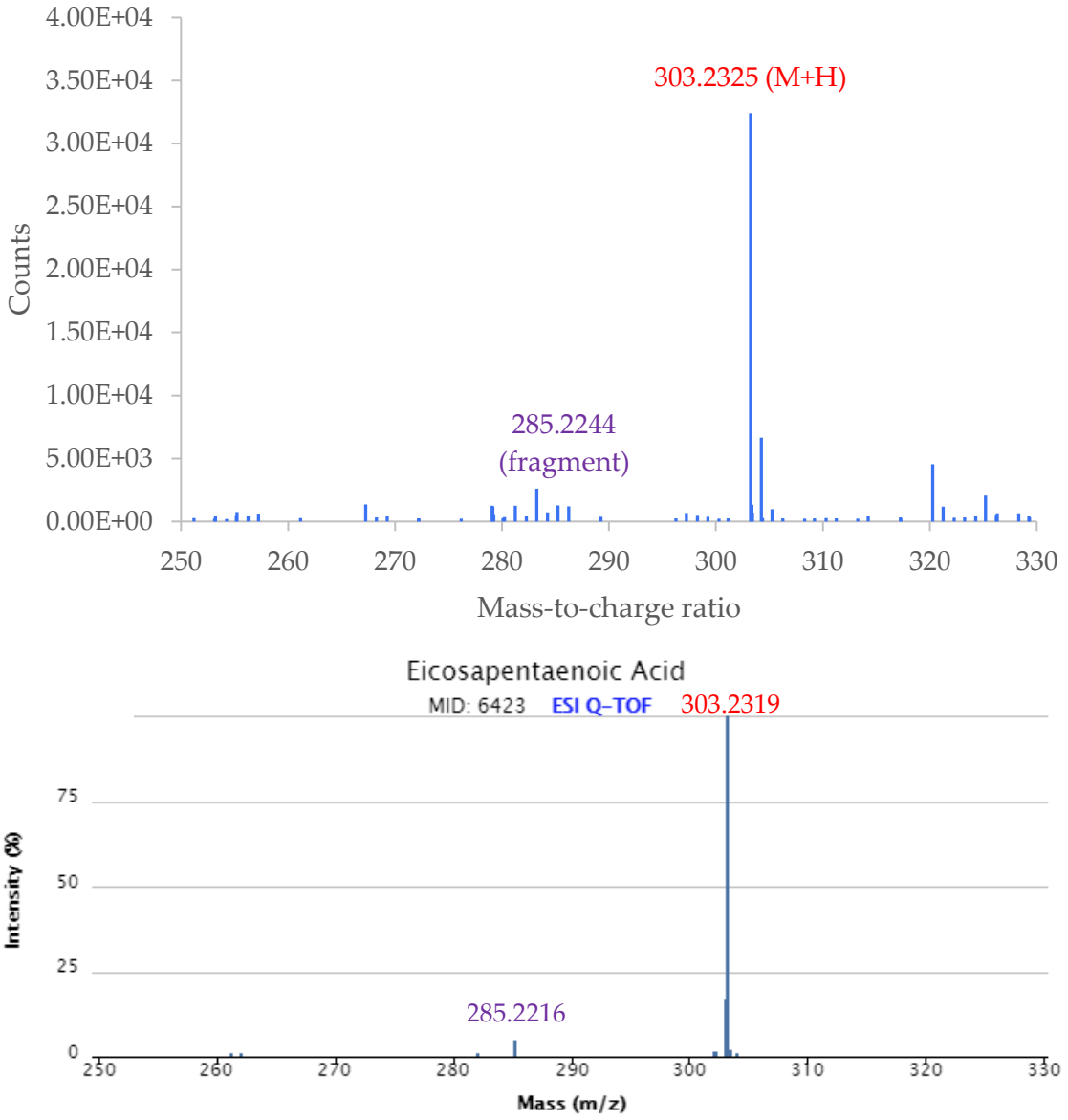

Figure B.4: Mass spectrum of marker 303.2317 m/z at a retention time of 16.20 minutes in QC sample (top) compared to the mass spectrum of eicosapentaenoic acid found on METLIN (bottom)

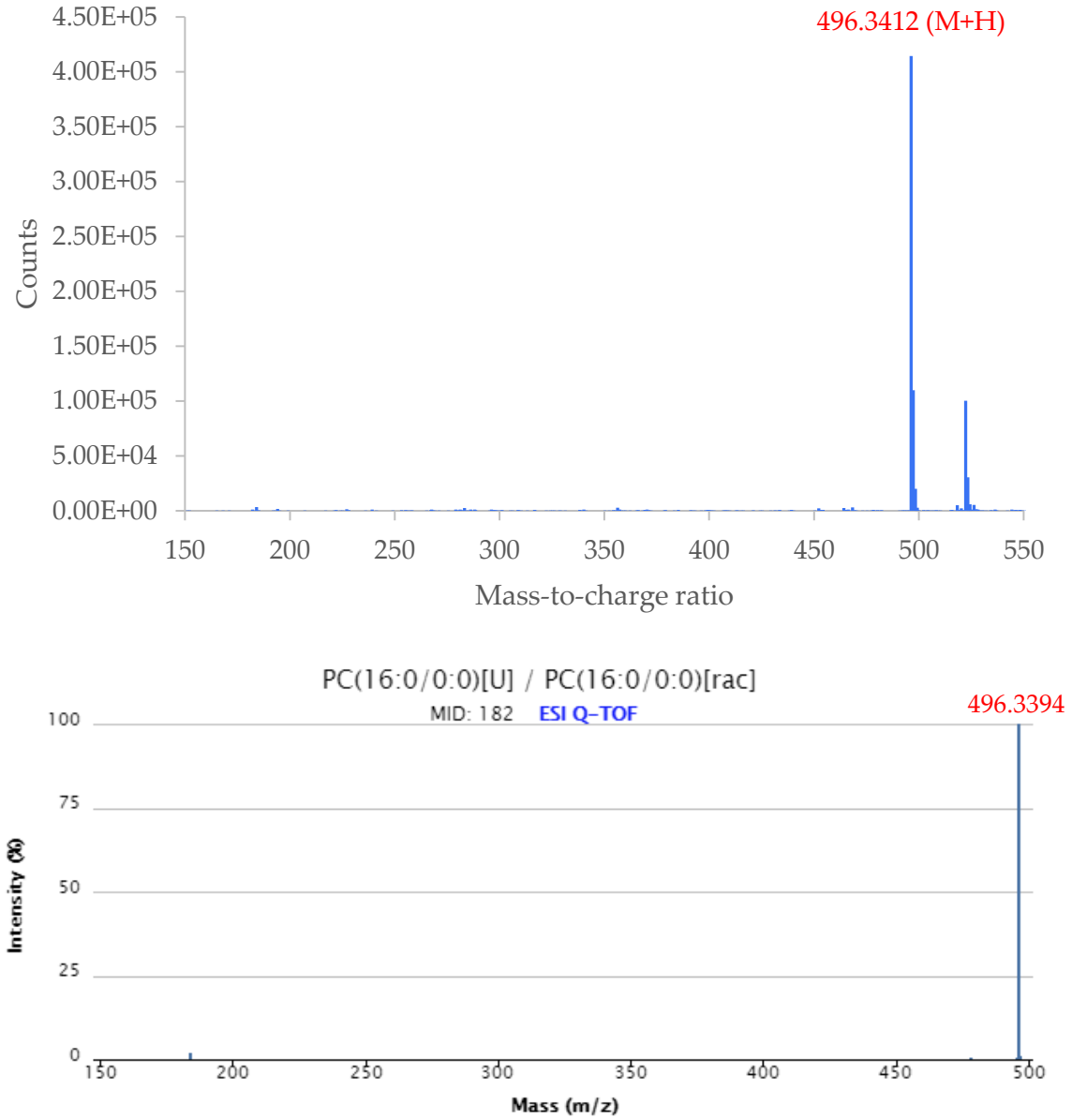

Figure B.5: Mass spectrum of marker 496.3403 m/z at a retention time of 15.47 minutes in QC sample (top) compared to the mass spectrum of PC(16:0/0:0) found on METLIN (bottom)

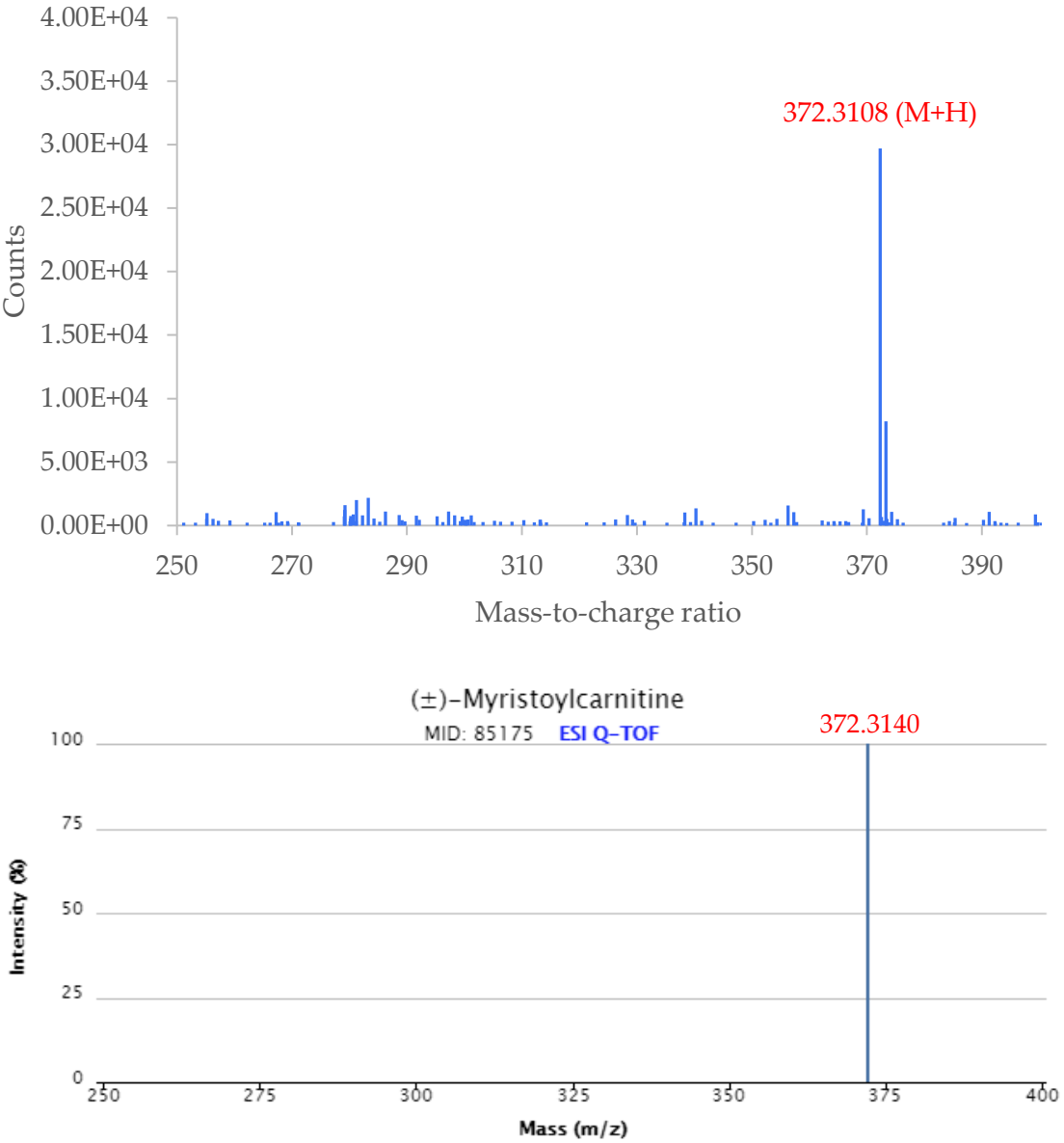

Figure B.6: Mass spectrum of marker 372.3107 m/z at a retention time of 12.90 minutes in QC sample (top) compared to the mass spectrum of myristoyl carnitine found on METLIN (bottom)

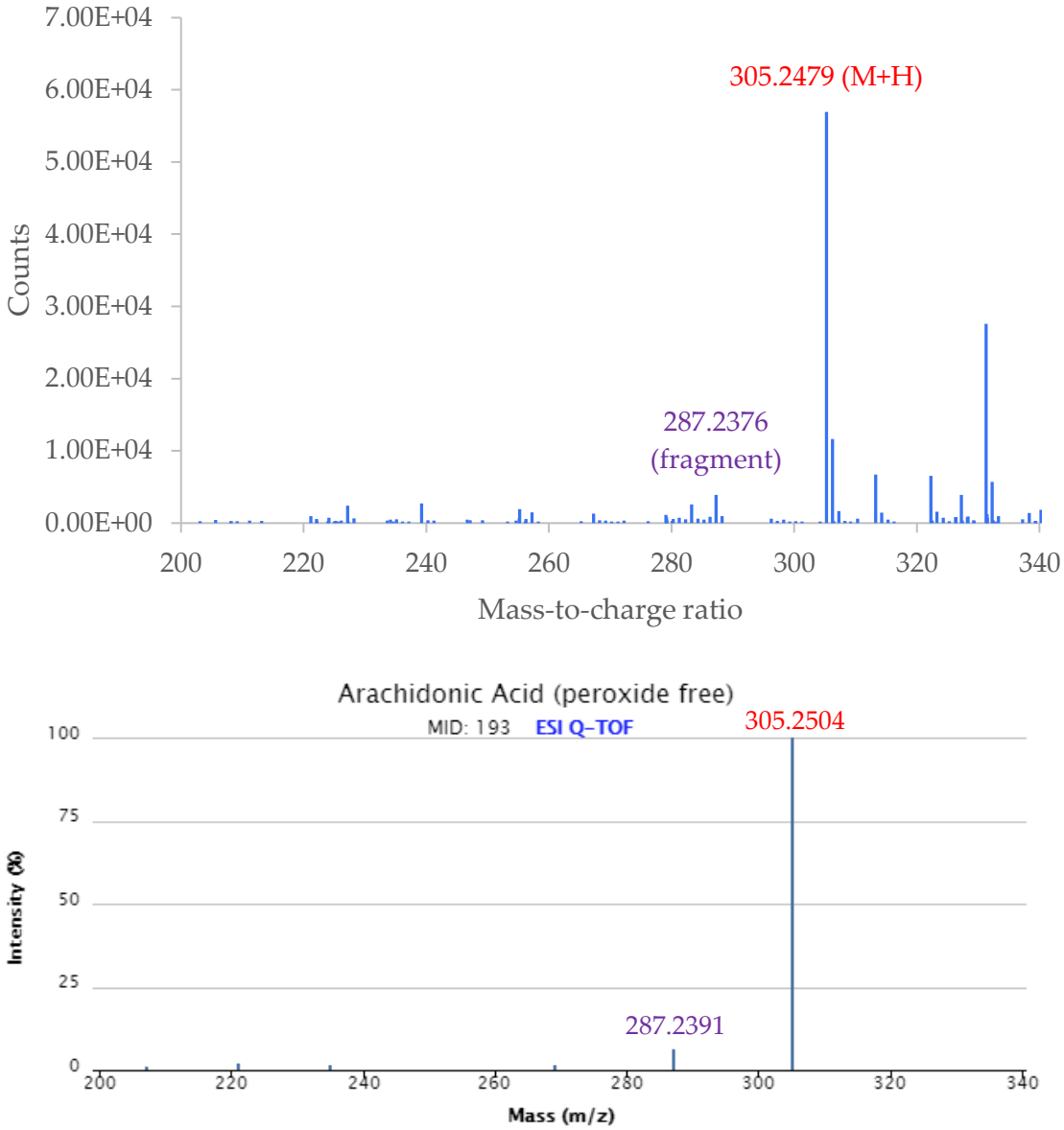

Figure B.7: Mass spectrum of marker 305.2474 m/z at a retention time of 18.06 minutes in QC sample (top) compared to the mass spectrum of arachidonic acid found on METLIN (bottom)

Appendix C

Mass spectra comparisons for tentative identifications of markers in raw beef adulterated with turkey

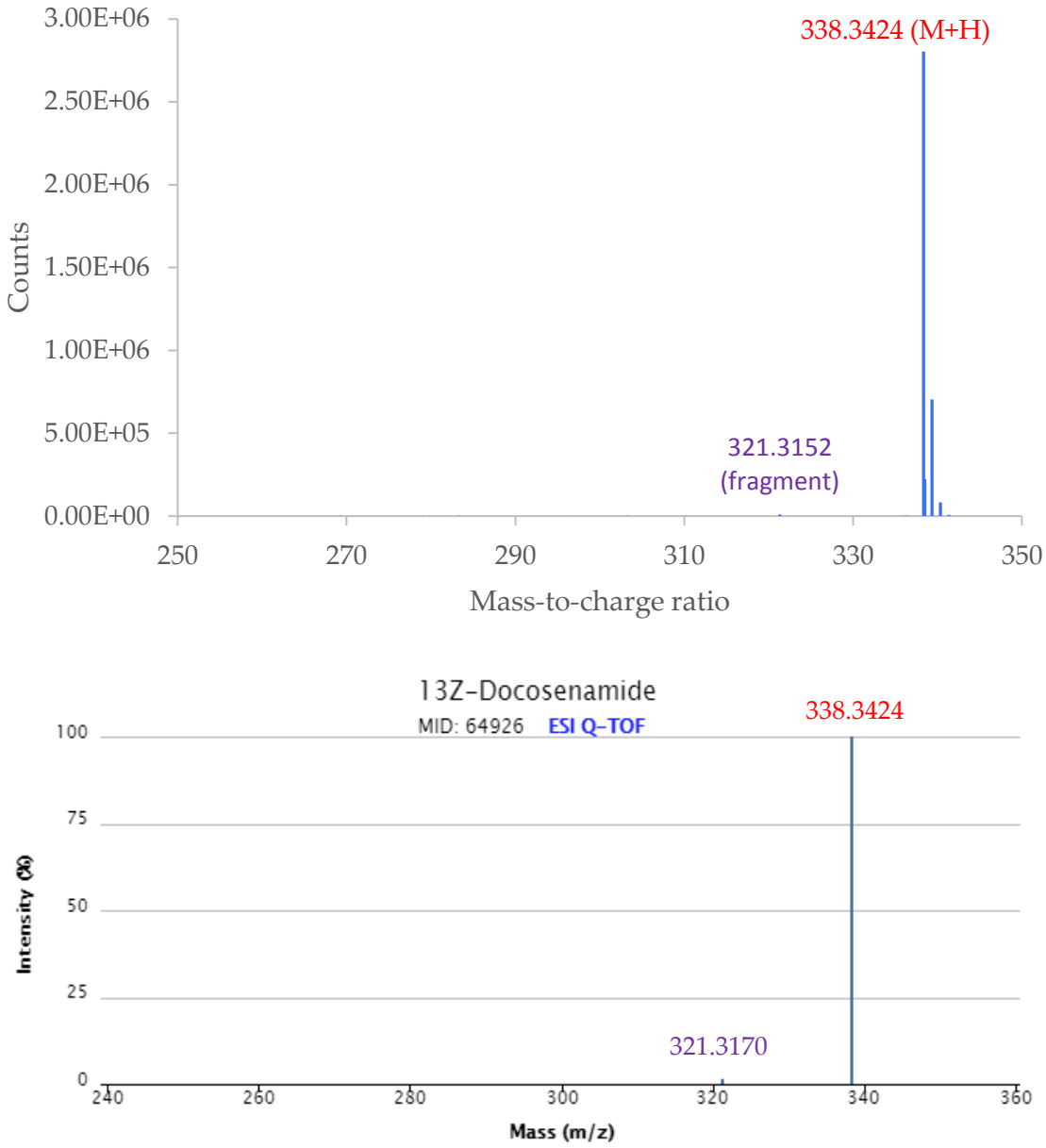

Figure C.1: Mass spectrum of marker 338.3422 m/z at a retention time of 26.99 minutes in QC sample (top) compared to the mass spectrum of 13Z-docosenamide found on METLIN (bottom)

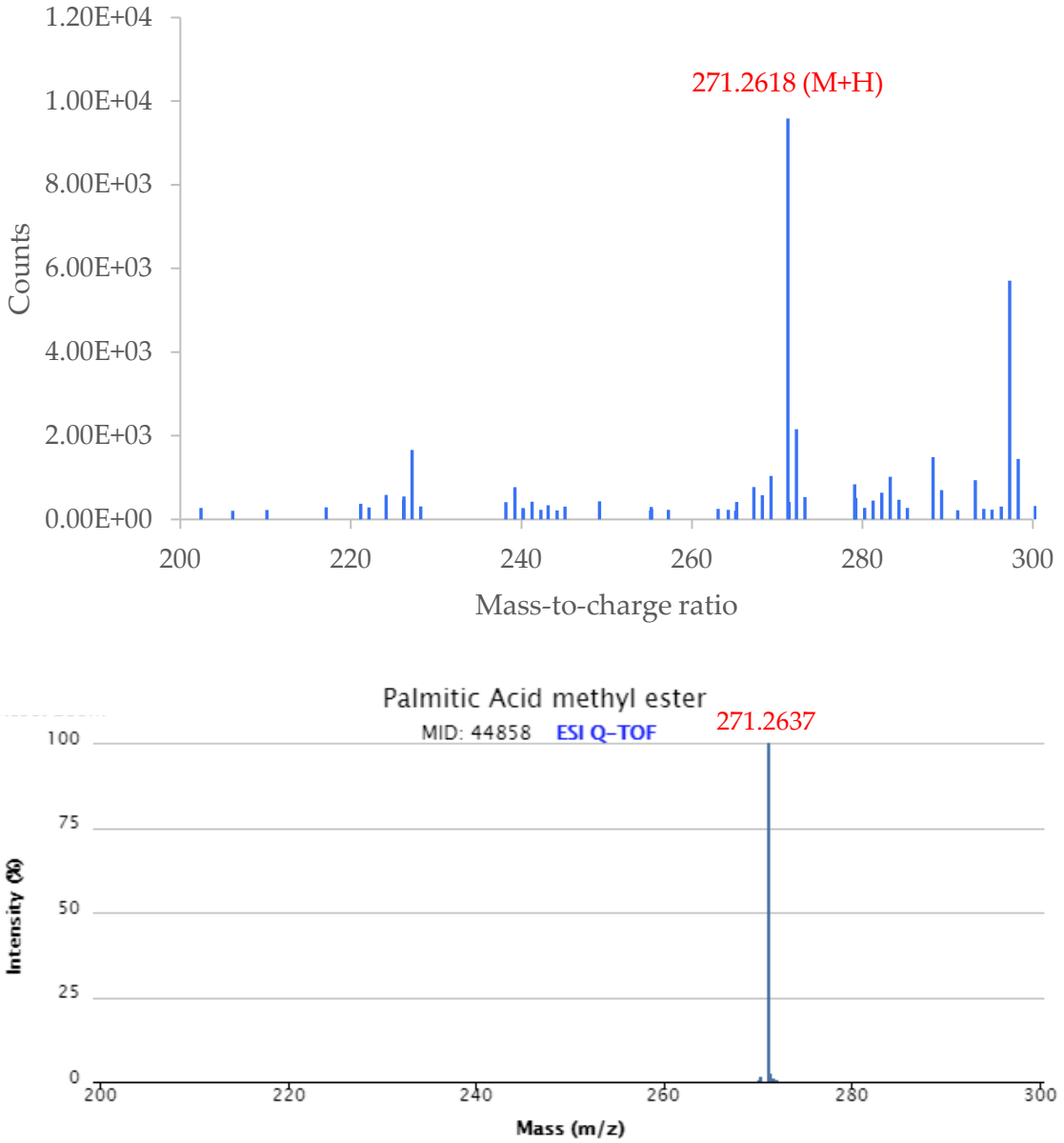

Figure C.2: Mass spectrum of marker 271.2629 m/z at a retention time of 26.14 minutes in QC sample (top) compared to the mass spectrum of palmitic acid methyl ester found on METLIN (bottom)

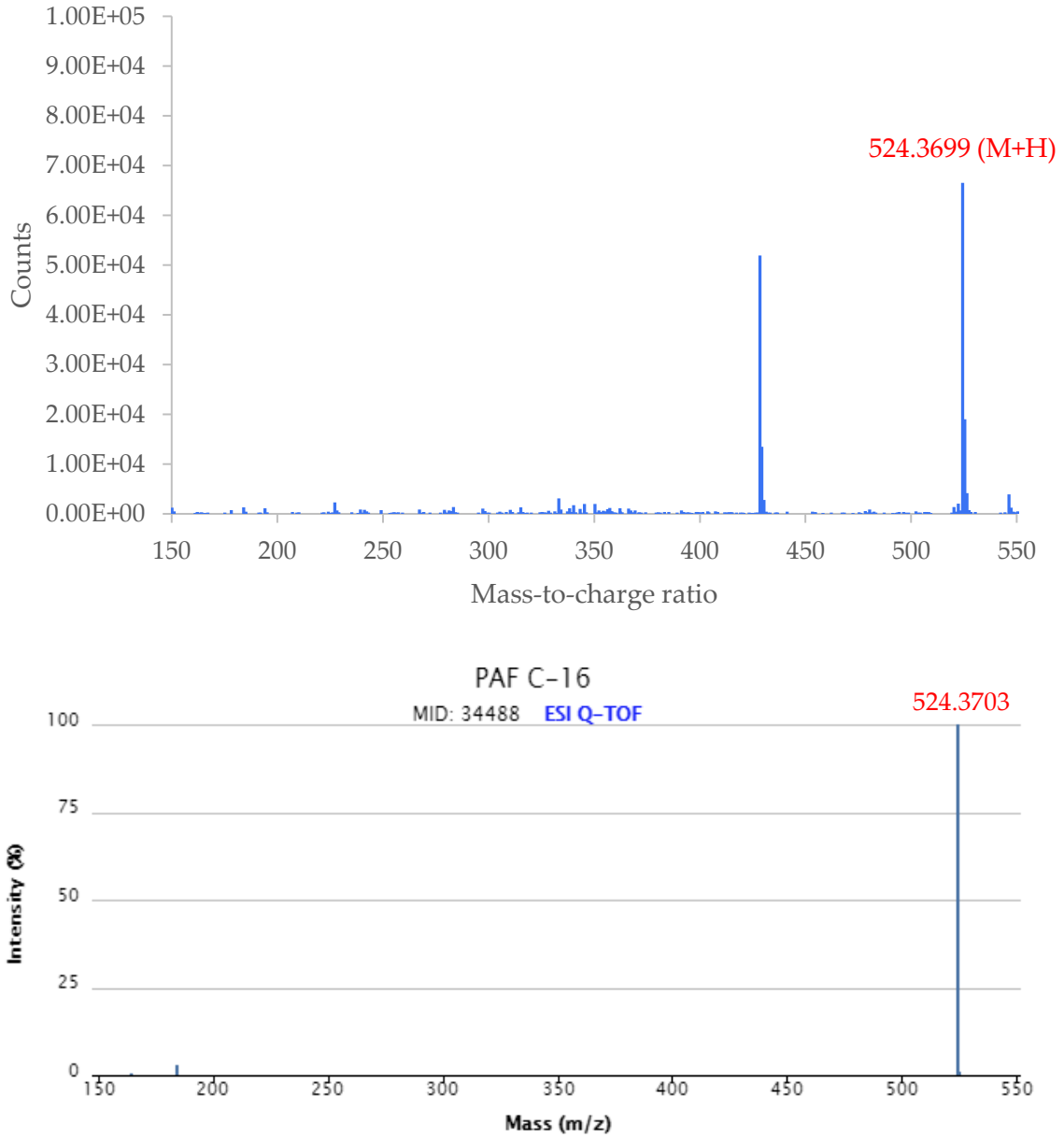

Figure C.3: Mass spectrum of marker 524.3706 m/z at a retention time of 20.62 minutes in QC sample (top) compared to the mass spectrum of PAF C-16 found on METLIN (bottom)

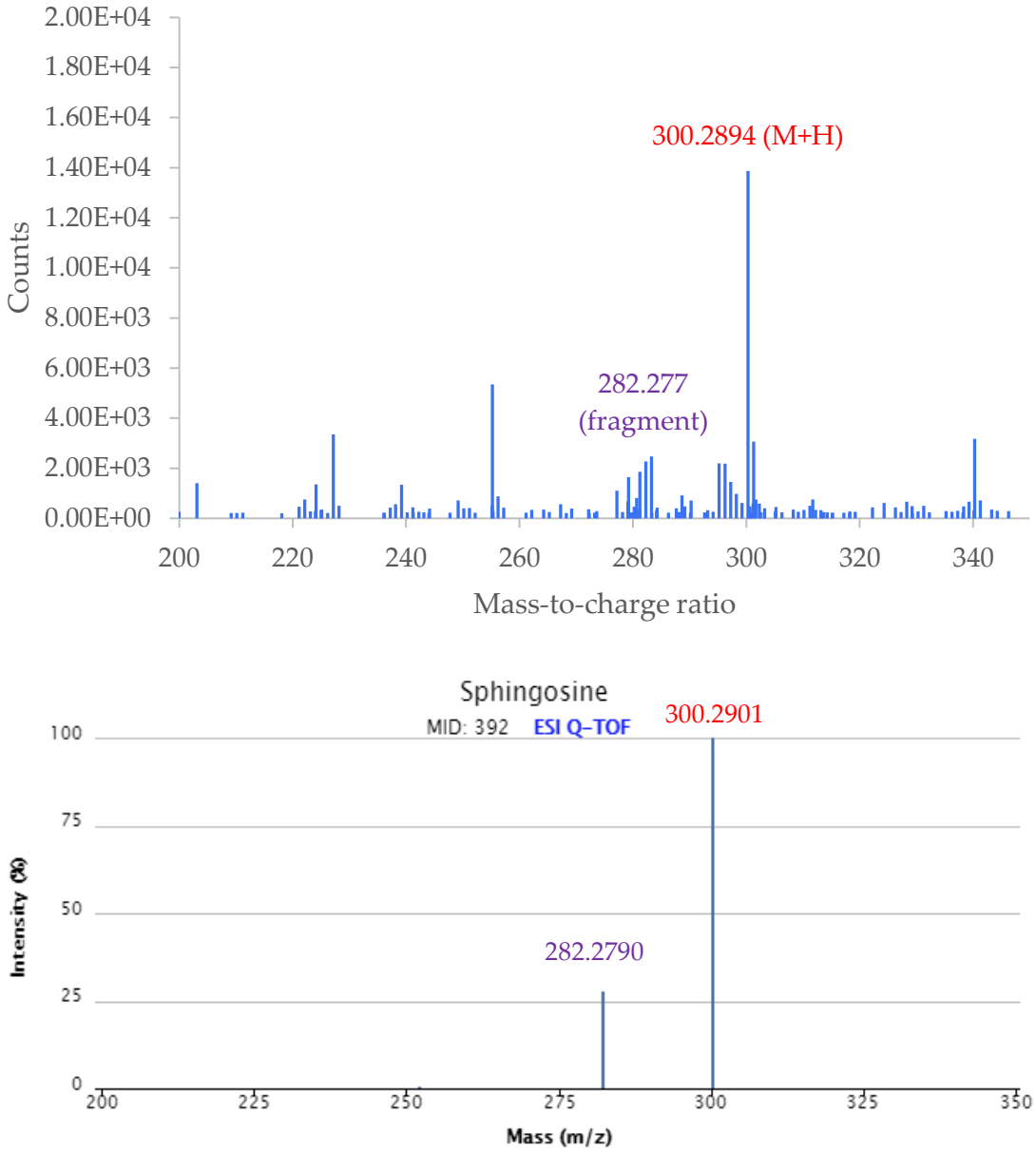

Figure C.4: Mass spectrum of marker 300.2893 m/z at a retention time of 12.44 minutes in QC sample (top) compared to the mass spectrum of sphingosine found on METLIN (bottom)

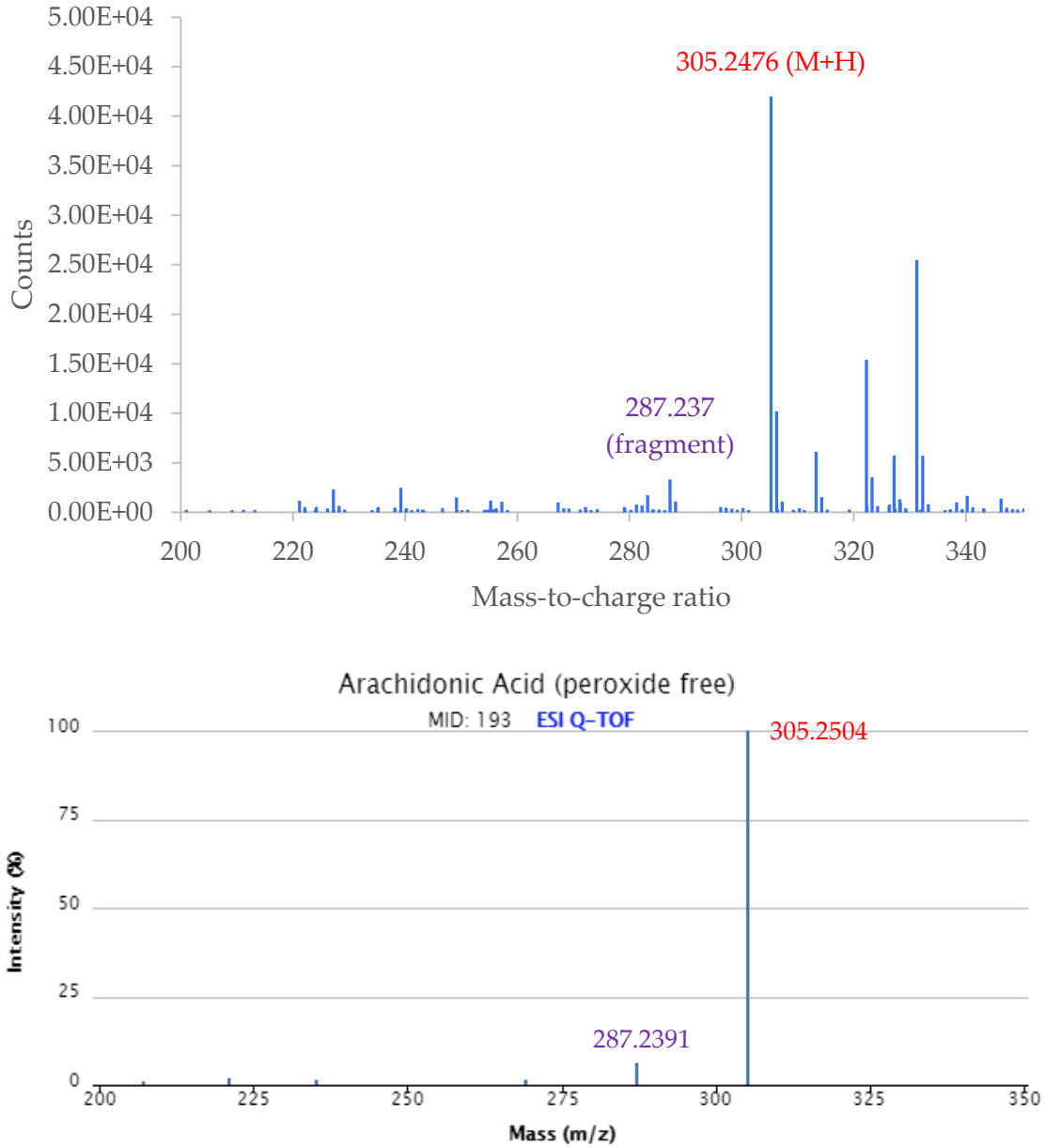

Figure C.5: Mass spectrum of marker 305.2475 m/z at a retention time of 18.02 minutes in QC sample (top) compared to the mass spectrum of arachidonic acid found on METLIN (bottom)

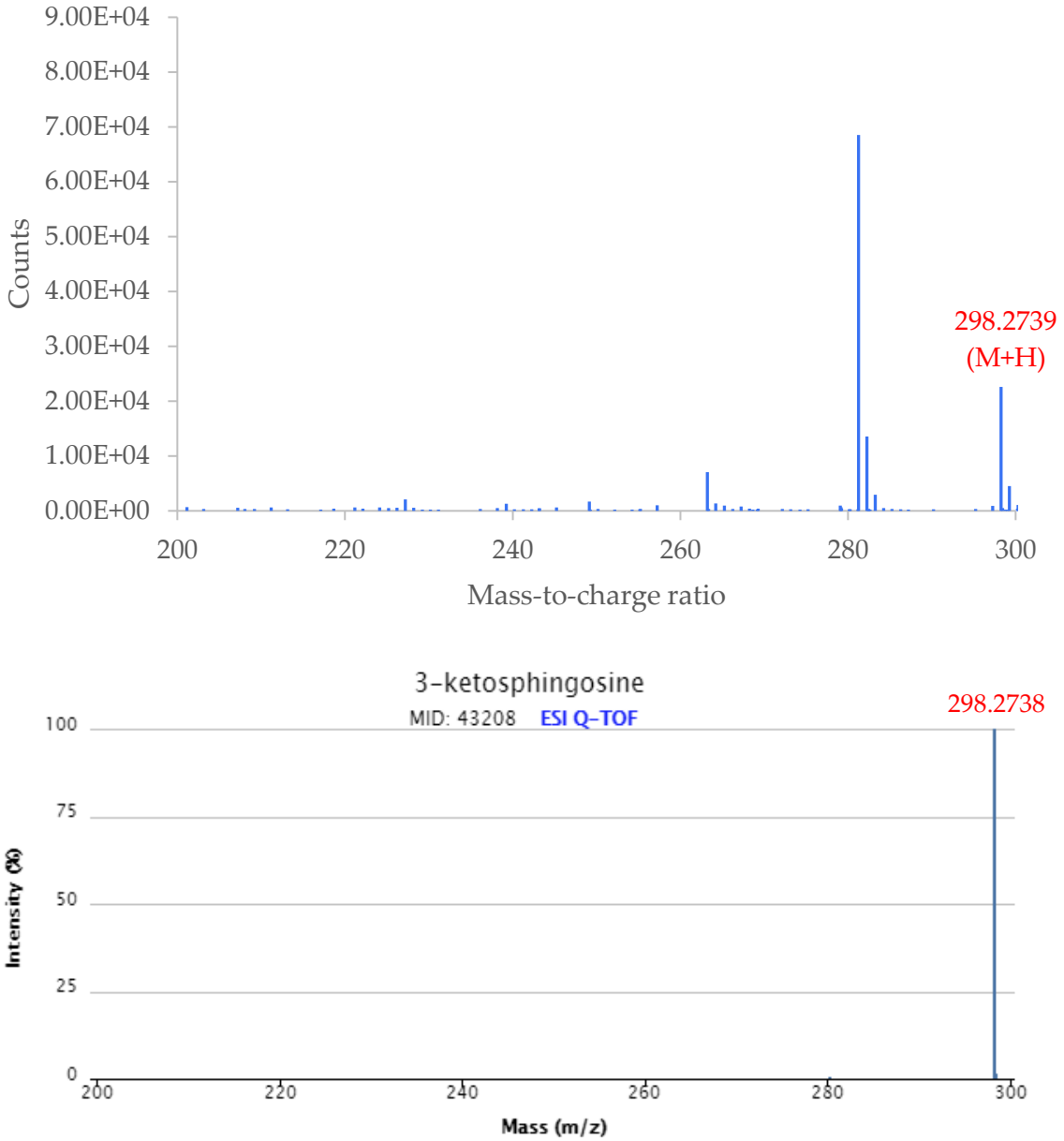

Figure C.6: Mass spectrum of marker 298.2740 m/z at a retention time of 18.51 minutes in QC sample (top) compared to the mass spectrum of 3-ketosphingosine found on METLIN (bottom)

Appendix D

Mass spectra comparisons for tentative identifications of markers in cooked beef adulterated with pork

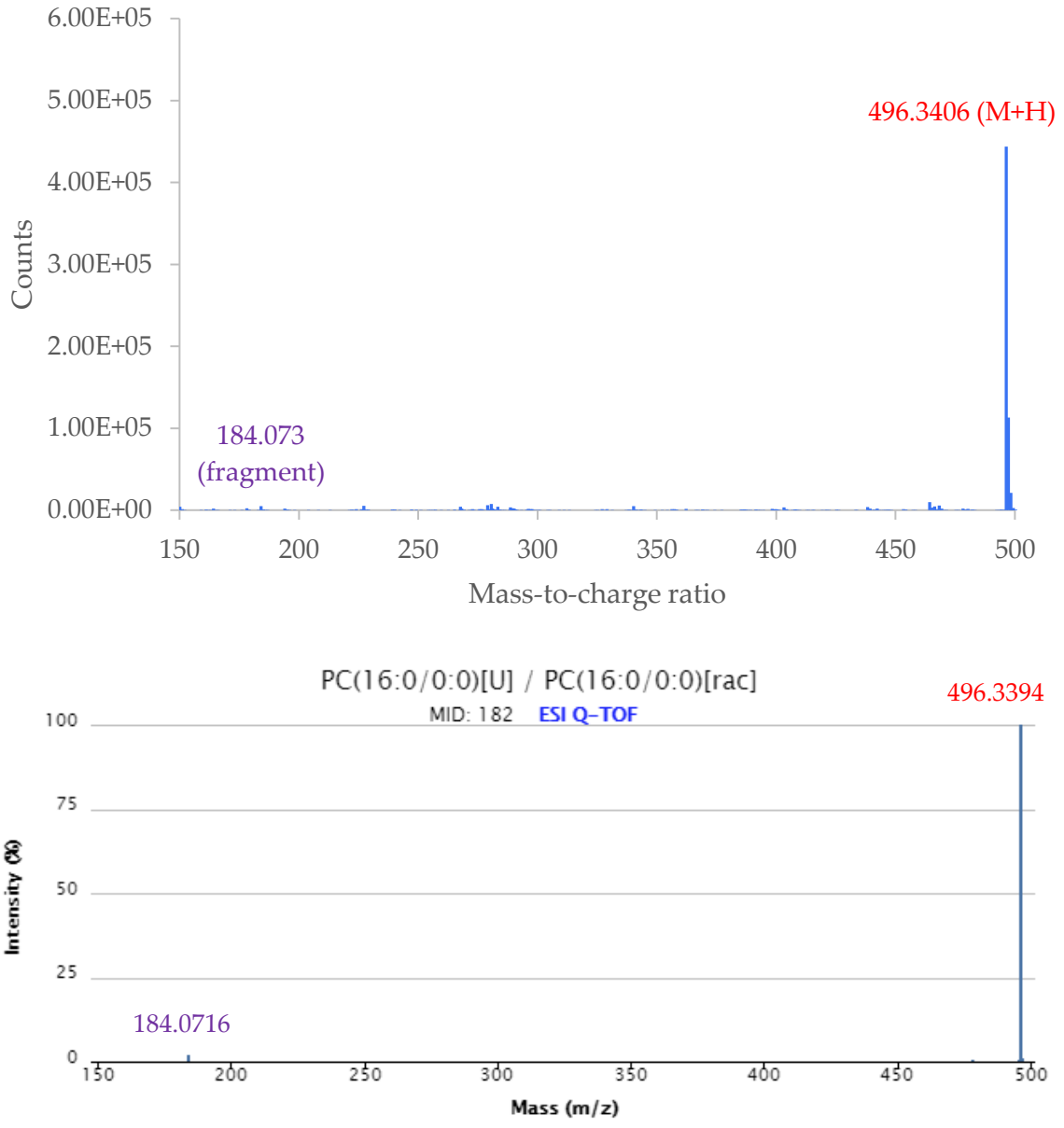

Figure D.1: Mass spectrum of marker 496.3401 m/z at a retention time of 14.48 minutes in QC sample (top) compared to the mass spectrum of PC(16:0/0:0) found on METLIN (bottom)

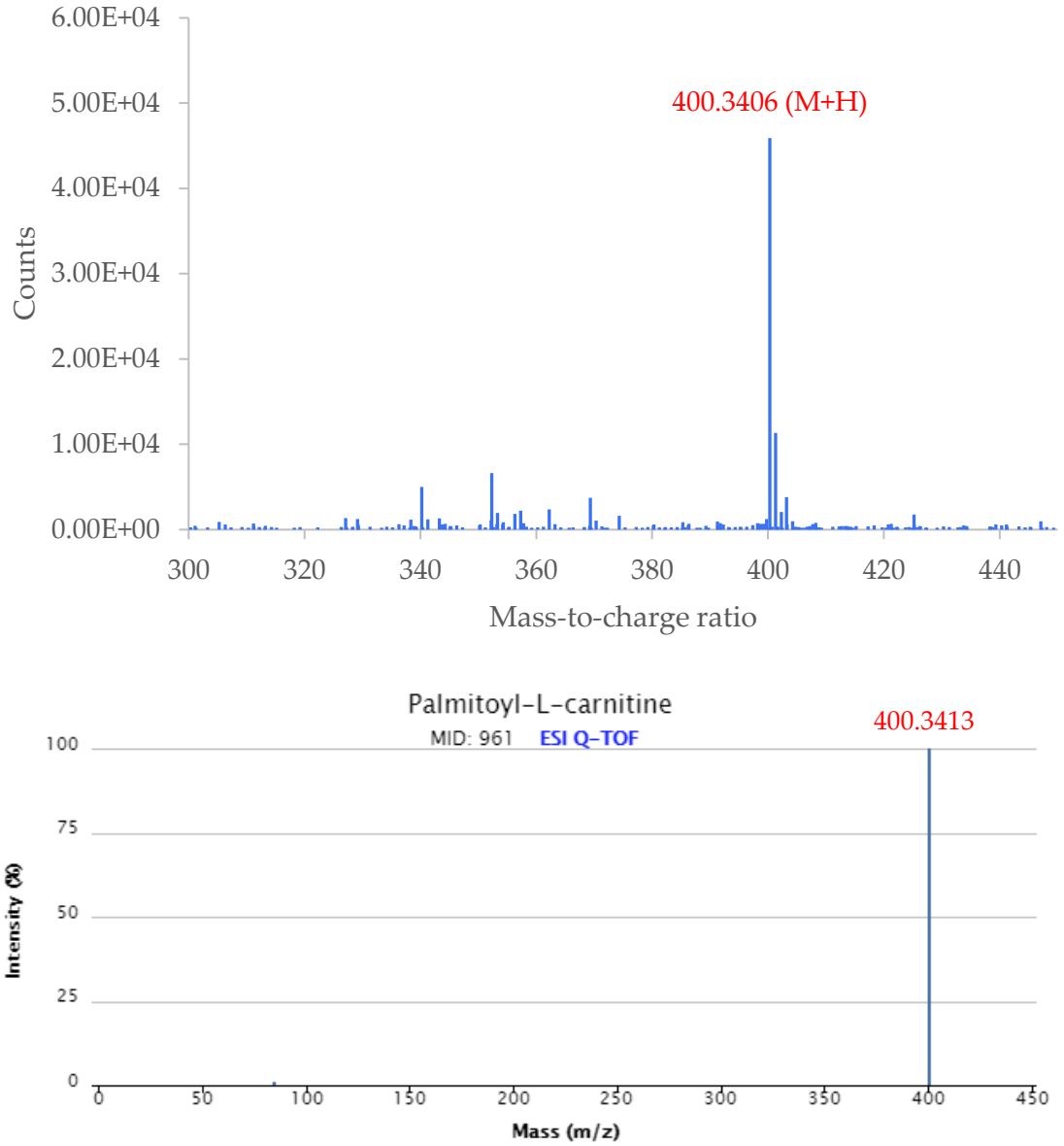

Figure D.2: Mass spectrum of marker 400.3414 m/z at a retention time of 17.92 minutes in QC sample (top) compared to the mass spectrum of palmitoyl carnitine found on METLIN (bottom)

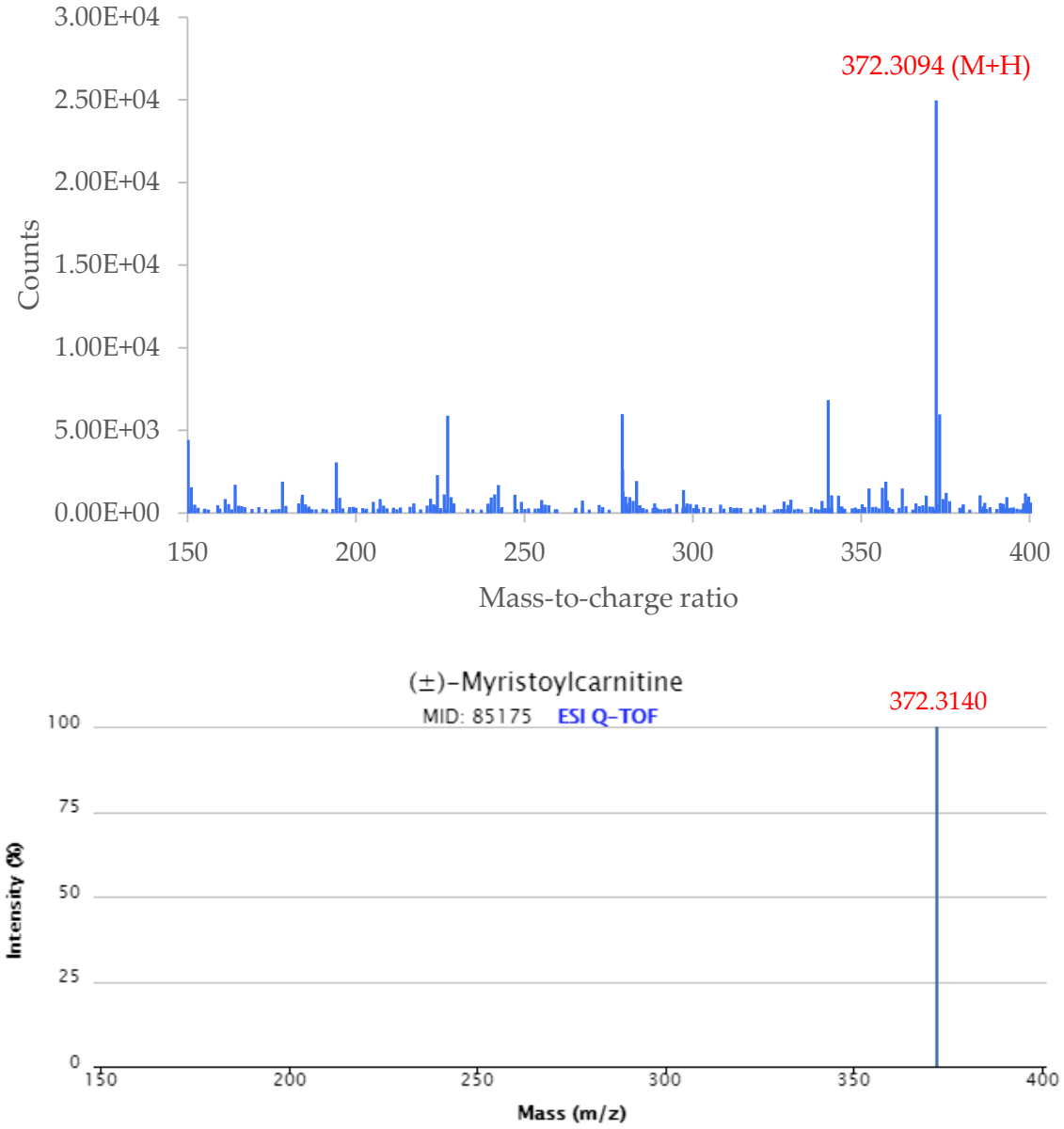

Figure D.3: Mass spectrum of marker 372.3108 m/z at a retention time of 13.75 minutes in QC sample (top) compared to the mass spectrum of myristoyl carnitine found on METLIN (bottom)

Appendix E

Mass spectra comparisons for tentative identifications of markers in cooked beef adulterated with lamb

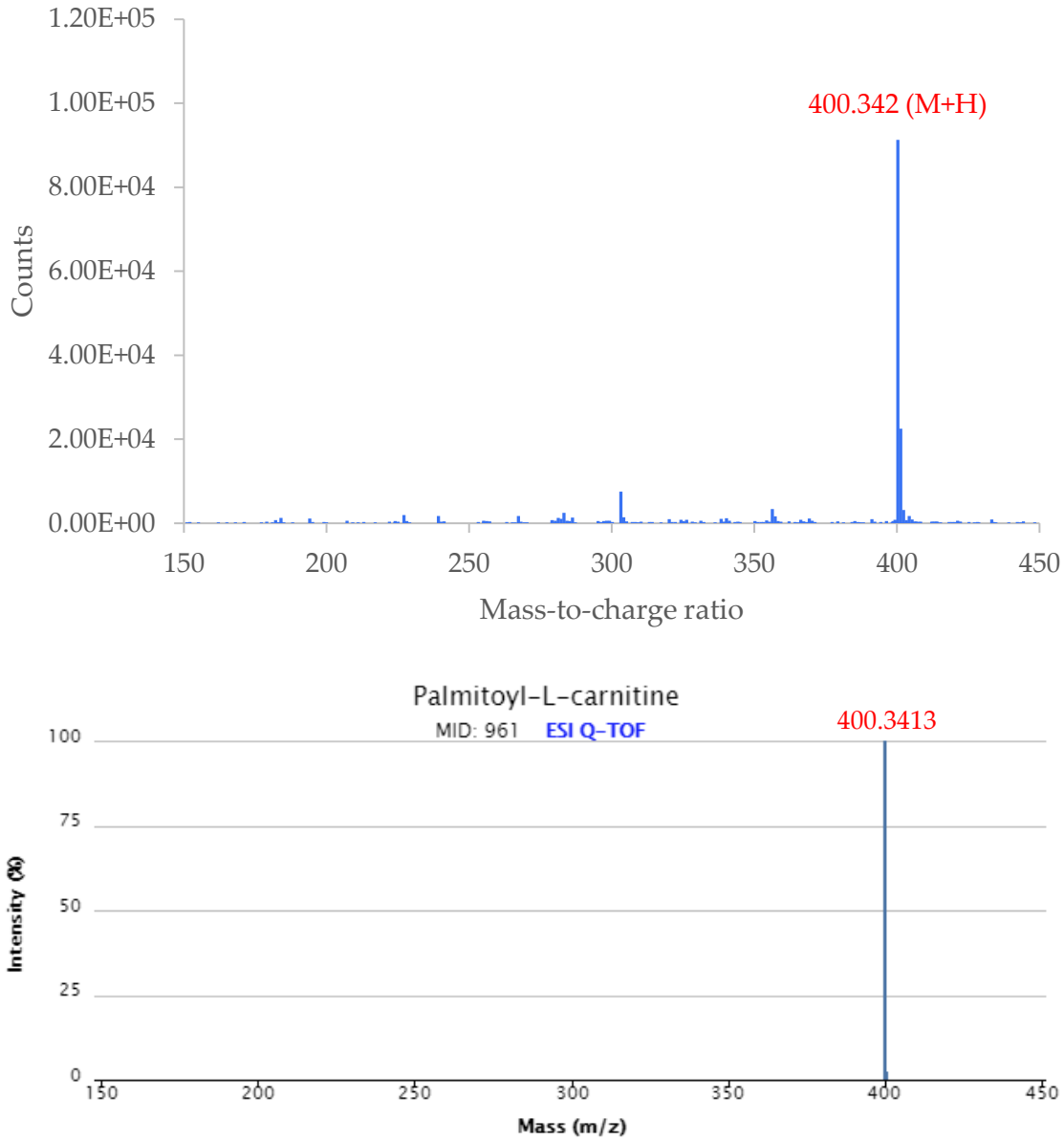

Figure E.1: Mass spectrum of marker 400.3422 m/z at a retention time of 16.20 minutes in QC sample (top) compared to the mass spectrum of palmitoyl carnitine found on METLIN (bottom)

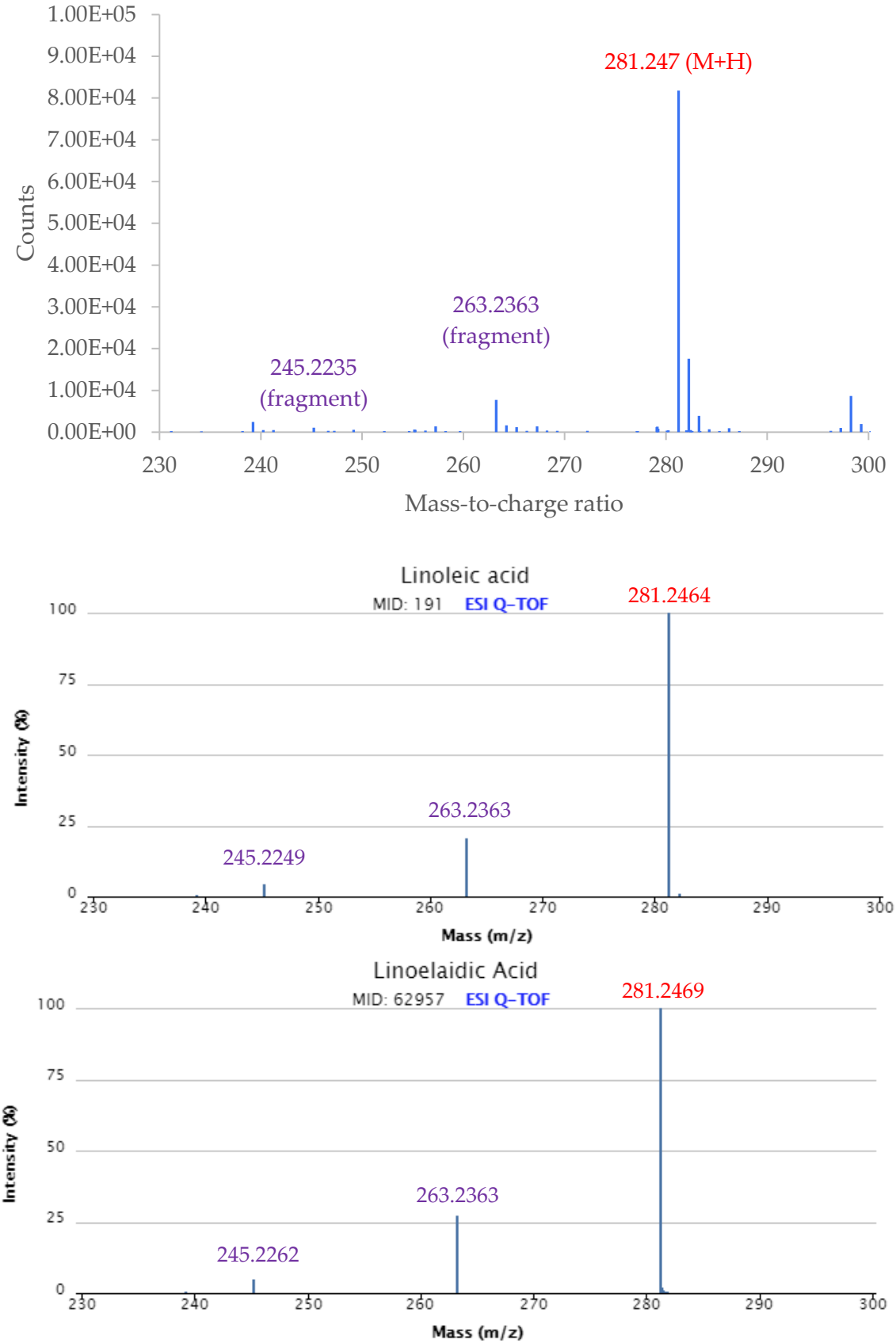

Figure E.2: Mass spectrum of marker 281.2472 m/z at a retention time of 18.50 minutes in QC sample (top) compared to the mass spectra of linoleic acid and linoelaidic acid found on METLIN (bottom)

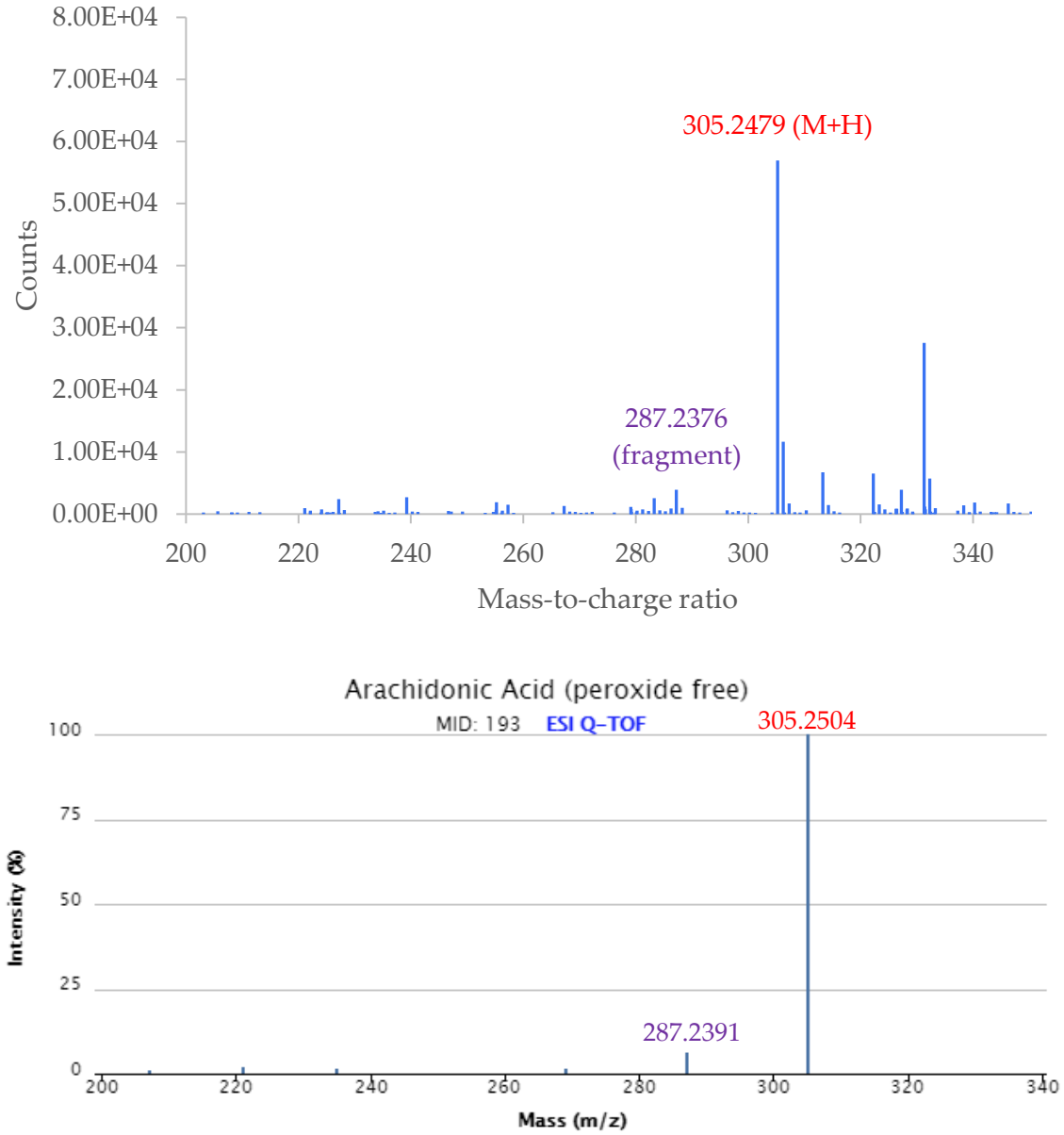

Figure E.3: Mass spectrum of marker 305.2474 m/z at a retention time of 17.99 minutes in QC sample (top) compared to the mass spectrum of arachidonic acid found on METLIN (bottom)

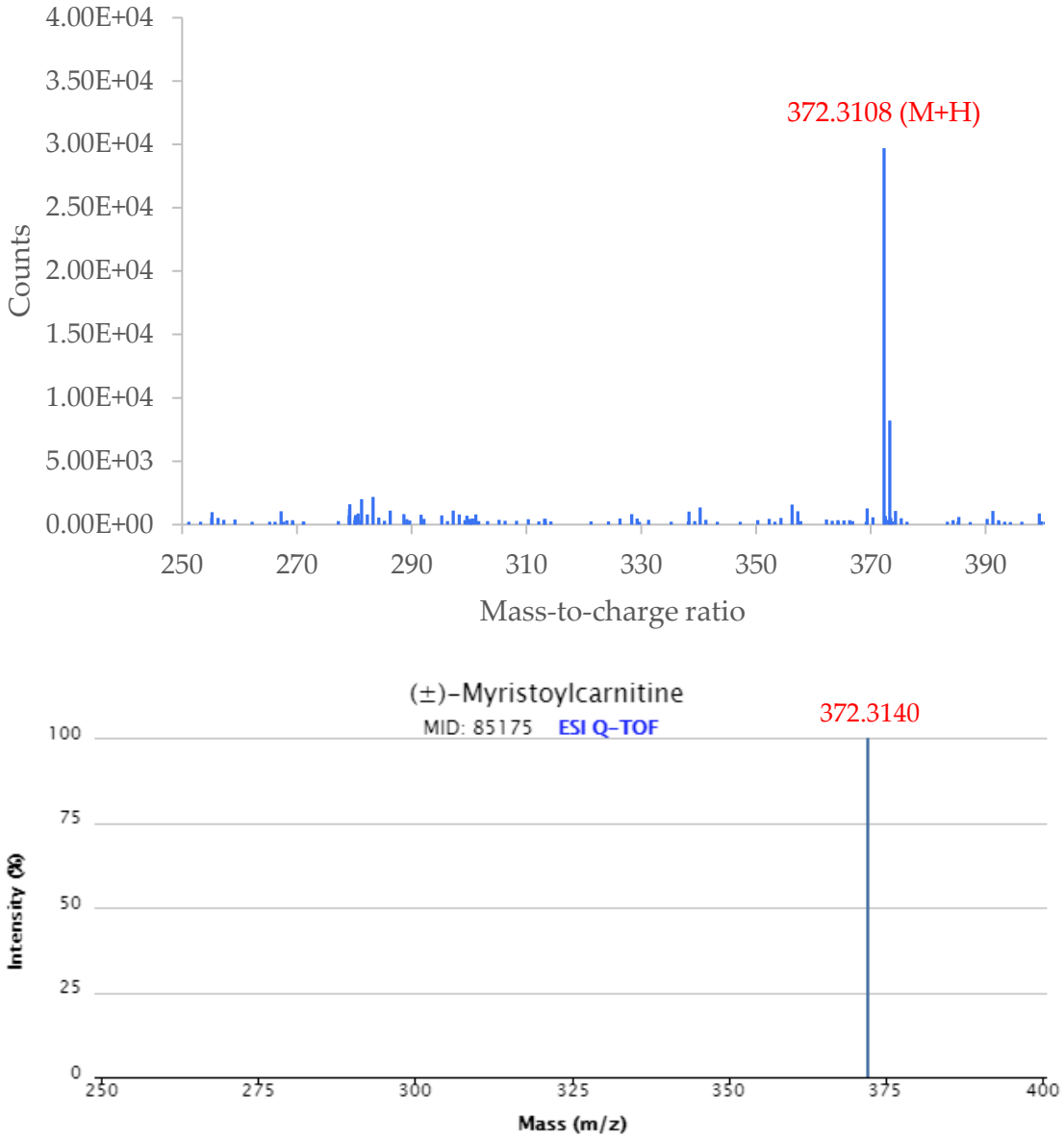

Figure E.4: Mass spectrum of marker 372.3108 m/z at a retention time of 12.85 minutes in QC sample (top) compared to the mass spectrum of myristoyl carnitine found on METLIN (bottom)

Appendix F

Mass spectra comparisons for tentative identifications of markers in cooked beef adulterated with turkey

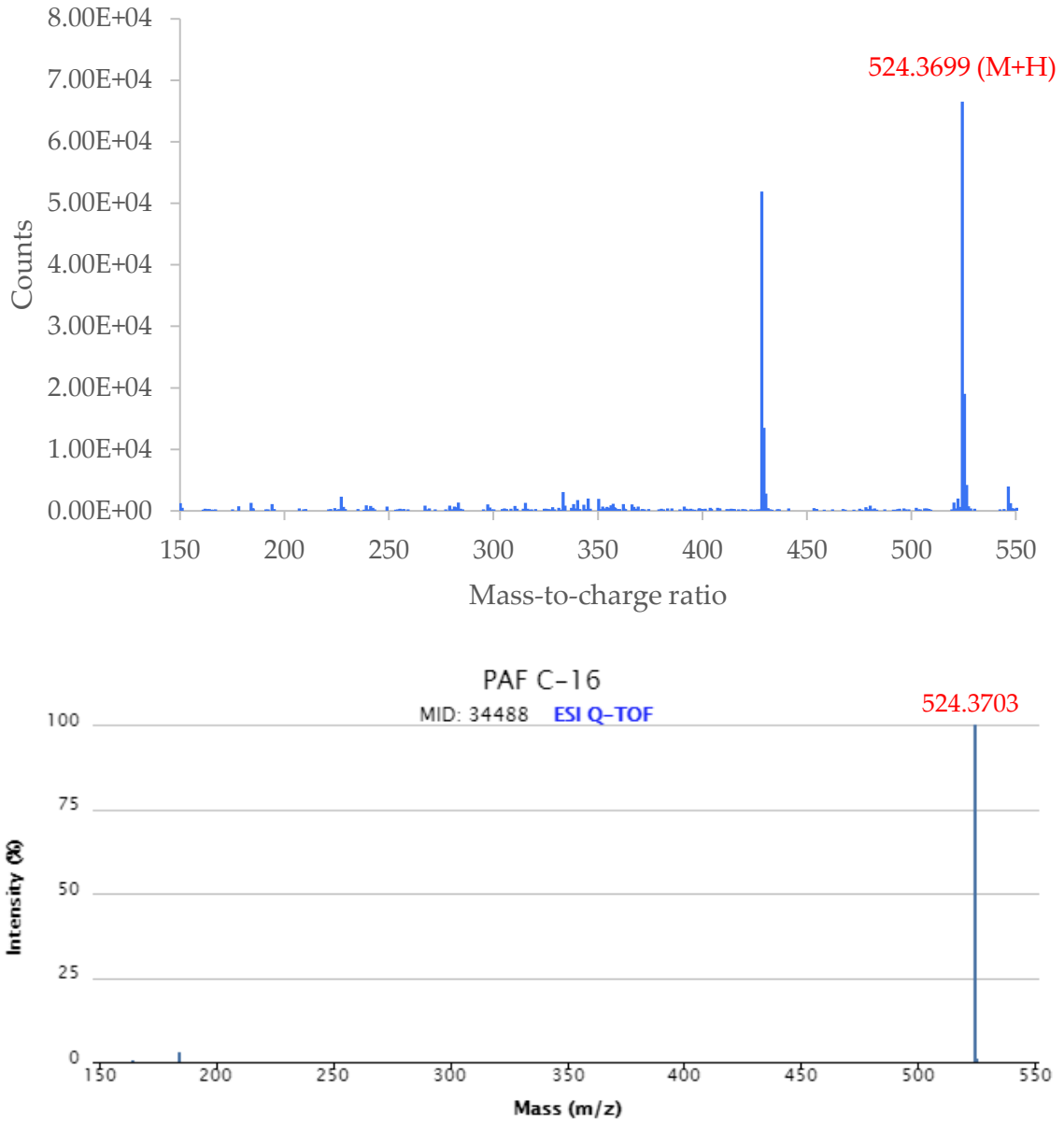

Figure F.1: Mass spectrum of marker 524.3707 m/z at a retention time of 20.63 minutes in QC sample (top) compared to the mass spectrum of PAF C-16 found on METLIN (bottom)

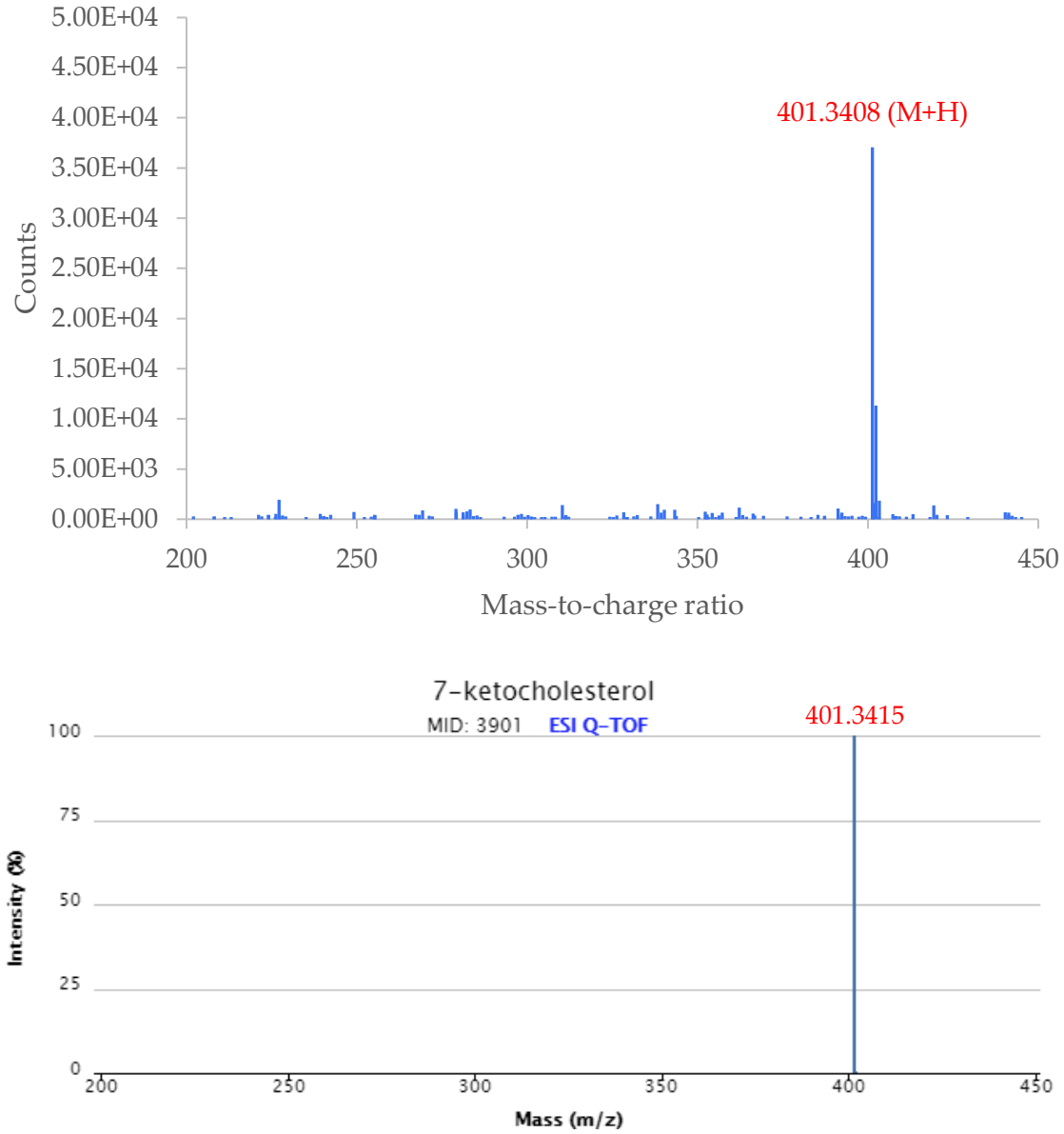

Figure F.2: Mass spectrum of marker 401.3412 m/z at a retention time of 26.42 minutes in QC sample (top) compared to the mass spectrum of 7-ketocholesterol found on METLIN (bottom)

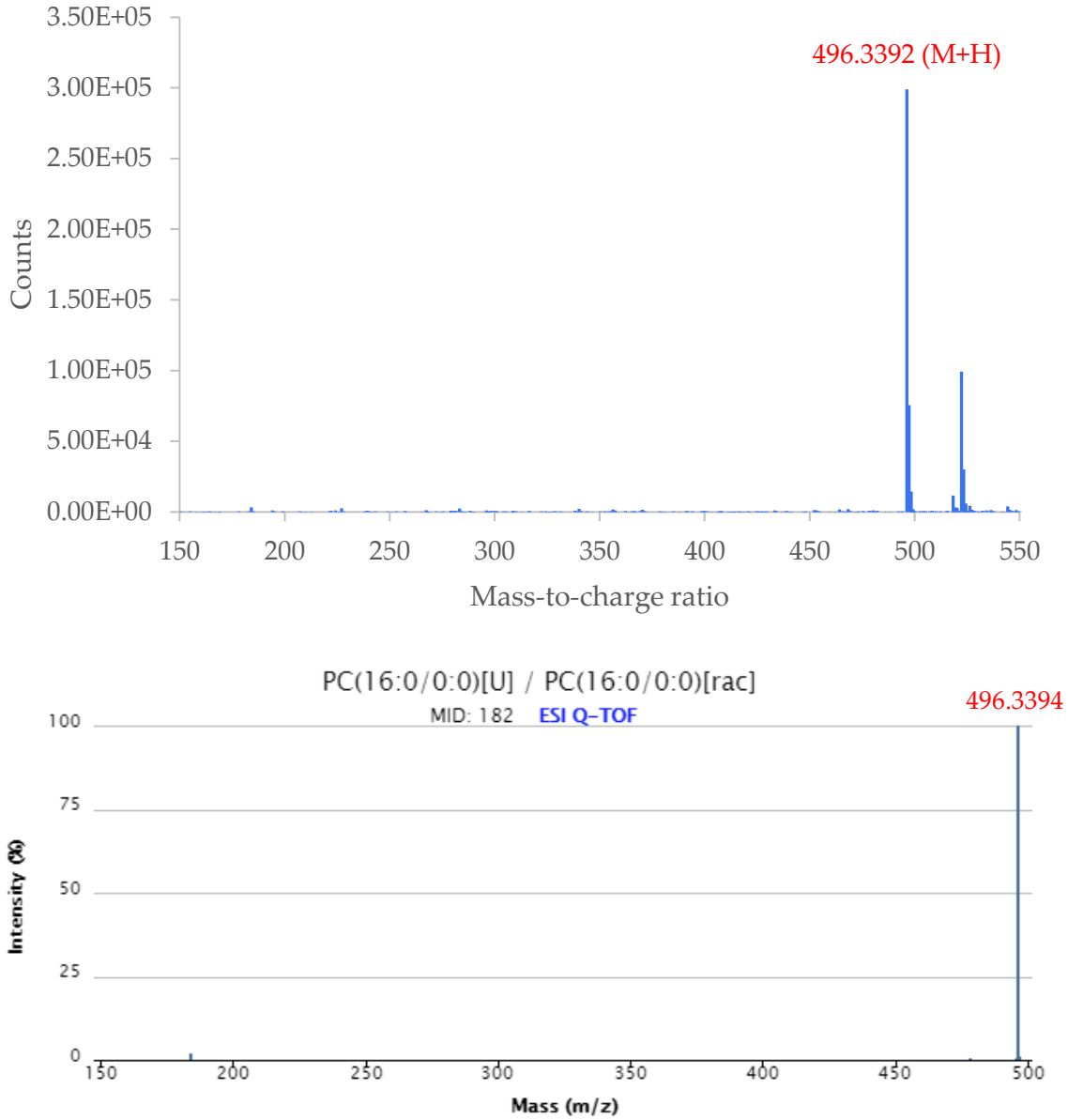

Figure F.3: Mass spectrum of marker 496.3399 m/z at a retention time of 15.43 minutes in QC sample (top) compared to the mass spectrum of PC(16:0/0:0) found on METLIN (bottom)

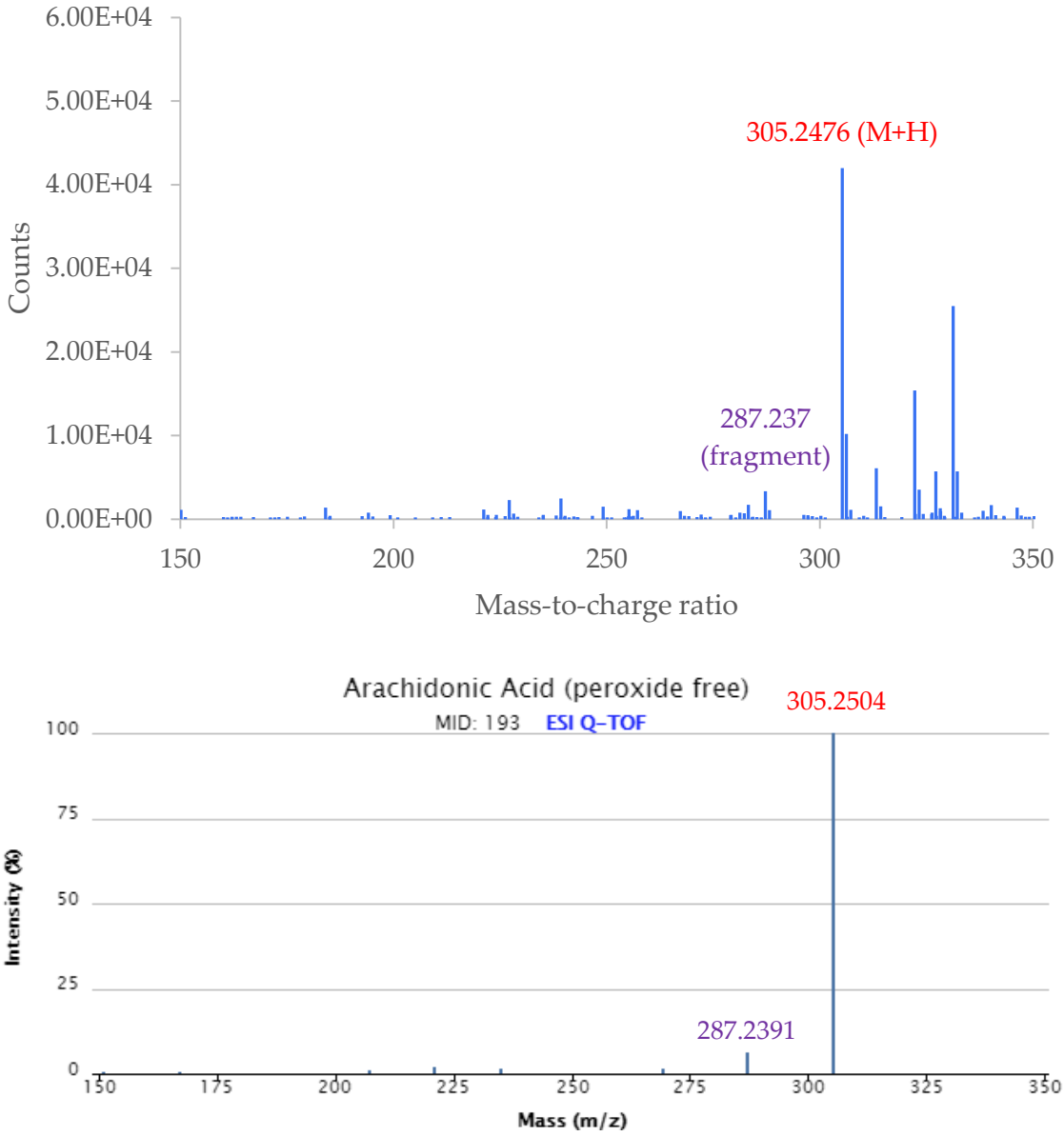

Figure F.4: Mass spectrum of marker 305.2474 m/z at a retention time of 18.01 minutes in QC sample (top) compared to the mass spectrum of arachidonic acid found on METLIN (bottom)

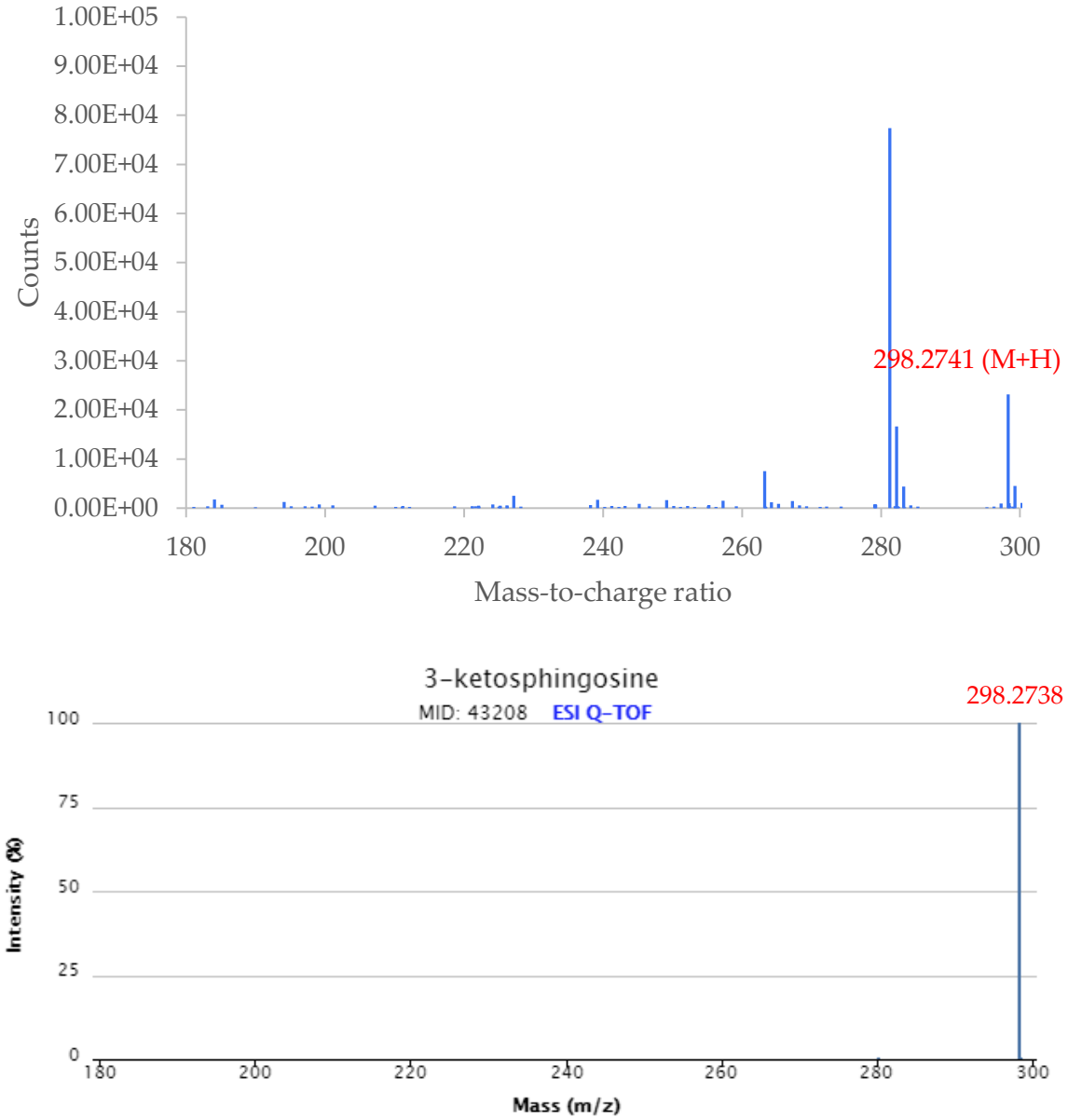

Figure F.5: Mass spectrum of marker 298.2738 m/z at a retention time of 18.53 minutes in QC sample (top) compared to the mass spectrum of 3-ketosphingosine found on METLIN (bottom)

Appendix G

Mass spectra comparisons for tentative identifications of markers in chicken muscle tissue stored at room temperature

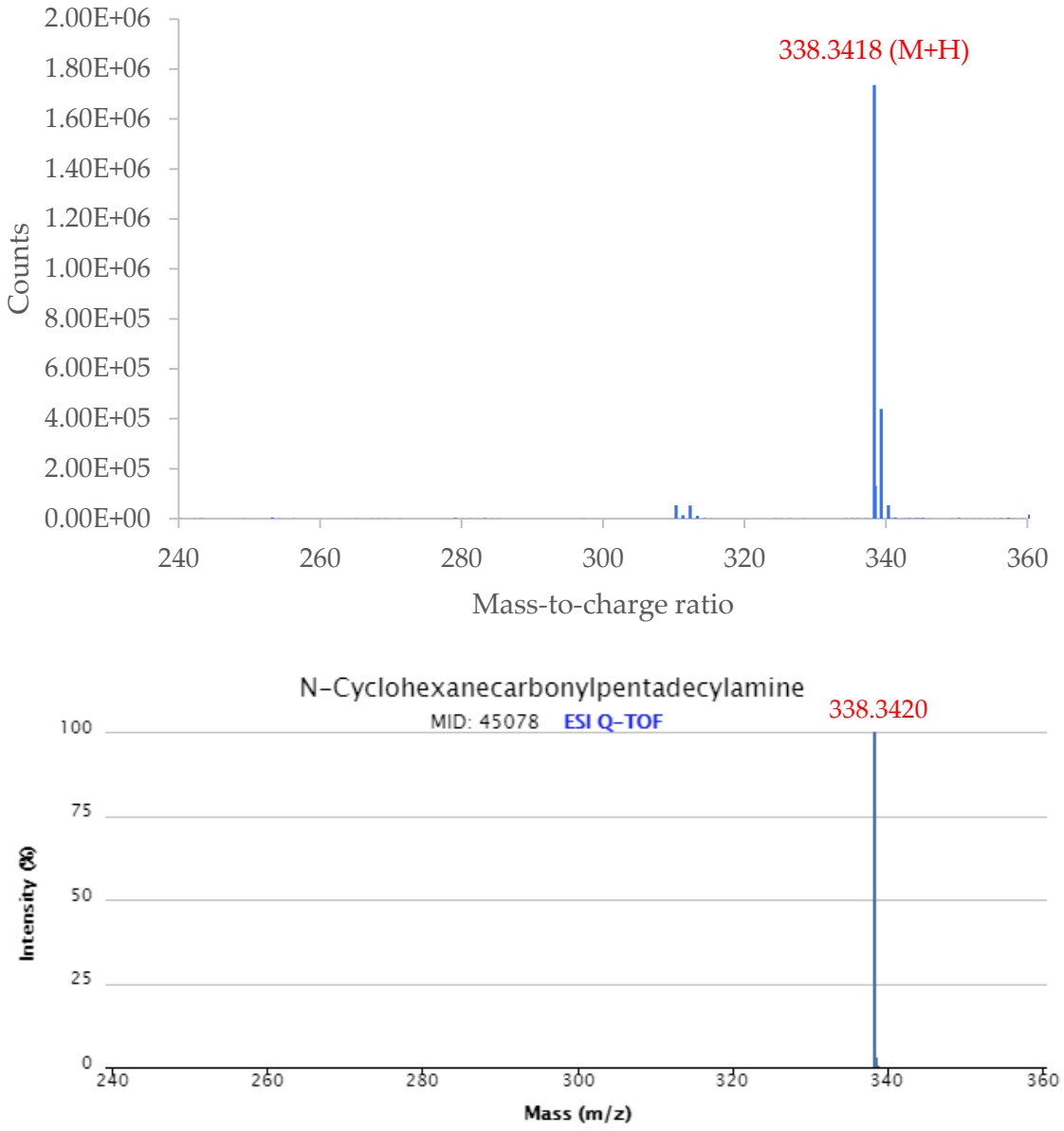

Figure G.1: Mass spectrum of marker 338.3416 m/z at a retention time of 23.81 minutes in QC sample (top) compared to the mass spectrum of N-cyclohexanecarbonylpentadecylamine found on METLIN (bottom)

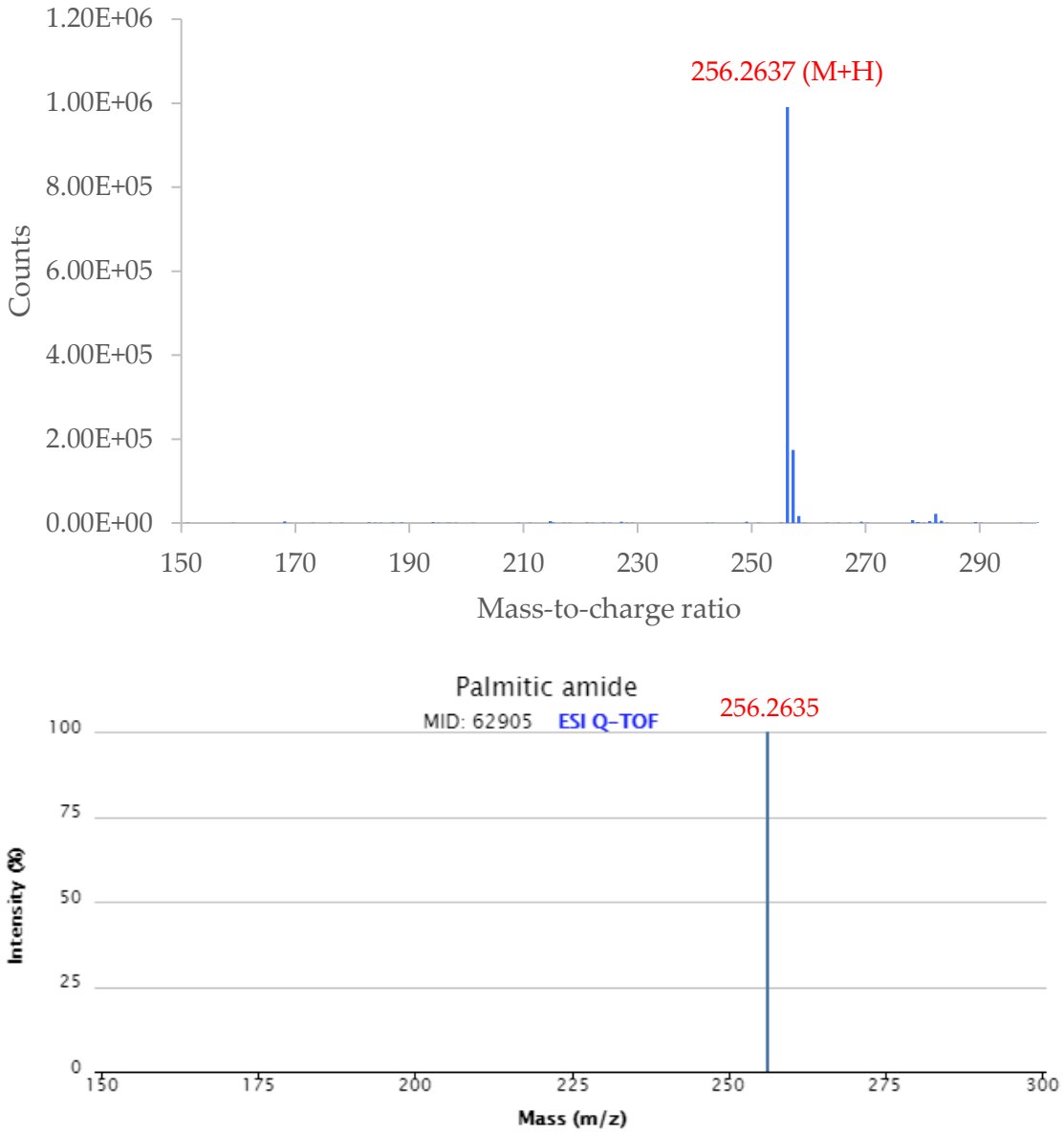

Figure G.2: Mass spectrum of marker 256.2631 m/z at a retention time of 20.21 minutes in QC sample (top) compared to the mass spectrum of palmitic amide found on METLIN (bottom)

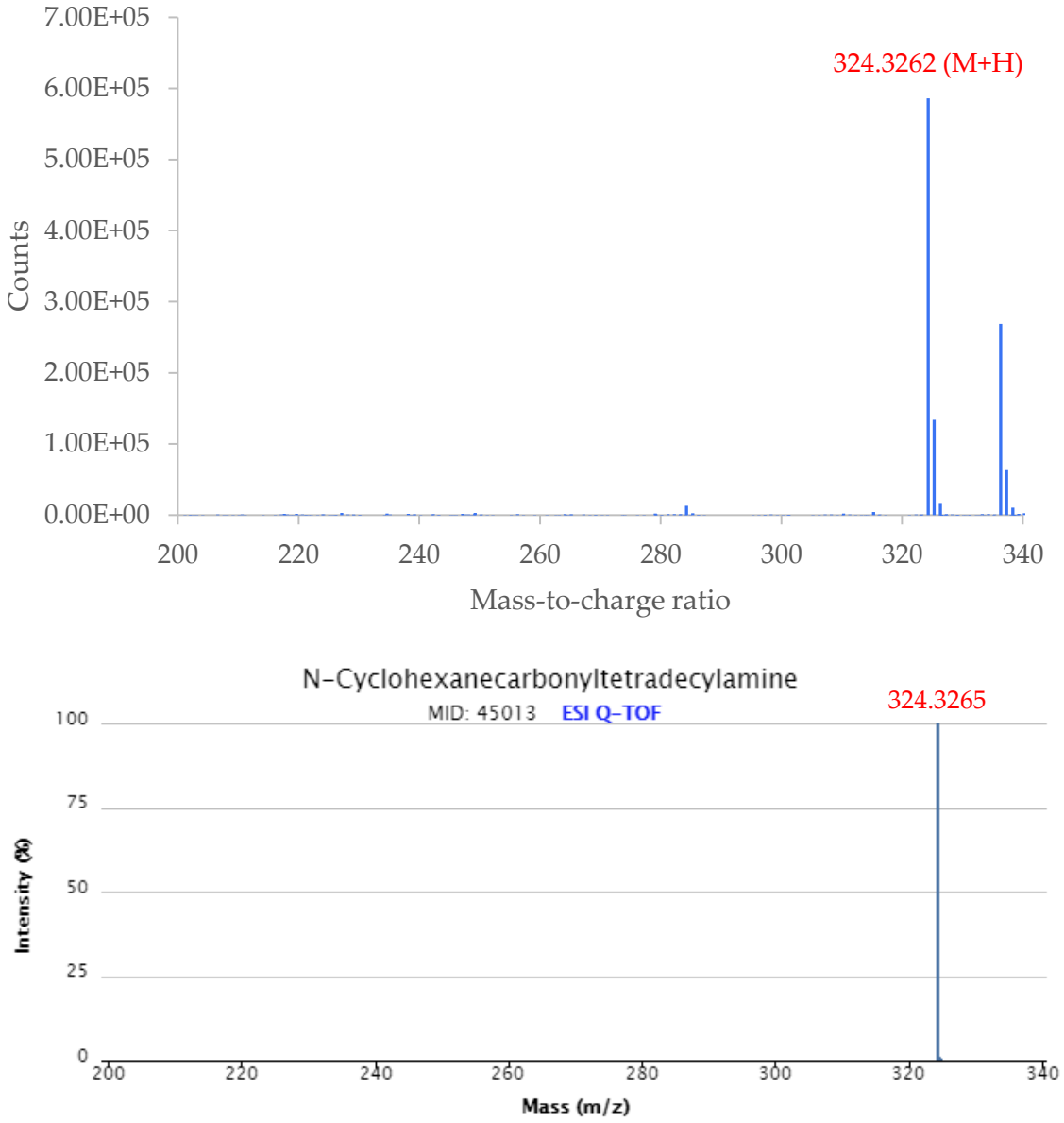

Figure G.3: Mass spectrum of marker 324.3254 m/z at a retention time of 21.55 minutes in QC sample (top) compared to the mass spectrum of N-cyclohexanecarbonyltetradecylamine found on METLIN (bottom)

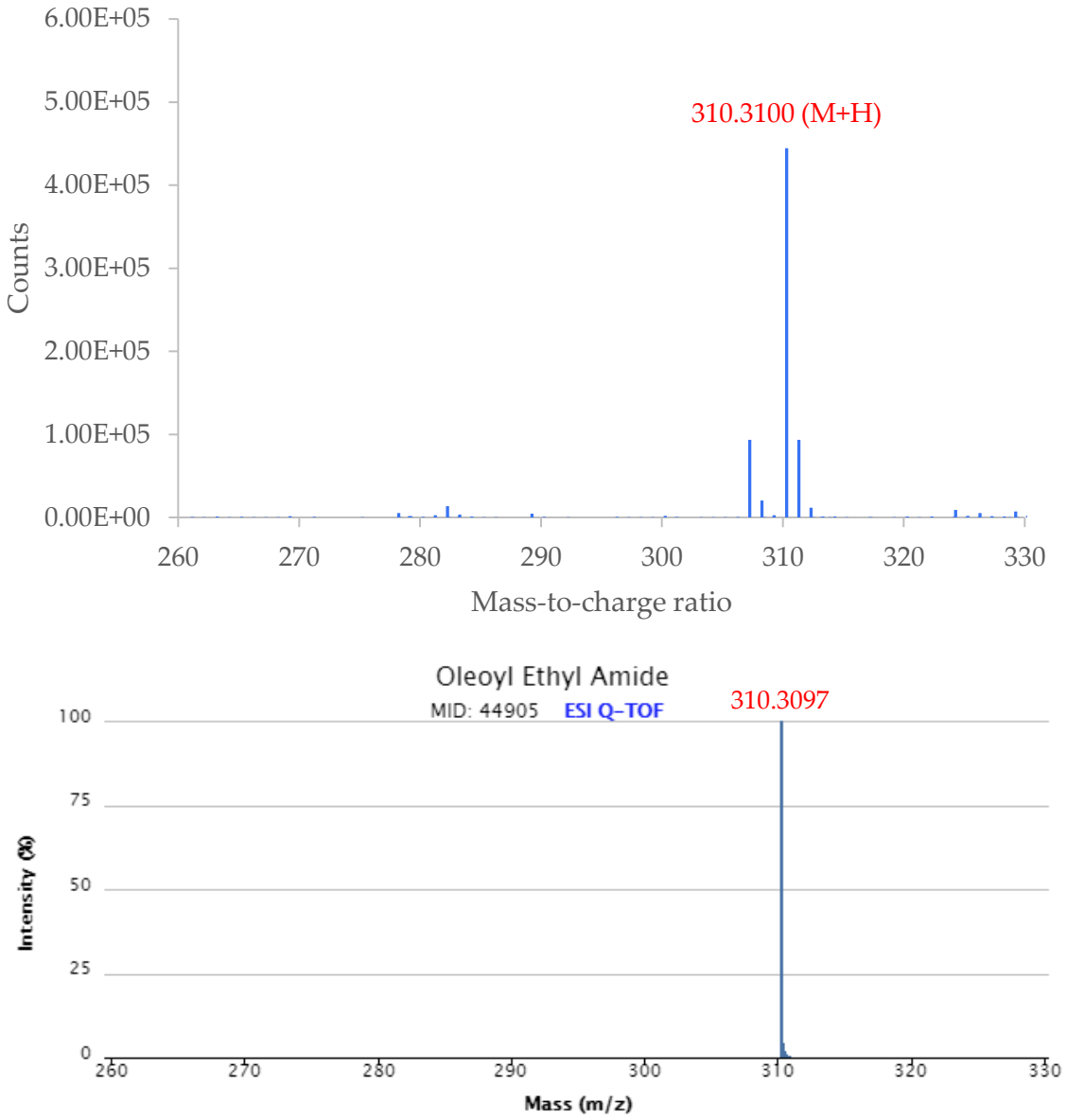

Figure G.4: Mass spectrum of marker 310.3097 m/z at a retention time of 20.19 minutes in QC sample (top) compared to the mass spectrum of oleoyl ethyl amide found on METLIN (bottom)

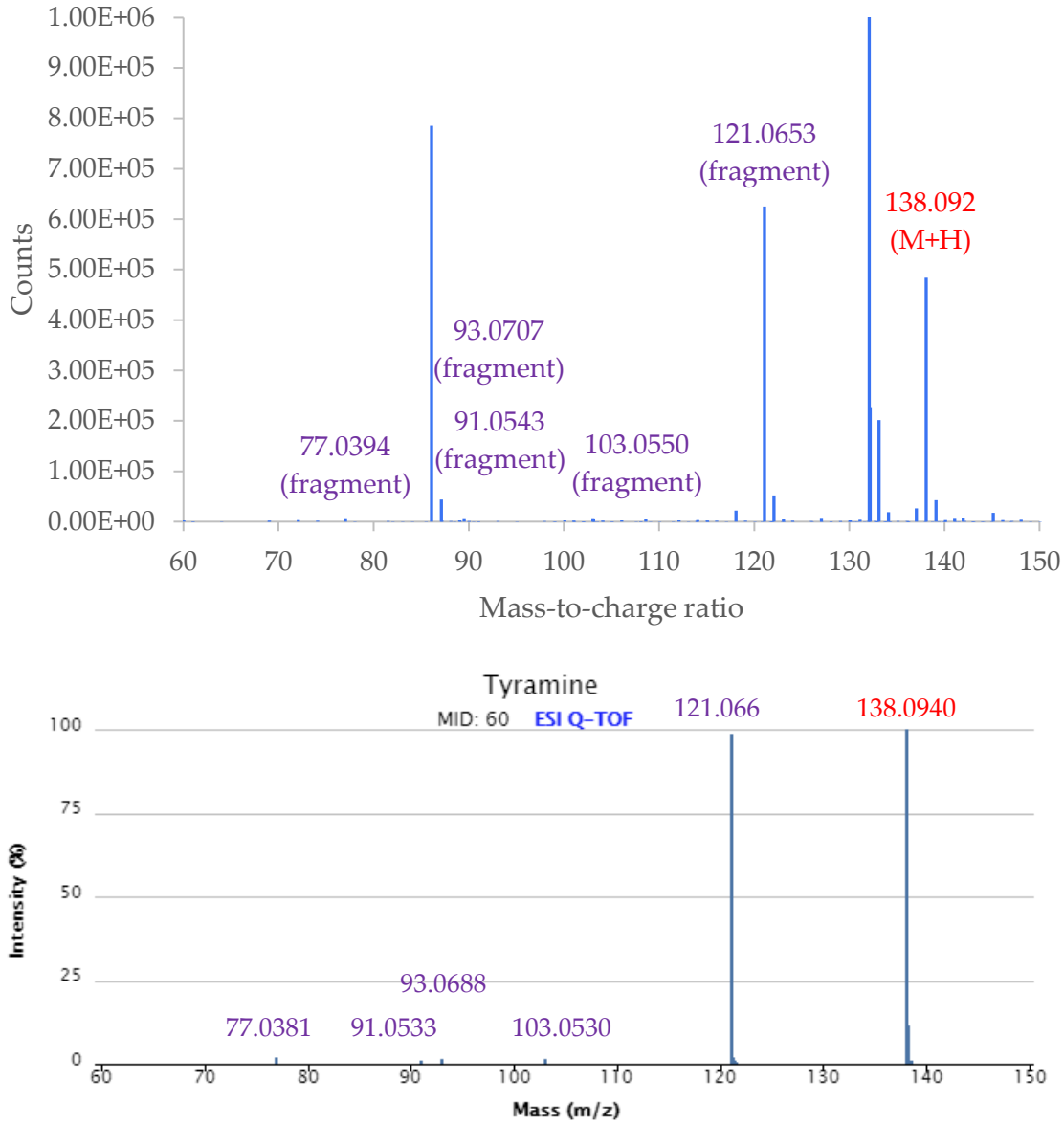

Figure G.5: Mass spectrum of marker 138.0911 m/z at a retention time of 1.50 minutes in QC sample (top) compared to the mass spectrum of tyramine found on METLIN (bottom)

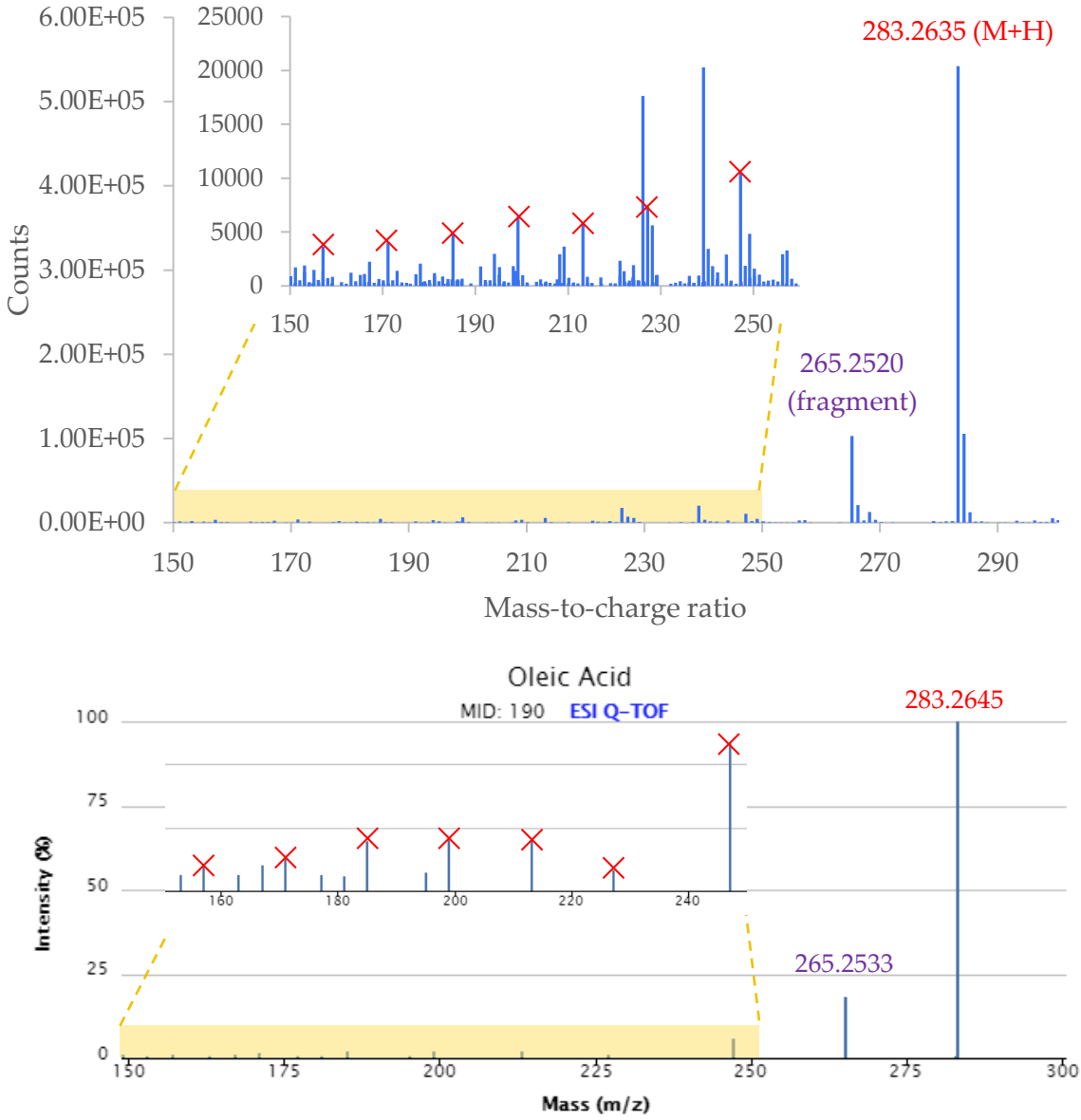

Fragment in raw data spectrum	Fragment in reference spectrum
157.1204	157.1233
171.1388	171.1404
185.1553	185.1518
199.1732	199.1740
213.1848	213.1869
227.1917	227.2016
247.2405	247.2430

Figure G.6: Mass spectrum of marker 283.2630 m/z at a retention time of 20.94 minutes in QC sample (top) compared to the mass spectrum of oleic acid found on METLIN (bottom). Table shows matching fragments in zoomed in spectra

Appendix H

Mass spectra comparisons for tentative identifications of markers in chicken muscle tissue stored at 4°C

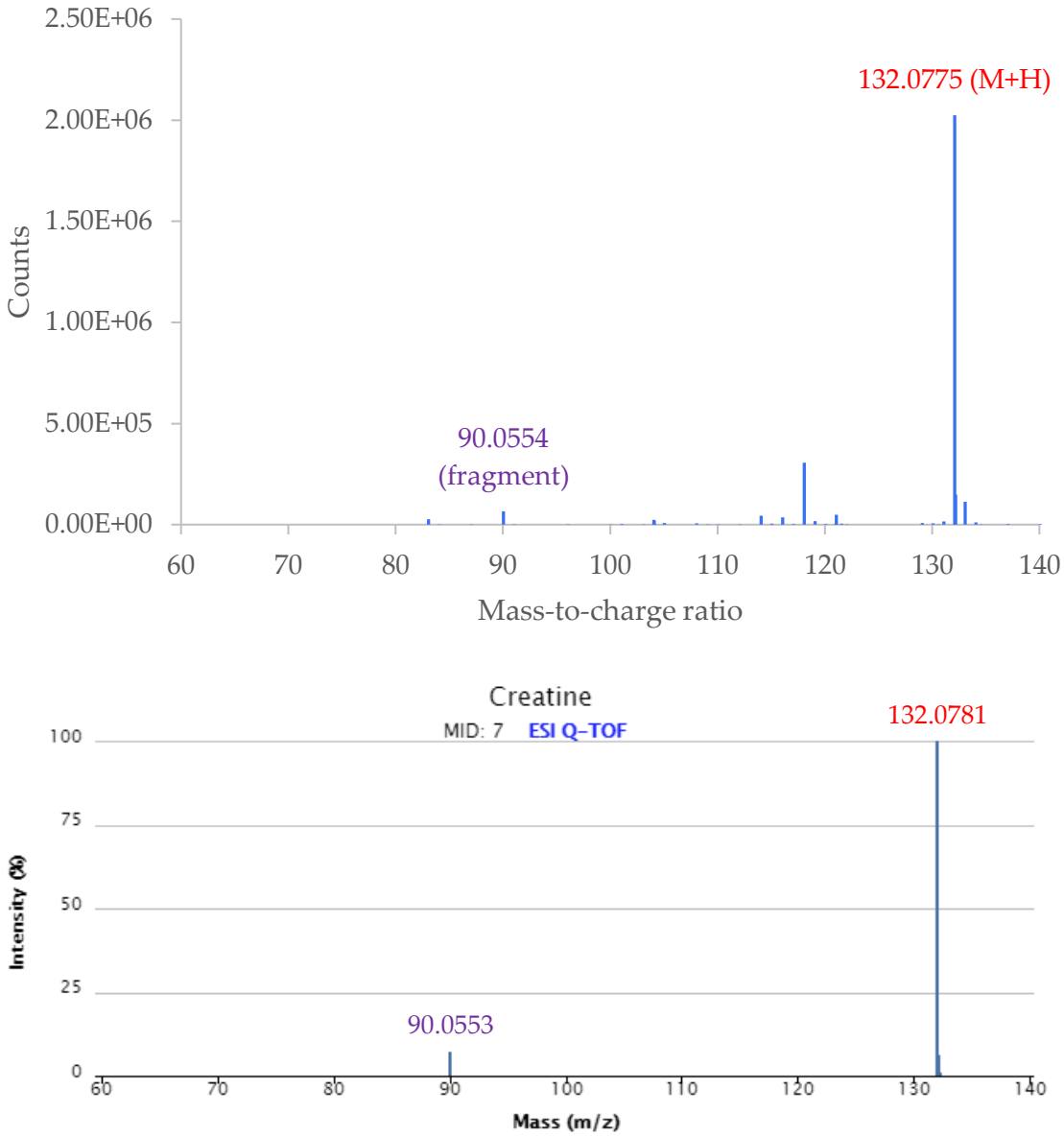

Figure H.1: Mass spectrum of marker 132.0771 m/z at a retention time of 1.03 minutes in QC sample (top) compared to the mass spectrum of creatine found on METLIN (bottom)

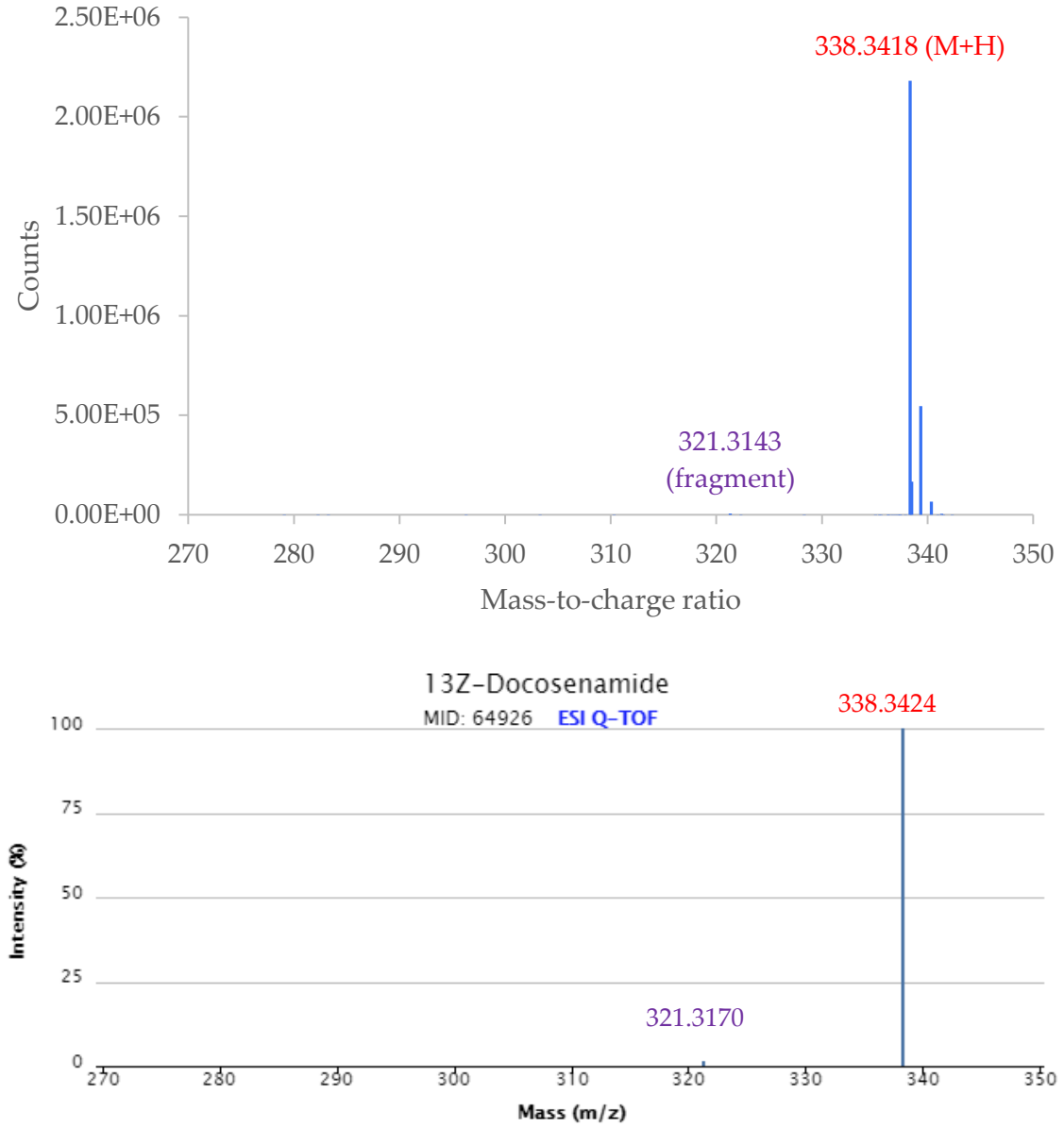

Figure H.2: Mass spectrum of marker 338.3424 m/z at a retention time of 27.68 minutes in QC sample (top) compared to the mass spectrum of 13Z-docosenamide found on METLIN (bottom)

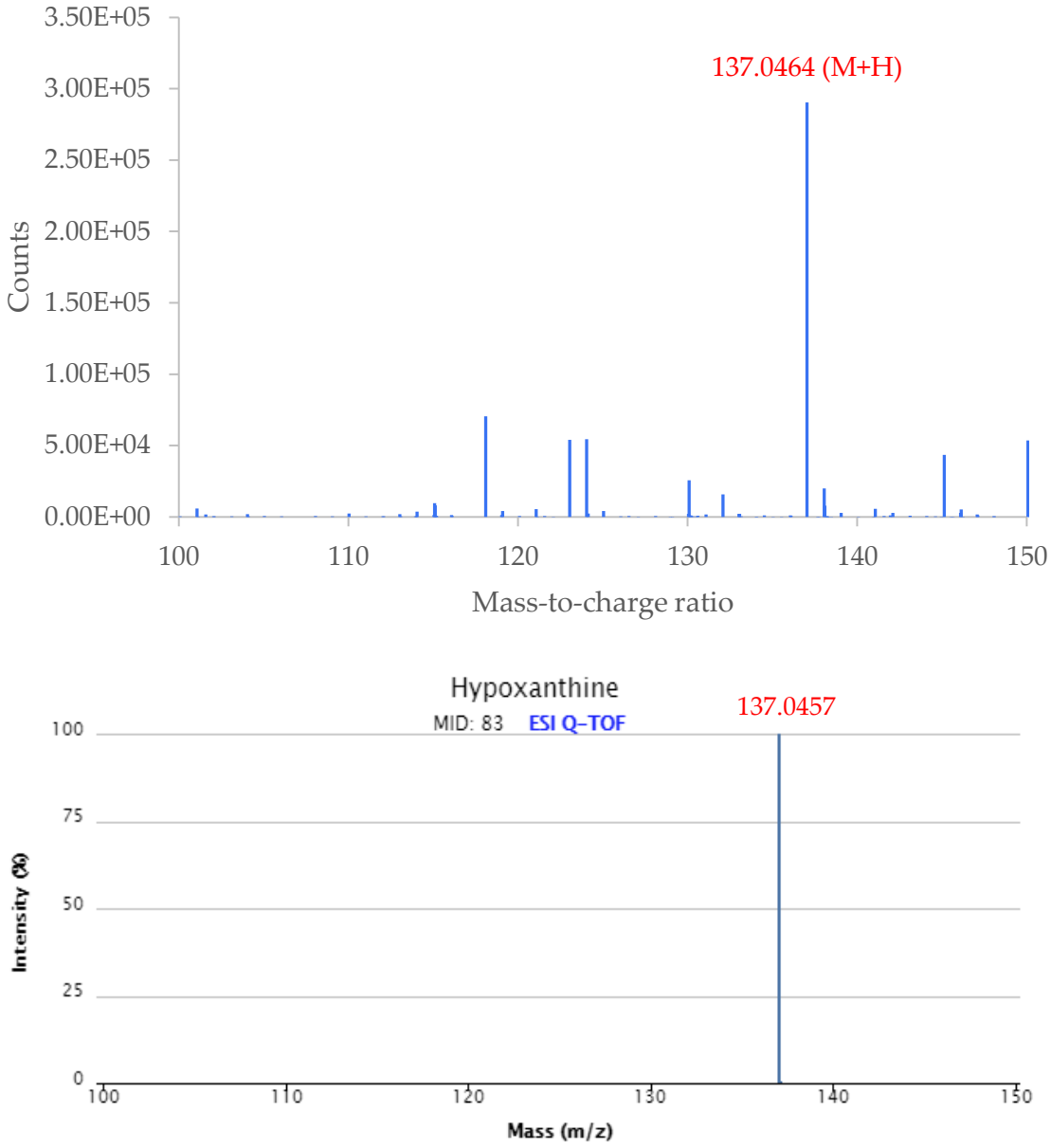

Figure H.3: Mass spectrum of marker 137.0458 m/z at a retention time of 1.32 minutes in QC sample (top) compared to the mass spectrum of hypoxanthine found on METLIN (bottom)

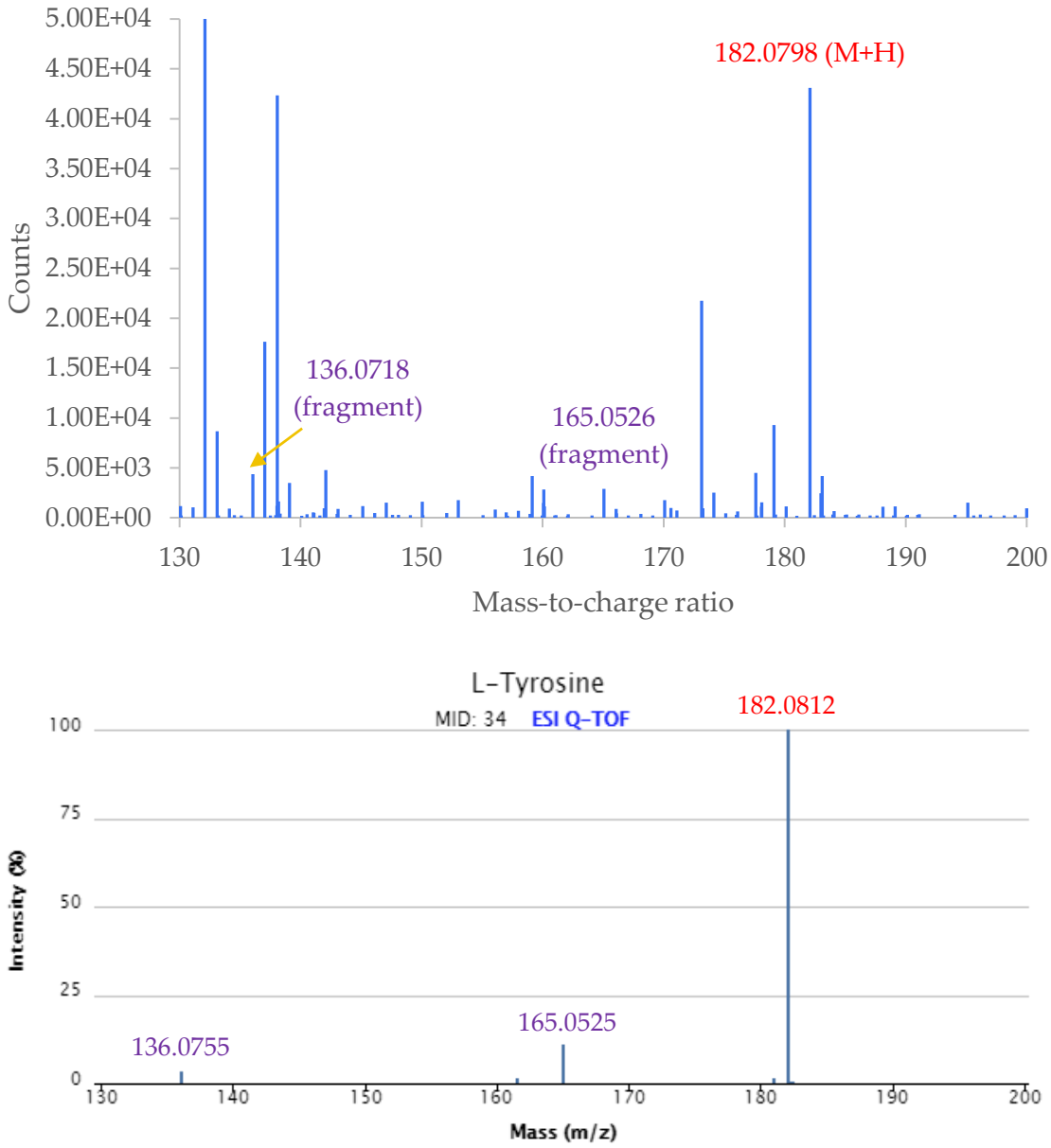

Figure H.4: Mass spectrum of marker 182.0809 m/z at a retention time of 1.38 minutes in QC sample (top) compared to the mass spectrum of tyrosine found on METLIN (bottom)

Appendix I

Mass spectra comparisons for tentative identifications of markers in chicken muscle tissue stored at room temperature and 4°C

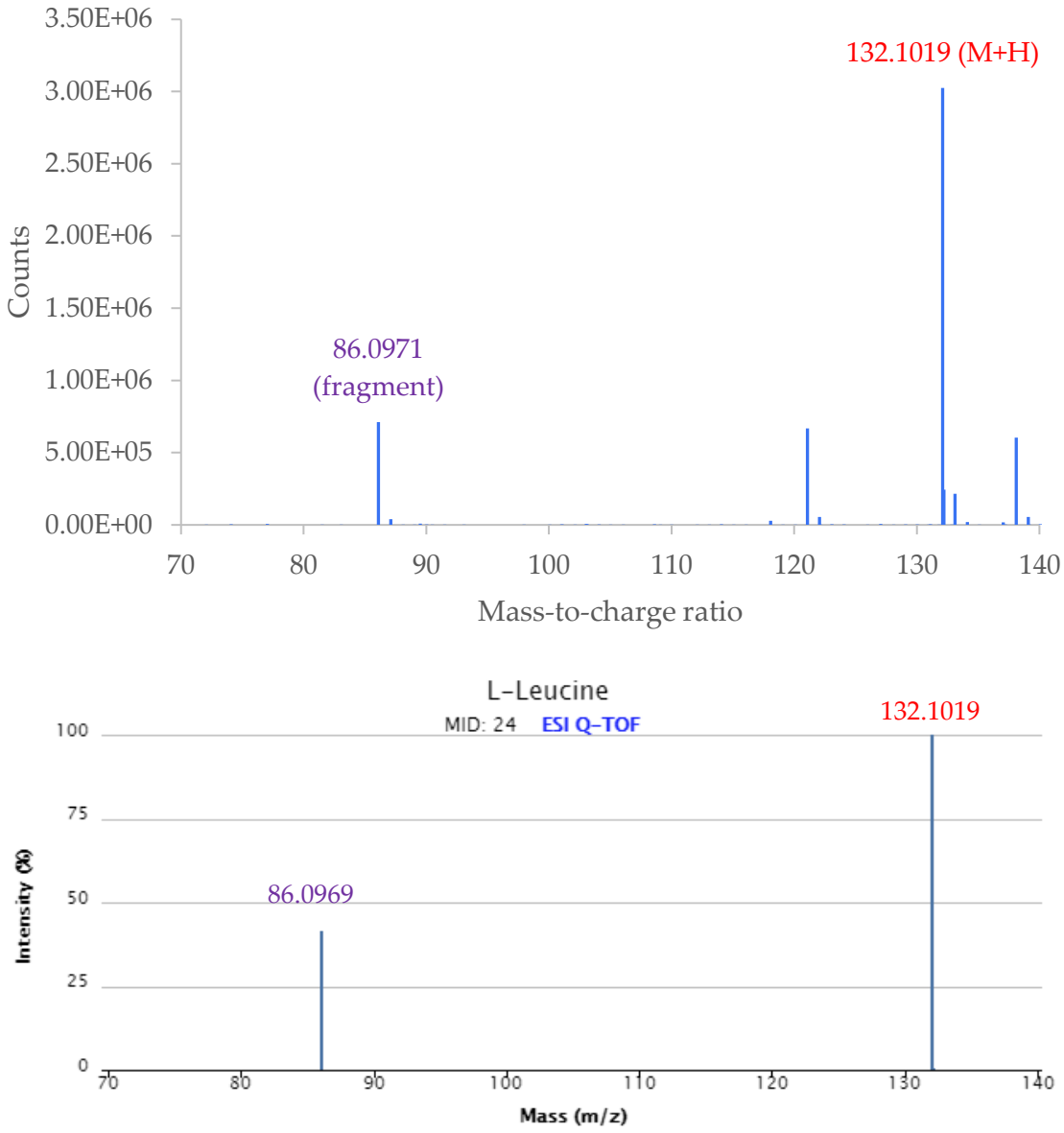

Figure I.1: Mass spectrum of marker 132.1020 m/z at a retention time of 1.50 minutes in QC sample (top) compared to the mass spectrum of leucine found on METLIN (bottom)

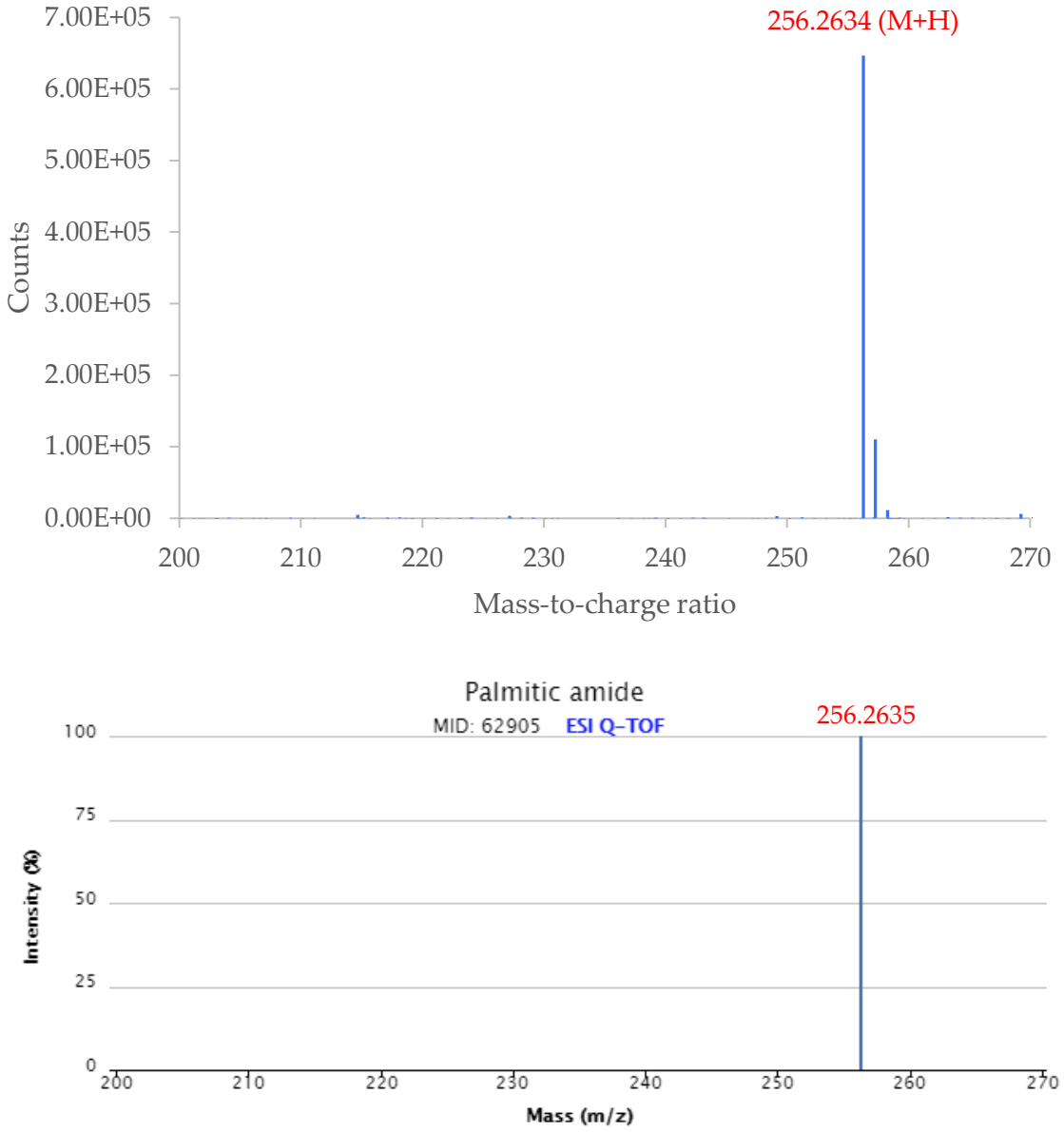

Figure I.2: Mass spectrum of marker 256.2630 m/z at a retention time of 19.90 minutes in QC sample (top) compared to the mass spectrum of palmitic amide found on METLIN (bottom)

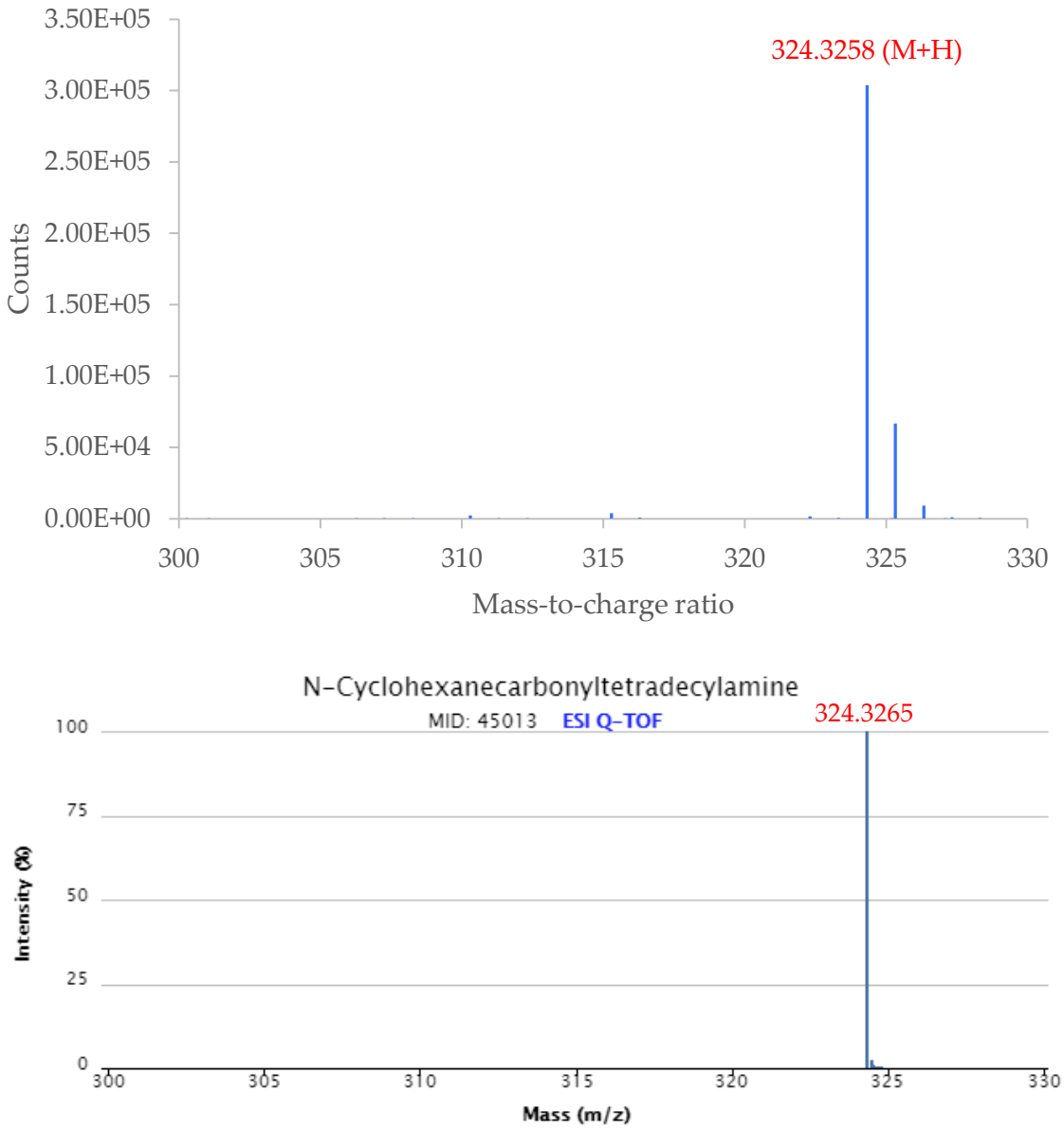

Figure I.3: Mass spectrum of marker 324.3254 m/z at a retention time of 21.43 minutes in QC sample (top) compared to the mass spectrum of N-cyclohexanecarbonyltetradecylamine found on METLIN (bottom)

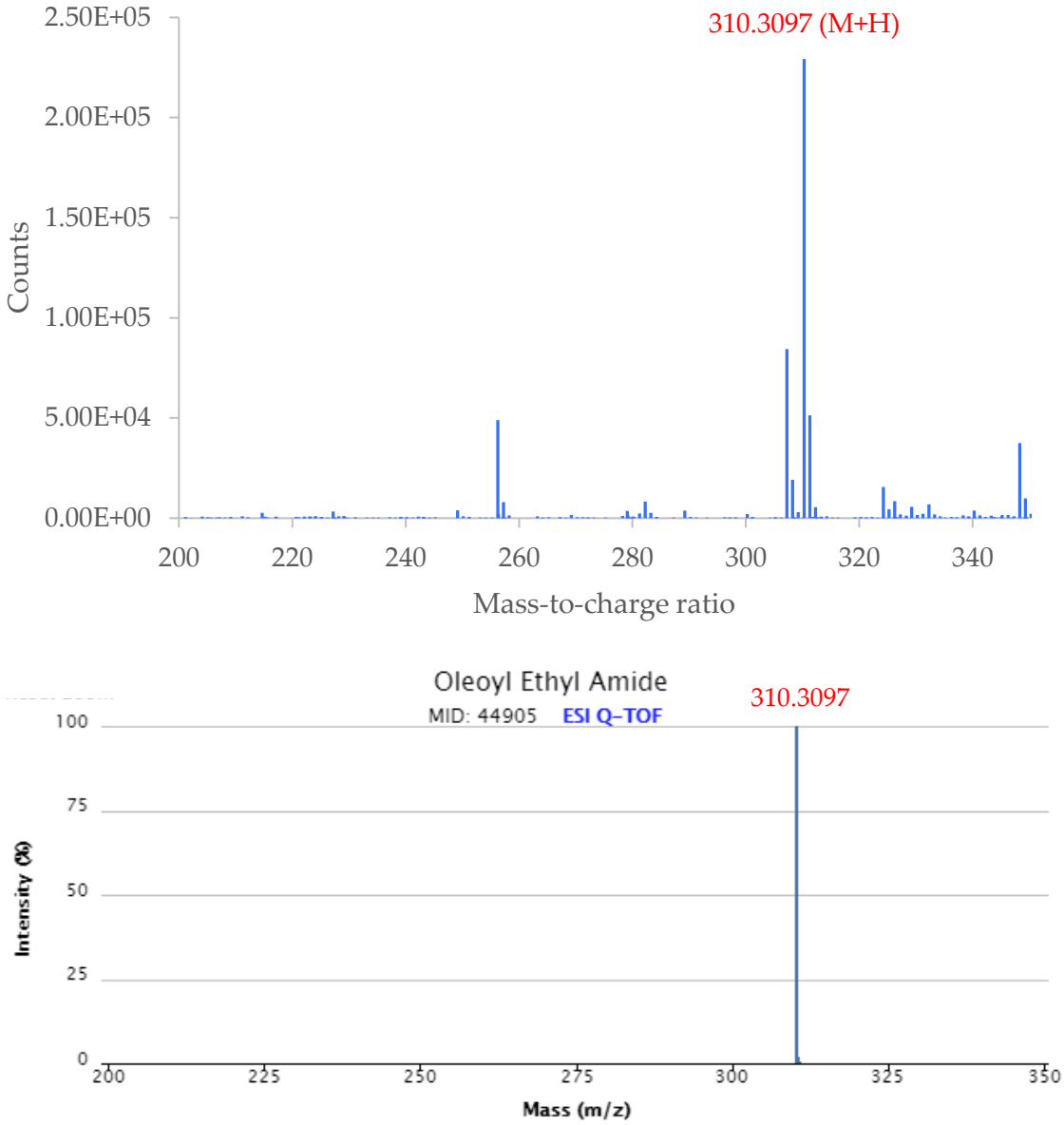

Figure I.4: Mass spectrum of marker 310.3098 m/z at a retention time of 20.08 minutes in QC sample (top) compared to the mass spectrum of oleoyl ethyl amide found on METLIN (bottom)

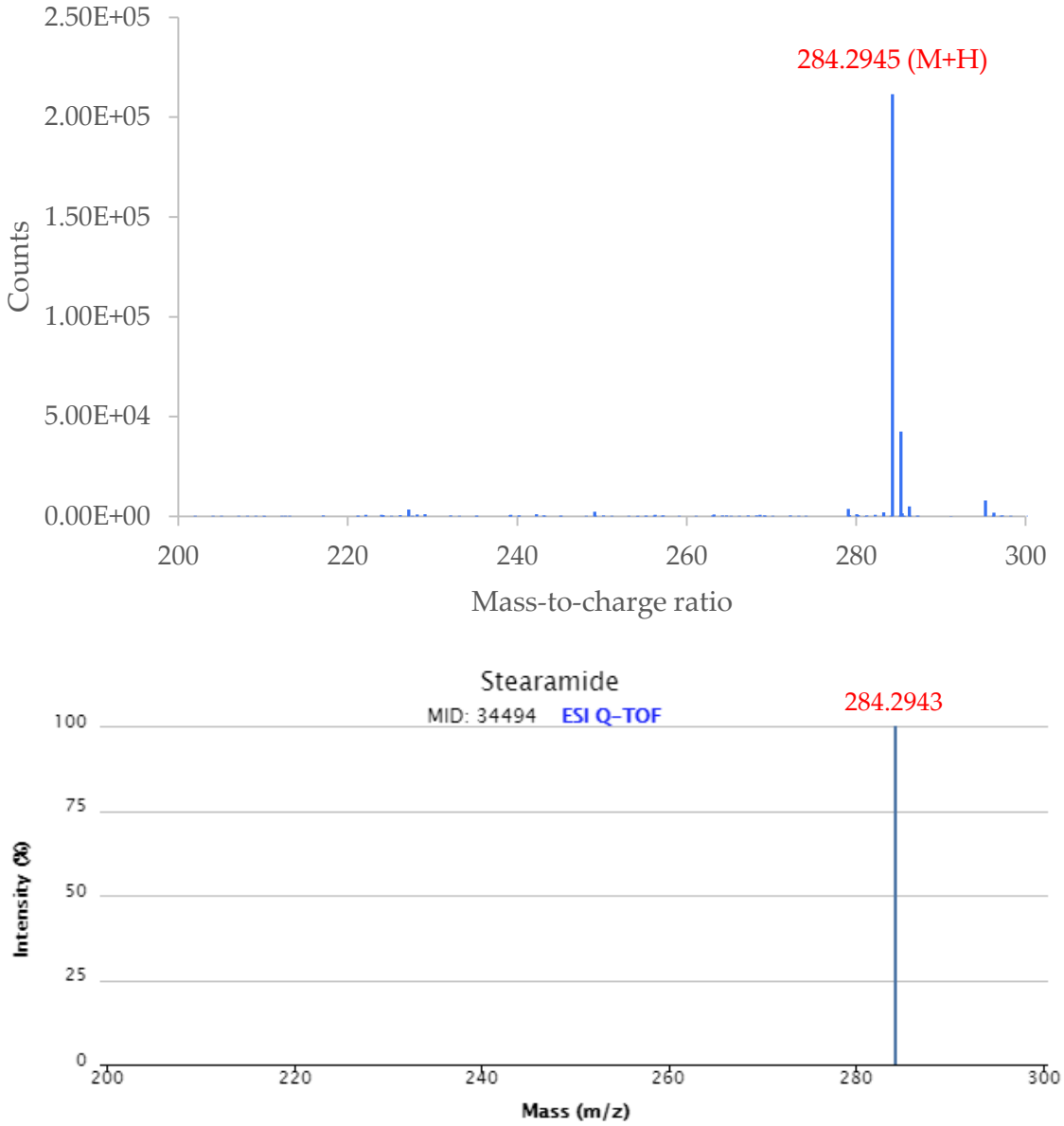

Figure I.5: Mass spectrum of marker 284.2941 m/z at a retention time of 24.58 minutes in QC sample (top) compared to the mass spectrum of stearamide found on METLIN (bottom)

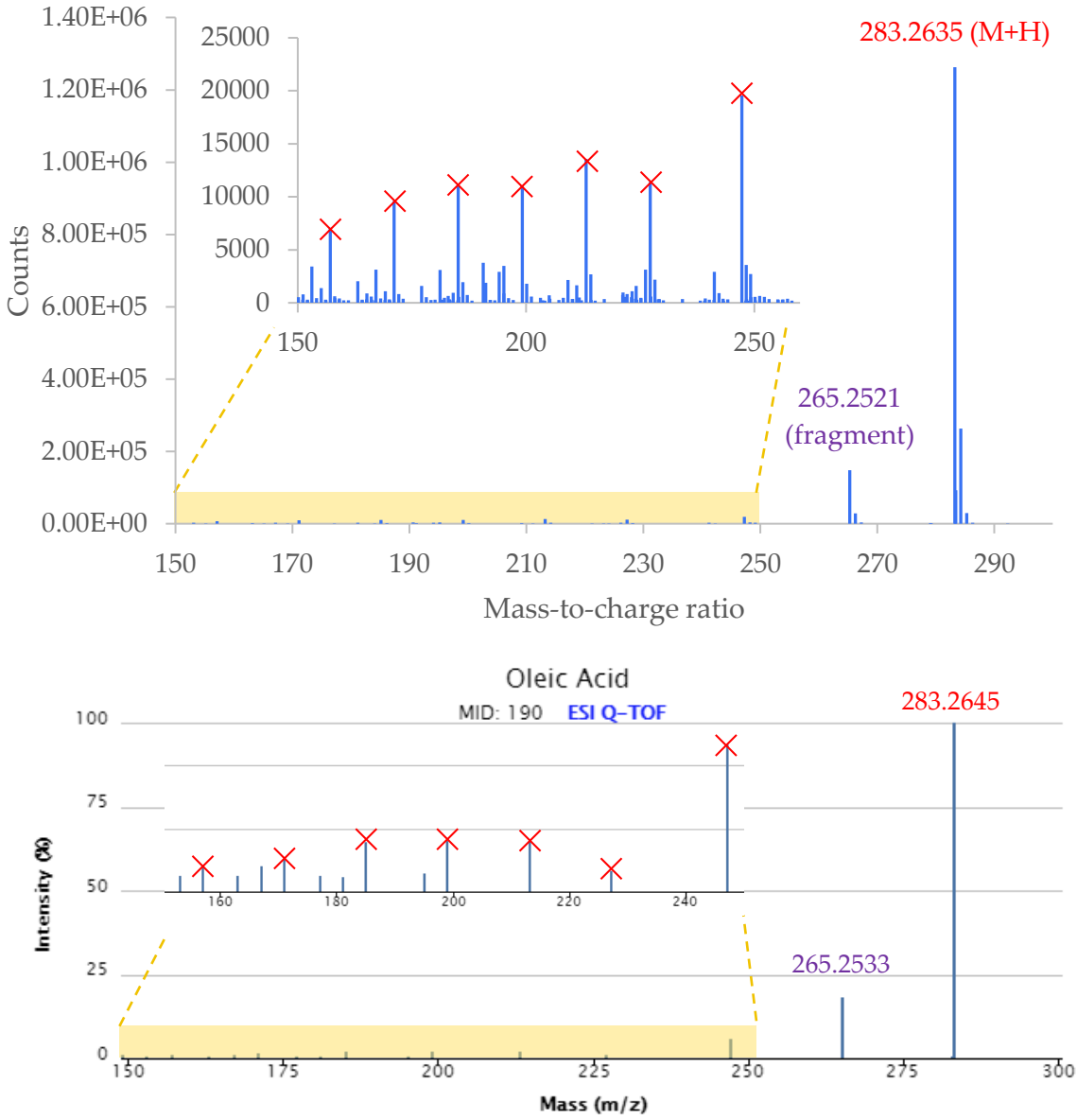

Fragment in raw data spectrum	Fragment in reference spectrum
157.1223	157.1233
171.1379	171.1404
185.1579	185.1518
199.1751	199.1740
213.1842	213.1869
227.1964	227.2016
247.2416	247.2430

Figure I.6: Mass spectrum of marker 283.2632 m/z at a retention time of 14.65 minutes in QC sample (top) compared to the mass spectrum of oleic acid found on METLIN (bottom). Table shows matching fragments in zoomed in spectra

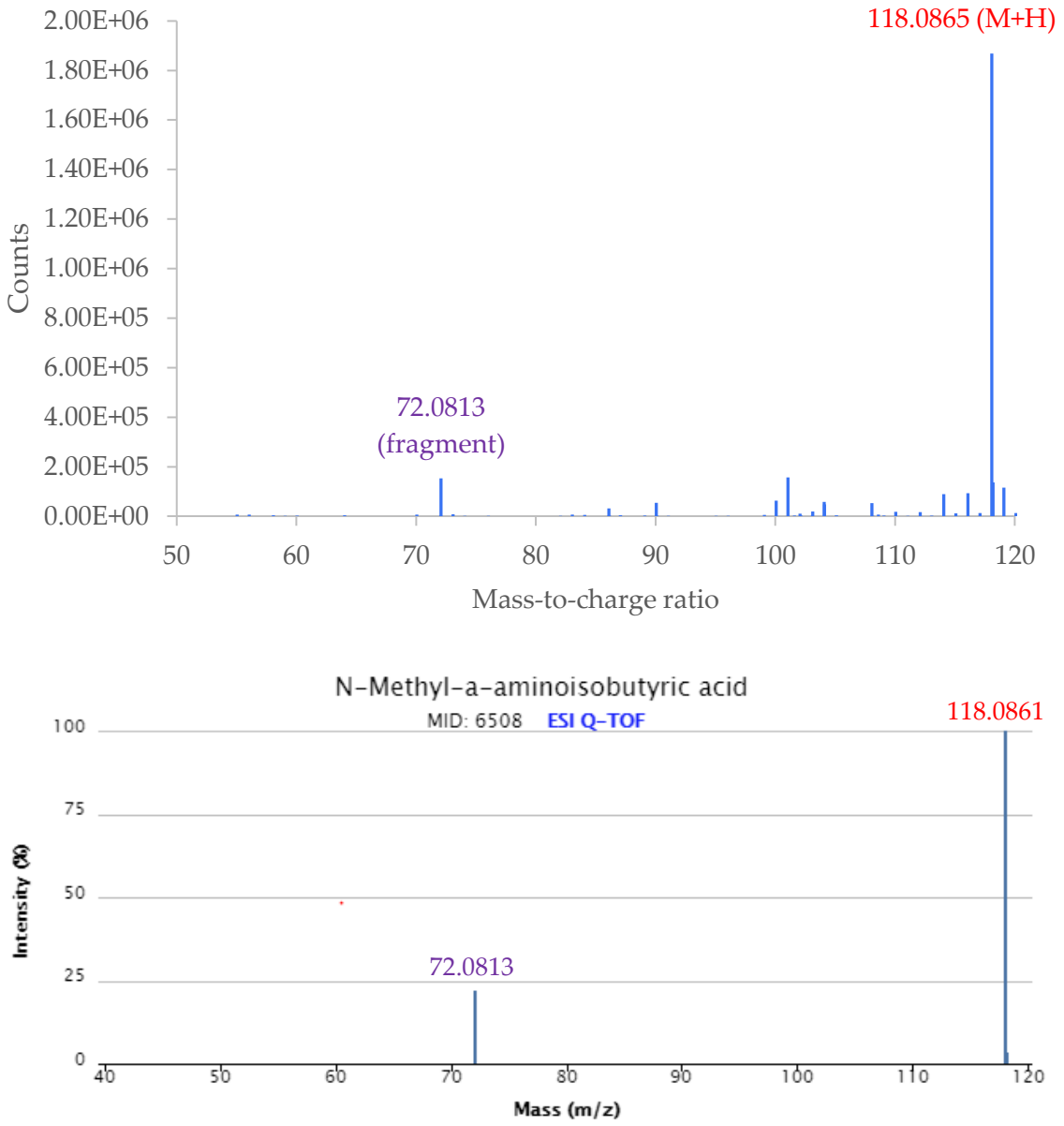

Figure I.7: Mass spectrum of marker 118.0867 m/z at a retention time of 1.04 minutes in QC sample (top) compared to the mass spectrum of N-methyl-α-aminoisobutyric acid found on METLIN (bottom)